552
4/23/80

Ab. 1442

DOE/ET/21050-1/2

COMBINED CYCLE SOLAR CENTRAL RECEIVER HYBRID POWER SYSTEM STUDY

Final Technical Report, Volume II

November 1979

Work Performed Under Contract No. ET-78-C-03-2051

Bechtel National, Inc.
San Francisco, California

MASTER

U.S. Department of Energy

Solar Energy

DISCLAIMER

This report was prepared as an account of work sponsored by an agency of the United States Government. Neither the United States Government nor any agency Thereof, nor any of their employees, makes any warranty, express or implied, or assumes any legal liability or responsibility for the accuracy, completeness, or usefulness of any information, apparatus, product, or process disclosed, or represents that its use would not infringe privately owned rights. Reference herein to any specific commercial product, process, or service by trade name, trademark, manufacturer, or otherwise does not necessarily constitute or imply its endorsement, recommendation, or favoring by the United States Government or any agency thereof. The views and opinions of authors expressed herein do not necessarily state or reflect those of the United States Government or any agency thereof.

DISCLAIMER

Portions of this document may be illegible in electronic image products. Images are produced from the best available original document.

DISCLAIMER

"This book was prepared as an account of work sponsored by an agency of the United States Government. Neither the United States Government nor any agency thereof, nor any of their employees, makes any warranty, express or implied, or assumes any legal liability or responsibility for the accuracy, completeness, or usefulness of any information, apparatus, product, or process disclosed, or represents that its use would not infringe privately owned rights. Reference herein to any specific commercial product, process, or service by trade name, trademark, manufacturer, or otherwise, does not necessarily constitute or imply its endorsement, recommendation, or favoring by the United States Government or any agency thereof. The views and opinions of authors expressed herein do not necessarily state or reflect those of the United States Government or any agency thereof."

This report has been reproduced directly from the best available copy.

Available from the National Technical Information Service, U. S. Department of Commerce, Springfield, Virginia 22161.

Price: Paper Copy $24.00
Microfiche $3.50

DOE/ET/21050-1/2
Distribution Category UC-62e

VOLUME II

TECHNICAL REPORT

COMBINED CYCLE SOLAR CENTRAL RECEIVER HYBRID POWER SYSTEM STUDY

Final Technical Report

prepared by
Bechtel National, Inc.
San Francisco, CA

Subcontractors: Foster Wheeler Development Corporation
Northrup, Inc.
Westinghouse Electric Corporation,
Combustion Turbine Systems Division

Utility Advisor: Public Service Company of New Mexico

for the
United States Department of Energy
San Francisco Operations Office

November, 1979

Contract No.:
DE-AC03-78ET21050
Bechtel Job No. 13007

THIS PAGE

WAS INTENTIONALLY

LEFT BLANK

ABSTRACT

This study develops the conceptual design for a commercial-scale (nominal 100 MWe) central receiver solar hybrid power system with combined cycle energy conversion. A near-term, metallic heat pipe receiver and an advanced ceramic tube receiver hybrid system are defined through parametric and market potential analyses.

Comparative evaluations of the cost of power generation, the fuel displacement potential, and the technological readiness of these two systems indicate that the near-term hybrid system has better potential for commercialization by 1990. Based on the assessment of the conceptual design, major cost and performance improvements are projected for the near-term system. Constraints preventing wide-spread use were not identified. Energy storage is not required for this system and analyses show no economic advantages with energy storage provisions.

It is concluded that the solar hybrid system is a cost effective alternative to conventional gas turbines and combined cycle generating plants, and has potential for intermediate-load market penetration at 15 percent annual fuel escalation rate. Due to their flexibility, simple solar/nonsolar interfacing, and short startup cycles, these hybrid plants have significant operating advantages. Utility company comments suggest that hybrid power systems will precede stand-alone solar plants.

THIS PAGE

WAS INTENTIONALLY

LEFT BLANK

CONTENTS

Section			Page
1	INTRODUCTION		1-1
	1.1	Project Objective	1-2
	1.2	Technical Approach	1-2
		1.2.1 Technical Requirements	1-3
		1.2.2 The Preconceptual Reference Solar Hybrid Power Systems	1-3
		1.2.3 Market Analysis	1-10
		1.2.4 Parametric Analysis	1-12
		1.2.5 Selection of Preferred System	1-13
		1.2.6 Conceptual Design of Commercial-Scale Hybrid Plant	1-14
		1.2.7 Assessment of Commercial-Scale Hybrid Plant	1-15
	1.3	Project Team	1-16
2	MARKET ANALYSES		2-1
	2.1	Introduction	2-1
	2.2	Baseline Cost/Performance Data and Economic Assumptions	2-2
		2.2.1 Baseline Data for Solar Hybrid Systems	2-2
		2.2.2 Baseline Data for Conventional Technologies	2-5
		2.2.3 Regional Variation of Data	2-5
		2.2.4 Economic Assumptions	2-8
	2.3	Economic Comparisons	2-10
		2.3.1 Levelized Busbar Electricity Cost Calculations	2-10
		2.3.2 Economic Comparisons	2-13
		2.3.3 Sensitivity Analysis	2-19
		2.3.4 Optimistic Scenario	2-23
	2.4	Market Assessment	2-27
		2.4.1 Methodology	2-27
		2.4.2 Market Assessment Results	2-36
	2.5	Conclusions	2-47

Section		Page

3	PARAMETRIC ANALYSES	3-1
3.1	Introduction	3-1
3.2	Collector Subsystem	3-3
3.2.1	Field Design and Input Data	3-5
3.2.2	Field Analysis	3-10
3.3	Receiver Subsystem	3-24
3.3.1	Receiver Concepts	3-24
3.3.2	Receiver Size	3-38
3.3.3	Receiver Materials	3-41
3.3.4	Receiver Thermal Performance Analysis	3-46
3.3.5	Absorber Panel Stress (Life) Analysis	3-66
3.3.6	Receiver Structural Support Analysis	3-68
3.3.7	Tower Analysis	3-69
3.3.8	Riser/Downcomer Analysis	3-70
3.3.9	Pumps, Piping, and Valve Analysis	3-75
3.3.10	Heat Exchanger Analysis	3-77
3.3.11	Receiver Outlet Temperature Analysis	3-77
3.3.12	Receiver Pressure Drop Analysis	3-77
3.4	Energy Storage Subsystem	3-80
3.5	Nonsolar Subsystem	3-83
3.5.1	Nonsolar Subsystem Concepts	3-83
3.5.2	Nonsolar Subsystem Size	3-91
3.5.3	Nonsolar Subsystem Materials	3-94
3.5.4	Fuels Selection	3-94
3.5.5	Nonsolar Thermal Performance Analysis	3-102
3.6	Electrical Power Generation Subsystem	3-103
3.6.1	Combined Cycle Overview	3-103
3.6.2	EPGS Size	3-109
3.6.3	EPGS Cycle Selection	3-110
3.7	Master Control	3-132
3.7.1	Master Control Concepts	3-133
3.7.2	Master Control Analysis	3-141
3.8	System Analyses	3-157
3.8.1	Plant Size	3-157
3.8.2	Solar Multiple and Field/Receiver Power Ratio	3-158
3.8.3	Storage Capacity	3-158
3.8.4	Solar Fraction	3-173

Section		Page

4	SELECTION OF PREFERRED SYSTEM	4-1
4.1	Selection Process	4-1
4.2	Selection Criteria	4-1
4.3	System Selection	4-2
4.3.1	Modifications to Preconceptual Reference Designs	4-3
4.3.2	Comparison of Strawman and Advanced Strawman Systems	4-4
4.3.3	Selected Plant Summary	4-11
5	CONCEPTUAL DESIGN AND COST/PERFORMANCE ESTIMATES	5-1
5.1	System Performance	5-2
5.1.1	Design Point Performance, Hybrid Operation	5-2
5.1.2	Fossil-Only Performance	5-5
5.1.3	Annual Average Performance	5-5
5.2	Collector Subsystem	5-8
5.2.1	Requirements	5-8
5.2.2	Conceptual Design	5-8
5.2.3	Performance	5-14
5.3	Receiver Subsystem	5-20
5.3.1	Requirements	5-20
5.3.2	Receiver Conceptual Design	5-20
5.3.3	Tower Conceptual Design	5-47
5.3.4	Riser and Downcomer Conceptual Design	5-58
5.4	Storage Subsystem	5-66
5.5	Nonsolar Subsystem	5-66
5.6	Electric Power Generation Subsystem	5-66
5.6.1	Performance	5-66
5.6.2	Gas Turbine-Generator	5-76
5.6.3	Steam Turbine-Generator	5-84
5.6.4	Heat Recovery Steam Generator	5-87
5.6.5	Gas Turbine Auxiliary Systems	5-88
5.6.6	Steam Cycle Auxiliary Systems	5-93
5.6.7	Site Power Distribution	5-96
5.7	Master Control Subsystem	5-101
5.7.1	Requirements	5-101
5.7.2	Collector Subsystem Controls	5-102
5.7.3	Receiver Subsystem Controls	5-106
5.7.4	EPGS Controls	5-108
5.7.5	Fuel Supply Controls	5-111
5.7.6	Master Control	5-111

Section		Page

5.8	Plant Arrangement	5-119
5.8.1	Plot Plan	5-119
5.8.2	Major Equipment	5-120
5.8.3	Architectural Considerations	5-120
5.9	System Operation	5-125
5.9.1	Daily Operating Cycle	5-125
5.9.2	Startup and Shutdown Sequence	5-127
5.9.3	System Transients	5-129
5.10	Cost Estimates	5-131
5.10.1	Introduction	5-131
5.10.2	Costing Geographical Boundaries	5-133
5.10.3	Capital Costs	5-138
5.10.4	Operating and Maintenance Costs	5-138
5.10.5	Project Schedule	5-150
6	ASSESSMENT OF COMMERCIAL-SCALE SOLAR CENTRAL RECEIVER HYBRID POWER SYSTEM	6-1
6.1	Potential Improvements	6-1
6.1.1	Performance	6-1
6.1.2	Fossil Fuel Displacement Potential	6-6
6.1.3	Cost Reduction	6-20
6.1.4	Economies of Scale	6-22
6.2	Potential Limitations	6-26
6.2.1	Environmental Effects	6-26
6.2.2	Land Use Constraints	6-30
6.2.3	Natural Resources Constraints	6-32
6.2.4	Status of Materials Technology	6-35
6.2.5	Power Conversion Equipment Availability	6-36
6.2.6	Manufacturing and Market Capacity Constraints	6-37
6.2.7	Legal, Regulatory, Fiscal, and Institutional Constraints	6-39
6.2.8	Safety Considerations	6-44
6.3	Market Analysis Update	6-45
6.3.1	Busbar Costs and Market Potential	6-46
6.3.2	Utility Survey	6-53
6.4	Summary Assessment and Conclusions	6-58
6.4.1	The Conceptual Design	6-58
6.4.2	Potential Improvements	6-59
6.4.3	Potential Constraints to Widespread Application	6-59
6.4.4	Conclusions	6-60
7	REFERENCES	7-1

ILLUSTRATIONS

Figure		Page
1-1	Reference System Schematic	1-7
2-1	Sample Busbar Cost Functions	2-12
2-2	Screening Curves, 1990, 12 Percent Fuel Escalation Rate	2-15
2-3	Screening Curves, 1990, 15 Percent Fuel Escalation Rate	2-16
2-4	Screening Curves, 2000, 12 Percent Fuel Escalation Rate	2-17
2-5	Screening Curves, 1990, Variable Fuel Escalation Rates	2-18
2-6	Sensitivity of Modified Strawman Levelized Busbar Cost to +1 Percent Variation in Cost/Performance Components Specific to Hybrid Systems	2-21
2-7	Sensitivity of Modified Strawman Levelized Busbar Cost to +1 Percent Variation in Cost Components Common to All Technologies	2-22
2-8	Screening Curves, Optimistic Scenario	2-26
2-9	1990 Incremental Load Duration Curve for the Pacific Southern Region	2-29
2-10	Capacity Allocation Process	2-30
2-11	Allocation Process Under Constrained Coal/Nuclear Scenarios	2-35
2-12	Simulated Market Penetration of Modified Strawman in Pacific Southern Region, 15 Percent Fuel Escalation Rate	2-38
2-13	Simulated Market Penetration of Modified Strawman in Pacific Southern Region, 15 Percent Fuel Escalation Rate	2-39
2-14	Simulated Market Penetration of Modified Strawman in South Mountain Region, 15 Percent Fuel Escalation Rate	2-40
2-15	Simulated Market Penetration of Modified Strawman in South Central Region, 15 Percent Fuel Escalation Rate	2-41

Figure		Page
2-16	Simulated Market Penetration of Modified Strawman in Middle Atlantic Region, 15 Percent Fuel Escalation Rate	2-42
2-17	Simulated Market Penetration of Modified Strawman in Pacific Southern Region, 12 Percent Fuel Escalation Rate	2-43
3-1	Layout of Collector Field "A"	3-7
3-2	Layout of Collector Field "G"	3-9
3-3	Normalized Field Cost with Heliostats at $50/m²	3-12
3-4	Normalized Field Cost with Heliostats at $100/m²	3-13
3-5	Normalized Field Cost with Heliostats at $150/m²	3-14
3-6	Normalized Field Cost with Heliostats at $200/m²	3-15
3-7	Focal Plane Flux Map for North Receiver of "G" Field for Equinox Noon at Barstow, CA	3-18
3-8	Focal Plane Flux Profile for North Receiver of "G" Field for Equinox Noon at Barstow, CA	3-19
3-9	Cavity Flux Map for North Receiver of "G" Field for Equinox Noon at Barstow, CA	3-20
3-10	Cavity Flux Profile for North Receiver of "G" Field for Equinox Noon at Barstow, CA	3-21
3-11	Focal Plane Flux Map for West Receiver of "G" Field for 10:00 a.m., Equinox at Barstow, CA	3-22
3-12	Cavity Flux Profile for West Receiver of "G" Field for 10:00 at.m., Equinox a Barstow, CA	3-23
3-13	Receiver Plan Arrangement	3-28
3-14	Heat Pipe Receiver Schematic for Strawman System (East, West, and South Receivers)	3-29
3-15	Panel Configuration for Strawman System (East, West, and South Receivers)	3-31
3-16	Schematic of Heat Pipe for Strawman System	3-32
3-17	Typical Heat Pipe Layout for Strawman System	3-33
3-18	Schematic of Heat Pipe Installation	3-34
3-19	Ceramic Receiver Schematic for Advanced Strawman System	3-36

Figure		Page

3-20	North Receiver Air Flow Distribution, Strawman System	3-52
3-21	Panel Depth vs Pressure Drop, Strawman Receiver	3-55
3-22	Effect of Receiver Pressure Drop and Pressure Ratio on Ceramic Receiver Size, Advanced Strawman System	3-59
3-23	Effects of Air Outlet Temperature on Ceramic Receiver Size, Advanced Strawman System	3-60
3-24	Typical Aperture Sizing Parameters	3-63
3-25	Receiver Efficiency vs Temperature at Constant Air Flow	3-65
3-26	Receiver Efficiency vs Rated Power at Constant Outlet Temperature	3-67
3-27	Riser Piping Layout Concept	3-71
3-28	Cost Effect of Strawman Piping Pressure Loss	3-73
3-29	Cost Effect of Strawman Receiver Outlet Temperature	3-78
3-30	Cost Effect of Advanced Strawman Receiver Outlet Temperature	3-79
3-31	Cost Effect of Strawman Receiver Pressure Loss	3-81
3-32	Cost Effect of Advanced Strawman Receiver Pressure Loss	3-82
3-33	Conventional Gas Turbine Combustor	3-84
3-34	Combustion System Temperature History	3-87
3-35	Low NO Emission Combustor Concepts	3-89
3-36	Strawman Daily Heat Rate Variation	3-93
3-37	Simple Open-Cycle Gas Turbine Net Efficiency vs Compressor Pressure Ratio for Various Turbine Inlet Temperatures	3-105
3-38	Simple Open-Cycle Gas Turbine Specific Power vs Compressor Pressure Ratio for Various Turbine Inlet Temperatures	3-106
3-39	Gas and Water/Steam Temperature Profiles in Heat Recovery Boilers	3-108

Figure		Page
3-40	Cost Effect of Strawman Compressor Pressure Ratio	3-115
3-41	Cost Effect of Advanced Strawman Compressor Pressure Ratio	3-117
3-42	Cost Effect of Strawman Main Steam Pressure/Temperature	3-121
3-43	Cost Effect of Advanced Strawman Main Steam Pressure/Temperature	3-122
3-44	Cost Effect of Strawman Compressor Intercooling	3-125
3-45	Cost Effect of Advanced Strawman Compressor Intercooling	3-126
3-46	Dual-Pressure HRSG Temperature Profile	3-128
3-47	Typical Dual-Pressure Steam Cycle Diagram	3-130
3-48	Master Control Block Diagram	3-134
3-49	Collector Subsystem Control Schematic	3-147
3-50	Receiver and EPGS Subsystem Control Block Diagram	3-142
3-51	Heliostat Positions Used to Analyze Tracking Singularity Rates	3-146
3-52	Heliostat Axes Tracking Angle Pattern for Sample 1 (53N,15W)	3-147
3-53	Heliostat Axes Tracking Angle Pattern for Sample 2 (37N, 41W)	3-148
3-54	Heliostat Axes Tracking Angle Pattern for Sample 3 (17N, 46W)	3-149
3-55	Heliostat Axes Tracking Angle Pattern for Sample 4 (4S, 45W)	3-150
3-56	Heliostat Axes Tracking Angle Pattern for Sample 5 (21S, 35W)	3-151
3-57	Heliostat Axes Tracking Angle Pattern for Sample 6 (12S, 20W)	3-152
3-58	Heliostat Axes Tracking Angle Pattern for Sample 7 (6S, 7W)	3-153
3-59	Heliostat Axes Tracking Angle Pattern for Sample 8 (7N, 1W)	3-154

Figure		Page

3-60	Heliostat Axes Tracking Angle Pattern for Sample 9 (22N, 1W)	3-155
3-61	Heliostat Axes Tracking Angle Pattern for Sample 10 (37N, 1W)	3-156
3-62	Effects of Energy Storage at Different Times of Day	3-160
3-63	Energy Savings From Storage vs Solar Multiple	3-162
3-64	Increased Solar System Cost vs Solar Multiple, 1990 Plant	3-164
3-65	Value of Storage vs Solar Multiple, 1990 Plant, 100 Percent Turnaround Efficiency	3-165
3-65	Value of Storage vs Solar Multiple, 1990 Plant, 60 Percent Turnaround Efficiency	3-166
3-66	Value of Storage vs Fuel Escalation Rate, 1990 Plant, Solar Multiple 2.0	3-168
3-68	Hours of Storage vs Solar Multiple, Peak Insolation Day	3-170
3-69	Typical Schematic Incorporating Energy Storage in Solar Hybrid Plant	3-172
4-1	Screening Curve Cost Comparison, 1990, 12 Percent Fuel Escalation Rate	4-5
4-2	Screening Curve Cost Comparison, 1990, 15 Percent Fuel Escalation Rate	4-7
4-3	Screening Curve Cost Comparison, 2000, 12 Percent Fuel Escalation Rate	4-8
4-4	Screening Curve Cost Comparison, 2000, 15 Percent Fuel Escalation Rate	4-9
5-1	Stair-Step Diagram, Design Point Hybrid Operation	5-4
5-2	Stair-Step Diagram, Fossil Operation	5-6
5-3	Stair-Step Diagram, Annual Average	5-7
5-4	'H' Field Radial Stagger Layout	5-10
5-5	Normalized Field Cost, Heliostats at $160/m²	5-11
5-6	Normalized Field Cost, Heliostats at $69.5/m²	5-11
5-7	Back View of Heliostat (Northrup II)	5-12

Figure		Page
5-8	Front View of Heliostat (Northrup II)	5-12
5-9	North Focal Plane Flux Map (Wind at 0 m/sec)	5-19
5-10	North Focal Plane Flux Map (Wind at 16 m/sec)	5-19
5-11	Receiver Plan Arrangement	5-23
5-12	Cavity Design	5-25
5-13	Panel Design	5-27
5-14	North Cavity Airflow Distribution	5-34
5-15	Aperture Sizing	5-40
5-16	Receiver Losses at Rated Power Operation	5-43
5-17	Receiver Power Output at Equinox	5-46
5-18	Receiver Power Throughout Year	5-46
5-19	Tower Geometry	5-50
5-20	Typical Floor Diaphragm Framing Plan	5-51
5-21	Receiver Cavity Arrangement Plan	5-52
5-22	Tower Foundation Plan	5-54
5-23	OBE Horizontal Response Spectra, Elevation 190 Meters (639 Feet)	5-56
5-24	OBE Vertical Response Spectra, Elevation 190 Meters (630 Feet)	5-57
5-25	Artist's Concept of Riser(C) and Downcomer (H) Piping Arrangement	5-60
5-26	Selected Downcomer Design Concept	5-61
5-27	Air Piping Between Gas Turbine and Solar Receiver	5-64
5-28	Heat Balance Diagram, Hybrid Mode	5-69
5-29	Heat Balance Diagram, Long-Term Fossil Mode	5-71
5-30	Heat Balance Diagram, Solar-Only Mode	5-73
5-31	Variable-Pressure Operating Characteristics	5-75
5-32	Variation of Heat Rate as a Function of Plant Load	5-77

Figure		Page
5-33	Effect of Altitude on Net Plant Performance	5-78
5 34	Gas Turbine (Westinghouse W-501)	5-79
5-35	Catalytic Combustor Schematic	5-82
5-36	Typical Steam Turbine Cutaway Drawing	5-85
5-37	Perspective Drawing of HRSG	5-89
5-38	Fuel Storage and Supply System	5-90
5-39	Circulating Water, Chemical Treatment, and Cooling Tower Blowdown System	5-97
5-40	Single-Line Diagram	5-99
5-41	Collector Subsystem Control Configuration	5-104
5-42	Conceptual Master Control System	5-113
5-43	Typical 10-Loop Master Control	5-116
5-44	Control System Overview with Redundant Control Processors	5-117
5-45	Partial Site Plan	5-121
5-46	Elevations	5-123
5-47	Solar Power to Receivers During Startup (Equinox Morning)	5-128
5-48	Power Split Among Cavities During Startup (Equinox Morning)	5-128
5-49	Cost Account Boundaries	5-135
5-50	Solar Hybrid Plant Construction Schedule	5-151
6-1	"I" Field Radial Stagger Layout	6-4
6-2	Energy Storage Subsystem Schematic	6-9
6-3	Increased Solar Energy Contributions Due to Energy Storage	6-10
6-4	Potential for Increased Solar Fraction through Increased Field/Receiver Power Ratio	6-14
6-5	Percent of Incremental Energy Collection Used as a Function of Field/Receiver Power Ratio	6-15

Figure		Page
6-6	Reduction in Levelized Cost Due to Field/Receiver Power Ratios Exceeding 1.0	6-16
6-7	Capital Cost Effects of Economies of Scale	6-25
6-8	Levelized Busbar Costs for Solar Hybrid Plants	6-50
6-9	Simulated Market Penetration for Pacific Southern Region	6-52

TABLES

Table		Page
1-1	Preconceptual Design Data	1-5
1-2	Preconceptual System Performance	1-6
2-1	Capital Cost Estimate for Reference Solar Hybrid Systems	2-3
2-2	Operating and Maintenance Cost Estimate for Reference Solar Hybrid Systems	2-6
2-3	Baseline Performance Data for Reference Solar Hybrid Systems	2-6
2-4	Baseline Performance Data and Cost Estimates for Conventional Technologies	2-7
2-5	Economic Assumptions	2-9
2-6	Optimistic Scenario Assumptions	2-25
2-7	Key Market Potential Determinants	2-46
3-1	Collector Field Descriptions	3-6
3-2	Geometric Performance Efficiency, "G" Field	3-17
3-3	Geometric Data Summary for Ceramic Receiver, Advanced Strawman	3-39
3-4	Weight Data Summary for Ceramic Receiver, Advanced Strawman	3-40
3-5	Heat Pipe Receiver Materials Data	3-42
3-6	Heat Pipe Receiver Materials Composition	3-43
3-7	Heat Pipe Receiver Materials Evaluation	3-45
3-8	Receiver Performance Parametric Values	3-47
3-9	Net Heat Flux Into Panels, North Receiver, Strawman System	3-49
3-10	Net Power to Air, North Receiver, Strawman System	3-50
3-11	Power Transported by Individual Heat Pipes, North Receiver, Strawman System	3-51

Table		Page

3-12	Peak Heat Pipe Metal Temperature, Evaporation Section, North Receiver, Strawman System	3-54
3-13	Strawman Heat Pipe Receiver Parametric Cases	3-56
3-14	Advanced Strawman Receiver Operating Conditions	3-57
3-15	Advanced Strawman Receiver Parametric Cases	3-61
3-16	Receiver Thermal Losses	3-64
3-17	Constant Air Flow vs Constant Receiver Outlet Temperature	3-76
3-18	Fuel Characteristics	3-100
3-19	Alternative Fuels Analysis	3-101
3-20	EPGS Parametric Values	3-111
3-21	Economic Evaluation of Strawman Parametric Cases	3-112
3-22	Economic Evaluation of Advanced Strawman Parametric Cases	3-113
3-23	Exhaust Temperature vs Pressure Ratio	3-119
3-24	High-Temperature Energy Storage Systems	3-169
4-1	Modified Strawman Capital Cost Summary	4-12
4-2	Modified Strawman System Perfcrmance	4-13
5-1	System Performance	5-3
5-2	Heliostat Error Tolerances	5-17
5-3	Mean and Standard Deviation Wind-Induced Error	5-17
5-4	North Receiver Wind Effect Summary	5-18
5-5	West Receiver Wind Effect Summary	5-18
5-6	Receiver Subsystem Requirements	5-21
5-7	Incident Heat Flux, Panel Zones	5-30
5-8	Receiver Weight Breakdown	5-31
5-9	Power Transported by Individual Heat Pipes	5-33
5-10	Allowable Membrane Stresses in Inconel 617	5-36

Table		Page

5-11	Design Temperatures for Components of the Panel Shell	5-38
5-12	North Cavity Performance	5-42
5-13	Power vs Day of Year at Noon	5-44
5-14	Power vs Time of Day at Equinox	5-45
5-15	Subsystem Status for Various Plant Operating Modes	5-103
5-16	EPGS Controls	5-109
5-17	Construction Cost Summary	5-139
5-18	Construction Cost Estimate	5-140
6-1	Conceptual Design Energy Storage Subsystem Sizing Data	6-11
6-2	Potential Legal and Regulatory Constraints	6-40
6-3	Capital Cost Comparison	6-47
6-4	Operating and Maintenance Cost Comparison	6-47
6-5	Revised Performance Data	6-49
6-6	Typical Utility Economic Assumptions	6-54

Section 1

INTRODUCTION

This report was prepared by Bechtel National, Inc. to present the technical results of the Combined Cycle Solar Hybrid Power System Study Project. This project is part of the Department of Energy's Solar Central Receiver Hybrid Power System program.

The report has been organized to treat the work of each technical task in separate sections, generally following the outline instructions provided by Sandia Laboratories, Livermore, Technical Manager of the project. A data list and appendices are also included. The tasks presented are:

- Task 2 - Market Analysis
- Task 3 - Parametric Analysis
- Task 4 - Selection of Preferred System Configuration
- Task 5 - Commercial Plant Conceptual Design Cost/Performance Estimates
- Task 6 - Assessment of Commercial-Sacle Solar Central Receiver Hybrid Power System

Task 1, Review and Analysis of Preliminary Specifications, has been completed. Comments resulting from this review have already been sent to DOE and are therefore not covered in this report.

1.1 PROJECT OBJECTIVE

The overall objective of this project is to select and assess a commercial-scale hybrid power system concept with the maximum potential worth to a utility. This worth is to include minimum cost of energy in terms of mills per kilowatt-hour and maximum savings in capital and operating costs of displaced conventional power generation.

1.2 TECHNICAL APPROACH

The overall technical approach to this study project was as follows:

- Technical requirements were established by the U.S. Department of Energy, San Francisco Operations Office
- Based on these requirements, near-term and advanced reference designs and cost estimates were prepared for a solar hybrid concept
- A market analysis of the two designs was undertaken, based on the utility screening/load duration curve method
- Parametric analyses and economic evaluations were done on the hybrid systems and subsystems
- The near-term and advanced systems were comparatively evaluated, based on low-cost energy production, market potential, acceptable solar fraction, and low development risk
- From the evaluation, one of the systems was selected for conceptual design and assessment
- A commercial system conceptual design was developed and a cost estimate was prepared
- The technical and economic aspects, and marketability of the commercial system were assessed

1.2.1 Technical Requirements

The technical requirements for the project, which were specified by the U.S. Department of Energy, San Francisco Operations Office (DOE/SAN), are complied in a document titled: "Solar Central Receiver Hybrid Power System; Requirement Definition" (Ref 1-1).

1.2.2 The Preconceptual Reference Solar Hybrid Power Systems

In the solar hybrid power system concept selected for the study, solar energy supplies a portion of the energy requirements of a combined cycle power plant. The combined cycle technology, although already in commercial use, is open to further improvements. Therefore, two levels of system conditions were selected for study in the initial tasks, reflecting different levels of technological readiness. These two levels, designated "Strawman" and "Advanced Strawman," form the preconceptual reference solar power systems for studies in Tasks 2, 3, and 4:

- Strawman. This system uses near-term technology and is based on a metallic solar receiver and a gas turbine that is typical of the current level of technology. The air-cooled receiver uses metallic heat pipes to transport solar-generated thermal energy into the air stream. The receiver outlet temperature is 816C (1500F) and the gas turbine inlet temperature is 1093C (2000F).

- Advanced Strawman. This system, representing a further level of technological advancement, is based on a ceramic tube receiver and on a gas turbine that is still under development. The receiver outlet temperature is 1093C (2000F) and the gas turbine inlet temperature is 1316C (2400F).

Design and performance data and a schematic for these systems are presented in Tables 1-1 and 1-2 and Figure 1-1. (A more detailed list of characteristics is contained in Appendix A.) Preconceptual features of the two systems were defined in order to:

- Establish the base cases and ranges of variation for parametric studies
- Prepared cost estimates for market studies
- Calculate economic sensitivity factors to be used in parametric studies

Collector Subsystem. The collector fields of both the Strawman and Advanced Strawman systems are elliptical. In each case the receiver tower is offset to the south of the geometric center of the field. Each heliostat has a reflective area of 38.6 m^2 (415 ft^2). The Strawman and Advanced Strawman systems have 5682 and 7095 heliostats, respectively.

Receiver Subsystem. This subsystem consists of a tower, a solar receiver, and riser/downcomer piping in the tower. The receivers for each reference system have four cavities, facing north, south, east, and west. Air is delivered to the cavities from the discharge of the gas turbine compressor via the riser pipe. The air at the receiver inlet is 378C (712F) for both baseline designs, due to the heat of compression at a pressure ratio of 12:1.

TABLE 1-1

PRECONCEPTUAL DESIGN DATA

Parameter	Strawman Design	Advanced Strawman Design
Reflective Area per Heliostat, m^2	38.6	38.6
Number of Heliostats	5496	7071
Field Arrangement	Elliptical, South Offset Tower	
Receiver Type	Multicavity	
Absorber Type	Heat Pipe	Ceramic Tube
Height of Aperture Above Ground Level, m (ft)	175(574)	196(643)
Riser Pipe Diameter, m (in)	1.52(60)	1.22 (48)
Downcomer Pipe Diameter, m (in)	1.83(72)	1.83(72)
Compressor Pressure Ratio	12:1	12:1
Net Power Hybrid Mode, MWe		
Gas Turbine	68.4	64.7
Steam Turbine	31.6	35.3

TABLE 1-2

PRECONCEPTUAL SYSTEM PERFORMANCE

Parameter	Strawman Design	Advanced Strawman Design
Solar Receiver Outlet Temperature, °C (°F)	816 (1500)	1093 (2000)
Gas Turbine Inlet Temperature, °C (°F)	1093 (2000)	1316 (2400)
Fossil Fuel	Distillate No. 2	
EPGS Thermal to Net Electric Conversion Efficiency, %	43.5	47.7
Design Point Solar Capacity Fraction, %	56.3	71.9
Annual Average Daytime Solar Fraction, %	31.2	40.8
Assumed Average Nighttime Operation on Fossil Fuel, Hrs	2.0	2.0
Annual Average Solar Fraction, %	26.4	34.5
Plant Capacity Factor, %	48.0	48.0
Solar Capacity Factor, %	12.7	16.6

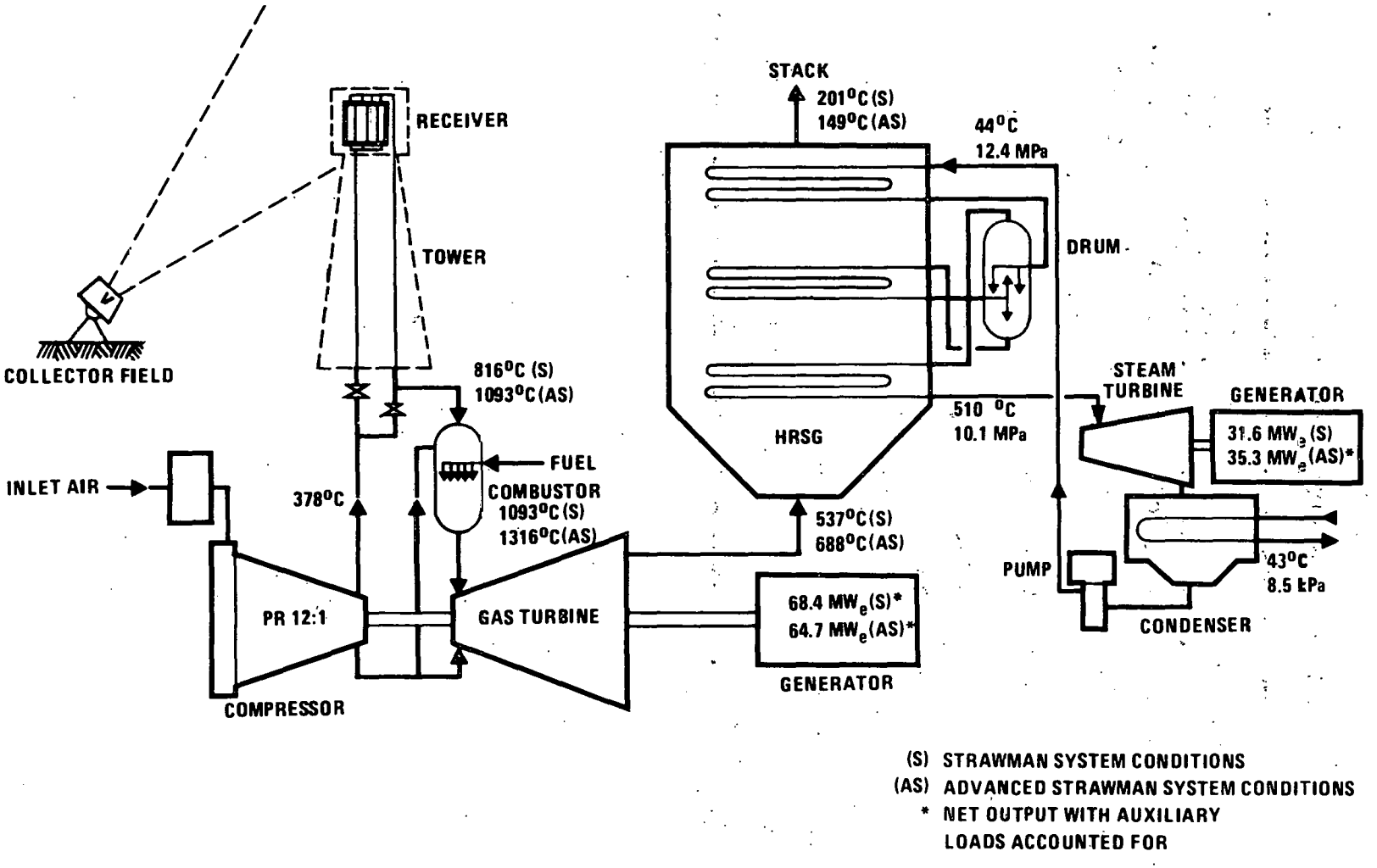

Figure 1-1 REFERENCE SYSTEM SCHEMATIC

The Strawman receiver design uses metallic heat pipes to transmit the solar heat to the air ducts, called panels, located at the rear wall of each receiver cavity. Heat is transferred to the air which flows over the finned condensing section of the heat pipes inside the receiver panels. The air flow is controlled to achieve a uniform 816C (1500F) outlet temperature from each of the panels at the design point. The heated air is delivered back to the combustor via the downcomer pipe. A pressure loss of 27.6 kPa (4 psi) is allowed in the receiver and a total of 27.6 kPa (4 psi) pressure loss is taken in the riser/downcomer.

The Advanced Strawman receiver design uses vertical ceramic U-tubes along the rear wall of each cavity to absord the solar radiant flux. The air flowing inside the tubes is heated to an outlet temperature of 1093C (2000F). Allowable pressure losses are 69.0 kPa (10 psi) for the receiver and 34.5 kPa (5 psi) for the riser/downcomer piping.

Electric Power Generation Subsystem. The electric power generation subsystem consists of the gas turbine cycle and the steam cycle. The front end of the gas turbine cycle is the compressor, which feeds the air to the receiver. After the air is heated in the solar receiver, its temperature is further boosted in the combustor, using fossil fuel. Both preconceptual baseline designs have the combustor in series with the receiver. The air with combustion products is then expanded through the gas turbine-generator to produce approximately two-thirds of the plant's electrical output.

The exhaust from the gas turbine, which still contains significant energy, is ducted into a heat recovery steam generator (HRSG) where this residual energy is extracted from the air. This energy is then used to power the steam-Rankine bottoming cycle.

A simple, single-pressure, nonreheat steam cycle is used for both preconceptual baseline designs with 10.1 MPa/510C (1450 psig/950F) main steam conditions. Water is pumped from the condenser hotwell through the economizer, evaporator, and superheater sections of the HRSG. The superheated steam is then expanded through a non-extraction steam turbine to generate about one-third of the total plant output. Heat is rejected from the condenser through a wet cooling tower located outside the heliostat field.

At the design point (equinox noon), the solar heat input is 56.3 percent for the Strawman design and 71.9 percent for the Advanced Strawman design. These values reflect the ratios of the temperature rise in the solar receiver compared to the total temperature rise from the compressor outlet to the turbine inlet.

The high energy conversion efficiencies of 43.5 percent and 47.7 percent, net, for the Strawman and Advanced Strawman, respectively, are indicative of the advantages of combined cycle plants. A 48 percent capacity factor was used to represent conventional combined cycle plants in intermediate-load service.

However, the plants can be operated up to 24 hours a day at the rated output of 100 MWe net.

Energy Storage. The reference systems do not have energy storage provisions, since the gas turbines can respond rapidly to load changes and this obviates the need for buffer storage. In addition, according to preliminary estimates, long-term energy storage is, at best, marginally economic. Further evaluations during the project confirmed these initial findings.

Modified Strawman. As the preliminary system selection process progressed, it became apparent that certain technical and economic advantages could be gained by modifying the reference Strawman system. These modifications included reduced receiver and rise/downcomer pressure drops, a dual-pressure heat recovery steam generator, an increased receiver outlet temperature, and larger heliostats. A modified Strawman system incorporating the first two of these modifications was used as the basis of the market analysis work and in economic evaluations.

1.2.3 Market Analysis

When selecting the type of technology for any addition of generating capacity, utilities must consider many economic, technical, and institutional factors. These might include:

- Existing and projected growth of system load
- Timing and duration of the load (existing and projected

- The mix of the existing generating capacity
- The projected cost of power generation and distribution
- Confidence in the technical reliability of the technology
- The availability and cost of energy sources
- Institutional factors constraining the choices

Some of the factors lend themselves to rigorous quantitative analyses. Assessment of others can only be qualitative. The weight of each factor and the overall decision-making process varies from one utility to another.

The method frequently used by utility planners in the early planning stages to identify the economically viable alternatives for any part of the system load is the screening/load duration curve method. This was used in the market analysis to test the economic viability of the reference systems. In the screening curves produced, the solar hybrid plant is compared with competing conventional technologies.

The Bechtel computer program ALLOCATE was used to calculate the screening curves and to estimate the market share where solar hybrid power systems could compete successfully. The two inputs to the program were:

- Levelized annual plant costs
- Plant operating characteristics

The levelized annual cost components were calculated by Bechtel's computer program RESOURCE, based on economic guidelines and data from EPRI and DOE, and on specific plant costs and operating characteristics from published and Bechtel in-house materials.

During the market studies, utility companies were contacted to verify the analytical approach and the validity of the input data.

1.2.4 Parametric Analysis

A large data base was required to allow rational selection of the preferred system for the subsequent conceptual design and assessment tasks. To establish this data base, parametric analyses were performed to evaluate the cost impact of major design, performance, and cost variables of the solar hybrid power systems.

The approach used in these parametric studies was to establish a reference value or point based on a preconceptual system design (see Subsection 1.2.2) and then to choose two additional points, one above and one below the reference, to establish the trend of change. The figure of merit selected to gauge the effects of the variations was the equivalent capital cost. This included the estimated capital cost and the capitalized value of the operating and maintenance costs, including the cost of fuel.

The analyses included evaluation of the following design variables:

- Collector field configuration
- Receiver design concept and configuration
- Power cycle design and operating conditions

Although variations are also conceivable in the master control subsystem and in the site electric power distribution, it is not expected that these will significantly affect the economics of the solar hybrid power systems. Consequently no separate analyses were conducted for these portions of the plant. However, the cost impacts on them by changes in other design variables were considered.

1.2.5 Selection of Preferred System

The preferred commercial power system evolved from the preconceptual reference designs through parametric analyses, economic evaluations, and system-level studies. The major criteria during the evaluations were: cost of energy production, market potential, fossil fuel displacement potential (solar fraction), and development risk.

Major system-level studies included selecting the reference fuel, assessing the economic value of energy storage, and selecting the solar fraction. Other system-level considerations included plant size and solar multiple and field/receiver power ratio.

The reference Strawman and Advance Strawman designs were modified as a result of the parametric analyses and system-level studies, and the final economic evaluation of the two systems took into consideration the cost impact of these changes.

1.2.6 Conceptual Design of Commercial-Scale Hybrid Plant

The conceptual design of the preferred commercial power system was developed around a commercially available gas turbine produced by Westinghouse (Model W-501), and a single-casing, nonreheat steam turbine, also produced by Westinghouse. The combined net output of these units in the hybrid mode is 112.6 MWe, which is slightly higher than the DOE-specified 100 MWe nominal output for the commercial solar hybrid power system. However, there is an extensive technical and economic data base available for these turbines, and due to the comparatively small capacity difference, any extrapolation to a 100 MWe power level can be made without introducing significant scaling errors.

The overall conceptual design was developed to provide system data and component functional specifications to assess system performance; estimate capital, operating, and maintenance costs; and prepare an accurate construction schedule. The system was also consistent with the technical requirements in Reference 1-1 and with the selected gas and steam turbines.

1.2.7 Assessment of Commercial-Scale Hybrid Plant

Assessment of the preferred commercial hybrid power system included identifying potential future improvements, identifying potential constraints to wide-spread use, and updating the market analysis.

It was recognized at the beginning of the project that the performance of the combined cycle solar hybrid concept could be improved significantly and that costs would be reduced as a result. Costs will also be reduced as the central receiver technology matures and as economies of scale are introduced.

The potential for performance improvements and cost savings were analyzed for the system as a whole and for the subsystems.

Potential technical and socioeconomic constraints were also identified and assessed in terms of their impact on successful introduction and wide-spread use of the solar hybrid concept. Among the major technical issues examined were the environmental effects, safety, materials technology, and manufacturing and marketing capacity. The major socioeconomic constraints examined were land used, natural resources, legal/regulatory, and institutional constraints.

The earlier market analyses were updated using the busbar cost of electricity calculated for the conceptual design. In addition, several utility companies were contacted to confirm the market

analysis methodology and comment on the prospective use of solar hybrid plants. The utilities represented each of the four regions considered in the market analysis effort.

1.3 PROJECT TEAM

Bechtel National, Inc. (BNI) was the prime contractor for the project. In addition to the responsibility for overall management, BNI was also responsible for the following specific technical efforts:

- System integration
- Market analysis
- Parametric studies and conceptual design of the electric power generation subsystem and the master control subsystem
- Conceptual design of site electric power distribution, site arrangement, site structures, and utilities
- Conceptual design of the receiver tower structure
- Preparation of a development plan
- Technical and economic assessment of the preferred system

Northrup, Inc., as a subcontractor, was responsible for the conceptual design and parametric analysis of the collector subsystem. In addition, Northrup was responsible for defining the collector field-related portions of the master control subsystem. Foster Wheeler Development Corporation, also a subcontractor, was responsible for the conceptual design and parametric analysis of the receiver. The Combustion Turbine

System Division of Westinghouse was a consultant on the combined cycle power conversion system and equipment technology. The Public Service Co. of New Mexico served as a utility advisor. Informal discussions were also held with the Pacific Gas and Electric Co. on power generation planning. The Solar Energy Research Institute, Electric Power Research Institute, and several utilities from representative regions of the U.S. participated by responding to a questionnaire on utility economics and on potential use of solar hybrid plants.

THIS PAGE

WAS INTENTIONALLY

LEFT BLANK

Section 2

MARKET ANALYSES

2.1 INTRODUCTION

This section describes the analyses performed to assess the economic viability of both the Modified Strawman and Advanced Strawman systems in four regions of the country. In these analyses first-generation solar hybrid plants are compared to conventional power technologies.

First, baseline capital and operating costs were estimated, based on the preconceptual reference designs for the hybrid plants, assuming that they were first-of-a-kind, and on published data for the conventional technologies. From these estimates, annualized busbar electricity costs were generated, using Bechtel's computer program RESOURCE. These busbar costs, along with plant operating characteristics, were used as input to the program ALLOCATE, which produced the utility screening curves and load duration curves used for analyzing market penetration.

Market penetration of the solar hybrid systems was estimated under nine economic scenarios, in four regions, in the 1990 to 2020 time frame.

2.2 BASELINE COST/PERFORMANCE DATA AND ECONOMIC ASSUMPTIONS

The baseline cost estimates for both hybrid and conventional technologies assume a Western plant location (Pacific Southern region). Capital and operating cost estimates for the conventional technologies are adapted from the EPRI Technical Assessment Guide (Ref. 2-1). For the regional market assessments, baseline estimates were adjusted to account for variations in labor and material costs and for some variations in performance characteristics.

The financial and economic data, such as discount rates, fixed charge rates, and escalation rates, were derived from the Requirements Definition Document. A set of typical utility financial/economic data was also developed and used for comparison purposes.

2.2.1 Baseline Data for Solar Hybrid Systems

Table 2-1 shows the baseline capital cost estimates for the first 100 MWe Strawman and Advanced Strawman hybrid systems. The estimates, expressed in 1978 dollars, include:

- Direct field construction cost
- Indirect field cost and engineering services
- Contingency
- Allowance for funds during construction (AFDC)

TABLE 2-1

CAPITAL COST ESTIMATE FOR REFERENCE SOLAR HYBRID SYSTEMS
(1000's, End of Year 1978 Dollars)

Account/Description	Strawman		Advanced Strawman	
	Non-Solar Portion	Solar Portion	Non-Solar Portion	Solar Portion
DIRECT FIELD CONSTRUCTION COST				
4100 Site, Structures and Miscellaneous Equipment	2,200	100	2,200	100
4200 Turbine Plant Equipment				
Gas Turbine	7,800		6,600	
Heat Recovery Steam Generator	7,700		5,600	
Steam/Turbine/Miscellaneous	9,300		10,000	
4300 Electric Plant Equipment	2,500	200	2,500	200
4400 Collector Equipment				
Heliostats*†		21,300		28,600
Computer*		2,000		2,000
Cable*		1,000		1,000
4500 Receiver Equipment				
Receiver*		15,300		20,700
Tower*		3,200		4,000
Riser/Downcomer		2,800		3,100
4700 Nonsolar Energy Subsystem Equipment	500		500	
Total Direct Field Construction Cost	30,000	45,900	27,400	59,700
INDIRECT FIELD COST AND ENGINEERING SERVICES				
4800 Distributables and Indirect Costs				
Indirect Field Cost	6,800	1,600	5,600	2,200
Engineering Services	4,400	4,800	4,000	6,200
Total Construction Cost Excluding Contingency and AFDC	93,500		105,100	
CONTINGENCY	14,000		15,800	
AFDC**	21,500		24,200	
Total Construction Cost	129,000		145,100	
Modifications (Strawman only)	(1,100)		—	
Total Construction Cost	127,900		145,100	

*Subcontracted item.
**Allowance for funds during construction.
†Assumes heliostats @ $93.42/m^2 per Northrup preconceptual estimate.

Capital costs for 1990 were estimated using a nominal capital cost escalation rate of 10 percent per year. The estimate for the Strawman plant was reduced by 1.1 million dollars to reflect modifications to the reference system decided upon during preliminary system selection. Specifically, the receiver and riser/downcomer pressure drop was reduced to 41.4 kPa (6 psi) and a dual-pressure steam bottoming cycle was incorporated. This Modified Strawman was then used in the estimate of operating costs and in all economic comparisons. It is emphasized that the capital costs of Table 2-1 are for a first-of-a-kind plant only; since real cost reductions are expected for "n^{th} plants," this estimate is conservative.

Annual operating and maintenance cost estimates for the Modified and Advanced Strawman systems are shown in Table 2-2.

The estimates are based on the DOE guideline of 1 percent of total capital cost. Fixed operating and maintenance costs do not vary with capacity factor, but variable operating and maintenance costs are assumed to be directly proportional to capacity factor. (For this study, capacity factor is defined as the fraction of the year the plant operates at rated capacity. Part-load operation is not considered.) The O&M costs for 1990 are based on an operating and maintenance escalation rate of 8 percent per year. The O&M costs do not include fuel costs, which are calculated separately.

Table 2-3 summarizes the major performance data used in calculating electricity production costs for the solar hybrid plants.

2.2.2 Baseline Data for Conventional Technologies

Baseline cost estimates and performance data were compiled for four conventional power technologies:

- Combustion turbine (distillate oil-fired)
- Combined cycle (distillate oil-fired)
- Coal with flue gas desulfurization
- Light water reactor

To ensure compatibility with commonly accepted utility industry practice, the baseline data in Table 2-4 were adapted from the EPRI Technical Assessment Guide (Ref. 2-1).

2.2.3 Regional Variation of Data

Four regions representing a range of capital costs, fuel costs, and insolation levels were selected for the market assessments:

- Middle Atlantic Region: Pennsylvania, New York, and New Jersey
- South Central Region: Texas, Oklahoma, Arkansas, and Louisiana
- South Mountain Region: Nevada, Utah, Colorado, Arizona, and New Mexico

TABLE 2-2

OPERATING AND MAINTENANCE COST ESTIMATE
FOR REFERENCE SOLAR HYBRID SYSTEMS

Account	Modified Strawman		Advanced Strawman	
	1978	1990	1978	1990
Nonsolar system				
Fixed ($1000/yr)	109	274	92	232
Variable (mill/kWh)	1.04	2.62	0.88	2.22
Solar system				
Fixed ($1000/yr)	671	1690	940	2367

Table 2-3

BASELINE PERFORMANCE DATA FOR REFERENCE SOLAR HYBRID SYSTEMS

System Characteristics	Modified Strawman	Advanced Strawman
Capacity, MW	100	100
Life, yr	30	30
Heat rate, daytime average, kJ/kWh (Btu/kWh)	8101(7679)	7760(7355)
Heat rate, nighttime average, kJ/kWh (Btu/kWh)	8169(7743)	7831(7423)
Average annual solar fraction, %	31.2	40.8
Breakpoint solar capacity factor, %	48	48

TABLE 2-4

BASELINE PERFORMANCE DATA AND COST ESTIMATES FOR CONVENTIONAL TECHNOLOGIES*
(South Mountain and Pacific Southern Regions)

Technology	Plant Characteristics			Capital Cost ($/kW)		Fixed O&M Cost ($/kW-yr)		Variable O&M Cost (Mills/kWh)	
	Capacity (MWe)	Life (Yrs)	Heat Rate (Btu/kWh)	1978	1990	1978	1990	1978	1990
Combustion Turbine	75	30	14,000	157	493	0.49	1.23	2.02	5.09
Combined Cycle	250	30	8,700	295	926	1.18	2.97	1.25	3.15
Coal with Flue Gas Desulfurization	1,000	30	10,400	745	2,338	2.58	6.50	1.64	4.13
Light Water Reactor	1,000	30	10,400	825	2,589	2.84	7.15	0.72	1.81

*Source: EPRI Technical Assessment Guide.

- Pacific Southern Region: California

The Middle Atlantic and South Central regions are U.S. census regions, while the South Mountain and Pacific Southern regions are the southern parts of the Mountain and Pacific census regions, respectively.

The baseline cost and performance data for both the hybrid and conventional power plants correspond to the Pacific Southern region. For the South Mountain region, the only variation is in the average annual solar fraction of the hybrid systems. Costs remain the same.

For the South Central and Middle Atlantic regions, however, all cost and performance data were adjusted from the baseline values to reflect variations in material and labor cost and in performance characteristics. The costs are lower in the South Central region and higher in the Middle Atlantic region, and the solar fraction is less in both regions. The adjustments are based on the recommendations of the EPRI Technical Assessment Guide.

2.2.4 Economic Assumptions

The financial and economic data, such as discount rates and fixed charge rates, used in calculating electricity production costs are presented in Table 2-5. The DOE financial/economic data

TABLE 2-5

ECONOMIC ASSUMPTIONS

Parametric Description	DOE	Typical Utility
Financial Institutional Assumptions		
Discount rate (%)	10	9
Economic life (yrs)	30	30
Fixed charge rate (%)	18	15
Projected relative price behavior		
Expected inflation rate (%)	6	6
Capital escalation rate (%)	10	6
O&M esclation rate (%)	8	6
Fuel escalation rate (%)		
Coal	6,8,10,12,15	6.4
Distillate oil	6,8,10,12,15	7.6
U_3O_8	6,8,10,12,15	8.0
Fuel price (1978 $/MBtu)		
Coal		
Base price	1.00	
Pacific Southern		1.02
South Mountain		1.02
South Central		.48
Middle Atlantic		1.01
No. 2 distillate		
Base price	2.35	
Pacific Southern		2.49
South Mountain		2.69
South Central		2.49
Middle Atlantic		2.59
U_3O_8		.53

shown in the first column are used in all systems studies, baseline economic comparisons, and market assessments. They reflect guidelines set forth in the DOE Requirements Definition Document. The typical utility data, which are similar to financial/economic data presented in the EPRI Technical Assessment Guide, are used in one scenario of the economic comparisons and market assessments.

2.3 ECONOMIC COMPARISONS

The levelized busbar electricity cost, a commonly accepted economic criterion in the electric utility sector, was used to compare the Modified and Advanced Strawman systems with each other and with the four selected conventional power technologies. Since levelized costs are highly dependent on capacity factor, all comparisons are presented for a range of capacity factors. The sensitivity of the Modified and Advanced Strawman busbar costs to variations in cost/performance and economic parameters was also examined.

2.3.1 Levelized Busbar Electricity Cost Calculations

Levelized busbar electricity costs are computed in current dollars using DOE financial/economic data and busbar costing methodology. For conventional technologies, levelized busbar costs are expressed in dollars per kilowatt per year as a linear function, f_1, of capacity factor (CF):

$$f_1(CF) = F + (V \cdot 87.6 \cdot CF)$$

where:

F = levelized fixed cost (levelized capital charges plus levelized fixed operating and maintenance costs in $/kW-yr)

V = levelized variable cost (levelized fuel cost plus levelized variable operating and maintenance cost in $/kW-hr)

CF = capacity factor (%)

The upper curve in Figure 2-1, designated $f_1(CF)$, illustrates a conventional technology levelized busbar cost function. The linear levelized cost functions imply several simplifying assumptions:

- Levelized variable O&M and fuel costs are strictly proportional to capacity factor
- Utility system interfaces and dispatching need not be explicitly considered
- Reliability and availability need not be explicitly considered

The levelized busbar cost functions for the hybrid systems are complicated by the intermittent solar energy contribution. The shaded region of Figure 2-1 illustrates the feasible range of levelized busbar electricity cost functions for a hypothetical solar hybrid plant. If the plant is never operated during periods of useful insolation, the levelized cost function corresponds to $f_2(CF)$. (This represents the levelized cost function of a conventional combined cycle plant burdened with the cost of idle solar equipment.) If the plant is operated during all periods of useful insolation, the cost function is $f_4(CF)$.

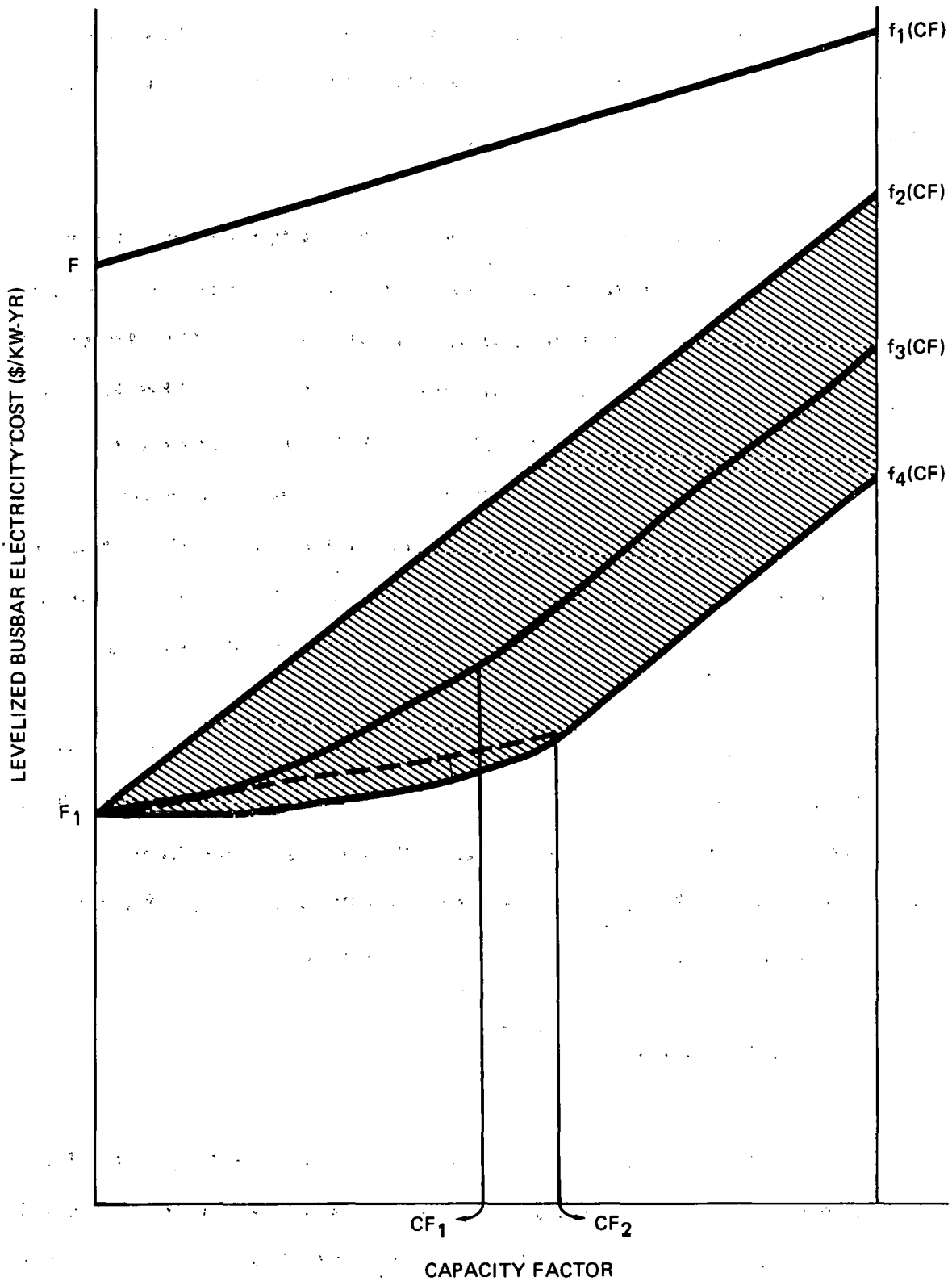

Figure 2-1 SAMPLE BUSBAR COST FUNCTIONS

If an intermediate dispatching strategy is adopted, a typical cost function is $f_3(CF)$. The varying slopes of $f_3(CF)$ and $f_4(CF)$ reflect the variation in receiver power over the year, the flattest portions corresponding to periods of greatest fuel savings.

Comparison of $f_4(CF)$ to $f_3(CF)$ shows that dispatching the plant less during periods of useful insolation shifts the cost curve upward and moves the solar/nonsolar breakpoint to the left (from CF_2 to CF_1). The capacity factor corresponding to the knee of the hybrid cost function (e.g. CF_1 or CF_2), is hereafter referred to as the breakpoint capacity factor. For the economic comparisons that follow, levelized cost functions corresponding to $f_4(CF)$ are used. This strategy maximizes the average annual solar fraction and minimizes the fossil fuel consumption.

A linear approximation, represented by the dashed segment in Figure 2-1, has been assumed for the curved portion of $f_4(CF)$. In addition, the earlier stated assumptions in the linear conventional technology cost functions apply equally to the piecewise linear solar hybrid cost functions.

2.3.2 Economic Comparisons

Economic comparisons between the solar hybrid systems and the selected conventional technologies were carried out by computing the parameters of the linear levelized cost functions for each

and superimposing the resulting set of cost curves, usually called screening curves by the utility industry. The lower envelope of each set of screening curves indicates the technology with the minimum levelized busbar cost at each capacity factor.

The results of the analyses are shown in Figures 2-2 through 2-5. Specifically, Figure 2-2 reflects the baseline cost/performance data, a 12 percent fuel escalation rate for all fuels, and a plant startup of 1990. With these conditions the Advanced Strawman exhibits a slight cost advantage over the Modified Strawman at capacity factors exceeding 35 percent, while the converse is true below 35 percent.

Figure 2-3 shows the same screening curves with a 15 percent fuel escalation rate. The cost advantage of the Advanced Strawman over the Modified Strawman is increased slightly, while there is a large decrease in cost relative to the combined cycle system for both hybrid systems. In this scenario, however, the hybrid system costs increase relative to coal and nuclear system costs.

Figure 2-4 reflects plant startup in the year 2000 and a fuel escalation rate of 12 percent. It shows that the effects of a later startup date are similar to those of a higher escalation rate. Again, the hybrid systems look better relative to the combined cycle and combustion turbine systems, and worse relative to the coal and nuclear systems.

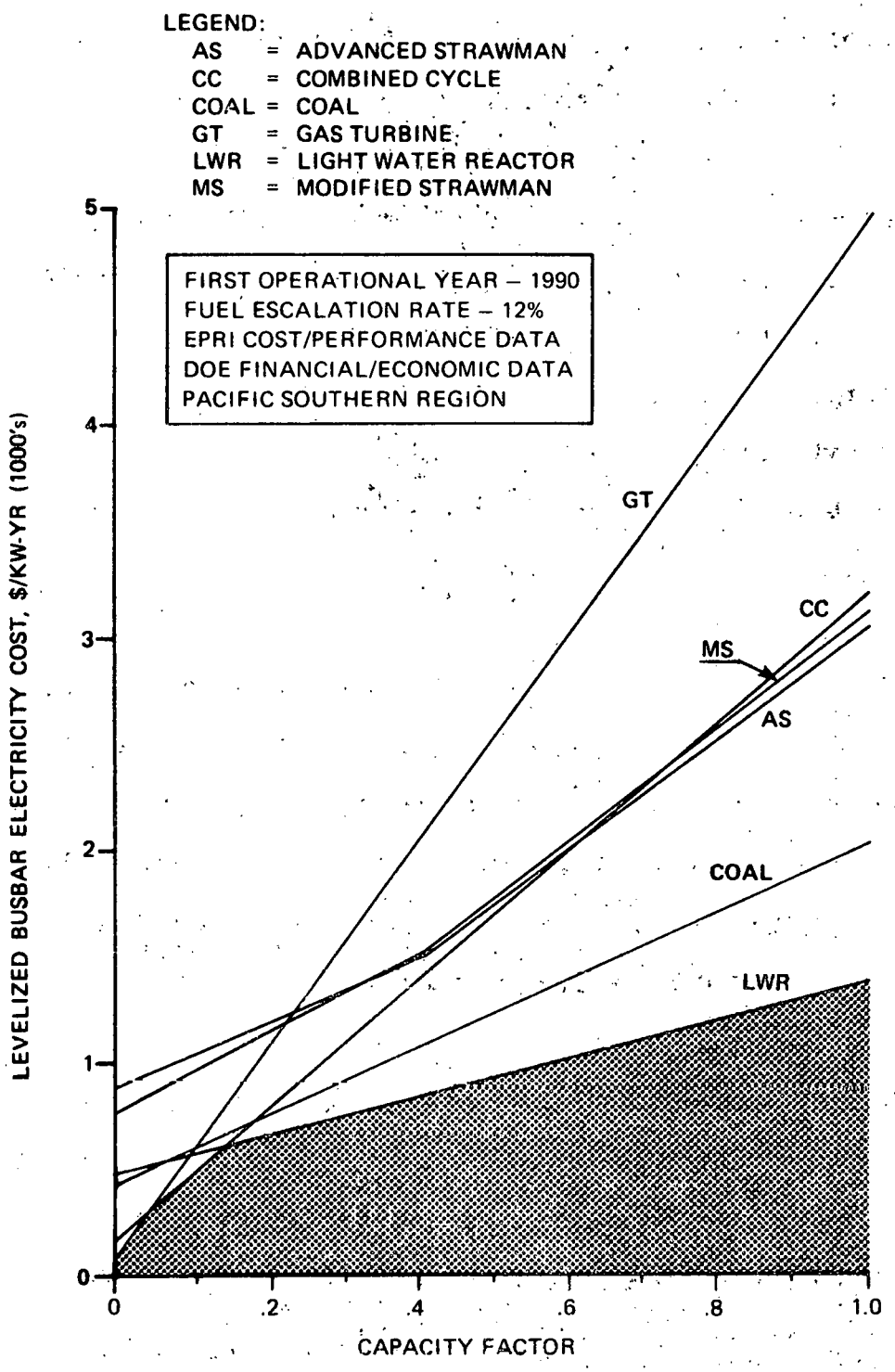

Figure 2-2 SCREENING CURVES, 1990, 12 PERCENT FUEL ESCALATION RATE

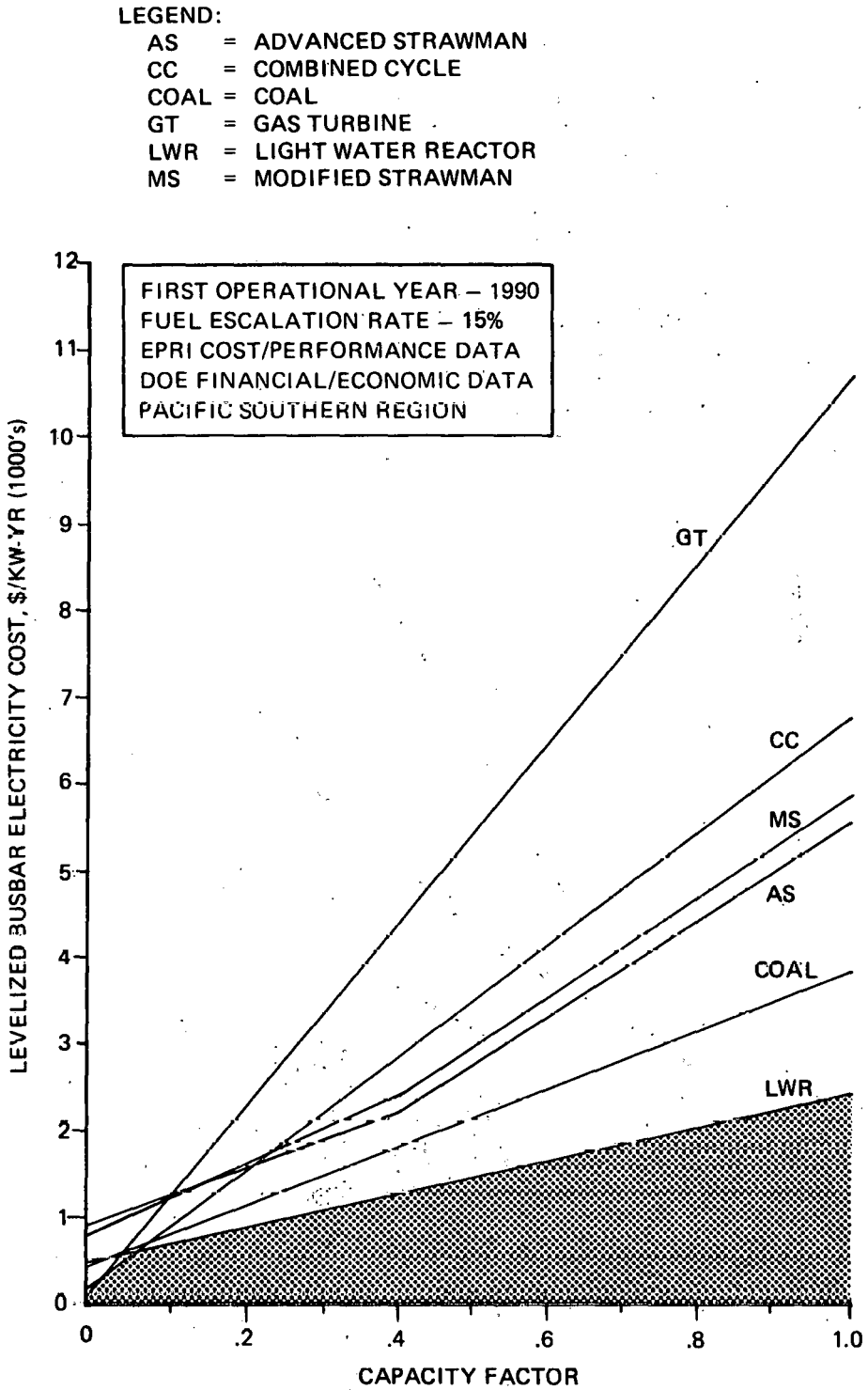

Figure 2-3 SCREENING CURVES, 1990, 15 PERCENT FUEL ESCALATION RATE

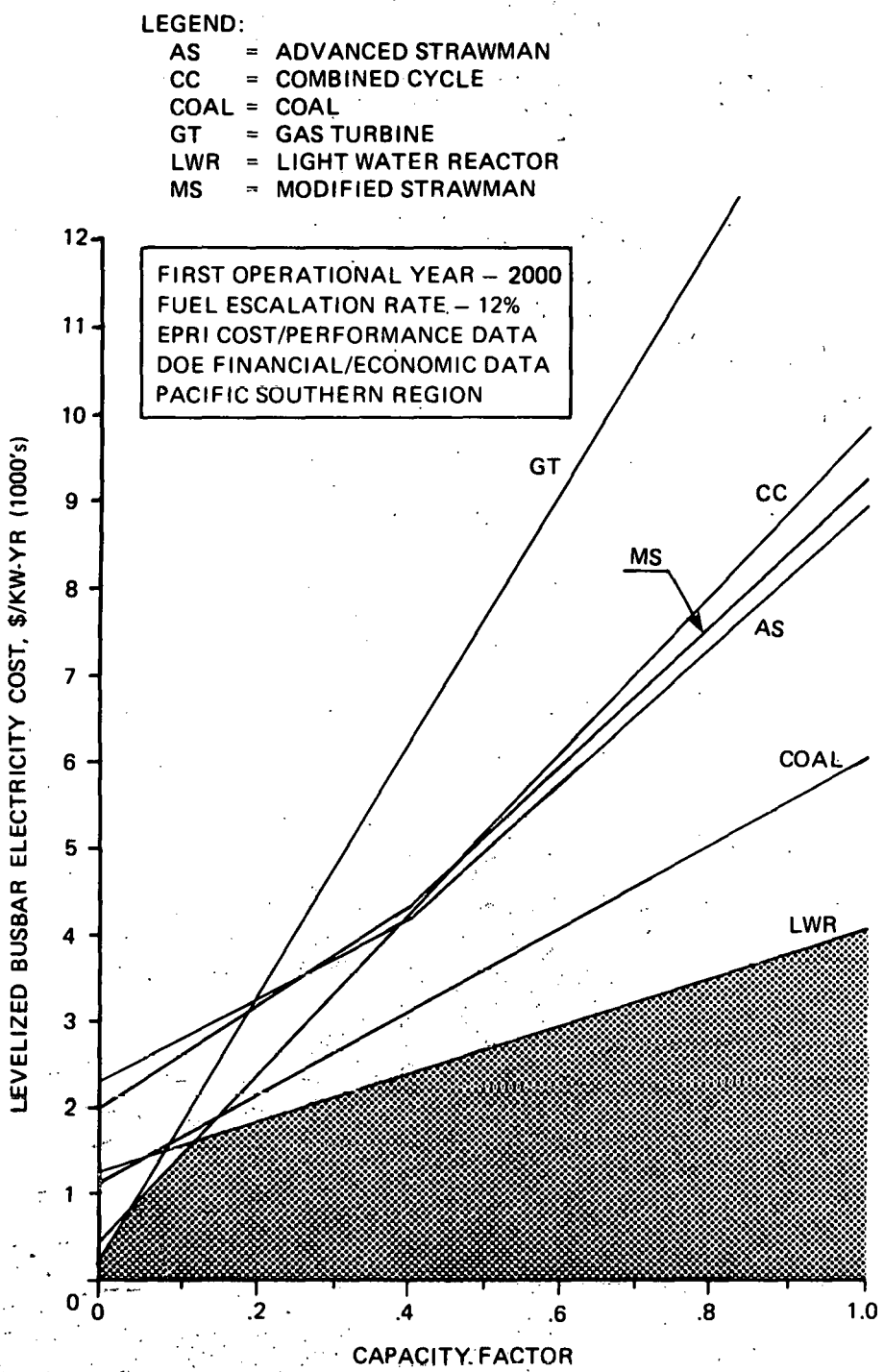

Figure 2-4 SCREENING CURVES, 2000, 12 PERCENT FUEL ESCALATION RATE

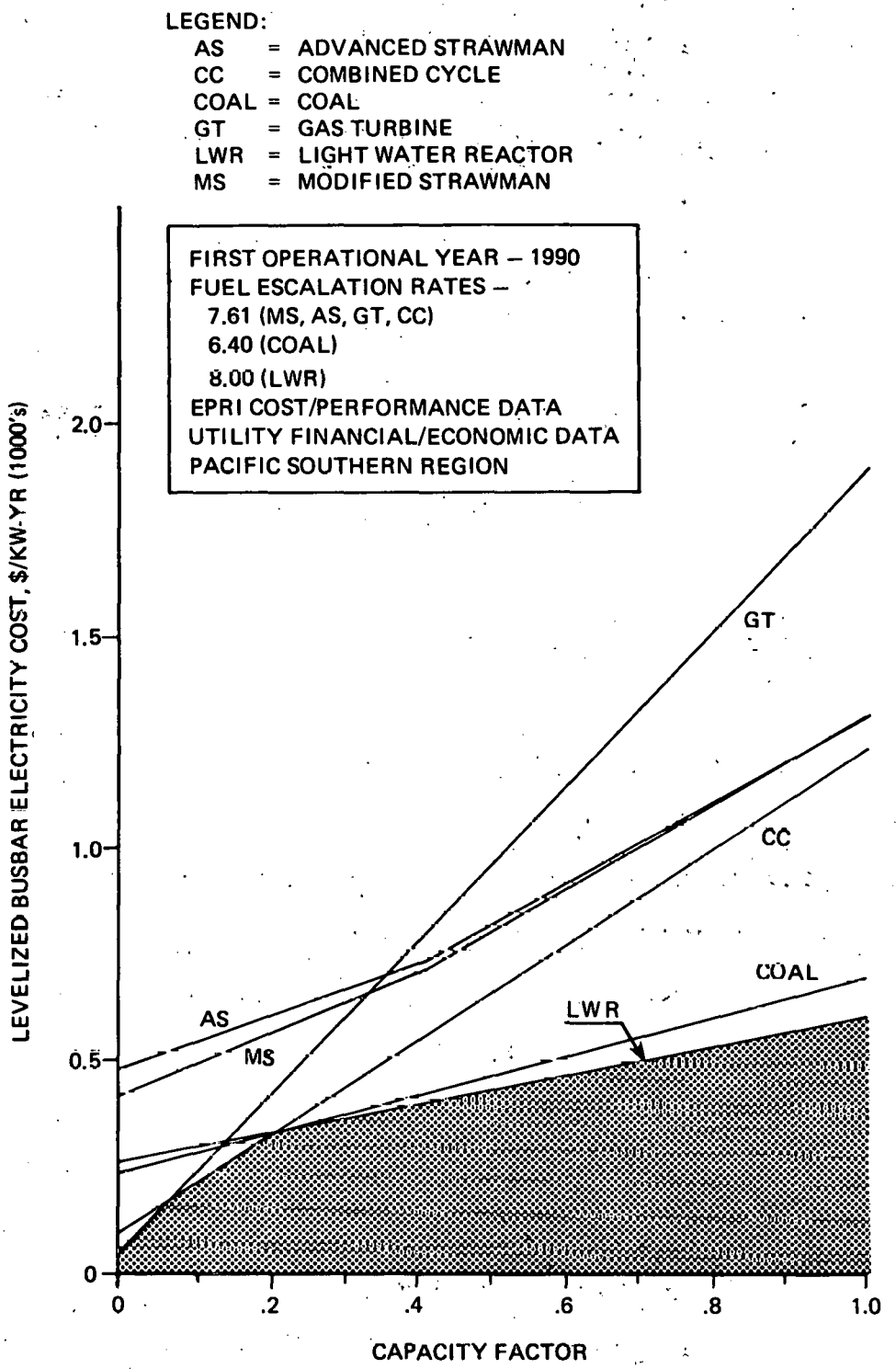

Figure 2-5 SCREENING CURVES, 1990, VARIABLE FUEL ESCALATION RATES

Figure 2-5 shows the effects on the levelized cost functions of the typical utility financial/economic data outlined in the second column of Table 2-5. It was found that their effects were generally consistent with those of the DOE financial/economic data. The generally lower escalation rates for all fuels in the typical utility data tend to:

- Increase costs for the Advanced Strawman relative to the Modified Strawman
- Increase costs for the hybrid systems relative to combined cycle and combustion turbine systems
- Decrease costs relative to coal and light water reactor systems

2.3.3 Sensitivity Analysis

Sensitivity analyses were performed to quantify the relative importance of selected life cycle cost parameters. The percentage change in Modified Strawman and Advanced Strawman levelized busbar costs for a +1 percent change in a selected cost/performance or financial/economic parameter was used as an index of sensitivity. Specifically, percentage changes in levelized busbar cost are computed for changes in:

- Capital cost
- Fixed operating and maintenance cost
- Variable operating and maintenance cost
- Daytime average heat rate
- Solar fraction

- Fuel cost
- Discount rate
- Fixed change rate
- Escalation rate (capital, operating and maintenance, and fuel)

Figure 2-6 shows the sensitivity analysis results for some of these parameters specific to the Modified Strawman system. Sensitivities to changes in capital cost, fixed and variable O&M cost, daytime average heat rate, and solar fraction are graphed as functions of capacity factors.

As seen from the graphs, when the capacity factor increases, percentage changes in levelized cost for a +1 percent change in capital and fixed operating costs decreases, while the percentage change in levelized cost for a +1 percent change in variable O&M cost increases. Percentage changes in daytime average heat rate and solar fraction (which affect only the slope of the flat segment of f_4 (CF) in Figure 2-1) reach a maximum at the breakpoint capacity factor of 40.8 percent. The discontinuity in these last two curves reflects the piecewise linear levelized cost function used for the hybrid plants. As a whole, the graphs do not indicate strong sensitivity to any of these parameters.

Figure 2-7 shows the sensitivity of hybrid levelized busbar costs to variations in cost components common to several of the technologies under consideration (fuel cost for distillate oil-

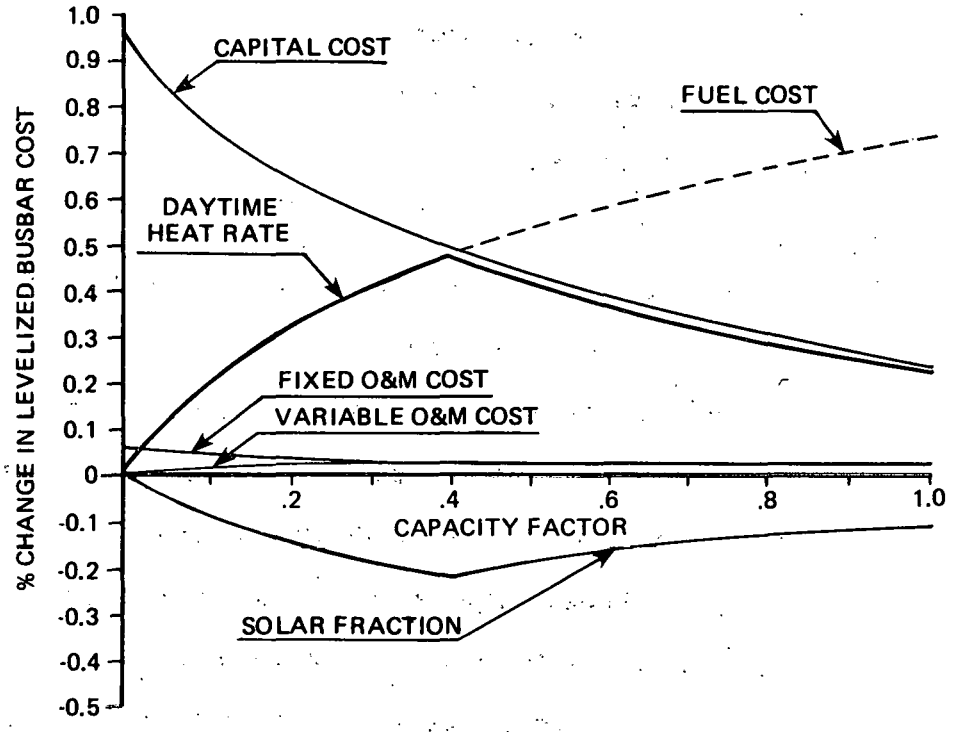

Figure 2-6 SENSITIVITY OF MODIFIED STRAWMAN LEVELIZED BUSBAR COSTS TO +1% VARIATION IN COST/PERFORMANCE COMPONENTS SPECIFIC TO HYBRID SYSTEMS

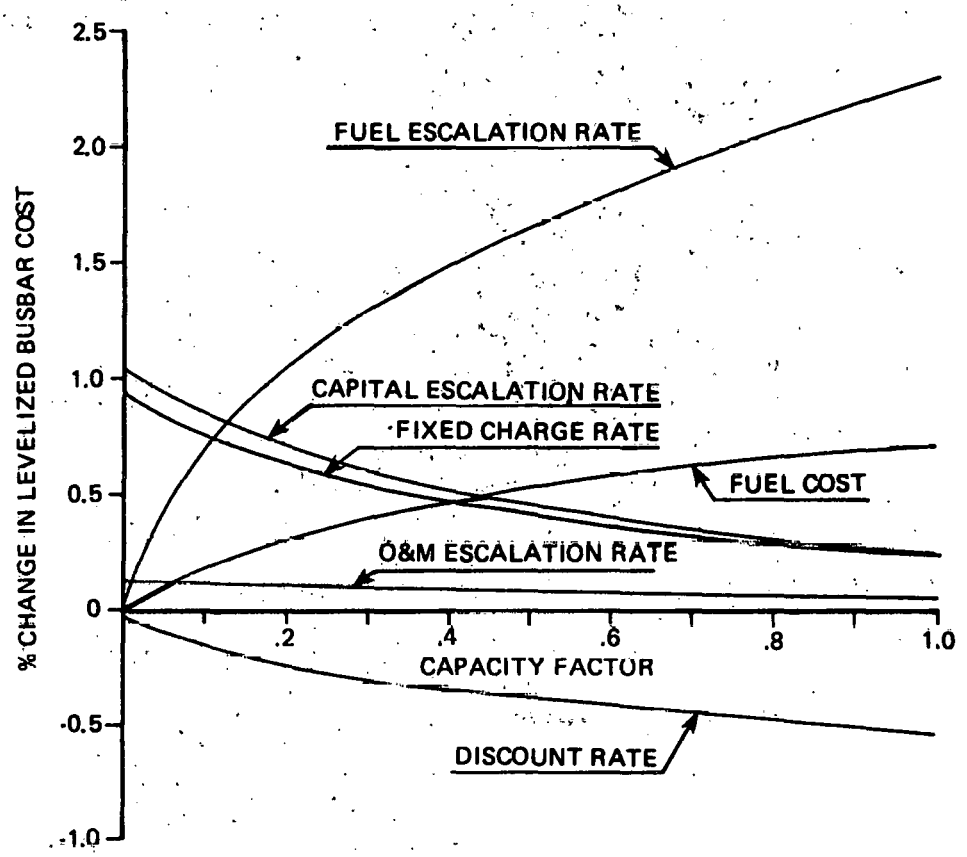

Figure 2-7 SENSITIVITY OF MODIFIED STRAWMAN LEVELIZED BUSBAR COSTS TO +1% VARIATION IN COST COMPONENTS COMMON TO ALL TECHNOLOGIES

fired plants, discount rate, fixed charge rate, and escalation rates).

As before, the impact of the capacity factor on the results is the most significant. Levelized costs are more sensitive to variations in fixed-cost-related items at lower capacity factors and variable-cost-related items at higher capacity factors. The distillate oil escalation rate is the most significant levelized cost component.

It is also important to examine the relative sensitivity of hybrid and conventional technology levelized busbar costs to changes in cost/performance and financial/economic parameters. Thus, if a 1 percent increase in the fuel-oil escalation rate raises hybrid levelized cost by $1/kW-yr but raises the levelized costs of oil-fired conventional technologies by $10/kW-yr, the hybrid systems are more competitive at higher fuel oil escalation rates. Details of comparative sensitivity analyses for the Modified Strawman, Advanced Strawman, combined cycle, and coal power systems are contained in Volume III. The results are similar to those implied by the screening curves of Subsection 2.3.2.

2.3.4 Optimistic Scenario

After identifying the key variables from the sensitivity analyses, optimistic, but plausible, scenarios were constructed

which enhance hybrid economic viability relative to coal and nuclear technologies. One such set of optimistic parameters is shown in Table 2-6. Basically this set of parameters reflects:

- Higher discount rate
- Lower fixed charge rate (reflecting favorable tax treatment)
- Lower 1978 oil price and escalation rate
- Lower heliostat cost ($68/m²)
- Higher plant capacity (350 MWe)

The screening curves resulting from this set of parameters are shown in Figure 2-8.

Increasing the plant capacity rating to 350 MWe was assumed to reduce the capital cost for the nonsolar parts of the hybrid plant according to a 0.7 exponential scaling factor. Figure 2 8 shows that the hybrid/coal levelized cost differential at the breakpoint capacity factor (at maximum solar contribution) is reduced by at least 50 percent compared with the screening curves of Figures 2-2 to 2-5. In fact, if pessimistic parameters were also assumed for coal and nuclear plants, the differential can be reduced even more.

TABLE 2-6

OPTIMISTIC SCENARIO ASSUMPTIONS

Parameter Description	Strawman	Advanced Strawman
Plant Capacity (MWe)	350	350
Economic		
Discount Rate (%)	10	10
Fixed Charge Rate (%)	15	15
Capital Escalation Rate (%)	6	6
O&M Escalation Rate (%)	6	6
Fuel Escalation Rate (%)	7.6	7.6
Plant Cost		
Capital Including AFDC* ($/kW)	1038	1190
Fixed Operating Cost ($/kW-yr)	7.80	10.32
Variable Operating Cost (mills/kWh)	0.88	1.04
Fuel Cost ($/MBtu)	2.35	2.35

*Allowance for funds during construction.

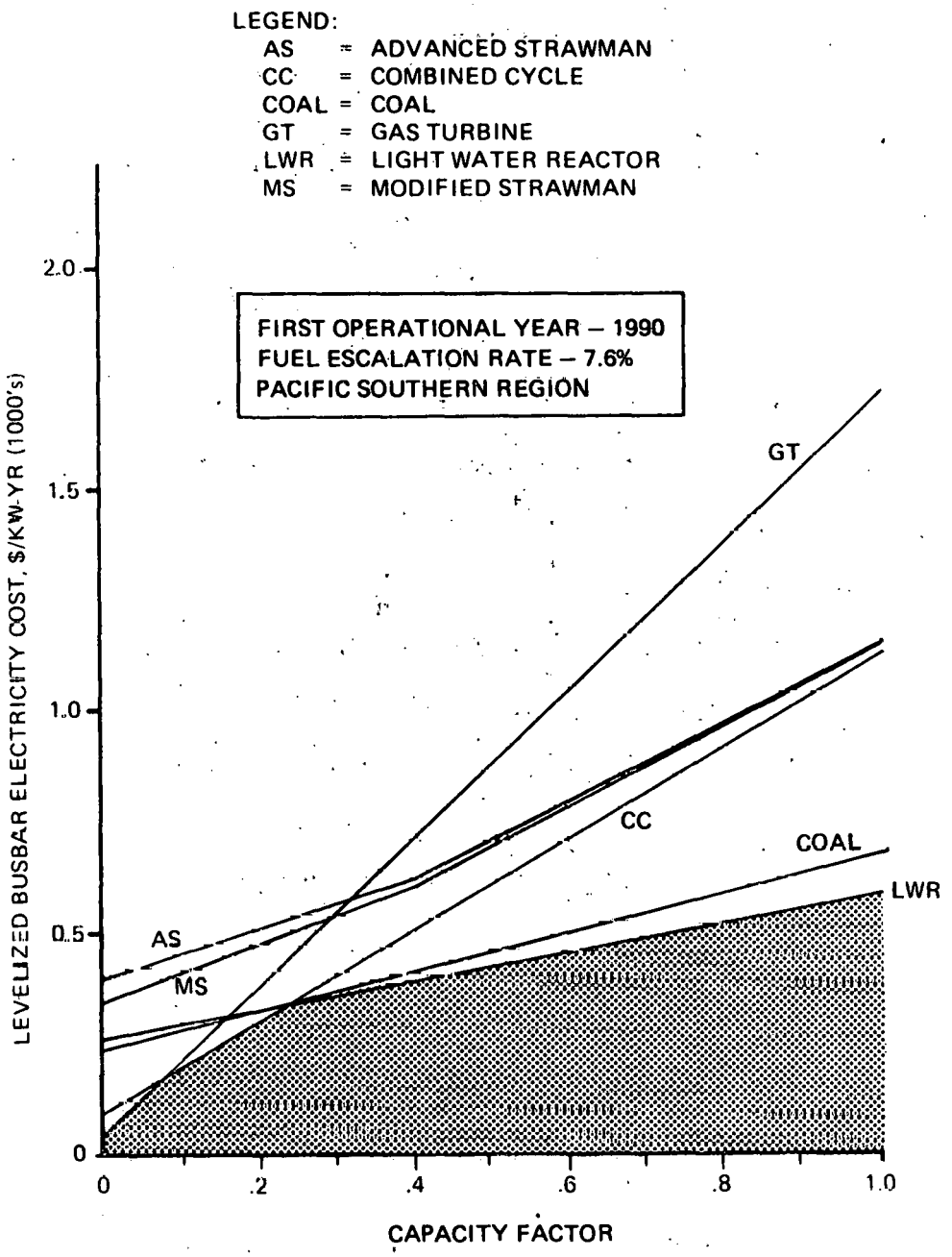

Figure 2-8. SCREENING CURVES, OPTIMISTIC SCENARIO

2.4 MARKET ASSESSMENT

Screening curve analyses are used in the early stages of capacity expansion studies to narrow the selection to a small group of promising candidates. These then become the subject of a more detailed analysis, often involving a generation expansion planning model. These models are used to determine preferred generating capacity mixes given the utility's generation requirements.

Since this study does not address a particular utility, it was decided that extending the screening curve analysis was more appropriate than using a production planning model. Regional screening curves, in conjunction with regional demand forecasts, can be used to project least-cost generation mixes over the 1990 to 2020 time frame. In the analysis that follows, this technique is used to simulate regional market penetration for the Modified Strawman concept under three economic scenarios.

2.4.1 Methodology

One of the most important utility investment objectives is to minimize the levelized busbar electricity cost. Under the assumption that utilities tend to allocate investment capital to minimize revenue requirements, the screening curves can be used to project the rate of market penetration for an emerging

technology. Bechtel's market potential computer simulation model, ALLOCATE, incorporates this approach.

Capacity Allocation Process. The first step of the simulation process was development of incremental load duration curves for the years 1990, 2000, 2010, and 2020. These curves plot incremental generating capacity relative to annual hours of operation (i.e., the capacity factors). The area under the duration curve represents the total incremental demand.

The 1990 curve for the Pacific Southern region is shown in Figure 2-9. Since the regional analyses do not focus on a specific utility, the ALLOCATE model uses a deterministic function for the duration curve in lieu of a curve fit to actual utility data points.

For this study, regional demand forecasts were adapted from forecasts used by the MITRE Corporation of McLean, Virginia in recent R&D benefit/cost studies for DOE (Ref. 2-2).

Levelized busbar electricity costs were incorporated through regional utility screening curves similar to those depicted in Figures 2-2 to 2-5. These show busbar cost vs. capacity factor and they establish an envelope of the least cost technology at each capacity factor. The ALLOCATE program apportions the incremental demand to the least-cost technologies, as shown in Figure 2-10. Point estimates for capacity mixes, electricity

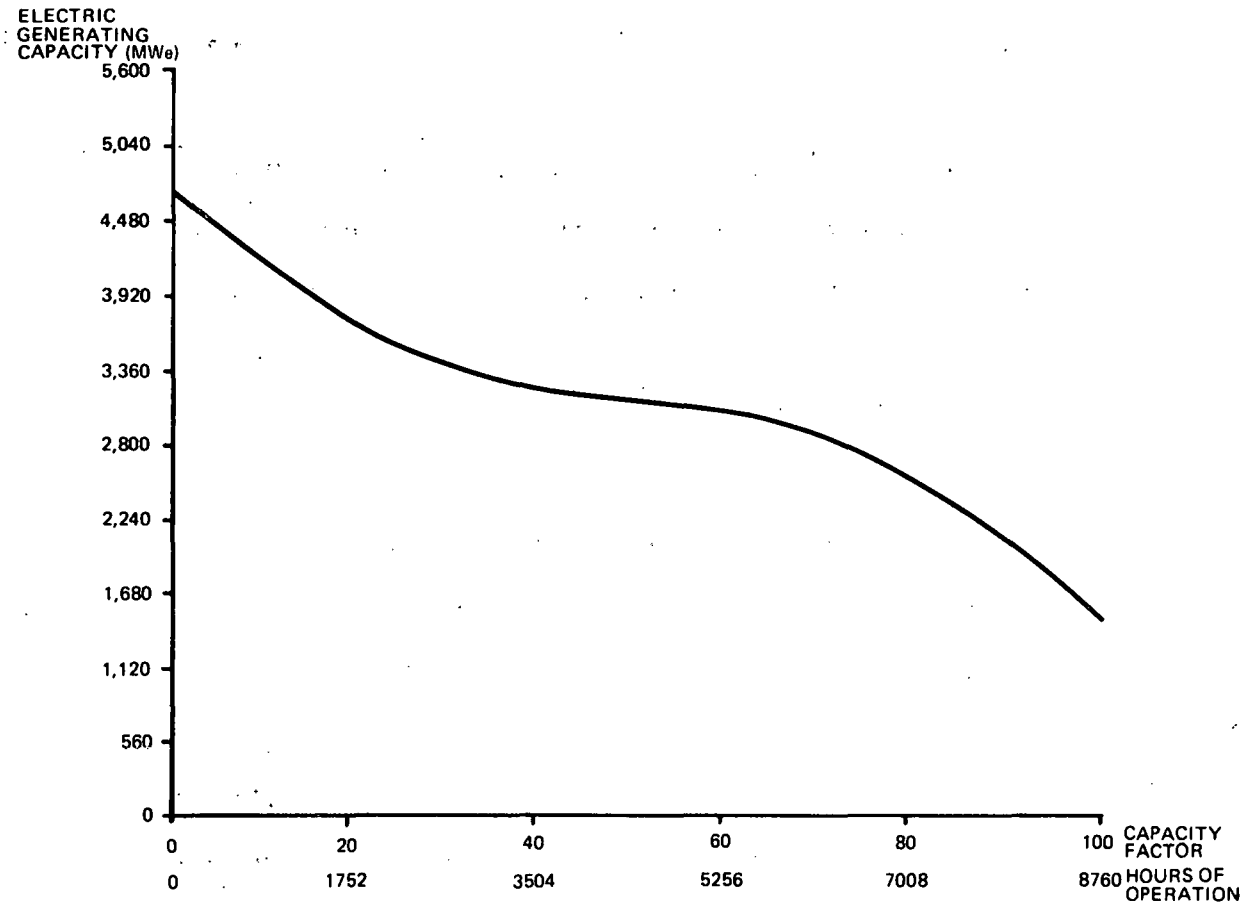

Figure 2-9 1990 INCREMENTAL LOAD DURATION CURVE FOR THE PACIFIC SOUTHERN REGION

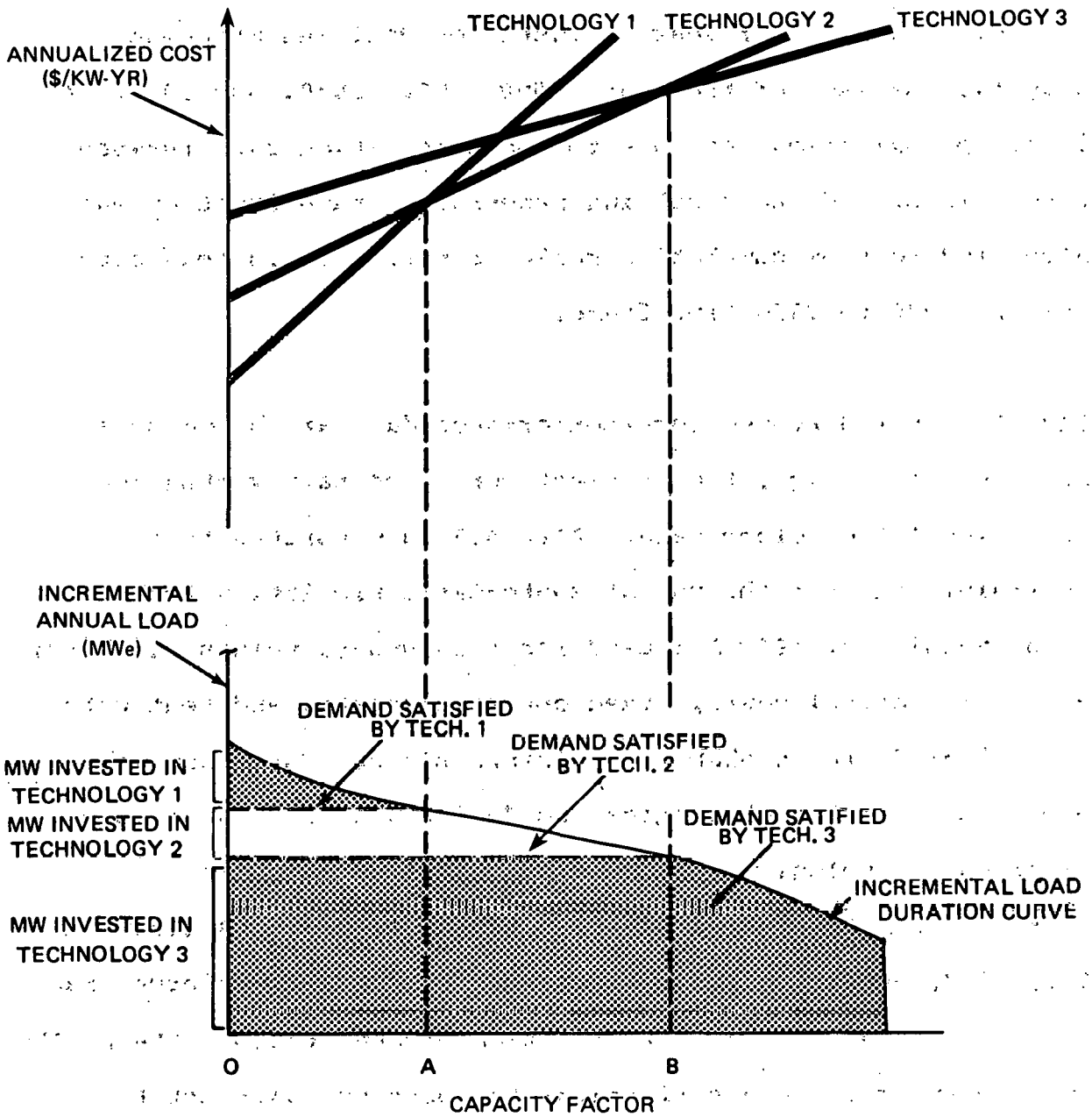

Figure 2-10 CAPACITY ALLOCATION PROCESS

production, load ranges, capacity factors, and power generation costs are simultaneously determined.

For this study, market penetration projections were expressed in terms of megawatts per year of installed Modified Strawman capacity, for each of the years 1990, 2000, 2010, and 2020. A linear approximation was made to the penetration rate between these points, and the resulting penetration rate function was integrated to show cumulative market penetration in megawatts over the 1990 to 2020 time frame.

Since the hybrid system cost/performance data are based on a preconceptual design, they reflect more uncertainty than the conventional technology data. ALLOCATE incorporates this uncertainty through the use of Monte-Carlo simulation techniques. In the version of ALLOCATE used for this study, values for hybrid fuel cost, capital costs, fixed operating costs, and heat rate were selected from probability distributions. Fuel cost is common to several technologies, so fuel costs for conventional oil-fired technologies were assumed to follow the same distribution. At each of the selected decision years (1990, 2000, 2010, and 2020), the allocation process was performed many times, giving a frequency distribution of penetration rates. The sample mean of these distributions was used to construct the penetration rate functions described above.

The penetration profiles are merely mathematical transformations of the screening curve data and are therefore based on the same assumptions as the economic comparisons:

- Levelized variable O&M and fuel costs are strictly proportional to capacity factor
- Utility system interfaces and dispatching need not be explicitly considered
- Reliability and availability need not be explicitly considered

In addition, it was assumed that:

- Only conventional technologies were considered, excluding advanced concepts such as fusion and fuel cells
- Minimization of revenue requirements is the utility's sole investment objective
- No capital, equipment availability, or statutory constraints (market imperfections) are imposed
- Load following, capacity factor downgrading, and other utility system interface and operational considerations are not included

In fact, under scenarios represented by the screening curves in Section 2.3 (Figures 2-2 to 2-5), these assumptions completely exclude both the hybrid systems and coal-fired systems from the power generation market. This interpretation, however, does not completely conform to utility expectations. For example, discussions with Pacific Gas and Electric Company revealed that utilities expect coal and nuclear technologies to dominate the long-term baseload market, since the statutory limitations of the

National Energy Act of 1978 preclude new oil-fired units from base-load and high-intermediate-load duty in most cases (Ref. 2-3). But it is expected that oil-fired plants should be viable for some time to come in low-intermediate and peaking applications.

A recent study of the utility industry by Arthur D. Little, Inc. also states:

> "...we expect more oil and gas fired capacity to be in service in 1990 and that capacity to be used more intensively than government policy pronouncements might suggest. In fact, we expect slightly more oil and gas fired capacity to be in service in 1990 than today, but that it will be used less intensively; i.e., more in peaking and intermediate-load service." (Ref. 2-4)

These industry expectations formed the basis for a constrained penetration analysis addressing only the low-intermediate and peaking markets.

Constrained Penetration Analysis. To be able to make utility choices based on other than economic reasons, it is necessary to incorporate what the economists refer to as "intangibles and market imperfections" into the analysis. For example, the screening curves of Figure 2-2 imply that nuclear plants alone will account for all new base-load capacity in 1990. They do not reflect restrictions imposed, for example, by the nuclear regulatory process (a market imperfection) or the government

mandate to rely more heavily on coal. The constrained penetration analysis is a means of incorporating market imperfections in a "pure economic choice" technique.

Briefly, the base load of the coal and nuclear plants is estimated with exogenous capacity forecasts that include the effects of intangibles and market imperfections. This base-load market is allocated to a surrogate coal/nuclear technology. Then the remaining peaking and low-intermediate market is to be satisfied by a least cost mix of combined cycle, combustion turbines, and solar hybrid technologies on the basis of pure economic choice. The effect of constraints on coal/nuclear capacity additions can be examined through parametric variation of the exogenous coal/nuclear capacity forecast.

The analytical tools used to implement this approach are shown in Figure 2-11. The incremental peaking and low-intermediate demand corresponds to the unshaded area under the incremental load duration curve. The shaded coal/nuclear portion was estimated based on a regional capacity expansion forecast by the United States Department of Commerce (Ref. 2-5) for 2000, 2010, and 2020 for each of the four regions studied. The ratio of coal/nuclear capacity addition to the total capacity addition is called the "forecasted incremental coal/nuclear capacity fraction." The point, CF*, on the graph corresponds to the lower bound of coal/nuclear capacity factors limited by operational considerations.

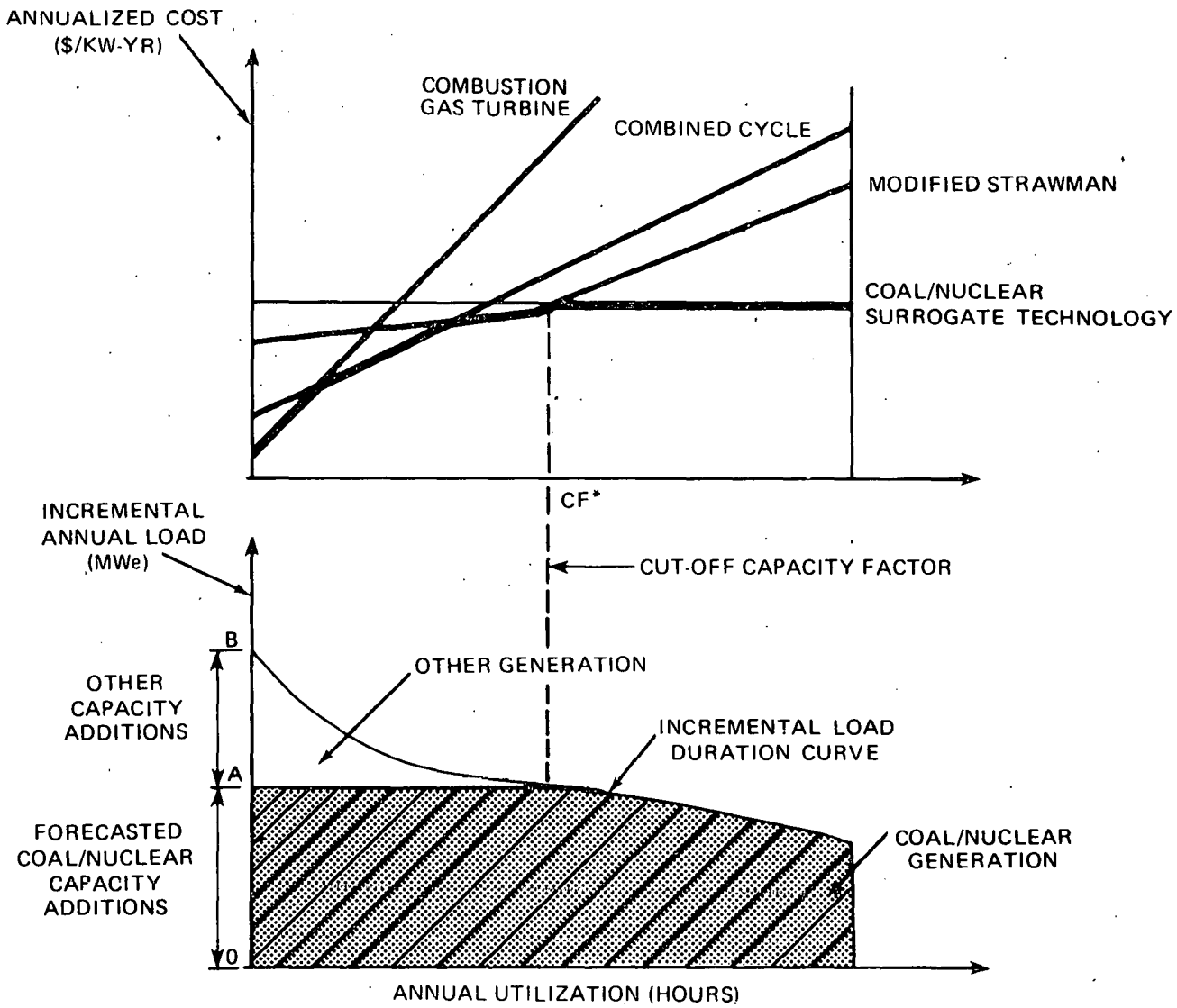

Figure 2-11 ALLOCATION PROCESS UNDER CONSTRAINED COAL/NUCLEAR SCENARIOS

Incremental demand filled by the capacity, OA, is excluded from allocation to other technologies through the introduction of a surrogate coal/nuclear technology represented by the flat cost curve in Figure 2-11. The variable cost of the surrogate coal/nuclear technology is fixed at zero while its fixed cost, F*, is set equal to the minimum of the combustion turbine, combined cycle, or Modified Strawman levelized costs at CF*. This guarantees that all demand in the shaded region of the load duration curve is allocated to the coal/nuclear surrogate while competition on a least-cost basis for the remaining demand (the unshaded area) is unaffected. As the simulation proceeds, F* is continuously adjusted to exclude the same coal/nuclear demand fraction.

2.4.2 Market Assessment Results

Constrained market penetration simulations were performed for a matrix of cost/performance data sets and coal/nuclear incremental capacity fractions for each region. The cost/performance data sets were drawn from the EPRI regional data and are summarized as follows:

- EPRI regional cost/performance data, DOE/SAN financial/economic data, 12 percent fuel escalation rate
- EPRI regional cost/performance data, DOE/SAN financial/economic data, 15 percent fuel escalation rate
- EPRI regional cost/performance data, typical utility financial/economic data

In the Pacific Southern and South Mountain regions, where the forecasted incremental coal/nuclear capacity fraction is less than 1 (this agrees with PG&E), the simulation was performed for the forecasted fractions and a ±10 percent variation from the forecasted fractions. In the South Central and Middle Atlantic regions, where the forecasted coal/nuclear incremental capacity fraction is 1, the simulation was performed for coal/nuclear fractions of 0.9, 0.8, and 0.7. The Modified Strawman is used in the penetration analyses to represent both hybrid technologies.

The lower curve in Figure 2-12 shows simulated market penetration in the Pacific Southern region over the 1990 to 2020 time frame for the forecasted coal/nuclear fractions, DOE financial/economic data, and 15 percent fuel escalation rate. It represents the simulation results using raw demand data unadjusted for incremental reserve requirements and retired capacity. The other curves show the effect of annual retirement of 1.5 and 3 percent of the installed capacity.

Since a detailed treatment of retirements is beyond the scope of this study, the remaining penetration results are presented for the raw demand data only. The reader may use the results shown in Figure 2-11 to judge the impact of different retirement rates.

Figures 2-13 to 2-17 show the market penetration simulation results for all cases where penetration exceeds 50 MWe prior to

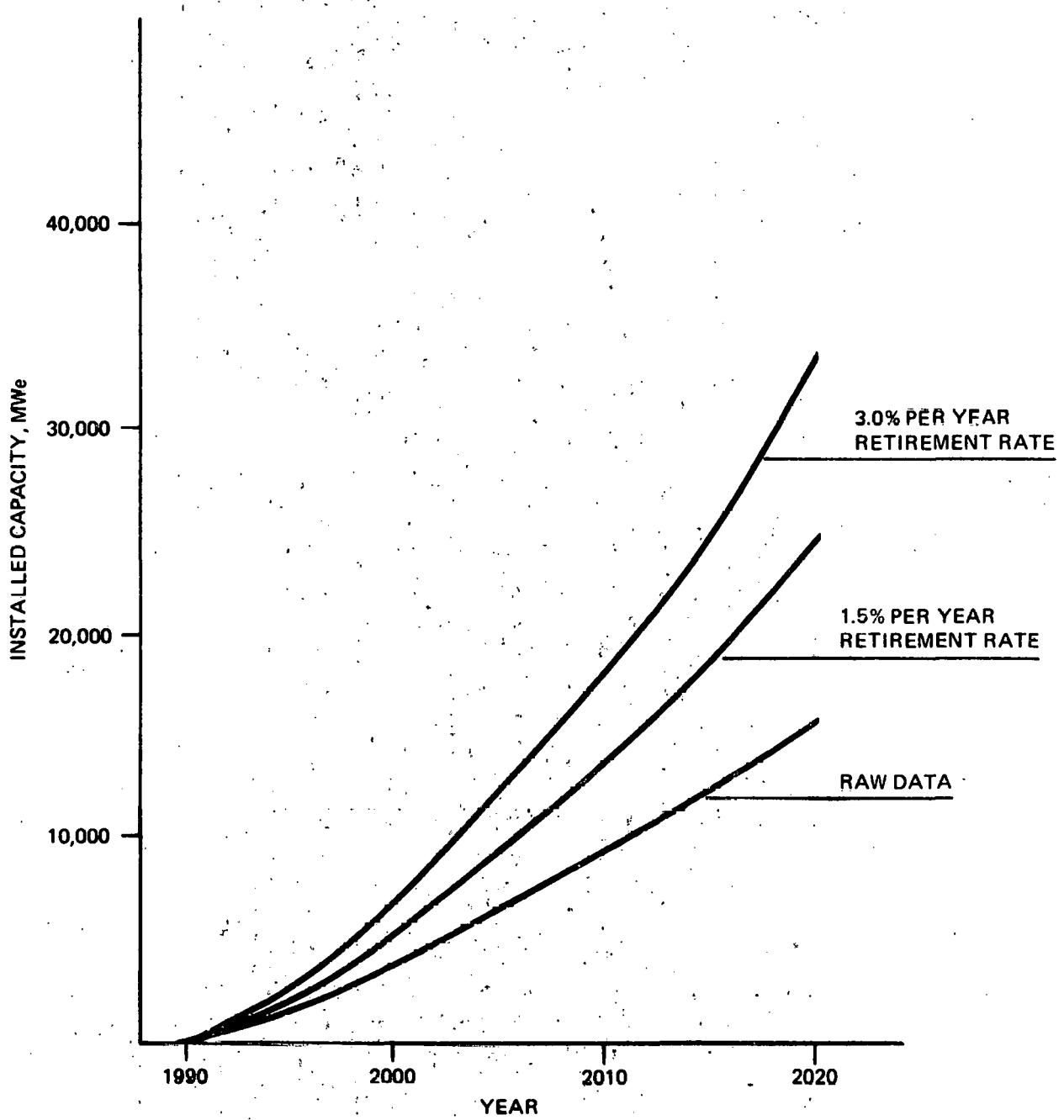

Figure 2-12 SIMULATED MARKET PENETRATION OF MODIFIED STRAWMAN IN PACIFIC SOUTHERN REGION, 15 PERCENT FUEL ESCALATION RATE

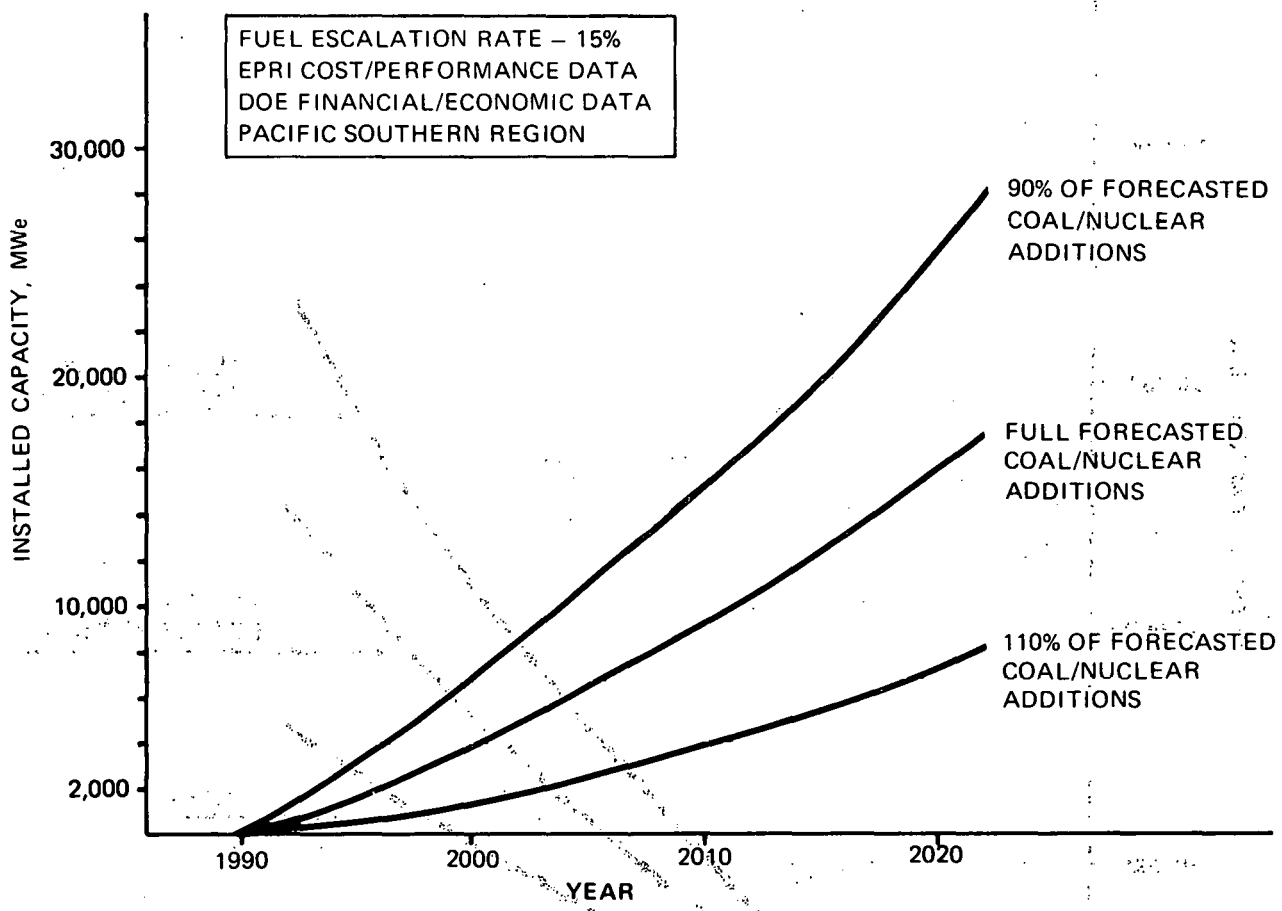

Figure 2-13 SIMULATED MARKET PENETRATION OF MODIFIED STRAWMAN IN PACIFIC SOUTHERN REGION, 15 PERCENT FUEL ESCALATION RATE

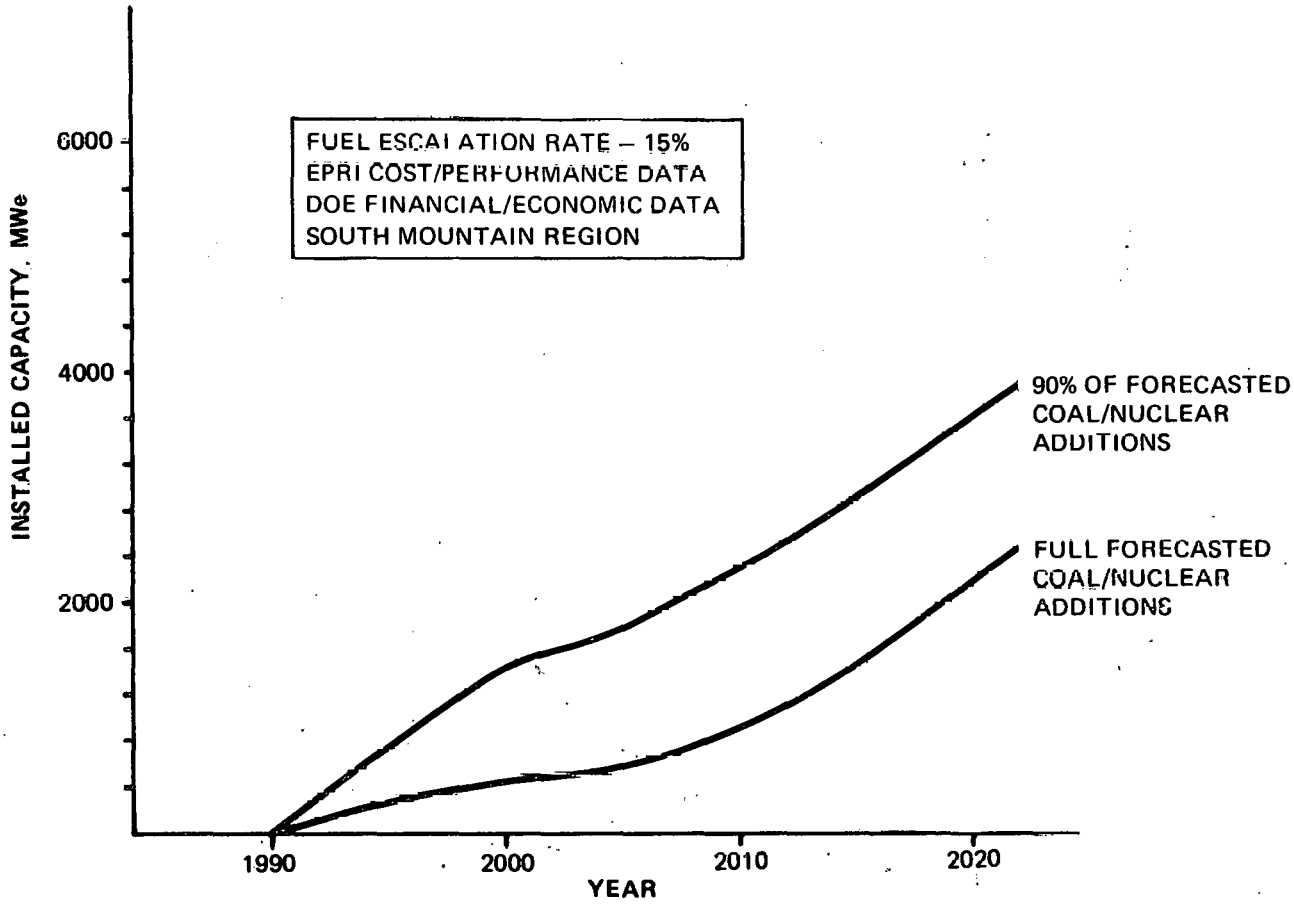

Figure 2-14 SIMULATED MARKET PENETRATION OF MODIFIED STRAWMAN IN SOUTH MOUNTAIN REGION, 15 PERCENT FUEL ESCALATION RATE

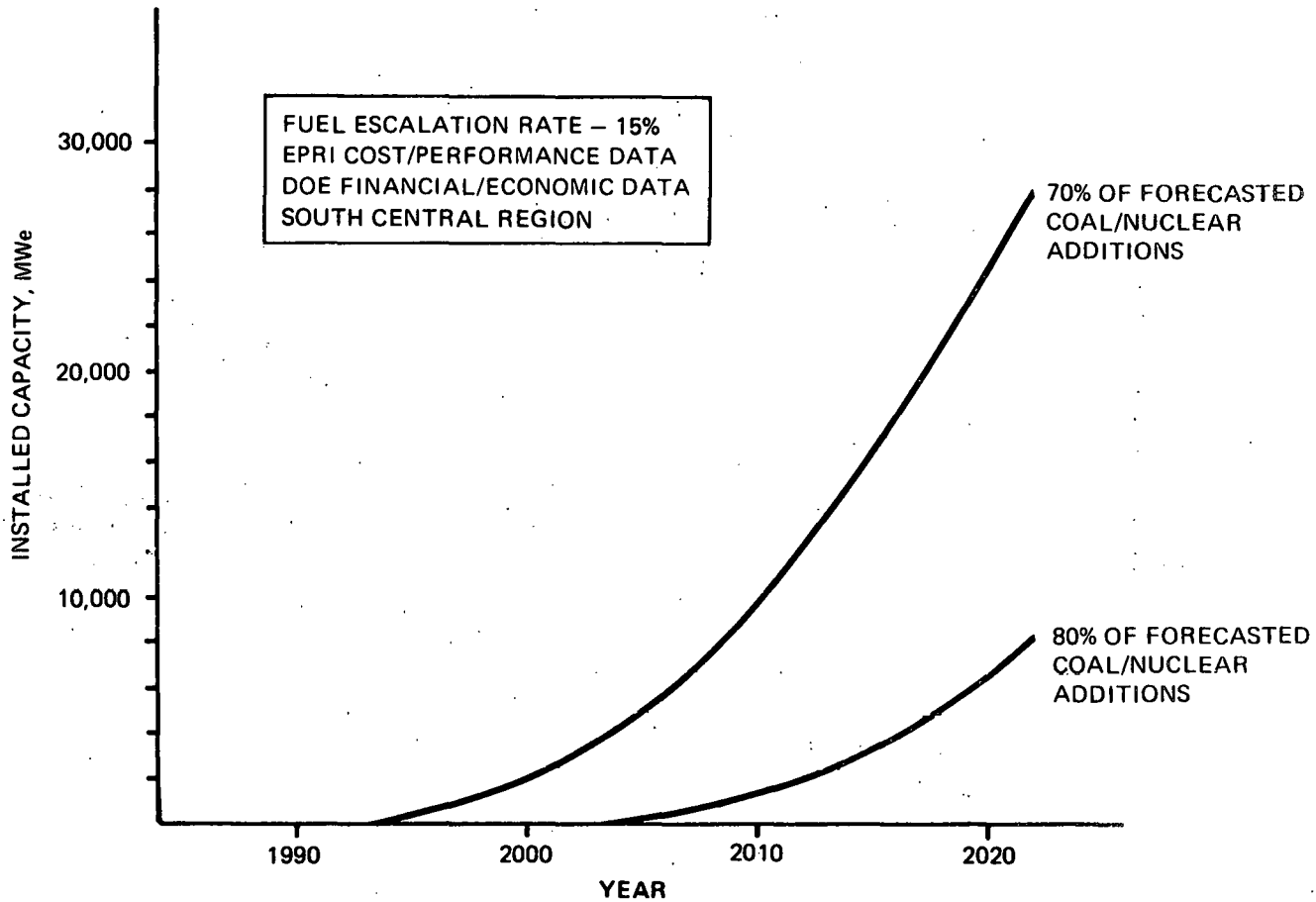

Figure 2-15 SIMULATED MARKET PENETRATION OF MODIFIED STRAWMAN IN SOUTH CENTRAL REGION, 15 PERCENT FUEL ESCALATION RATE

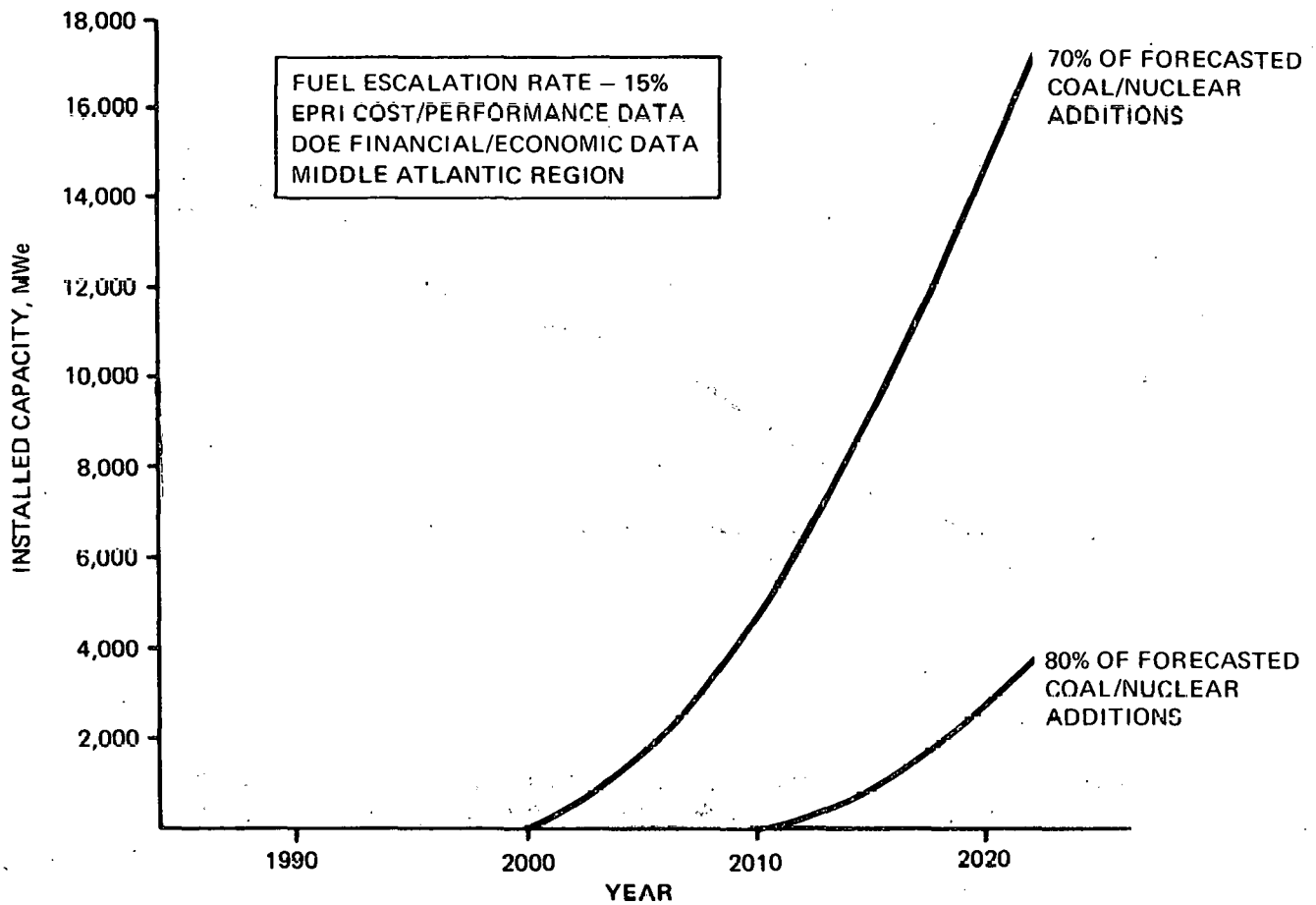

Figure 2-16 SIMULATED MARKET PENETRATION OF MODIFIED STRAWMAN IN MIDDLE ATLANTIC REGION, 15 PERCENT FUEL ESCALATION RATE

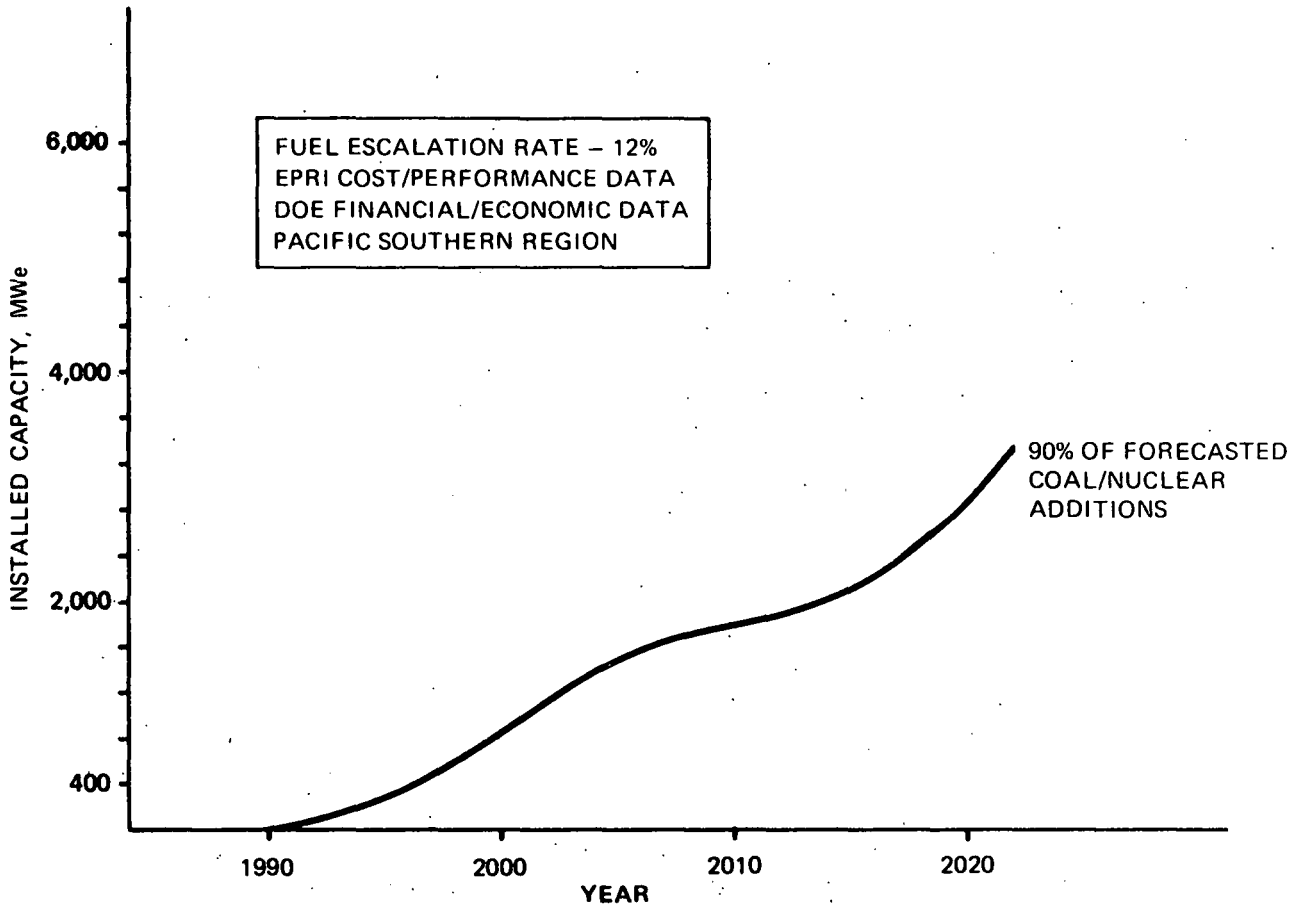

Figure 2-17 SIMULATED MARKET PENETRATION OF MODIFIED STRAWMAN IN PACIFIC SOUTHERN REGION, 12 PERCENT FUEL ESCALATION RATE

the year 2020. The fraction of forecasted incremental coal/nuclear capacity corresponding to each curve is indicated.

Significant penetration (over 50 MWe) is observed for all regions under the DOE financial/economic data and a 15 percent escalation rate for all fuels. Inter-regional comparisons for this economic scenario show that market penetration is greatest in the Pacific Southern region, followed by the South Mountain, South Central, and Middle Atlantic regions. The Pacific Southern region is the only one showing significant penetration for all values of the coal/nuclear incremental capacity fraction.

In light of the sensitivity analyses, however, the results for the 15 percent fuel escalation rate scenario must be presented in the proper perspective. Although the higher rate enhances hybrid economic feasibility relative to combustion turbines and combined cycles, the opposite is true relative to coal and nuclear plants. Thus, the constrained penetration analysis (which excludes coal and nuclear plants) probably gives more reasonable results for lower fuel escalation rates.

Using the DOE financial/economic data and 12 percent fuel escalation rate, solar hybrid penetration is reduced for all regions; the Pacific Southern region exhibits the only significant market penetration and even there, the coal/nuclear additions are constrained to 90 percent of the forecasted level. Smaller penetration is observed, prior to 2020, in the South

Mountain and South Central regions under constrained coal/nuclear scenarios. Under typical utility financial/economic data (7.6 percent fuel oil escalation), penetration is further inhibited, exceeding zero by the year 2020 only in the Pacific Southern region.

Table 2-7 ranks the regions in terms of key market potential determinants with the regions listed in order of decreasing market potential. Since all technologies in the constrained penetration analysis were oil fired, oil price levels are only significant under the typical utility financial/economic data, which recognizes regional differences in fuel prices.

Although the scope of the study does not allow a formal analysis of the sensitivity of penetration rate to these parameters, limited conclusions can be inferred from the market penetration curves and Table 2-7:

- Since Table 2-7 lists the regions in order of decreasing market penetration, a strong correlation is implied between market potential and the incremental coal/nuclear capacity fraction.
- Solar fraction and relative prices are less important than incremental coal/nuclear capacity fraction.
- Total incremental demand (total market size) is relatively unimportant.
- Regions of highest market potential do not necessarily correspond to those of highest average annual insolation.

TABLE 2-7

KEY MARKET POTENTIAL DETERMINANTS*

Determinant	Region			
	Pacific Southern	South Mountain	South Central	Middle Atlantic
Equipment price and wage level	2	2	1	3
Oil price level	1	3	1	2
Incremental demand	3	4	1	2
Incremental coal/nuclear capacity factor	1	2	4	3
Solar fraction	2	1	3	4

* 1 = Best
4 = Worst

2.5 CONCLUSIONS

From the market analyses conducted on the Modified Strawman and Advanced Strawman systems in four regions of the country, the following conclusions can be drawn on the economic viability of hybrid power systems:

- If only economic factors are considered, at a 12 percent fuel escalation rate, solar hybrid plants do not appear economically competitive. Coal and nuclear plants will share the base-load and intermediate-load markets, and oil- and gas-fired combustion turbines and combined cycles will capture the peaking market.

- At fuel escalation rates higher than 12 percent, hybrid plant economics improve relative to combustion turbine and combined cycle plants but do not improve relative to coal and nuclear plants. This relationship holds true over time.

- Economic parameters can be varied to reflect "optimistic" scenarios where hybrid plant economics improve relative to conventional plants.

- At a 15 percent fuel escalation rate and with a preassigned coal/nuclear capacity fraction, all regions experience significant market penetration by hybrid plants for the peaking and low-intermediate-load markets. It is greatest in the Pacific Southern region, followed by the South Mountain, South Central, and Middle Atlantic regions.

- At a 15 percent fuel escalation rate and with an unconstrained coal/nuclear capacity fraction, the Pacific Southern region is the only one showing significant market penetration.

- At a 12 percent fuel escalation rate, the Pacific Southern region exhibits the only significant market penetration, and even then requires a 10 percent reduction in the preassigned coal/nuclear capacity fraction.

It is clear, from these observations, that the market for the solar hybrid power plant is highly dependent on the anticipated fuel escalation rates and the external constraints placed on coal and nuclear plants. These analyses do not consider the effects of competition from other advanced technologies currently under development. It must also be emphasized that the market analysis is conservative. For example, the cost estimates were based on a first-of-a-kind installation. Although difficult to quantify, the construction of subsequent plants should realize cost savings from experience and from mass production of key components, such as the heliostat. In addition, the assumption of zero retirement rate of existing installed capacity in the utility systems is conservative. There will obviously be some degree of retirement, and this should favorably affect the market penetration. These purely economic conclusions may also be influenced by provisions of the National Energy Act of 1978, which is expected to accelerate the commercialization of solar power.

Section 3

PARAMETRIC ANALYSES

3.1 INTRODUCTION

Parametric analyses were conducted for the collector subsystem, receiver subsystem, and electric power generation subsystem (EPGS). The collector subsystem studies, for the selection of field layout and tower height, were conducted relatively independently. The receiver subsystem studies and EPGS studies were integrated because of the significant interdependence of these two subsystems. Analysis of the energy storage subsystem was not undertaken, since preliminary studies showed that this subsystem was neither technically necessary nor economically justified. Preliminary analysis was conducted on 1) the nonsolar subsystem, primarily related to the Brayton cycle combustor and the type of fuel, and 2) the master control subsystem, primarily related to the collector subsystem. These subsystems were further evaluated during the subsequent conceptual design.

System-level studies were also undertaken, including plant size, storage capacity, and solar fraction. These studies are also summarized in this section.

The parametric analysis of the combined cycle solar hybrid power system was the largest single activity in the 12-month study. The purpose was to quantify, both technically and economically,

the relationships between plant cost and performance for those parameters that significantly impact the selection of the preferred system concept. Parameters that have a lesser impact on the system were evaluated during the conceptual design.

Baseline designs and cost estimates for the two preconceptual reference systems formed the reference points around which the sensitivity to changes in key parameters were measured. The systems, representing two levels of technology in the use of an air-cooled receiver with a combined cycle, are the Strawman and the Advanced Strawman systems. (These are defined in Section 1.)

After defining the two preconceptual baseline designs, the significant parameters to be evaluated and the ranges for evaluation were selected. In most cases, three values were selected for analysis, bracketing the baseline value both above and below.

The next step in the analysis was the development of point designs for the cases to be analyzed. For the receiver, Foster Wheeler developed the point designs sufficiently to estimate the cost and weight of each design. For the EPGS, the Bechtel computer program ME670A was used to define data for this subsystem and also at the system level.

Each parametric case was evaluated to ascertain its effect on system costs. The economic evaluations were based on equivalent

capital costs in 1990 dollars. These costs included direct field construction cost, indirect field cost and engineering services, contingency, and allowance for funds during construction. They also included the cost of fuel consumed over an assumed 30-year operating life and other operating costs.

Based on systems analysis and market potential discussions with various utilities, a 12 percent baseline fuel escalation rate was chosen for the economic evaluations. A 15 percent fuel escalation rate was also calculated to check system sensitivity to changes in fuel escalation rate. The evaluations are based on the preconceptual heliostat cost of $93.42/m² (installed, 1978) and an average daily operation of 12.875 hours, which corresponds to a 48 percent capacity factor at a 90 percent availability.

3.2 COLLECTOR SUBSYSTEM

The objective of the collector parametric studies was to identify the subsystem of least cost, considering the land, heliostats, and field wiring. Although the receiver tower is not part of the collector subsystem, its cost variation was logically included in these parametrics, since the tower height and collector field performance are closely interrelated. In addition, the sensitivity of the subsystem costs to variations in field configuration, field performance, and unit costs of the components was also analyzed.

During the parametric studies, two basic collector field layouts were considered:

- An elliptical field with a south offset receiver tower
- A north field

Initially, the study of a circular field with south offset receiver tower was also planned, but this study was abandoned in favor of a comparative evaluation of two different heliostat sizes.

The preconceptual reference plants of 100 MWe capacity require a solar contribution of 56.3 and 71.9 MWe for the Strawman and Advanced Strawman systems, respectively. With nominal field and EPGS performance efficiencies, this requires collector fields capable of intercepting about 200 to 250 MWt of insolation, respectively. Seven versions of the basic field configurations were laid out and their geometric performances were calculated for the solar angles at Barstow, California. With these field and performance data, normalized costs were calculated for a range of points in:

- Field layout
- Tower height
- Heliostat unit cost
- Land cost

The study effort was concluded by determining solar flux data, for selected configurations, at the receiver aperture and at the absorber surfaces. In addition, the annual energy collected was also determined from the available Barstow information.

3.2.1 Field Design and Input Data

The collector field designs studied in the project evolved from reviews of previous DOE-sponsored studies of central receiver solar thermal power systems. Since the elliptical field offered a better year-round performance, it was studied extensively, although a north field was included for comparison. Table 3-1 defines the seven fields selected for study.

The six elliptical field designs evolved through the following path:

- The "A" field (Figure 3-1) represents the first cut approach prepared for the project proposal. The solar-energy-collecting capacity of 6125 heliostats, each with 38.6 m² reflective area, approximates the requirements of the Strawman design option (nominal 50 percent of the plant design power) at noon of the best solar day. The field is based on 22 percent packing factor with a rectangular layout. The blocking and shading at the design point was assumed to be 1 percent.

- The "B" and "C" fields represent optimizations of the "A" field to reduce the blocking and shading below 1 percent during the central 6 hours of any day.

- The "D" field uses the benefits of low blocking and shading of the "C" field and was laid out with 6500 heliostats of 38.6 m² size. The total reflective area from these heliostats is at about the midpoint of the reflective areas required for the Strawman and Advanced Strawman concepts. The "D" field was characterized to

TABLE 3-1

COLLECTOR FIELD DESCRIPTIONS

Field Designator	Generic Field Type	Heliostat Size (m^2)	Number of Heliostats	Tower Heights (m)
A	Elliptical	Small (38.6)	6125	174, 204
B	Elliptical	Small (38.6)	6125	*
C	Elliptical	Small (38.6)	6125	180, 226
D	Elliptical	Small (38.6)	6500	140, 187, 235
E	Elliptical	Large (49)	5121	128, 170, 215
F	North	Large (49)	5121	125, 210, 285, 360
G	Elliptical (with south sector removed)	Large (49)	5121	190

*Not evaluated.

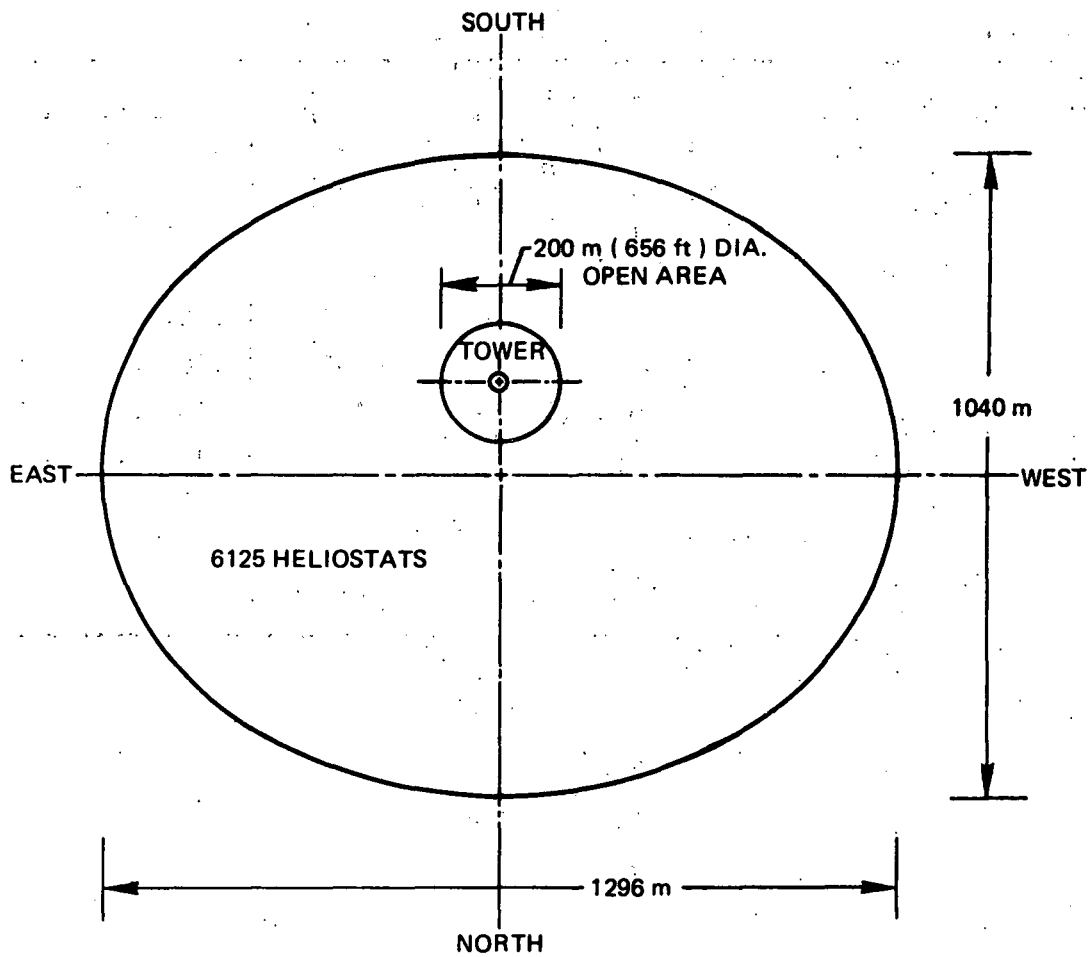

Figure 3-1 LAYOUT OF COLLECTOR FIELD "A"

provide all the necessary input for the parametric studies with the 38.6 m^2 heliostats.

- The "E" field has 5121 heliostats of 49 m^2 which gives the same total reflective area as the "D" field. This configuration was used in the comparison of the 38.6 and 49 m^2 heliostats and for comparison with the north field.

- Finally, the "G" field (Figure 3-2) evolved as a result of determining the radiant fluxes for the "E" field, where it became evident that the contribution of the south quadrant of the field was so small that an additional receiver configuration would be required. The "G" field arrangement permits a three-cavity receiver, with one common design being adequate for all three cavities.

As shown in Table 3-1, three receiver tower heights were typically selected for parametric optimization cases. The tallest tower has a 73.35° rim angle, which was found to give the optimum optical performance. The intermediate tower height was selected at approximately 5 percent blocking. The shortest tower was chosen to be shorter than the intermediate tower by the amount the intermediate tower was shorter than the tallest tower.

The collector field performance for each tower height was evaluated by computer, which required the determination of the coordinates of the heliostats and the sun position as inputs. The code calculates the cosine factors, shading, and blocking for each heliostat in the collector field. These values are averaged over a year for 36 sun positions and, with the inclusion of the tower shadow, yield the overall geometric performance efficiency. Since the atmospheric attenuation does not vary significantly

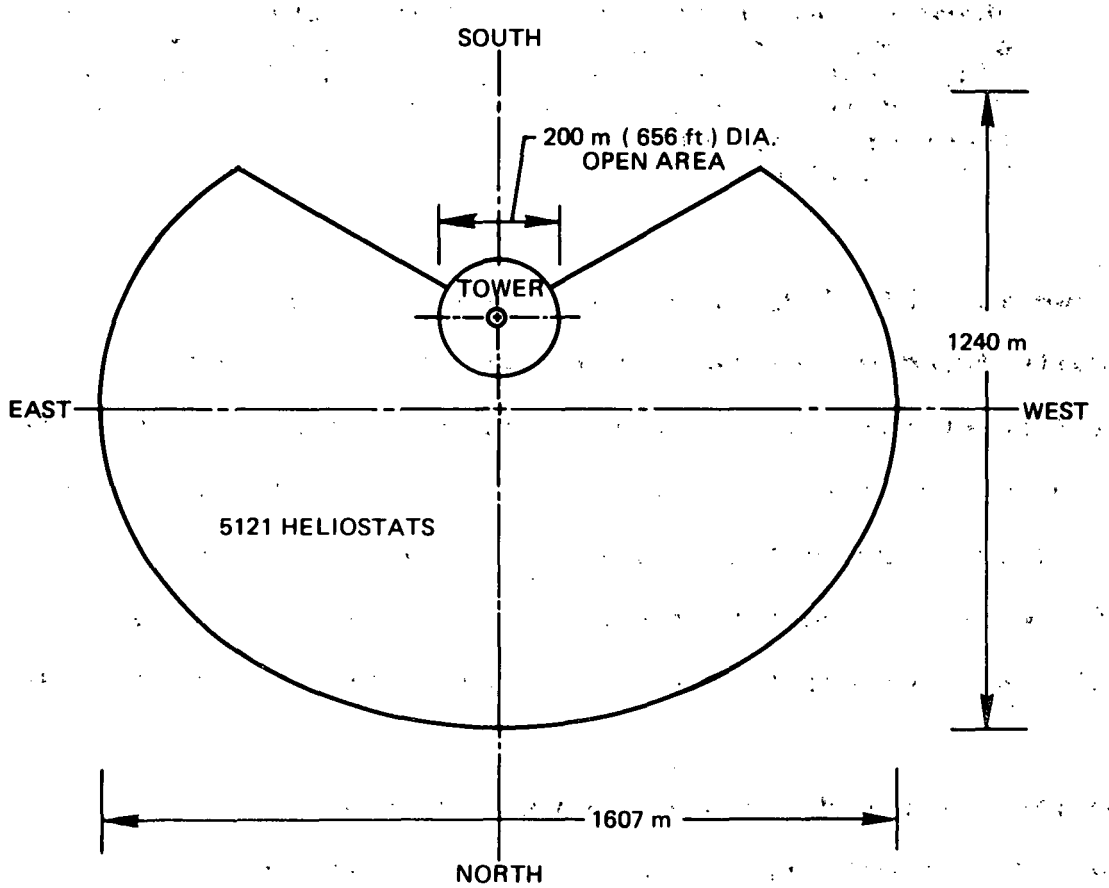

Figure 3-2 LAYOUT OF COLLECTOR FIELD "G"

over the range of field dimensions, it was only considered in calculations of the annual energy collected.

3.2.2 Field Analysis

To compare the cost of various solar subsystem configurations, it is necessary to normalize the costs for performance variation. The collector subsystem and tower costs were analyzed by use of the algorithm:

$$C_{CN} = \frac{C_H + C_T + C_L + C_W}{\eta}$$

where:

C_{CN} = the normalized collector subsystem cost

C_H = installed cost of heliostats

C_T = tower cost

C_L = land cost

C_W = field wiring cost

η = field efficiency

The inputs and variations of the terms of the algorithm were defined as follows:

- The heliostat costs (C_H) were derived by calculating the total reflective area and multiplying the resulting total area by the specific cost of heliostats ($/m²). The specific cost was varied over a range of $50 to $200 per m².
- The tower cost (C_T) was calculated from the Sandia algorithm (Ref. 3-1) for tower cost, modified to include the cost of riser and downcomer piping. The receiver

weight and seismic accelerations were held constant for all tower heights. Separate tower cost values were determined for each assumed tower height.

- The land cost (C_L) was initially varied between $3000 and $5000 per acre, but found to have only marginal effect on the normalized cost and was later set at a conservative $5000 per acre.

- The cost of wiring (C_W) was extrapolated from a previous preliminary design study of a 10 MWe central receiver pilot plant (Ref. 3-2).

- The field efficiency (η) is the integrated average of the geometric efficiency taken hourly from 6 a.m. to 6 p.m. for the year 1976 at Barstow, for times when the insolation was above 500 W/m^2.

Figures 3-3 through 3-6 show the results of the parametric analyses for heliostat costs of $50 to $200 per m^2. These graphs indicate that, considering the collector subsystem alone, the "E" field is the most cost-effective. The curves also show the expected trend that the more expensive the heliostats are, the higher the receiver tower optimum height. It is also evident that the cost of the "G" field is not significantly higher than the "E" field. This indicates that potential benefits to the overall system, such as simplified receiver design attendant to the "G" field, could be achieved with minimal cost penalty to the collector subsystem.

Flux profiles were calculated for the "E" field at the following time points:

North quadrant: noon winter and summer solstice, 8 and 10 a.m., noon, 2 and 4 p.m. at equinox

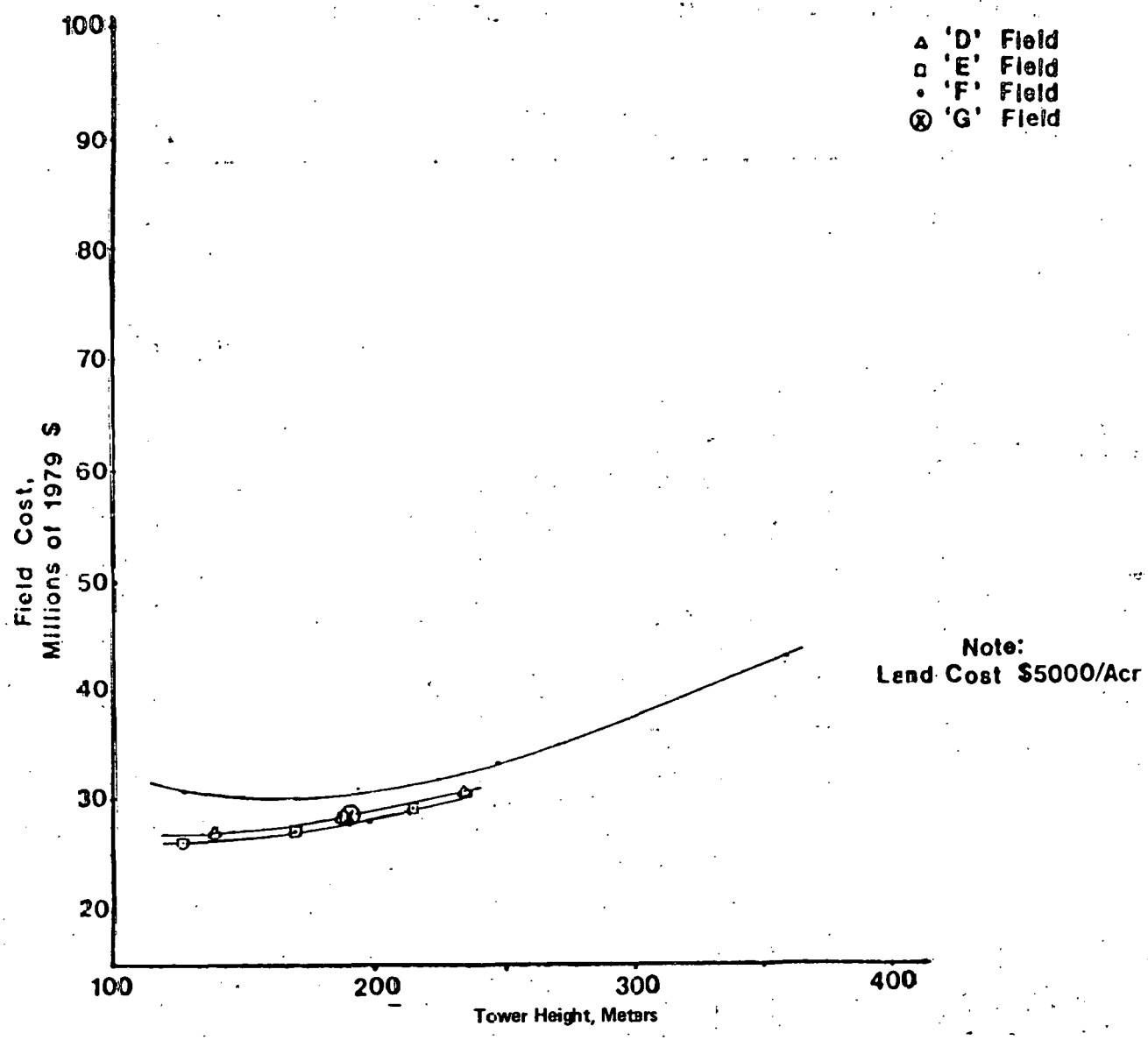

Figure 3-3 NORMALIZED FIELD COST WITH HELIOSTATS AT $50/m^2

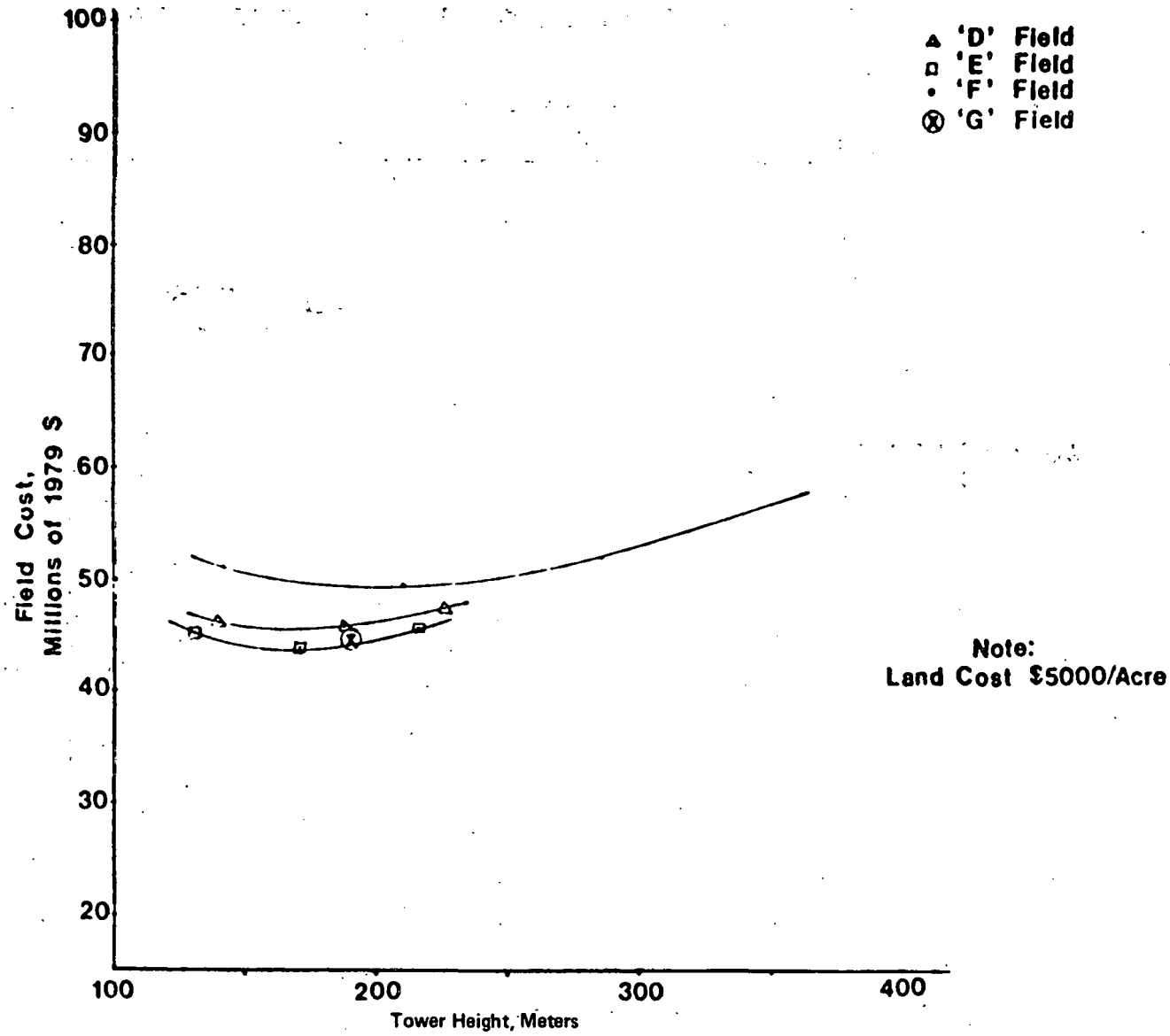

Figure 3-4 NORMALIZED FIELD COST WITH HELIOSTATS AT $100/m^2

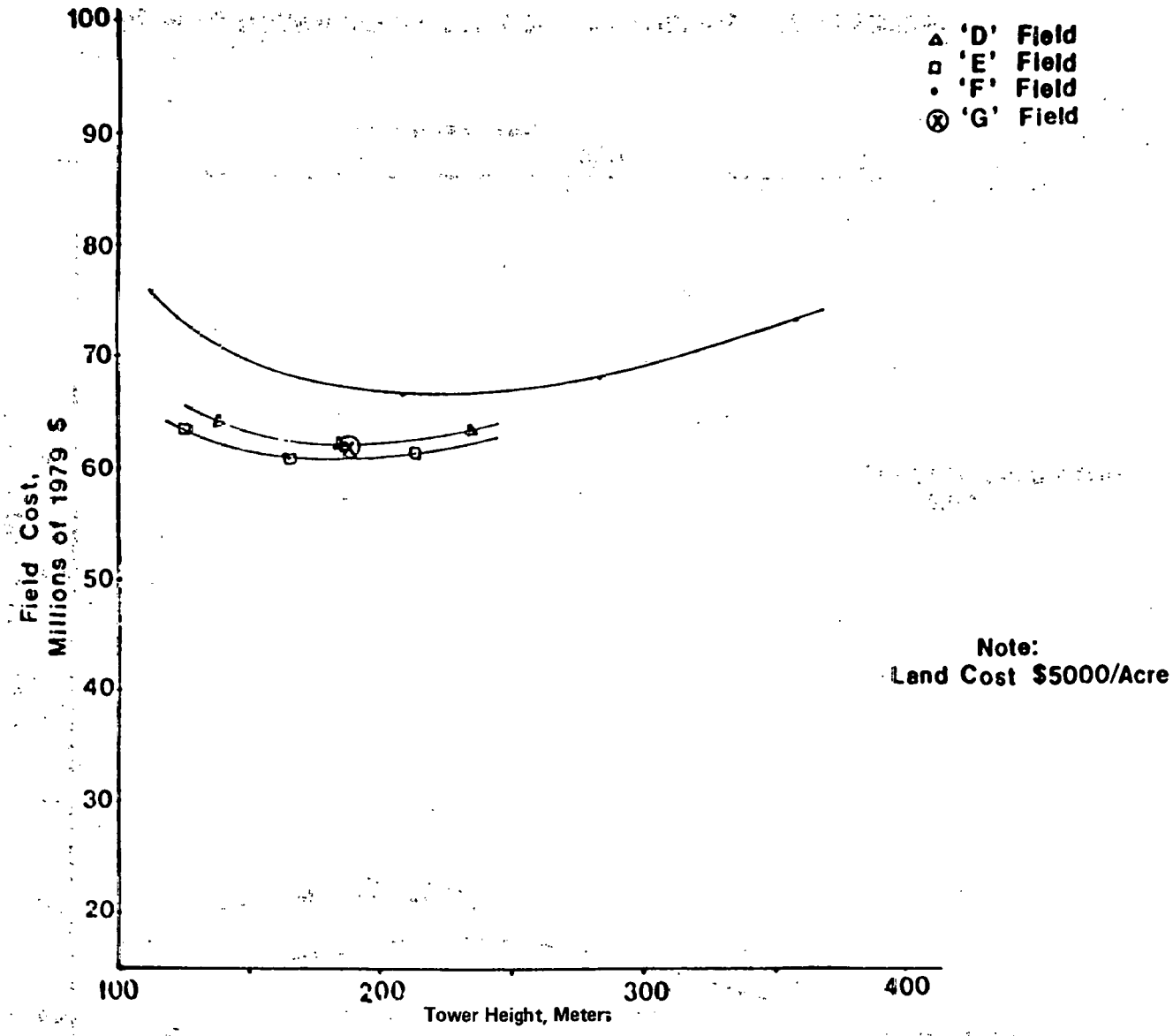

Figure 3-5 NORMALIZED FIELD COST WITH HELIOSTATS AT $150/m^2

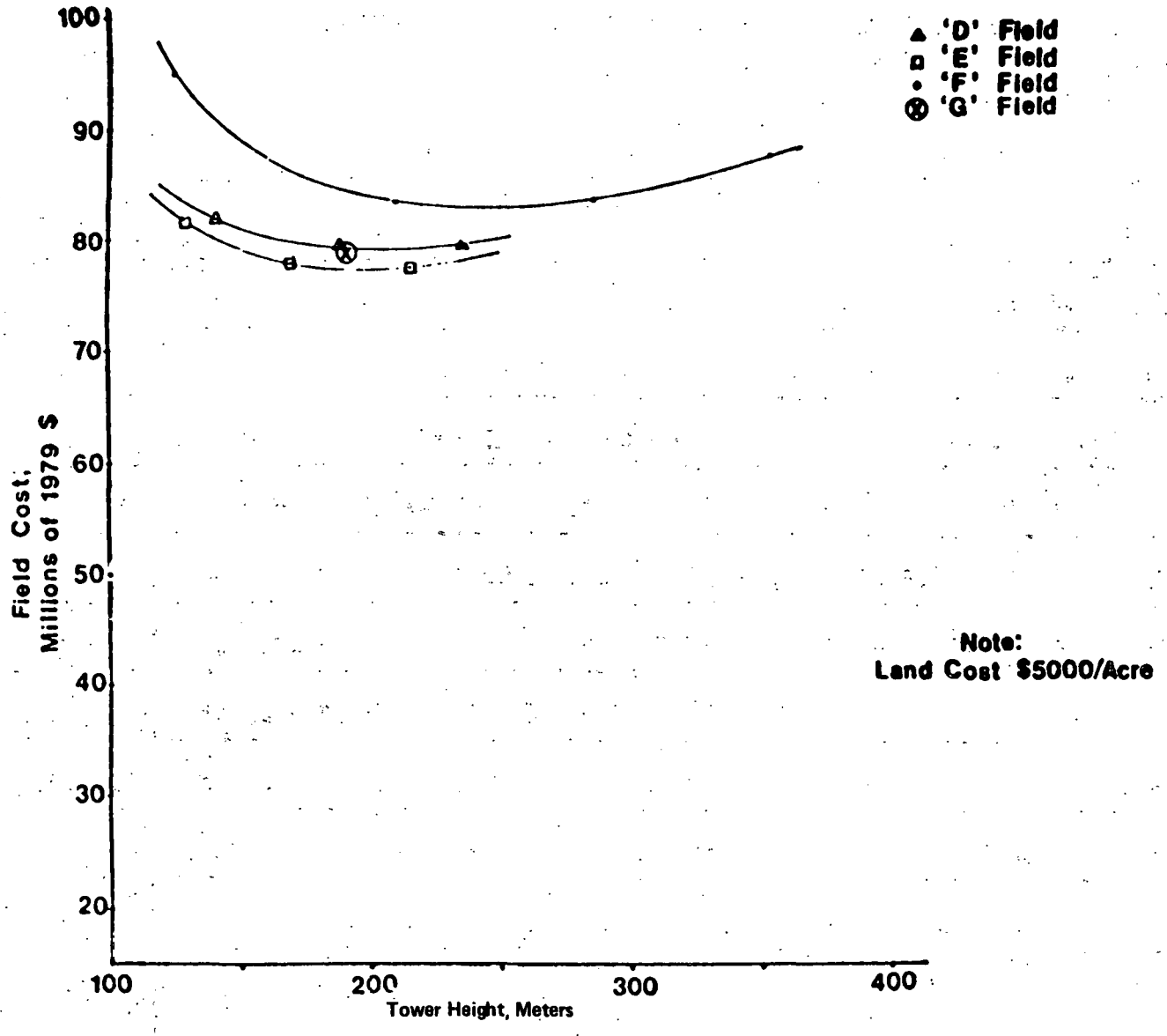

Figure 3-6 NORMALIZED FIELD COST WITH HELIOSTATS AT $200/m^2

West quadrant:	noon winter and summer solstice, 8 and 10 a.m., noon, 2 and 4 p.m. at equinox
East quadrant:	same as west quadrant at noon of solstices, mirror image of west receiver at equinox
South quadrant:	noon winter and summer solstices, noon equinox

The maximum energy collected in the south quadrant at noon, summer solstice, is about 32 MWt, which is about 30 percent below the maxima of the east and west quadrants. With such differences, it is clear that the south receiver cavity would have to have a different design from the east and west quadrants, which would mean three separate cavity designs in the receiver.

Attempts to eliminate this undesirable complexity led to the development of the "G" field configuration, which deletes the south receiver quadrant and redistributes the ineffective south field heliostats from a 120° segment south of the tower. The resulting field can achieve an improved field performance efficiency. In addition, by orienting the east and west cavities 22° north of the east-west axis, the maximum fluxes and cavity power in the remaining three cavities can be made nearly equal and thus they can be of a single design.

Considering these significant advantages, the "G" field was recommended for continuation into the conceptual design task. Significant performance characteristics of this field are shown in Table 3-2 and Figures 3-7 through 3-12.

TABLE 3-2

GEOMETRIC PERFORMANCE EFFICIENCY, "G" FIELD
Tower Height: 190 m (623.4 ft)

Solar Elevation Angle, Degrees	Solar Azimuth Angle, Degrees 0	±30	±60	±75	±90	±110
89.5	.8004	.8000	.7997	.7995	.7993	.7991
65	.8309	.8240	.8057	.7941	.7819	.7667
45	.8346	.8224	.7882	.7661	.7428	.7137
25	.7075	.8010	.7541	.6983	.6392	.6381
15	.4561	.7458	.6993	.6226	.4812	.5630
5	.1584	.6695	.5508	.5250	.2192	.5199

TARGET PLANE FLUX -KW/M2

	-15	-12	-9	-6	-3	0	3	6	9	12	15
15	25	48	83	123	158	172	158	123	83	48	25
12	48	97	172	267	352	387	352	267	173	97	48
9	83	173	322	524	726	816	726	525	322	173	83
6	124	269	526	925	1388	1620	1388	925	526	269	124
3	160	355	731	1393	2302	2810	2302	1393	731	355	160
0	175	392	825	1631	2818	3510	2818	1631	825	392	175
-3	161	358	736	1403	2318	2827	2318	1403	737	358	161
-6	126	272	533	938	1408	1643	1408	938	533	272	126
-9	85	176	328	535	742	833	742	535	328	176	85
-12	50	99	177	274	361	398	361	274	177	99	50
-15	26	50	85	127	163	177	163	127	85	50	26

10.1M [33FT]

10.1M [33FT]

TOTAL POWER = 61896.96 KWT

DAY - 80.00

TIME = 12.00

AZ = 0.00

ELEV = 55.11

JB

Figure 3-7 FOCAL PLANE FLUX MAP FOR NORTH RECEIVER OF "G" FIELD FOR EQUINOX NOON AT BARSTOW, CA

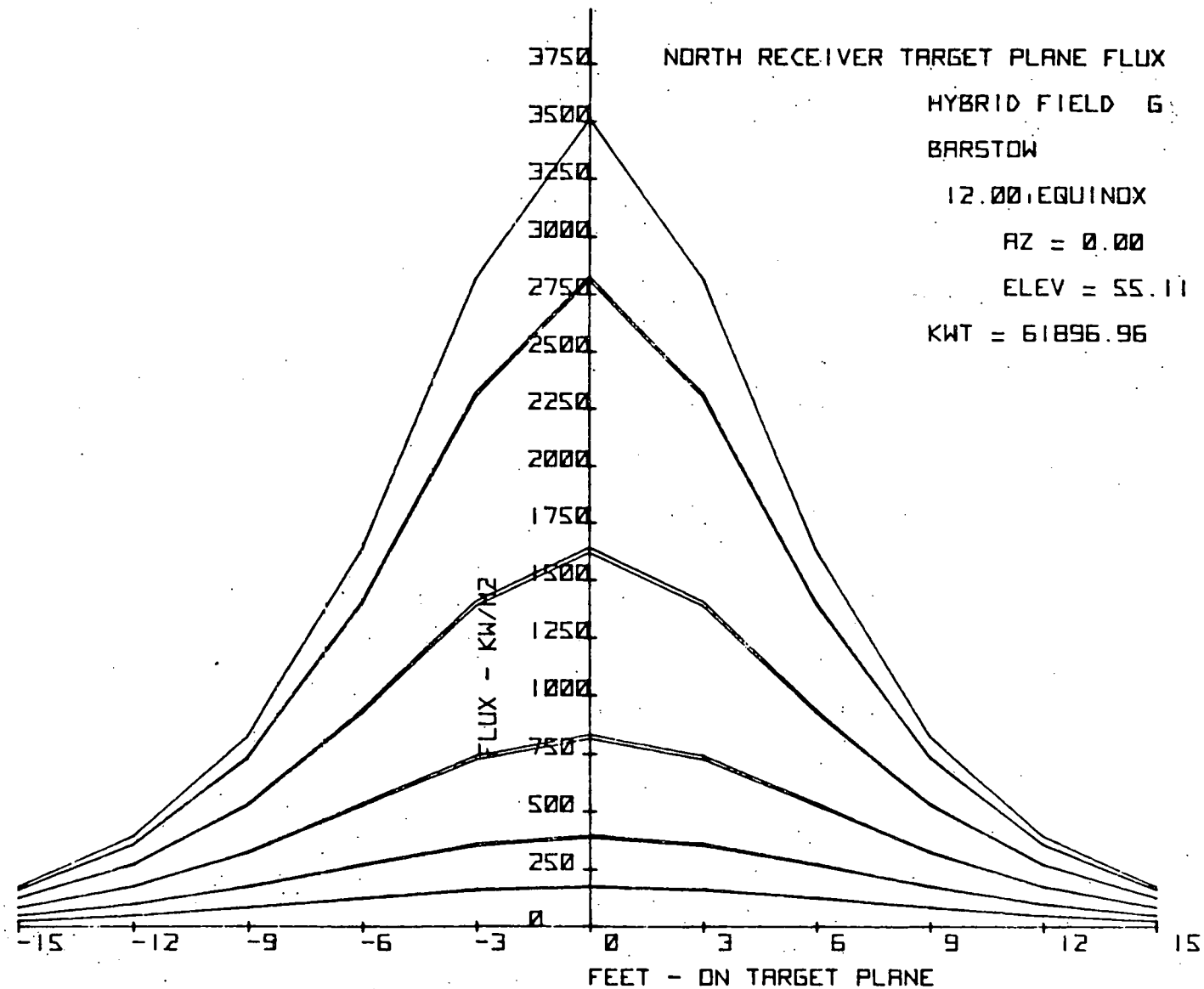

Figure 3-8 FOCAL PLANE FLUX PROFILE FOR NORTH RECEIVER OF "G" FIELD FOR EQUINOX NOON AT BARSTOW, CA

PANEL NO.

DISTANCE ABOVE APER. C.L.	1	2	3	4	5	6	7	8	9	10	11
35	4	20	35	24	24	32	24	24	35	20	4
30	15	36	62	81	109	141	109	81	62	36	15
25	54	108	150	174	199	222	199	174	150	108	54
20	126	239	358	449	518	553	518	449	358	239	126
15	273	476	691	866	985	1033	985	866	691	476	273
10	370	608	859	1068	1207	1258	1208	1063	859	608	370
5	323	509	703	867	975	1013	975	867	703	509	323
0	196	298	404	494	552	573	552	494	404	298	196
-5	86	127	170	206	229	237	229	206	170	127	86
-10	28	41	53	64	71	73	71	64	53	41	28
-15	0	10	13	15	17	17	17	15	13	10	7

TOTAL POWER = 61896.96 KWT

DAY - 80.00

TIME = 12.00

AZ = 0.00

ELEV = 55.11

INSOL. = 950 W/M2

JB

Figure 3-9 CAVITY FLUX MAP FOR NORTH RECEIVER OF "G" FIELD FOR EQUINOX NOON AT BARSTOW, CA

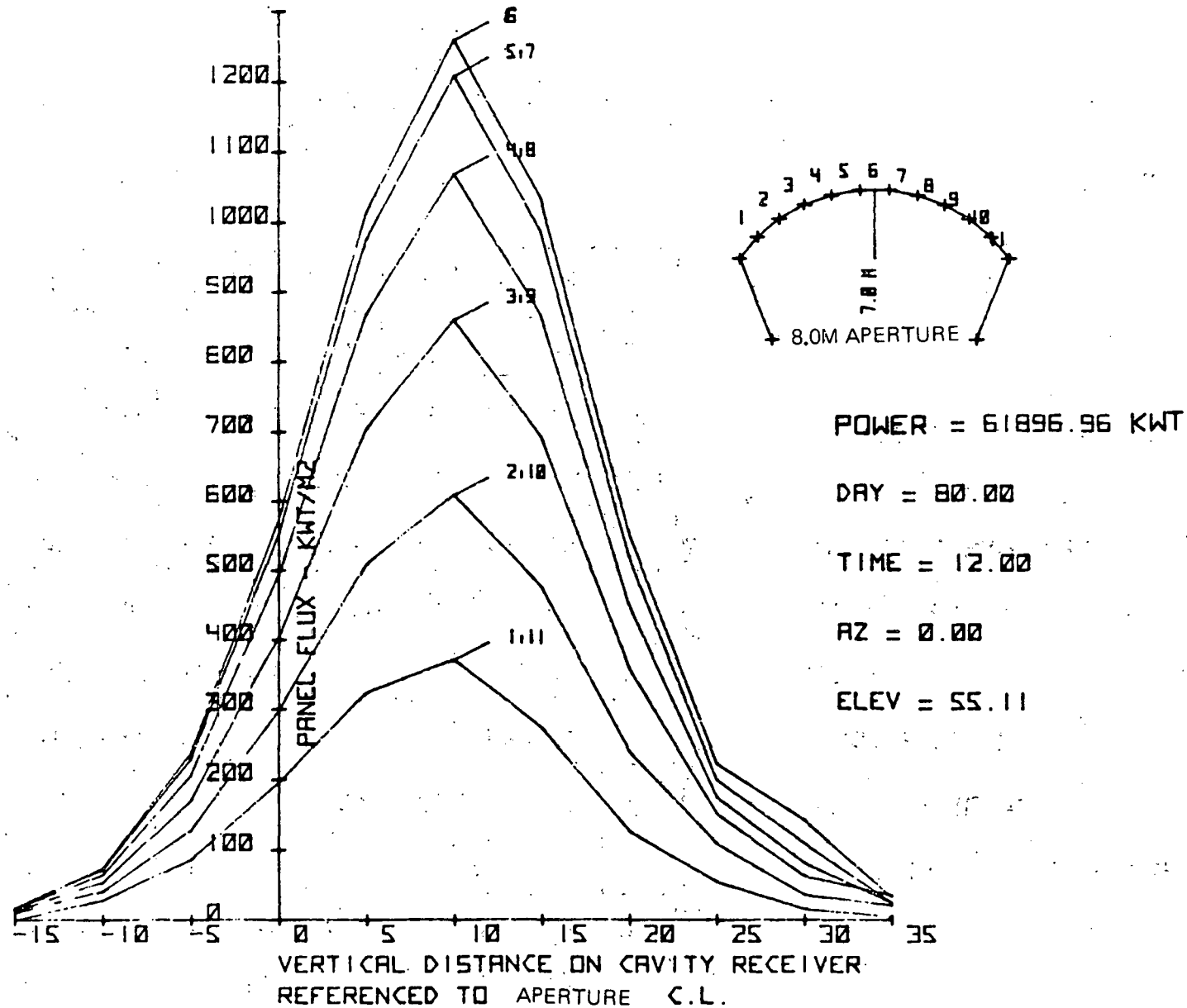

Figure 3-10 CAVITY FLUX PROFILE FOR NORTH RECEIVER OF "G" FIELD FOR EQUINOX NOON AT BARSTOW, CA

TARGET PLANE FLUX -KW/M2

	-15	-12	-9	-6	-3	0	3	6	9	12	15
15	20	40	70	105	136	148	135	104	69	39	20
12	40	82	149	237	318	352	317	235	147	81	39
9	70	150	289	490	689	792	694	485	284	147	68
6	106	238	491	910	1411	1658	1402	899	483	233	103
3	137	320	702	1414	2385	2901	2369	1396	689	314	134
0	150	355	797	1665	2906	3585	2887	1644	783	347	146
-3	137	320	701	1411	2377	2891	2362	1393	688	313	134
-6	106	238	490	907	1405	1650	1396	896	482	233	103
-9	70	149	288	489	696	788	692	483	284	147	68
-12	40	82	149	236	317	351	316	234	147	80	39
-15	20	40	69	105	136	148	135	104	68	39	20

10.1M [33FT]

10.1M [33FT]

TOTAL POWER = 60127.00 KWT

DAY - 80.00

TIME = 10.00

AZ = 45.16

ELEV = 45.16

22 DEG. PLANE ROTATION

JB

Figure 3-11 FOCAL PLANE FLUX MAP FOR WEST RECEIVER OF "G" FIELD FOR 10:00 A.M., EQUINOX, BARSTOW, CA

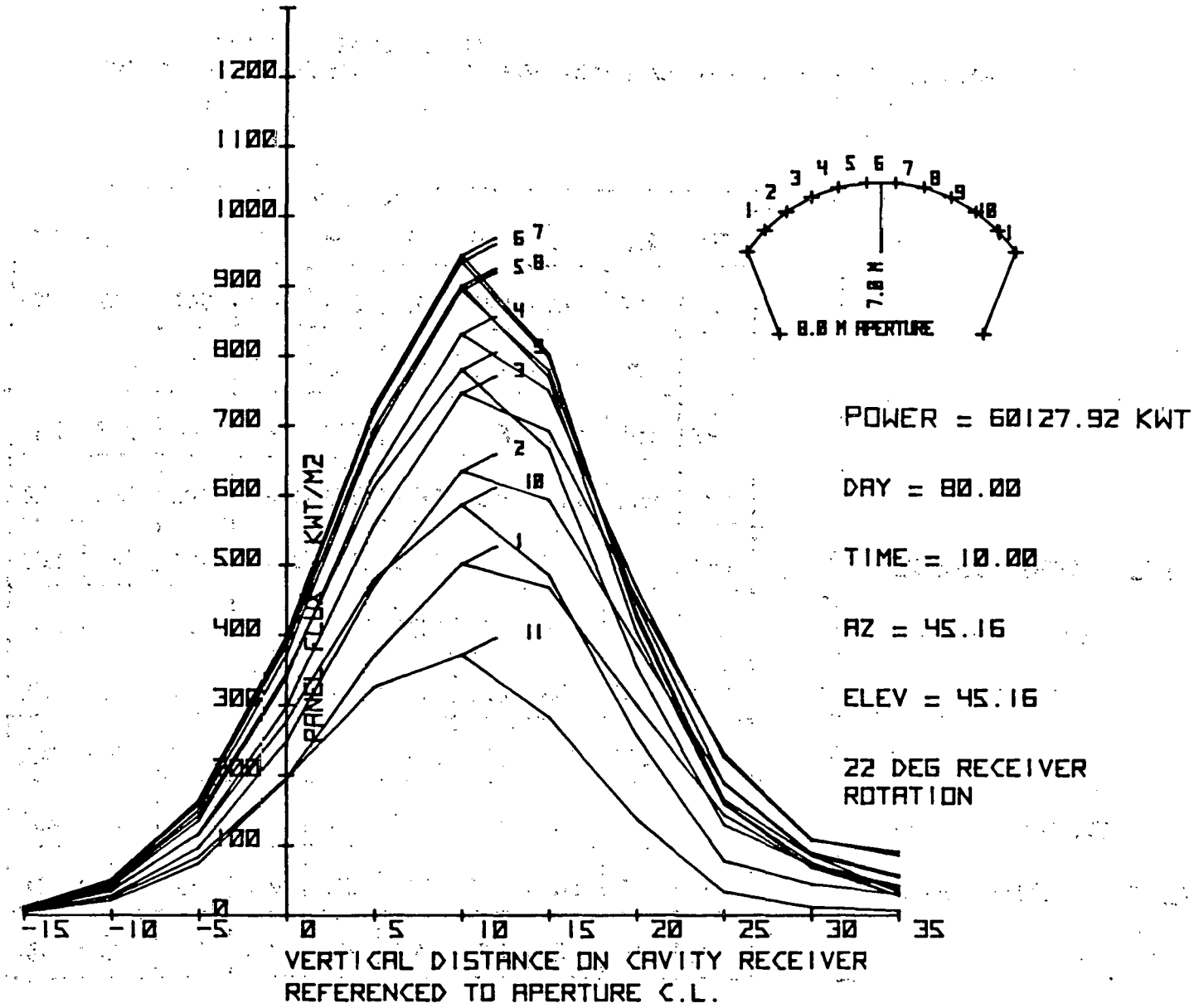

Figure 3-12 CAVITY FLUX PROFILE FOR WEST RECEIVER OF "G" FIELD FOR 10:00 A.M., EQUINOX, BARSTOW, CA

3.3 RECEIVER SUBSYSTEM

The objective of the receiver subsystem parametric studies was to define the most cost effective and technically suitable subsystem for the Strawman and Advanced Strawman designs. The receiver subsystem includes all components necessary to absorb the incident energy from the heliostat field and to introduce the energy into the power system. The components include the tower, the receiver, and the connecting piping.

The receiver parametric analysis addressed questions of cost, weight, size, surface requirements, materials, thermal efficiency (heat losses), air pressure drop, design complexity, operation and control, thermal transients, maintenance, and installation. This section summarizes the receiver concepts considered and discusses the parametric studies of receiver components. Work on the tower was confined to the economic aspects.

3.3.1 Receiver Concepts

Receivers selected for the combined cycle hybrid power systems must be able to operate at high temperatures to maximize the solar fraction and to take advantage of the excellent cycle efficiencies at elevated temperatures. The cycle working fluid, air, has low volumetric heat capacity, and has comparatively low heat transfer coefficients.

The capabilities of the receiver have a strong impact on the performance of the solar hybrid power system. In the chosen concept, where the receiver and the Brayton cycle combustor are in series, the solar fraction is determined by the ratio of the temperature rise across the receiver to the temperature rise from the compressor outlet to the gas turbine inlet. Thus, the closer the receiver outlet temperature is to the gas turbine inlet temperature, the higher the achievable solar fraction.

The peak receiver outlet temperature is constrained by material limitations:

- Metallic receivers: material properties and manufacturing process are better understood, but the upper limit of useful metal temperatures is about 871C (1600F).
- Ceramic receivers: much less is known about the material properties and manufacturing processes, but the upper limit of useful temperatures is above 1093C (2000F).

A metallic receiver was selected for the Strawman system, since metallic receivers should be ready for application in the 1985-1990 time frame. A ceramic receiver was selected for the Advanced Strawman system, although this receiver is less developed and would involve more R&D; the improved system performance gained at higher temperatures make this concept worth pursuing.

The metallic receiver concepts considered are:

- Nickel alloy tube-type receiver advanced by the Boeing Co. (Ref. 3-3)
- Heat pipe receiver, using nickel alloy advanced by Foster Wheeler Corp./Dynatherm Corp. (Ref. 3-4)

The ceramic receiver concepts considered are:

- SiC tube concept under development for EPRI by Black and Veatch, Consulting Engineers (Ref. 3-5)
- Bottom-opening ceramic matrix receiver under development by Sanders Associates (Ref. 3-6)
- Ceramic dome receiver under development by Lincoln Laboratories of MIT (Ref. 3-7).

In addition, an innovative concept, using a small particle heat exchanger, is being advanced by the Lawrence Berkeley Laboratory (Ref. 3-8). This concept is in the early laboratory testing stage and will require extensive development to prove its practicality.

Of the available receiver types, the heat pipe concept was selected for the Strawman system and the tube-type ceramic receiver concept was selected for the Advanced Strawman system.

The heat pipe receiver was selected because:

- It can accept high solar fluxes of 1 MWt/m^2 of projected absorber surface resulting in compact, light weight receivers

- It can achieve high heat transfer rates with low airside pressure loss
- It has a small difference between the peak receiving surface and the average air stream temperatures
- It can be of a modular design, which enhances reliability, maintainability, and operating flexibility
- It is expected to have a low capital cost

The tube-type ceramic receiver concept was selected for the Advanced Strawman primarily because it is a more conventional ceramic configuration, suitable for the Brayton cycle pressure conditions. The bottom-opening ceramic matrix receiver is not suitable for high-pressure air operation and will require an optical window with high transmissivity and adequate structural strength for direct power cycle air flow. The experimental-scale ceramic dome receiver holds promise, but will require further evaluation and development to make it suitable for commercial application.

Each receiver used in the parametric studies has four receiver cavities. It is shown in plan view in Figure 3-13. The north cavity in the figure is larger than the others because the north sector of the collector field delivers a larger proportion of the energy.

Strawman Receiver Concept. A typical arrangement of a Strawman heat pipe receiver cavity is shown in Figure 3-14. The incident solar radiation from the heliostat field enters the cavity through the aperture and impinges on the heat-absorbing surface

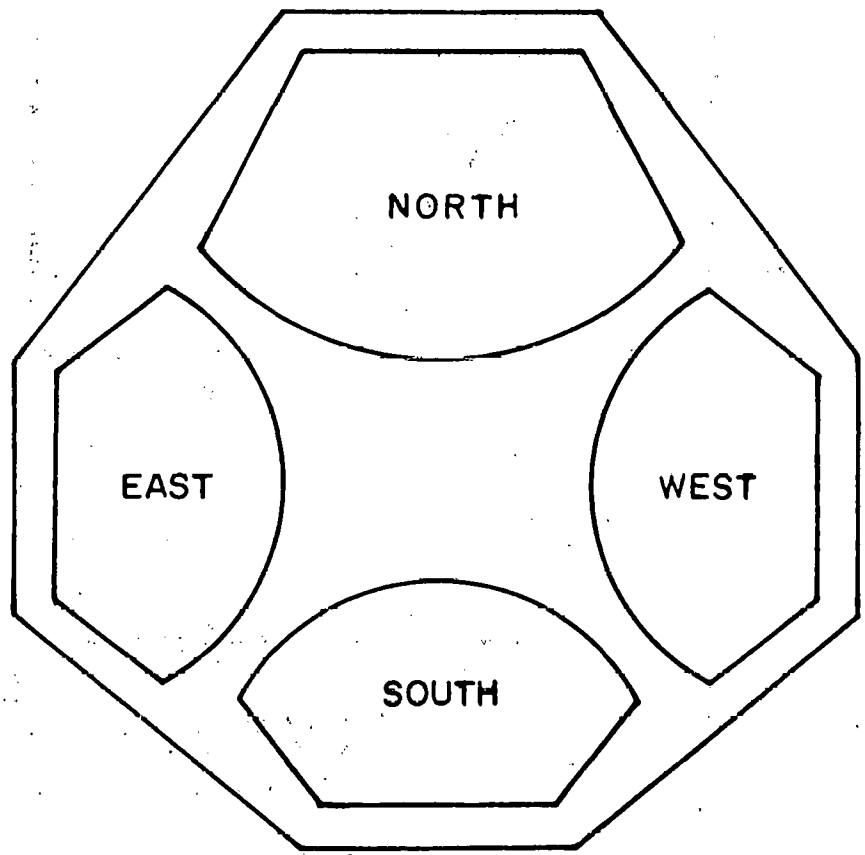

Figure 3-13 RECEIVER PLAN ARRANGEMENT

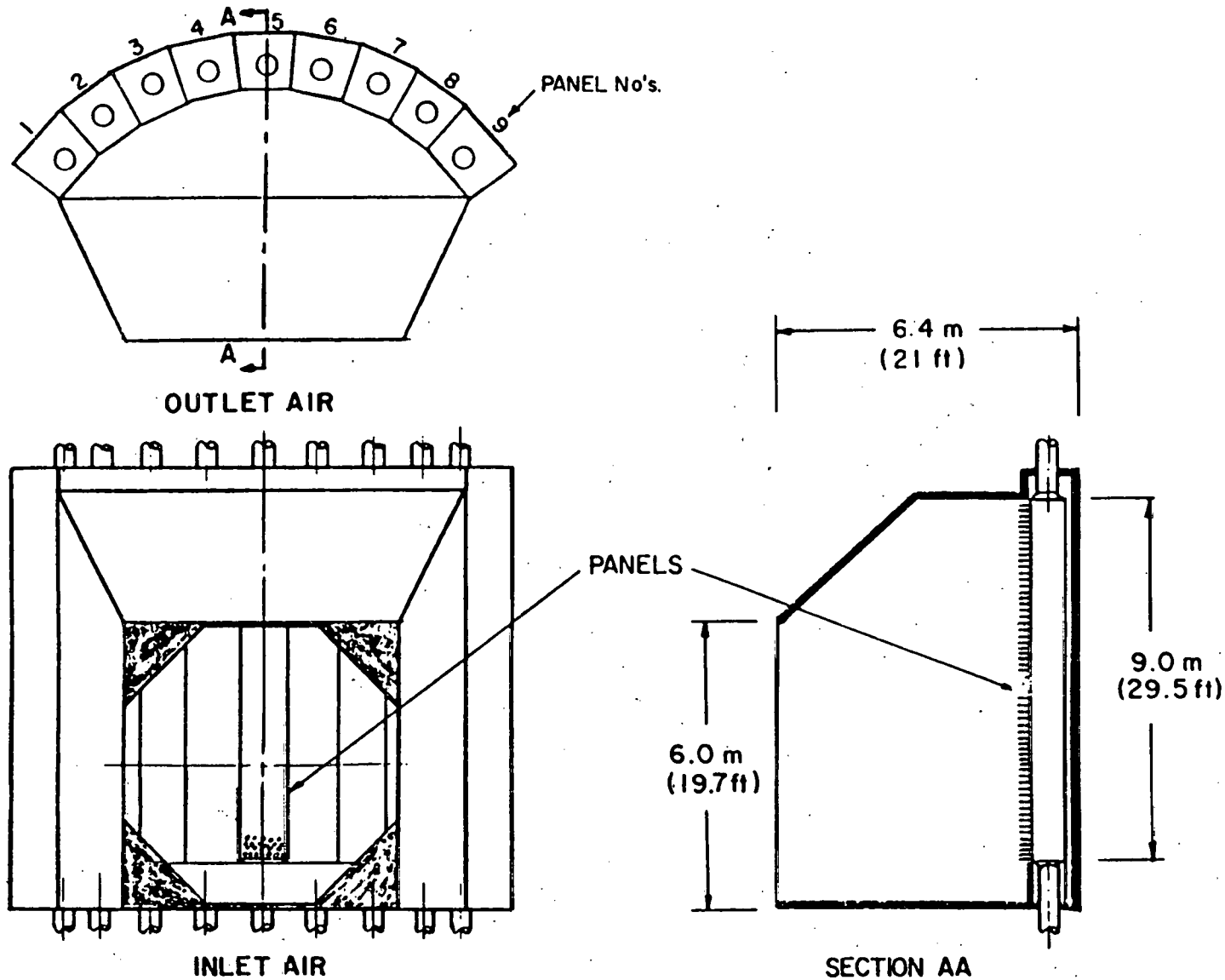

Figure 3-14 HEAT PIPE RECEIVER SCHEMATIC FOR STRAWMAN SYSTEM (EAST, WEST, AND SOUTH RECEIVERS)

along the back wall of the cavity. The back wall is made up of a number of panels, each configured as shown in Figure 3-15. The panels consist of rectangular air ducts fitted with sodium-filled heat pipes, inlet and outlet plenums, insulation, and support structure. Compressed air is introduced at the bottom of the panels and is gradually heated by thermal contact with the heat pipe fins as it passes upward to the outlet plenum. The compressed air also receives some heat from contact with the insulated front wall of the panel.

A 0.66 m (26.0 in.) diameter inlet manifold distributes the air to each panel via butterfly control valves located at the bottom inlet of each panel. A 0.76 m (30.0 in.) diameter outlet manifold collects the hot air leaving the panels.

A simplified schematic of a typical heat pipe, indicating the main functional features, is shown in Figure 3-16. The heat pipes are installed in a triangular-pitch grid, as shown in Figure 3-17. The heat pipes are attached to the panel walls in such a way that they can be removed from the back of the panel for servicing or replacement, as shown in Figure 3-18.

The evaporator surfaces of the heat pipes protrude from the front panel plate. The purposes of this protruding section are to:

- Provide enough area to keep the radiant flux in the evaporator section below design limits

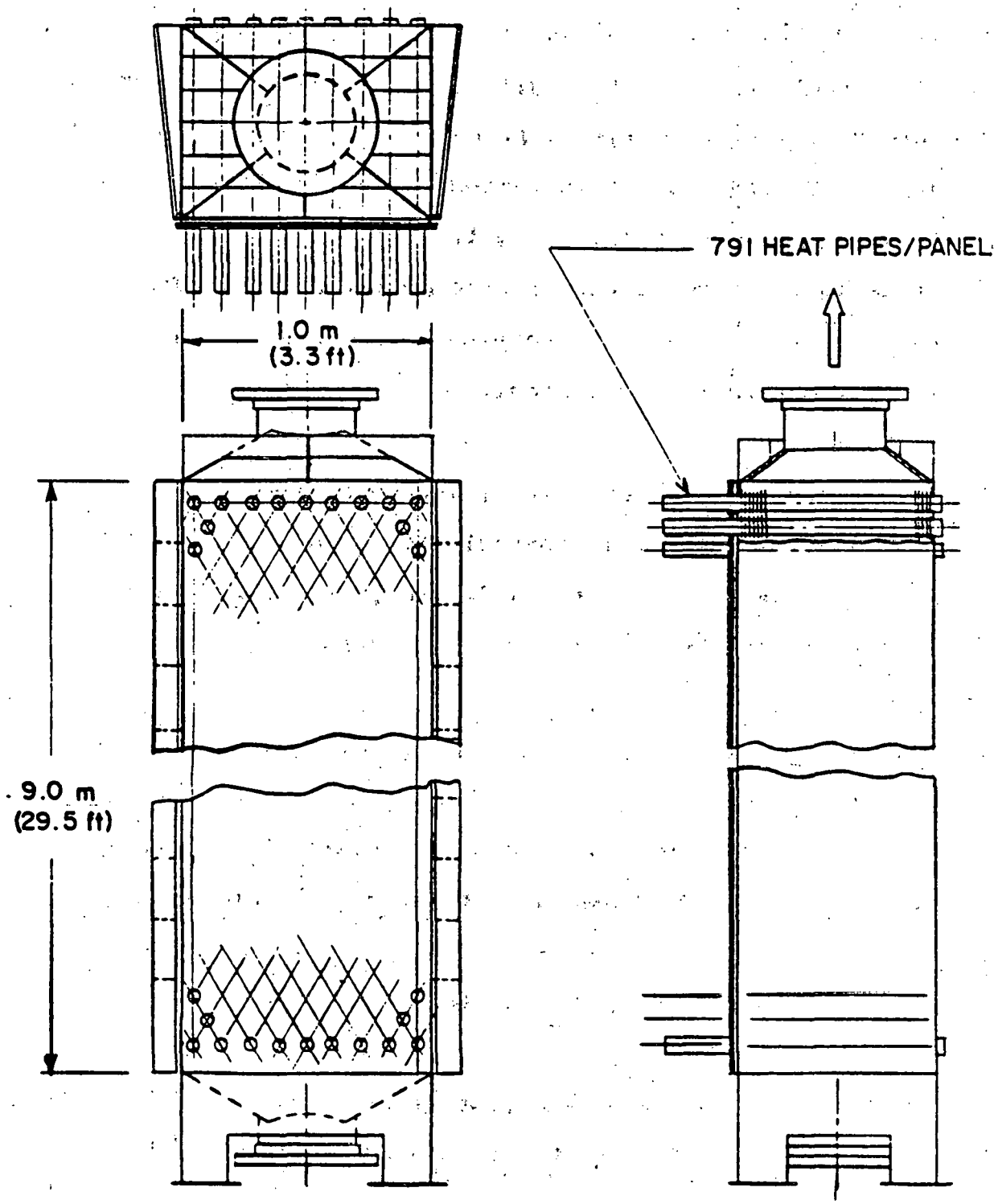

Figure 3-15 PANEL CONFIGURATION FOR STRAWMAN SYSTEM (EAST, WEST, AND SOUTH RECEIVERS)

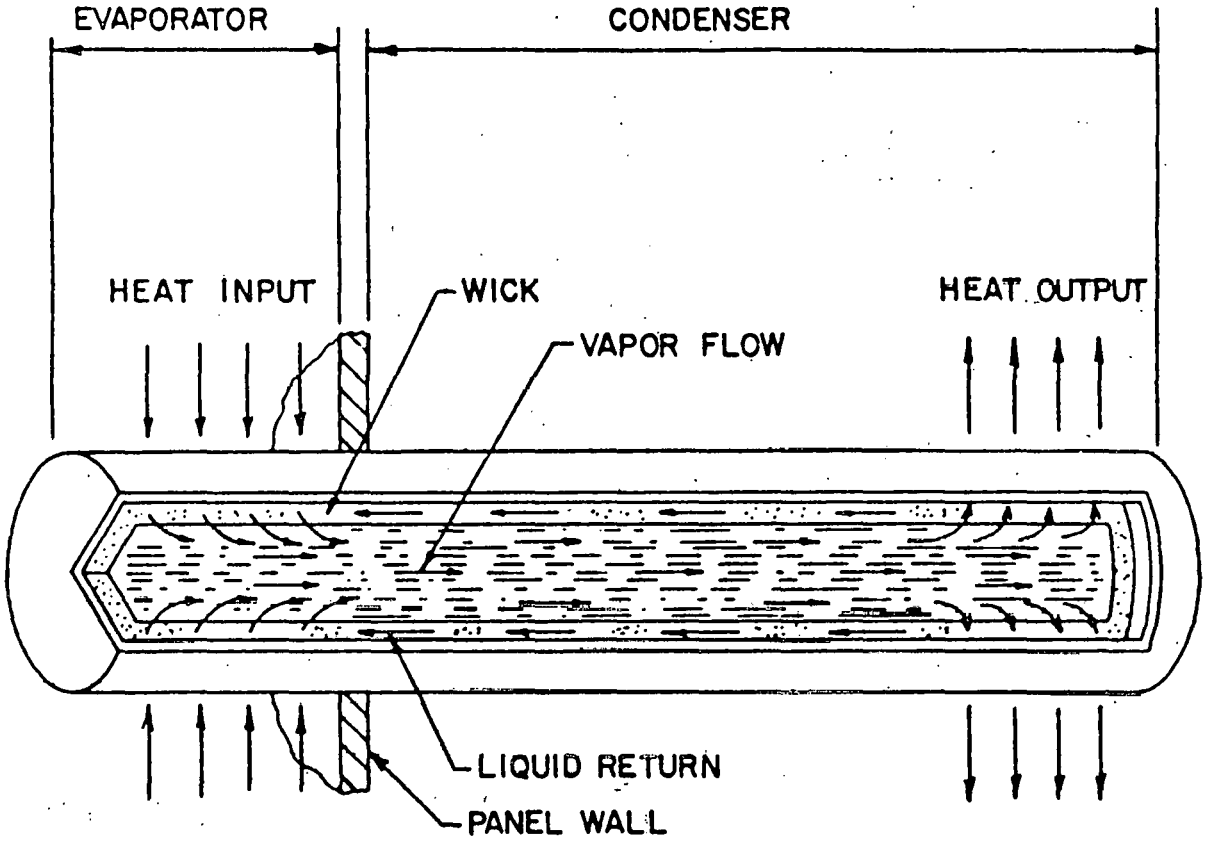

Figure 3-16 SCHEMATIC OF HEAT PIPE FOR STRAWMAN SYSTEM

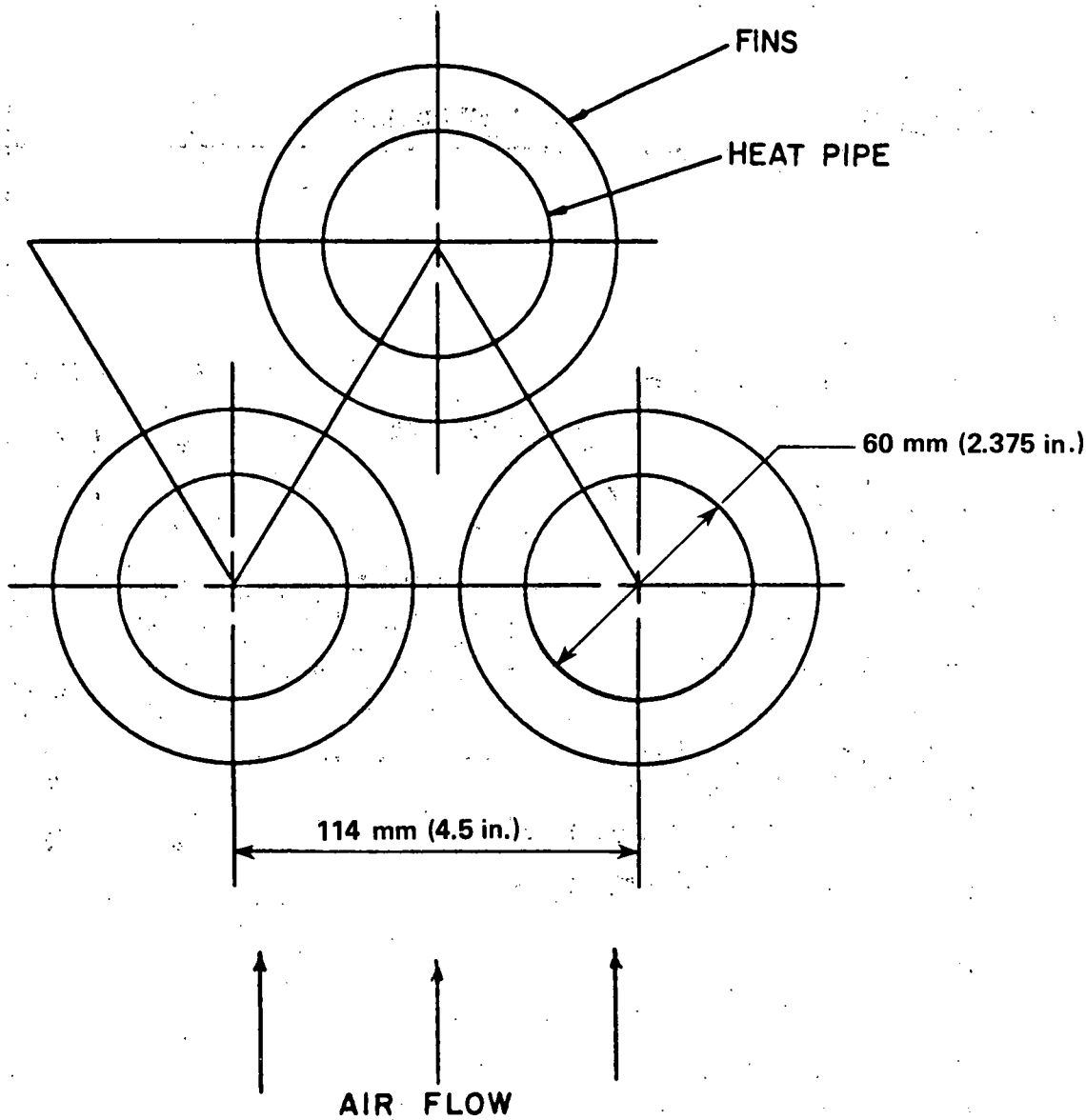

Figure 3-17 TYPICAL HEAT PIPE LAYOUT FOR STRAWMAN SYSTEM

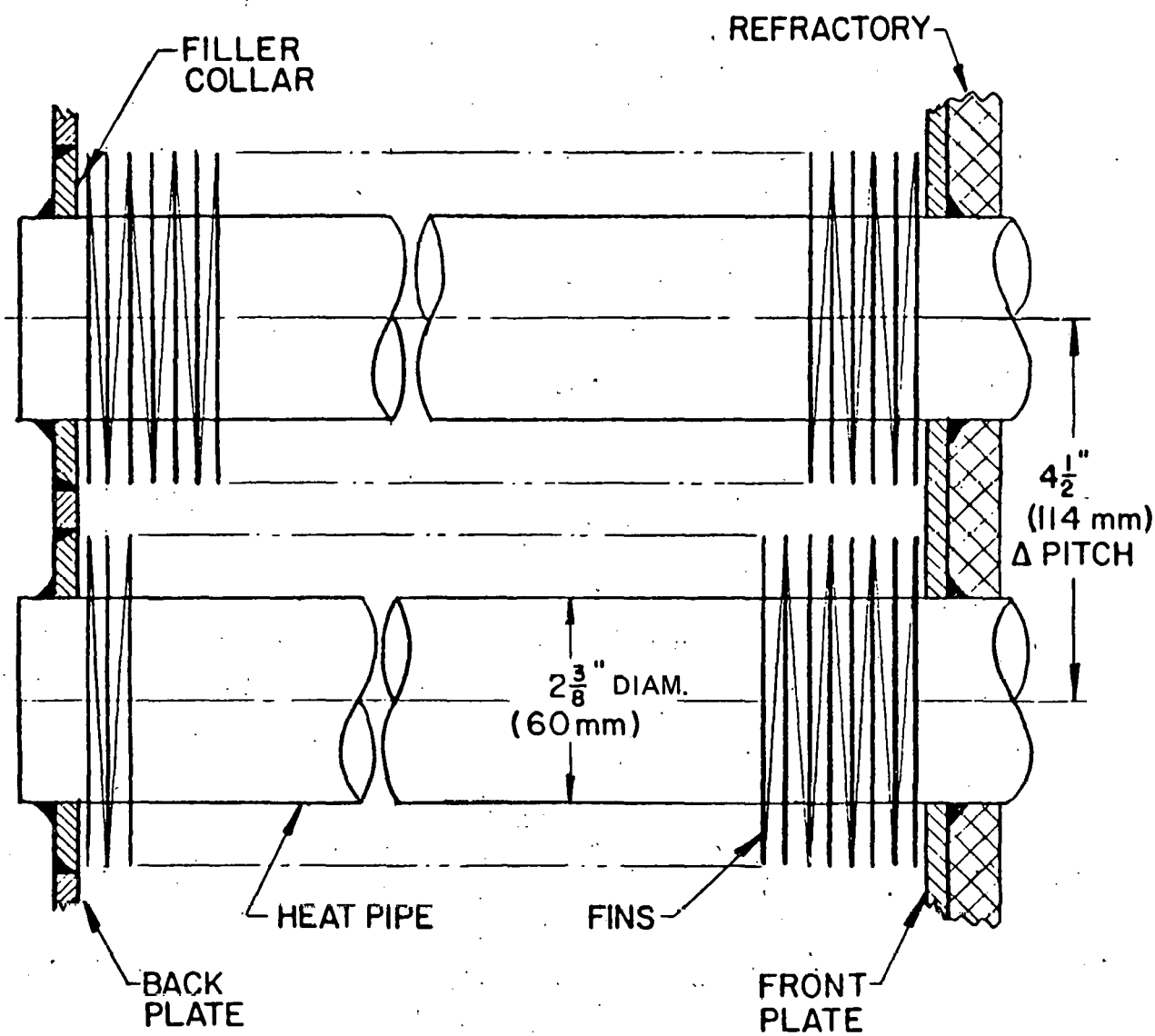

Figure 3-18 SCHEMATIC OF HEAT PIPE INSTALLATION

- Shade the front-panel wall area between heat pipes from direct exposure to the high solar radiant flux

As an additional protection, the panel area between heat pipes is covered with Fiberfrax, a ceramic fiber insulation, to prevent overheating of the panel walls. The Fiberfrax is a light, fluffy refractory fiber made by Carborundum Company and is capable of withstanding continuous temperatures up to 1427C (2600F).

Advanced Strawman Receiver Concept. A schematic view of the Advanced Strawman ceramic tube cavity is given in Figure 3-19. The receiver is designed to provide:

- High receiver efficiency by minimizing both conduction and reradiation losses
- Acceptable pressure drop
- Maximum tube operating temperature of 1316C (2400F)
- Minimized tensile tube stresses, along with adequate means of accommodating differential thermal expansion
- Air flow proportional to the anticipated energy received by each panel, thus reducing the possibility of hot spots and subsequent tube failure

In this design, the active heat absorbing surface is located in front of the curved rear wall of the cavities, opposite the cavity aperture. This surface consists of a single row of evenly spaced vertical U-tubes through which the compressed air flows as it is being heated. Air enters the tubes via a carbon steel header beneath the cavity floor. The return leg passes through the cavity floor and discharges into a common collecting header.

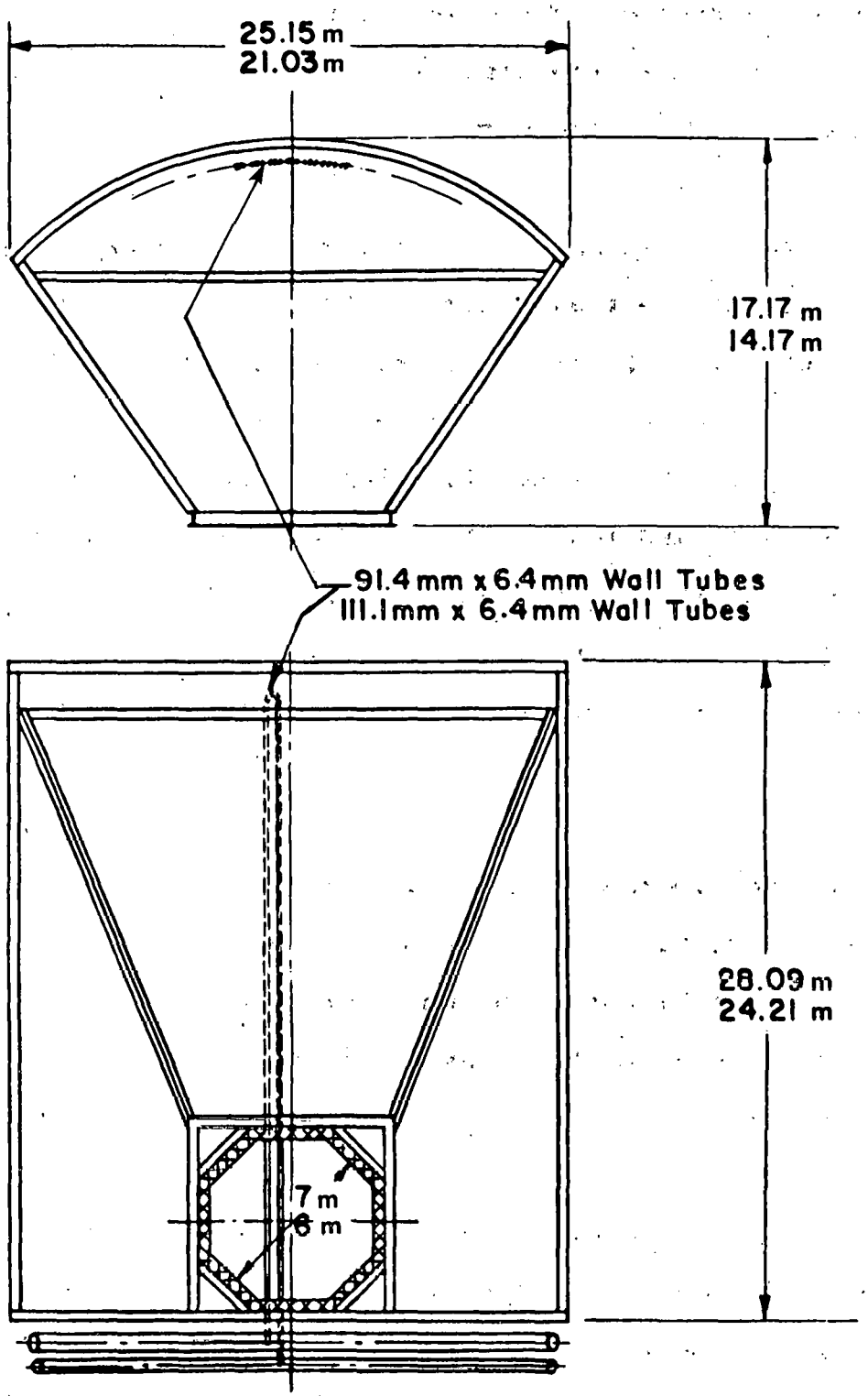

Figure 3-19 CERAMIC RECEIVER SCHEMATIC FOR ADVANCED STRAWMAN SYSTEM

The headers are located so as to reduce the effects of thermal differential expansion. The vertical tubes are also spaced and positioned to minimize the effects of thermal differentials in producing undesirable stresses.

Adequate selection of two, dimensionless parameters can ensure acceptable circumferential thermal tube stresses. The first of these parameters, a pitch-to-diameter ratio (S/D), yields optimum results at a value of about 3. At values substantially smaller than this (i.e., tubes closer together), insufficient flux passes between the tubes and leaves the rear portions of the tubes relatively cold, thus producing significant thermal stresses. Sides of the tubes remain colder for values of S/D much greater than 3, thereby producing significant tensile stresses in the tubes.

The second dimensionless parameter is the ratio of the tube-center-to-wall distance to the tube outside diameter (O/D). For very large and small values of this parameter, inadequate heating of the rear and side walls of the tubes will occur and high stresses result.

Based on analytical results, S/D and O/D values of 2.66 and 2, respectively, were adopted for the baseline design. Air flow to the U-tubes is proportioned by means of inlet orifices.

The entire cavity interior surface is lined with high-temperature Fiberfrax insulation, so that heat losses due to conduction may be kept at or below 2 percent of the thermal input to the air. Basic geometric data describing the north and south cavities are presented in Table 3-3. The cavity weights are summarized in Table 3-4.

3.3.2 Receiver Size

The Strawman and Advanced Strawman receivers add 100.67 MWt and 150.78 MWt, respectively, to the air stream. Of the four cavities, the north cavity receives approximately 34 percent of the total power delivered by the collector field. The south, east, and west cavities receive approximately 22 percent each.

Heat flux patterns for the design-point conditions of equinox noon were used, with appropriate scaling factors, for sizing and performance analysis of the receivers.

Strawman Receiver. Because of the excellent heat-transfer performance of the heat pipes, this receiver is capable of accommodating high radiant fluxes. The peak radiant fluxes absorbed by the heat pipes were limited to a conservative 1.0 MWt/m^2 (317,000 $Btu/hr\text{-}ft^2$) which resulted in a depth of 7.0 m (23.0 ft) for the north cavity and 5.5 m (18.0 ft) depth for the south, east, and west cavities. The north cavity has eleven panels, each 1.0 m (3.3 ft) wide by 11.0 m (36.0 ft) high. The

TABLE 3-3

GEOMETRIC DATA SUMMARY FOR CERAMIC RECEIVER, ADVANCED STRAWMAN

Data Item	Cavity	
	North	South
Height (overall), m (ft)	28.1 (92.2)	24.2 (79.4)
Width (overall), m (ft)	25.1 (82.5)	21.0 (69.0)
Radius, m (ft)	15.80 (51.8)	12.77 (41.9)
Aperture Area, m^2 (ft^2)	38.6 (415.5)	28.3 (304.4)
Working Area, m^2 (ft^2)	644.8 (6940)	457.6 (4925)
Tube O.D., mm (in.)	110.1 (4.375)	91.4 (3.6)
Tube I.D., mm (in.)	98.5 (3.875)	78.7 (3.1)
Active U-Tube Length, m (ft)	49.6 (162.8)	41.8 (137.2)
No. of Panels	11	9
U-Tubes/Panel	4	5
U-Tube Material	SiC	SiC

TABLE 3-4

WEIGHT DATA SUMMARY FOR CERAMIC RECEIVER, ADVANCED STRAWMAN
kg (lb)

Data Item	Cavity			
	North		South	
SiC Tubes	15,954	(35,172)	10,411	(22,952)
Fiberfrax Insulation	143,461	(316,278)	74,896	(165,117)
1/4 in. CS Casing	87,678	(193,297)	60,034	(132,352)
Total Mass per Cavity	163,874	(544,747)	145,341	(320,421)
Mass per Panel	9,137	(20,143)	6,841	(15,082)
Header Weight				
Hot	10,378	(22,880)	6,552	(14,445)
Cold	4,756	(10,486)	4,007	(8,834)
Structural Weight	84,921	(187,218)	47,854	(105,500)
Total Dry Weight (4 Cavities)	347,148	(765,331)	611,261	(1,347,600)

other cavities have nine panels, each 1.0 m (3.3 ft) wide by 9.0 m (29.5 ft) high.

Advanced Strawman Receiver. Because of the relative sensitivity of the SiC tubes to thermally induced tensile stresses, the peak tube heat fluxes were limited to 0.2 MWt/m² (63,500 Btu/hr-ft²) in the north cavity and to 0.19 MWt/m² (58,900 Btu/hr-ft²) in the south, east, and west cavities. These limitations, coupled with the maximum tube temperature of 1316C (2400F) and pressure drop of 0.1 MPa (15 psi) resulted in a cavity depth of 15.8 m (51.8 ft) for the north cavity, and 12.8 m (42.0 ft) for the south, east, and west cavities.

The flux maps of the heat pipe receiver were used as bases for the advanced receiver as well, except the values were ratiod to achieve the peak fluxes. This resulted in a north cavity with 11 panels, each 2.36 m (7.75 ft) wide and 24.8 m (81.4 ft) high. The south, east, and west cavities have 9 panels, each 2.43 m (8.0 ft) wide and 20.9 m (68.6 ft) high.

3.3.3 Receiver Materials

Strawman Receiver. Eight alloys were identified for evaluation as potential materials for the heat pipe receivers. Factors considered in the evaluation process were cost, welding and fabrication characteristics, and availability. Tables 3-5 and 3-6 show the characteristics of the candidate alloys. A

TABLE 3-5

HEAT PIPE RECEIVER MATERIALS DATA

Material	$/kg	Welding*	Fabrication	Comments
Incoloy 800H	5.48	Fair to Good	Fair to Good	Used for Inconel welding.
Inconel 600	8.80	Good	Good	For use in severely corrosive environments.
Inconel 601	8.05	Fair to Good**	Fair to Good	Improved over 600; better high temperature properties.
Inconel 617	14.87	Fair to Good**	Fair to Good	Improved over 625; very good high-temperature mechanical properties; not presently coded at high temperatures; high Co content.
Inconel 625	11.75	Good	Fair	Aging (brittle) at high temperature; unacceptable for high-temperature cyclic service.
Haynes 25	51.24	Poor	Poor; considerable work; hard	High Co content; not available in large quantities.
Haynes 188	43.80	Poor	Same as Haynes 25	Same as Haynes 25 but has less Co.
Hastelloy X	13.6	Fair	Fair	More expensive and not as good mechanical properties as Inconel 601.

* Welding costs for Incoloy and Inconels are similar; three times higher for Haynes.
** Caution due to aluminum content; use proper filler welding product.

TABLE 3-6

HEAT PIPE RECEIVER MATERIALS COMPOSITION

Material	Nickel (%)	Chromium (%)	Cobalt (%)	Molybdenum (%)	Aluminum (%)
Incoloy 800H	30.0-35.0	19.0-23.0	---	---	0.15-0.60
Inconel 600	72.0-76.0	14.0-17.0	---	---	---
Inconel 601	58.0-63.0	21.0-25.0	---	---	1.00-1.7
Inconel 617	54.0	22.0	12.5	9.0	1.0
Inconel 625	61.0	20.0-23.0	1.0 max	8.0-10.0	0.40
Haynes 25	10.0	20.0	51.0	---	---
Haynes 188	22.0	22.0	63.0	---	---
Hastelloy X	52.0	22.0	0.5-2.5	9.0	---
U.S. Imports (%) 1972	92	100	98	50	95

preliminary screening eliminated five candidate alloys for the following reasons:

- Haynes 25 and 188 have poor fabrication and welding characteristics, and high costs. Their high cobalt content makes them undesirable because of the current shortage of cobalt, which limits their availability in large quantities.
- Hastelloy X and Inconel 600 are more expensive and their mechanical properties are not as good as Inconel 601.
- Inconel 625 age-hardens and becomes brittle at high temperatures. Therefore, it is unacceptable for high-temperature cycling service.

To assist in further analysis of the remaining alloys, the maximum allowable stresses were assessed and preliminary panel cost and weights estimated (see Table 3-7). Finally, total panel costs (labor and material) and tower cost differentials were estimated for Incoloy 800H and Inconel 617. The results show that the additional material cost of Inconel 617 was more than balanced by lower labor costs. Considering all aspects, Inconel 617 was selected as the material for the panel.

Costs might be reduced by using Inconel 617 only in the high-temperature portion of the panel and a less expensive material in the lower-temperature portions of the panel.

Advanced Strawman Receiver. Silicon carbide (SiC) was selected as the tube material in the Advanced Strawman receiver. A survey of candidate materials indicated that this material could provide

TABLE 3-7

HEAT PIPE RECEIVER MATERIALS EVALUATION

Item	Incoloy 800H	Inconel 601	Inconel 617
Allowable Stress, MPa (psi)*			
At 760C (1400F)	24.8 (3600)	19.3 (2800)	48.3 (7000)
At 816C (1500F)	17.2 (2500)	13.1 (1900)	37.2 (5400)
At 871C (1600F)	11.0 (1600)	8.3 (1200)	18.6 (2700)
Material Required, kg (lb)	3500 (7700)	3818 (8400)	2045 (4500)
$/Panel	22,250	30,800	30,300
Properties Documentation	Very Good	Good	Fair to Poor
ASME Code	Sections III and VIII	Section VIII	None
Potential for Higher Design Temperatures	Poor	Poor	Fair to Good

* At temperatures in the creep range, the maximum allowable stress is the lowest of the following:

- 100 percent of the average stress for a creep rate of 0.1 percent per 1000 hours.
- 67 percent of the average stress for rupture at the end of 100,000 hours.
- 80 percent of the minimum stress for rupture at the end of 100,000 hours.

adequate service life at the desired high-temperature operation. Limitations of this material typical for ceramics include:

- Susceptability to brittle fracture
- Inability to sustain high tensile stresses
- Availability in short tube lengths only, necessitating numerous tube-to-tube joints
- Relatively unknown resistance to a thermally cycling environment

The most serious of the above limitations is the necessity for exposing numerous tube-to-tube joints to solar radiation during receiver operation. The tube joint integrity has yet to be proven experimentally for cyclic operation. And the cost of making these tube joints could approach 20 percent of the total receiver costs. Due to the virtual absence of data concerning the specific procedure to be followed in constructing these joints, the estimated receiver costs are subject to significant variation.

3.3.4 Receiver Thermal Performance Analysis

The thermal and hydraulic performance of the Strawman and Advanced Strawman receivers was analyzed to permit a rational assessment of sizes, weights, and costs for parametric analysis. Table 3-8 shows the parametric cases studied for the receiver subsystem. The receiver parametrics were incorporated into the EPGS parametrics, because of their strong interdependence. Solar

TABLE 3-8

RECEIVER PERFORMANCE PARAMETRIC VALUES

Receiver Type	Receiver Pressure Drop kPa (psi)	Receiver Outlet Temperature °C (°F)	System Pressure Ratio
Strawman Receiver (Heat Pipe)	13.8 (2)	760 (1400)	8
	27.6 (4)*	816 (1500)*	12*
	41.4 (6)	871 (1600)	16
Advanced Receiver (Ceramic)	69.0 (10)	982 (1800)	8
	103 (15)*	1093 (2000)*	12*
	155 (20)	1204 (2200)	16

*Baseline case.

flux data, inlet air temperature, and power handling requirements were the basic input data used in the thermal/hydraulic studies.

Strawman Receiver. As the first step in the analysis of the Strawman receiver, the net heat input into each receiver panel was calculated at height increments of 1 m (3.3 ft), based on the solar flux data. Separate matrices were prepared for the north and the south cavities. (The south cavity also represents the east and west cavities.) Table 3-9 shows the data matrix for the north cavity and is typical of the results obtained.

From these matrices the net energy input into the air along the length of each panel was determined. This was the basis for determining the heat transfer duty per heat pipe. Tables 3-10 and 3-11 show the matrices of energy to air-and-heat-pipe duties in the north cavity for the above described grid.

The air flows in the receiver panels are adjusted so that the outlet temperature at each panel is 816C (1500F). The resulting air flow distribution in the same cavity is shown in Figure 3-20. The nearly equal outlet temperature is desirable to keep the metal temperature safely below the maximum service temperature of the alloy. In practice, a coarse flow control is exercised by selecting appropriate panel depths. Fine control is achieved with butterfly valves at the panel inlets.

TABLE 3-9

NET HEAT FLUX INTO PANELS, NORTH RECEIVER, STRAWMAN SYSTEM

$\left(\begin{matrix} MW/m^2 \\ Btu/hr\text{-}ft^2 \end{matrix}\right)$

DISTANCE FROM BOTTOM OF PANEL (m)	Panel No. 6	5 and 7	4 and 8	3 and 9	2 and 10	1 and 11	
11.0	0.1280 40564.	0.1209 38311.	0.1106 35055.	0.0869 27544.	0.0474 15024.	0.0158 5008.	
10.0	0.2291 72615.	0.2212 70111.	0.2054 65103.	0.1675 53084.	0.1185 37559.	0.0529 16777.	
9.0	0.3713 117686.	0.3618 114682.	0.3334 105667.	0.2702 85635.	0.1896 60095.	0.0964 30548.	
8.0	0.5451 172773.	0.5325 168767.	0.4803 152241.	0.3847 121943.	0.2473 78374.	0.1185 37559.	
7.0	0.7387 234120.	0.7189 227861.	0.6446 204323.	0.5064 160504.	0.2970 94149.	0.1422 45071.	
6.0	0.8595 272431.	0.8319 263667.	0.7489 237376.	0.5728 181537.	0.3342 105918.	0.1612 51081.	
5.0	0.8848 280444.	0.8611 272932.	0.7742 245388.	0.5949 188548.	0.3476 110174.	0.1706 54086.	
4.0	0.8295 262916.	0.8003 253651.	0.7213 228612.	0.5609 177781.	0.3358 106418.	0.1627 51582.	
3.0	0.6383 202320.	0.6123 194057.	0.5538 175528.	0.4353 137968.	0.2805 88891.	0.1343 42567.	
2.0	0.3768 119439.	0.3626 114932.	0.3460 109674.	0.2805 88891.	0.2015 63851.	0.0948 30048.	
1.0	0.1722 54586.	0.1659 52583.	0.1580 50079.	0.1422 45071.	0.1074 34054.	0.0474 15024.	
0.0							
TOTALS/ PANELS	6.0458 1916266.	5.8531 1855170.	5.3162 1684992.	4.1910 1328380.	2.6250 832007.	1.2533 397255.	44.5229 14111850.
PERCENT	13.58	13.15	11.94	9.41	5.90	2.82	100.00

TABLE 3-10

NET POWER TO AIR, NORTH RECEIVER, STRAWMAN SYSTEM

(MW / Btu/hr)

DISTANCE FROM BOTTOM OF PANEL (m)	Panel No. 6	5 and 7	4 and 8	3 and 9	2 and 10	1 and 11	
11.0	0.1340 42479.	0.1266 40119.	0.1158 36710.	0.0910 28844.	0.0496 15733.	0.0165 5244.	
10.0	0.2399 76042.	0.2316 73420.	0.2151 68176.	0.1754 55590.	0.1241 39332.	0.0554 17568.	
9.0	0.3888 123241.	0.3789 120094.	0.3491 110655.	0.2829 89677.	0.1985 62932.	0.1009 31990.	
8.0	0.5708 180928.	0.5576 176733.	0.5030 159427.	0.4029 127699.	0.2589 82073.	0.1241 39332.	
7.0	0.7735 245171.	0.7528 238616.	0.6751 213967.	0.5303 168080.	0.3111 98593.	0.1489 47199.	
6.0	0.9001 285290.	0.8711 276113.	0.7843 248580.	0.5998 190106.	0.3499 110917.	0.1688 53492.	
5.0	0.9266 293681.	0.9017 285814.	0.8107 256971.	0.6229 197448.	0.3640 115375.	0.1787 56638.	
4.0	0.8687 275326.	0.8380 265624.	0.7553 239402.	0.5874 186173.	0.3516 111441.	0.1704 54016.	
3.0	0.6684 211870.	0.6411 203217.	0.5799 183813.	0.4558 144480.	0.2937 93086.	0.1406 44577.	
2.0	0.3946 125077.	0.3797 120357.	0.3624 114850.	0.2937 93086.	0.2110 66865.	0.0993 31466.	
1.0	0.1803 57163.	0.1737 55065.	0.1655 52443.	0.1489 47199.	0.1125 35661.	0.0496 15733.	
0.0							
TOTALS/ PANEL	6.0458 1916266.	5.8531 1855170.	5.3162 1684992.	4.1910 1328380.	2.6250 832007.	1.2533 397255.	44.5229 14111850.
PERCENT	13.58	13.15	11.94	9.41	5.90	2.82	100.00

TABLE 3-11

POWER TRANSPORTED BY INDIVIDUAL HEAT PIPES, NORTH RECEIVER, STRAWMAN SYSTEM

(kW)

DISTANCE FROM BOTTOM OF PANEL (m)	Panel No. 6	5 and 7	4 and 8	3 and 9	2 and 10	1 and 11
11.0	1.9	1.8	1.7	1.4	0.9	0.4
10.0	3.2	3.1	2.9	2.3	1.6	0.8
9.0	4.9	4.8	4.4	3.5	2.3	1.1
8.0	6.9	6.7	6.0	4.8	2.9	1.4
7.0	8.5	8.3	7.5	5.8	3.4	1.6
6.0	9.3	9.1	8.1	6.2	3.6	1.8
5.0	9.2	8.9	8.0	6.2	3.7	1.8
4.0	7.8	7.6	6.8	5.3	3.3	1.6
3.0	5.4	5.2	4.8	3.8	2.6	1.2
2.0	2.9	2.8	2.7	2.3	1.7	0.8
1.0	0.9	0.9	0.8	0.8	0.6	0.3
0.0						

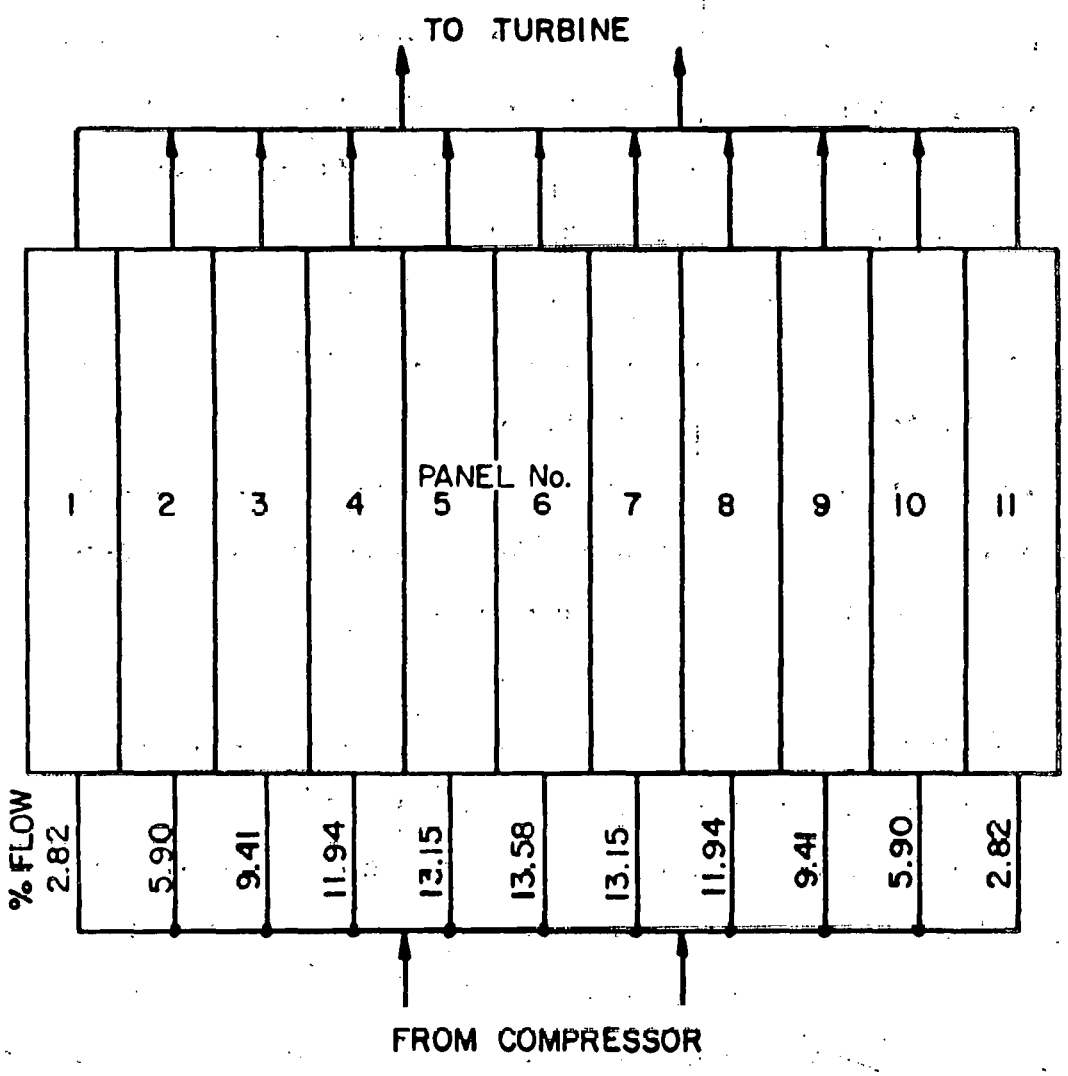

Figure 3-20 NORTH RECEIVER AIR FLOW DISTRIBUTION, STRAWMAN SYSTEM

As seen in Table 3-12, peak metal temperatures occur in the center panel (6) at about two-thirds panel height. The metal temperature appears to vary relatively little (about 19C or 33F) in the upper half of the panel. It is noted that the variation of panel depth is limited by the minimum heat pipe condenser section length needed to transfer the collected solar heat to the air stream. This limiting depth is indicated by a broken line on Figure 3-21. This figure also indicates the relationship between the panel depth and the air pressure drop.

The heat pipe receiver was analyzed for the parametric cases shown in Table 3-13. The weight and cost data shown was used as input to the tower and EPGS parametric analyses. (Economic parametric results are given in Table 3-21 in Subsection 3.6, Electric Power Generation Subsystem.)

Advanced Strawman Receiver. For performance analyses, the ceramic receiver cavities were divided into panels and zones similar to those used in the design of the heat pipe receiver. The heat fluxes in the ceramic receiver were obtained by multiplying the heat pipe receiver flux values by 0.197 and 0.185, respectively. This was necessary to compensate for the greater depth of the ceramic receiver. A summary of the baseline operating conditions resulting from these fluxes for both the north and south cavities is given in Table 3-14.

TABLE 3-12

PEAK HEAT PIPE METAL TEMPERATURE, EVAPORATION SECTION
NORTH RECEIVER, STRAWMAN SYSTEM

$\left(\begin{matrix}^{o}C \\ ^{o}F\end{matrix}\right)$

Distance From Bottom of Panel (m)	Panel No. 6	5 and 7	4 and 8	3 and 9	2 and 10	1 and 11
11.0	840.8 1545.4	838.9 1543.9	838.6 1541.6	853.3 1535.5	830.0 1526.0	822.9 1513.2
10.0	848.3 1558.9	847.6 1557.8	845.4 1551.3	840.0 1544.1	834.2 1535.5	825.7 1518.2
9.0	853.5 1568.2	852.7 1566.9	848.0 1558.4	838.8 1541.9	825.0 1517.0	813.5 1496.3
8.0	852.0 1565.6	850.6 1563.0	842.8 1549.0	828.4 1523.1	802.0 1475.6	783.6 1442.5
7.0	834.9 1534.8	832.2 1529.9	822.9 1513.2	802.6 1476.8	767.7 1413.9	745.6 1374.2
6.0	792.8 1459.0	789.6 1453.2	780.1 1436.2	757.0 1394.5	722.2 1331.9	697.8 1288.1
5.0	730.1 1346.1	726.7 1340.0	717.6 1323.7	696.8 1286.2	666.2 1231.1	640.4 1184.7
4.0	649.1 1200.4	644.9 1192.8	637.9 1180.2	621.9 1151.4	601.4 1114.5	575.1 1067.3
3.0	554.0 1029.2	550.7 1023.3	548.2 1018.7	538.7 1001.6	531.4 988.5	508.5 947.3
2.0	468.2 874.8	466.6 871.9	467.6 873.7	465.4 869.7	465.6 870.1	448.9 840.0
1.0	406.7 764.1	406.2 763.2	406.5 763.7	407.8 766.0	408.8 767.8	401.7 755.1
0.0						

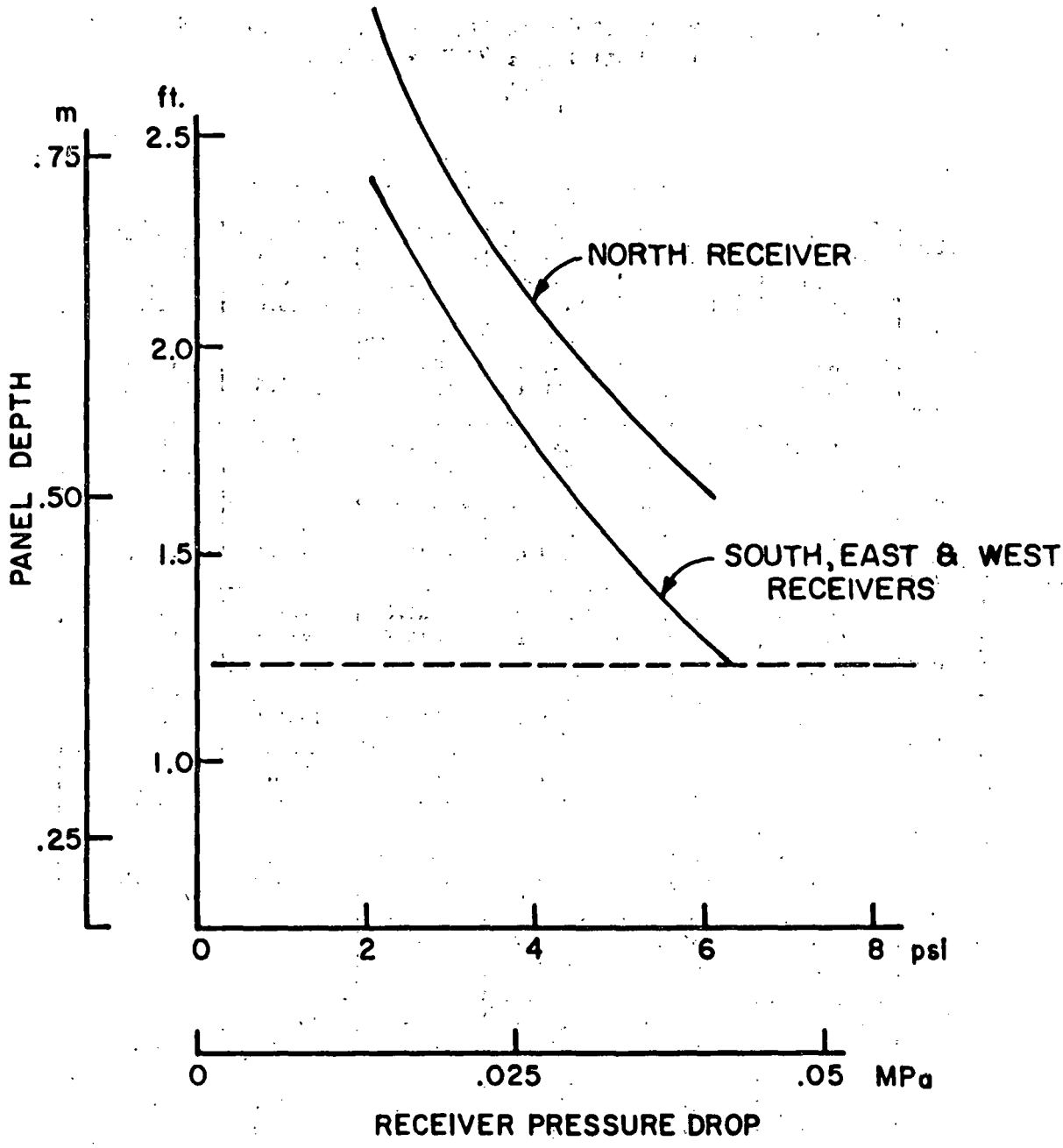

Figure 3-21 PANEL DEPTH VS. PRESSURE DROP, STRAWMAN RECEIVER (PRESSURE RATIO = 12)

TABLE 3-13

STRAWMAN HEAT PIPE RECEIVER
PARAMETRIC CASES

Outlet Temp., °C	816	816	816	816	816	760	854
°F	1500	1500	1500	1500	1500	1400	1570
System Pressure Ratio	8	12	12	12	16	12	12
Receiver Pressure Drop, MPa	0.028	0.014	0.014	0.042	0.028	0.028	0.028
psi	4	2	4	6	4	4	4
South Receiver Weight*	107.4	138	114.2	94.5	128.2	87.5	425.1
North Receiver Weight*	168.5	217.5	182.2	150.6	204.4	134.5	228.7
Total Receiver Weight*	490.7	631.4	524.8	434.1	589.0	397.0	653.8
Cost in Million Dollars**	13.3	16.9	14.0	11.9	15.4	11.0	17.0

*Weight in tons (2000 lb/ton or 907 kg/ton).
**Delivered but uninstalled cost.

TABLE 3-14

ADVANCED STRAWMAN RECEIVER OPERATING CONDITIONS

Parameter	Cavity	
	North	South
Inlet Temperature, °C (°F)	378 (712)	378 (712)
Outlet Temperature, °C (°F)	1093 (2000)	1093 (2000)
Pressure Ratio	12.0	12.0
Inlet Pressure, MPa (psia)	1.11 (161)	1.11 (161)
Outlet Pressure, MPa (psia)	1.01 (146)	1.01 (146)
Air Flow Rate, kg/h (lb/h)	233183 (514080)	150883 (332640)
Max. Air Velocity, m/s (ft/s)	79 (259)	80 (262)

Parametric analyses were performed to establish the effects of various operating variables on the cost and weight of the baseline Advanced Strawman design. The variables examined were system pressure ratio, air outlet temperature, and receiver pressure drop. Their effects on the cavity radius, and thus the cavity enclosure surface area, are shown in Figures 3-22 and 3-23. Throughout these calculations, the maximum allowable tube temperature was maintained at 1316C (2400F), regardless of the other operating conditions. This assumption was largely responsible for the sharp increase in cavity size for the 1204C (2200F) air outlet case resulting in substantial weight and cost penalties. A summary of the parametric cases is given in Table 3-15.

Aperture Size. The size and configuration of the cavity aperture must be selected through an optimization process which balances the "spillover" against the radiant and convection losses through the aperture. The optimum aperture size is that which results in the maximum power delivered to the air stream.

The spillover energy was calculated by integrating that part of the focal plane flux which falls outside a given aperture size. The larger the aperture, the less energy will be lost to spillage. Conversely, the radiation and convection losses become larger with increasing aperture size.

The radiation losses have two components:

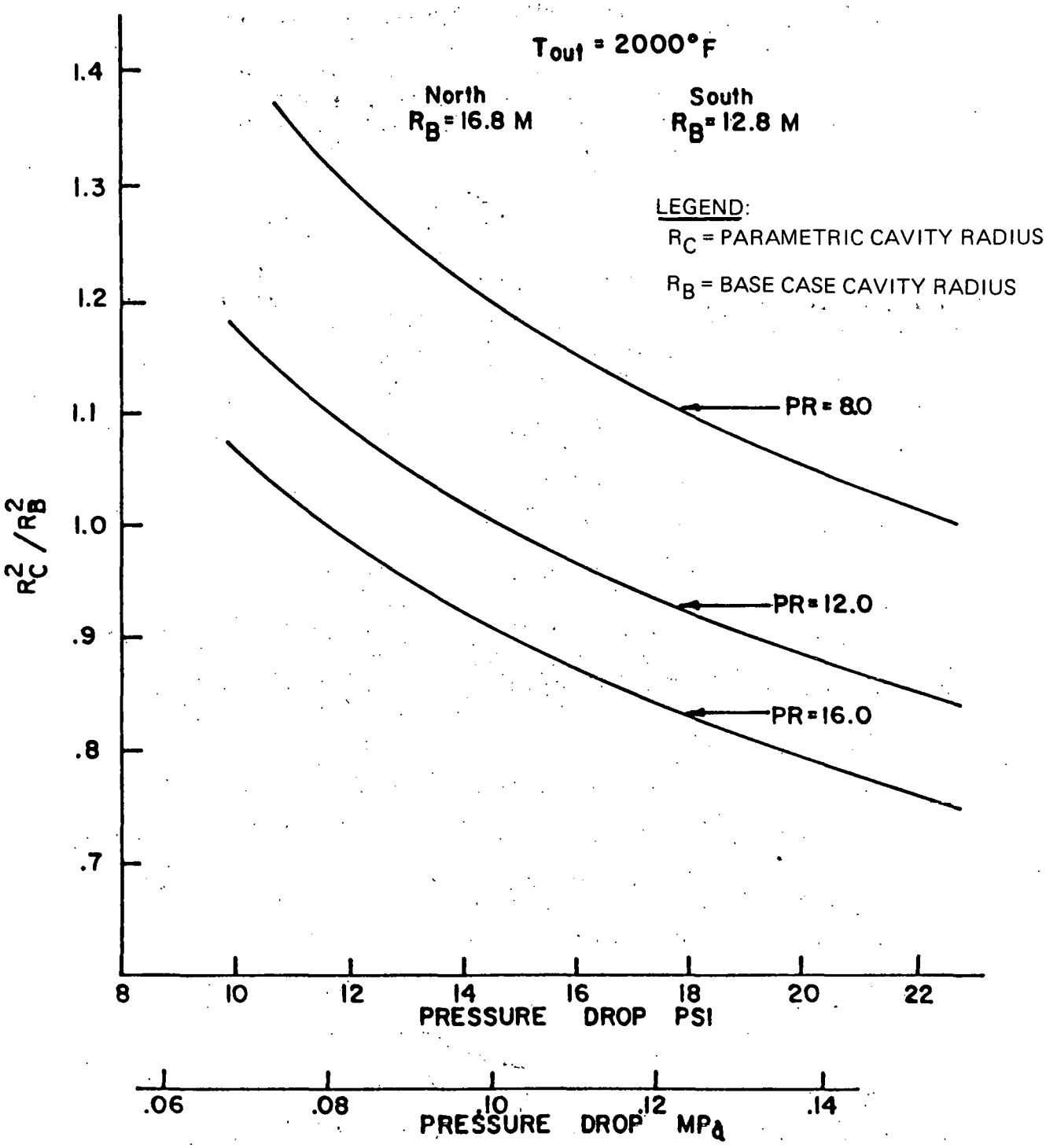

Figure 3-22 EFFECTS OF RECEIVER PRESSURE DROP AND PRESSURE RATIO ON CERAMIC RECEIVER SIZE, ADVANCED STRAWMAN SYSTEM

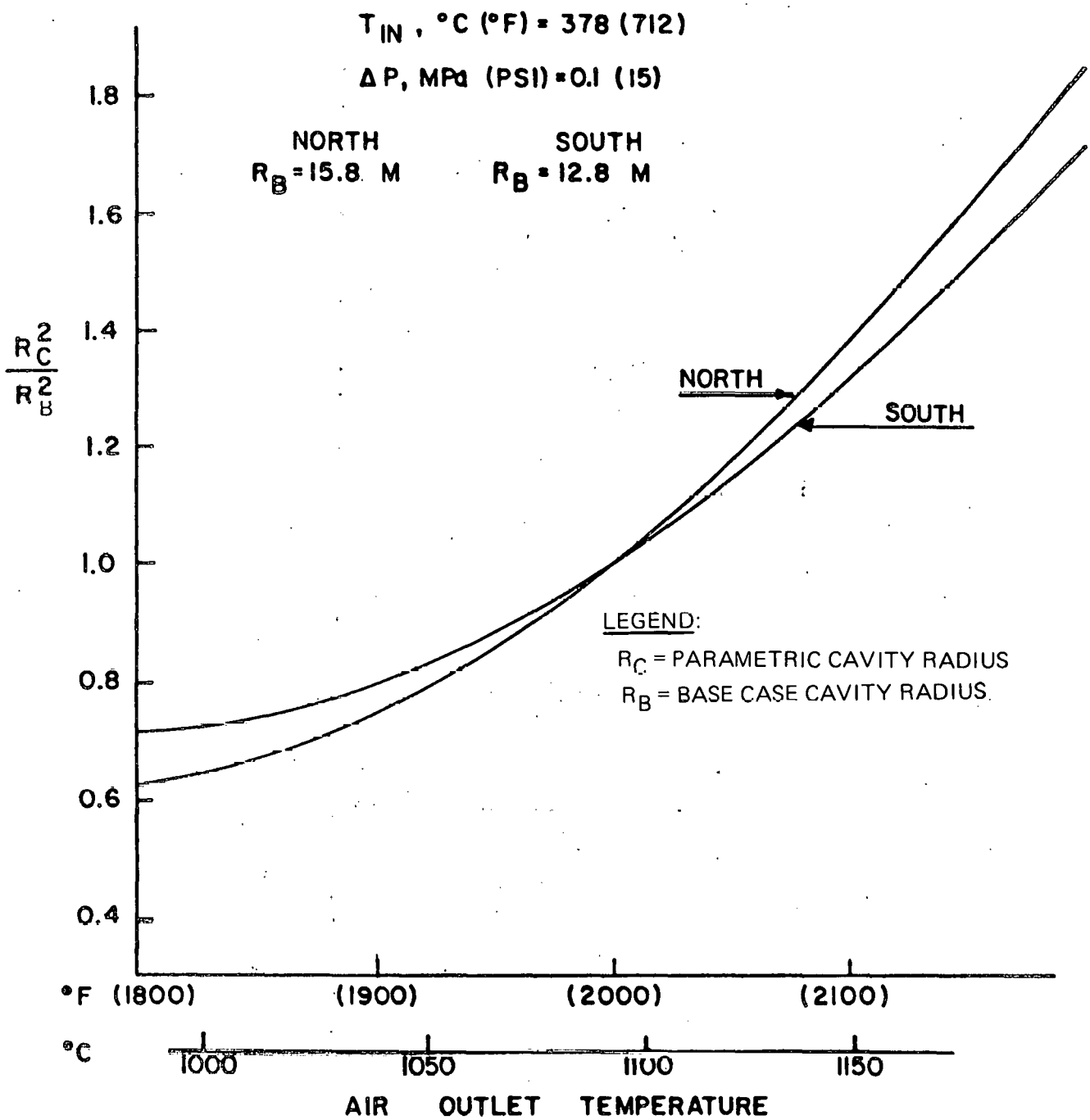

Figure 3-23 EFFECTS OF AIR OUTLET TEMPERATURE ON CERAMIC RECEIVER SIZE, ADVANCED STRAWMAN SYSTEM

TABLE 3-15

ADVANCED STRAWMAN RECEIVER PARAMETRIC CASES

Outlet Temp., °C	1093	1093	1093	1093	1093	982	1204
°F	2000	2000	2000	2000	2000	1800	2200
Pressure Ratio	8	12	12	12	16	12	12
Pressure Drop, MPa	.103	.069	.103	.138	.103	.103	.103
psi	15	10	15	20	15	15	15
Receiver Weight,*	1247.8	1341.5	1055.7	942.1	953.9	617.0	1576.4
Cost in Million Dollars**	19.554	19.513	18.065	17.064	17.152	12.819	31.021

*Weight in tons (2000 lb/ton or 907 kg/ton).
**Delivered but uninstalled cost.

- Reflection Losses: These depend on the cavity geometry and interior surface reflectivities. For first-cut analysis, the reflective losses were assumed to be 1 percent of the incident energy.

- Infrared Reradiation: This was calculated for the aperture area using the well-known relationship of radiant heat transfer. The radiating surface effective temperature was assumed to be the root-mean-temperature of the radiating areas. The receiving surfaces were assumed to be at ambient temperature.

The convection losses were calculated from the equation:

$$q_c = hA\,(T_W - T_A)$$

where:

q_c = the convection heat loss
A = the aperture area
T_W = the average temperature of the cavity
T_A = the ambient temperature
h = the effective heat transfer coefficient, which was correlated from experimental results as $h = 21.43 + 0.97V$, where V denotes the wind velocity (dimensions in metric units)

Finally there is a comparatively minor conduction loss through the walls of the cavity. This represents less than 10 percent of the total losses.

Spillage and heat loss calculations were conducted for aperture diameters up to 15 m (39.4 ft). The diameters were for the circle inscribed within the octagonal aperture configuration. Figure 3-24 shows the optimization process, and indicates that the optimum is between 6.5 and 7 m (21.4 and 23.1 ft). The receiver losses calculated for the design point are tabulated in Table 3-16. Figure 3-25 shows the variation of the receiver

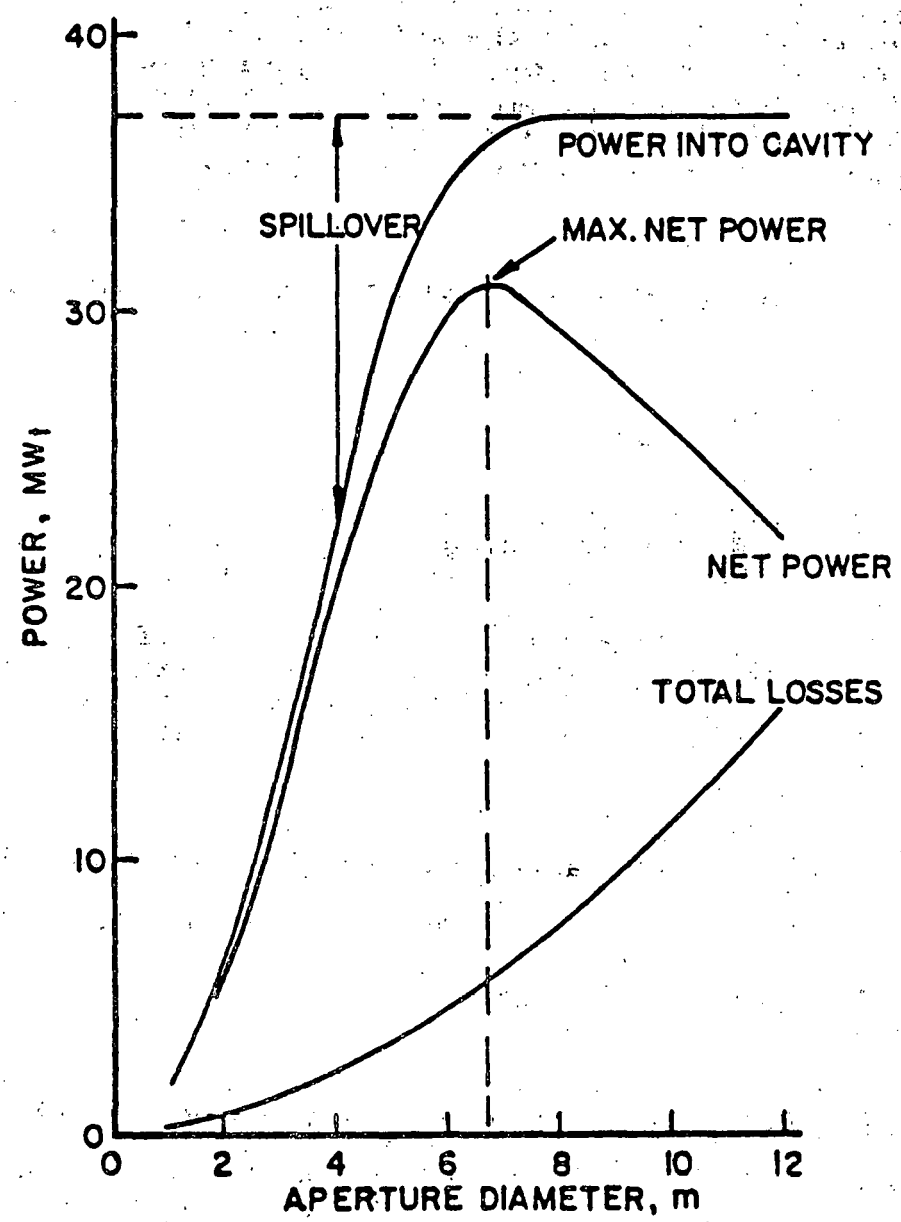

Figure 3-24 TYPICAL APERTURE SIZING PARAMETERS

TABLE 3-16

RECEIVER THERMAL LOSSES

Losses/Assumptions	Strawman Receiver	Advanced Receiver
Losses, %		
Conduction	0.70	1.83
Convection	1.72	2.63
Radiation	6.10	14.94
Total	8.52	19.40
Receiver Efficiency, %	91.50	80.60
Assumptions		
Wind Velocity, m/s (mph)	6.7 (15)	
Ambient Temperature, °C (°F)	15.5 (60)	
Inlet Air Temperature, °C (°F)	378 (712.1)	
Outlet Air Temperature, °C (°F)	816 (1500)	1093 (2000)

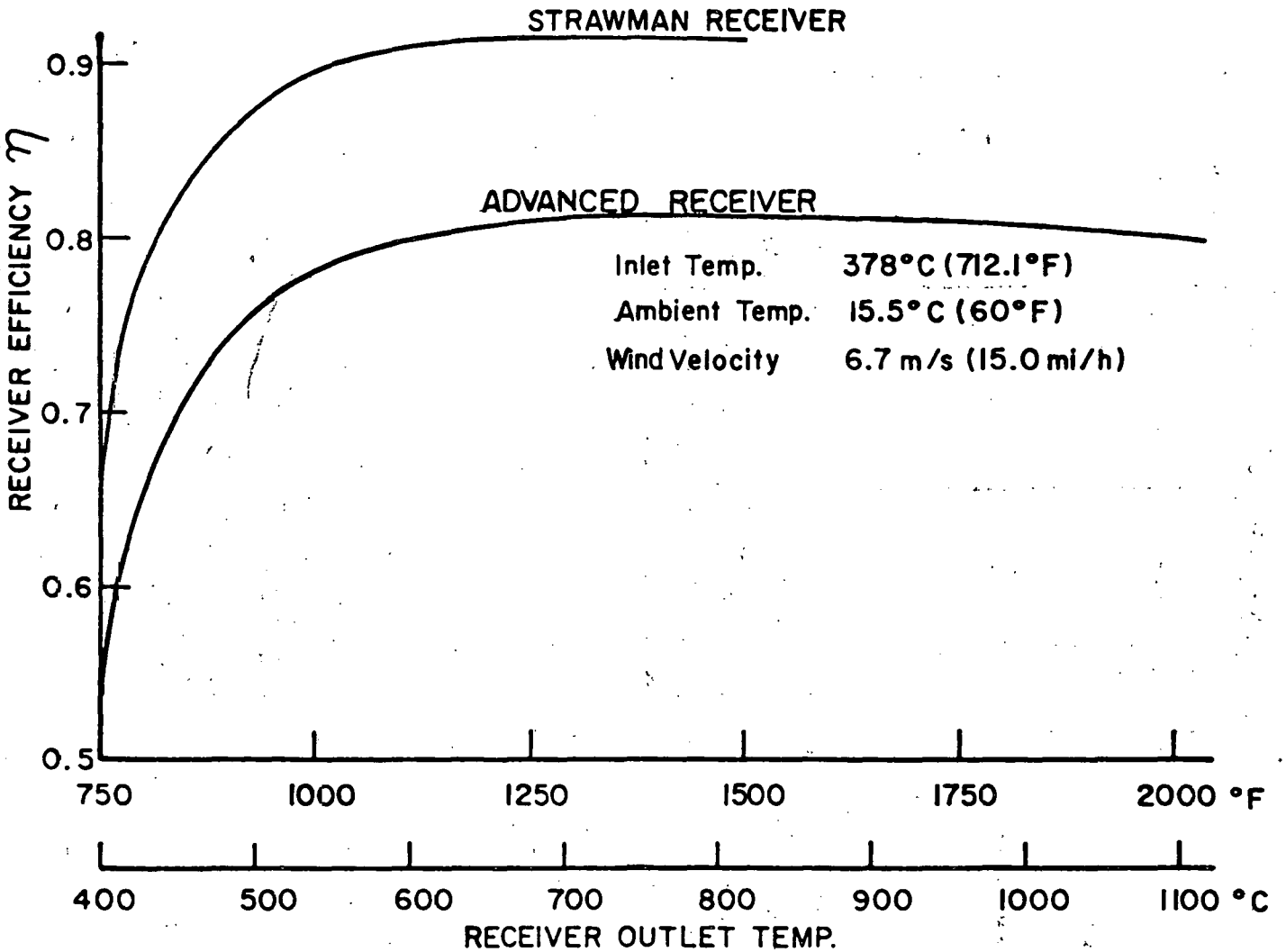

Figure 3-25 RECEIVER EFFICIENCY VS. TEMPERATURE AT CONSTANT AIR FLOW

efficiencies as a function of the operating temperature for constant airflow operation. Figure 3-26 shows the efficiency variation as a function of the percentage of rated power operations, assuming constant outlet temperature.

3.3.5 Absorber Panel Stress (Life) Analysis

The receiver panels are subjected to the following types of loading conditions:

- Pressure loads
- Thermal loads during normal operation
- Pressure and thermal cyclic loads resulting from diurnal startups and shutdowns and from cloud covers
- Dynamic loads (earthquake, flow-induced vibrations)
- Dead loads (weight, support reactions, etc.)

Initial stress calculations were performed mainly to define wall thicknesses for weight estimating and to identify feasibility issues. The particular receiver components considered to date in the analysis of major loads were:

- Panel Shell. Only internal pressure loads were considered in the design of the receiver panel walls and the two heads.
- Heat Pipes. The ends of the heat pipes protrude through the receiver shell and are directly exposed to the solar radiation. Therefore, a cyclic thermal analysis of the heat pipes was done to determine the allowable radiant fluxes. Only the cyclic thermal loads were considered in the analysis. A total of 13,000 cycles were used, corresponding to a 30-year life. The effects of cloud

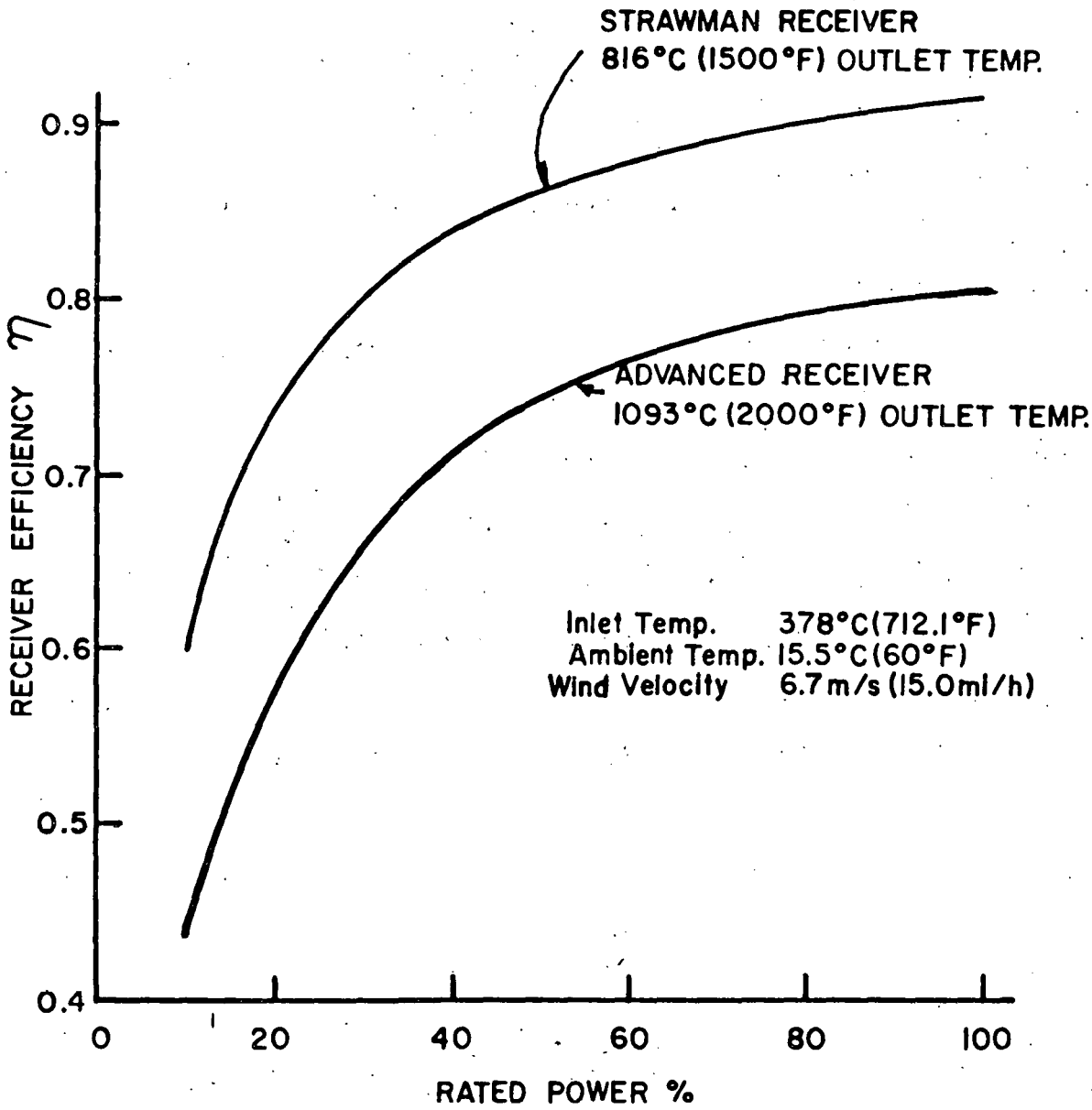

Figure 3-26 RECEIVER EFFICIENCY VS. RATED POWER AT CONSTANT OUTLET TEMPERATURE

covers and pressure loading on fatigue life were not considered.

- Headers. Only internal pressure loads were considered. Header thicknesses were based on primary hoop stress resulting from internal pressure. Stress concentration effects at the connection of the piping to the shell were not considered in the design.

The various panel components have been evaluated according to Section VIII-Division 2 of the ASME Boiler and Pressure Vessel Code. The ideas of Code Case 1592, as modified for solar applications, were used for high-temperature service.

3.3.6 Receiver Structural Support Analysis

The receiver will be supported by a platform on top of the tower. The walls of the cavity will be supported by the platform and will carry the roof periphery load. The wall structure will be truss work, covered with steel plate and insulated internally. The roof of the cavity will be supported by the receiver wall support structure. The roof also consists of truss work, covered with internally insulated steel plates.

Only the dead loads were considered in the design of the receiver structure for the parametric studies. Dynamic loads (wind and earthquake loads) will be considered in the later design phases.

3.3.7 Tower Analysis

During the parametric studies, the tower analysis was confined to cost evaluations. To make maximum use of available information, the tower costs were estimated from the equation provided by Sandia, based on the work of Stearns-Roger on solar tower design (Ref. 3-7). The equation in condensed form is:

$$\$TOTAL = \$TOWER + \$FOUNDATION + \$ACCESSORIES + \$ENG \ \& \ FEE$$

$$= 1.25 \left[(0.969) + (0.0002\ H_T) + (1.4 \cdot 10^{-6})\ M_{MAX} + (0.669 \cdot 10^{-6})\ (H_T)\ (H_T \cdot M_{MAX})^{0.4}\right]$$

The costs are in millions of 1978 dollars. The tower height, H_T, is measured in feet and is exclusive of the receiver height. The maximum moment, M_{MAX}, due to wind or earthquake, was found to be dominated by earthquake. The equation for M_{MAX} due to earthquake is:

$$M_{MAX} = \left[(5.71 \cdot 10^{-3})\ (\ddot{X}_g)^{1.5}\ (H_T)\right] \left[W_R(536 - H_T) + (5.34)\ (H_T)\ (H_T - 160)\right]$$

where:

W_R = receiver weight in kips
$\ddot{X}_g$ = peak acceleration, g's

Calculations of tower height for a given receiver power and number of heliostats was based on the assumptions of constant rim angle for the heliostat field and scaling relationships described in Appendix C.

3.3.8 Riser/Downcomer Analysis

Piping Concepts. The compressed air piping to and from the receiver requires careful design. This is because excessive piping pressure drop of small piping reduces the efficiency of the EPGS, and large-diameter piping associated with low-pressure losses increases the complexity of the piping and receiver tower design. In addition, the receiver outlet temperatures in the 816-1093C (1500-2000F) range require attention to insulation and piping flexibility.

Thermal expansion flexibility in the Strawman riser was accomplished by using a concept similar to a helical coil spring. Horizontal expansion loops absorb the expansion, as shown in Figure 3-27 for the riser. This arrangement has the advantage of maximizing the number of bending legs per piping elbow. The loops were sized to be supported from the inside of the main structural columns of the tower.

The riser pipe preconceptual design was based on a temperature rise from ambient to 427C (800F) and a bending stress limit of 69 MPa (10,000 psi). A 50 percent cold spring was assumed. The rolled and welded carbon steel riser pipe is externally insulated with 12.7 cm (5 in.) of calcium silicate with lagging.

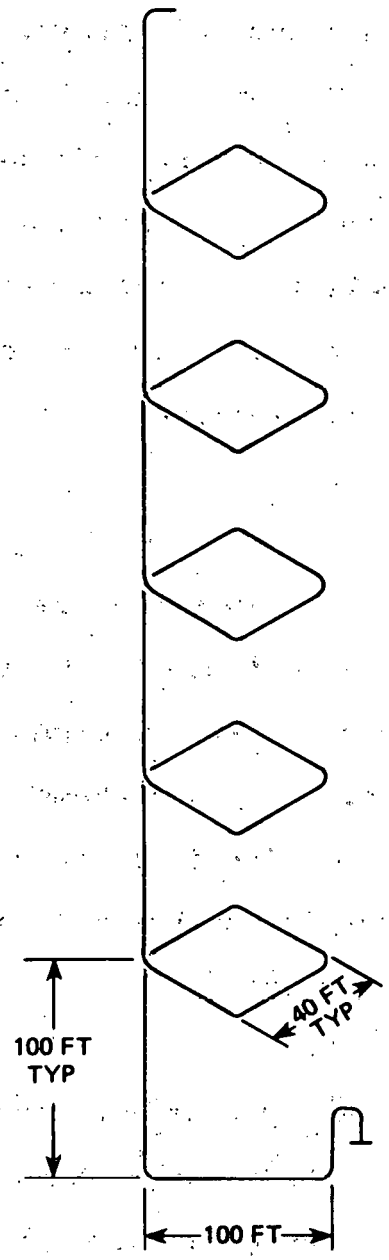

Figure 3-27 RISER PIPING LAYOUT CONCEPT

The Strawman riser has a 1.52 m (60 in.) diameter. The Advanced Strawman riser, with a taller tower but lower mass flow, has a 1.22 m (48.0 in.) diameter.

The downcomer has a carbon steel pipe as the pressure boundary with internal insulation and metal liner. The internal insulation with a more flexible thin liner results in less thermal expansion of the pressure boundary, since it is at a much lower temperature. The allowable stresses are higher, so thinner walls can be used and local hot spots can be easily detected on the bare pipe surface in the event of insulation breakdown.

The downcomer steel pipe of the Strawman design has a diameter of 1.83 m (72 in). The diameter of the flow channel in this design is approximately 1.44 m (57 in.). The Advanced Strawman baseline design also has the same steel pipe diameter, but the flow channel diameter is 1.35 m (53 in.).

Economic Evaluation of Piping Pressure Drop. The parametric evaluation of the economics of piping pressure drop included the considerations of losses in plant performance due to increased compressor horsepower, required by higher losses, and the savings accrued from reduced pipe sizes.

In the Strawman concept, as shown in Figure 3-28, the capital cost is lowest at a pressure drop of approximately 48.3 kPa (7 psi). But the additional cost of fuel consumed with

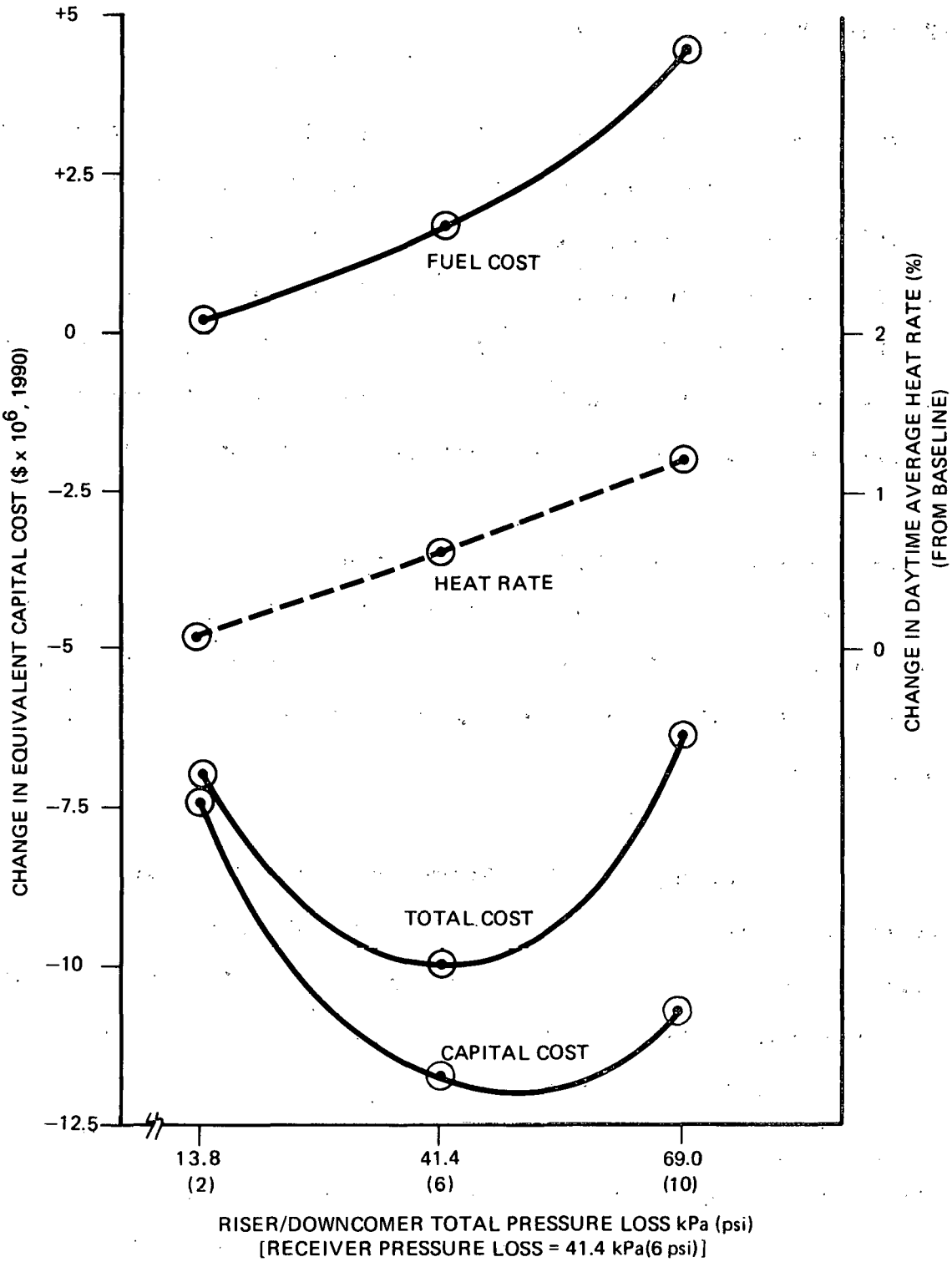

Figure 3-28 COST EFFECT OF STRAWMAN PIPING PRESSURE LOSS

increasing pressure losses causes the total cost to be lowest at 41.4 kPa (6 psi).

Although a similar detailed analysis was not done for the Advanced Strawman, conclusions drawn from the trends evident in the Strawman analysis indicate that a pressure drop of between 13.8 kPa (2 psi) and 34.5 kPa (5 psi) yields the lowest total cost. This is consistent with the higher ratio of receiver cost to riser/downcomer cost compared to the Strawman.

Receiver Bypass Analysis. The primary modes of operation investigated for the receiver were constant air flow and constant receiver outlet temperature.

At off-design conditions, the constant air flow mode results in receiver outlet temperatures below the design point outlet temperature, and hence lower receiver thermal losses. The receiver loop pressure drop, however, remains constant for this mode. The constant receiver outlet temperature mode utilizes a bypass control valve at the base of the receiver tower to bypass air directly to the combustor inlet to maintain constant receiver outlet temperature. This results in a lower overall pressure drop and a corresponding cycle heat rate reduction. However, for this mode, the receiver losses remain high throughout the day.

Computer runs were made to determine cycle efficiencies over a range of solar input levels throughout the day for both the

constant air flow and constant temperature modes. The results of these runs together with the receiver efficiency curves were used to determine the change in fuel consumption as a function of solar power to the receiver. Table 3-17 shows that the constant temperature case requires more fuel over at least 80 percent of the operating day. The bypass control valve and the associated instrumentation for the constant temperature represents additional capital expenditure. The constant air flow case is also beneficial for thermal cycling. The receiver temperature would increase and decrease daily at a relatively slow rate compared to constant outlet temperature operation, which would involve a rapid temperature increase in the morning and a similar rapid temperature decline in the evening.

In view of the above considerations, the constant air flow case was selected as the most cost effective mode of operation for the receiver.

3.3.9 Pumps, Piping, and Valve Analysis

The riser and downcomer piping, described in Subsection 3.3.8, are the major piping items in the concept. The only pump associated with the receiver is the Brayton cycle compressor. It is treated as part of the EPGS in Section 3.6.

TABLE 3-17

CONSTANT AIR FLOW VERSUS
CONSTANT RECEIVER OUTLET TEMPERATURE

Mode	Percent Rated Solar Power to Receiver (%)	Receiver Efficiency (%)	Heat Rate (Btu/kWh)	Rated Fossil Fuel Flow (%)	Change in Fossil Fuel Flow* (%)
Constant Air Flow	100	91.5	7853	100.00	Base
	80	91.5	7920	127.72	Base
	60	91.5	7977	155.15	Base
	40	90.0	8040	183.60	Base
	20	83.5	8105	212.52	Base
Constant Temperature	100	91.5	7853	100.00	0
	80	90.0	7868	127.89	+0.17
	60	87.5	7890	155.57	+0.42
	40	82.9	7930	183.77	+0.17
	20	68.5	7982	212.88	+0.36

*Differential expressed as percentage of rated fossil fuel flows.

3.3.10 Heat Exchanger Analysis

The heat recovery steam generator and cooling towers are discussed in Section 3.6 with the EPGS. There are no other heat exchangers in the combined cycle hybrid system.

3.3.11 Receiver Outlet Temperature Analysis

The receiver outlet temperature and the solar fraction are closely interrelated. The results of economic analyses show an advantage with lower receiver outlet temperature, and hence, lower solar fraction. This is true for both the Strawman and Advanced Strawman systems at a 12 percent fuel escalation rate, as shown in Figures 3-29 and 3-30. However, this conclusion is very sensitive to economic parameters. In the Strawman system with a 15 percent fuel escalation rate, there is an economic advantage with a higher receiver outlet temperature, keeping within technical limits. Subsequent evaluations with low cost heliostats confirmed this conclusion. In the Advanced Strawman system, the 15 percent fuel escalation rate did not reverse the conclusions.

3.3.12 Receiver Pressure Drop Analysis

Based on the parametric case input from the receiver designer on the cost effects of receiver pressure drop, a tradeoff study was

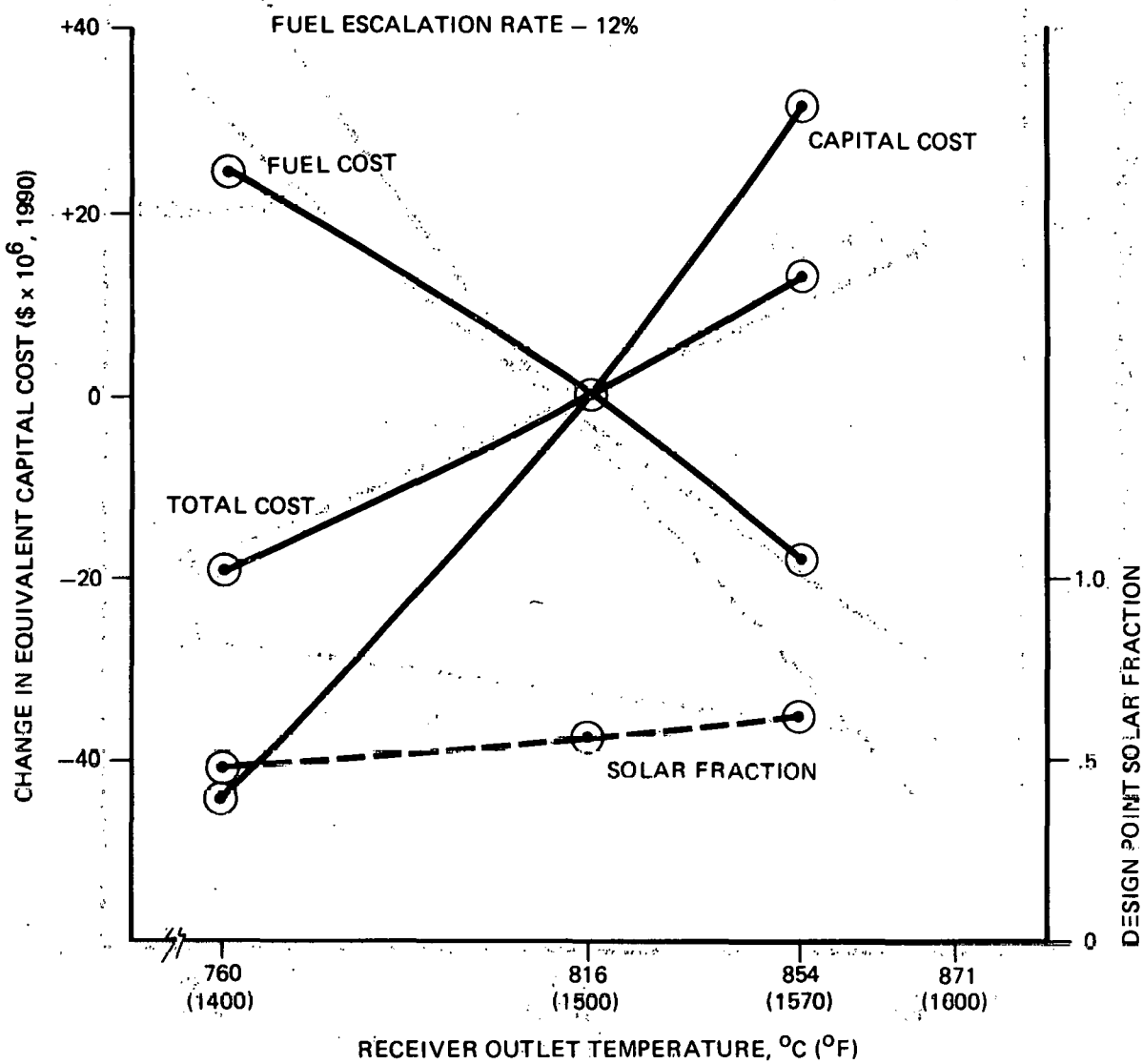

Figure 3-29 COST EFFECT OF STRAWMAN RECEIVER OUTLET TEMPERATURE

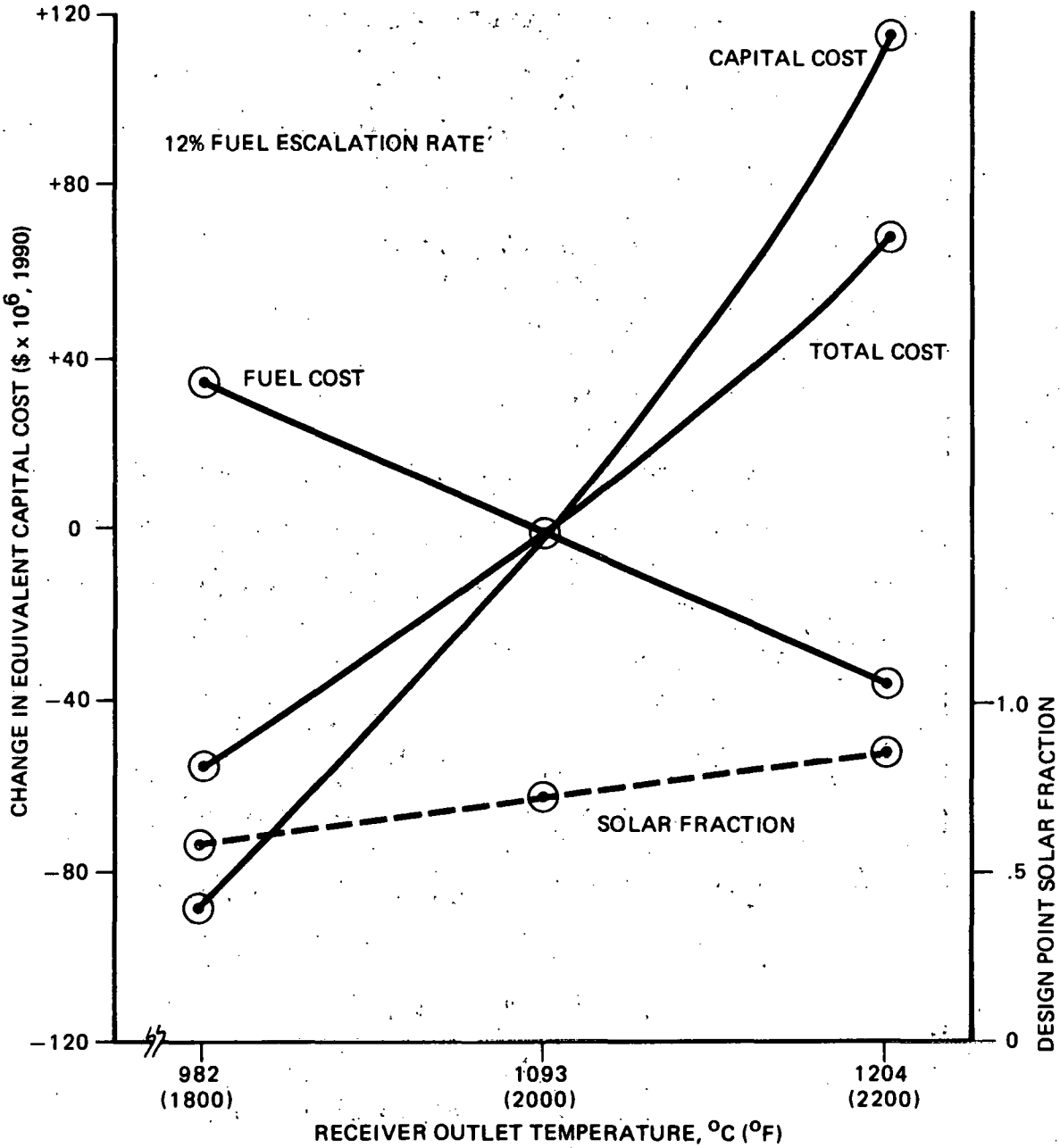

Figure 3-30 COST EFFECT OF ADVANCED STRAWMAN RECEIVER OUTLET TEMPERATURE

done to determine the optimum pressure drop, consistent with the overall system.

For the Strawman, receiver pressure drops of 13.8 kPa (2 psi) and 41.4 kPa (6 psi) were evaluated, and compared to the baseline. As shown in Figure 3-31, no economic optimum occurs in the range examined. However, the upper limit for reasons of heat transfer requirements is 41.4 kPa (6 psi).

For the Advanced Strawman, the same approach was used and at a pressure ratio of 12:1, an optimum pressure drop was found to be 75.8 kPa (11 psi). This can be seen in Figure 3-32. For the higher pressure ratios, which are more economical for the Advanced Strawman, an optimum pressure drop of 103.4 kPa (15 psi) was determined, based on analogous trends in the Strawman parametrics.

3.4 ENERGY STORAGE SUBSYSTEM

Based on system-level studies of storage capacity (described in Subsection 4.3.3), it was concluded that energy storage for the combined cycle solar hybrid plant is technically not required and economically not justified. Consequently, there were no parametric studies conducted to support any energy storage subsystem choices.

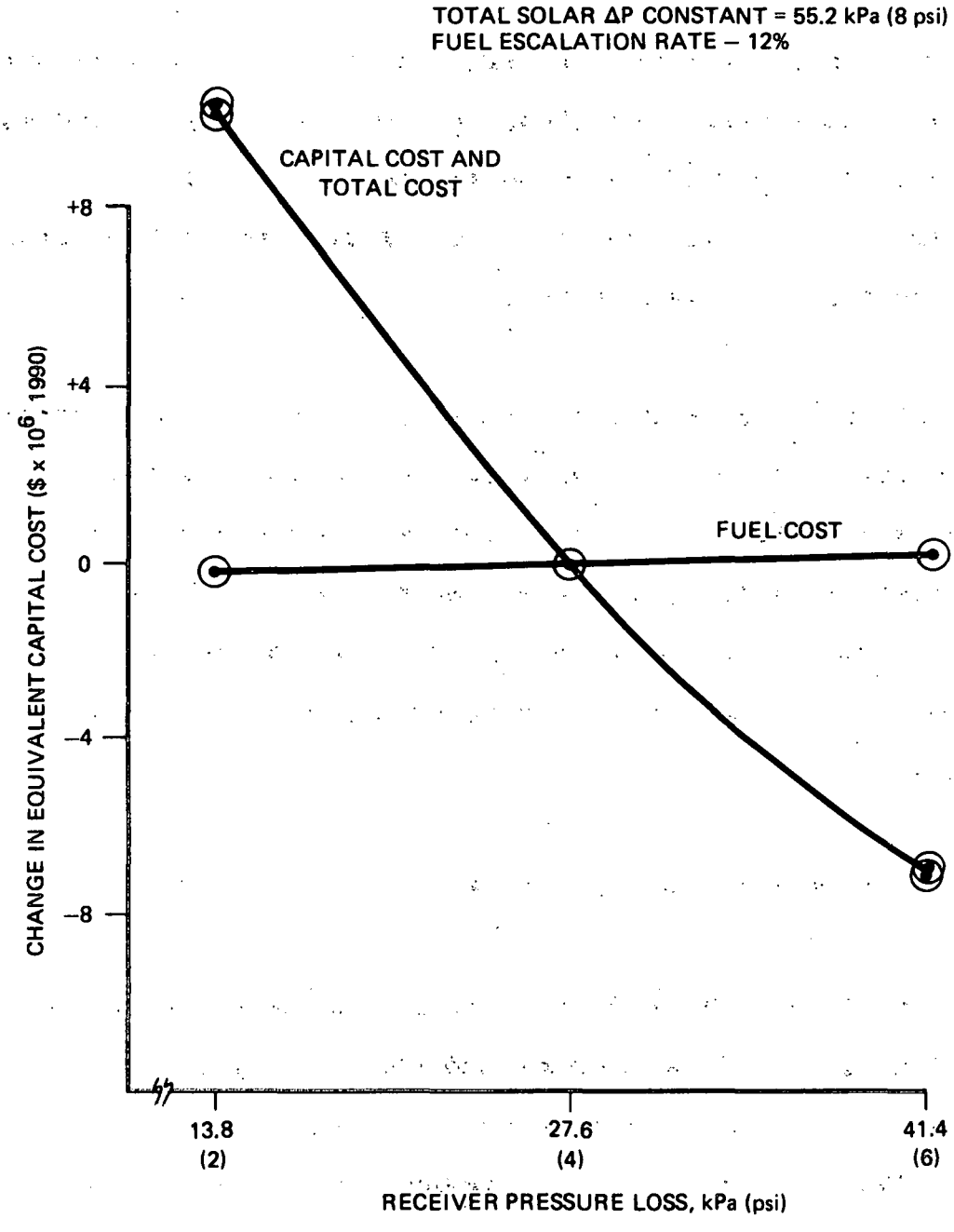

Figure 3-31 COST EFFECT OF STRAWMAN RECEIVER PRESSURE LOSS

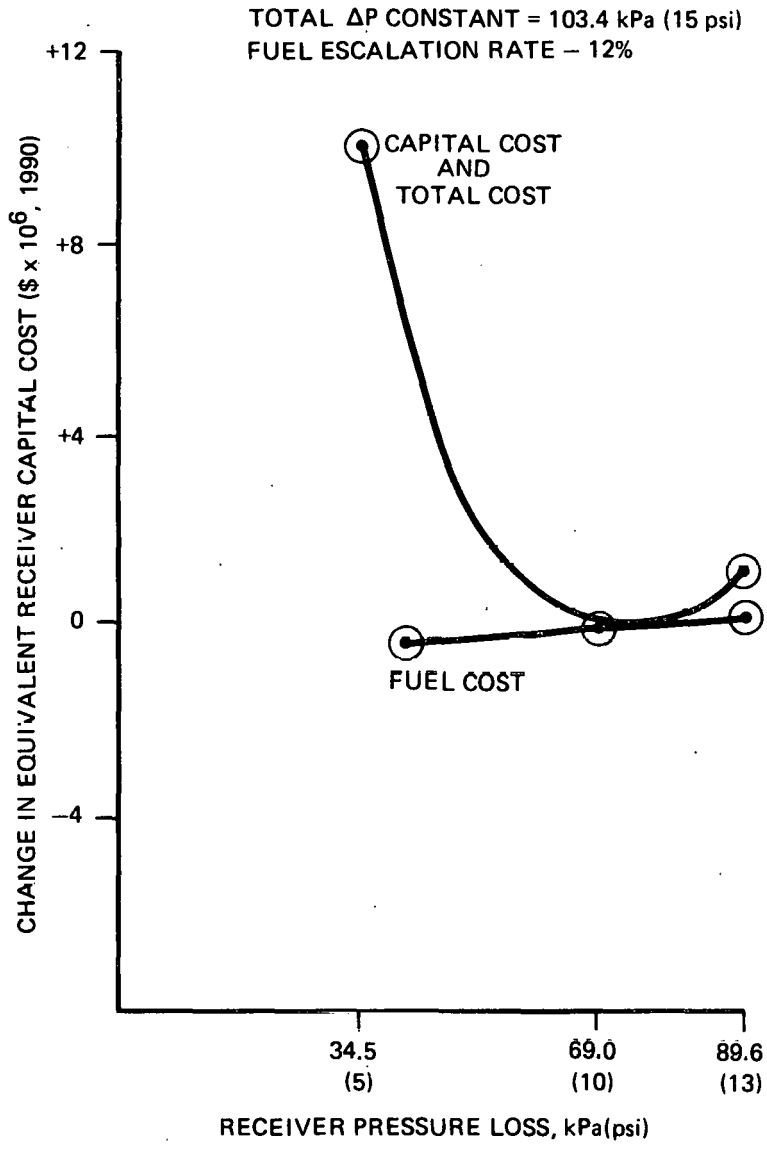

Figure 3-32 COST EFFECT OF ADVANCED STRAWMAN RECEIVER PRESSURE LOSS

3.5 NONSOLAR SUBSYSTEM

In the combined cycle energy conversion system concept, the main component of the nonsolar subsystem is the Brayton cycle combustor, which is an integral component of the EPGS. The other major components for the liquid or gas fuels are the fuel storage and transfer equipment, which do not warrant separate treatment as a plant subsystem.

The combustor, which converts the chemical energy in the fuel to thermal energy, is closely coupled to the gas turbine casing and is generally supplied with the gas turbine. The combustor, in this solar hybrid application, is subjected to service conditions that are signficantly different from conventional gas turbine installations. Consequently, they require special treatment. This section presents the required background material on gas turbine combustor technology as a basis for discussing alternatives for combustor arrangement and fuel types.

3.5.1 Nonsolar Subsystem Concepts

Conventional Gas Turbine Combustor Design. The combustor is a direct-fired air heater that operates in the range of 200 to 250 percent excess air for conventional fuels. A schematic diagram of a typical conventional combustor is shown in Figure 3-33. Typically, the combustor is a cylindrical can with a perforated metal liner within which the chemical reaction takes place.

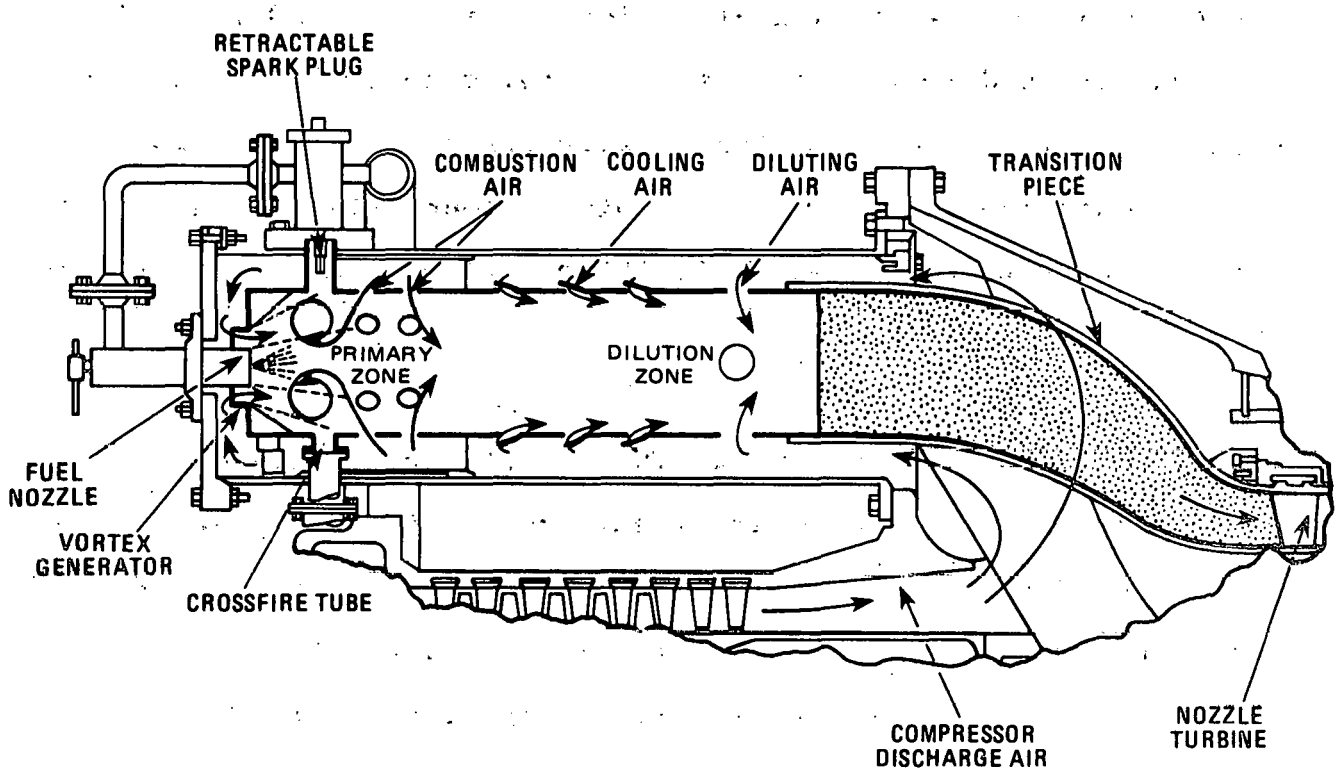

Figure 3-33 CONVENTIONAL GAS TURBINE COMBUSTOR

In the primary zone, fuel is mixed and burned with a portion of the air. Film air cooling protects the liner from overheating. The remainder of the air is added in the dilution zone to bring the temperature down to turbine inlet conditions. Additional cooling air is directed through small holes to cool the turbine nozzles and rotor for high-temperature designs. To meet lower power requirements the fuel flow rate is controlled to lower the turbine inlet temperature, while the air flow remains essentially constant.

Combustor Design Alternatives. Two significant issues must be considered when using a conventional gas turbine combustor for a solar hybrid plant, with its series arrangement of solar receiver and combustor. Both issues relate to the higher-than-conventional air inlet temperatures to the combustor.

First is the cooling of the combustor liner, which is critical to the operating life of the combustor. In conventional, close-coupled gas turbines, the air entering the combustor is at low enough temperatures to accomplish the necessary cooling. However, in the hybrid systems with receiver outlet temperatures of 816 to 1093C (1500 to 2000F), special provisions, such as bypass cooling, are required to cool the metallic combustor liner. Alternatively, an uncooled ceramic liner would have to be used. It is probable that current development work on ceramic liners could be accomplished by 1990.

The second issue is the thermal generation of nitrogen oxides (NO_x) resulting from the increased combustor inlet temperature. In conventional combustors, water and steam are injected along with the fuel to control thermal NC_x. This method is not expected to be sufficient to meet the requirements of the hybrid design or to meet future, more stringent, emission standards. Two alternative methods are under development to reduce the NO_x emissions:

- Lean premixed combustion
- Thermally supported catalytic combustion

Both of these have the potential for reducing emissions below the proposed EPA requirements by controlling the peak combustor temperature, which is the key variable in thermal NO_x production. Figure 3-34 illustrates NC_x emission using these methods in place of conventional combustion.

Lean premixed combustion controls the peak reaction temperature by assuring that a lean (higher than stoichiometric air-to-fuel ratio) mixture is introduced into the combustion chamber. This results in a lower peak temperature than with conventional combustion, but premixing the fuel with hot air introduces the potential for autoignition during the mixing process. This aspect needs further development to meet the operational requirement of commercial gas turbines.

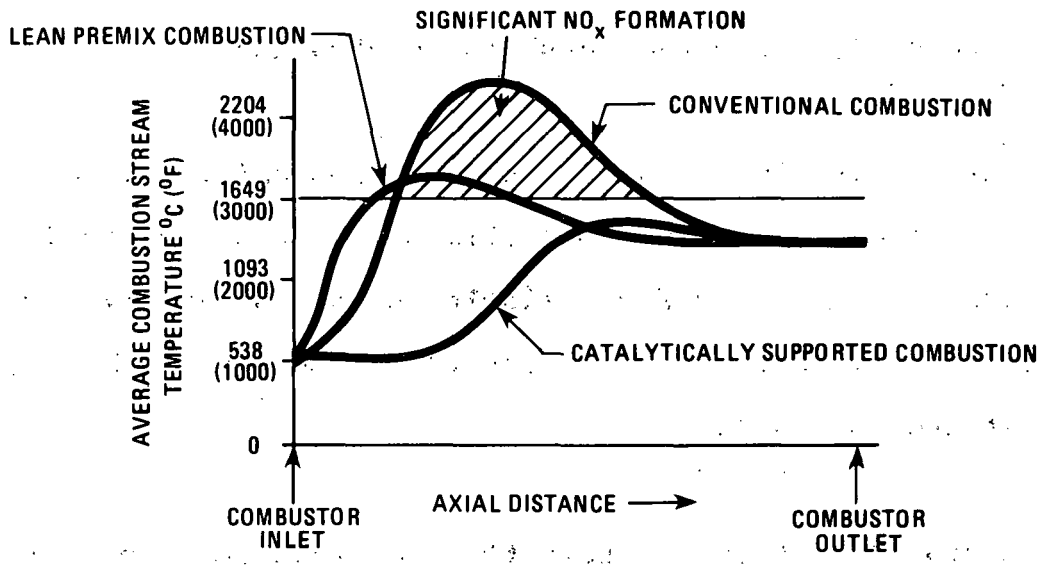

Figure 3-34 COMBUSTION SYSTEM TEMPERATURE HISTORY

Hybrid designs that combine the conventional and premixed processes, as shown schematically in Figure 3-35, are being evaluated as a compromise between emission control and operability.

The catalytic combustor could minimize thermal NO_x emissions. This method, which uses a noble metal catalyst on a ceramic honeycomb substrate, accomplishes the combustion at temperatures below the threshold for NO_x formation. The process is characterized by the lack of flame and a very even exhaust temperature. It also may be suitable for a wide range of fuels, although the effects of ash deposition on the catalyst have not yet been evaluated. Elevated inlet temperatures pose no problem for the catalytic combustor; in fact, a minimum inlet temperature is necessary to achieve high combustion efficiency.

Westinghouse, in conjunction with Englehard Industries, has been working on the development of a catalytic combustor for approximately seven years. Test results are very promising but further development work is necessary in mechanical design and operational characteristics. In Westinghouse's opinion, this type of unit can be available in the 1990 time frame.

<u>Series vs. Parallel Combustion Arrangement</u>. The choice between a parallel and series combustor arrangement has a potential impact on the solar fraction achievable in the combined cycle hybrid system. The preconceptual designs were based on a series

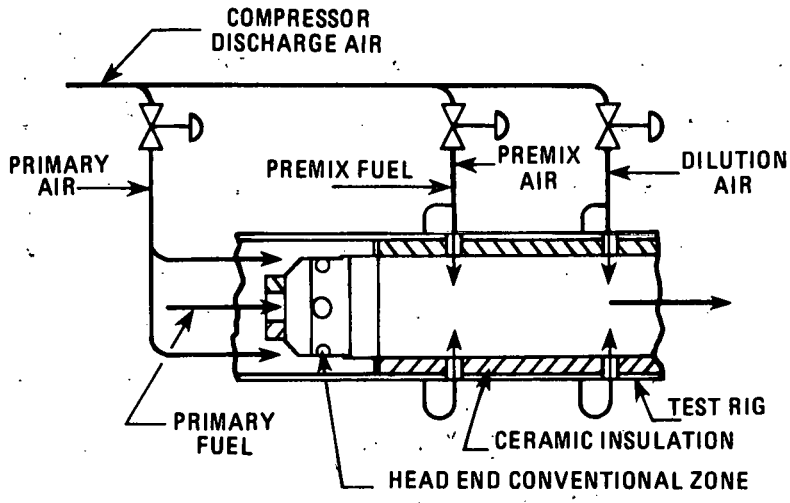

PREMIX HYBRID COMBUSTOR TEST RIG SCHEMATIC

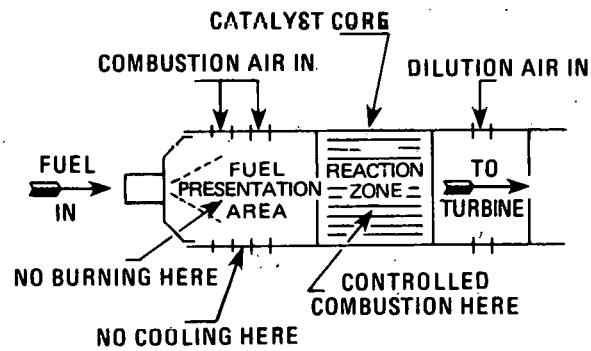

CATALYTIC COMBUSTOR SCHEMATIC

Figure 3-35 LOW NO_x EMISSION COMBUSTOR CONCEPTS

arrangement of the solar receiver and combustor. During parametric analysis, this was further evaluated. Factors which influence the choice of arrangement are:

- The relative temperatures of receiver outlet and turbine inlet
- Combustor development requirements
- Achievable solar fractions

The peak outlet temperature possible with metallic receivers is approximately 843C (1550F). Combined cycles with such a low gas turbine inlet temperature have cycle efficiencies below that for modern steam Rankine cycles. To be competitive it is desirable to use gas turbine inlet temperatures approaching 1093C (2000F). Until the ceramic receivers become available, the only way to achieve such temperatures is through raising the temperature of the receiver outlet air in combustors, placed in series with the receiver.

Analysis shows that with metallic receivers in a parallel arrangement, even using an optimistic value of 1649C (3000F) as the maximum combustor outlet temperature, a significant portion of the Brayton cycle air flow must bypass the solar receiver. With the reduced receiver air flow, this would actually result in a lower solar fraction for the same receiver outlet temperature and turbine inlet temperature.

The assumption that the parallel arrangement would permit the use of a conventional combustor is not justifiable, since the present-day commercial combustors themselves are not expected to meet the emissions regulations in 1990. Thus, development is required for either the parallel or series arrangement. And it seems appropriate to focus on the series arrangement, since it gives a better utilization of solar energy for the same type of solar receiver. It is also appropriate to focus on the catalytic combustor, as recommended by Westinghouse, because it is the most compatible with a series arrangement and shows a potential for the lowest emissions of the improved combustor concepts currently under development.

3.5.2 Nonsolar Subsystem Size

The sizing of the nonsolar (fossil-fired) generating capacity is straightforward. It does, however, require an understanding of the daily operational characteristics of the combined cycle solar hybrid system.

Daily Operational Characteristics. The design point for the solar system is 950 W/m² insolation at noon of the best day for the heliostat geometric efficiency. This sets the maximum (design point) solar fraction for the Strawman plant at 0.563. The three operational modes necessary to describe the normal daily operation of this plant are:

- Hybrid mode (design point)
- Short-term fossil mode
- Long-term fossil mode

Figure 3-36 shows the daily variation of heat rate and solar fraction for the Strawman system during these operating modes. The hybrid mode represents the maximum solar input and has the best heat rate due to a minimum of combustion losses. In the short-term fossil mode, when the solar input is lost temporarily, all the air continues to flow through the solar receiver, but there is no solar heat input. The long-term fossil mode is similar to short-term fossil mode, except the solar receiver and the tower piping are bypassed to reduce the pressure loss between the compressor and the turbine to a nominal 3.45 kPa (0.5 psi).

If the load demand for the plant is reduced by the utility system dispatcher, operation at part load is achieved by reducing the fossil fuel input and lowering the turbine inlet temperature. The resulting decrease in the turbine exhaust temperature decreases both pressure and temperature in the steam cycle. This part-load operating mode can minimize the fossil energy input while increasing the solar fraction to a value greater than the design point at reduced plant output. The allowable turndown ratio on the fuel system is the only major limit on the reduction of fossil input at part load. This will be studied further in conceptual design.

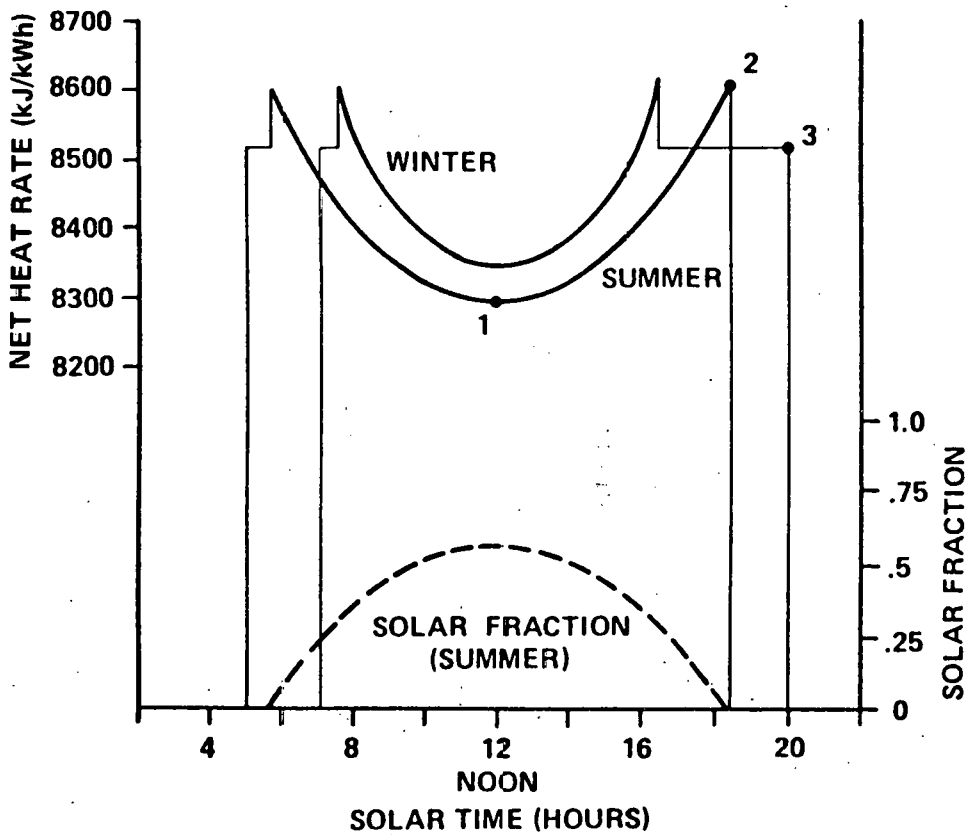

STRAWMAN HEAT RATE (kJ/kWh)	
HYBRID-DESIGN POINT(1)	8285
SHORT-TERM FOSSIL(2)	8612
LONG-TERM FOSSIL(3)	8515
DAYTIME AVERAGE	8441
SOLAR FRACTION-DESIGN POINT	.563

Figure 3-36 STRAWMAN DAILY HEAT RATE VARIATION

Design Point For Nonsolar Subsystem Sizing. Due to the operational charcteristics discussed above, the nonsolar subsystem must be capable of supplying 100 percent rated power in the short-term fossil operating mode, since this represents the maximum demand. The nonsolar generating capacity decision affects mainly the combustor and fuel storage provisions.

3.5.3 Nonsolar Subsystem Materials

No significant materials-related problems have been identified that are unique to the hybrid system. The gas turbine materials technology used for this study is consistent with the present state-of-the-art for commercial gas turbines. The type of fuel can influence the selection of the combustor liner and hot gas path components. But no evaluation of materials was attempted during the parametric analysis, since they play no major role in selecting the preferred system.

3.5.4 Fuels Selection

The gas turbines considered for the hybrid system concept are the same as in conventional combined cycle plants and generally use the same types of fuel. The fuel selection process involved identifying suitable candidates and selecting the reference fuel, after evaluating technical and economic factors. Although the evalautions described in this section show that the No. 2 distillate fuel oil is the preferred choice, the National Energy

Act of 1978 may require that combined cycle hybrid plants be fueled with coal-derived gases or oils, or that DOE approval be obtained to burn natural gas or petroleum distillates. The impact of the act will be further evaluated in light of the implementing regulations, which are currently being formulated.

Fuels Suitable for Gas Turbines. Gas turbine combustors directly mix fuel and air in the combustion process, and the hot combustion products are then expanded through the turbine. This makes it necessary to burn relatively clean fuels to meet emission requirements and to prevent erosion and corrosion of the turbine blades. In addition, requirements for fuel handling, injection, and rapid mixing also impact the use of certain fuels for gas turbines. The candidate fuels considered and their relevant characteristics are:

- Natural Gas. This is an ideal fuel for gas turbine power plants. It is delivered to the plant by pipeline from an offsite source. In the continental U.S. it is generally clean, so no special treatment is required. It is easily injected and burned in a combustor, since it readily mixes with air to provide an ignitable mixture with rapid flame propagation and high temperature.

- Hydrogen. This fuel has similar desirable attributes, but its availability, cost, transportation, large-volume storage, and safety aspects need further development.

- Distillate (No. 2) Oils. These are very compatible with gas turbine operation and include naphtha, kerosene, and diesel fuel. On-site storage is normally required, but no preheating is needed in temperate climates due to relatively low viscosity. Distillates are essentially ash free as refined and contain less than 1 percent sulfur, so usually no fuel treatment is required, provided adequate care is taken to prevent contamination during storage and handling. Atomization and mixing

within the combustor is relatively simple for this type of fuel.

- Residual and Crude Oils. These are also readily stored on site in tanks and pumped to the turbine combustor. Residual and crude oils are very viscous at ambient temperatures and require heating systems in the tanks and on piping to facilitate pumping. Residual and crude oils may also need cleaning to reduce alkali metal compounds or ash content. Alkali compounds can be removed by water washing followed by centrifuging. Ash can be removed by electrostatic precipitation, but more frequent inspection and cleaning to remove deposits in the hot gas path are needed for ash-bearing fuels. Residual and crude oils, even though heated to reduce viscosity, require more complex high-pressure, air-augmented injectors to properly atomize for combustion. A less viscous, lighter fuel is also required for startup.

- Coal-Derived Gas Fuels. These fuels are from conversion processes, using existing or advanced technologies, and are expected to be among the significant turbine fuels of the future. The gasification processes can be designed to use air and steam to produce low-Btu gas at about 5600 kJ/m^3 (150 Btu/ft^3) heating value, or to use oxygen and steam to produce medium-Btu gas at about 11,200 kJ/m^3 (300 Btu/ft^3). These gases are expected to be relatively clean fuels, suitable for easy injection and burning. They would be comparable to natural gas fuels from the turbine industry viewpoint. Gas turbines can be easily adapted to use either medium- or low-Btu gases. Medium-Btu gases can be pipe supplied from remote sites. Economics appear to dictate on-site or nearby production of the low-Btu gases.

- Coal-Derived Liquid Fuels. These have characteristics similar to residual or crude oils. Their properties are a function of the feedstock coal and the conversion process. These conversion processes are still in development and the product properties are not completely established as yet. However, in general these liquids tend to have high densities and viscosities, with the liquids often being near solids at ambient temperatures. They must be heated and stirred during storage. Further heating is required for pumping to the turbine combustor. Handling, injection, and combustion of coal-derived liquids are expected to require system complexities comparable to those now used for petroleum crude oil.

- Alcohols. These include methanol and ethanol, relatively clean-burning fuels, which are excellent gas turbine fuels. Whether derived from coal, biomass, or

other sources, alcohols have the potential for low emission and low maintenance. Existing gas turbines would require minor modifications. However, provisions for removal of any alkali metal contaminants will be required.

- Coal. This will not be feasible for hybrid plants in the 1990 time frame for direct combustion in gas turbine systems. Indirect heating of compressor discharge air by submerging pipes in a fluidized-bed coal combustor has been the subject of several studies. This type of coal combustion system may provide low emissions, but nonmetallic air piping development would be necessary for application to turbine inlet temperatures between 2000 and 2400F.

Fuels Chosen for Evaluation. To reduce the number of different fuels evaluated during the parametric analysis, the following criteria were applied to the range of fuels discussed above:

- Sufficient resource availability (1990-2000) for utility applications, after impact of the National Energy Act of 1978
- Commercial development status by 1990

Although natural gas is an ideal fuel for gas turbines, it appears unlikely that it will still be available for new utility applications after 1990 for a plant with a 30-year life.

Quantity production of hydrogen to fuel a number of hybrid plants is unlikely by 1990. It is probable, however, that commercial production of hydrogen will begin some time during the 30-year design life of a plant constructed in 1990.

Distillate oils and residual oils are expected to be available throughout the required time frame. However, if there is a shortage of petroleum oils, synthetic oils with approximately the same physical characteristics will probably be developed.

Development of coal-derived gas fuels, medium- and low-Btu, is well under way. Ease of transportation and greater purity makes the medium-Btu gas more desireable as a turbine fuel. It is expected that the commercial development of medium-Btu gas will precede commercialization of the low-Btu gases and is likely to be available in the 1990 time frame.

Development of coal-derived liquid fuels, such as solvent-refined coal and H coal, is currently under way. Commercial quantities are expected to be available during the operational life of a solar hybrid plant constructed in 1990.

Alcohol fuels should be available, since alcohol fuels from coal or biomass are now being introduced to displace gasoline for automotive use.

Fluidized bed combustion of coal for utility boiler applications may be developed by 1990, but successful development, in the same time frame, of tubing to indirectly heat the air to 1093 to 1316C (2000 to 2400F) for the gas turbine is doubtful.

It is recognized that candidate fuels still in the developmental phase complicate the evaluation process, since there is no reliable data available to support rigorous economic evaluations.

These considerations led to the selection of two petroleum-based and two coal-based fuels for further evaluation:

- No. 2 distillate oil
- No. 6 residual oil
- Coal-derived liquid (solvent-refined coal)
- Medium-Btu gas (Texaco process)

Evaluation Results. The characteristics of the four selected fuels are given in Table 3-18. A summary of the key input parameters and the results of the economic evaluations are given in Table 3-19.

Capital cost variations include both the differences in equipment requirements and differences in heat rates characteristic for different fuels. The residual oil and solvent-refined coal capital costs are higher, primarily because of more significant fuel handling equipment requirements and costs. The medium-Btu gas capital costs are less than those for the base case distillate oil, primarily because of a reduction in the solar system size due to a credit for the pressure energy in the medium-Btu gas.

TABLE 3-18

FUEL CHARACTERISTICS

Parameter	Distillate Oil (No. 2)	Residual Oil (No. 6)	Coal-Derived Liquid (SRC)	Medium-Btu Gas (Texaco)
Fuel Analysis (wt % for liquid) (mole % for gas)				25.52 CO_2
C	86.5	85.6	88.41	37.14 CO
H	12.5	9.7	5.15	32.87 H_2
N	0.2	1.58	1.84	0.95 N_2
S	0.8	2.3	0.78	0.30 H_2S
O	—	0.42	3.72	0.01 COS
Ash	—	0.12	0.1	3.14 CH_4
H_2O	—	0.28	—	0.09 H_2O
Heating Value (kJ/kg)	8353	7868	6742	1823

TABLE 3-19

ALTERNATIVE FUELS ANALYSIS

Item	Distillate Oil (No. 2)	Residual Oil (No. 6)	Solvent-Refined Coal	Medium-Btu Gas
1978 Fuel Price ($/$10^6$ Btu)	2.35	2.00	3.00	3.50
Real Escalation Rate (%)	11.61	12.03	10.5	10.5
Annual O&M Rate (%)	1.0	1.4	1.4	0.7
Strawman Daytime Average Heat Rate (kJ/kW)	8441	8362	8272	8367
Strawman Net Long-Term Fossil Heat Rate (kJ/kW)	8515	8403	8269	8417
Change in Equivalent Capital Cost (%)	Base	+.74	+1.1	+2.5

Operating and maintenance costs were based on the distillate oil case using an annual rate of 1 percent of initial capital cost, escalated at an 8 percent annual rate in accordance with DOE guidelines. The O&M rates for the other fuels were estimates using maintenance cost factors from a recent EPRI report (Ref. 3-9) and the assumption that maintenance constitutes 60 percent of total O&M costs, based on the Energy Conversion Alternatives Study (Ref. 3-10).

Fuel prices for distillate oil, residual oil, and coal-derived liquid fuel was obtained from the DOE Requirements Definition document. The medium-Btu gas price estimate is based on recent Bechtel studies. The fuel escalation rates are derived from the EPRI Technical Assessment Guide (Ref. 2-1).

The results indicate that the baseline fuel selection of No. 2 distillate oil is the most economical choice at this time.

3.5.5 Nonsolar Thermal Performance Analysis

The miscellaneous equipment associated with the nonsolar subsystem does not differ significantly from a conventional combined cycle plant, with the possible exception of the daily cycling operation. Nonsolar equipment performance has no significant impact on selection of the preferred system.

3.6 ELECTRIC POWER GENERATION SUBSYSTEM

The electric power generation subsystem (EPGS) is used to convert thermal energy input, either fossil or solar, to electric energy. The nominal EPGS production capacity is 100 MWe net. This production capacity must be attainable under both hybrid and fossil-only operating modes.

3.6.1 Combined Cycle Overview

The EPGS in a hybrid power system can operate on any of several thermodynamic power cycles. However, the combined cycle concept has been identified in DOE- and EPRI-sponsored studies (Refs. 3-4 and 3-8) as one of the most promising fossil cycles for this solar application. It has a high thermal efficiency and has been shown in these studies to promise a low busbar cost of electricity. It was therefore selected to be the EPGS for this study. (The basic combined cycle concept, as adopted for hybrid operation, is described in Subsection 1.2.2 and is shown schematically in Figure 1-1.)

The efficiency of the combined cycle is a function of the gas turbine and the steam turbine cycle efficiencies and the HRSG effectiveness. On an ideal basis, it may be expressed as follows:

$$E_c = E_t + (E_e)\ (1 - E_t)\ (E_s)$$

where:

E_c = Combined cycle efficiency

E_t = Topping Brayton (gas turbine) cycle efficiency

E_e = HRSG effectiveness

E_s = Bottoming steam turbine cycle efficiency

For the gas turbine cycle efficiency, E_t, the two parameters of significance are the compressor pressure ratio and turbine inlet temperature. The sensitivity of the simple gas turbine cycle to variations of these parameters is shown in Figure 3-37. The curves indicate that the efficiency is higher at higher inlet temperature, but the incremental gain is declining with increasing temperature to a point where negligible gain in efficiency results for inlet temperatures above 1316C (2400F). Efficiency is also higher with higher compressor pressure ratios, to peaks that occur at progressively higher pressure ratios as the gas turbine temperatures increase.

The equipment size, and hence the cost, is a function of the specific power parameter; the higher the specific power, the lower the cost. Figure 3-38 shows the specific power parameter as a function of compressor pressure ratio and turbine inlet temperature. The points of optimum specific power of various turbine inlet temperatures are also indicated on the graphs. The compressor pressure ratio for maximum specific power is shown to

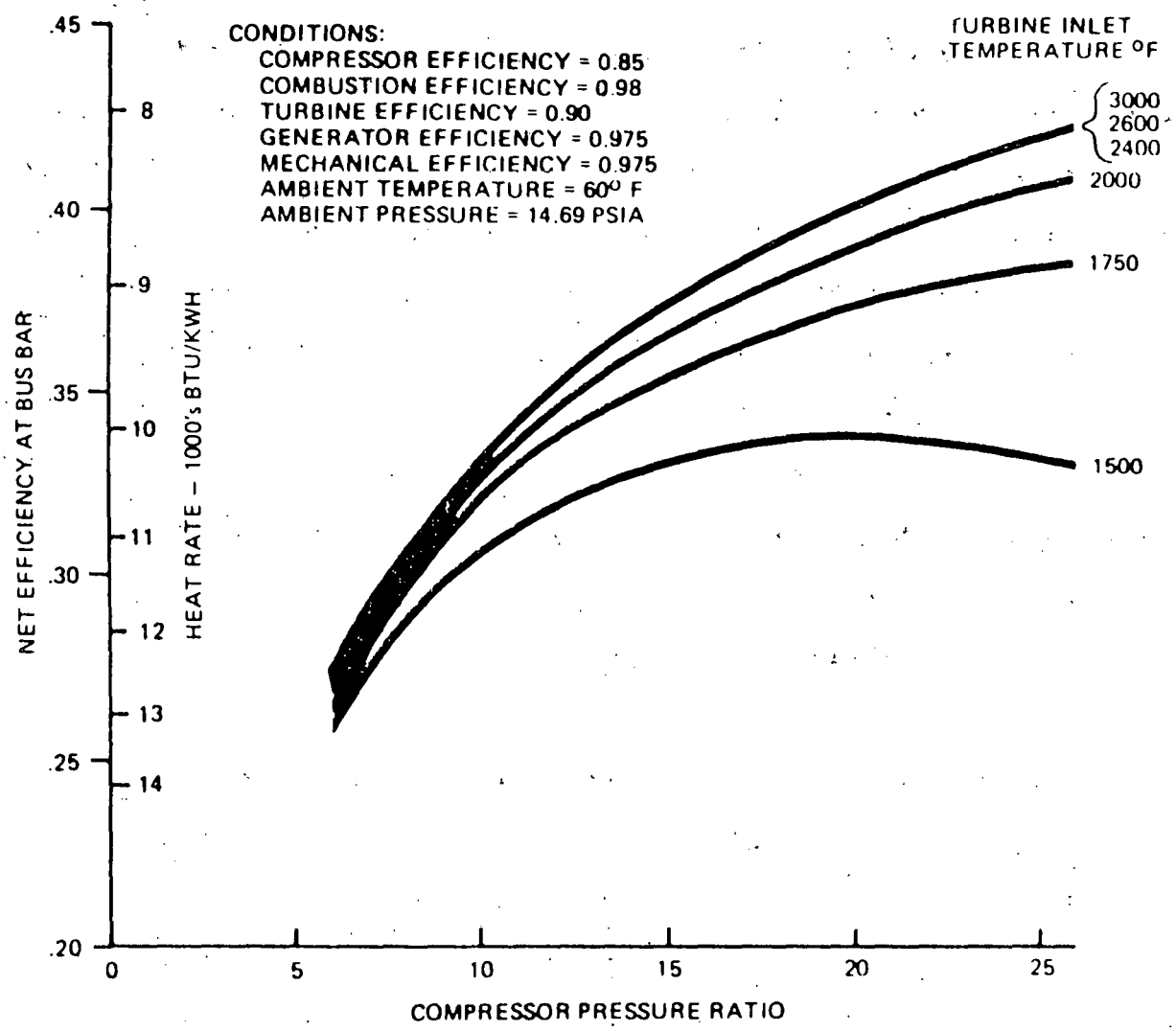

Figure 3-37 SIMPLE OPEN-CYCLE GAS TURBINE NET EFFICIENCY VS. COMPRESSOR PRESSURE RATIO FOR VARIOUS TURBINE INLET TEMPERATURES

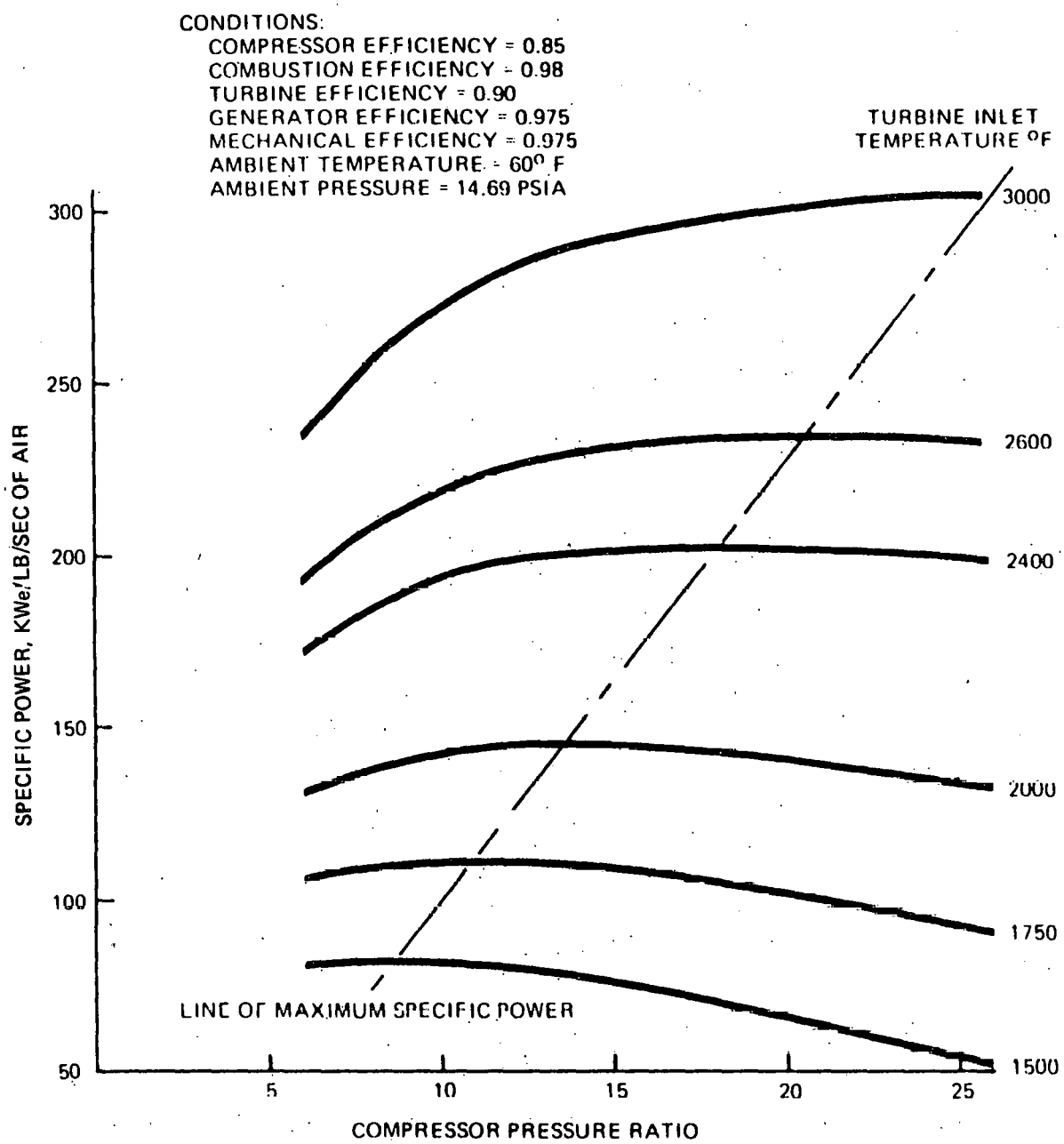

Figure 3-38 SIMPLE OPEN-CYCLE GAS TURBINE SPECIFIC POWER VS. COMPRESSOR PRESSURE RATIO FOR VARIOUS TURBINE INLET TEMPERATURES

be less than that for maximum efficiency at a given turbine inlet temperature.

For a given inlet temperature, the gas turbine exhaust temperature decreases with increased pressure ratios. As a result, the peak steam turbine cycle temperature also decreases with increasing compressor pressure ratio, with a resultant decrease in steam cycle efficiency, E_s. Thus the optimum efficiency of the combined cycle is achieved at conditions other than the optimum for either the gas or the steam turbine cycle.

The HRSG is designed to recover the residual thermal energy from the gas turbine exhaust gases and use it to heat and evaporate the feedwater and to superheat the steam. The energy recovery effectiveness of the HRSG is denoted by the index E_e. The practical limit of the effectiveness is set by the minimum practical air temperature at the stack, which is between 135 and 150C (270-300F).

Another potential limitation to full energy recovery is the minimum practical approach temperature at the beginning of the boiling process, generally known as the "pinch point temperature difference." The effects of this limitation can be seen in Figure 3-39, which is the temperature profile of the steam cycle along with the gas turbine cycle temperature profiles of the Strawman and Advanced Strawman concepts. In the case of the Advanced Strawman concept, the energy requirements of the

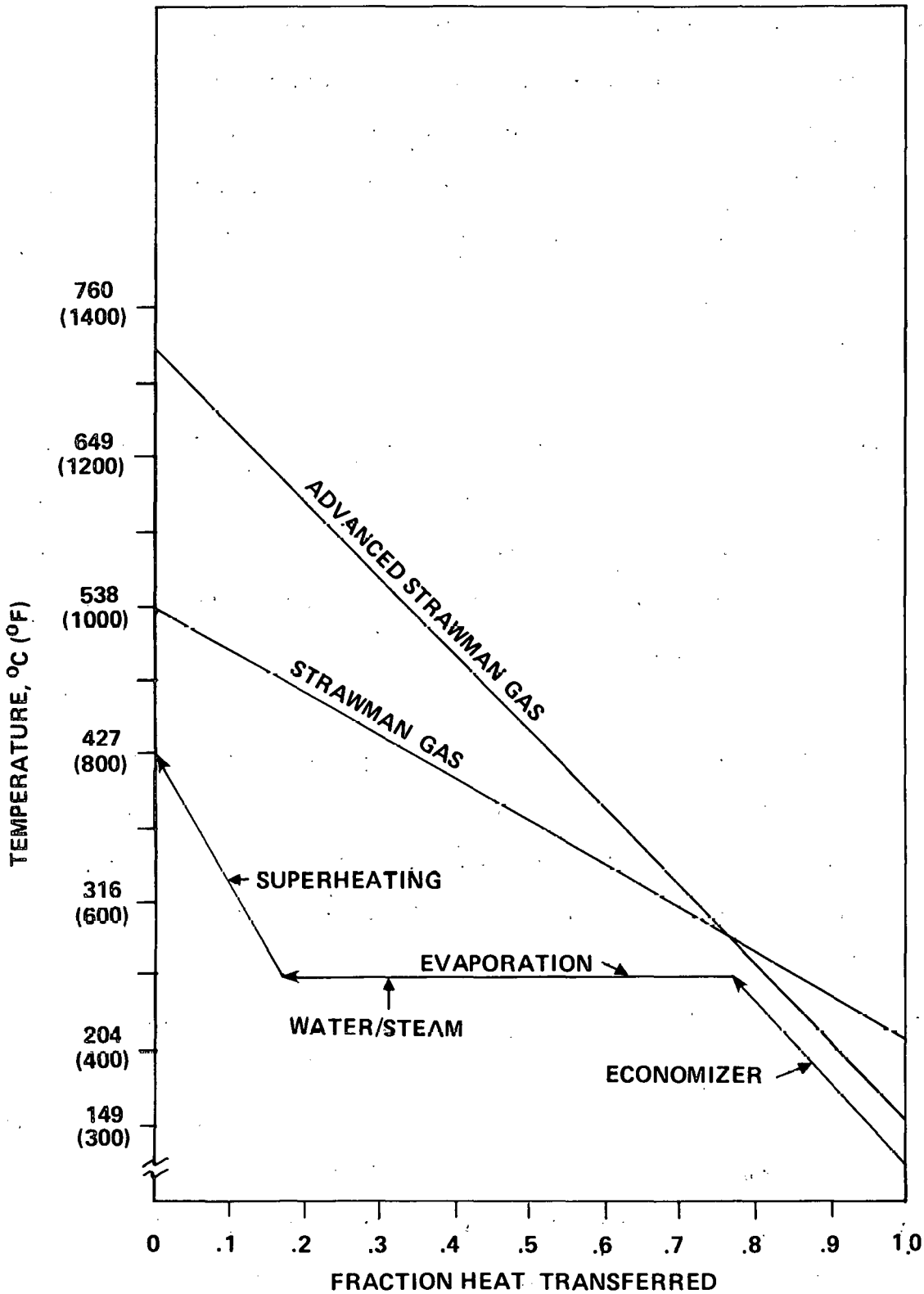

Figure 3-39 GAS AND WATER/STEAM TEMPERATURE PROFILES IN HEAT RECOVERY BOILERS

feedwater heating match the energy available from the air stream. Thus, the air can be cooled to the optimum level. For the Strawman, however, the energy from the air cannot be fully recovered by feedwater heating, due to the pinch point temperature difference limits. This results in higher cold end losses, and consequently a lower HRSG effectiveness.

3.6.2 EPGS Size

In combined cycle power systems, the size of the EPGS is governed by the size and number of gas turbines used. This is because the steam turbine output for an unfired HRSG is directly related to the Brayton cycle exhaust energy and represents 30 to 40 percent of the total plant output.

Depending on the manufacturer, large industrial single-shaft gas turbines are produced in typical sizes of 50 MWe, 75 MWe, and 100 MWe. For larger plants, multiple gas turbines are used, generally with one HRSG per gas turbine, feeding a single steam turbine. The use of a single large steam turbine offers the advantages of higher efficiency and the possible use of steam reheat. The heat rate of larger combined cycle plants is expected to be lower than that for a 100 MWe plant, and the part-load heat rate would also be better. For these reasons, the optimum plant size is expected to be larger than 100 MWe. For conventional combined cycle plants, the optimum appears to be approximately 300 to 400 MWe.

Nevertheless, in the parametric studies the reference EPGS subsystem was assumed to have a net generating capacity of 100 MWe, which is in accordance with current DOE technical guidance.

3.6.3 EPGS Cycle Selection

The parameters chosen for the EPGS subsystem and the selected ranges are shown in Table 3-20. The selection of the EPGS cycle conditions is the result of a series of individual tradeoff studies.

Results of these analyses are given in Tables 3-21 and 3-22. The evaluations were based on the preconceptual heliostat cost of $93.42/m² (installed, 1978) and an average daily operation of 12.875 hours, which corresponds to a 48 percent capacity factor at a 90 percent availability. It should be noted that the cost values represent cost increments from the baseline cases due to the parametric changes in design and/or operating conditions.

Compressor Pressure Ratio. Compressor pressure ratio, which determines the peak air pressure and the power absorbed by the compressor, is a key variable in gas turbine performance. As it was discussed in Subsection 3.6.1, this parameter is also closely related to gas turbine inlet temperature. The net power output of the gas turbine-generator is determined by the size of the equipment and the practical efficiencies that can be achieved for

TABLE 3-20

EPGS PARAMETRIC VALUES

Parameter	Strawman	Advanced Strawman
Pressure Ratios	8, 12, 16	8, 12, 16
Main Steam Conditions, MPa/C (Psia/F)	5.86/454 to 12.4/510 (850/825 to 1800/950)	8.62/482 to 12.4/510 (1250/900 to 1800/950)
Receiver Outlet Temperature, C (F)	760, 815, 870 (1400, 1500, 1600)	982, 1093, 1204 (1800, 2000, 2200)
Air System ΔP, kPa (Psi)	27.6, 55.2, 82.7 (4, 8, 12)	68.9, 103, 138 (10, 15, 20)
No. of Fossil Fuel Types (Liquid & Gas)	4	4

TABLE 3-21

ECONOMIC EVALUATION OF STRAWMAN PARAMETRIC CASES

Operating Conditions							Cost Effect				
Compressor Pressure Ratio	Air System Pressure Drop, PSI ΔP_{Total}*	Solar Rec'r Pressure Drop, PSI ΔP_{Total}*	Design Point Solar Fraction	Steam Conditions Pressure, PSIG	Steam Conditions Temperature, F	Other	Δ Capital Costs (1990 $ x10⁶)	Differential Equivalent Capital Cost Due to Fuel Escalation, 1990$x10⁶ 12%	Differential Equivalent Capital Cost Due to Fuel Escalation, 1990$x10⁶ 15%	Total Differential Equivalent Capital Costs, 1990$x10⁶ 12%	Total Differential Equivalent Capital Costs, 1990$x10⁶ 15%
PR = 8	8	4	.593	1800	950	-	26.7	-12.1	-26.7	14.6	0
	8	4	.593	1450	950	-	12.7	-8.9	-19.6	3.8	-6.9
	8	4	.593	1250	900	-	7.4	-0.4	-0.9	7.0	6.5
PR = 12	8	4	.563	1450	950	-	BASE	BASE	BASE	BASE	BASE
	8	4	.563	1250	900	-	-4.9	1.3	2.8	-3.6	-2.1
	8	4	.563	850	825	-	-3.6	3.9	8.6	-4.7	0
PR = 16	8	4	.530	1250	885	-	1.3	16.3	35.8	17.6	37.1
	8	4	.530	850	885	-	-7.5	15.4	33.9	7.9	26.4
PR = 12	4	2	.563	1450	950	-	15.5	-2.6	5.6	12.9	9.9
	4	3	.563	1450	950	-	12.6	-2.5	-5.4	10.1	7.2
	12	4	.563	1450	950	-	-0.9	1.5	3.3	0.6	2.4
	12	6	.563	1450	950	-	-11.6	1.6	3.5	-10.0	-8.1
	16	6	.563	1450	950	-	-10.7	4.3	9.5	-6.4	-1.2
	8	2	.563	1450	950	-	10.4	-0.2	-0.3	10.2	10.1
	8	6	.563	1450	950	-	-7.2	0.2	0.3	-7.0	-6.9
PR = 12	8	4	.520	1450	950	†Tro = 1570 F	31.5	-18.1	-39.7	13.8	-7.8
	8	4	.483	1450	950	Tro = 1400 F	-43.8	24.7	54.2	-19.1	10.4
PR = 12	8	4	.506	1450	950	Fired HRSG	-5.3	11.7	25.8	6.4	20.5
	8	4	.469	1450	950/950	Fired HRSG Reheat	-9.5	27.5	60.4	18.0	50.9
	8	4	.508	1800	950	Fired HRSG	10.4	7.3	16.0	17.7	26.4
	8	4	.465	1800	950/950	Fired HRSG Reheat	6.4	26.7	58.8	33.1	65.2
PR = 16	8	4	.444	1800	950	Fired HRSG	-2.9	30.9	67.8	28.0	64.9
PR = 8	8	4	.540	1450	950	Intercooled	42.4	9.1	19.9	51.5	62.3
PR = 12	8	4	.529	1450	950	Intercooled	34.6	15.4	33.9	50.0	78.5
PR = 16	8	4	.520	850	825	Intercooled	35.5	25.7	56.4	61.2	91.9
PR = 12	8	4	.557	1450	950	After Cooled 300 F	139.8	-10.6	-23.4	129.2	116.4
	8	4	.483	1450	950	Parallel Combustor (2000 F)	-67.7	50.6	111.1	-17.1	43.4
	8	4	.563	1450	950	Dual Press HRSG	4.0	-19.9	-43.7	-15.9	-39.7
	8	4	.563	1450	950	Dual Press HRSG Reheat	7.1	-25.6	-56.2	-18.5	-49.1

*To convert to kPa multiply psi values by 6.89
†Tro = Receiver Outlet Temperature

TABLE 3-22

ECONOMIC EVALUATION OF ADVANCED STRAWMAN PARAMETRIC CASES

Operating Conditions							Cost Effect				
Compressor Pressure Ratio	Air System Pressure Drop, PSI ΔP_{Total}*	Solar Rec'r Pressure Drop, PSI ΔP_{Total}*	Design Point Solar Fraction	Steam Conditions: Pressure, PSIG	Steam Conditions: Temperature, F	Other	Δ Capital Cost (1990 $x10^6$)	Differential Equivalent Capital Cost Due to Fuel Escalation, 1990 $x10^6$		Total Differential Equivalent Capital Costs, 1990$x10^6$	
								12%	15%	12%	15%
PR=8	15	10	.737	1800	950	-	51.4	18.2	40.0	69.6	91.4
	15	10	.737	1450	950	-	38.5	21.2	46.6	59.7	85.1
	15	10	.737	1250	900	-	38.9	27.8	61.1	66.7	100.0
PR=12	15	10	.719	1800	950	-	12.7	-2.5	-5.5	10.2	7.2
	15	10	.719	1450	950	-	BASE	BASE	BASE	BASE	BASE
	15	10	.719	1250	900	-	-0.7	5.0	10.9	4.3	10.2
PR=16	15	10	.704	1800	950	-	3.7	-11.4	-25.1	-7.7	-21.4
	15	10	.704	1450	950	-	-7.9	-9.0	-19.3	-16.9	-27.7
	15	10	.704	1250	900	-	-12.5	-4.3	-9.4	-16.8	-21.9
PR=12	10	5	.719	1450	950	-	11.6	-3.0	-6.6	8.6	5.0
	10	8	.719	1450	950	-	9.2	-2.9	-6.4	6.3	2.8
	20	10	.719	1450	950	-	-1.6	2.9	6.5	1.3	4.9
	20	15	.719	1450	950	-	-7.9	3.2	7.1	-4.7	-0.8
	15	5	.719	1450	950	-	10.0	-0.3	-0.6	9.7	9.4
	15	13	.719	1450	950	-	1.2	0.3	0.6	1.5	1.8
	25	20	.719	1450	950	-	-10.7	5.8		-4.9	
PR=12	15	10	.856	1450	950	†Tro=2200F	116.5	-36.5	-80.2	80.0	36.3
	15	10	.590	1450	950	Tro=1800F	-89.3	34.7	76.4	-54.6	-12.9
PR=8	15	10	.737	1800	950/950	Reheat	67.5	12.3	27.0	79.8	94.5
PR=12	15	10	.719	1450	950/950	Reheat	11.2	-5.4	-11.4	5.8	-0.2
PR= 8	15	10	.759	1450	950	Intercooled	67.6	37.5	82.6	105.1	150.2
PR=12	15	10	.753	1450	950	Intercooled	24.6	16.1	35.4	40.7	60.0
PR=16	15	10	.748	1450	950	Intercooled	11.1	7.9	17.5	19.0	28.6
PR=12	15	10	.433	1450	950	Parallel Combustor (2400F)	-109.3	88.4	194.4	-20.9	85.1

*To convert to kPa multiply psi values by 6.89
†Tro = Receiver Outlet Temperature

the cycle components. Representative values selected for this analysis are:

- Compressor efficiency = 0.85
- Combustion efficiency = 0.98
- Turbine efficiency = 0.90
- Mechanical efficiency = 0.975
- Generator efficiency = 0.975
- Combustor pressure loss fraction = 0.05

For parametric analysis a base pressure ratio of 12 was selected for both plants. Parametric cases were evaluated for pressure ratios of 8 and 16. To simplify the analysis of pressure ratio as a separate parameter, the same main steam conditions of 10.1 MPa (1450 psia) and 510C (950F) were assumed throughout.

For the Strawman design, the economic optimum pressure ratio is approximately 12, as shown in Figure 3-40. One would expect that the high cost of solar energy collection equipment would drive the pressure ratios higher to achieve lower heat rates. However, the design complexity and cost penalties of the higher pressures in the heat pipe receivers tend to favor the lower-than-thermodynamically-optimum pressure ratio. The solar fraction also increases with decreasing pressure ratios, because the compressor discharge temperature also decreases, allowing a greater temperature rise in the receiver.

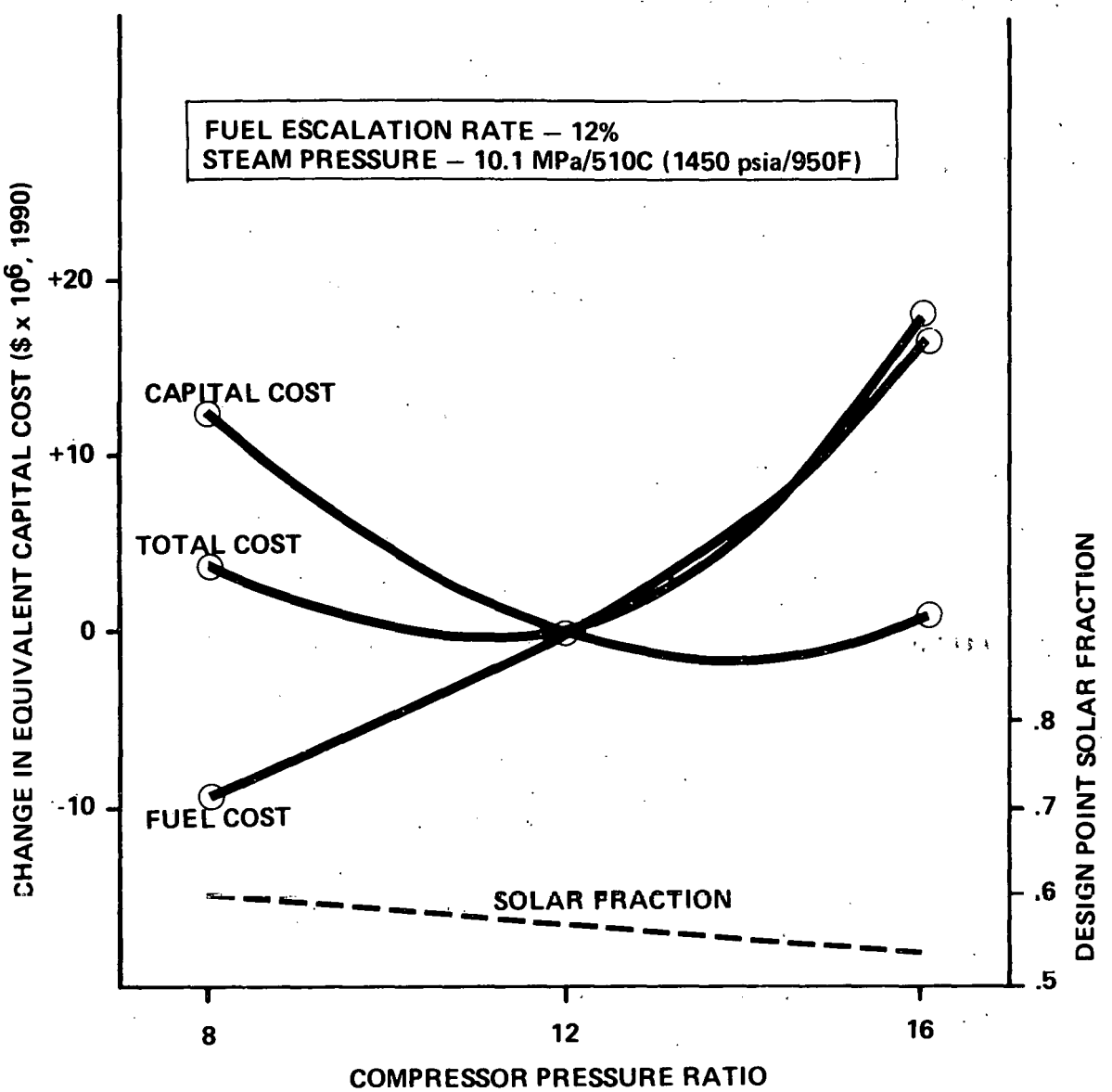

Figure 3-40 COST EFFECTS OF STRAWMAN PRESSURE RATIO

The Advanced Strawman favors a pressure ratio above 16, as shown in Figure 3-41. In addition to better performance, the higher pressure in the receiver allows higher heat transfer rates to the air in the receiver tubes, which lowers both the cost and weight of the receiver. Although the optimum appears to be above the range examined, the total cost curve in this range is quite flat, indicating that little additional economic gain can be expected with pressure ratios above 16:1. There are greater uncertainties associated with ceramic receivers designed for higher pressures. In light of these uncertainties, the pressure ratio of 16:1 was selected.

Main Steam Pressure and Temperature. The pressure level at the steam turbine throttle is one of the most significant parameters for determining the performance of the steam bottoming cycle. Temperature was not studied as an independent parameter, but pressure/temperature combinations were selected for analysis that are typical of standard steam turbine designs in the 25 to 50 MWe range.

The pressure ratio is also a significant factor in the selection of the steam conditions, because the gas turbine exhaust (HRSG inlet) temperature (T_{EXH}) is related to the turbine pressure ratio by the adiabatic expansion equation:

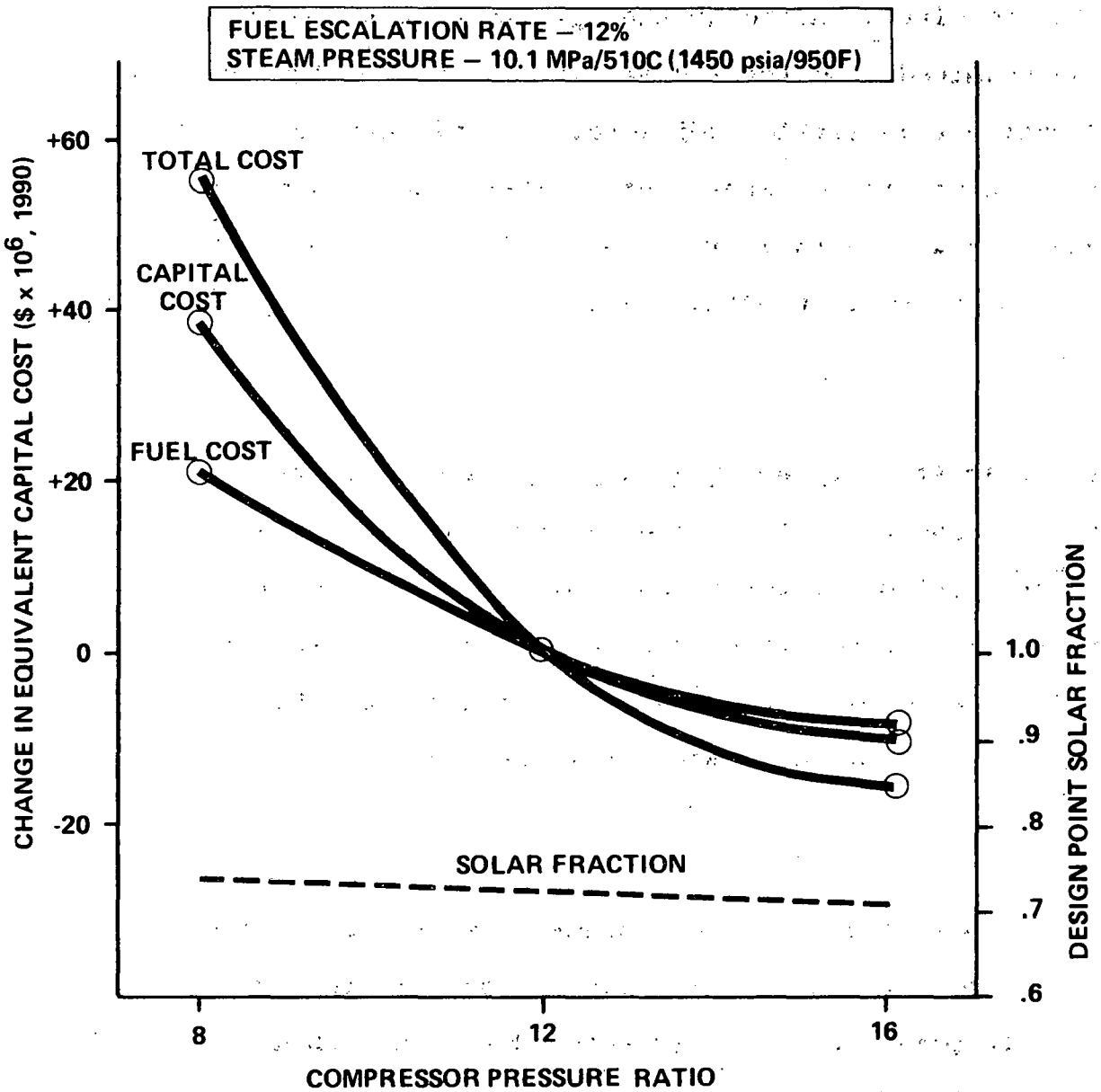

Figure 3-41 COST EFFECTS OF ADVANCED STRAWMAN COMPRESSOR PRESSURE RATIO

$$T_{EXH} = T_{IN} \left(\frac{P_{EXH}}{P_{IN}} \right)^{\frac{k}{k-1}}$$

where:

T_{IN} = gas turbine inlet temperature

$\frac{P_{EXH}}{P_{IN}}$ = reciprocal of the turbine pressure ratio

k = specific heat ratio

Calculated values for the gas turbine exhaust temperatures, based on the Strawman and Advanced Strawman gas turbine inlet temperatures, are shown in Table 3-23.

To extract the maximum heat from the gas turbine exhaust, it is desirable to minimize the HRSG gas outlet temperature. The technical limit is the acid dewpoint temperature at the end of the gas path in the HRSG on the metal tube surface. This metal temperature should be maintained above 121C (250F) to minimize cold end corrosion. A minimum HRSG exhaust temperature of 149C (300F) was selected for parametric analysis.

The pinch point temperature difference is also a significant factor. (This is discussed in Subsection 3.6.1.) For practical designs, the minimum pinch point temperature difference should not be less than 16.7C (30F). This consideration was of particular significance in the Strawman design.

The optimum steam pressure and temperature combination for the Strawman with a pressure ratio of 12 is approximately

TABLE 3-23

EXHAUST TEMPERATURE VS. PRESSURE RATIO

Compressor Pressure Ratio	Exhaust Temperature, C(F)	
	Strawman	Advanced Strawman
8	614 (1137)	781 (1438)
12	538 (1001)	688 (1270)
16	491 (915)	629 (1165)

6.0 MPa/441C (850 psia/825F), as shown in Figure 3-42. This case is pinch point limited with an evaporator temperature of 287C (549F) and a HRSG gas outlet temperature of 172C (342F). Methods for reducing the gas outlet temperature have been investigated and are presented in the following discussions on "Supplemental Firing of HRSG" and "Dual-Pressure Steam Cycle".

For the Advanced Strawman, with the optimum pressure ratio of 16, the best combination of pressure and temperature is between 10.1 MPa/510C (1450 psia/950F) and 8.7 MPa/482C (1250 psia/900F), as shown in Figure 3-43. These cases are not pinch point limited, since the calculated pinch points are between 22 and 28C (40 and 50F).

Supplemental Firing of HRSG. A burner system can be added to the HRSG to effectively increase the HRSG gas inlet temperature and to increase the power output of the steam turbine. The advantages of supplemental firing are:

- It can increase the total power output for the same gas turbine size.
- The operational flexibility can be increased, especially for part-load operation.
- It can overcome the pinch point limitation in the HRSG with a small amount of supplemental firing.

The primary disadvantage is that the supplemental heat input is utilized at the efficiency of the bottoming cycle, typically less

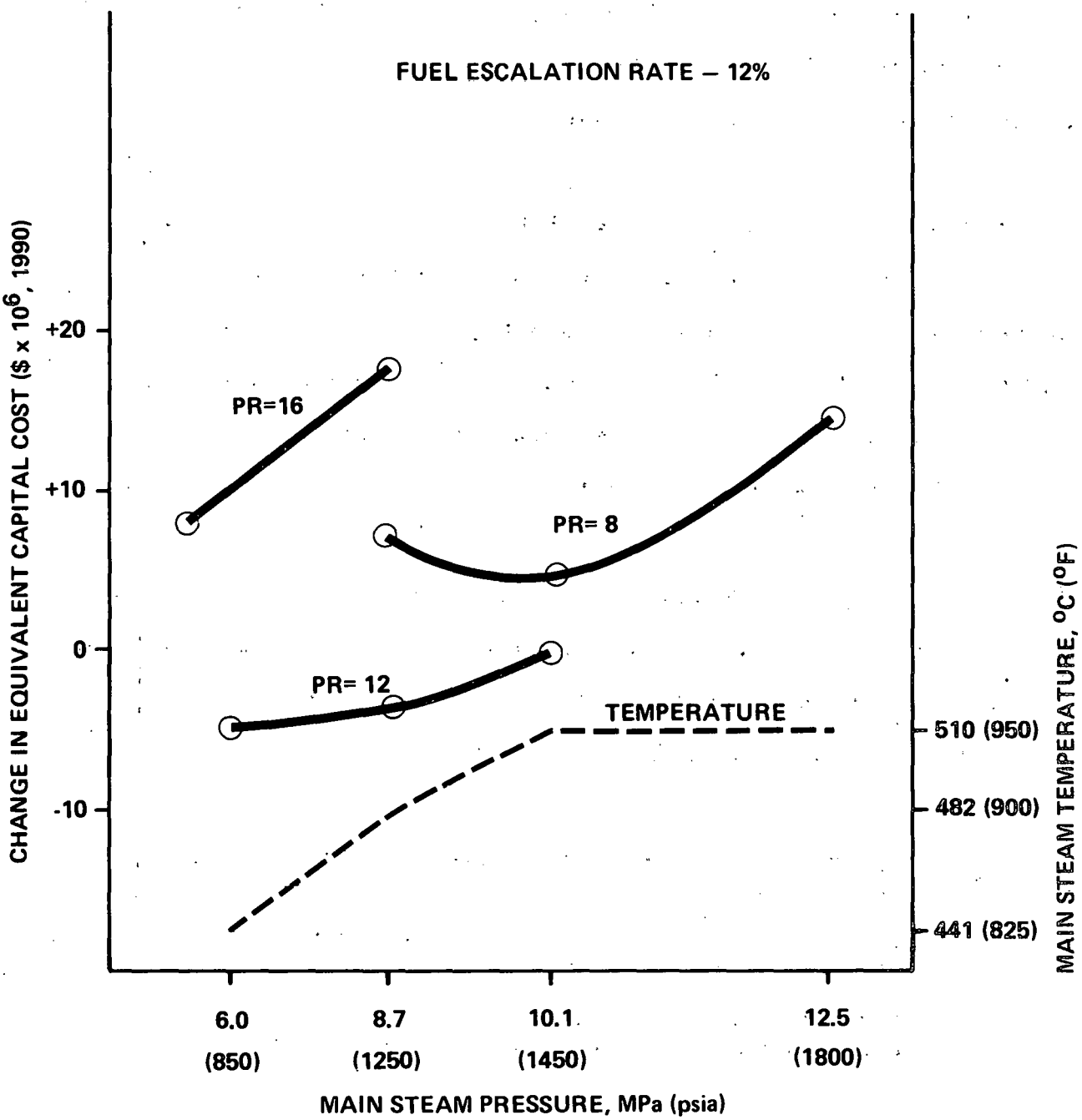

Figure 3-42 COST EFFECT OF STRAWMAN MAIN STEAM PRESSURE/TEMPERATURE

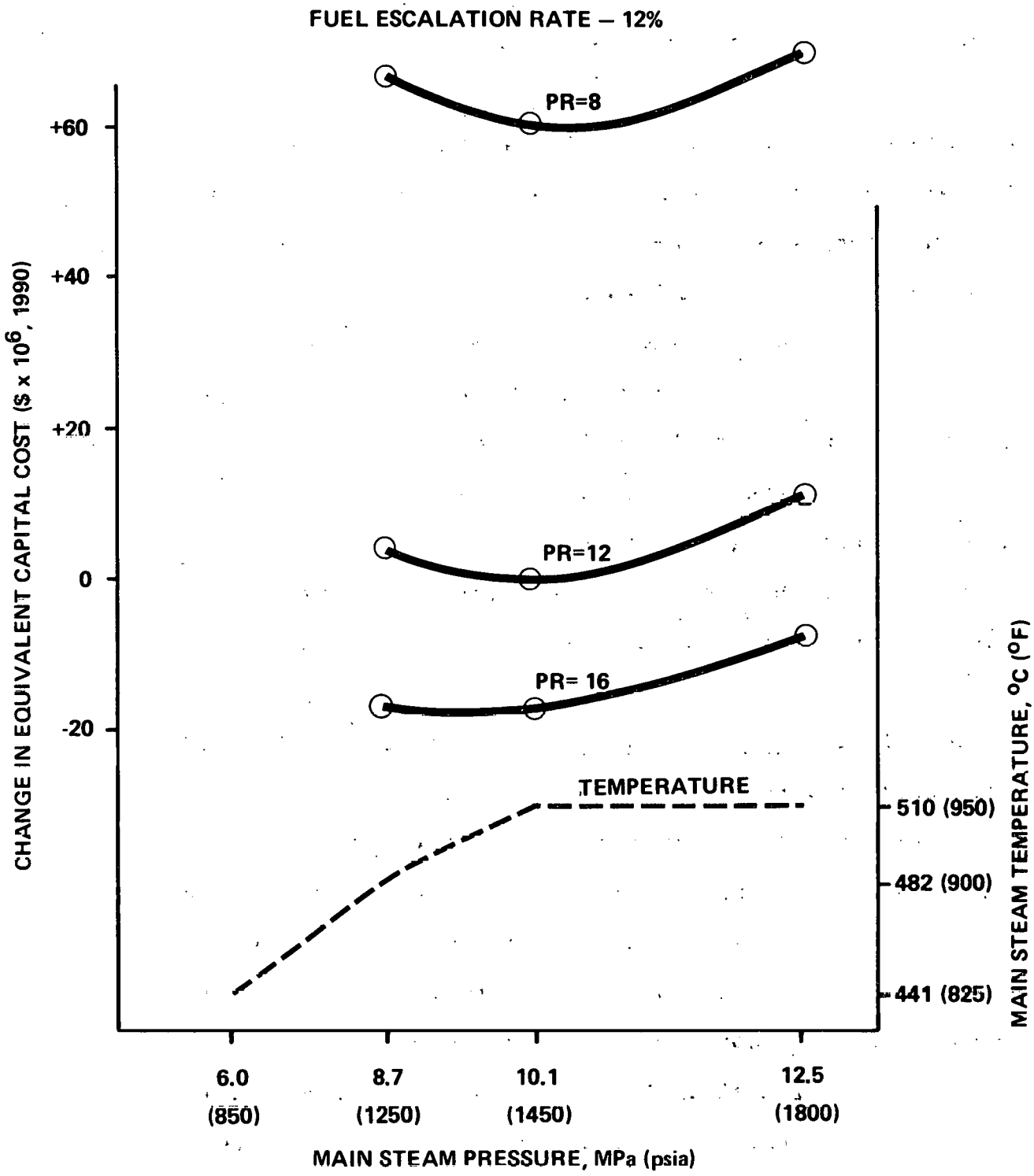

Figure 3-43 COST EFFECT OF ADVANCED STRAWMAN MAIN STEAM PRESSURE/TEMPERATURE

than 30 percent. Thus, both the net heat rate of the overall plant and its capital cost are higher.

A range of cases of supplemental firing were evaluated for the Strawman design including several combinations of steam pressure/temperature and the use of a reheat turbine. For the baseline 12 percent fuel escalation rate, none of the cases showed any economic advantage. Some economic advantage was observed in analyses using low-cost heliostats ($68 per m^2). It should also be noted that this firing of the HRSG also decreases the solar fraction. No fired HRSG cases were evaluated for the Advanced Strawman (since these cases were not pinch point limited), but the above reasoning for the Strawman is generally valid for the Advanced Strawman as well.

Intercooling and Aftercooling. Intercooling and aftercooling of the air during the compression process can have advantages in some Brayton cycles. Intercooling involves cooling the compressor air at an intermediate compressor stage. With intercooling the size of the compressor and the power consumption can be reduced, yielding a large gain in specific power. Conversely, aftercooling is used to reduce the temperature of the compressor outlet air. Both of these methods result in lower receiver inlet temperature, and the solar fraction is increased for a hybrid plant in relation to the amount by which the compressor discharge temperature is reduced. A higher pressure ratio is generally more favorable to intercooling. The

disadvantage is that, because of the low temperature, the extracted energy cannot be practically used in the power cycle.

The intercooling cases evaluated use an intercooler gas outlet temperature of 66C (150F) and a single stage of intercooling. As evident from the results shown in Figures 3-44 and 3-45 for the Strawman and the Advanced Strawman, intercooling does not offer economic advantages in the hybrid plant. (The relative equivalent capital costs are all positive, indicating that they are more expensive than the base case.)

Aftercooling of the compressor discharge does not impact the compressor specific power but does produce heat that is useful to the steam cycle. The Strawman design was evaluated with an aftercooler air outlet temperature of 149C (300F). The heat rejected to the aftercooler was used to generate additional intermediate-pressure steam for a dual-pressure steam cycle. The aftercooler significantly increased the solar fraction and increased the relative output of the steam turbine. However, there was a loss in plant performance, since the rejected heat was utilized at the bottoming cycle efficiency.

Steam Turbine Reheat. Steam turbine reheat can improve the efficiency of the steam bottoming cycle and has an economic advantage in most steam power plants. However, a survey of turbine manufacturers concluded that efficient steam turbines with reheat are not generally available below about 75 MWe.

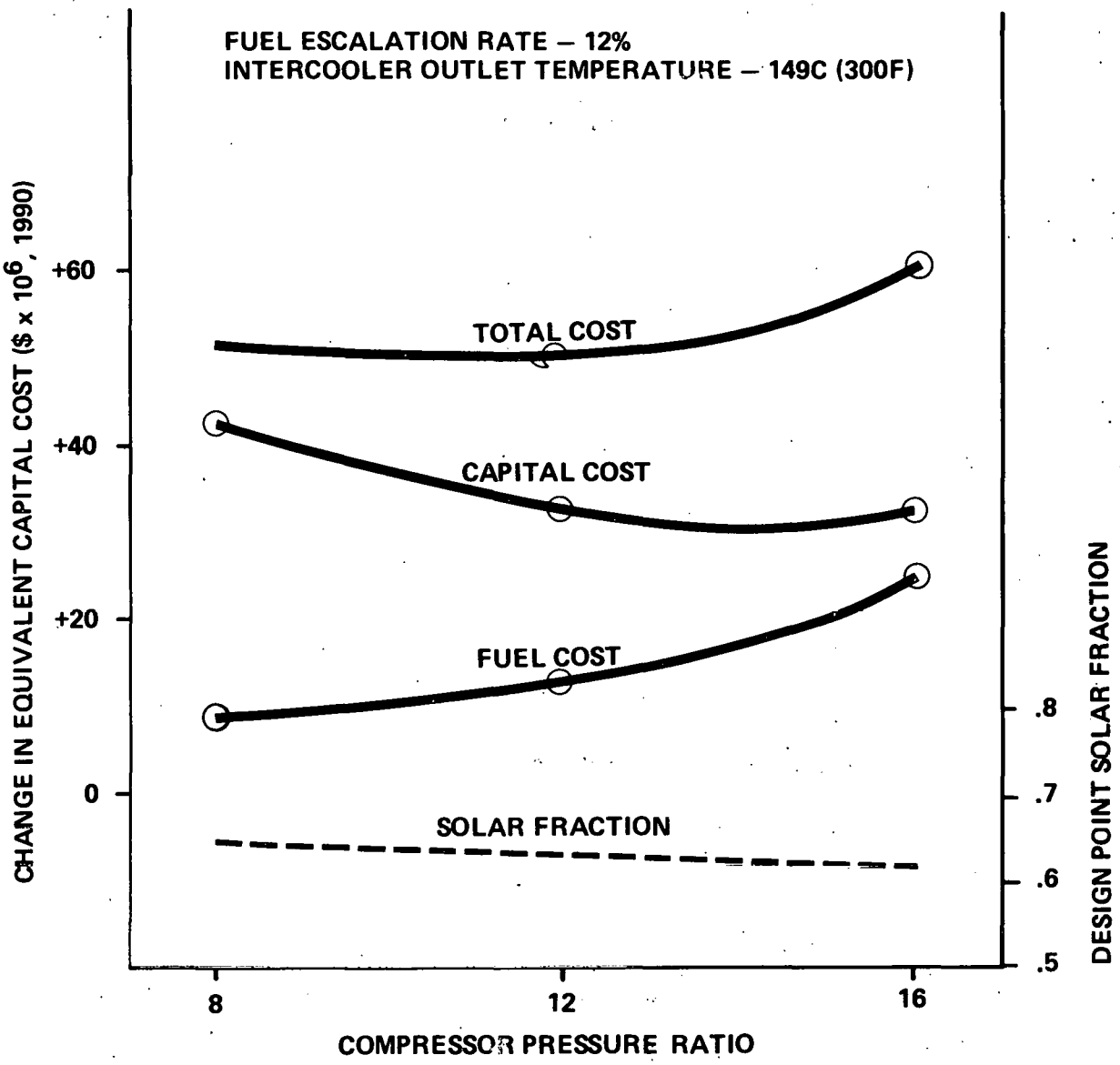

Figure 3-44 COST EFFECT OF STRAWMAN COMPRESSOR INTERCOOLING

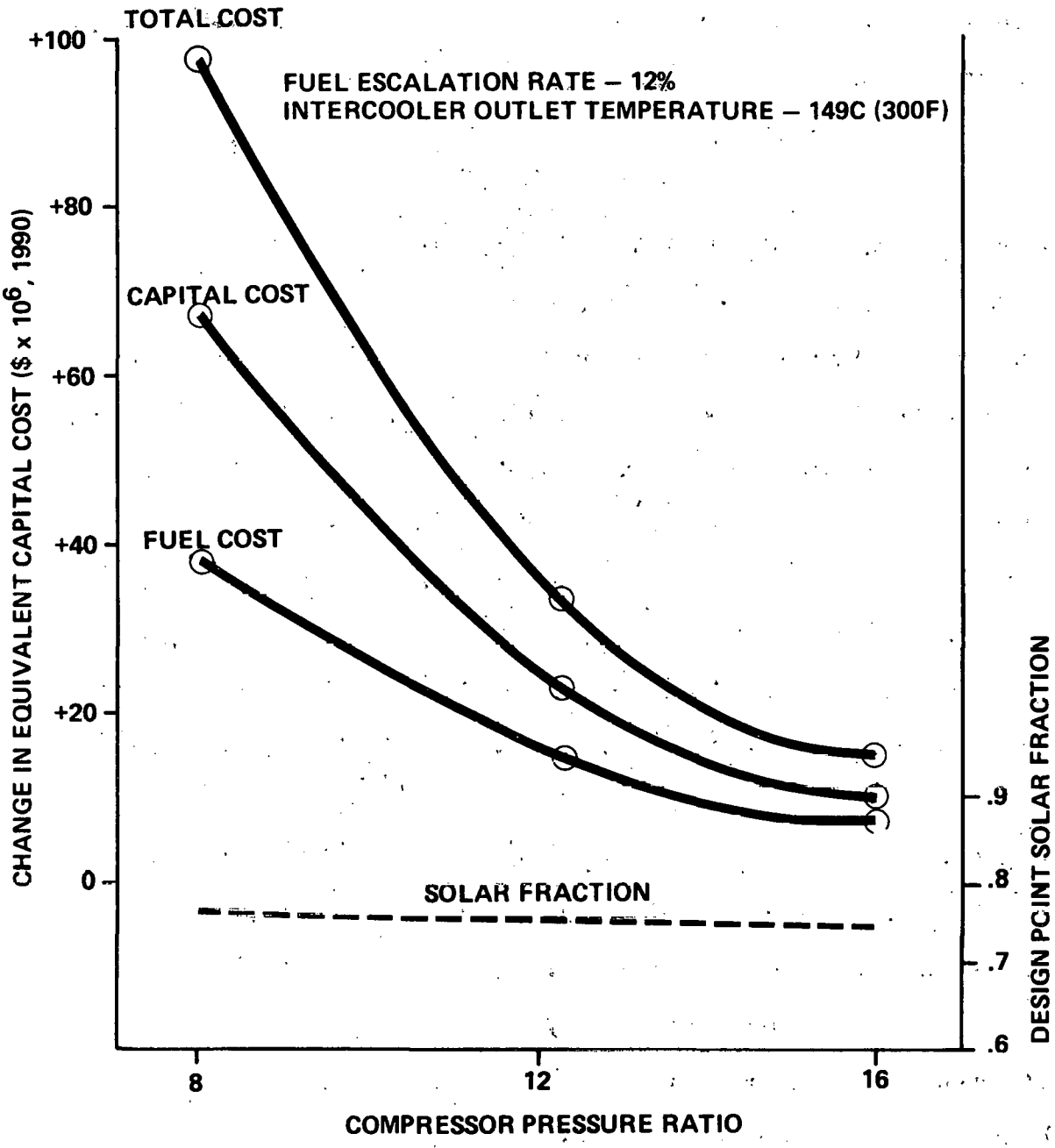

Figure 3-45 COST EFFECT OF ADVANCED STRAWMAN COMPRESSOR INTERCOOLING

Several manufacturers stated that they could supply such units, but that it would not be a standard design. There has been little incentive for developing small reheat turbines, but a few units of 50 MWe capacity or less have been built and are operating successfully.

Reheat was evaluated for both the Strawman and the Advanced Strawman. For the baseline Strawman, with 1043C (200F) turbine inlet temperature and unfired HRSG, not enough high-temperature heat is available in the gas turbine exhaust for reheat to be effective. Reheat can be successfully applied to the Advanced Strawman, since the pinch point does not interfere. A slight economic advantage was also found for the reheat cases evaluated. For the purposes of this study, it was concluded that steam turbine reheat should be considered an improvement with overall plant ratings above 200 MWe.

Dual-Pressure Steam Cycle. A steam cycle which uses two evaporators and produces steam at two different pressures for use in the steam turbine is one way to extract more energy from the Strawman HRSG to circumvent the pinch point limitation. This cycle arrangement has been used in studies involving integrated combined cycle/coal gasification plants, which require intermediate-pressure (IP) process steam. In the approach shown in Figure 3-46 a small amount of superheat is added to the IP steam to match the temperature of the turbine expansion line at the IP induction port. The result is a double pinch point and a

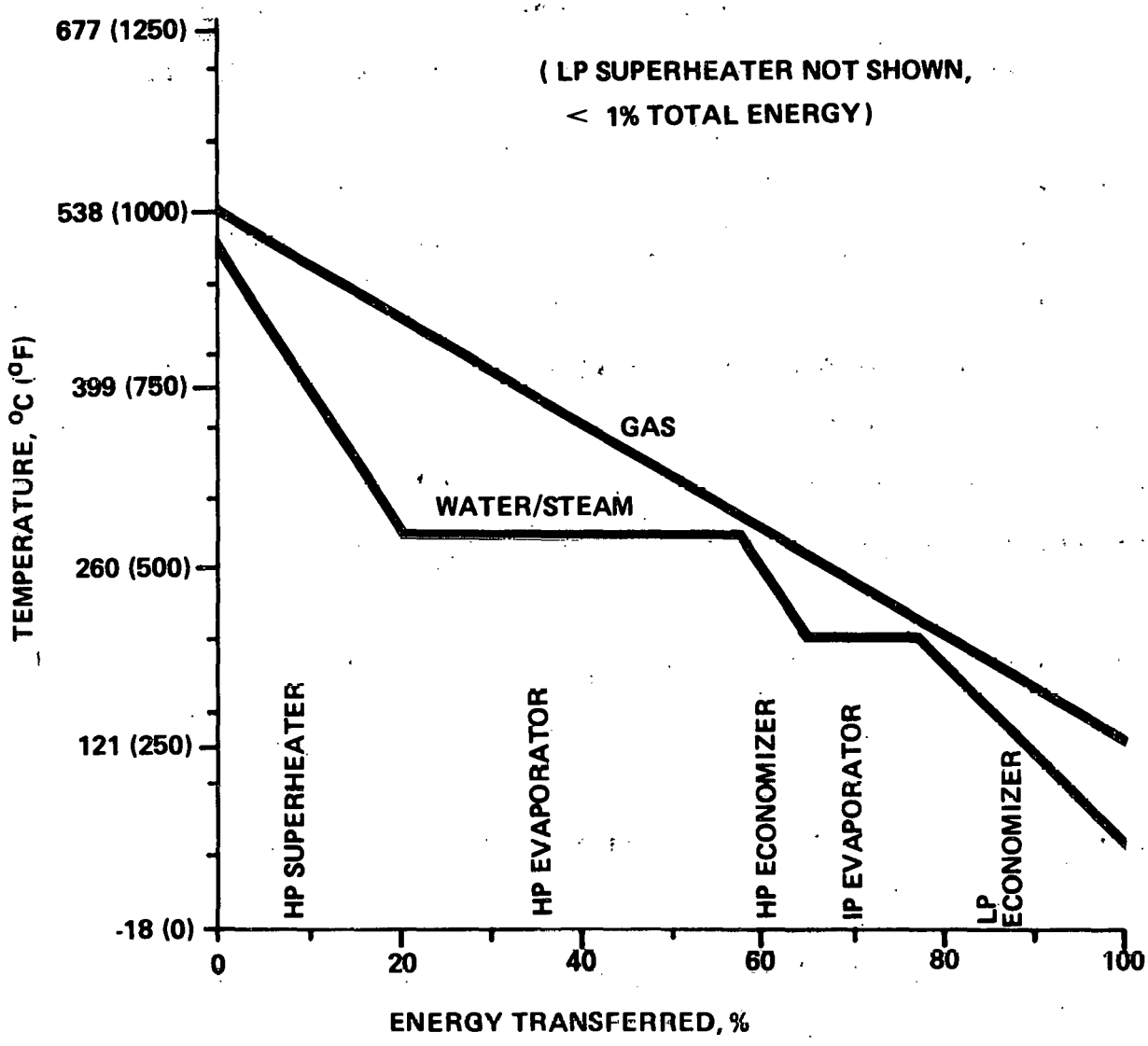

Figure 3-46 DUAL-PRESSURE HRSG TEMPERATURE PROFILE

better match between the gas and water/steam temperature profiles. A diagram of this cycle is shown in Figure 3-47.

Westinghouse studies of combined cycles with dual pressure indicated that, in general, the optimum main steam pressure for cycles like the Strawman design was approximately 6.9 MPa (1000 psia); the maximum attainable temperature is approximately 510C (950F) for a pressure ratio of 12 and using a 28C (50F) approach temperature at the HRSG gas inlet. Subsequent analysis of higher and lower pressures confirmed that this is approximately optimum when the net output for a given heat input was used as the figure of merit. The optimum IP steam pressure is usually between 20 and 25 percent of the main steam pressure, according to Westinghouse studies.

Preliminary estimates show that the optimum dual-pressure cycle will result in a 13 percent increase in steam turbine output over the baseline with no increase in the heat input. The calculated net heat rate for the cycle is approximately 7948 kJ/kWh (7534 Btu/kWh), corresponding to a net cycle efficiency of approximately 45.3 percent.

A reheat version of the same dual-pressure cycle was also examined. The discharge from the high-pressure turbine section is combined with saturated steam from the IP drum and the mixture is routed through the reheater. A small gain in overall cycle

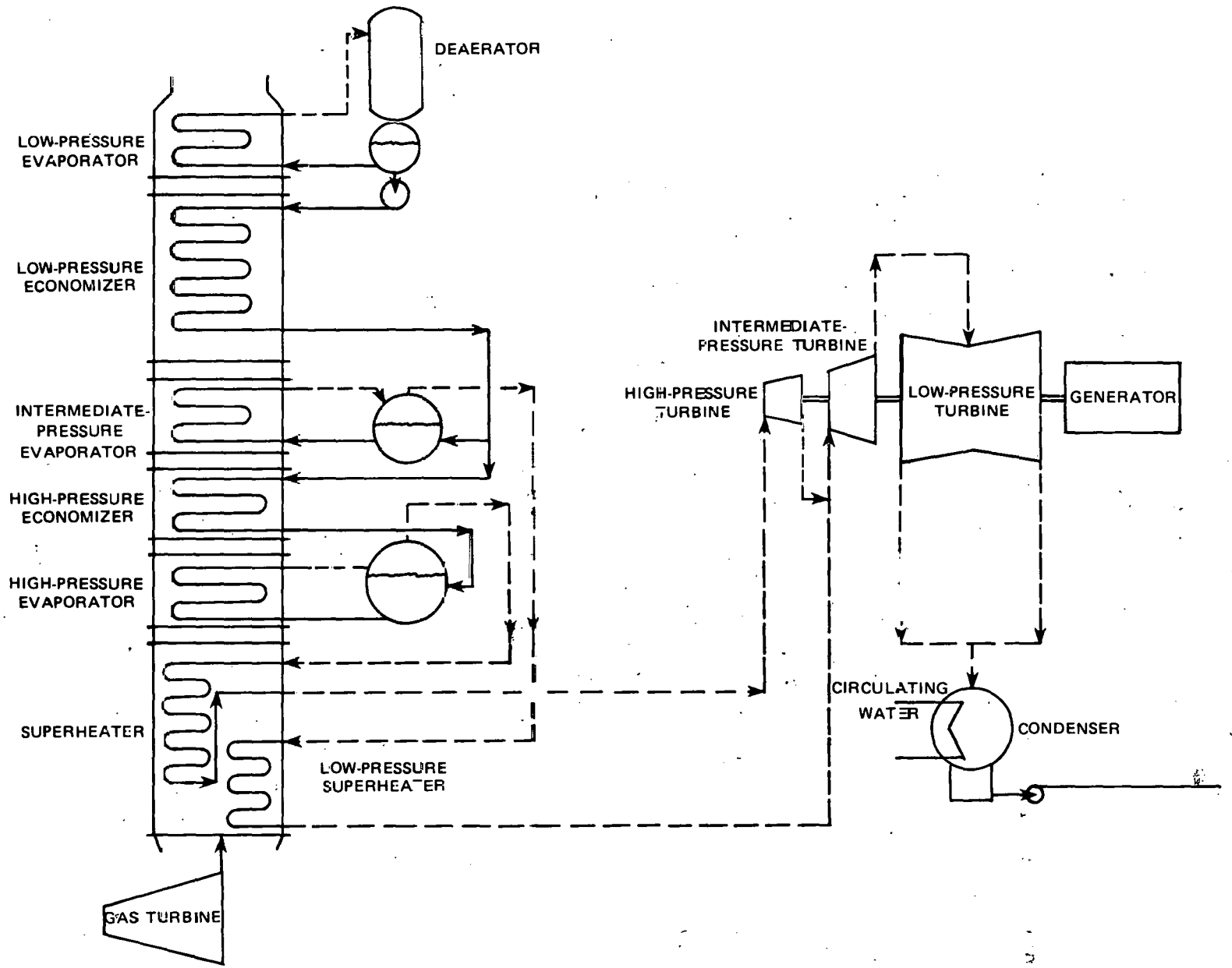
DEAERATOR
LOW-PRESSURE EVAPORATOR
LOW-PRESSURE ECONOMIZER
INTERMEDIATE-PRESSURE EVAPORATOR
HIGH-PRESSURE ECONOMIZER
HIGH-PRESSURE EVAPORATOR
SUPERHEATER
LOW-PRESSURE SUPERHEATER
GAS TURBINE
INTERMEDIATE-PRESSURE TURBINE
HIGH-PRESSURE TURBINE
LOW-PRESSURE TURBINE
GENERATOR
CIRCULATING WATER
CONDENSER

performance was found for this case, with a calculated heat rate of 7859 kJ/kWh (7449 Btu/kWh).

An additional advantage of the dual-pressure steam cycle is the ability to run at reduced gas turbine inlet temperatures. A calculation was made for a turbine inlet temperature of 871C (1600F) using a constant HRSG surface area and configuration, and decreasing the main steam temperature and pressure to match the steam flows at wide open turbine throttle valves. Under these conditions, the net power output would be 56.5 MWe with a heat rate of 9850 kJ/kWh (9340 Btu/kWh). The solar fraction with a receiver outlet temperature of 816C (1500F) would be 0.89. The capability to operate the hybrid plant to run at reduced output with high solar fraction significantly adds to the value of solar hybrid systems for utility companies. The economic advantage achievable for this cycle is shown in Table 3-21.

Conclusions. The results of the parametric analyses indicate that the preferred EPGS arrangement for the 100 MWe Strawman plant should have:

- A pressure ratio of 12
- A dual-pressure steam cycle with 6.9 MPa (1000 psia) and 1.7 MPa (250 psia) with 510C (950F) main steam temperature
- A total pressure drop of riser/downcomer and receiver of 82.7 kPa (12 psi), equally split between receiver and piping
- A gas turbine inlet temperature of 1093C (2000F)

The preferred EPGS arrangement for the 100 MWe Advanced Strawman plant should have:

- A pressure ratio of 16
- A single-pressure steam cycle with 8.7 MPa (1450 psig) and 510C (950F) main steam
- A total pressure drop of riser/downcomer and receiver of 137.9 kPa (20 psi), of which 103.4 kPa (15 psi) is for the receiver
- A gas turbine inlet temperature of 1316C (2400F)

3.7 MASTER CONTROL

The purpose of this subsystem is to coordinate the operation of the other subsystems and to allow the plant to respond as a whole to external signals such as load demand. The master control subsystem is also used for data logging and performance trending of system parameters.

Most of the work on the master control subsystem is concerned with collector subsystem control, which is identical in both the Strawman and the Advanced Strawman systems. Due to the conceptual level of the designs, only general control concepts have been evaluated for the receiver subsystem.

3.7.1 Master Control Concepts

The major considerations for design of the master control subsystem are:

- Compatibility with other subsystem controls
- Transient response time requirements
- Operational flexibility
- Simplicity and reliability
- Maximum stability
- Cost effectiveness

The block diagram of the baseline preconceptual master control subsystem, applicable to both the Strawman and Advanced Strawman concepts, is shown in Figure 3-48. It consists of a hybrid control system, which has an analog control for the receiver and combined cycle portions of the plant. This is consistent with current power plant practice and easily compatible with the analog control circuitry of the gas turbine, steam turbine, and HRSG. A central computer is provided for the collector subsystem since it has a digital control profile. An interface device is needed for analog-to-digital conversion and an operator's control panel is provided.

Two alternative concepts have been proposed. The first is a large computerized centralized processing unit (CPU) which has overall control of the plant and is capable of such functions as

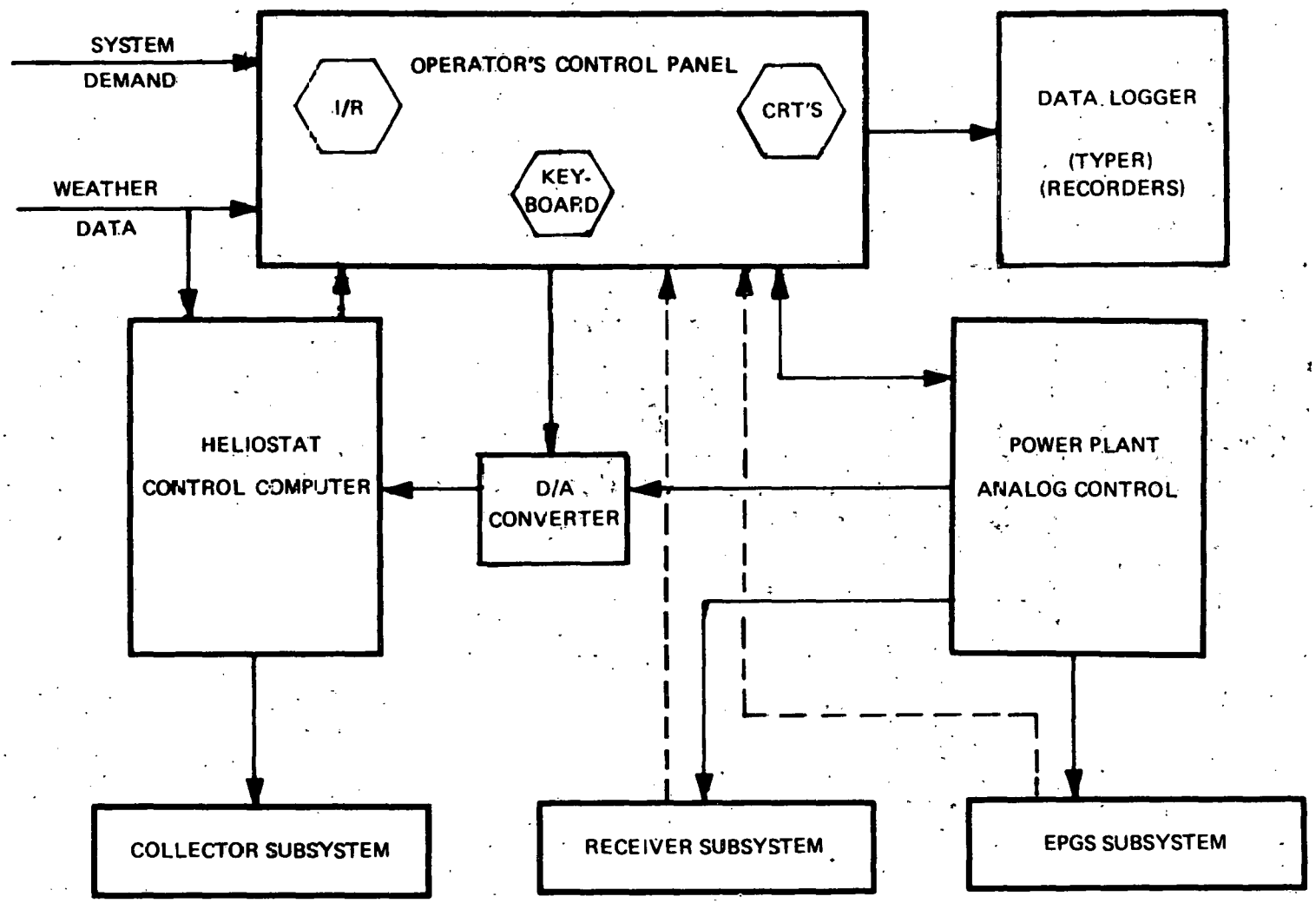

Figure 3-48 MASTER CONTROL BLOCK DIAGRAM

automatic startup and load following. A centralized computer system has been proposed by Westinghouse on their PACE combined cycle plants but utility acceptance was limited.

The other approach is to use an overall digital philosophy but to use microprocessors dedicated to important control loops rather than a large CPU. This has the advantage of easy coordination, maximum reliability, and low cost. Westinghouse's Instrument Systems Division has recently proposed this approach for combined cycle control. An evaluation of these proposed concepts for use in the solar hybrid system was conducted during the conceptual design task.

Collector Subsystem Control Concepts. Concepts for collector subsystem control range from master computer control of all heliostat positions, to master computer controls providing only trigger signals to heliostat positional control by "smart" heliostat controllers at each heliostat. Intermediate concepts between these extremes feature heliostat group control by heliostat field controllers. Master computer control of all heliostat positions, which would have to perform 5000 to 6000 mirror steering algorithms per second, would represent a massive computing and communication load.

The basic tradeoffs for the collector subsystem segment of the master control subsystem center on the degree of decentralization of the computation of the heliostat steering algorithm.

The two basic candidate configurations of collector subsystem control, intermediate and decentralized, are shown in Figure 3-49.

Both systems meet the control requirements for the collector subsystem and are different primarily in the state-of-the-art of their development. They can be considered as sequential evolutionary steps of the same basic system. The intermediate system uses components and software currently in production for technically similar equipment at most points and only slightly modified production components for the remainder. The decentralized system combines the "heliostat-essential" elements of the field and heliostat controllers into a unitized, so-called "smart heliostat controller" for low-cost high-volume production.

In the intermediate heliostat control approach, an array of about 200 heliostats is controlled through a heliostat field controller (HFC). This consists of a minicomputer-multiprogrammer network interfaced at the minicomputer to the heliostat array controller (HAC) and at the multiprogrammers with the individual heliostat controllers. The HAC calculates and transmits to the HFC:

- Solar vector direction cosine data
- Operating mode specification data
- Target coordinate data

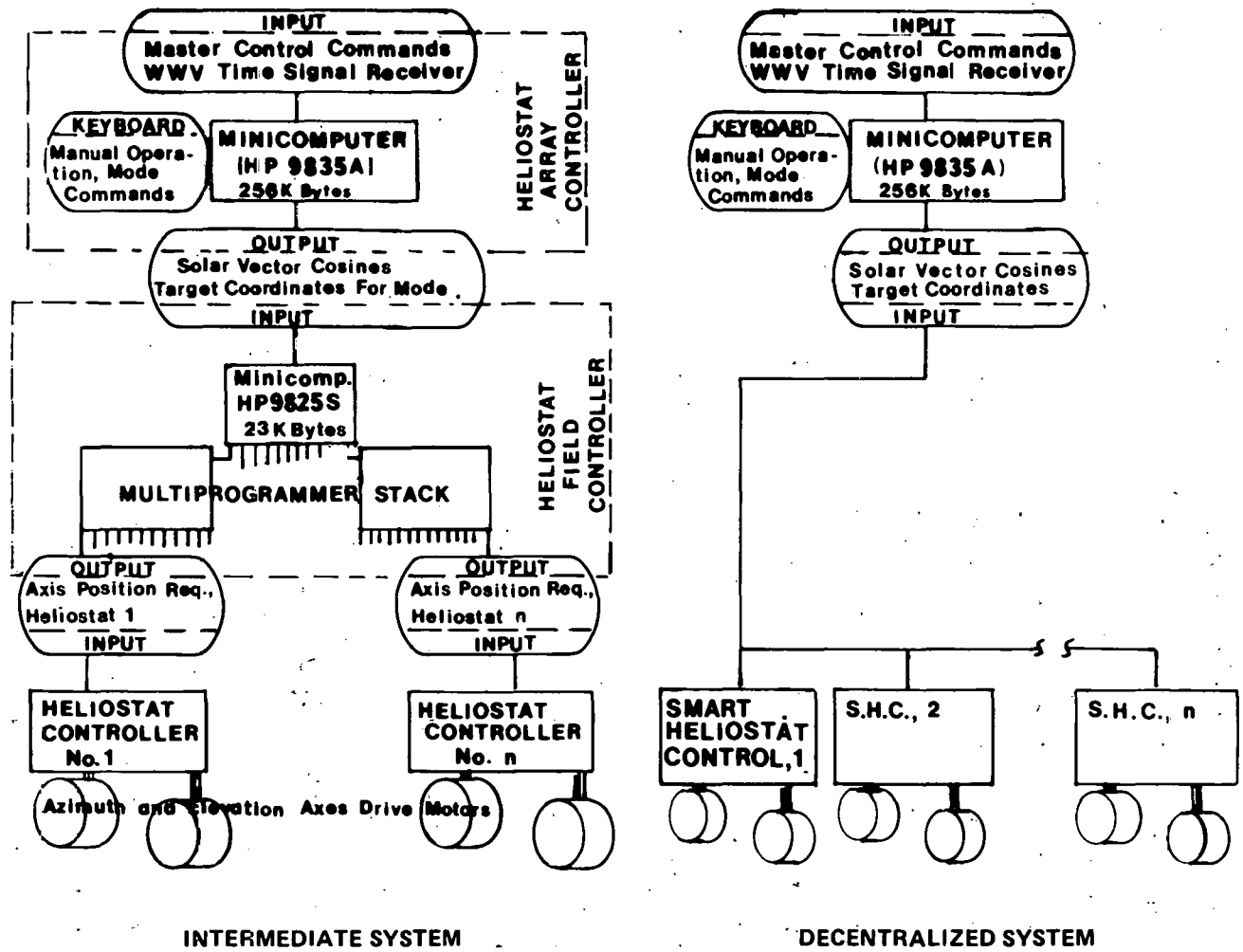

INTERMEDIATE SYSTEM

DECENTRALIZED SYSTEM

Figure 3-49 COLLECTOR SUBSYSTEM CONTROL SCHEMATICS

The HFC (nominally an HP 9825S minicomputer) then performs the steering algorithms for each heliostat in its group and communicates the individual requirements to the multiprogrammer for communication, execution, and verification interaction with the HAC. Both the minicomputer and multiprogrammer are widely used in process control and data acquisition applications. The 200 heliostat field grouping permits mode control and flux control for subsystem segments as small as 4 percent of the heliostats. This is well within the 10 percent specified in the Requirement Definition. The size of the HFC minicomputer is approximately one-tenth of the HAC computer - 23,000 byte storage vs. 256,000 byte storage. Both computers are equipped with 217,000 byte magnetic tape storage which will likely by accessed only as mode changes are made.

The HAC (a 256,000 byte memory version of the HP9835A minicomputer) interfaces with the master control and a time signal generator at its input, and with the approximately 25 field controller computers at its output. It performs an ongoing update of the solar vector calculation and transmits the updated direction cosines approximately once a second to the field controllers. The HAC program routines also establish the required target X,Y,Z coordinates for the field for the applicable operational mode. The target coordinates vary with the operational mode and are acted upon by the steering algorithm to achieve the desired reflected beam and axis positioning.

In the decentralized heliostat control approach, the controllers employ the technology currently used in so called "X-Y plotters". In both the heliostat control and plotter applications, the required positions of two independently powered axes are calculated externally and communicated to an internal microprocessor control at the heliostat, which executes the required positional drive response. The microprocessor control electronics of the plotters serve as foundation for the design of the heliostat control. In addition to providing fast and accurate response to calculated position commands, the plotter control has an override mode, which is basically similar to the acquisition and stow modes of a heliostat.

Similar to the plotter technology, the heliostat drives use stepper motors and calculated positions based on step count rather than either AC or DC motors with encoder position monitoring. Baseline position knowledge derived from limit switches at the ends of travel in the plotter would be used with the heliostats.

<u>Collector Subsystem Control System Selection</u>. The intermediate collector control system has the advantages of:

- Low capital cost
- Low operation and maintenance cost
- High reliability
- System flexibility

By using proven methods and equipment for technically similar applications, the collector control can take off from a base of current industrial practice and technical maturity with a minimum of development.

For near-term minimum cost, equipment already widely produced was selected. For high reliability and flexibility, the same manufacturer's proven equipment was chosen for all three controller levels. The intermediate system is available for immediate application with prototype heliostats, the hybrid critical experiment, and/or the first full hybrid plant. Operational experience with the intermediate system in one or more of the early solar installations is desirable before establishing the detailed configuration of the decentralized control.

The evolutionary step to the decentralized control involves: 1) simplifying the design to narrow the electronics to only those required by the heliostats and 2) combining the computational and response functions at the heliostat controller.

Receiver Control Concepts. As discussed in Subsection 3.3.9, the best approach to the operation of the receiver is to use constant air flow, which simplifies the necessary controls. The flow to the panels of a receiver cavity can be set by fixed dampers at the inlet to each panel. The required daily adjustments in the distribution of flows to individual cavities can be accomplished

with butterfly valves in the riser branch pipes. The outlet temperature from each panel is monitored and if the maximum allowable temperature is exceeded, a signal is given to defocus the heliostats. The receiver bypass is conceptually a series of block valves. Figure 3-50 shows the relationship between the receiver control blocks and master control subsystem.

EPGS Control Concepts. The control concept for the EPGS is very similar to that for a conventional combined cycle plant. The controls for the HRSG, the steam cycle, the electrical equipment, and the balance of plant equipment is identical to the conventional plant. The gas turbine, especially the combustor, presents some conditions unique to this type of plant, although not really new in concept. Figure 3-50 shows the relationship between the EPGS control blocks and the master control subsystem.

3.7.2 Master Control Analysis

Collector Subsystem Control. Primary control requirements for the collector subsystem are stated in the Requirement Definition as follow:

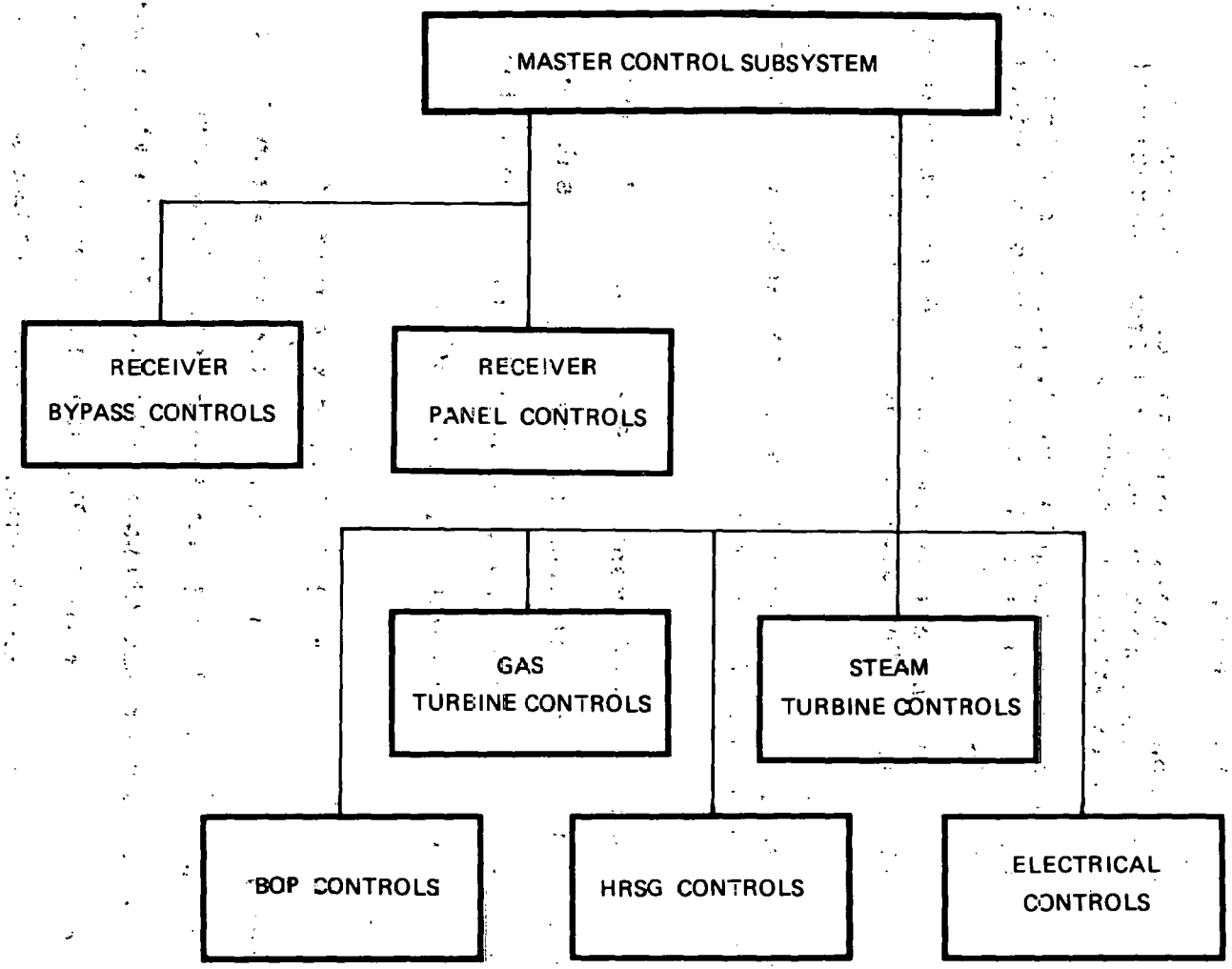

Figure 3-50 RECEIVER AND EPGS SUBSYSTEM CONTROL BLOCK DIAGRAM

- Performance

  Maximum pointing error for each axis must be 0.75 mrad (2.58 arc-min) at solar positions above 0.26 rad (14.9°) solar elevation angle.

- Operation

  - Flux must be variable between zero and maximum with step changes no larger than 10 percent of collector energy.

  - Positions to stow, cleaning, or maintenance orientation must be achieved from operational positions within 15 minutes.

  - Field control singularity (i.e., over-the-shoulder limits or gimbal lock) must be resolved within 10 minutes.

  - Orientation must be available to master control at all times. Calculated angles acceptable.

- Safety

  The collector field must be defocusable to less than 3 percent flux in 120 seconds.

Achieving the specified performance, operational, and safety requirements has been accomplished in the collector subsystem by incorporating key supportive features in the heliostat drive mechanical equipment, drive motors, and controls.

The pointing accuracy budget of 0.75 mrad per axis is split between mechanical backlash (0.38 mrad in the elevation drive and 0.45 mrad in the azimuth drive) and the control dead band (0.3 mrad). One step of the stepper motor results in the minimum potential control increment of 0.0075 mrad for the elevation axis and 0.0089 mrad for the azimuth axis. Control pulses as large as

30 steps are possible within the span of the control dead band and will be typical while operating in the tracking mode.

Control of flux variations with steps no larger than 10 percent is accomplished by sizing the collector segment serviced by each HFC. The conceptual design selection of 200 heliostat groups for unit HFC control results in flux steps of 4 percent of full power, well within the specified limit.

Positioning to stow, cleaning, or maintenance orientations within 15 minutes is accomplished with margin by the stepper motor speed of 1000 steps per second selected for slew operation. This results in time for full travel of 3.14 rad (180°) in elevation of 6.9 minutes and of 4.71 rad (270°) in azimuth of 10.4 minutes. For the Superior Model M112-FJ326 stepper motor of the Northrup II heliostat, rated torque is maintained over the range of 1 to 1500 steps per second. This heliostat is of the same generic design as the MDAC 49 m^2 heliostats (McDonnell Douglas Astronautics Company) and offers ready access to more detailed design data. This spans the planned motor speed range of the heliostat: tracking speed (250 steps per second) to slew speed (1000 steps per second).

To ensure that the collector resolves any field singularities within 10 minutes, a study was made of the heliostat tracking angles and tracking angle rates for summer, equinox, and winter for the heliostat positions around the field periphery and those

near the north-south centerline. Sample positions are shown on Figure 3-51 overlaid on the layout of the "G" field. Samples are identified from 1 to 10 taken counterclockwise around the western half of the layout. Results of the tracking angles and their seasonal variations are shown in Figures 3-52 through 3-61.

The first evident singularity is in the summer curve for Sample 3 and occurs at 17.5 hours. The heliostat does not lose tracking because the required azimuth rate of 332°/hr is within the azimuth tracking speed of 460°/hr. Samples 4, 5, 6, and 7 encounter both positive and negative singularities, but not of sufficient magnitude to lose tracking. Samples 8, 9, and 10 follow the benign pattern of samples 1 and 2, typical of heliostats generally north of the tower. With the "G" field, the singularity specification is met and exceeded, since heliostats continue tracking through periods of singularity.

Defocusing within 120 seconds is accomplished with a large margin, due to the slew speed needed to meet the "stow, cleaning, maintenance" requirement.

Receiver and EPGS Control. The analysis of control for these subsystems was limited to the identification of significant control issues for consideration in the conceptual design. These issues are:

- The reaction of the receiver and the combustor control systems to the rapid cloud passage transient

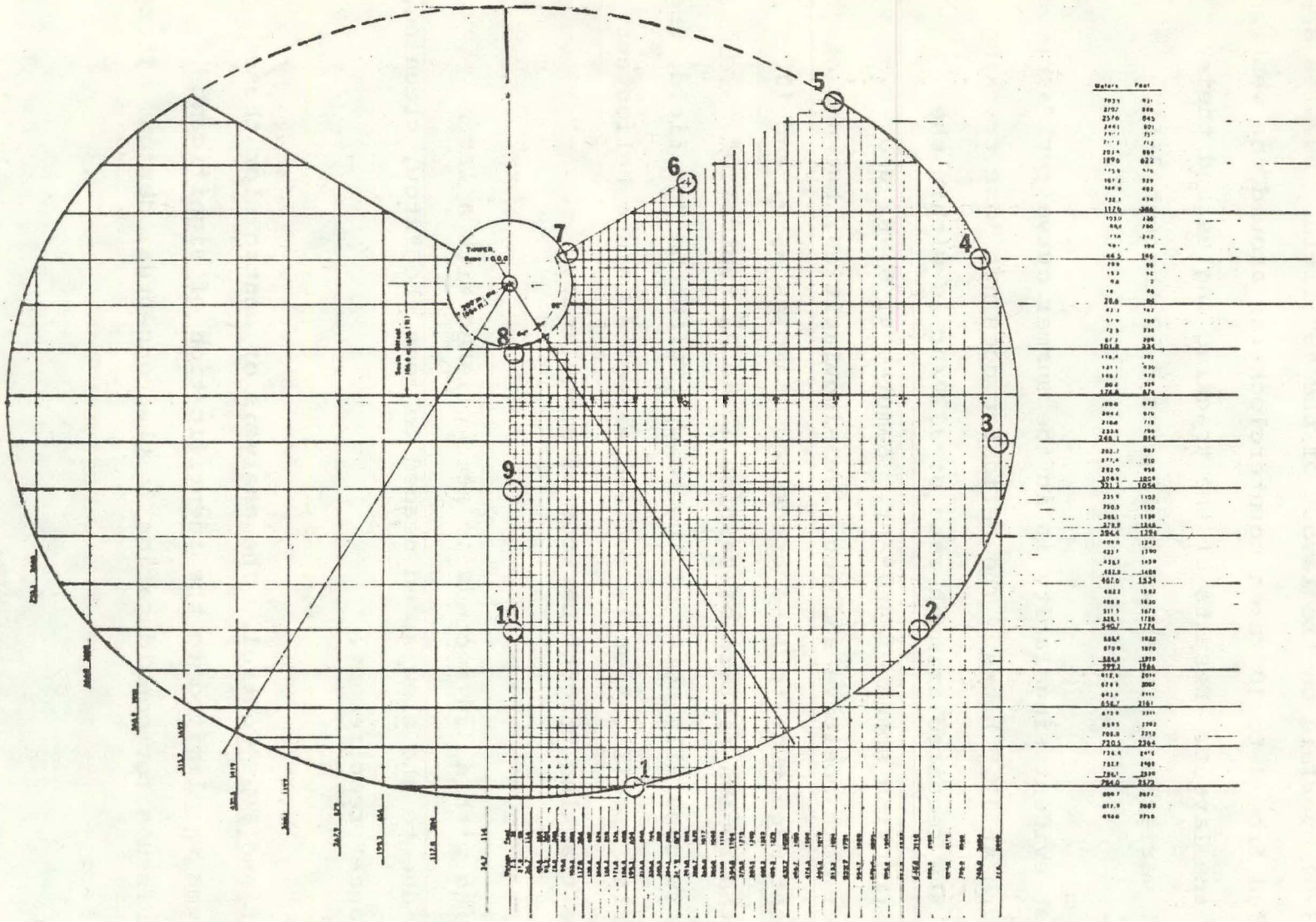

Figure 3-51 HELIOSTAT POSITIONS USED TO ANALYZE TRACKING SINGULARITY RATES

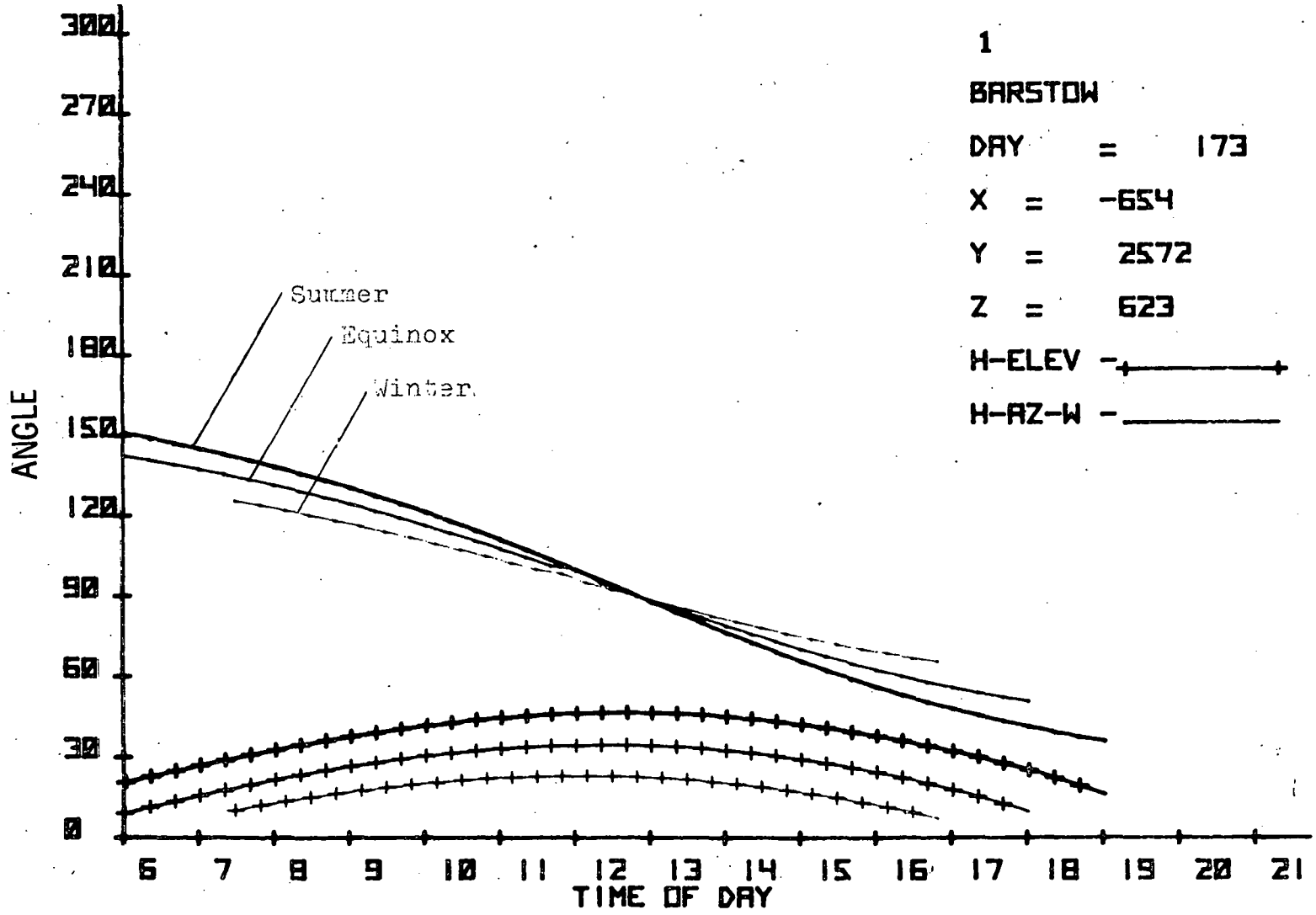

Figure 3-52 HELIOSTAT AXES TRACKING ANGLE PATTERN FOR SAMPLE 1 (53N, 15W)

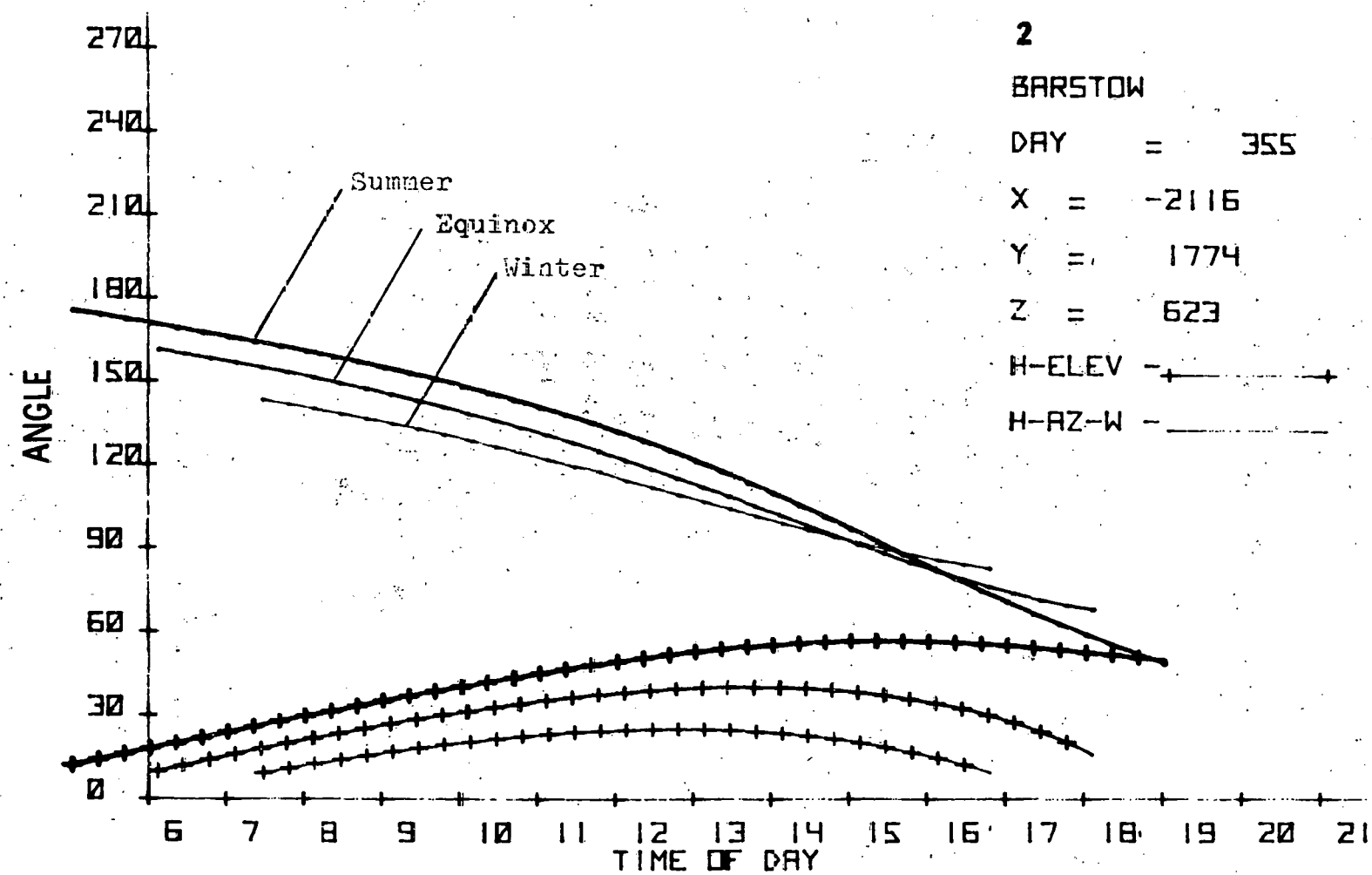

Figure 3-53 HELIOSTAT AXES TRACKING ANGLE PATTERN FOR SAMPLE 2 (37N, 41W)

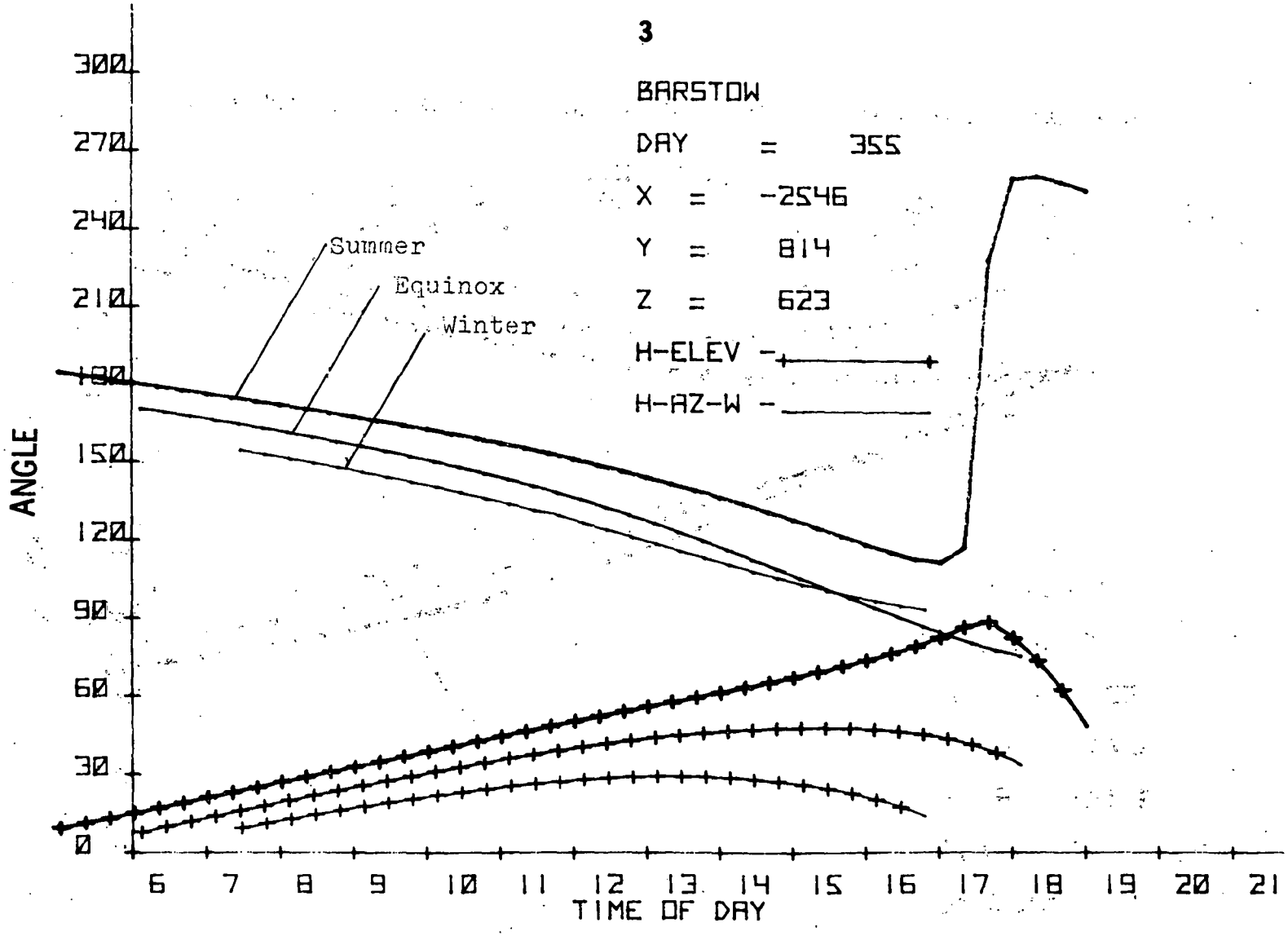

Figure 3-54 HELIOSTAT AXES TRACKING ANGLE PATTERN FOR SAMPLE 3 (17N, 46W)

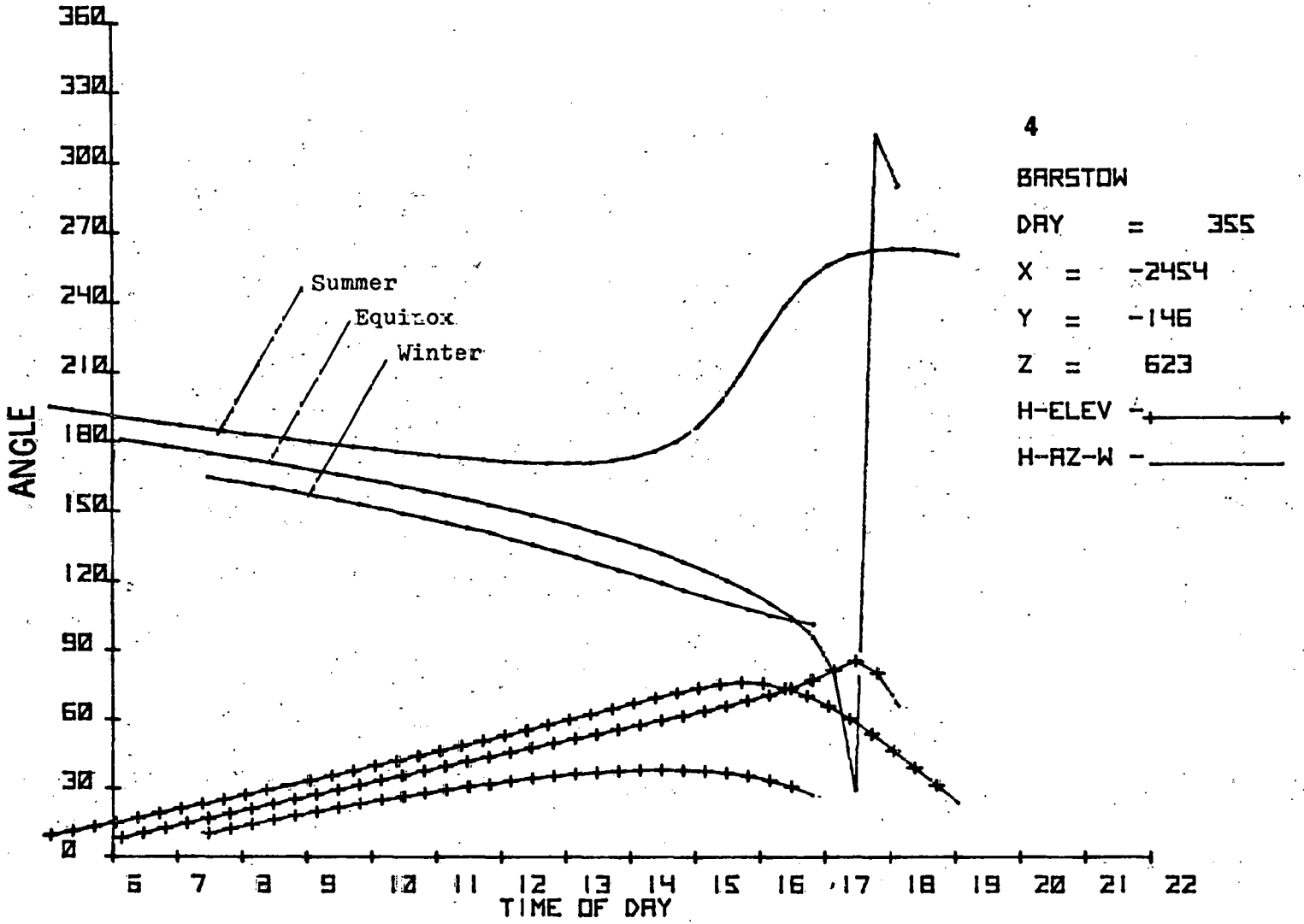

Figure 3-55 HELIOSTAT AXES TRACKING ANGLE PATTERN FOR SAMPLE 4 (4S, 45W)

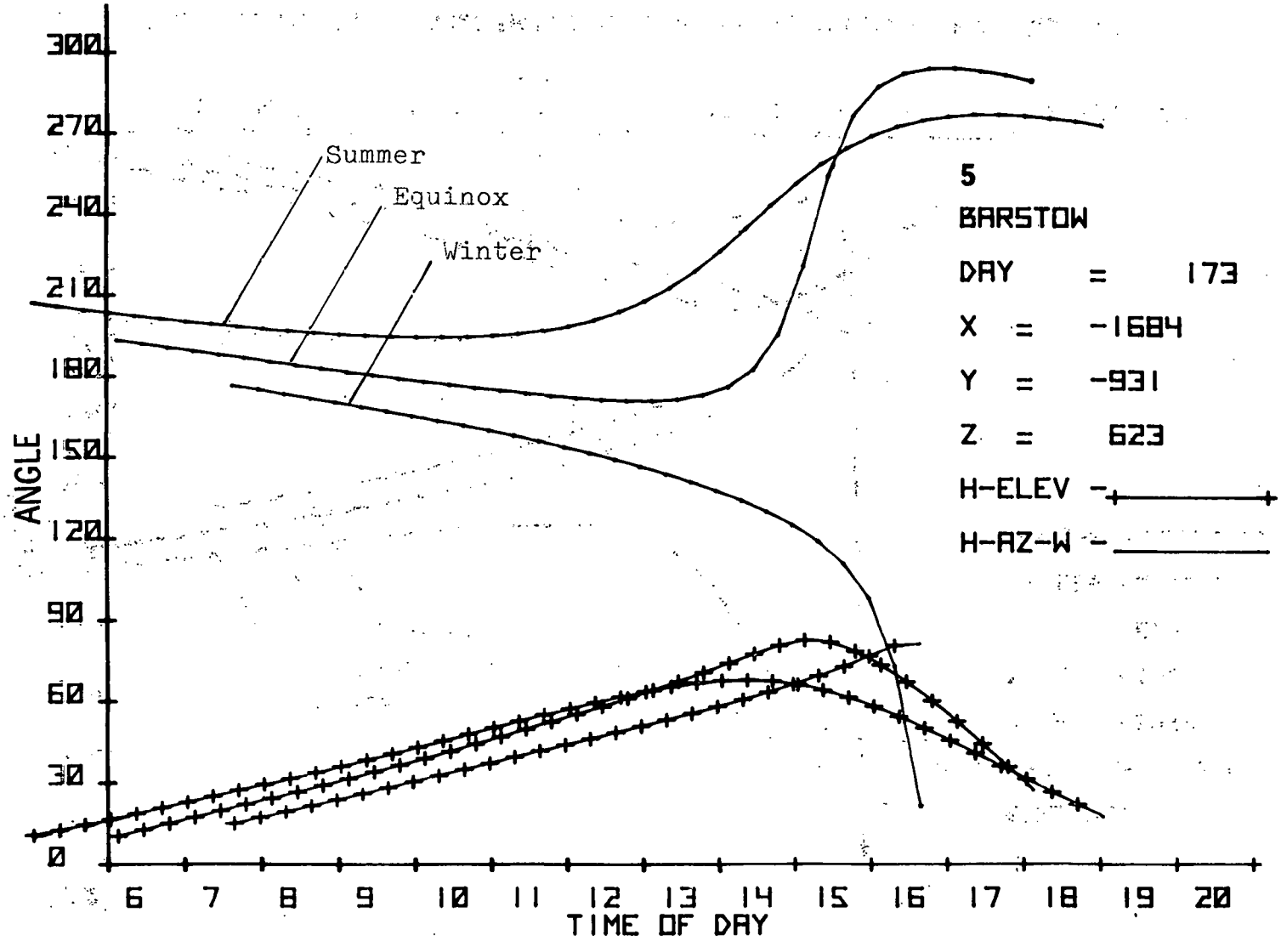

Figure 3-56 HELIOSTAT AXES TRACKING ANGLE PATTERN FOR SAMPLE 5 (21S, 35W)

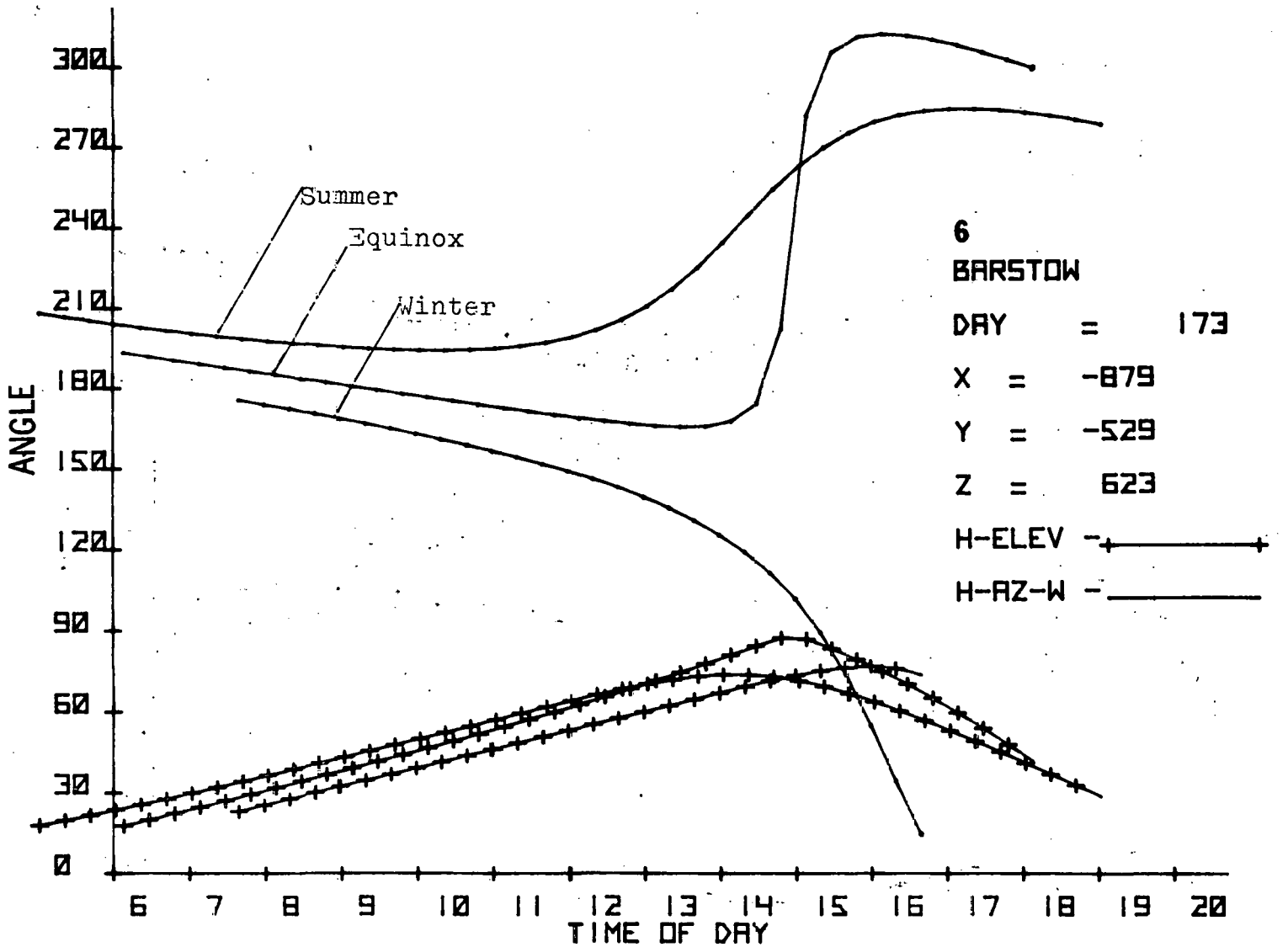

Figure 3-57 HELIOSTAT AXES TRACKING ANGLE PATTERN FOR SAMPLE 6 (12S, 20W)

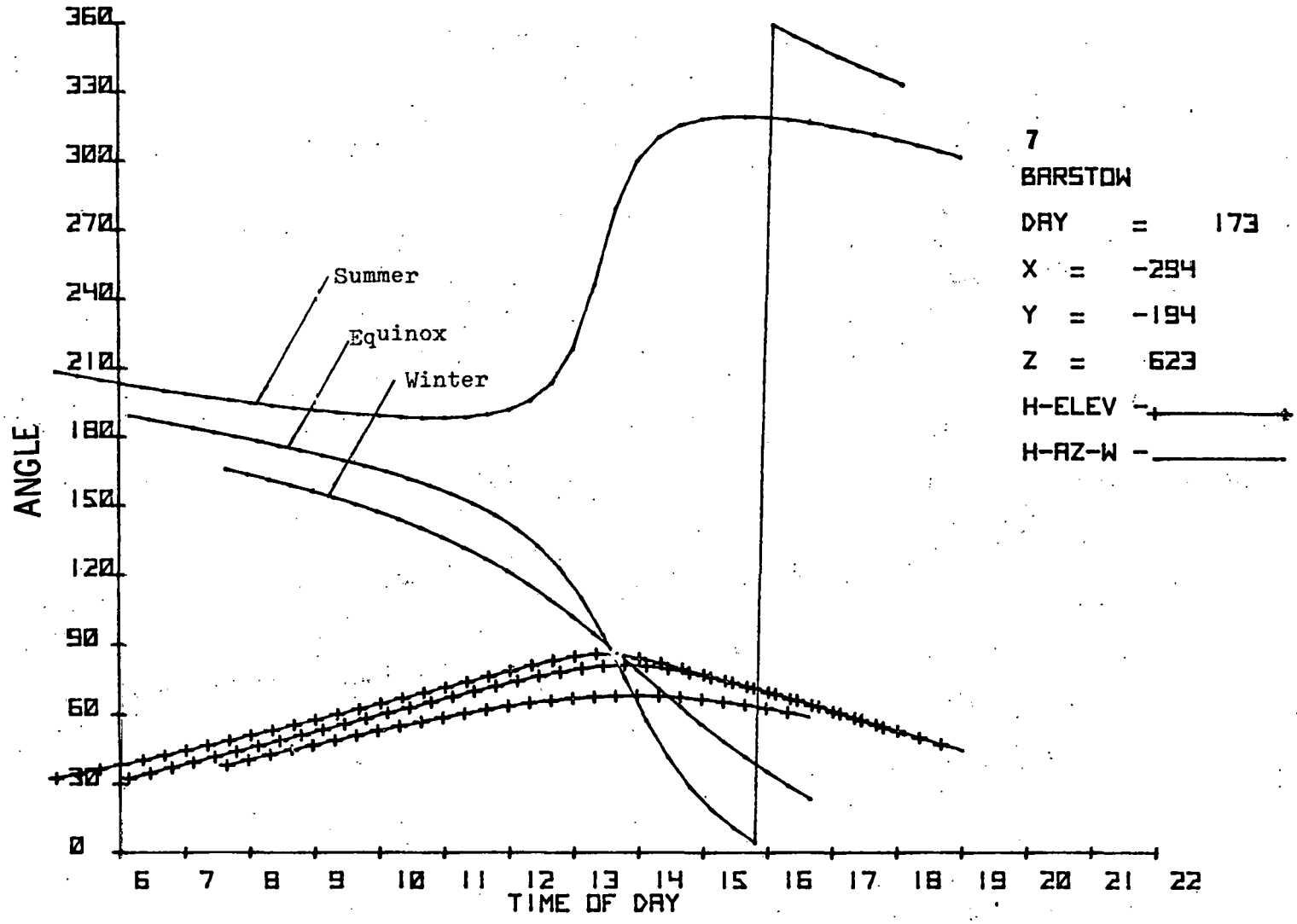

Figure 3-58 HELIOSTAT AXES TRACKING ANGLE PATTERN FOR SAMPLE 7 (6S, 7W)

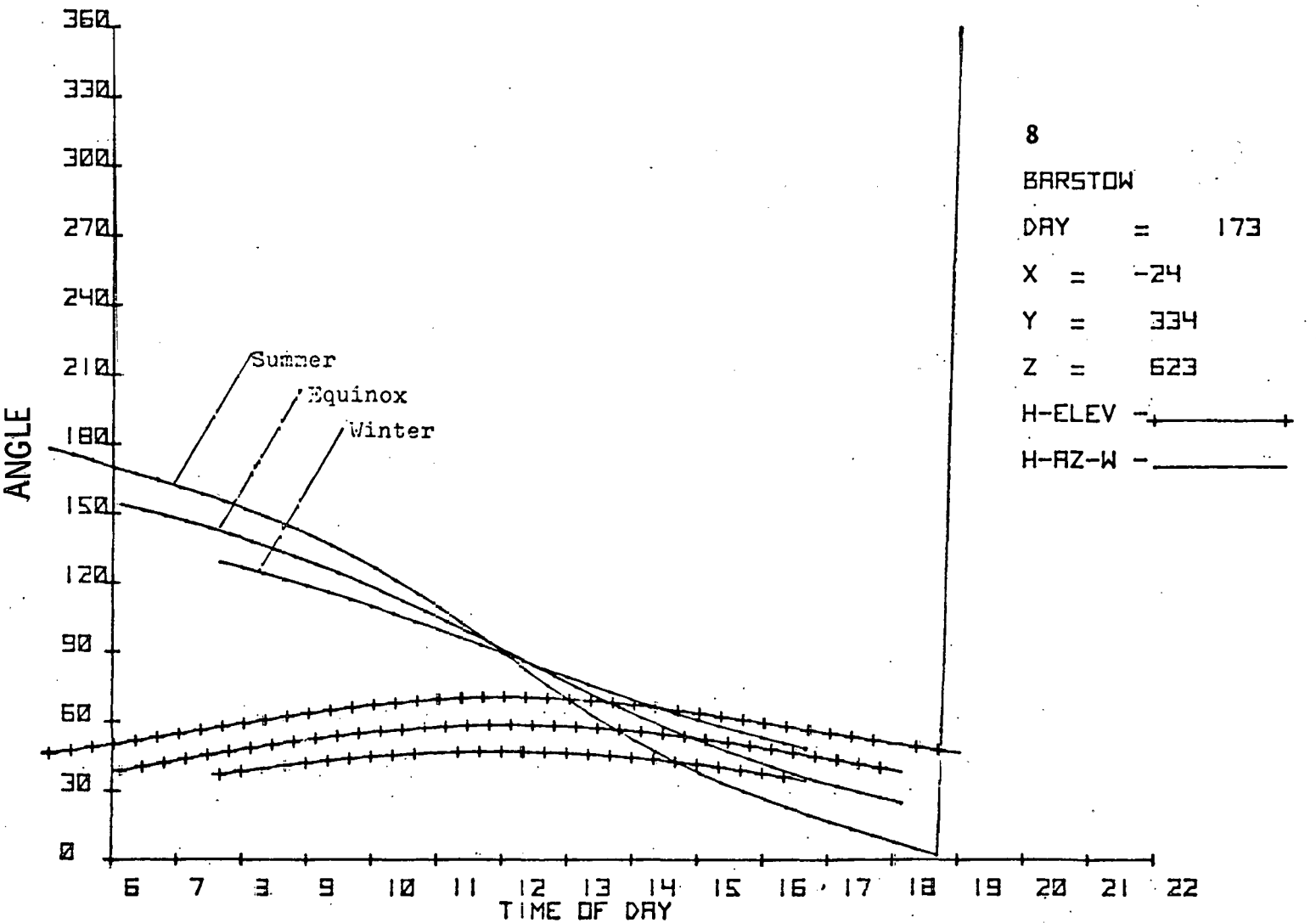

Figure 3-59 HELIOSTAT AXES TRACKING ANGLE PATTERN FOR SAMPLE 8 (7N, 1W)

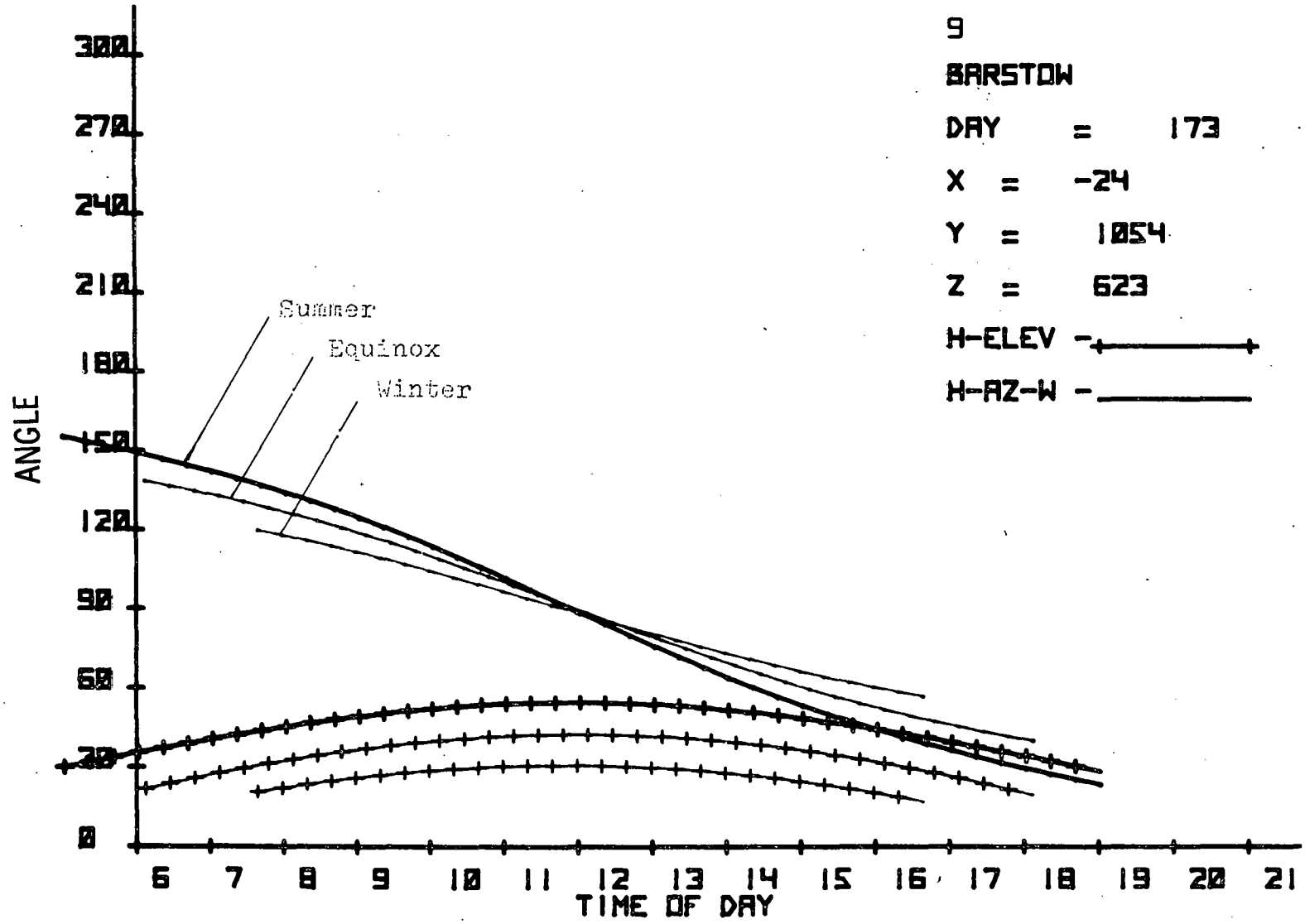

Figure 3-60 HELIOSTAT AXES TRACKING ANGLE PATTERN FOR SAMPLE 9 (22N, 1W)

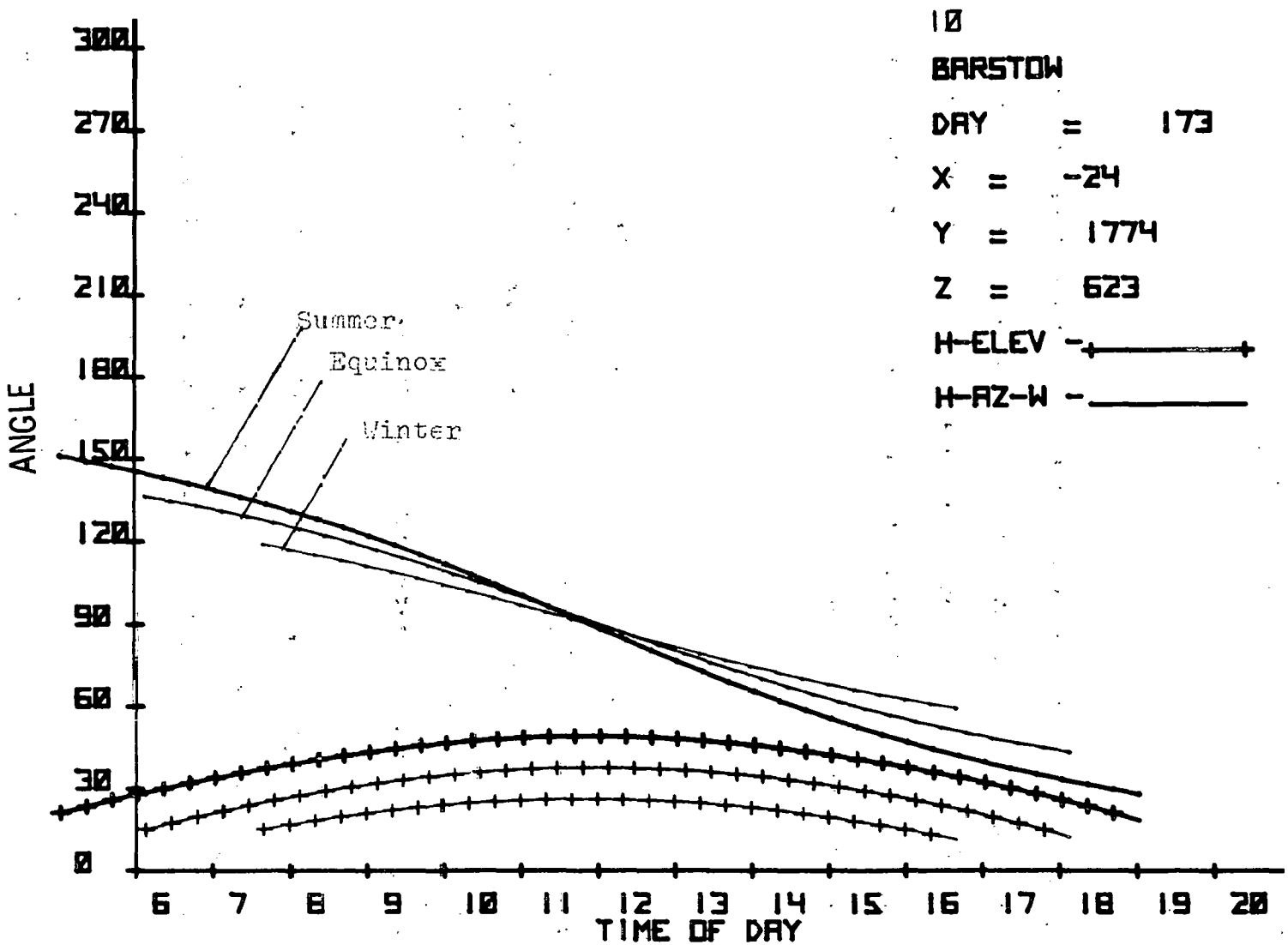

Figure 3-61 HELIOSTAT AXES TRACKING ANGLE PATTERN FOR SAMPLE 10 (37N, 1W)

- The reaction of the system to a large leak, especially involving sodium from the heat pipes
- The reaction of the receiver and gas turbine to the loss of electrical load on the generators

3.8 SYSTEM ANALYSES

System-level studies performed include energy storage capacity and the solar fraction. System considerations analyzed in the parametric analysis phase and dealt with in more detail in the conceptual design phase include plant size and the solar multiple and field/receiver power ratio.

3.8.1 Plant Size

The solar hybrid power plant selected for study in the preconceptual design studies was a 100 MWe plant, according to project specifications. Recognizing that this may not be the optimum size, key cost and performance sensitivities to plant size were identified during parametric analyses.

Using the single-receiver tower approach, scaling studies show that solar system energy costs and performance have relatively minor sensitivity to size, until atmospheric attenuation effects become significant at plant sizes around several hundred megawatts. Conversely, the combined cycle costs (in dollars per installed kilowatt) and cycle efficiencies improve significantly in the 100 MWe to 300 MWe range. Therefore, the optimum plant

size is expected to be larger than 100 MWe. (See also Subsection 3.6.2 on EPGS size.)

3.8.2 Solar Multiple and Field/Receiver Power Ratio

Since energy storage is not recommended, large increases in the solar multiple are not required. However, small increases in the solar multiple corresponding to field/receiver power ratios of greater than one could improve both the solar fraction and the plant economics. This concept was further investigated during conceptual design.

3.8.3 Storage Capacity

The solar/fossil combined cycle hybrid system that Bechtel originally proposed for this study in June, 1978 did not include an energy storage subsystem. This is because the excellent response time of fossil fuel injection into the combined cycle plant obviates the need for buffer storage.

A systems study was conducted to investigate the economic feasibility of long-term energy storage. The primary thrust of this investigation was directed at determining the "value" of energy storage, rather than the technical details and costs of a specific energy storage system. This value is defined as the equivalent capital cost of the fuel savings associated with the incorporation of storage, less the associated increased capital

cost of the solar system, not including the energy storage system cost itself. The increased cost to the solar system includes a larger collector field, receiver, tower, and additional riser/downcomer piping. This value is therefore also the breakeven cost of the energy storage system itself.

Energy Savings. The effects of adding energy storage to the hybrid plant are shown schematically in Figure 3-62. For the Strawman plant, the maximum electrical megawatts generated by the solar system directly is 53 MWe due to the 53 percent solar fraction at the design point with maximum receiver outlet temperature. As the solar system size is increased, surplus energy is diverted to energy storage. Fossil fuel energy savings result from displacement of fossil energy during the day and evening by the energy from storage.

A computer program STORSIM was developed to compute the annual fossil energy savings. Hour-by-hour "energy delivered to the receiver" data, prepared for an elliptical field with a 180 m (591 ft) tower, was used as input to the program. The program assumes constant system efficiencies for the receiver and electric power generation subsystems and also assumes that direct solar insolation levels of greater than 950 W/m² results in energy spillage. The hourly data is based on a reference Barstow weather tape for the entire year of 1976, with actual insolation levels and cloudy periods included.

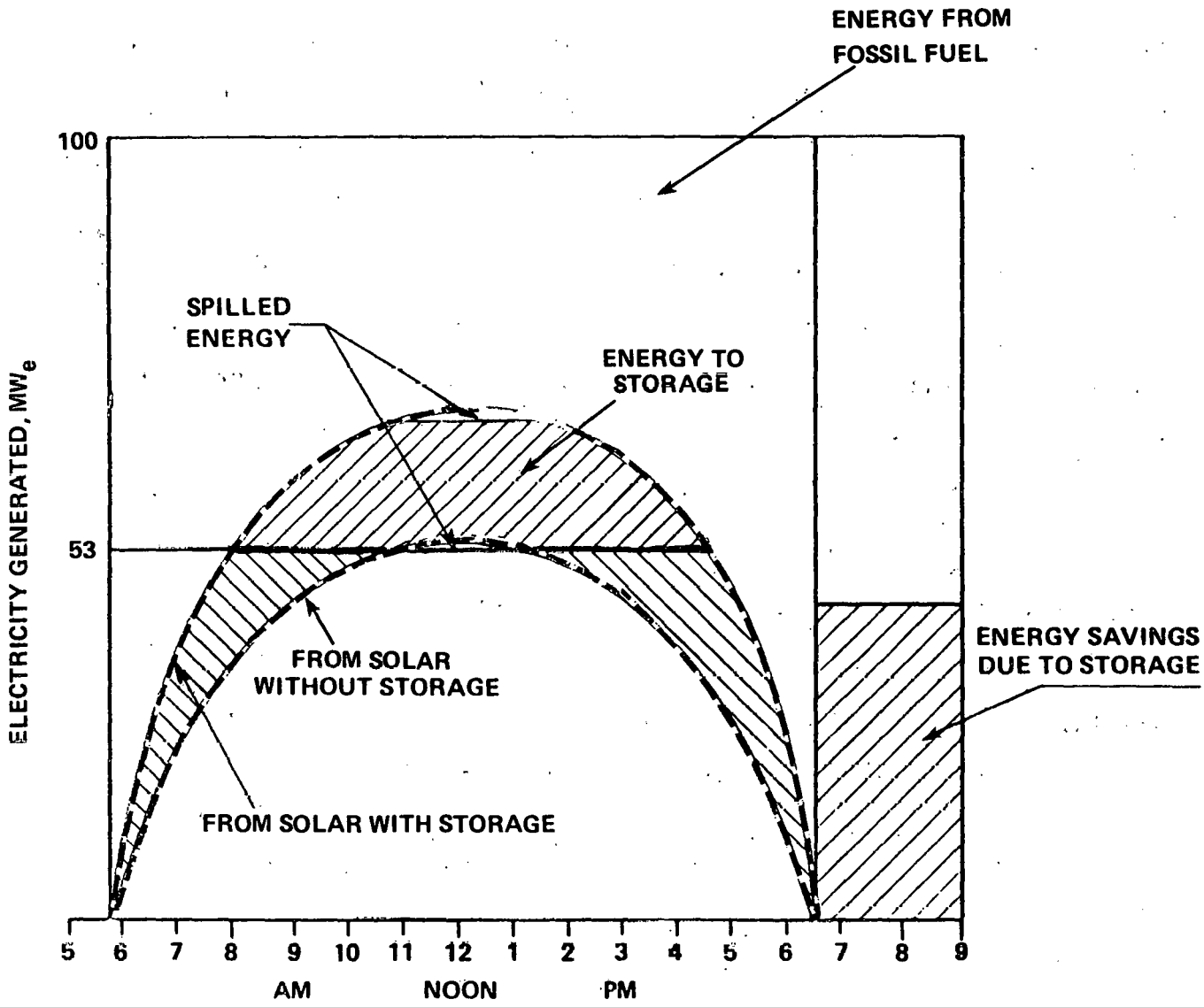

Figure 3-62 EFFECTS OF ENERGY STORAGE AT DIFFERENT TIMES OF DAY

Results of the STORSIM program runs are summarized in Figure 3-63 for solar multiples up to 2.5. Since the fossil fuel energy savings depend upon the storage system turnaround efficiency, a range of efficiencies of 40 percent to 100 percent is included to cover the majority of currently proposed energy storage concepts. As a first approximation, the energy savings shown assume a 100 percent plant availability.

Value of Storage. A second computer program VALSTOR was written to compute the value of storage. This program computes the equivalent capital cost of the plant lifetime fossil fuel savings for a plant starting operation in 1990 for a range of solar multiples up to 2.5. It also computes the increased solar system cost for the same range of solar multiples and subtracts this cost from the equivalent capital cost fuel savings to determine the value of storage. The program uses the preconceptual baseline Strawman plant performance and costs. Solar system cost variations are computed using the following assumptions:

1. Tower cost: Sandia tower equation (Ref. 3-11)
2. Receiver cost:

$$W_{Ri} = K_{RW} \left(\frac{P_i}{P_R}\right)^{1.1}$$

$$C_{Ri} = K_{RC} \left(\frac{P_i}{P_R}\right)^{0.9}$$

3. Collector field cost:

$$C_{Ci} = K_C \left(\frac{P_i}{P_R}\right)^{1.05}$$

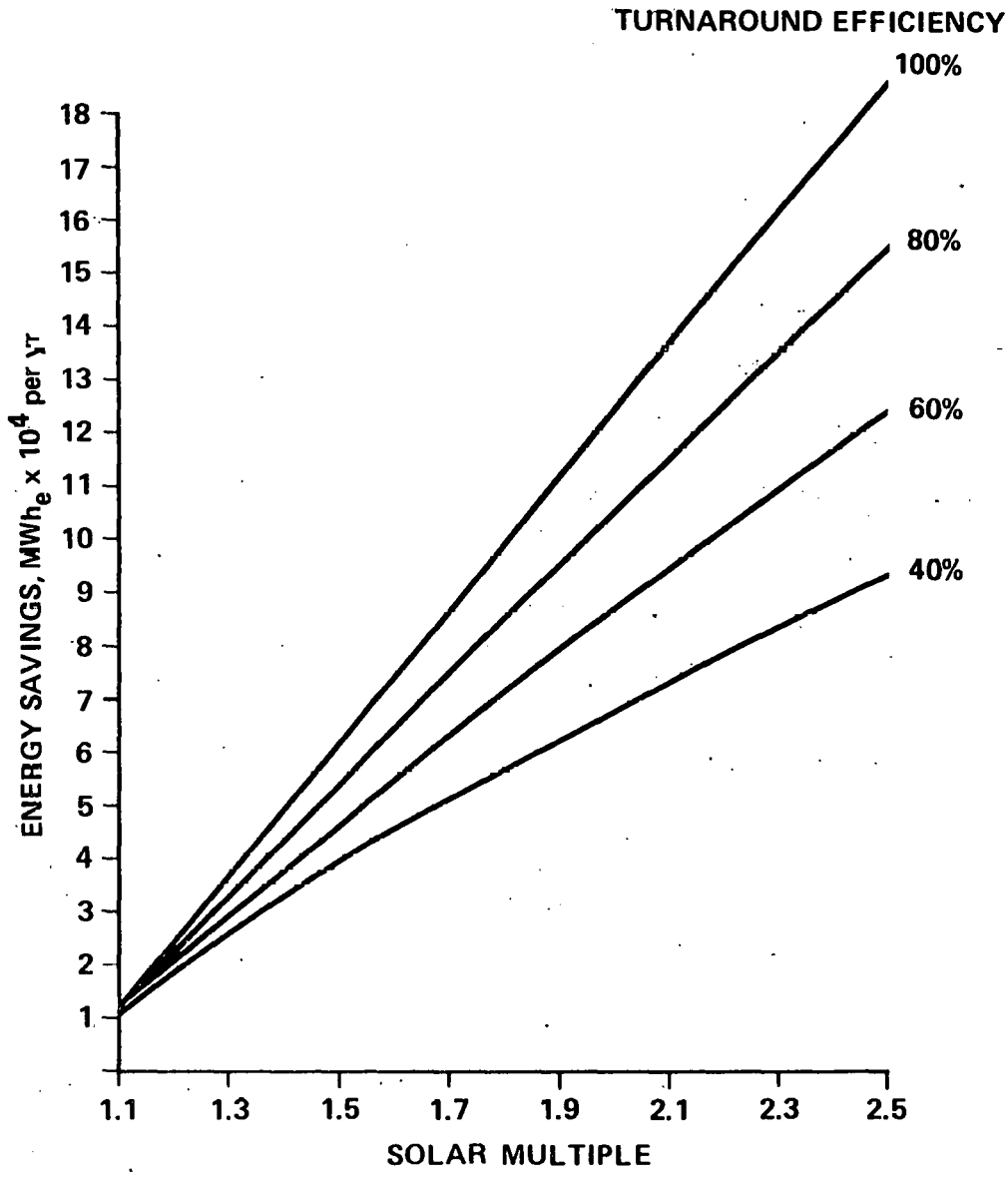

Figure 3-63 ENERGY SAVINGS FROM STORAGE VS. SOLAR MULTIPLE

4. Riser/downcomer cost:

$$C_{Di} = K_D \left(\frac{P_i}{P_R}\right)^{0.7}$$

where:

W_{Ri} = Receiver weight

P_i = Parametric power

P_R = Reference power

C_{Ri} = Receiver cost

C_{Ci} = Collector field cost

C_{Di} = Riser/downcomer cost

K_{RW}, K_{RC}, K_C, and K_D = Proportionally constants

A plot of increased solar system cost and marginal solar system cost versus solar multiple is given in Figure 3-64 in 1990 dollars. It can be seen that over the solar multiple range of interest, the solar system cost is essentially linear with power delivered to the receiver.

The value of energy storage for a range of fossil fuel escalation rates is shown in Figures 3-65 and 3-66. In Figure 3-65, which shows a 100 percent energy storage system turnaround efficiency, a fuel escalation rate of 12.5 to 13 percent is necessary before a positive value of storage can be realized. In Figure 3-66, which shows a 60 percent turnaround efficiency, a fuel escalation rate of 13 to 14 percent is necessary. The actual turnaround efficiency of energy storage subsystems is expected to be somewhere between 60 and 100 percent. Hence, a fuel escalation rate of between 12.5 and 14 percent would be necessary to realize

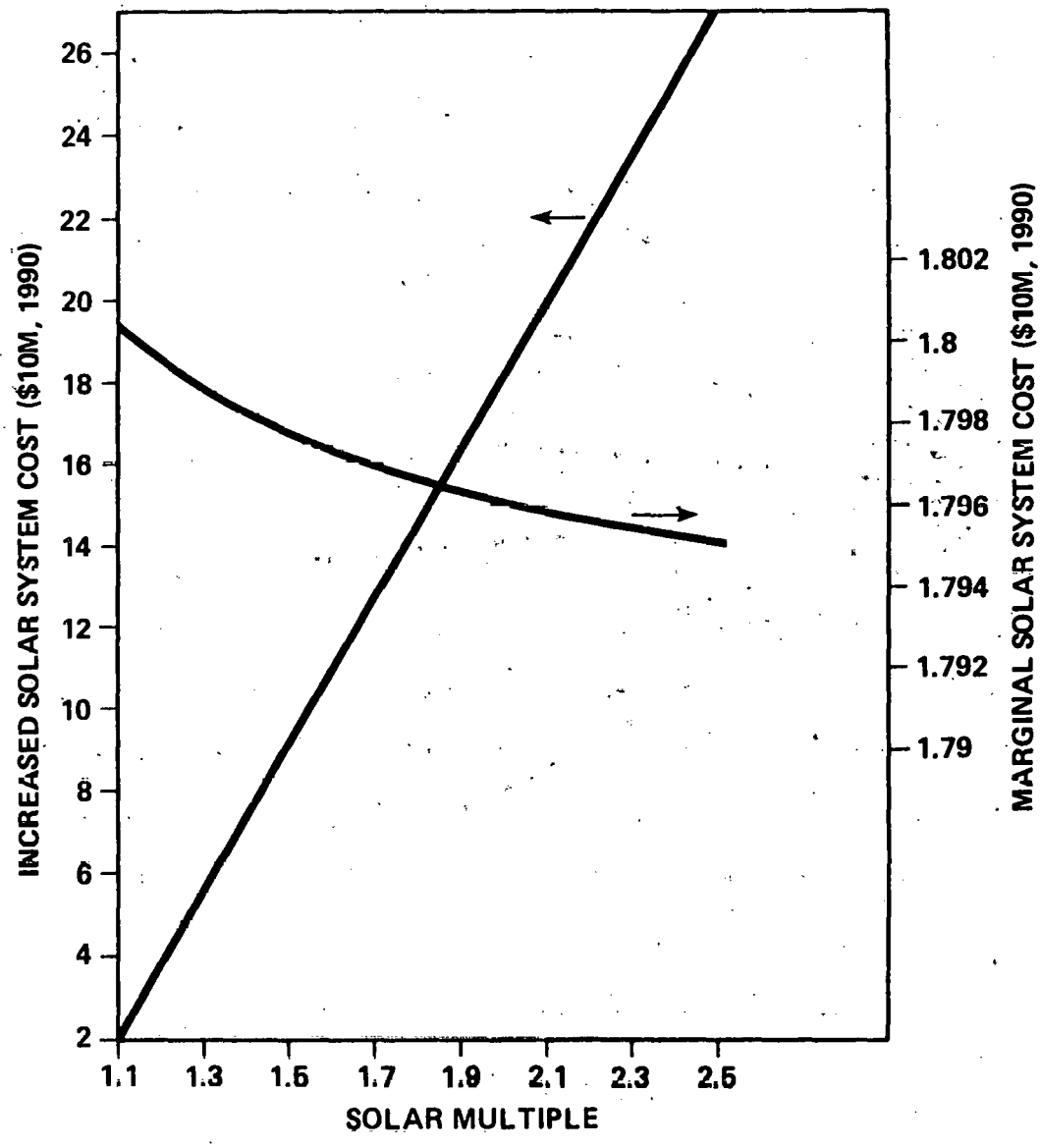

Figure 3-64 INCREASED SOLAR SYSTEM COST VS. SOLAR MULTIPLE, 1990 PLANT

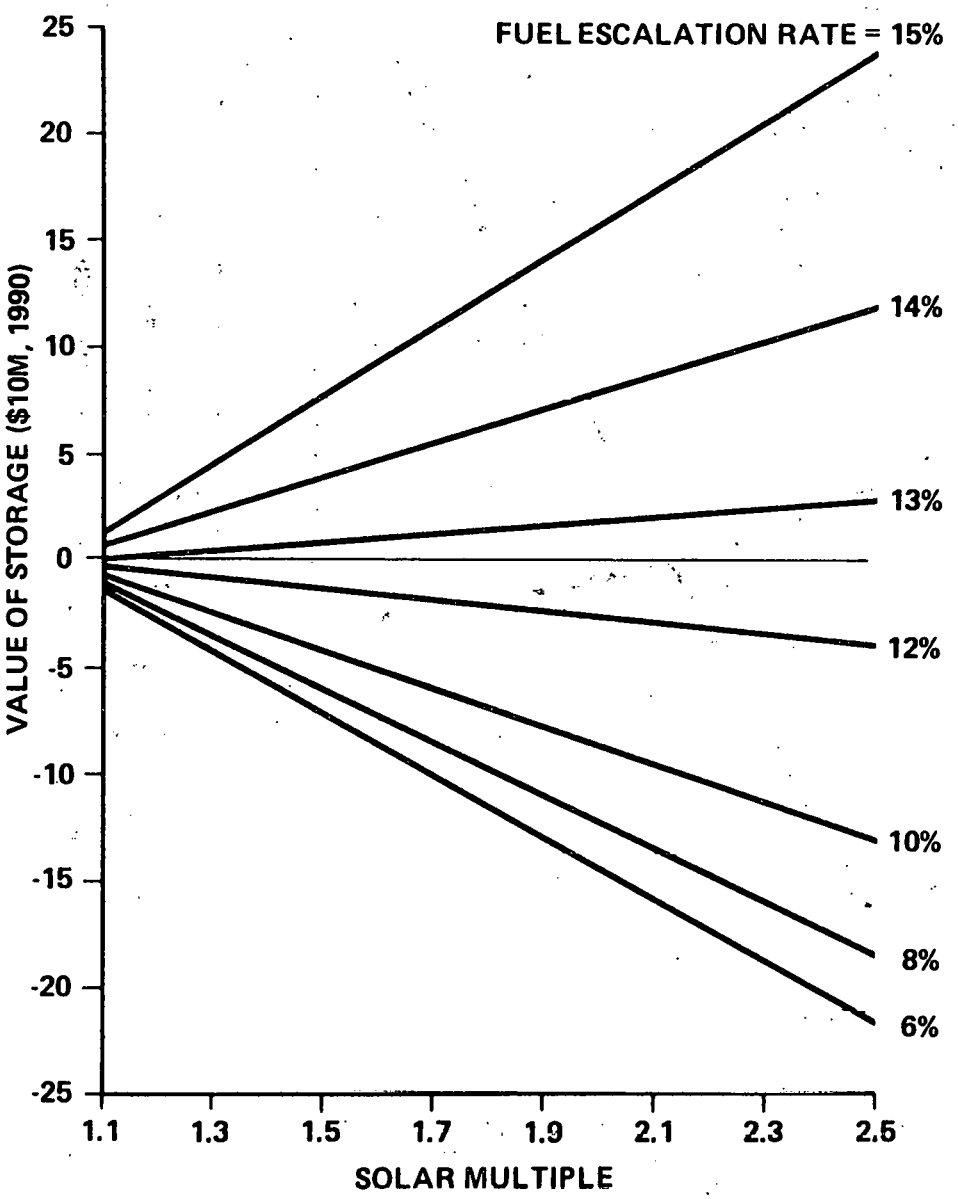

Figure 3-65 VALUE OF STORAGE VS. SOLAR MULTIPLE, 1990 PLANT, 100 PERCENT TURNAROUND EFFICIENCY

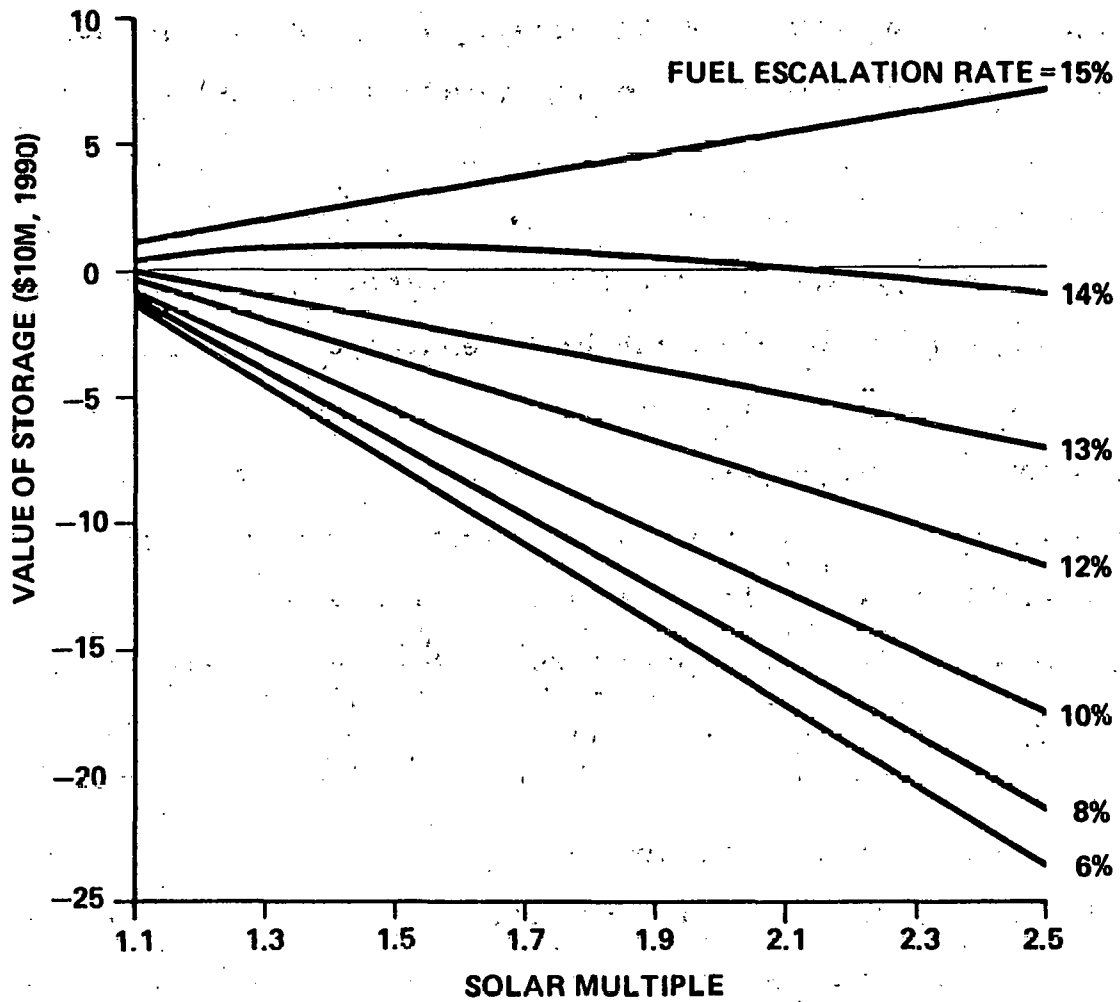

Figure 3-66 VALUE OF STORAGE VS. SOLAR MULTIPLE, 1990 PLANT, 60 PERCENT TURNAROUND EFFICIENCY

a positive value of storage. This is illustrated further in Figure 3-67, where information from Figures 3-65 and 3-66 has been replotted for a solar multiple of 2.

Since the escalation rate of distillate oil expected by utility companies is 12 percent or less, it is apparent that the addition of energy storage would not be economical for a 1990 plant, even if the capital cost of the energy storage system itself were zero.

Economic Evaluation. Typical cost and performance values (Ref. 3-3) for three different high-temperature energy storage systems are shown in Table 3-24. Using the values for the lowest-cost storage system in conjunction with Figures 3-65, 3-66, and 3-67, it can be deduced that the cost of energy storage itself would increase the breakeven fuel escalation rate by 0.5 to 1 percent. This results in overall breakeven rates between 13 and 15 percent.

For reference purposes, Figure 3-68 was generated using the STORSIM program for the peak insolation day. This figure relates the hours of storage necessary to accommodate any solar multiple on the peak insolation day for a range of storage system turnaround efficiencies. Each hour of storage is defined as being capable of delivering 100 MWh of electric energy to the power grid.

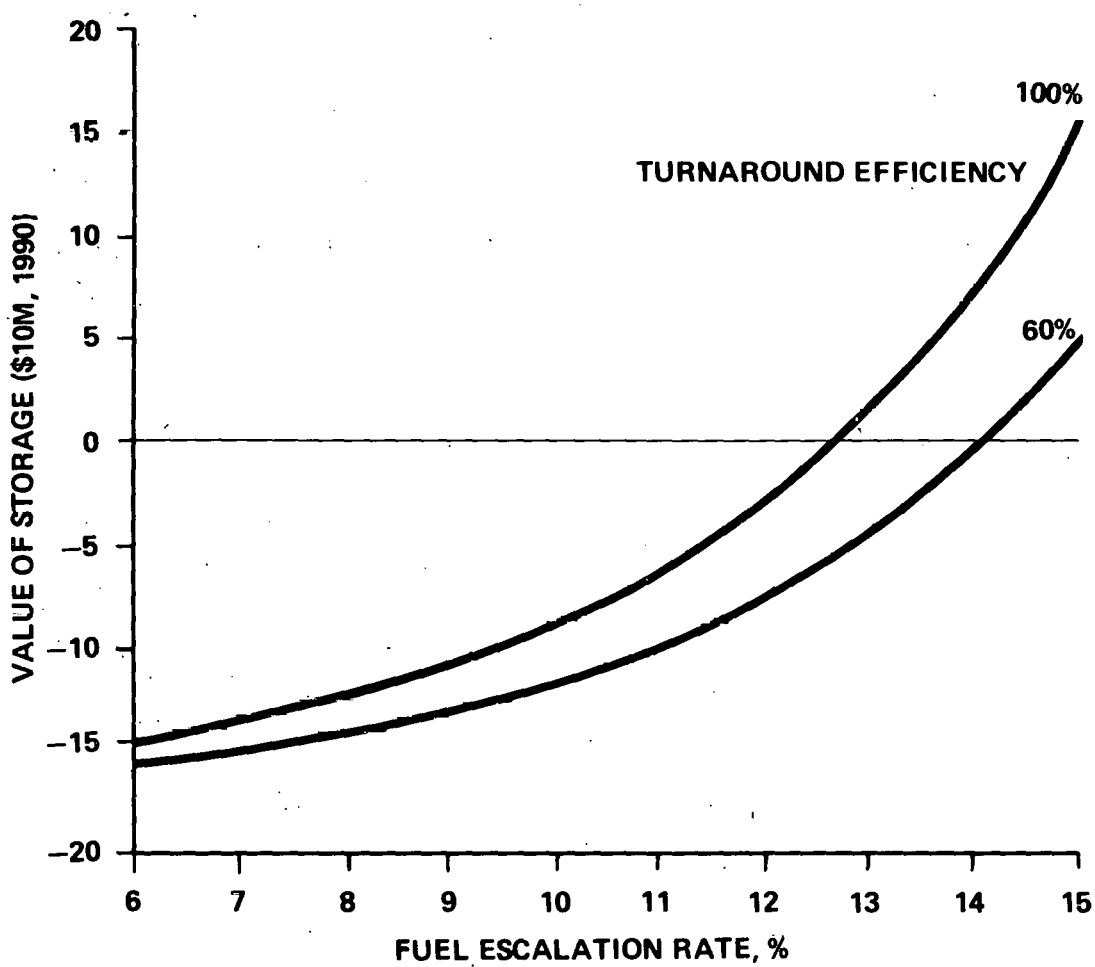

Figure 3-67 VALUE OF STORAGE VS. FUEL ESCALATION RATE, 1990 PLANT, SOLAR MULTIPLE 2.0

TABLE 3-24

HIGH-TEMPERATURE ENERGY STORAGE SYSTEMS*
100 MWe PLANT

Item	Storage System		
	Thermal, Phase Change	Thermal Sensible Heat	Thermochemical
Turnaround efficiency (%)	62	72	57
Cost in $1975			
Stored energy cost ($/kWh)	16.3	48.7	5
Discharge rate cost ($/kW)	66	44	441
Cost of 6 hours Storage ($/kW)	164	336	472
Cost in $1990 (millions)	68.5	140.3	197.2

*Source: "Closed-Cycle, High-Temperature Central Receiver Concept for Solar Electric Power," EPRI ER629, Boeing Engineering and Construction, January 1978.

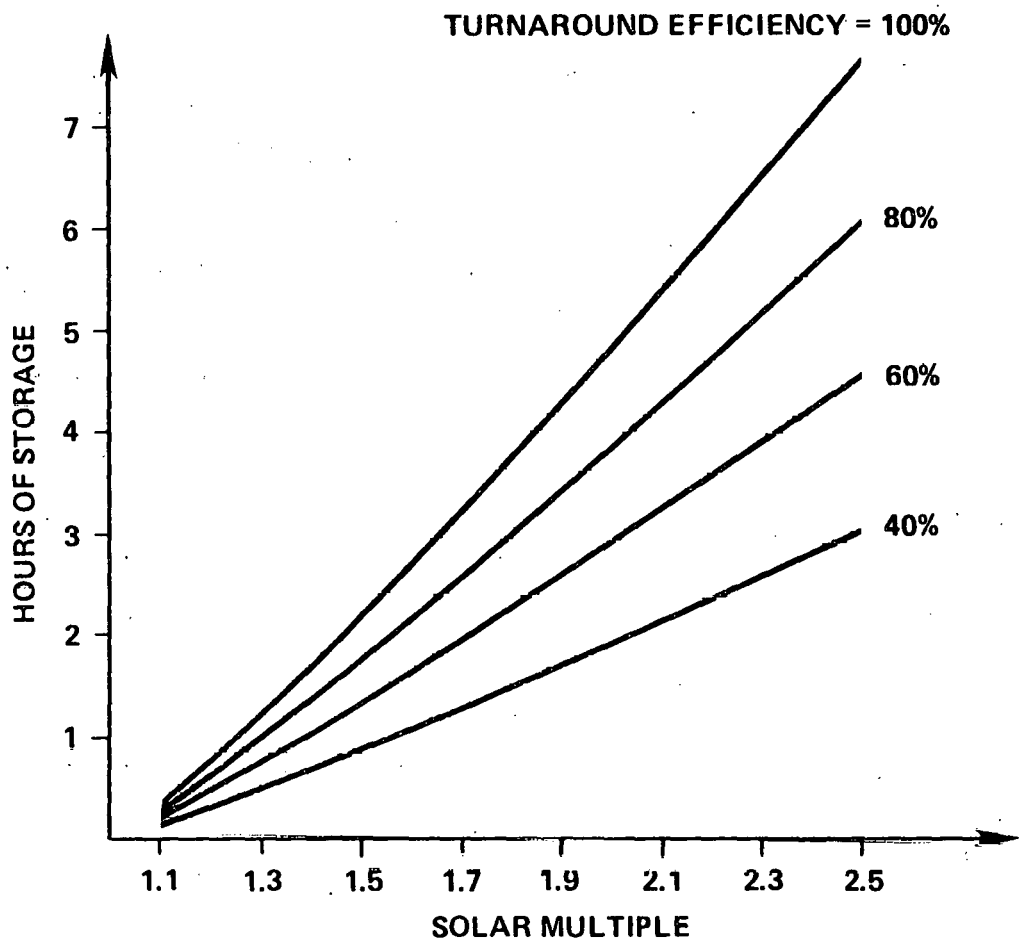

Figure 3-68 HOURS OF STORAGE VS. SOLAR MULTIPLE
PEAK INSOLATION DAY

Although energy storage does not appear to be economical for a 1990 plant based on the above assumptions, the hybrid plant can accommodate energy storage at a later date and/or if the capital cost and escalation rate assumptions change.

Figure 3-69 shows a typical schematic of how energy storage would probably be incorporated into the solar hybrid plant. The combined cycle plant compressor air flow is maintained to the receiver from sunrise until the receiver air outlet temperature reaches the design value of 816C (1500F) at the 53 MWe level. Then the variable-speed storage system compressor is activated to maintain the maximum 816C (1500F) receiver outlet temperature. The receiver air flow increases, reaching a peak at noon and then decreases until the storage system compressor reaches zero flow at the 53 MWe level. At this point, energy can be extracted from storage by diverting flow from the receiver through energy storage in the reverse direction.

Conclusions. The following statements summarize the study results regarding energy storage in the hybrid plant:

- In view of the excellent response time of the hybrid combined cycle concept, buffer storage is not required for any operational reason.
- Considering typical energy storage system costs, the value of energy storage would be positive only with fuel escalation rates exceeding 13 to 15 percent for a 1990 plant. This compares to present projections of long-range fuel escalation rates of 12 percent or less.
- High temperature energy storage technology is in the early stages of development. Although cost and

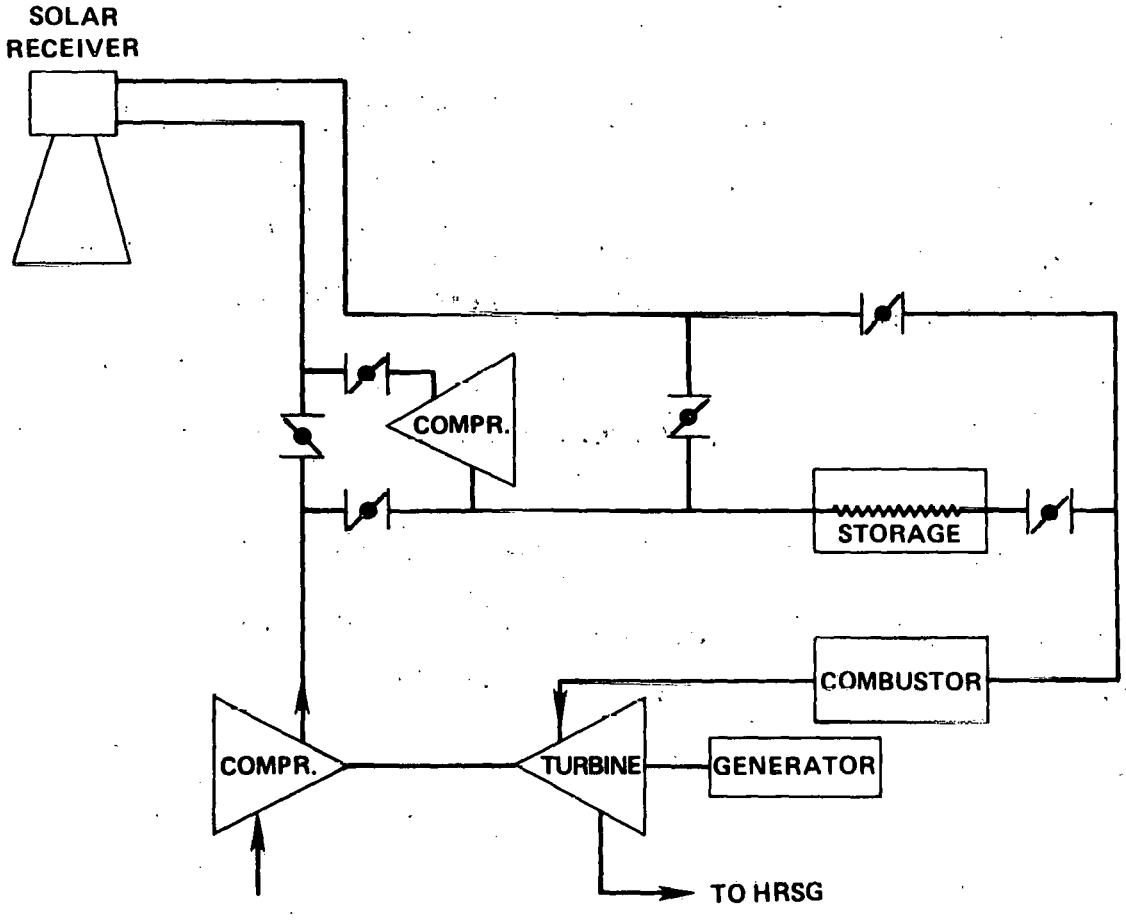

Figure 3-69 TYPICAL SCHEMATIC INCORPORATING ENERGY STORAGE IN SOLAR HYBRID PLANT

performance estimates are available from some studies, many technical and economic uncertainties exist. R&D, as well as design and evaluation of high temperature storage systems, should be pursued.

Considering the above, it was recommended that energy storage not be incorporated into the plant at this time.

3.8.4 Solar Fraction

The solar fraction is an important selection criterion, since it is directly related to the potential for fossil fuel displacement. It is determined by the temperature rise across the receiver relative to the total temperature rise from the receiver inlet to the gas turbine inlet. The upper limit of solar fraction is then set by the maximum temperature achievable at the receiver outlet.

If the Strawman design is modified by raising the receiver outlet temperature from 816C (1500F) to 843C (1550F), the design point solar fraction can be raised from 56.3 percent to 60.4 percent. This represents the maximum achievable solar fraction with this system at a solar multiple of 1.0, since it is based on the highest attainable receiver outlet temperature.

At a 12 percent fuel escalation rate, the 60.4 percent solar fraction is obtained at a slight overall cost penalty for the 1990 plant. At a 15 percent fuel escalation rate, there would be a slight overall cost advantage.

In the Advanced Strawman plant, with a receiver outlet temperature of 1093C (2000F), a design point solar fraction of 71.9 can be reached, but this system involves considerably more development risk.

Higher solar fractions could be achieved by increasing the number of heliostats beyond those needed for peak operation, and spilling energy when the receiver outlet temperature would otherwise exceed 843C (1550F). Considering the results of energy storage studies, a large increase in the solar multiple does not appear to be economical for a 1990 plant. However, a study was performed during conceptual design to determine whether a small solar multiple would be an economical way to achieve a higher solar fraction. The results are discussed in Section 5.

Section 4

SELECTION OF PREFERRED SYSTEM

4.1 SELECTION PROCESS

To select the most economical and technically feasible solar hybrid system, the evaluation process was as follows:

- Establish preconceptual reference designs and cost estimates for a near-term (Strawman) and a longer-term (Advanced Strawman) system (see Section 1)
- Undertake parametric analysis and economic evaluation of the various subsystems that make up these reference systems and modify the reference systems as appropriate (see Section 3)
- Do a market analysis for the two reference systems as modified (see Section 2)
- Do economic evaluations at the system level
- Select the preferred system based primarily on the criterion of long-term low-cost energy production, as well as other selection criteria and the results of the parametric analysis

This section discusses the selection criteria, the economic evaluations, and selection of the preferred hybrid system.

4.2 SELECTION CRITERIA

The economic evaluation and ultimate system selection of the solar hybrid designs were based on the following criteria:

- Energy production cost

- Market potential
- Fossil fuel displacement potential (solar fraction)
- Development risk

The primary selection criterion was low-cost energy production, which considered capital costs, life cycle costs for fuel, and operating and maintenance costs. The solar fraction, which determines the amount of fossil fuel displaced, is determined by the temperature rise across the receiver relative to the total temperature rise from the receiver inlet to the gas turbine inlet. The goal of a high solar fraction must be weighed against the associated development risk.

Other items, such as environmental impact, resource requirements, utility operational requirements, reliability, maintenance requirements, and potential safety hazards, were considered implicitly in the evaluation effort.

4.3 SYSTEM SELECTION

After parametric analyses the reference hybrid systems were modified to incorporate results of the studies. In a cost comparison during final system selection, cost impacts of these modifications were taken into consideration. Finally, the preferred system was selected, based on the established criteria.

4.3.1 Modifications to Preconceptual Reference Designs

As a result of system-level studies and parametric analyses, the following conclusions were reached on the design of the Strawman and Advanced Strawman systems:

- Energy storage is neither economically nor technically desirable, and is not recommended in the selected plant.
- The No. 2 distillate oil used in the reference designs is the most economical fuel when compared to solvent-refined coal, medium-Btu gas, and residual oil.
- Constant air flow is a more efficient mode of operation than constant receiver outlet temperature, allowing lower receiver outlet temperature at off-design conditions.
- A small increase in field/receiver power ratio from the baseline value of 1.0 may result in a small overall cost improvement.

The following modifications to the Strawman design were recommended as a result of the parametric analyses:

- Collector: A larger heliostat of 49 m^2 (527 ft^2) was recommended over the baseline size of 38.6 m^2 and a modified elliptical field with the south sector removed.
- EPGS: A dual-pressure steam bottoming cycle was incorporated instead of the baseline single-pressure cycle to achieve a thermal cycle efficiency of 44.95 percent.
- Receiver: The riser/downcomer and receiver pressure drops were modified to 41.1 kPa (6 psi) each over the baseline values of 13.8 kPa and 27.6 kPa, respectively. The receiver outlet temperature was raised to 843C (1550F) over the baseline value of 816C, with a minor cost penalty. This raises the design point solar fraction to 60.4 percent from 56.3 percent.

The following modifications to the Advanced Strawman design were recommended as a result of the parametric analyses:

- Collector: A larger heliostat of 49 m^2 (527 ft^2) was recommended over the baseline size of 38.6 m^2 and a modified elliptical field with the south sector removed.
- Receiver: The riser/downcomer pressure drop was modified to 34.5 kPa (5 psi) from the baseline value of 17.2 kPa. (The baseline value of 103.5 kPa (15 psi) for receiver pressure drop was found to be optimum.)
- EPGS: The compressor pressure ratio was raised from 12 to 16.

4.3.2 Comparison of Strawman and Advanced Strawman Systems

The Strawman and Advanced Strawman systems were compared on the basis of cost, market potential, solar fraction, and development risk.

Cost and Market Potential. During the market analysis work, screening curves were prepared to compare costs of the Modified Strawman and Advanced Strawman systems with those of conventional technologies. (The Modified Strawman in those evaluations incorporated a dual-pressure heat recovery steam generator and reduced riser/downcomer and receiver pressure drops.) During system-level evaluations, these hybrid data were compared to the performance of a conventional combined cycle system at the same state of technological development as the Advanced Strawman concept. Figure 4-1 shows the results of this evaluation, indicating that for 1990 operation and a 12 percent fuel

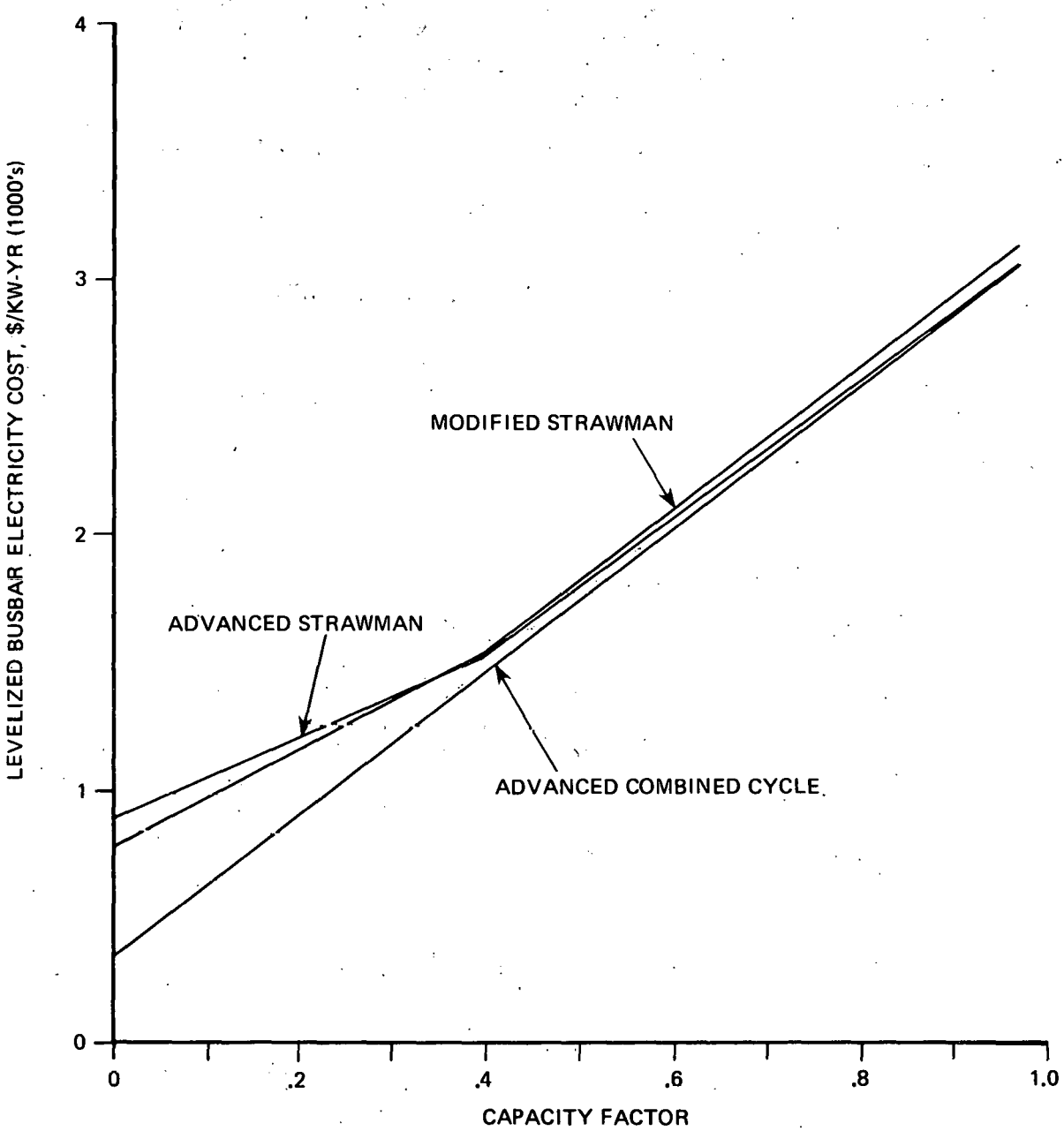

Figure 4-1 SCREENING CURVE COST COMPARISON, 1990, 12 PERCENT FUEL ESCALTION RATE

escalation rate, there is essentially no cost difference between the Modified Strawman and the Advanced Strawman in the intermediate-load range.

When all the modifications recommended for these systems were then considered, the costs of the Modified Strawman plant increased slightly and the costs of the Advanced Strawman decreased slightly. In the 48 percent capacity range, the Modified Strawman costs increased by 0 to 1 percent, and the Advanced Strawman costs decreased by 2 to 3 percent. This results in costs for the two plants that are within approximately 4 percent of each other, which is considered to be within the margin of error for cost estimates. Therefore, the two plant costs may be considered to be equal at a 12 percent fuel escalation rate and with plant startup in 1990.

The levelized busbar electricity costs for the two plants are also close to those of the advanced combined cycle plant, although the ACC plant is slightly cheaper. It is expected that the market would be shared, rather than captured entirely by the ACC plant. Figures 4-2, 4-3, and 4-4 show hybrid system costs with higher fuel escalation rates and/or a first operation year of 2000. Under those conditions the solar plants become cheaper than the ACC plant, and the Advanced Strawman becomes more economical than the Modified Strawman.

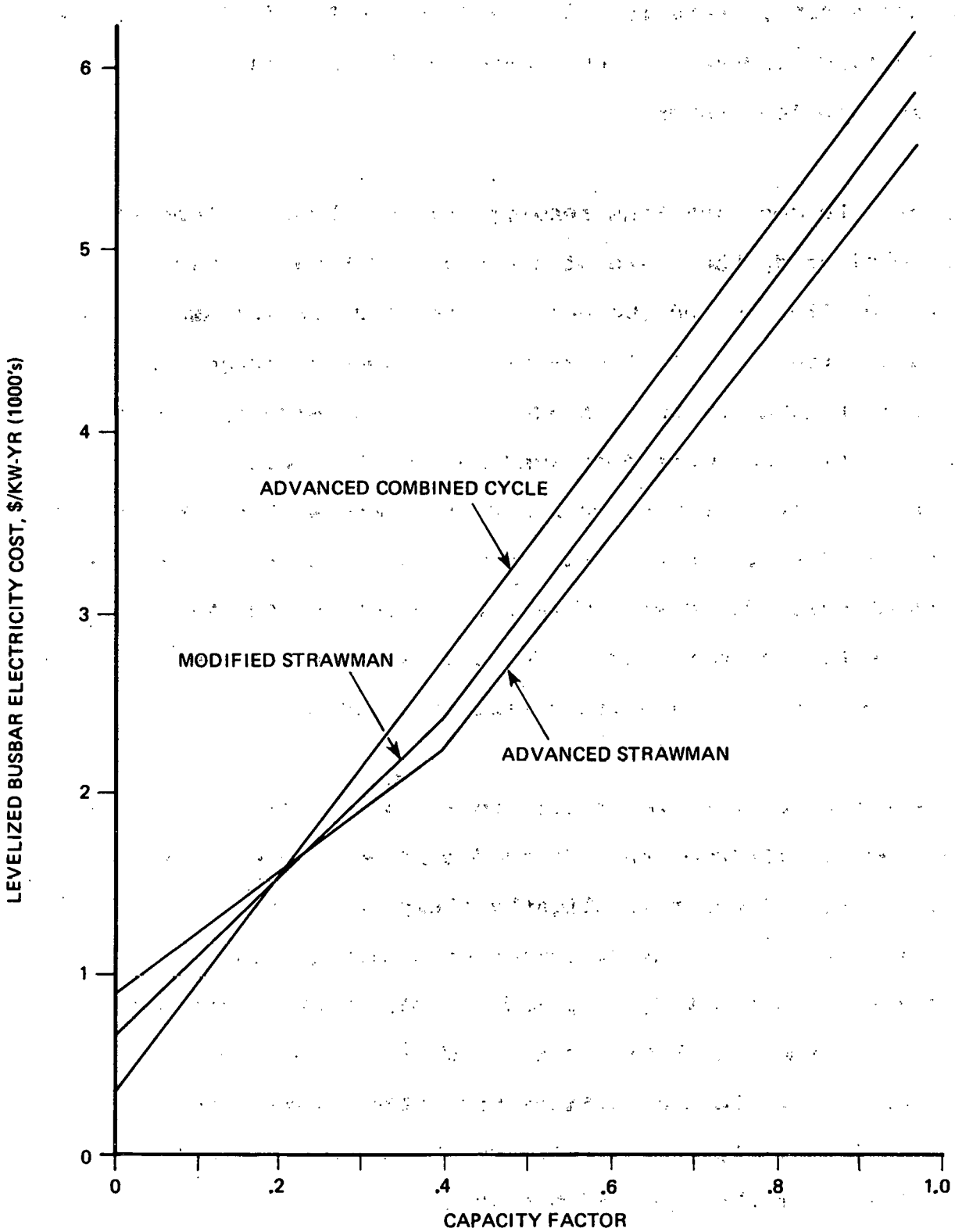

Figure 4-2 SCREENING CURVE COST COMPARISON, 1990, 15 PERCENT FUEL ESCALATION RATE

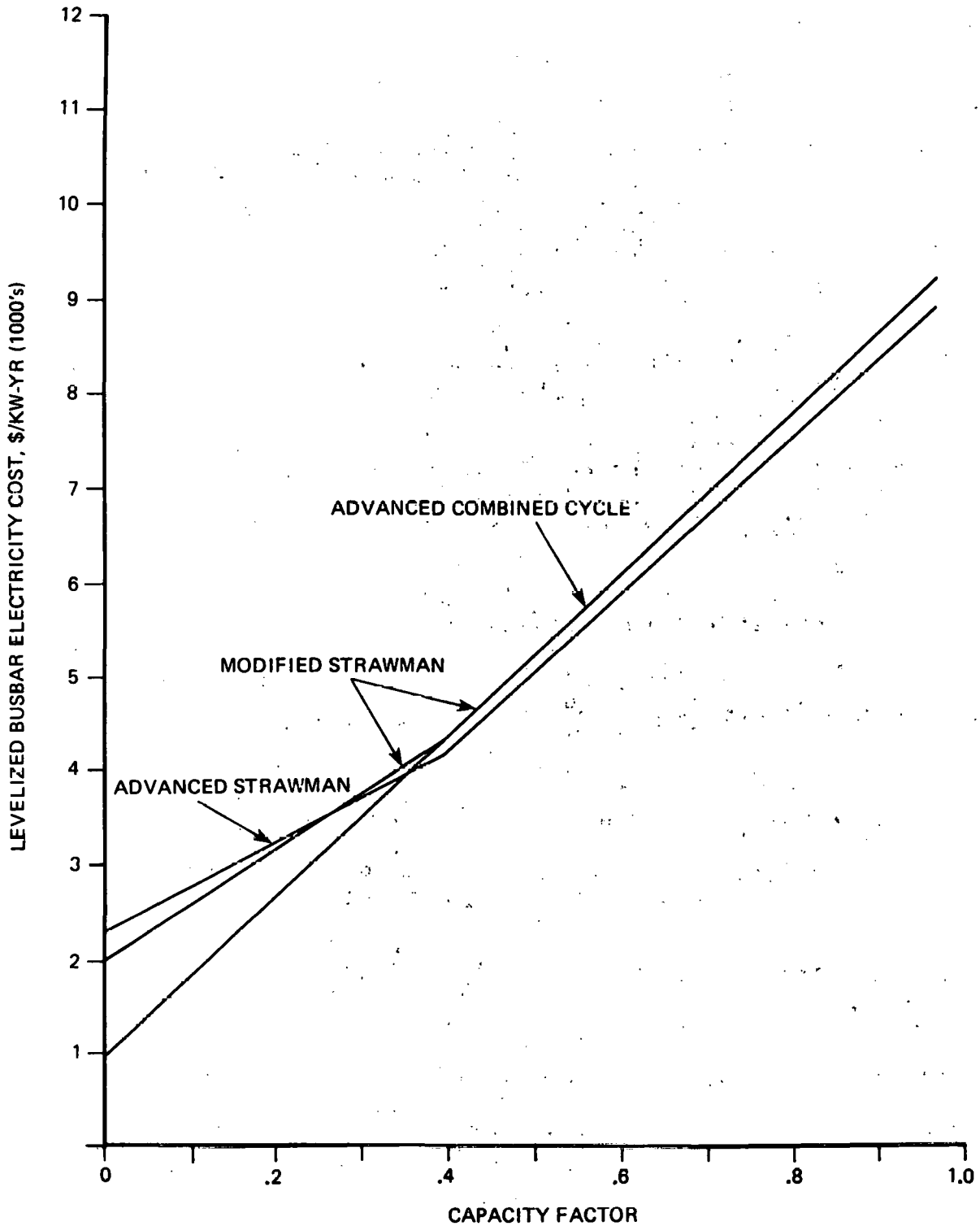

Figure 4-3 SCREENING CURVE COST COMPARISON, 2000, 12 PERCENT FUEL ESCALATION RATE

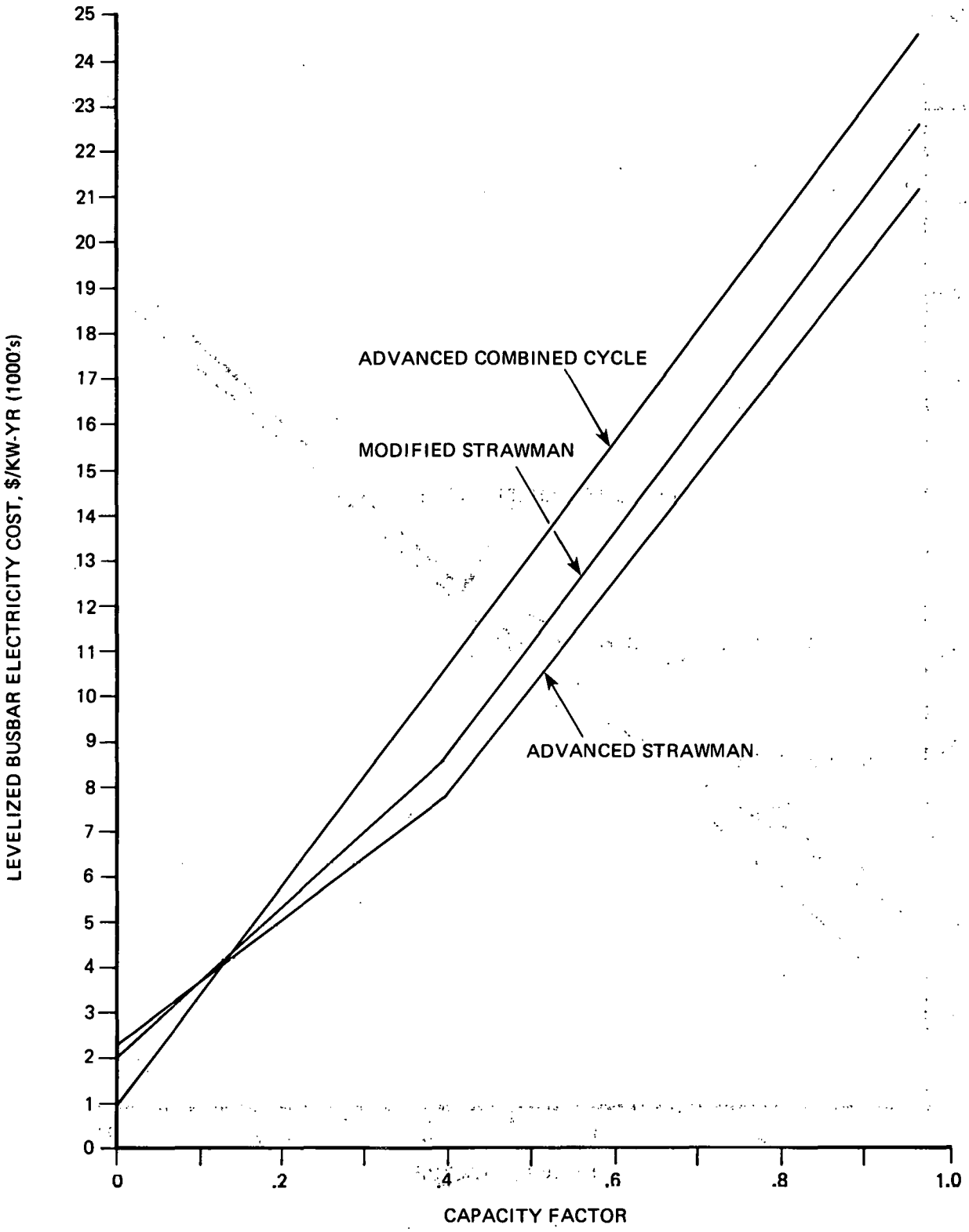

Figure 4-4 SCREENING CURVE COST COMPARISON, 2000, 15 PERCENT FUEL ESCALATION RATE

Solar Fraction. The two hybrid systems incorporating all recommended modifications have the following design point and annual average solar fractions:

	Modified Strawman	Modified Advanced Strawman
• Design point:	60.4	70.4
• Annual average:	28.3	33.0

These values are all above the anticipated National Energy Act requirement of 25 percent solar energy input to obtain an exemption for burning distillate oil.

Development Risk. The development risk associated with the Modified Advanced Strawman design is much greater than with the Modified Strawman design. With the former there are several problems to be resolved with regard to the high-temperature ceramic receiver, the high-temperature industrial turbine, and the combustor. These problems may be resolved by 1990, but this is uncertain. The Modified Strawman plant, with its lower temperature levels, presents much less of a risk.

Conclusions. The two hybrid designs have essentially equal economics, comparable market potential, and acceptable solar fractions. However, the development risks associated with the Modified Advanced Strawman are much greater. It was therefore decided to proceed with the Modified Strawman for conceptual design of the 1990 plant. It was also recommended that the high-

temperature ceramic receiver for the Advanced Strawman design be developed in parallel to provide a second-generation plant that may be more economical under higher fuel escalation rates.

4.3.4 Selected Plant Summary

The costs and performance of the selected Modified Strawman plant are summarized in Tables 4-1 and 4-2. These data reflect incorporation of all changes resulting from the system- and subsystem-level studies. The selected plant design was further developed during the conceptual design to reflect actual equipment size, performance, and cost data, and minor system- and subsystem-level studies.

TABLE 4-1

MODIFIED STRAWMAN SYSTEM PERFORMANCE

Parameter	Value
Solar Receiver Outlet Temperature, °C (°F)	843(1550)
Gas Turbine Inlet Temperature, °C (°F)	1093(2000)
Fossil Fuel	Distillate Oil
EPGS Thermal to Net Electric Conversion Efficiency, %	44.95
Design Point Solar Capacity Fraction, %	60.4
Annual Average Daytime Solar Fraction	33.5
Assumed Average Nighttime Operation on Fossil Fuel, Hrs	2.0
Annual Average Solar Fraction, %	28.3
Plant Capacity Factor, %	48.0
Solar Capacity Factor, %	13.6

TABLE 4-2

MODIFIED STRAWMAN CAPITAL COST SUMMARY
($1000)

Cost Item	Nonsolar Combined Cycle Portion	Solar Portion
Site, Structures, Miscellaneous	2,200	100
Turbine Plant	27,000	
Electric Plant	2,500	200
Collector Equipment		25,200
Receiver, Tower, Riser/Downcomer		21,600
Nonsolar Equipment	500	
Indirect Field Cost	7,300	1,800
Engineering, Home Office, and Fee	4,700	4,900
Subtotal	44,200	53,800
Contingency @ 15%	14,700	
Total	112,700	

THIS PAGE

WAS INTENTIONALLY

LEFT BLANK

Section 5

CONCEPTUAL DESIGN AND COST/PERFORMANCE ESTIMATES

This section describes the conceptual design of the commercial-scale solar hybrid power plant, including the collector subsystem, receiver subsystem, electric power generation subsystem, and master control subsystem. It presents performance estimates for the conceptual design, describes the plant arrangement, and outlines daily system operation. Estimates of capital and operating costs were generated based on this conceptual design, and a top level project construction schedule was established.

System requirements for the conceptual design were specified in the Requirement Definition document (Ref. 5-1) and are summarized below:

• Nominal plant capacity	100 MWe net
• Availability	90 percent
• Plant life	30 years
• Reference site	Barstow, CA
• First year of operation	1990
• Solar system design point	Best solar angle

In addition to these requirements, a plant capacity factor of 48 percent was established, placing the hybrid plant in the intermediate-load range.

Conceptual design was based on a Westinghouse commercial gas turbine unit, since design and performance data are available on this unit. For this reason, the nominal net plant capacity was increased from 100 MWe to 112.6 MWe. Collector design was based on a Northrup II 50.54 m^2 heliostat instead of the generic 49 m^2 design, also due to availability of data.

5.1 SYSTEM PERFORMANCE

System performance for hybrid, fossil-only, and annual average operation is summarized in Table 5-1. The solar fraction and net cycle efficiency of the conceptual design are both lower than those of the selected system in preconceptual design. This is primarily because the airflow requirement for turbine cooling is significantly higher than was initially estimated and the cooling air bypasses the receiver.

5.1.1 Design Point Performance, Hybrid Operation

The performance of the solar hybrid power system conceptual design at the design point is shown in the stair-step diagram in Figure 5-1. It is based on solar energy input at the best sun angle, which is 45 degrees elevation, 0 degree azimuth and it is calculated for the "H" heliostat field (a radial stagger arrangement) with 145 m (475 ft) aperture centerline elevation. The solar angles correspond to equinox noon at Barstow, CA.

TABLE 5-1

SYSTEM PERFORMANCE

Performance Characteristic	Design Point Hybrid Operation	Fossil Operation	Annual Average
Solar fraction	0.536		0.282
Electrical output, MWe			
Gross	115.9	116.3	116.1
Net	112.6	113.6	112.9
Heat rate, kJ/kWh (Btu/kWh)			
Gross	7987(7570)	8363(7926)	8184(7757)
Net	8223(7794)	8562(8116)	8410(7971)
Thermal efficiency, %			
Gross	45.1	43.1	44
Net	43.8	42.1	42.8

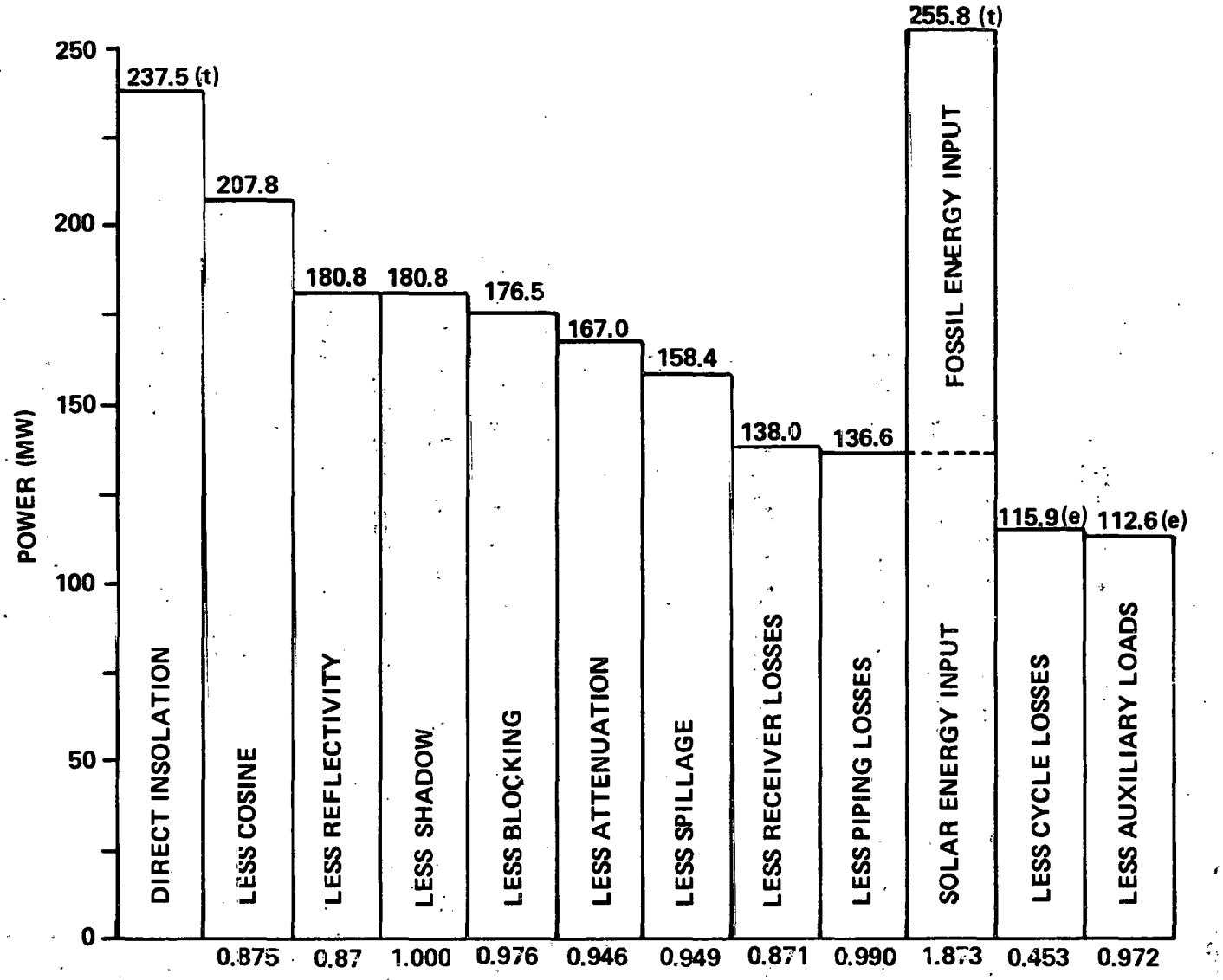

Figure 5-1 STAIR-STEP DIAGRAM, DESIGN POINT HYBRID OPERATION

The piping loss shown in Figure 5-1 represents the solar input lost due to heat leak in the downcomer piping. The loss in the riser piping is included with the cycle losses, since it represents the loss from the heat of compression.

5.1.2 Fossil-Only Performance

The stair-step diagram for fossil-only operation for the same ambient conditions is shown in Figure 5-2. The output and heat rate are slightly higher than for hybrid operation.

5.1.3 Annual Average Performance

The stair-step diagram for annual average performance is shown in Figure 5-3. For this calculation, the solar component of the power plant was assumed to be operating only when the insolation level is in excess of 500 W/m^2. The 3.5 percent excess heliostat area at the design point was found to result in approximately 0.5 percent of excess annual solar energy, due to heliostat turndown when the receiver focal plane thermal power limit is exceeded.

The annual average geometric efficiency of the field was developed using the 1976 Barstow data and the geometry of the "H" field (see Section 5.2). The design point values for reflectivity, atmospheric attentuation, and receiver efficiency were used in calculating the annual performance. Spillage was estimated from efficiency variation calculated for the equinox

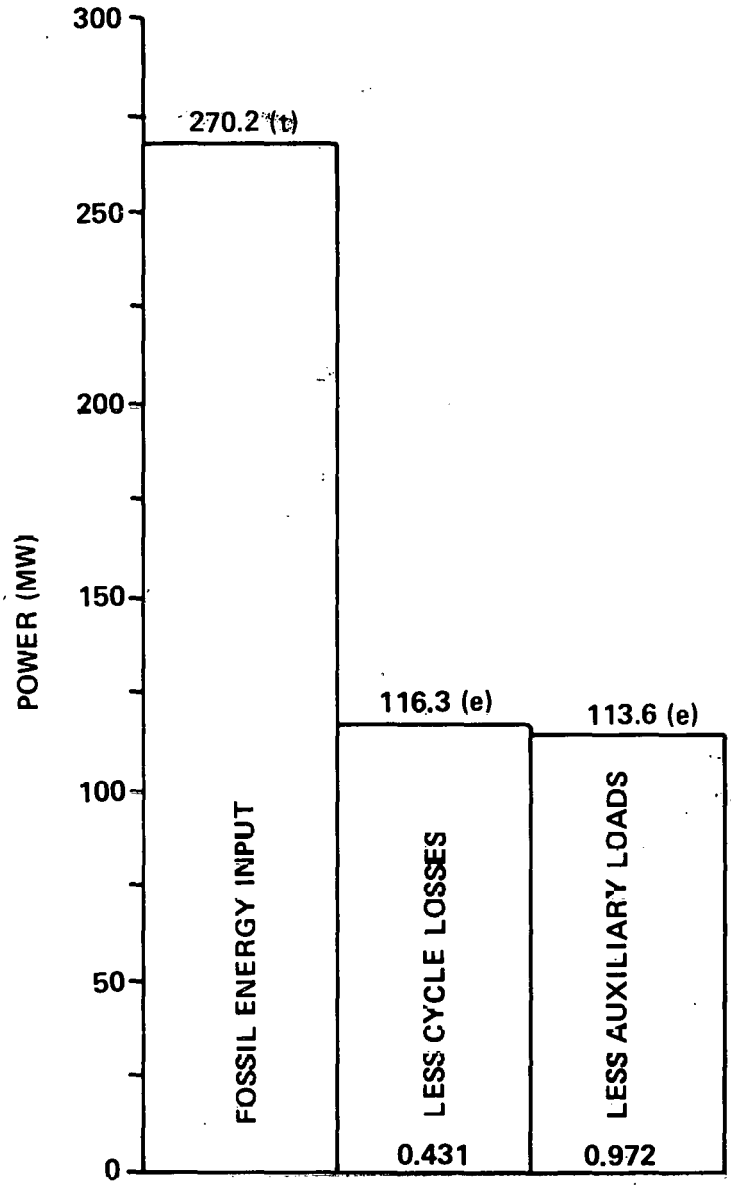

Figure 5-2 STAIR-STEP DIAGRAM, FOSSIL OPERATION

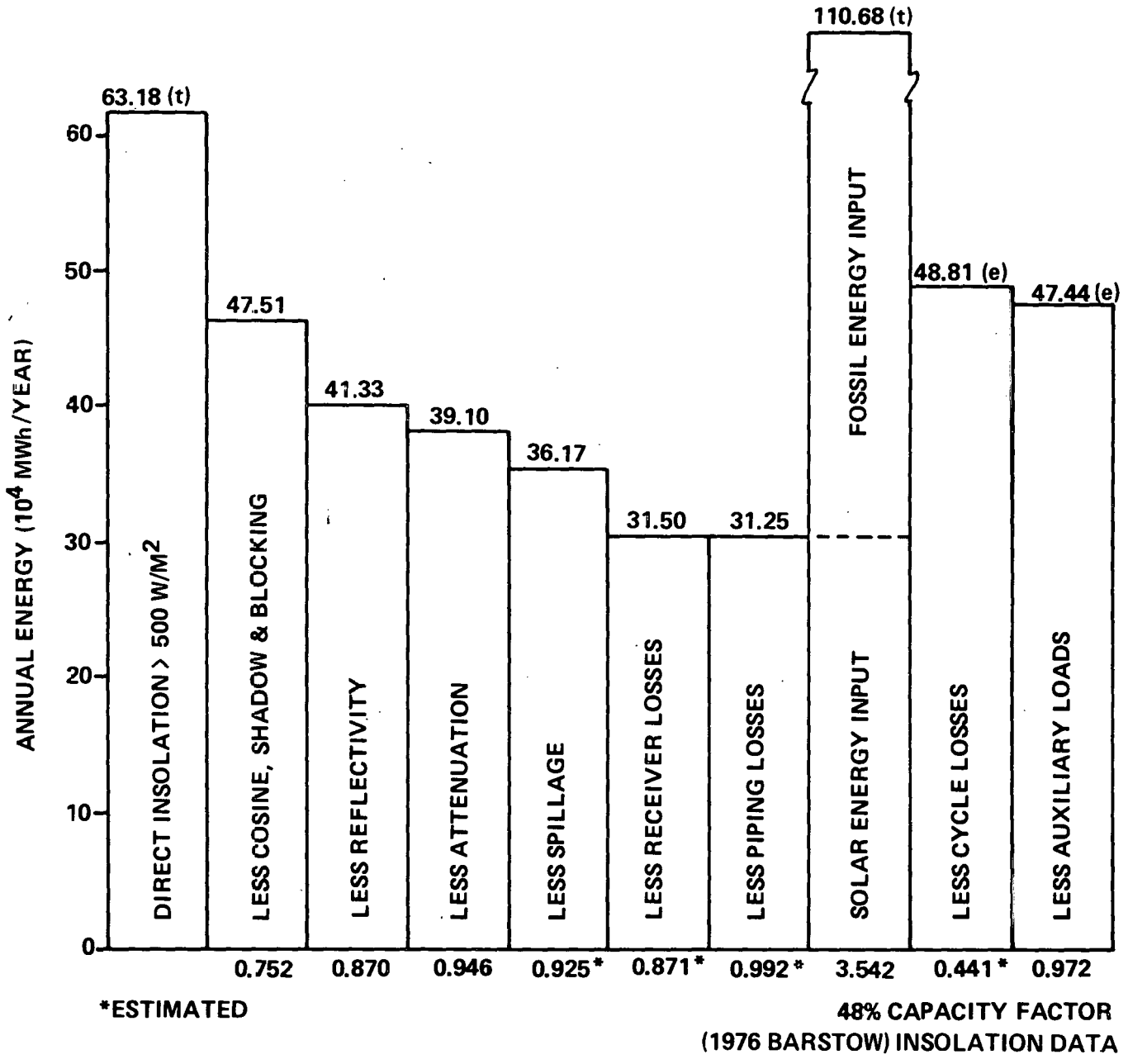

Figure 5-3 STAIR-STEP DIAGRAM, ANNUAL AVERAGE

day. The piping losses are adjusted for the lower average air temperature at the receiver outlet.

An annual capacity factor of 48 percent was used to calculate the electric output. With 90 percent availability, this represents an average of approximately 2 hours per day operation in the fossil-only mode.

5.2 COLLECTOR SUBSYSTEM

The collector subsystem consists of heliostats deployed in the collector field, supporting power and control elements, a heliostat alignment system, and field lightning protection. The collector design requirements, conceptual design, and performance characteristics are described in this section.

5.2.1 Requirements

The subsystem requirements are stated in the Requirement Definition document (Ref. 5-1). In addition to these general requirements, the total solar power collected and reflected to the aperture plane at design point must be 147 MWt.

5.2.2 Conceptual Design

Field Layout. The preferred collector field selected in preconceptual design ("G" field) was laid out in a rectangular grid pattern, as described in Section 3. From this layout, the

radial stagger "H" field (Figure 5-4), was developed from the spacing relationships used by the University of Houston and Sandia, Livermore. For a three-cavity receiver, the "H" field performs about 6 percent better than the "G" field at the lower tower heights. Costs for the "H" field are compared to those of several other fields in Figures 5-5 and 5-6 at two specific heliostat costs, corresponding to the 1990 first and eightieth plants. Since the radial-staggered field is expected to have lower costs and higher performance, the "H" field was selected as the reference layout in the conceptual design.

Collector. Design of the collector itself was outside the scope of this study. As a result, no novel collector designs are offered to reduce manufacturing cost or increase performance. The best projected performance was assumed for all collector components regardless of source. This approach endeavored to eliminate any penalty on the system performance resulting from any single design inadequacy.

Studies performed during the parametric analyses indicated that larger heliostats will result in a less expensive collector subsystem. Heliostat dimensions and characteristics selected for the conceptual design were those of the 50.54 m^2 Northrup II unit. (See Figures 5-7 and 5-8.) This was used mainly because of the availability of extensive data related to design details and performance projections. It is comparable in reflector area with other designs undergoing evaluation in the current heliostat development effort.

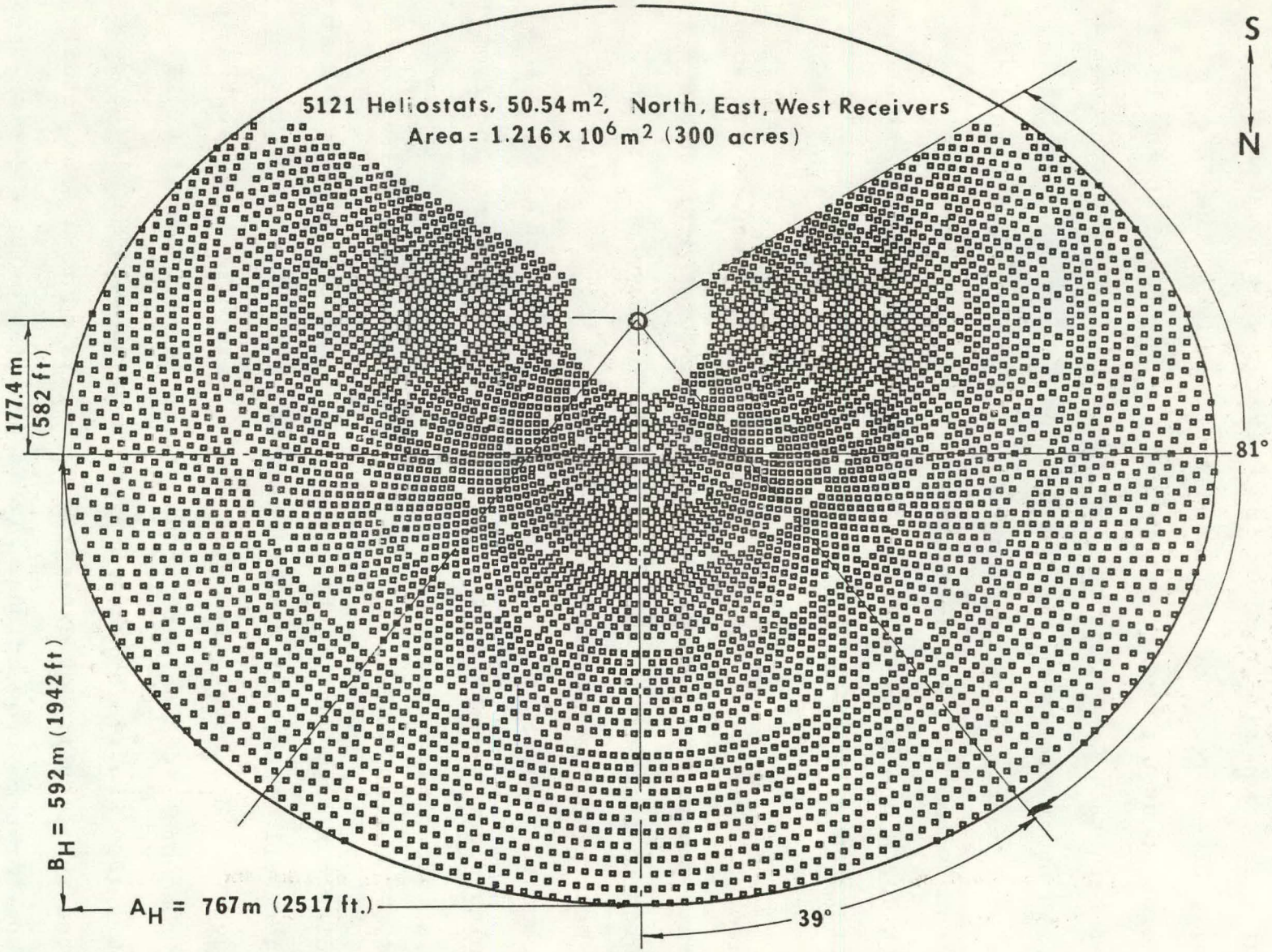

Figure 5-4 'H' FIELD RADIAL STAGGER LAYOUT

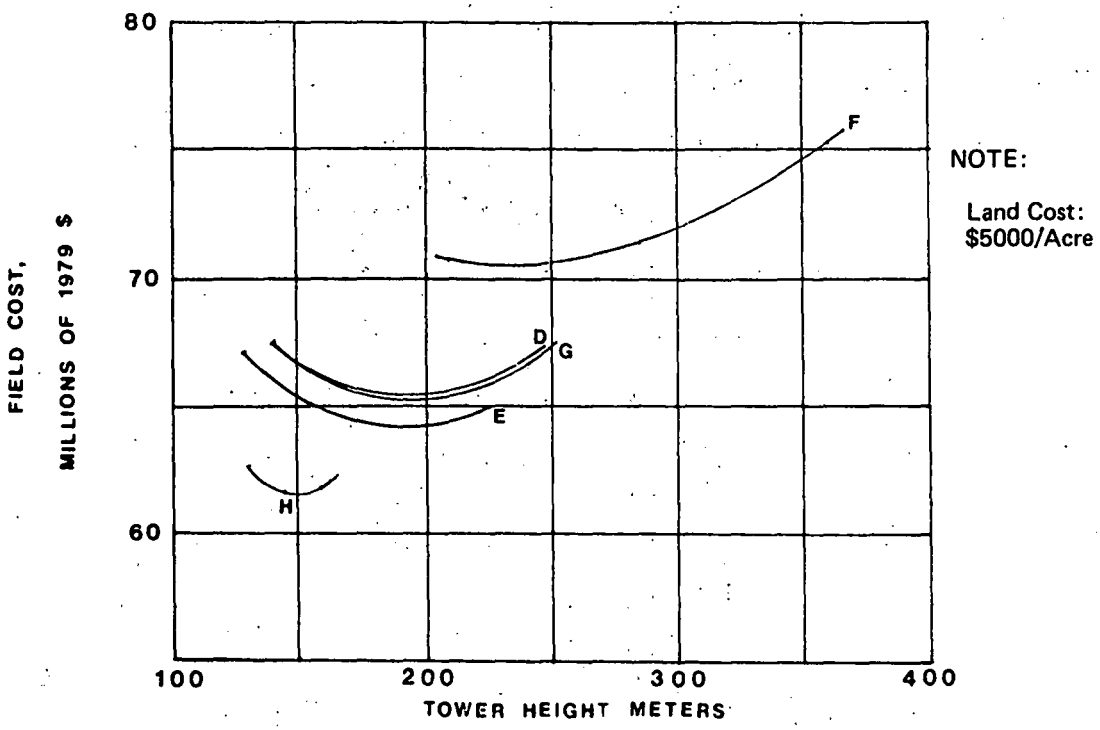

Figure 5-5 NORMALIZED FIELD COST, HELIOSTATS AT $160 /m2

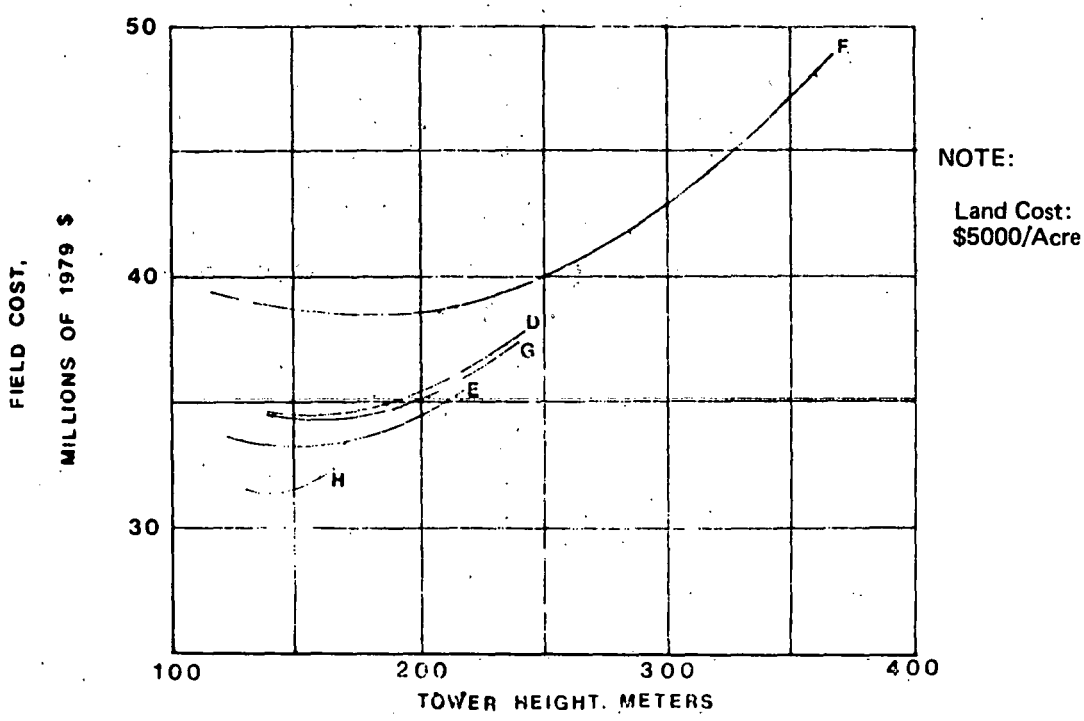

Figure 5-6 NORMALIZED FIELD COST, HELIOSTATS AT $69.6 /m2

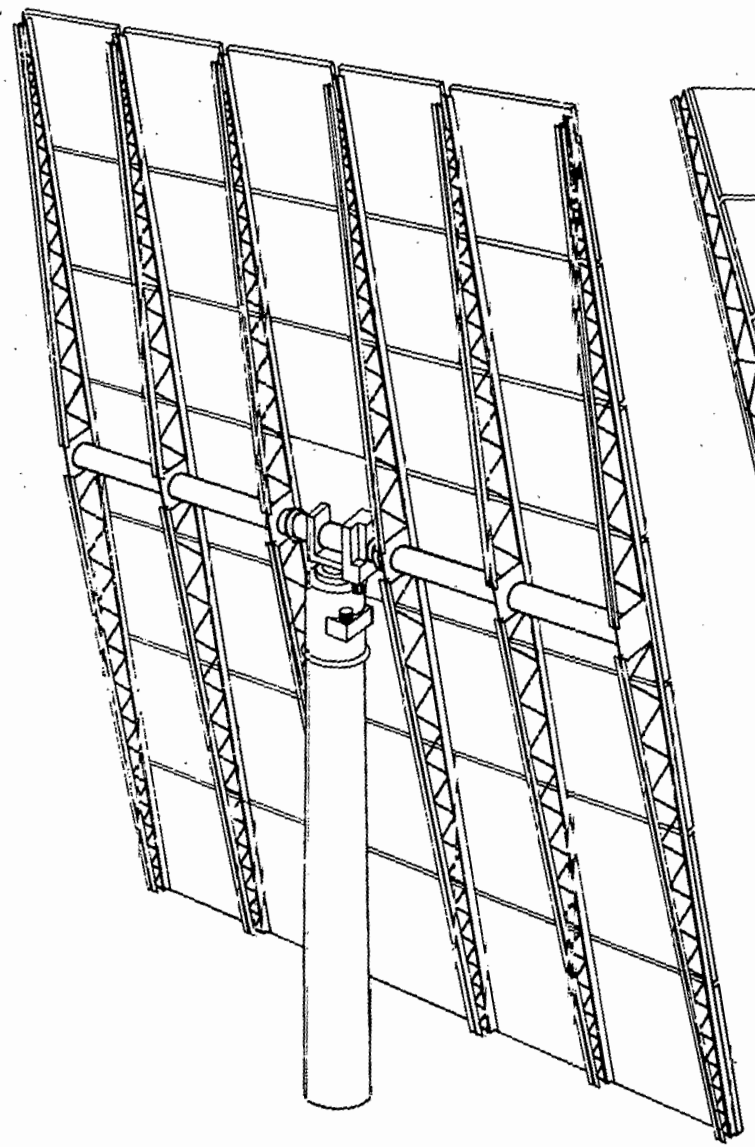

Figure 5-7 BACK VIEW OF HELIOSTAT (NORTHRUP II)

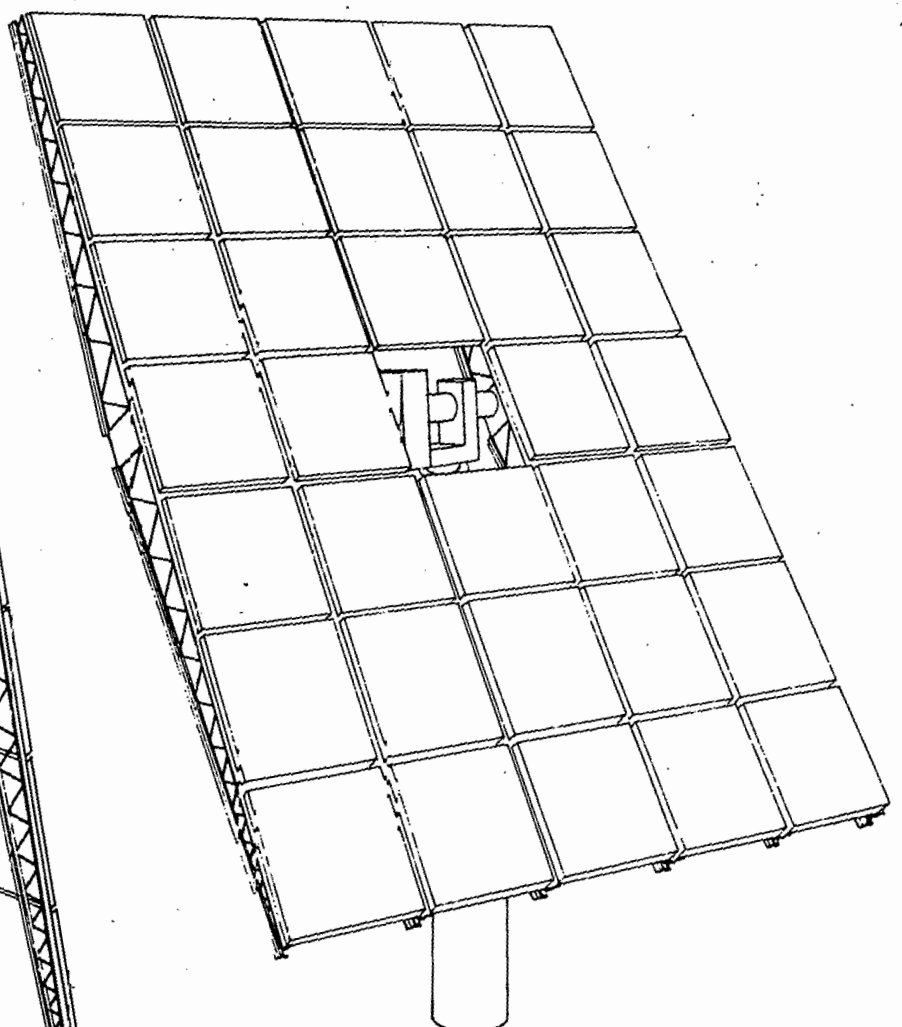

Figure 5-8 FRONT VIEW OF HELIOSTAT (NORTHRUP II)

The heliostat design uses a single support from the foundation to the drive unit. The drive unit positions the mirror support rack and the mirror modules in a precise position. The pedestal supports the drive and gimbaled components, limiting deflections to 0.66 mrad under normal operating conditions. The pedestal is capable of unyielding support in winds up to 40 m/sec (90 mph) with the rack stowed, and 22 m/sec (50 mph) with the rack in any orientation.

The tracking drive unit contains the drive motor, gears, and controls. The drive design uses a two-stage worm-gear drive system which is capable of large gear reductions with the minimum number of components.

The mirror support rack uses a trussed spar, designed to minimize weight while providing rigidity for minimum deflection. The spars are attached to the torque tube using tapered bolts giving an attachment method that will remain solid for the expected life of the plant.

The mirror modules use 1.21 m by 1.21 m (4 ft by 4 ft) facets of silvered glass, which allows procurement in the most common glass size. The glass is 94 mm (3/32 in.) thick with the lowest iron content available at production time. The estimated reflectivity used in the system study was .87, which is conservative in the 1990 time frame. The facet support is still in development. Most current designs use either a glass-glass or a glass-foam-steel sandwich.

5.2.3 Performance

To achieve economic performance of the collector subsystem, 95 percent of the reflected solar radiation must be collected at an incident angle of less than 60 degrees on the receiver. Table 5-2 shows collector error tolerances required to meet these goals and manufacturer test results indicating the capability of current heliostat designs to meet these tolerance limits.

Heliostat manufacturers suggest that their products will be capable of 30-year life under the following environmental conditions:

Ambient temperature	32 to 120F
Wind speed	26 mph at a 1.3 gust factor
Stowage initiation	36 mph
Wind rise rate during stowage	1.3 mph/min, heliostat to withstand a maximum wind of 50 mph without catastrophic failure
Wind profile	$V_z = V_o \left(\frac{z}{10}\right)^{.15}$ z = height above ground, m V_z = wind velocity at height z V_o = wind velocity at 10 m above ground

The heliostat components are designed so that stresses resulting from dynamic forces will not exceed structural capabilities. The maximum pressure exerted by the base of the pedestal foundation footing upon the soil is less than 71.8 kPa (1500 psf) at .6 m (2 ft) and 239 kPa (5000 psf) at 1.5 m (5 ft) below the surface.

The heliostats can satisfy operational requirements in a sustained surface wind up to 8.9 m/sec (20 mph) and gusts up to 11.6 m/sec (26 mph) at all elevation angles and can remain operational with gusts up to 16 m/sec (36 mph). In a nonoperational mode, the heliostats can survive 22.4 m/sec (50 mph) wind at worst azimuth and elevation angles. It can be moved to stowed position in 15 minutes and thereafter can survive wind gusts up to 40.2 m/sec (90 mph). Mirror samples have survived impacts from 19 and 25 mm (.75 and 1.0 in) diameter hail stones at measured velocities of 20 m/sec (65 fps) and 25 m/sec (75 fps), respectively. (Survival means that the specimen withstood six impacts with no damage.)

Using the wind load methodology of ASCE Paper 3269 (Ref. 5-2), a facet-by-facet analysis was performed to determine the aiming error as a function of wind speed and elevation angle. Northrup computer codes "BEAMSUM" and "BEAMRAD" were used in the computations. Both frontside and backside wind impacts were evaluated. Wind speeds from 0 to 16 m/sec (0 to 36 mph) were considered.

The analysis considered the combined effects of the following:

- Beam bending, which varies with 1) facet position from top to bottom of the heliostat, 2) elevation angle, 3) wind speed, and 4) wind direction (front vs. back)
- Differential beam bending between adjacent beams to which a given mirror is attached
- Support column bending due to both the drag force and elevation moment (With a frontside wind, these two

effects tend to be compensatory, and with a backside wind they are additive.)

- Support column bending (For facets below the elevation axis, the combined effects of beam bending and column bending are compensatory, and for facets above the elevation axis they are additive.)

The wind-induced mean error and standard deviation for the entire field of heliostats are given in Table 5-3.

The error indicated at 0 m/sec wind speed is due to the gravity loads of the mirror modules and beams, which were also included in this analysis. Torsional deflections of the heliostat torque tube were also examined, but were found to be small relative to the column and beam bending, so were not further considered.

The calculated errors due to the wind were then combined with the other potential errors (mirror waviness, backlash, tracking error, etc.) to yield a total system error for five wind speeds. Northrup's "Flux" computer code was used to evaluate the effects of these errors on spillage, target plane distribution, and the receiver flux distribution for the "H" field at equinox noon. The results are presented in Tables 5-4 and 5-5.

Even with the conservative assumptions used in the analysis, increases in spillage due to wind were relatively modest. As evident from Figures 5-9 and 5-10, the flux profiles are rather dramatically changed by the wind. However, this effect is generally beneficial and results in reduced tube temperatures, thermal stresses, and receiver heat losses.

TABLE 5-2

HELIOSTAT ERROR TOLERANCES

Tolerance Item	Tolerance Target	Tested Heliostat Accuracy
Reflectivity	-	.91
Beam pointing error, mrad	1.5	2.5
Reflective surface deflection, mrad	1.7	1.7
Optical spreading, mrad	-	1.4
Foundation settling, mrad	.05	-
Plastic structural deformation, mrad	.5	-

TABLE 5-3

MEAN AND STANDARD DEVIATION WIND-INDUCED ERROR

Wind Speed (m/sec)	Mean Error (mrad)	Standard Deviation (mrad)
0	0.091	0.076
3	0.098	0.088
7	0.172	0.136
11	0.375	0.371
16	0.789	0.844

TABLE 5-4

NORTH RECEIVER WIND EFFECT SUMMARY

Wind Speed (m/sec)	Peak Target Plane Flux (kW/m^2)	Peak Receiver Plane Flux (kW/m^2)	Energy Spillage (%)
0	4,132	1,081	1.99
3	4,077	1,075	2.00
7	3,717	1,037	2.08
11	2,840	937	2.44
16	1,871	816	3.35

TABLE 5-5

WEST RECEIVER WIND EFFECT SUMMARY

Wind Speed (m/sec)	Peak Target Plane Flux (kW/m^2)	Peak Receiver Panel Flux (kW/m^2)	Energy Spillage (%)
0	2,748	1,100	3.11
3	2,653	1,082	3.14
7	2,518	1,056	3.18
11	2,015	951	3.47
16	1,425	796	4.19

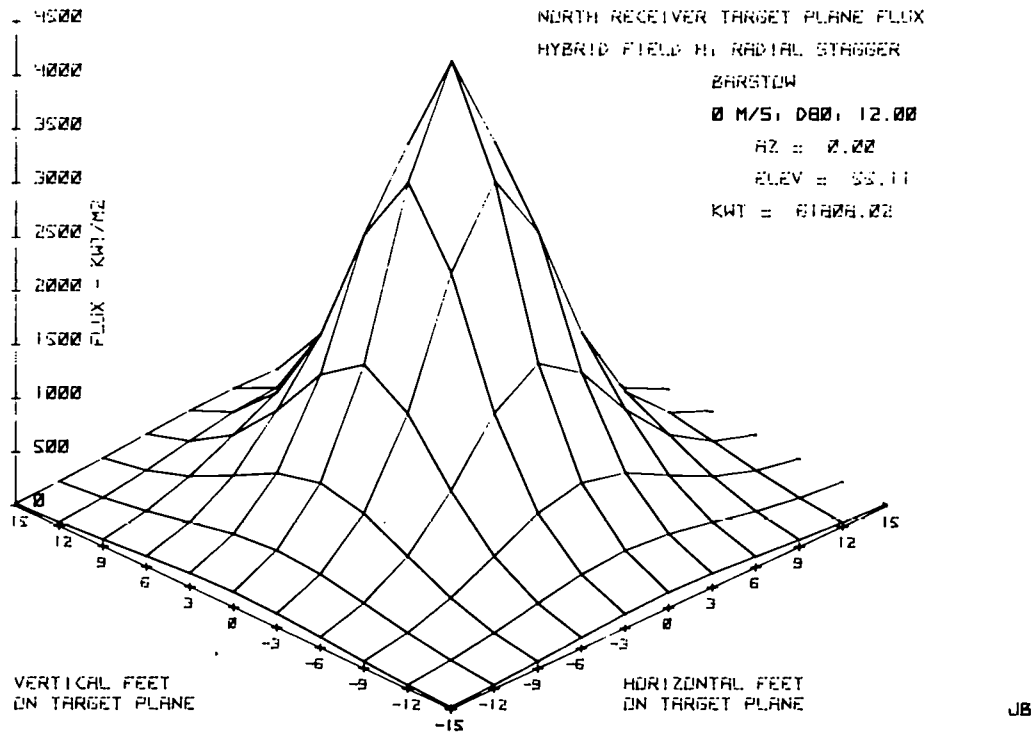

Figure 5-9 NORTH FOCAL PLANE FLUX MAP (WIND AT 0 m/sec)

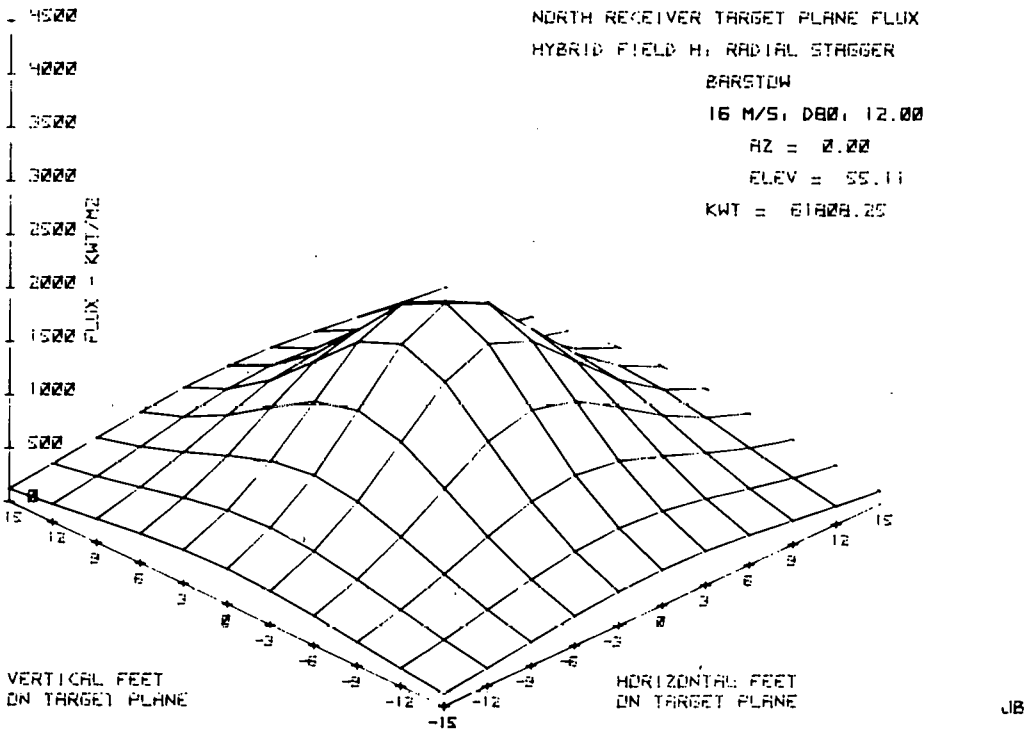

Figure 5-10 NORTH FOCAL PLANE FLUX MAP (WIND AT 16 m/sec)

5.3 RECEIVER SUBSYSTEM

The receiver subsystem consists of the receiver proper, the receiver tower, and the riser/downcomer piping. The latter connects the receiver with the gas turbine. Valves and controls for the safe and efficient operation of the solar hybrid power system are also included. The requirements, conceptual design, and performance for this subsystem are described in this section.

5.3.1 Requirements

The receiver subsystem requirements listed in Table 5-6 are consistent with those in the Requirement Definition document (Ref. 5-1). In addition to these specific requirements, the receiver must satisfy the following:

- High efficiency by minimizing heat losses caused by reradiation, reflection, convection, and conduction
- Maximum use of existing hardware and manufacturing techniques
- Low capital cost
- Suitable cyclic service
- Minimum development requirement

5.3.2 Receiver Conceptual Design

The function of the receiver is to transform the incident solar energy from the heliostat field into thermal energy and transport the thermal energy to the air stream. The receiver design

TABLE 5-6

RECEIVER SUBSYSTEM REQUIREMENTS

Characteristic	Value
Receiver configuration	Multicavity, heat pipe panels
Design point	Equinox noon
Number of cavities	3
Total power to cavity focal plane, MWt	152.2
Total power to receiver air, MWt	138.0
Average air temperature, C(F)	
At receiver inlet	363.9 (687)
At receiver outlet	843.3 (1550)
Air pressure at receiver inlet, MPa(psig)	1.055 (153)
Receiver pressure drop, kPa(psi)	43.37 (6)
Air flow rate, kg/sec (lb/sec)	257.6 (568)
Design life, years	30
Plant cycles	13,000
Plant availability, %	90

considered factors such as cost, weight, size, surface requirements, materials, thermal efficiency (heat losses), air pressure drop, design complexity, operation and control, thermal transients, maintenance, and installation. The receiver design work involved:

- Thermal hydraulic analyses to establish panel size, flow path, pressure drop, heat-transfer coefficients, and metal temperatures
- Receiver performance analyses to calculate receiver losses (reflection, reradiation, convection, and conduction losses) and receiver power output throughout the year
- Receiver thermal stress analyses to determine wall thickness of components
- Mechanical design analyses to establish panel configuration, method of panel support, cavity enclosure configuration, and support structure

Description. The receiver consists of three cavities mounted on top of the receiver tower, and oriented as shown in plan view in Figure 5-11. The configuration of the cavity is shown in Figure 5-12. Each cavity consists of absorber panels, enclosure, inlet and outlet manifolds, insulation, and support structure. The cavity back walls each have 11 factory-assembled panels, which are shown in Figure 5-13. Because of stress, seismic, and thermal expansion considerations, the panels are hung from the cavity structure and are welded together on site. This eliminates the need for very thick side panel walls and eliminates the previously required gaps between panels to accommodate thermal expansion. Materials savings of about 20 percent resulted from this change. Simplicity of panel design

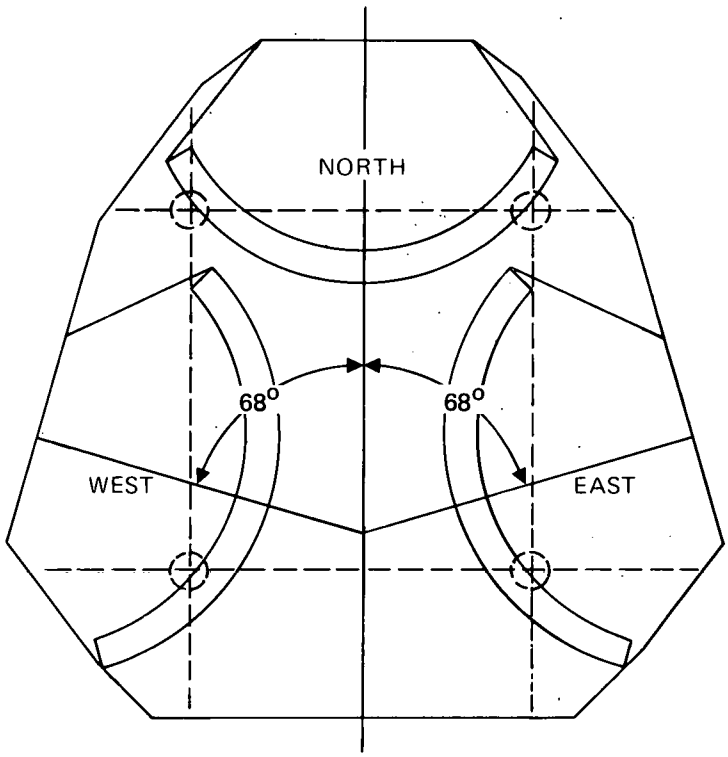

Figure 5-11 RECEIVER PLAN ARRANGEMENT

and elimination of high stresses at the corners of the panels are additional advantages.

Each panel is a rectangular air duct fitted with 1,147 heat pipes, installed in an 11.1 mm (4.375 in.) triangular-pitch pattern. The heat pipes are attached to the front and back plates of each panel. This permits removal for servicing or replacement from the back of the panel and eliminates the need for separately replaceable panels. The heat pipe design and operating principles are described in Section 3.

A 0.66 m (26 in.) diameter inlet manifold distributes the air to each panel via butterfly control valves at the bottom inlet of each panel. A 0.76 m (30 in.) diameter outlet manifold collects the hot air leaving the panels. The manifolds are outside the cavity. Welded piping connections are used.

The interior surfaces of the cavity are lined with insulation (Fiberfrax in high-temperature zones) to keep the conductive heat losses low. This insulation also protects the cavity enclosure and structural support steel members from excessive temperatures. The outer surfaces are covered with weatherproofed insulation and corrugated aluminum sheeting.

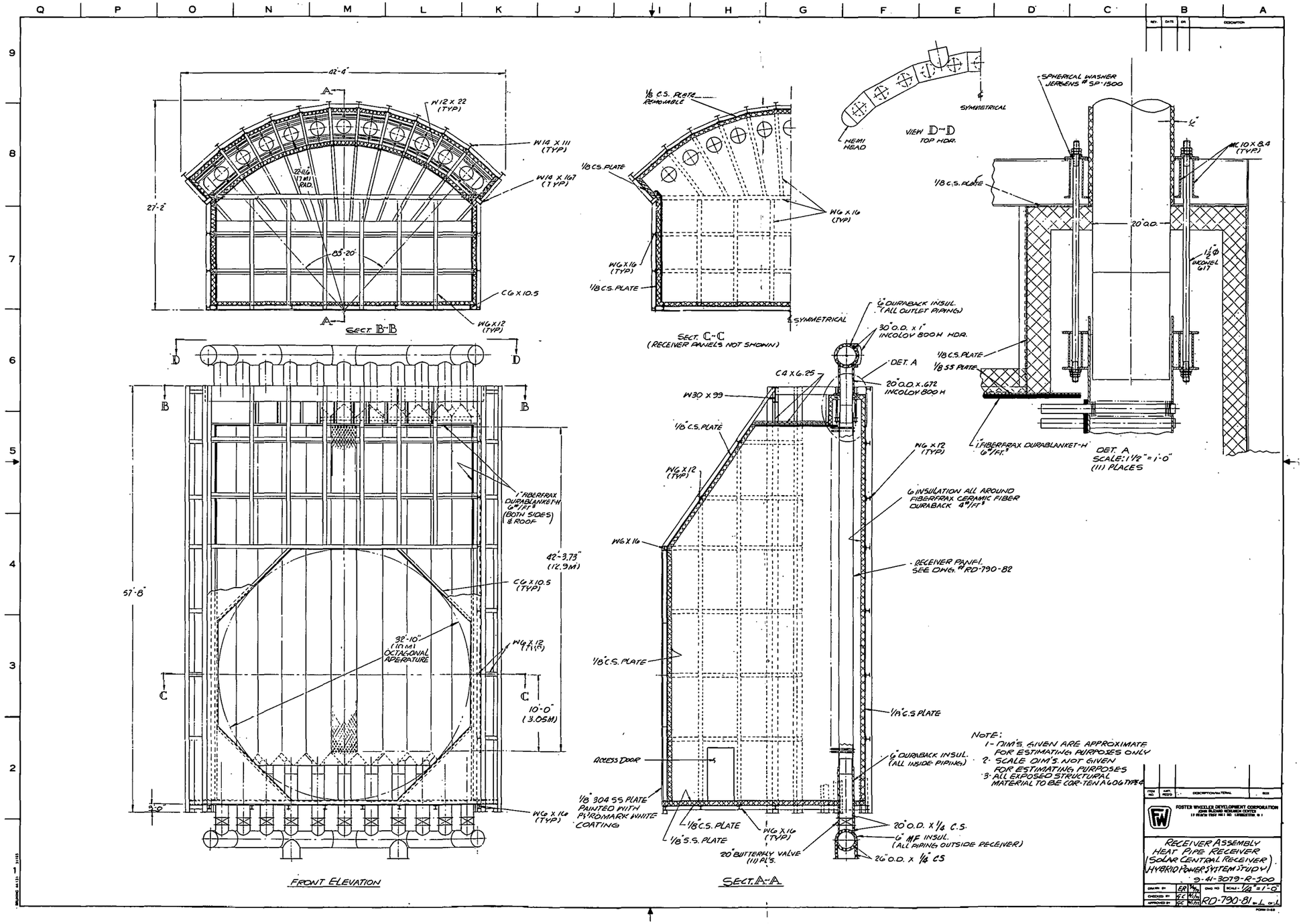

Figure 5-12 CAVITY DESIGN

THIS PAGE

WAS INTENTIONALLY

LEFT BLANK

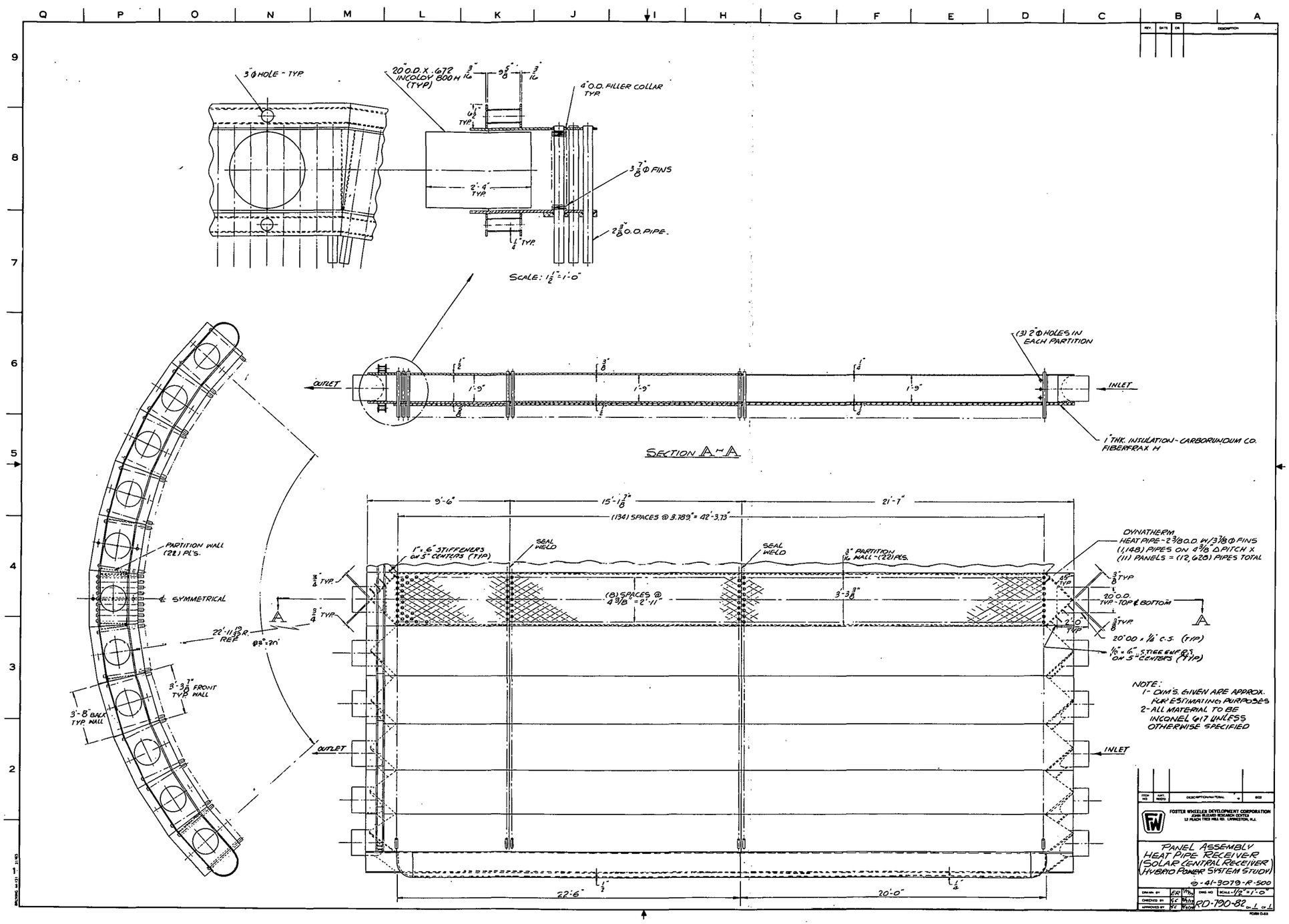

Figure 5-13 PANEL DESIGN

THIS PAGE

WAS INTENTIONALLY

LEFT BLANK

Size. The receiver must provide 138 MW to the system air at the design point of equinox noon. The maximum power delivered by the mirror field to the cavity aperture plane is 61.90 MW at the north cavity (equinox noon), and 60.13 MW at the west and east cavities (equinox 10 a.m. and 2 p.m., respectively). The difference between these peak values is small enough for all cavities to be of the same design, which minimizes design, fabrication, and installation costs.

The selected receiver material, Inconel 617, has an upper useful temperature limit of about 871C (1600F). This limits the peak radiant heat fluxes absorbed by the receiver to 1.26 MW/m^2 (400,000 $Btu/hr\text{-}ft^2$) which resulted in a cavity depth of 7.0 m (23 ft). Table 5-7 gives the matrix of direct solar heat flux incident on the panels of the north cavity at equinox noon. Reflected radiation from the inner cavity walls was not included in the calculations, since it will have little effect on the high heat flux areas near the middle. Eleven panels 1.0 m (3.3 ft) wide by 13.0 m (42.5 ft) high are required to absorb incident solar energy.

Weight. The receiver weight estimate includes the weight of panels, heat pipes, insulation, structural members, manifolds, and other receiver components. The weight breakdown is shown in Table 5-8.

TABLE 5-7

INCIDENT HEAT FLUX, PANEL ZONES
(MW/m^2)

DISTANCE FROM BOTTOM OF PANEL m	ft	PANEL NUMBER 6	5 & 7	4 & 8	3 & 9	2 & 10	1 & 11
		0.1410	0.1090	0.0810	0.0620	0.0360	0.0150
	40	0.2220	0.1990	0.1740	0.1500	0.1080	0.0540
10		0.5530	0.5180	0.4490	0.3580	0.2390	0.1260
	30	1.0330	0.9850	0.8660	0.6910	0.4760	0.2730
		1.2580	1.2080	1.0680	0.8590	0.6080	0.3700
	20	1.0130	0.9750	0.8670	0.7030	0.5090	0.3230
5		0.5730	0.5520	0.4940	0.4040	0.2980	0.1960
	10	0.2370	0.2290	0.2060	0.1700	0.1270	0.0860
0	0	0.0730	0.0710	0.0640	0.0530	0.0410	0.0280

TABLE 5-8

RECEIVER WEIGHT BREAKDOWN

Component	Weight	
	kg	lb
Structural steel	176,691	388,720
Carbon steel plate	48,427	106,540
Stainless steel plate	8,132	17,890
Incoloy 800H plate	44,905	98,790
Inconel 617 bar	1,055	2,320
Inconel 617 plate	114,245	251,340
Heat pipes	288,182	634,000
Valves	2,550	5,610
Durablanket-H insulation	2,345	5,160
Duraback insulation	24,136	53,100
Mineral fiber insulation	1,090	2,400
Lagging	450	990
Total	712,209	1,566,860

Thermal Hydraulic Analysis. For purposes of thermal hydraulic analysis, each panel was divided into nine axial zones. Then, using the solar flux data matrix of Table 5-7, the net power into the air along the length of the panels, and the heat pipe duties were calculated. As seen in Table 5-9, the maximum heat pipe energy transport requirement is 11.7 kW, which is well within the measured heat transport capabilities of the type of heat pipes proposed for the receiver. The total mass flow of air to the receiver, 257.6 kg/sec (568 lb/sec), is distributed to the three cavities in proportion to the heat input to each cavity. Thus, at equinox noon, 36.22 percent goes to the north cavity and 31.89 percent each to the west and the east cavities.

The airflow to each panel is adjusted in proportion to the collected energy, so that the outlet temperature at each panel is 843C (1550F). The airflow distribution in the north cavity at equinox noon is shown in Figure 5-14. The calculated peak metal temperature of 888C (1631F) occurs in the heat pipe boiling sections in the center panel, about two-thirds from the bottom of the panel. This temperature is above the nominal limit of 871C (1600F). But the boiling region has no pressure forces, so the elevated temperatures are acceptable.

Structural, Thermal Stress, and Mechanical Design Analysis. Structural analysis of the receiver subsystem includes both thermal stress analysis and mechanical design analysis.

TABLE 5-9

POWER TRANSPORTED BY INDIVIDUAL HEAT PIPES
(kW)

DISTANCE FROM BOTTOM OF PANEL m	ft	PANEL NUMBER 6	5 & 7	4 & 8	3 & 9	2 & 10	1 & 11
		1.31	1.01	0.75	0.58	0.33	0.14
	40	2.06	1.85	1.62	1.39	1.00	0.50
10		5.14	4.81	4.17	3.33	2.22	1.17
	30	9.60	9.15	8.04	6.42	4.42	2.54
		11.69	11.22	9.92	7.98	5.65	3.44
	20	9.41	9.06	8.05	6.53	4.73	3.00
5		5.32	5.13	4.59	3.75	2.77	1.82
	10	2.20	2.13	1.91	1.58	1.18	0.80
0	0	0.68	0.66	0.59	0.49	0.38	0.26

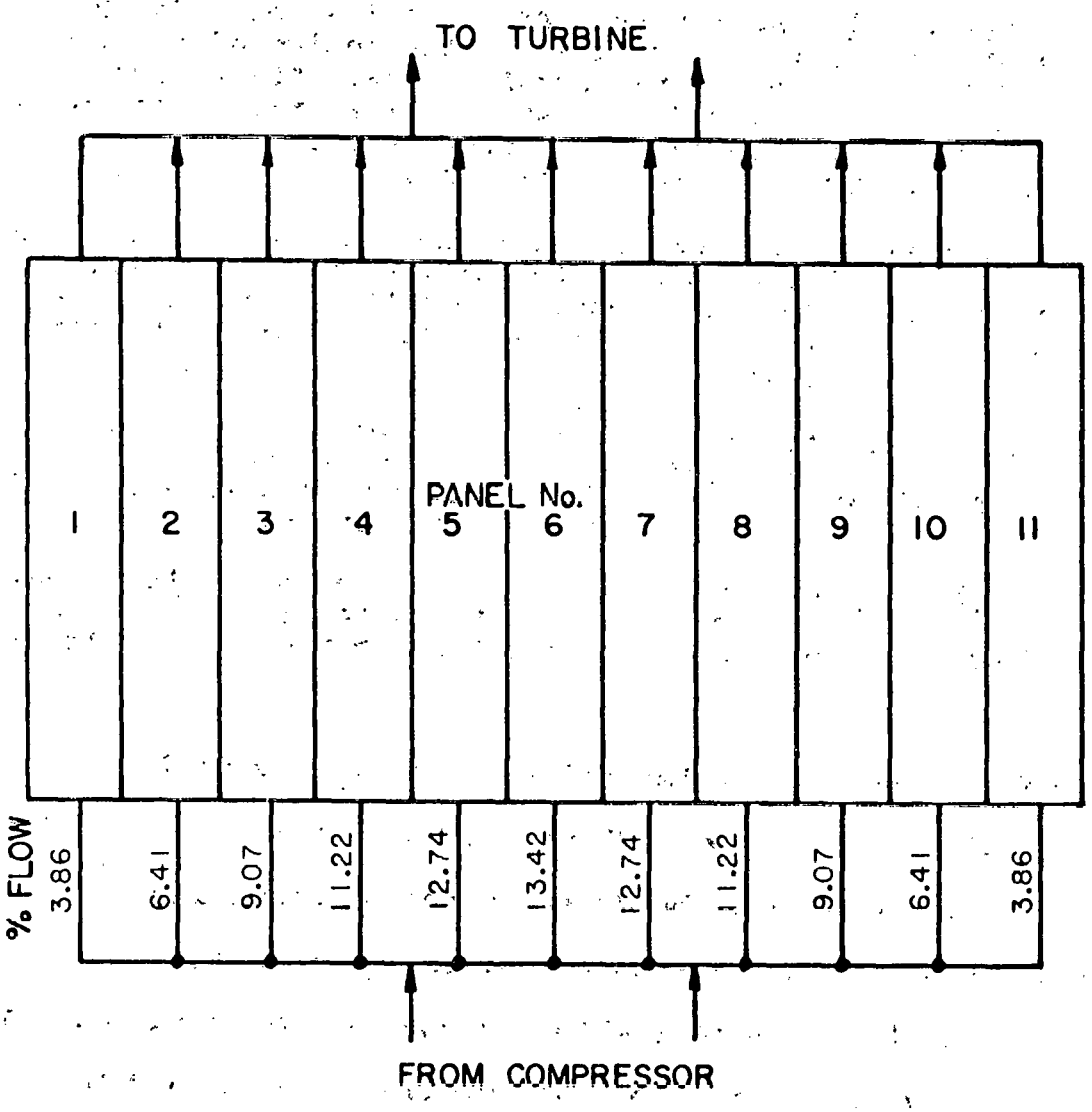

Figure 5-14 NORTH CAVITY AIRFLOW DISTRIBUTION

The following loads were used in the analyses of particular receiver components:

- Panel Shell. An internal pressure load of 0.954 MPa (138.3 psig) was considered in the design of the panel shell walls and the two nozzle heads. The design temperature varies from 364C (687F) at the inlet to 843C (1550F) at the outlet. The panel shell components are also subjected to thermal stresses.

- Heat Pipes. The loadings relevant to heat pipes include the external pressure, internal pressure, and axial load resulting from load transfer from the front and back walls. The heat pipes are also subjected to thermal stresses.

- Piping and Headers. An internal pressure load of 0.954 MPa (138.3 psig) was considered. Design temperatures of 364C (687F) and 843C (1550F) were used for inlet and outlet pipes, respectively.

- Support Frame. The panel shell is supported by hangers and by the support frame. The loading for the support frame consists of the dead loads and the seismic loads.

The allowable stresses for Inconel 617, based on supplier data and the requirements of the ASME Boiler and Pressure Vessel Code, are shown in Table 5-10. The design stress intensities (difference between the maximum and minimum principal stresses) due to membrane forces were limited to the tabulated values. The stress intensity due to the combined membrane forces and bending moments was limited to 1.5 times the tabulated values. The maximum allowable thermal gradients were determined so that the stress intensity due to the combined membrane, bending, and thermal gradient loads did not exceed three times the allowable stresses in Table 5-10.

TABLE 5-10

ALLOWABLE MEMBRANE STRESSES IN INCONEL 617*

Design Temperature C(F)	Allowable Stress MPa (ksi)
316 (600)	165.5 (24.0)
427 (800)	151.7 (22.0)
538 (1000)	144.8 (21.0)
649 (1200)	131.0 (19.0)
760 (1400)	48.3 (7.0)
816 (1500)	37.2 (5.4)
871 (1600)	18.6 (2.7)

*Based on supplier data and ASME Boiler and Pressure Vessel Code, Section VIII, Division 1 (Appendix P).

The panel shell (Figure 5-13) consists of a front plate, a rear plate, and side panels made of cylindrical shells. The heat pipes act as supports for the front and rear plates. The front plate is protected from direct solar radiation by a 25 mm (1 in.) refractory wall. Since the panel shell temperature varies along its length, it was divided into three axial regions for analytical purposes. The design temperatures in these regions are shown in Table 5-11. The thickness of each of the components of the panel shell was computed at these temperatures.

The inlet and outlet nozzles consist of pyramidal shells supported at three intermediate locations by stiffeners. The pressure loads on the nozzles are the same as those on the panel shell. Design temperatures are 364C (687F) for the inlet nozzle and 843C (1550F) for the outlet nozzle. The inlet nozzle is made of carbon steel (SA-515, GR.70) and the outlet nozzle is made of Inconel 617. At the design temperature, the allowable membrane stresses for the carbon steel is 114 MPa (16.6 ksi). An estimate over the expected temperature distributions during a cloud cover passage showed that the thermal gradients are within allowable limits for the panel shell and nozzles.

The heat pipes, made of Inconel 617, are the only major receiver components exposed to direct solar radiation. The heat pipes also support the front and back walls against the internal panel pressure. Their outer diameter is 60.325 mm (2.375 in.). The wall thickness, 3.81 mm (0.15 in.), was computed by limiting the primary membrane stress intensity, due to internal and external

TABLE 5-11

DESIGN TEMPERATURES FOR COMPONENTS OF THE PANEL SHELL

Component	Design Temperature, C(F)		
	Lower Region	Mid Region	Upper Region
Front wall	677 (1250)	843 (1550)	871 (1600)
Rear wall	649 (1200)	816 (1500)	843 (1550)
Side panels	649 (1200)	816 (1500)	843 (1550)

pressures and the support reaction forces from the front and back walls, to 18.6 MPa (2.7 ksi).

The piping and header arrangement is shown in Figure 5-12. The pipe wall thicknesses are based on primary hoop stresses resulting from internal pressure without stress concentration effects at the nozzle connections.

The support frame for the panel shell shown in Figure 5-12 was designed in accordance with the AISC Manual (Ref. 5-3). The loading consists of the dead loads from the panel shell and earthquake loads. The earthquake loads are included as an equivalent static load of 2.15g acting in the vertical direction, corresponding to the operation base earthquake at 2 percent damping. The horizontal forces due to earthquake and wind are transferred to the tower by ties connecting the panel shell to points on the tower top, or dissipated by horizontal seismic dampers so that their effect is not felt by the support frame.

Receiver Performance Analysis. Receiver heat losses are proportional to the aperture area. Thus, selecting the aperture size and configuration involves a trade-off between the spillover and the amount of energy lost due to reradiation, reflection, and convection losses. The optimum aperture was defined as that which can collect the highest net power. Figure 5-15 shows the process used to optimize the aperture size for the north facing cavity, based on an octagonal aperture.

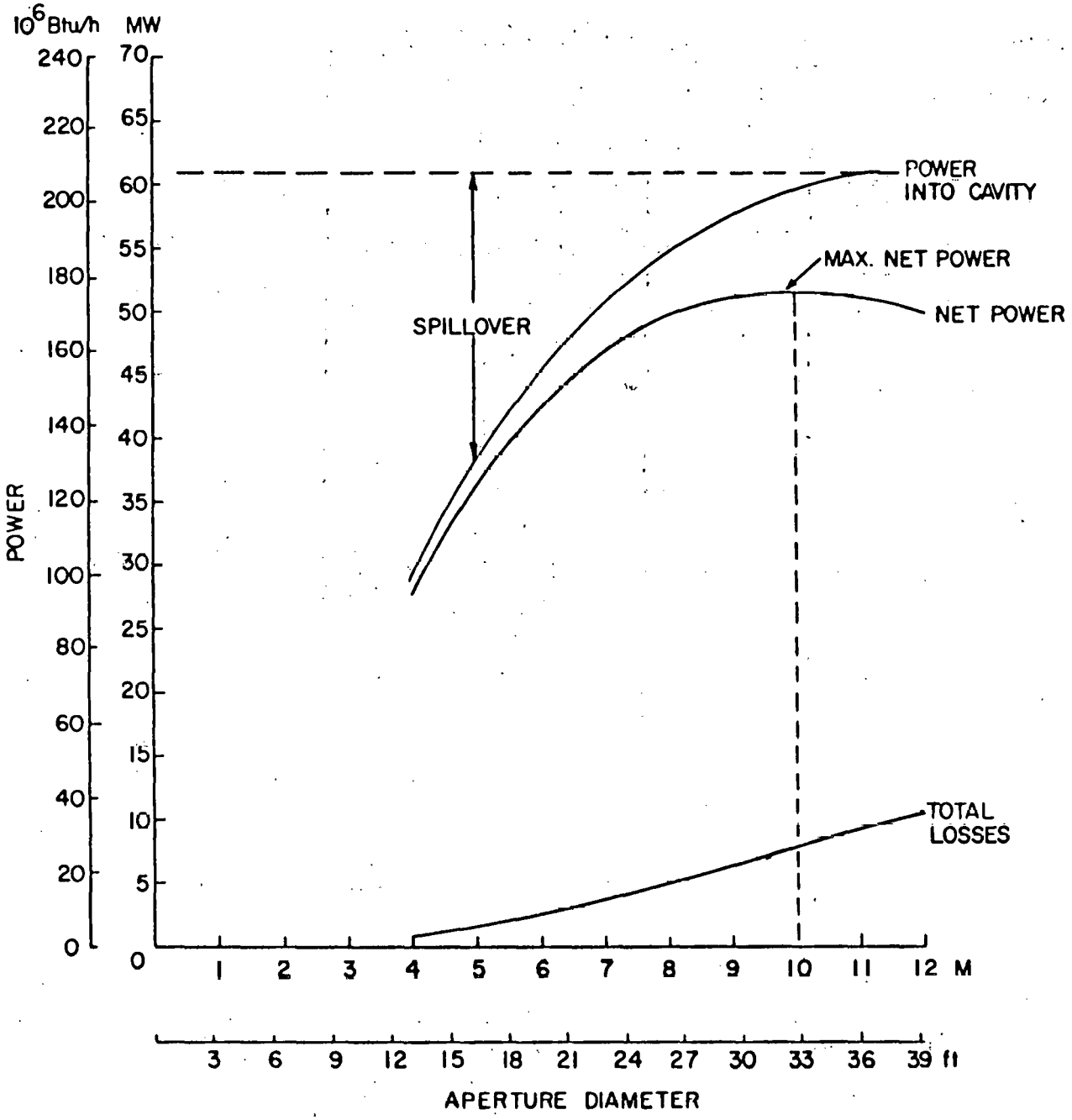

Figure 5-15 APERTURE SIZING

In principle the best aperture would be circular. However, it is somewhat more expensive to fabricate. Thus, only square and octagonal apertures were considered during the aperture optimization process. Aperture diameters up to 12 m (39.4 ft) were considered. (Diameter is the size of the circle inscribed within the aperture.) Table 5-12 shows the performance of the north cavity with square and octagonal apertures. The table shows that an octagonal aperture of 83 m^2 (892 ft^2) is more efficient and, therefore, it was selected for all three cavities.

Using the same size aperture for the north, east, and west cavities, the receiver heat losses were calculated as a function of wind speed and ambient temperatures. The results are plotted in Figure 5-16.

The performance of the north, east, and west cavities was calculated for noon on winter and summer solstices and equinox. The results are shown in Table 5-13 and Figure 5-17. The cavity performances as functions of the time of day, calculated at equinox, are shown in Table 5-14 and in Figure 5-18. As seen from these tables, the receiver delivers 141.18 MW to the system air at the design point of equinox noon. This represents a margin of 2.3 percent over the 138 MW required at equinox noon.

TABLE 5-12

NORTH CAVITY PERFORMANCE

Characteristic	Square Aperture	Octagonal Aperture
Area, m^2	92.16	82.84
Power at aperture plane, MW	61.90	61.90
Spillover, MW	1.92	2.40
Power into cavity, MW	59.97	59.49
*Aperture efficiency, %	96.89	96.12
Losses: Conduction, MW	0.31	0.31
Convection, MW	1.77	1.59
Radiation, MW	5.52	5.04
Reflection, MW	0.99	0.88
Total cavity losses, MW	8.58	7.83
Net power to air, MW	51.39	51.66
**Cavity efficiency, %	85.69	86.84
***Overall efficiency, %	83.00	83.50

Assumptions	
Wind velocity, m/sec (mph)	6.7 (15.0)
Ambient temperature, C(F)	15.5 (60.0)
Inlet air temperature, C(F)	363.9 (687.0)
Outlet air temperature, C(F)	843.3 (1550.0)

$$*\text{Aperture efficiency, } \eta_a = \frac{\text{Power through aperture}}{\text{Power that reaches aperture plane}}$$

$$**\text{Cavity efficiency, } \eta_c = \frac{\text{Net power to air}}{\text{Power through aperture}}$$

$$***\text{Overall efficiency} = \frac{\text{Net power to air}}{\text{Power at aperture plane}} = \eta_a \cdot \eta_c$$

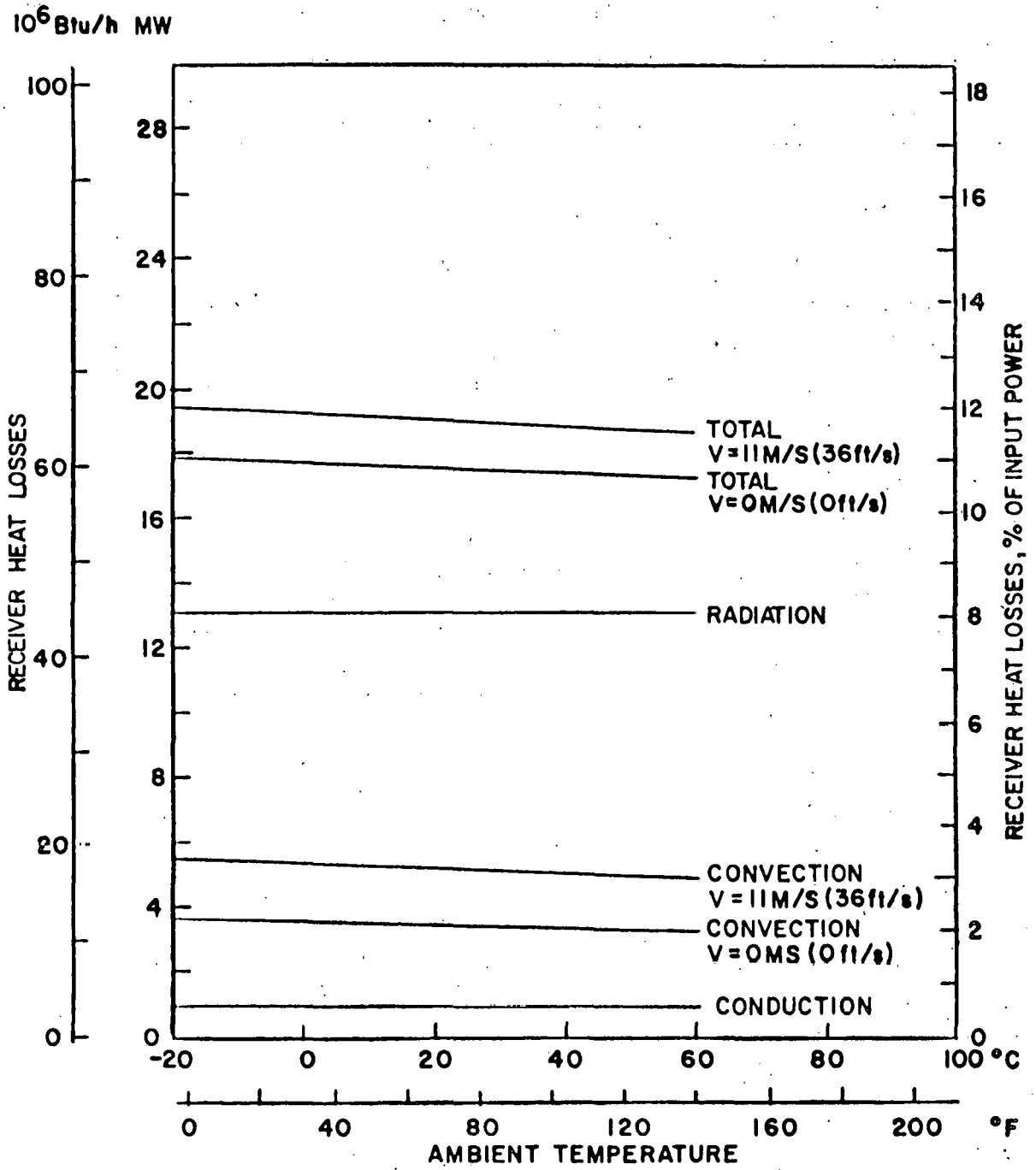

Figure 5-16 RECEIVER LOSSES AT RATED POWER OPERATION

TABLE 5-13

POWER VS. DAY OF YEAR AT NOON

Season of Year	Receiver	Power From Mirror Field Megawatts	Power Into Aperture Megawatts	Net Power To Air Megawatts
Summer Day 173	North	56.43	51.41	44.85
	West	55.17	50.05	43.67
	East	55.17	50.05	43.67
	Total	166.77	151.51	132.19
Equinox Day 80	North	61.90	59.49	51.66
	West	54.50	51.31	44.76
	East	54.50	51.31	44.76
	Total	170.90	162.11	141.18
Winter Day 355	North	56.10	53.87	46.95
	West	48.13	43.99	38.40
	East	48.13	43.99	38.40
	Total	152.36	141.85	123.75

TABLE 5-14

POWER VS. TIME OF DAY AT EQUINOX

Time of Day	Cavity	Power From Mirror Field Megawatts	Power Into Aperture Megawatts	Net Power To Air Megawatts
8 a.m.	North	51.18	46.02	40.18
	West	59.67	56.92	49.52
	East	32.97	26.91	23.23
	Total	143.82	129.85	112.93
10 a.m.	North	58.32	54.38	47.38
	West	60.13	57.18	49.74
	East	45.72	39.95	34.85
	Total	164.17	151.51	131.97
12 Noon	North	61.90	59.49	51.66
	West	54.50	51.31	44.76
	East	54.50	51.31	44.76
	Total	170.90	162.11	141.18
2 p.m.	North	58.32	54.38	47.38
	West	45.72	39.95	34.85
	East	60.13	57.18	49.74
	Total	164.17	151.51	131.97
4 p.m.	North	51.18	46.02	40.18
	West	32.97	26.91	23.23
	East	59.67	56.92	49.52
	Total	143.82	129.85	112.93

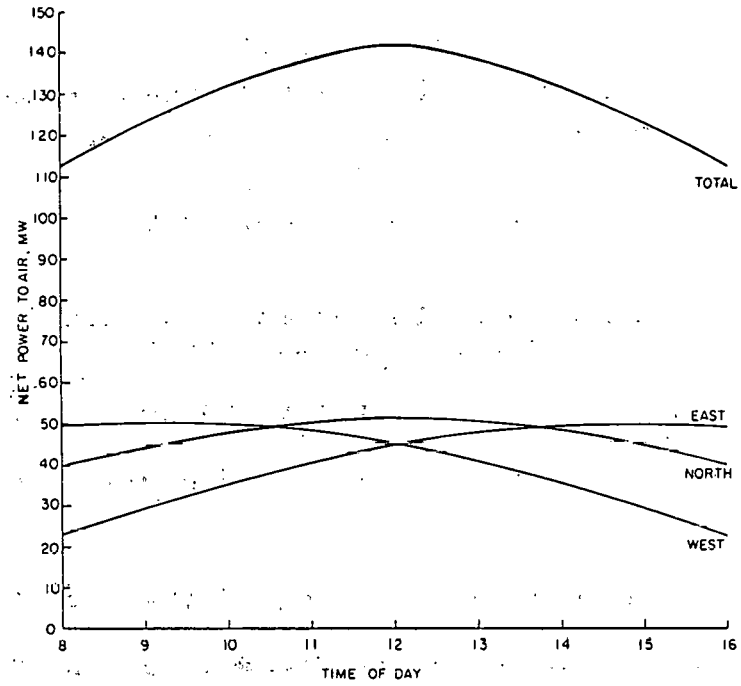

Figure 5-17 RECEIVER POWER OUTPUT AT EQUINOX

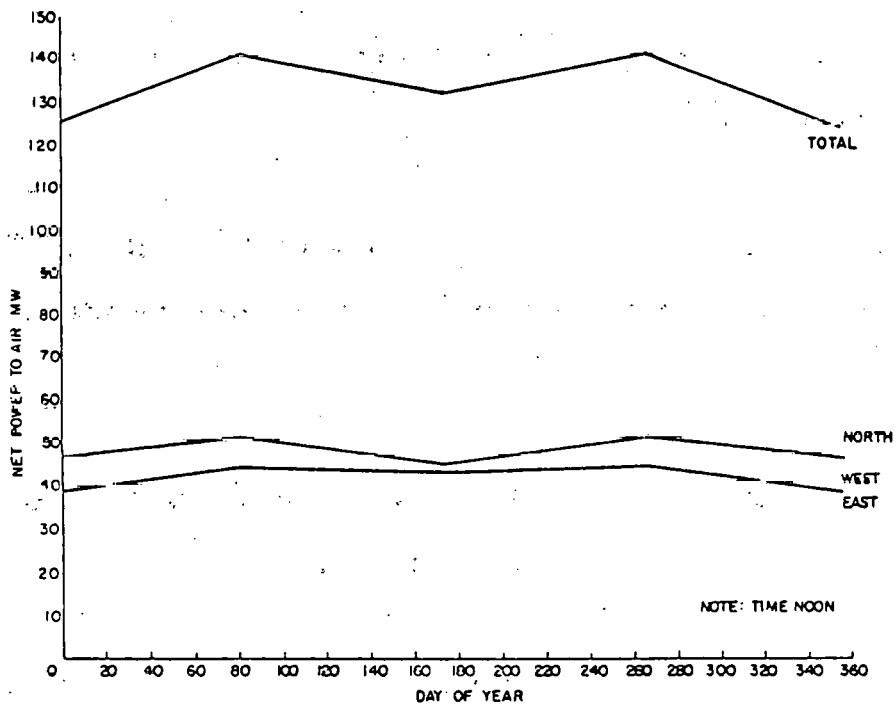

Figure 5-18 RECEIVER POWER OUTPUT THROUGHOUT YEAR

5.3.3 Tower Conceptual Design

Introduction. The main functions of the receiver tower are to:

- Support the receiver weight estimated to be 726,000 kg (800 tons)
- Hold the position of the aperture within acceptable limits of the heliostat aiming point
- Provide support for the riser and downcomer piping
- Allow access to the receiver and piping for maintenance

The design was based on a tower height of 190 m (623 ft) required for the "G" field. To meet the requirement of the "H" field, the tower height was reduced to 145 m (475 ft) by eliminating the bottom 45 m (148 ft) of the original design. Lack of time prevented an optimization of the shorter tower, so the design is quite conservative.

The tower design meets the requirements of the Uniform Building Code and national industry codes for steel and concrete structures.

Design Loads. The following loads were used for the conceptual design of the tower and its foundations:

- Dead Loads. These include weights of framing and permanent equipment such as receivers, piping, and controls.
- Live Loads. These are superimposed loads due to use and occupancy not including wind, earthquake, or dead loads.

- Wind Loads. These are based on wind speeds of 14 m/sec (32 mph) under operational conditions and 40 m/sec (90 mph) under survival wind conditions at a height of 10 m (30 ft) above ground. The calculated wind pressures were adjusted for round members in the structure.

- Seismic Loads. A peak ground acceleration of .15g under operating conditions and 0.25g under survival conditions were used. The tower was assumed to be located in UBC Zone 3. This peak ground acceleration was combined with the response spectrum given by NRC Reg. Guide 1.6 and damping values given for the operating basis earthquake in NRC Reg. Guide 1.61.

- Temperature. The project design criteria require that the plant has to remain operational in the ambient air temperature range from -30 to +50C (-2 to +120F).

Selected Tower Design. Following a review of recent comparative studies on receiver tower designs (Refs. 5-4 and 5-5), a square profile steel tower was selected for the hybrid plant. While most designs for steel receiver towers use rolled structural steel shapes, these are more efficient in building construction with close floor spacing and moderate beam spans. For tall solar towers, custom built-up sections would be required.

Offshore platform towers have similar requirements to those for a solar central receiver tower. The all-welded offshore structures are made of large-diameter welded or seamless piping. Successful tests have been made of the three-dimensional structural pipe joints at the University of California at Berkeley. The design of these structures is covered by an American Petroleum Institute code (API-RP2A) (Ref. 5-6). Several such towers have been built in the last few years. The main advantages of using large-diameter steel piping for the tower design include:

- A higher length-to-radius-of-gyration ratio for the same weight per unit length, permitting a higher allowable stress for the same effective member length
- A reduction in wind pressure loads, permitted by ANSI A58.1 for round cross sections
- Possibility of wider spacing between intermediate floor diaphragms
- A significant reduction in the number of members and connections
- An inherently greater rigidity due to welded construction, resulting in smaller deflections under wind and seismic loading
- Lower transportation costs with nested piping
- Potential for reduced fabrication costs due to automatic welding
- Less field fabrication after shop welding of the three-dimensional joints

The tower design employing this offshore platform technology is shown in Figure 5-19. K-bracing, effective in both tension and compression, is used to cut the span of the beams by half. Horizontal floor diaphragms are spaced at 15 m (50 ft) intervals for column bracing and to support piping, stairs, and the elevator guide rails. A typical floor diaphragm, which uses both pipe and rolled sections, is shown in Figure 5-20.

The column center lines are spaced at 18.3 m (60 ft) at the top to best support the combined receiver weight. The cavities were arranged as shown in Figure 5-21 to place the combined center of gravity at the center of the tower plan. Pipe diameters vary from a minimum of .41 m (16 in.) to a maximum of 2.13 m (84 in.)

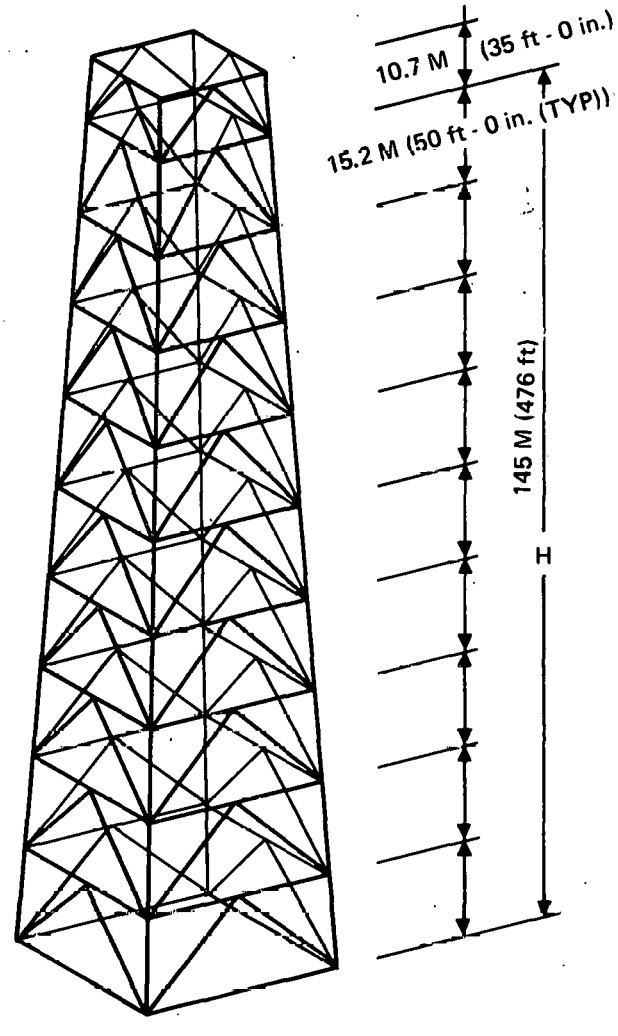

Figure 5-19 TOWER GEOMETRY

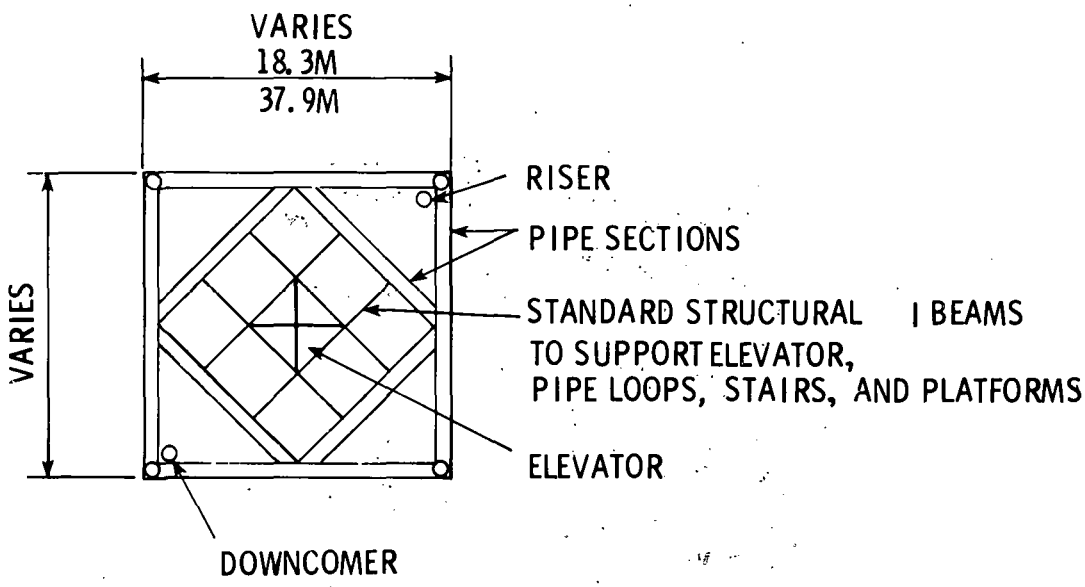

Figure 5-20 TYPICAL FLOOR DIAPHRAGM FRAMING PLAN

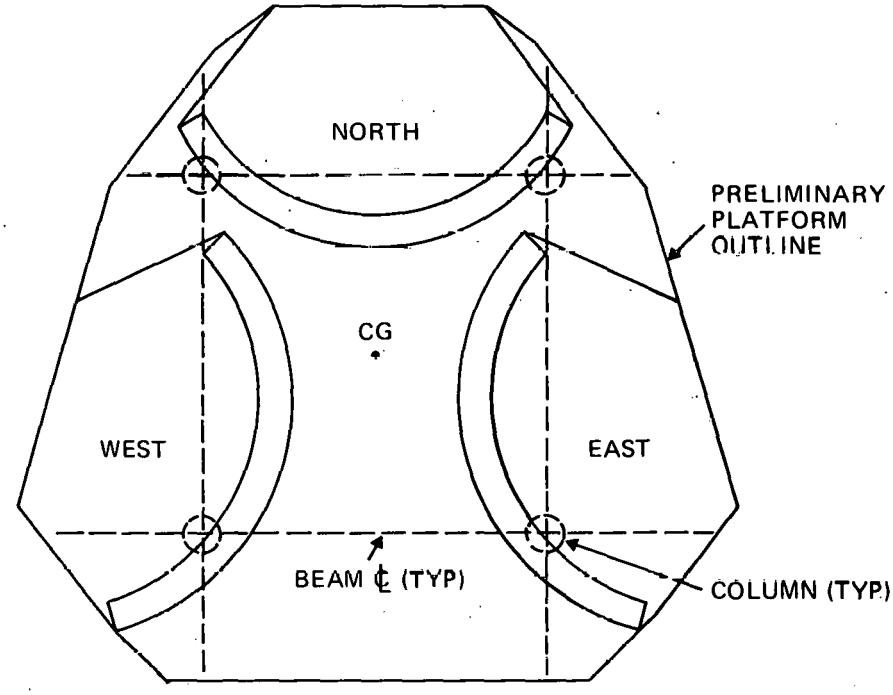

Figure 5-21 RECEIVER CAVITY ARRANGEMENT PLAN

and thicknesses vary from a minimum of 9.5 mm (0.375 in.) to a maximum of 32 mm (1.25 in.) for the larger diameter pipe.

All three-dimensional pipe-to-pipe connections can be prefabricated and shipped to the site. Straight pipes can be shipped to the site and welded to the prefabricated joints, thus reducing field labor and ensuring the proper taper.

The tower will have adequate aircraft obstruction lights, lightning protection, access platform stairs, ladders, piping supports, and lighting in accordance with the regulations of FAA and OSHA.

Foundation Design. The foundation consists of four 3 m (10 ft) thick concrete footings with 4.6 m by 4.6 m by 3 m (15 ft by 15 ft by 10 ft) deep concrete pilasters. The footings are tied together by a 3 m by 3 m (10 ft by 10 ft) concrete tie-beam, as shown in Figure 5-22. In addition to resistance to downward loads, the foundations also provide resistance against uplift (overturning) caused by winds. The uplift forces are transmitted to the foundations by embedding the lower columns in the pilasters, and are transmitted from the steel to the concrete by welded studs. The footings are embedded approximately 6 m (20 ft) below the ground. The pilaster and tie-beams can be cast one at time, thus allowing reuse of the forms to reduce costs. The reinforced concrete design is in accordance with the requirements of ACI Standard 318-71, Building Code Requirements for Reinforced Concrete.

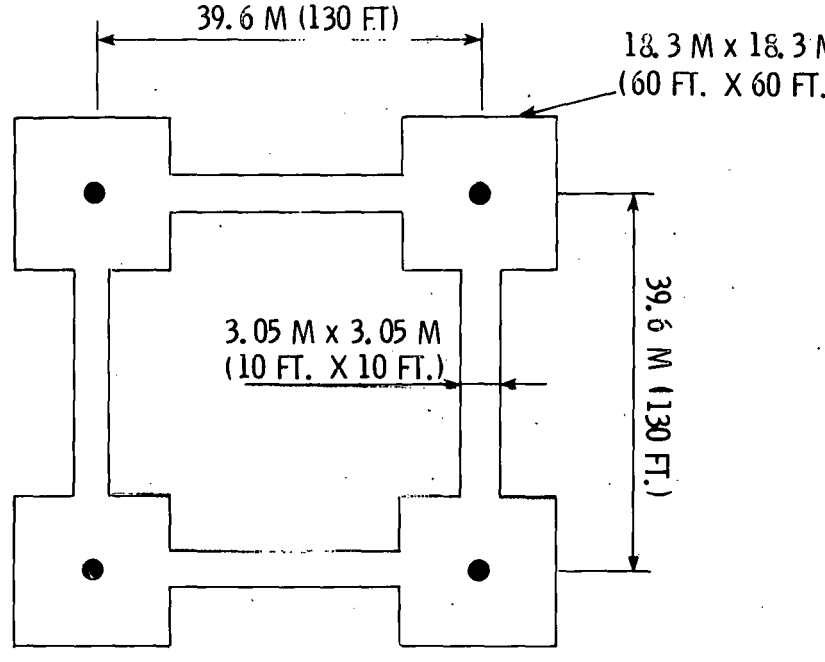

Figure 5-22 TOWER FOUNDATION PLAN

Analysis of Tower Design. A three-dimensional model of the tower was analyzed statically and dynamically using the NASTRAN computer program (Ref. 5-7). Top-of-tower horizontal displacements under operating and survival wind conditions were found to be 38 mm (1.5 in.) and .36 m (14 in.), respectively. Preliminary response spectra, shown in Figures 5-23 and 5-24, represent typical smoothed curves provided for equipment design. As seen from these curves, the tower resonance frequency is approximately 6 cycles/sec for the horizontal and 2 cycles/sec for the vertical excitation. The peak accelerations are quite low. The maximum lateral displacement at the tower top due to the operating basis earthquake (CBE) is .25 m (10 in.). At this condition the maximum acceleration is .22g.

The 2 and 4 percent damping values used for the response spectra correspond to recommendations for welded or hung equipment connection and bolted equipment connection, respectively. A 2 percent structural damping has been assumed for the welded steel tower.

The operating seismic event was analyzed, with a 0.15g ground acceleration, since in actual practice this often governs the design. The smaller factors of safety allowable for survival conditions results in a less stringent design criteria.

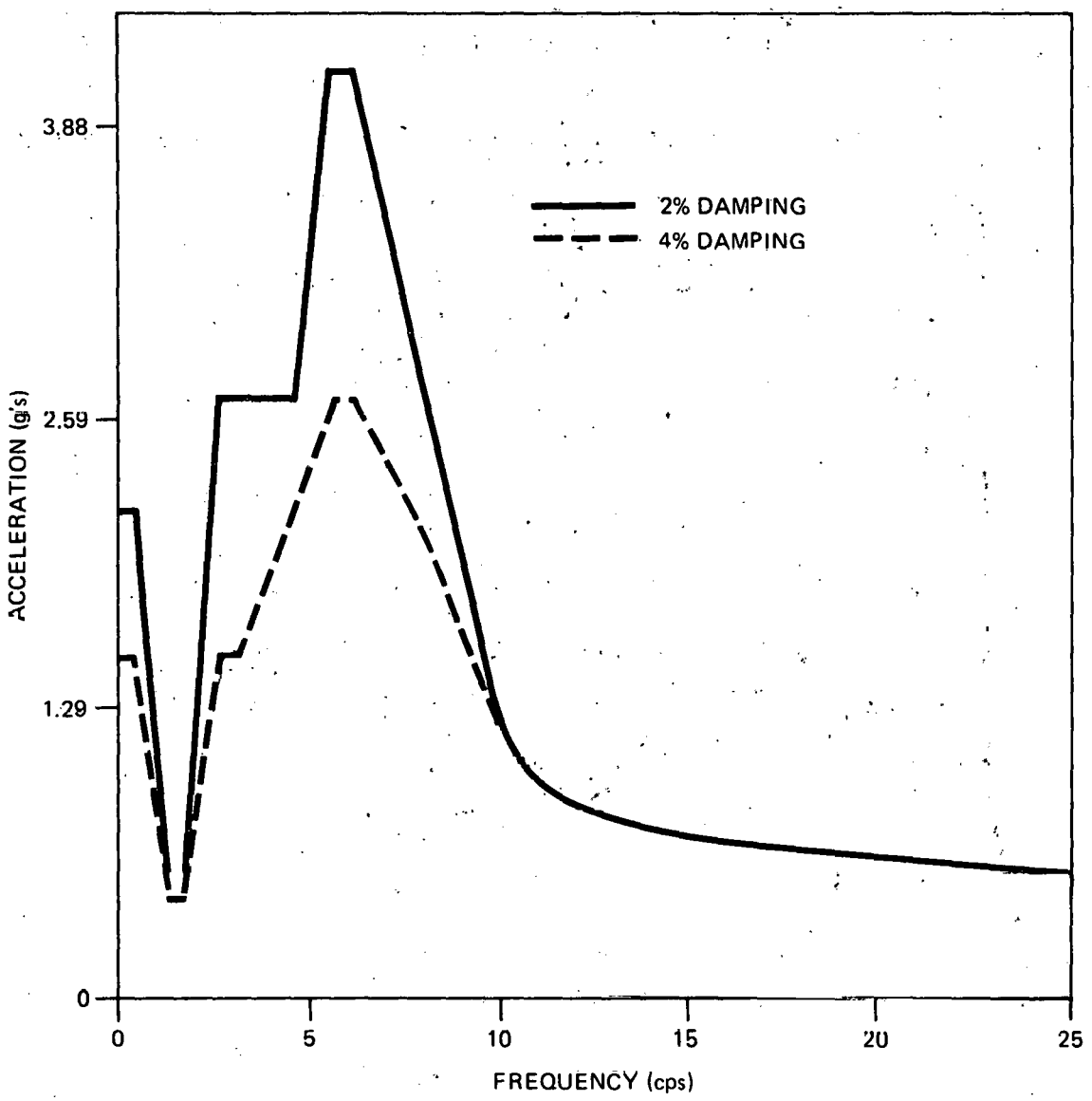

Figure 5-23 OBE HORIZONTAL RESPONSE SPECTRA– ELEVATION 190 METERS (630 FEET)

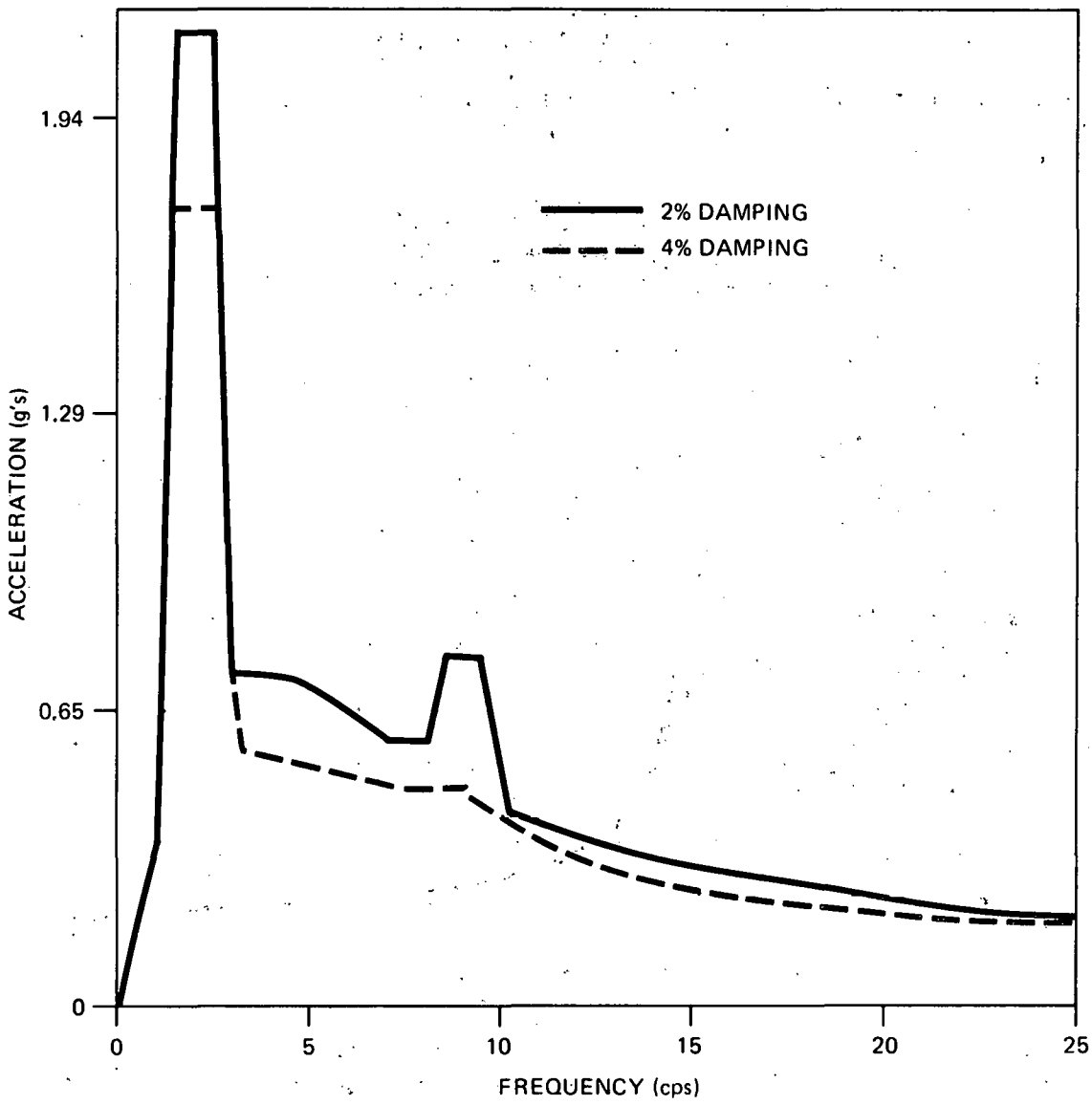

Figure 5-24 OBE VERTICAL RESPONSE SPECTRA– ELEVATION 190 METERS (630 FEET)

5.3.4 Riser and Downcomer Conceptual Design

The riser and downcomer, which convey the air to and from the receiver, form the interfaces between the receiver subsystem and the EPGS. They connect the receiver on top of the tower with the gas turbine at the tower base.

The total pressure drop allowed in the piping, based on parametric analysis, is 41.4 kPa (6 psi). Heat leak through the insulation results in a 4.4C (8F) temperature loss in both the riser and downcomer. This is approximately 1 percent of the design point temperature rise in the receiver.

Riser. The riser piping, operating with compressor discharge air at approximately 368C (695F) and 1.09 MPa (160 psia), is made of rolled and welded carbon steel piping with 5 cm (2 in.) of external insulation (Durablanket made by Carborundum). The pipe diameter is 1.3 m (51 in.) and the wall thickness is 1.6 cm (0.625 in.), in accordance with the Code for Power Piping (ANSI B31.1). In place of the expansion loops assumed in the parametric analysis, expansion joints are used to allow for thermal growth. This minimizes the length and weight of piping.

The riser will either operate at about 368C (695F) in the hybrid mode or will be near ambient temperature when the receiver is bypassed in the fossil-only mode. Based on conceptual-level analyses, the piping is not expected to need any slower warmup period than the receiver.

Two connections are provided at the compressor discharge of the gas turbine. These join into a single pipe near the turbine and run horizontally above the ground to the tower. In the tower the riser runs parallel to one of the main tower columns to a point just below the receiver platform, where the pipe branches into six flow paths, two to each receiver cavity. Figure 5-25 is an artist's concept of the piping arrangement around the receiver, showing both riser and downcomer. The diameter of the branch piping is specified to give nearly the same air velocity as the main riser pipe, which has a design velocity of approximately 33 m/sec (108 ft/sec).

Downcomer. The downcomer piping, which handles air at the receiver outlet of 843C (1550F), is exposed to more severe service conditions, which include significant thermal transients. Several design alternatives were evaluated, covering the range from high-temperature alloys, such as Inconel 617, to refractory lined steel pipe, often used for furnace transfer piping in a similar temperature environment.

The selected design, shown in Figure 5-26, consists of an internally insulated steel pipe with a metallic inner liner, made of rolled and welded Inconel 617 plate with a diameter of 1.45 m (57 in.) and a thickness of 6 mm (0.25 in.). The actual pressure boundary on the outside is formed by a 1.67 m (66 in.) diameter 19 mm (.75 in.) wall carbon steel pipe, which operates at a maximum temperature of about 120C (250F). Between the liner and the pipe there is an 89 mm (3.5 in.) thick Durablanket ceramic

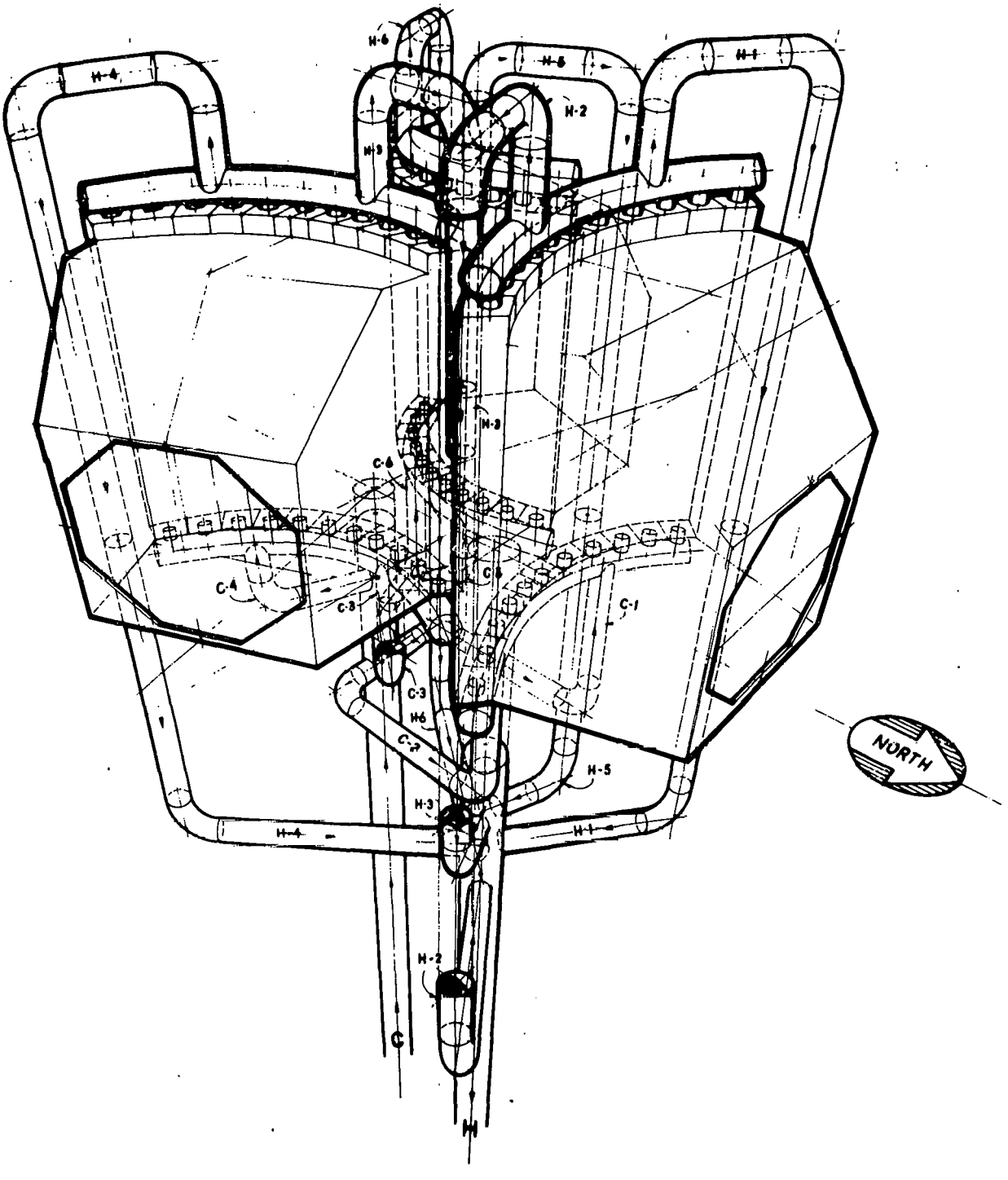

Figure 5-25 ARTIST'S CONCEPT OF RISER (C) AND DOWNCOMER (H) PIPING ARRANGEMENT

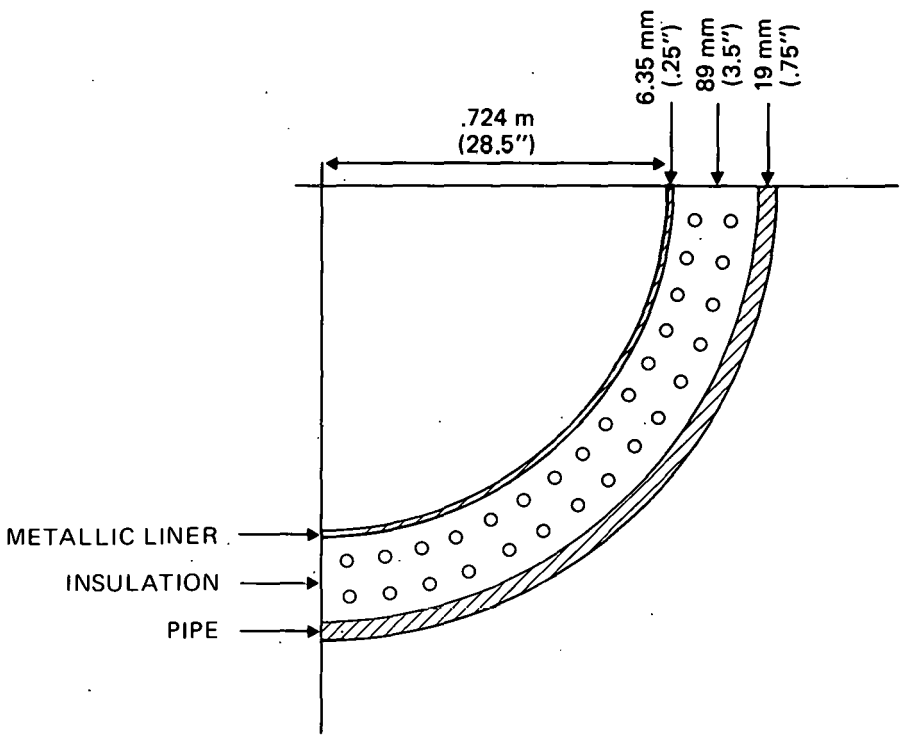

Figure 5-26 SELECTED DOWNCOMER DESIGN CONCEPT

fiber insulation, .10 kg/m³ (8 lb/ft³), manufactured by Carborundum.

The layout of the downcomer pipe is nearly parallel to the riser. Six pipes connect to the top of the receiver cavities, as shown in Figure 5-25, and join to a single large pipe. At the gas turbine, the downcomer is branched into two pipes for connection to the combustor plenum chamber. The design point air velocity is nearly constant at 49 m/sec (160 ft/sec), through all the pipes.

Design and development work is required before this internally insulated piping concept can be used with confidence in a commercial power plant. Connections to the receiver and the gas turbine, anchoring of the liner and the insulation without producing hot spots, and details of the expansion provisions of the liner need further development work. However, this concept appears to be the most cost effective and is similar in principal to those proposed for other conceptual designs (Refs. 5-8, 5-9, and 5-10).

The constant receiver airflow operational philosophy results in slow thermal transients during the diurnal solar variation. However, during cloud transients, the downcomer air temperature is expected to drop from a maximum of 843C (1550F) to approximately 370C (700F) in as little as 5 minutes. If necessary, the severity of these transients can be reduced

through bypassing the solar receiver or using early warning of cloud approach to moderate the effects.

Valves. Valves, shown in Figure 5-27, are required in the riser and downcomer piping to handle the operational requirements of the solar/nonsolar interface.

The valves in the riser piping are of conventional design. The riser isolation valve (V1) is closed only during long-term fossil operation. The cavity distribution valves (V3 through V9) are used to adjust the air flow with the diurnal variation in the solar input to the three cavities. Thermal relief valves (not shown) will be necessary on the inlet side of each panel for equipment protection.

Service conditions of the valves exposed to the downcomer air are more severe. The downcomer isolation valve (V2) must be able to withstand the 843C (1550F) air for several hours each day, but will not be operated at temperatures much above compressor discharge to isolate the receiver. The bypass valve (V3) is exposed to a large temperature differential when closed, and some cooling air flow will probably be required. The atmospheric dump valves (V10 through V15) are used to prevent compressor surge by dumping a portion of the total airflow when valves V2 and V3 restrict the airflow through the turbine during loss of load trips of the gas turbine. Further study during preliminary design may allow these valves to be moved to the cold side of the receiver.

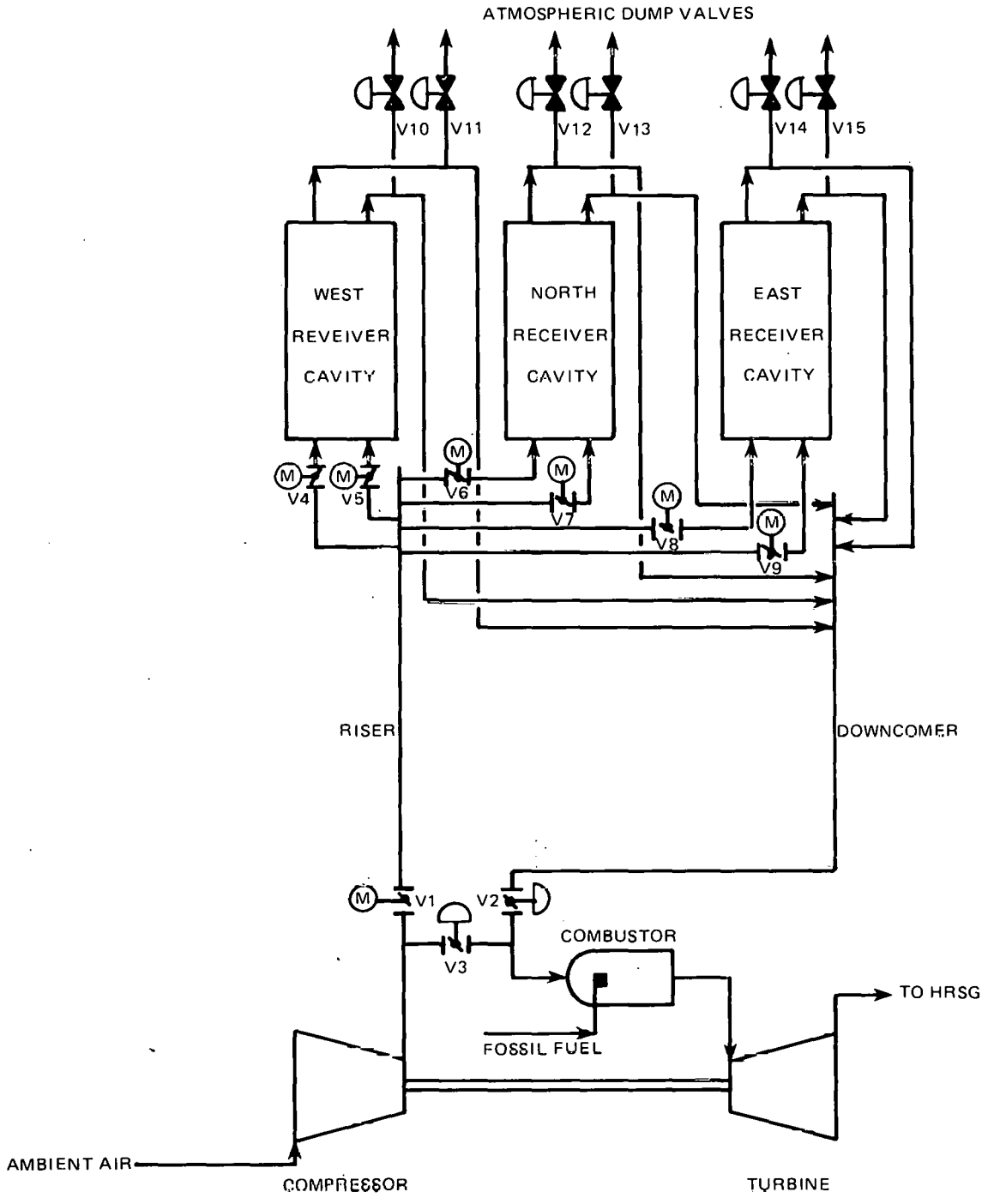

Figure 5-27 AIR PIPING BETWEEN GAS TURBINE AND SOLAR RECEIVER

Inquiries to valve vendors yielded a few examples of valves built to withstand the temperature conditions in the downcomer. The Clow Corporation recommended their Tricentric valve which has been used for other high-temperature air applications. The downcomer isolation valve (V3) included an internally insulated steel body and a hydraulic operator.

Valves for the 843C (1550F) air are not in the commercial equipment category as yet, although in the opinion of Clow Corporation, valves can be built to withstand the solar hybrid service requirements.

Expansion Joints. Expansion joints serve to compensate for thermal expansion of the steel pipe resulting from temperature changes of approximately 390C (700F) for the riser and 95C (170F) for the downcomer. Using expansion joints instead of piping loops to absorb the thermal growth of the riser and downcomer piping was found to be the economic choice over the preconceptual design. These joints are relatively inexpensive, and with good design practice, can provide reliable service. An estimate of the required number of joints and budgetary quotes were obtained from Pathway Corp.

5.4 STORAGE SUBSYSTEM

The conceptual design hybrid system has no energy storage provisions. As discussed in Subsection 4.3.3, the value of storage is negative under the economic parameters used in this study project.

5.5 NONSOLAR SUBSYSTEM

The nonsolar subsystem, consisting of the combustor and the fuel storage and supply provisions, is treated under the EPGS, because it is an integral part of the gas turbine and its auxiliaries.

5.6 ELECTRIC POWER GENERATION SUBSYSTEM (EPGS)

Primary functions of the EPGS include thermal to electric energy conversion, fossil fuel handling and combustion, waste heat rejection, and site power distribution. The energy conversion function is served by three major components: the gas turbine-generator, the heat recovery steam generator (HRSG), and the steam turbine-generator.

5.6.1 Performance

The three basic operating modes of the EPGS are:

- Hybrid mode (fossil and solar heat inputs)
- Fossil-only mode (long term or short term)

- Solar-only mode

The nominal capacity in the hybrid mode is 112.6 MWe net. The plant output in the fossil-only mode is slightly above 113 MWe net. Heat balance diagrams prepared for each mode provide detailed cycle characteristics. Additional information on these three modes is given in the EPGS data list in Volume III.

Hybrid Mode. Figure 5-28 is the heat balance diagram for the hybrid operating mode showing the flow parameters at design point. Total steam production is approximately 43 kg/sec (340,000 lb/hr). The high- and low-pressure steam represent approximately 84 and 16 percent of the total, respectively. Gross electrical output of the combined cycle is 115,940 kW, with the gas turbine-generator accounting for about 64 percent of the output. Net plant heat rate is approximately 8229 kJ/kWh (7794 Btu/kWh) and reflects the auxiliary power demand of about 3340 kW.

Long-Term Fossil Mode. This mode represents plant operation without solar energy input and with the receiver bypassed. As shown in Figure 5-29, the major differences between this mode and the hybrid mode are the increased fuel requirement, slightly higher gas turbine exhaust temperature, and a slight decrease in total steam production. The relative proportions of high- and low-pressure steam remain the same as in the hybrid mode. Gross electrical output in this mode is slightly higher (116,340 kW), but the relative contributions of the gas and steam turbine-

generators remain unchanged. The net plant heat rate is about 8562 kJ/kWh (8116 Btu/kWh), which is about 4 percent higher than that of the hybrid mode. The long-term fossil mode is part of the daily startup and shutdown sequences and will be used, in addition, to supply electric energy on cloudy days.

Solar-Only Mode. In this mode the hybrid plant can only produce a fraction of its rated output. It was analyzed to define the lower limit of hybrid operation with minimum fossil fuel input. As indicated in Figure 5-30, steam production in this mode decreases to about 21 kg/sec (166,000 lb/hr), and steam pressures and temperatures at the turbine inlet are lower. High-pressure steam production is 74 percent of the total. Gross electric output is about 43.1 MW, with the gas turbine accounting for 68 percent of the output.

Short-Term Fossil Mode. This mode differs from the long-term fossil mode, since the compressor discharge air continues to be routed through the receiver. It is used, for example, when insolation is only temporarily interrupted due to cloud passage. In this mode the fuel requirement increases by about 1 percent and the plant gross output decreases by about 0.2 percent. These changes are due to losses in the receiver and associated piping.

Performance Variation. Part-load operation of the hybrid power system is achieved by reducing the fossil fuel input to the gas turbine combustion chamber. Figure 5-31 shows the variation of steam cycle pressures at less than full power operation. The

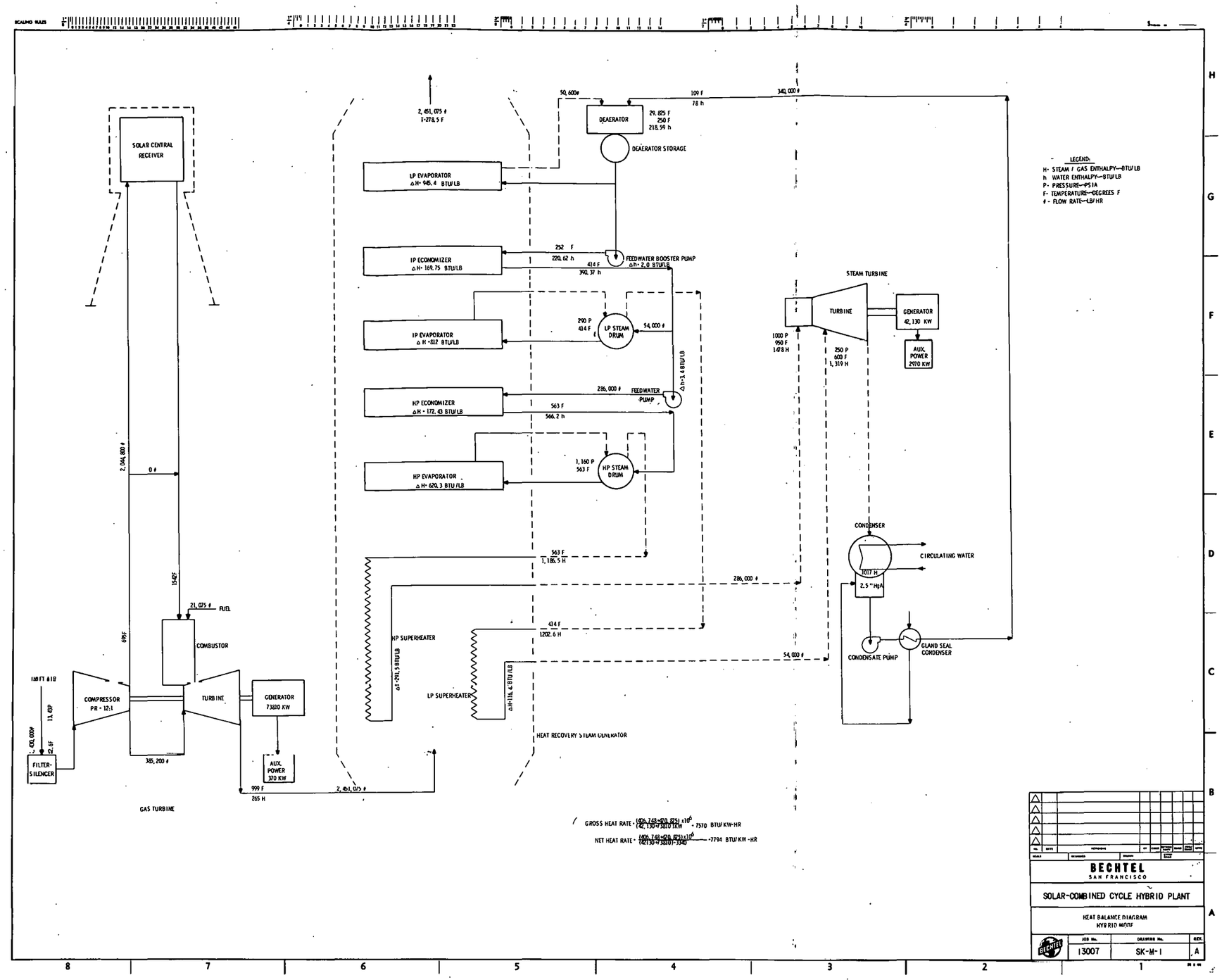

Figure 5-28 HEAT BALANCE DIAGRAM, HYBRID MODE

THIS PAGE

WAS INTENTIONALLY

LEFT BLANK

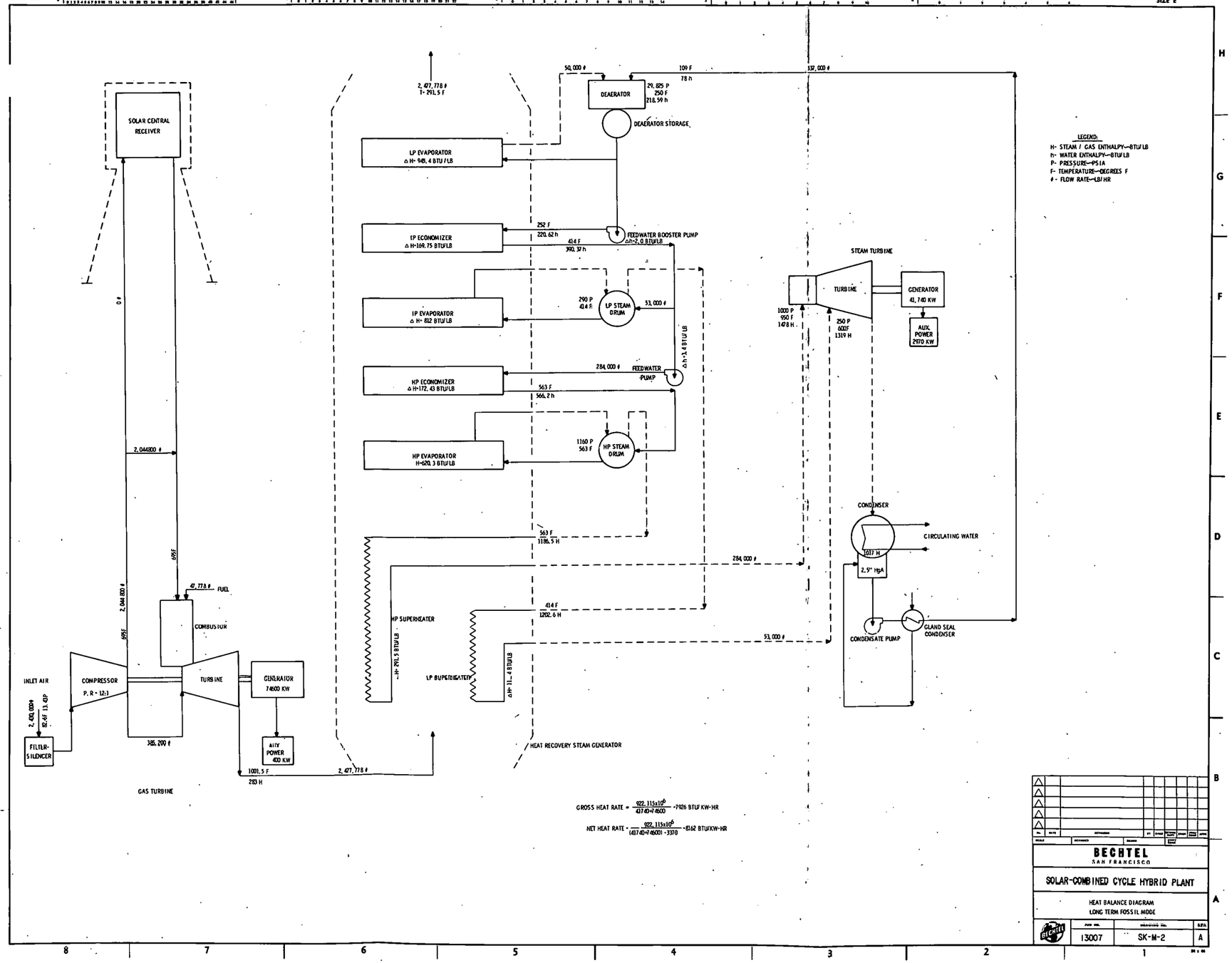

Figure 5-29 HEAT BALANCE DIAGRAM, LONG-TERM FOSSIL MODE

THIS PAGE

WAS INTENTIONALLY

LEFT BLANK

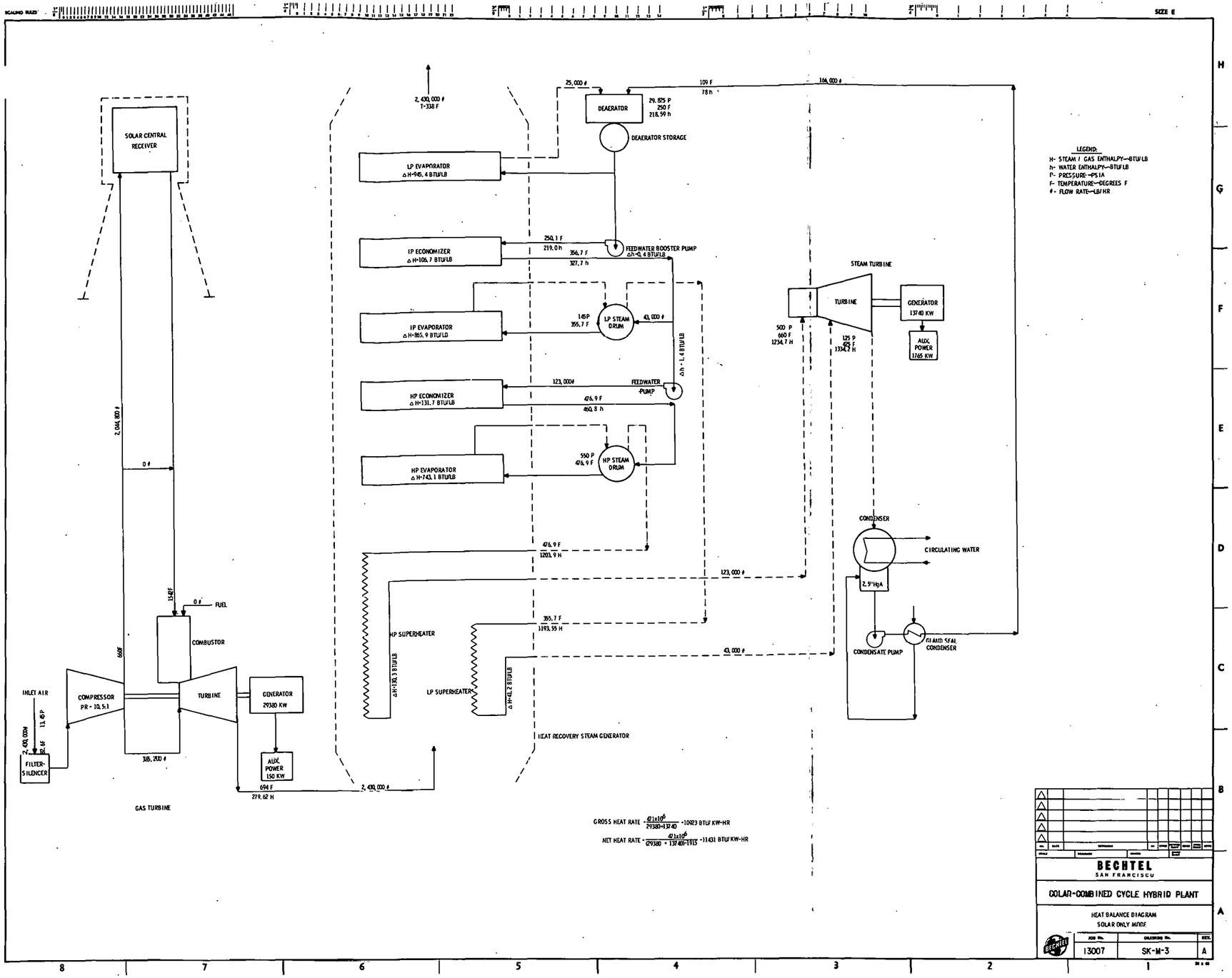

Figure 5-30 HEAT BALANCE DIAGRAM, SOLAR-ONLY MODE

THIS PAGE

WAS INTENTIONALLY

LEFT BLANK

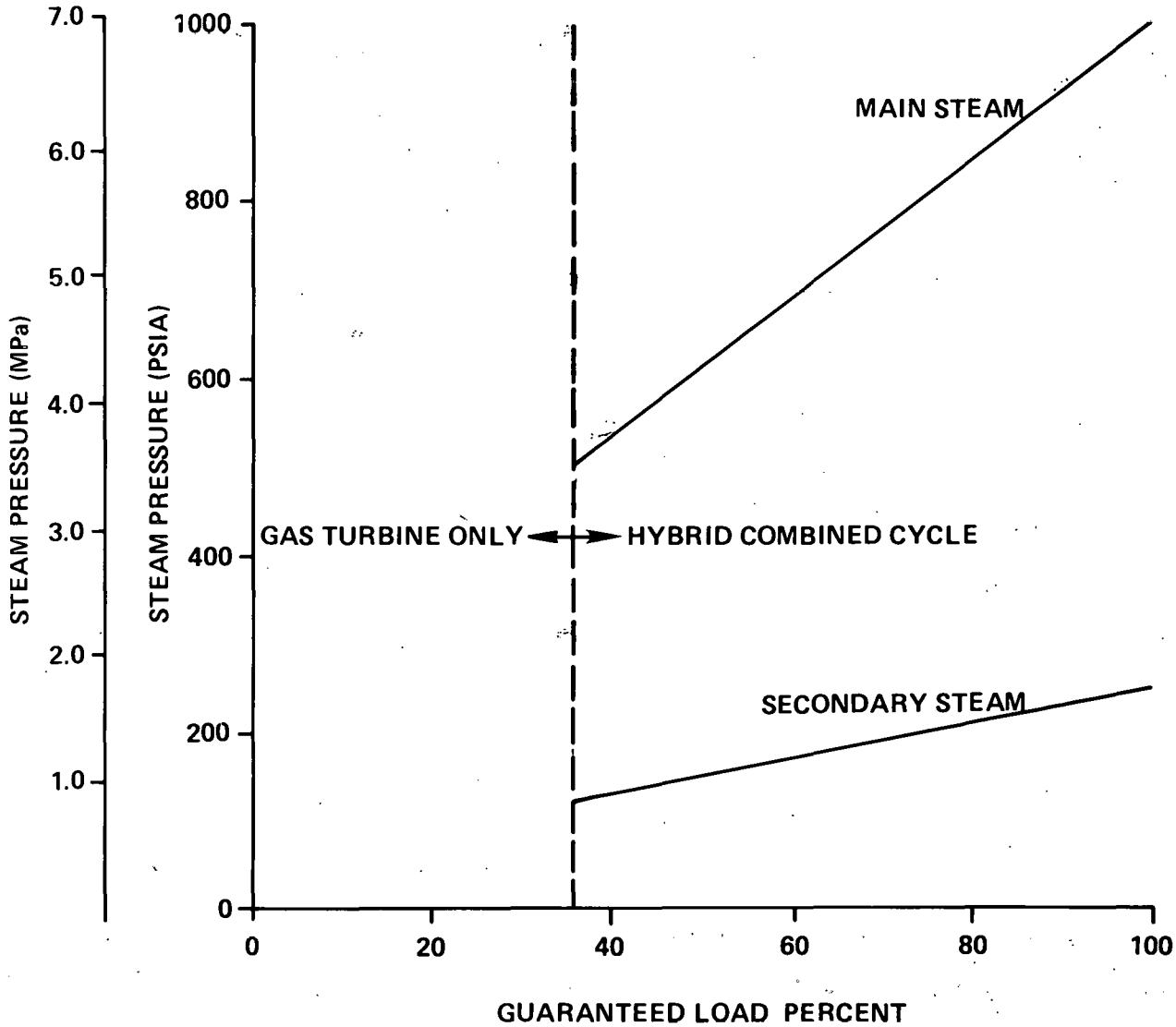

Figure 5-31 VARIABLE-PRESSURE OPERATING CHARACTERISTICS

lower operating limit is dictated by steam turbine design and represents the point below which operation of the steam turbine would be impractical. Below 35 percent of rated output, only the gas turbine would be operated; condensate-feedwater would be recirculated to the HRSG evaporators, maintaining the steam cycle in a hot standby condition, ready for startup should an increase in power demand occur.

Figure 5-32 shows the variation in net heat rate as a function of plant load. As the figure shows, the heat rate increases in all modes at part load, indicating poorer performance. The figure also shows the maximum plant output variation due to changes in wet and dry bulb temperatures. Plant output variation due to changes in relative humidity can also be derived from this figure. Figure 5-33 shows the effects of altitude above mean sea level on plant output and heat rate.

5.6.2 Gas Turbine-Generator

The gas turbine is a Westinghouse W-501 combustion turbine and consists of three basic elements: the axial flow compressor, a combustion system, and a power turbine. These are combined into a single assembly, shown in Figure 5-34, that can be shipped complete with rotor in place. The turbine rating is 86 MWe.

The hydrogen-cooled generator and exciter are equipped with integral lube oil and cooler piping and necessary instrumentation. The generator and combustion turbine are solid

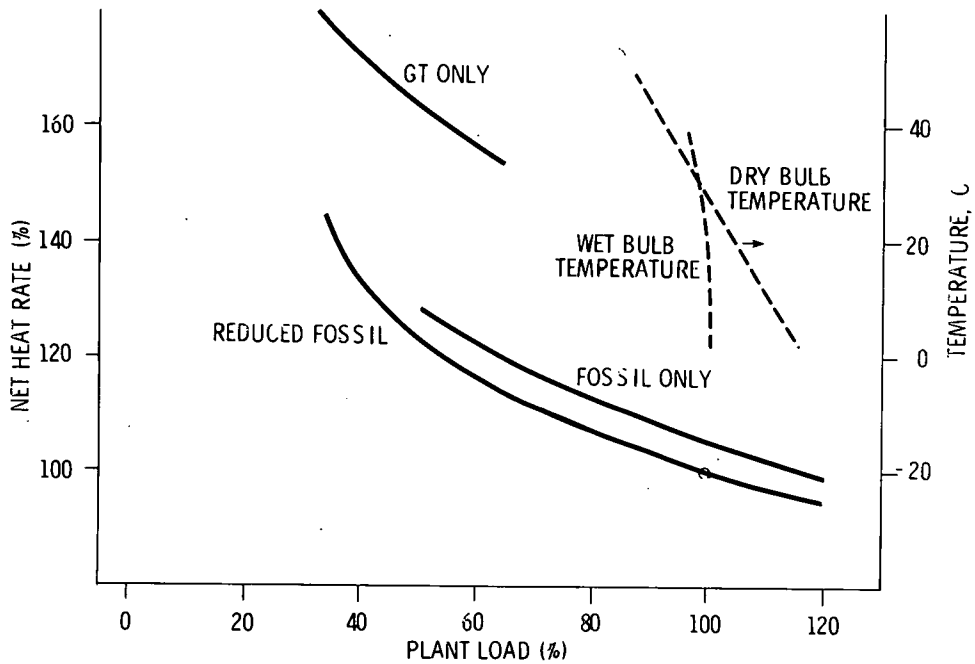

Figure 5-32 VARIATION OF HEAT RATE AS A FUNCTION OF PLANT LOAD

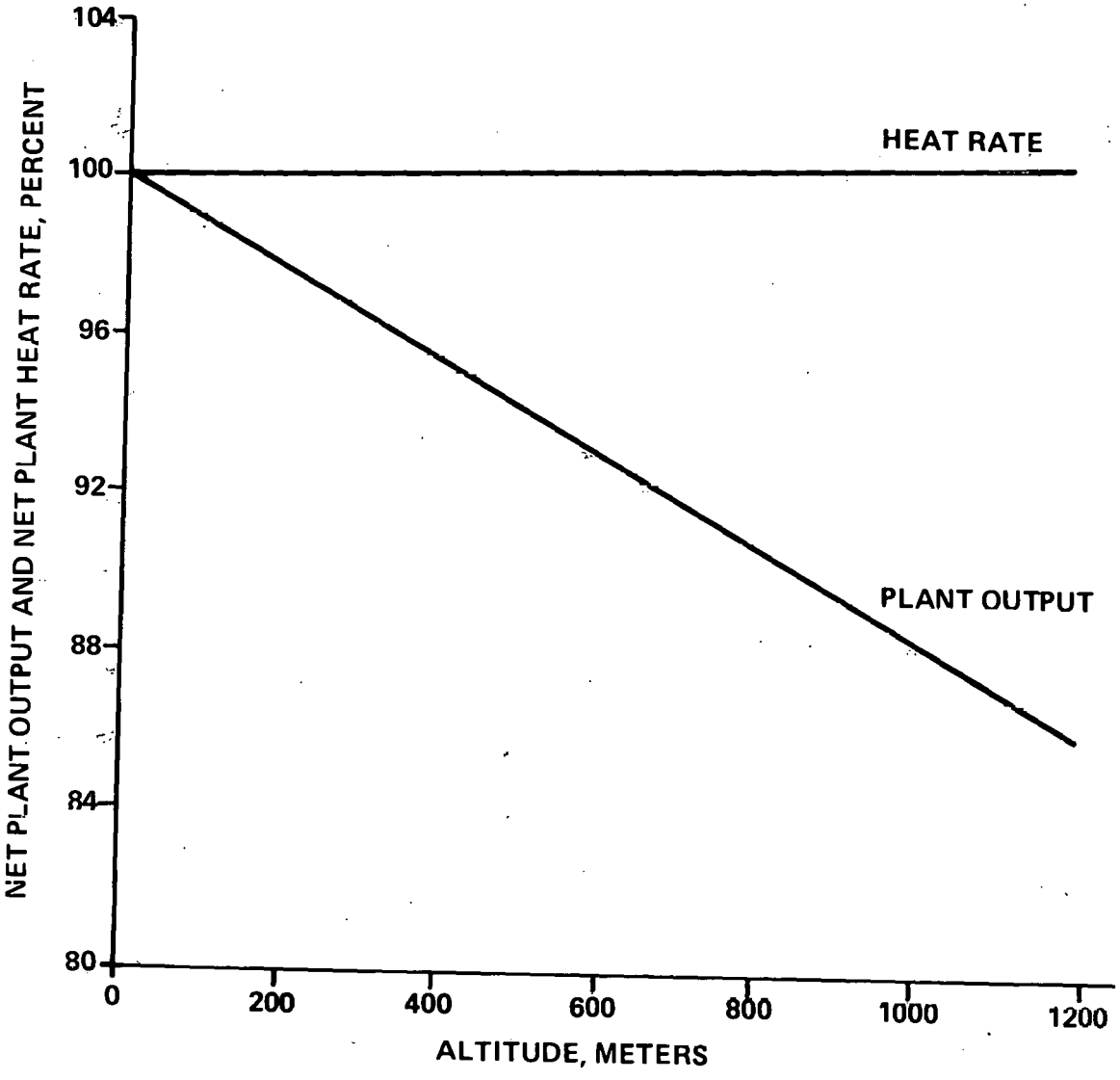

Figure 5-33 EFFECT OF ALTITUDE ON NET PLANT PERFORMANCE

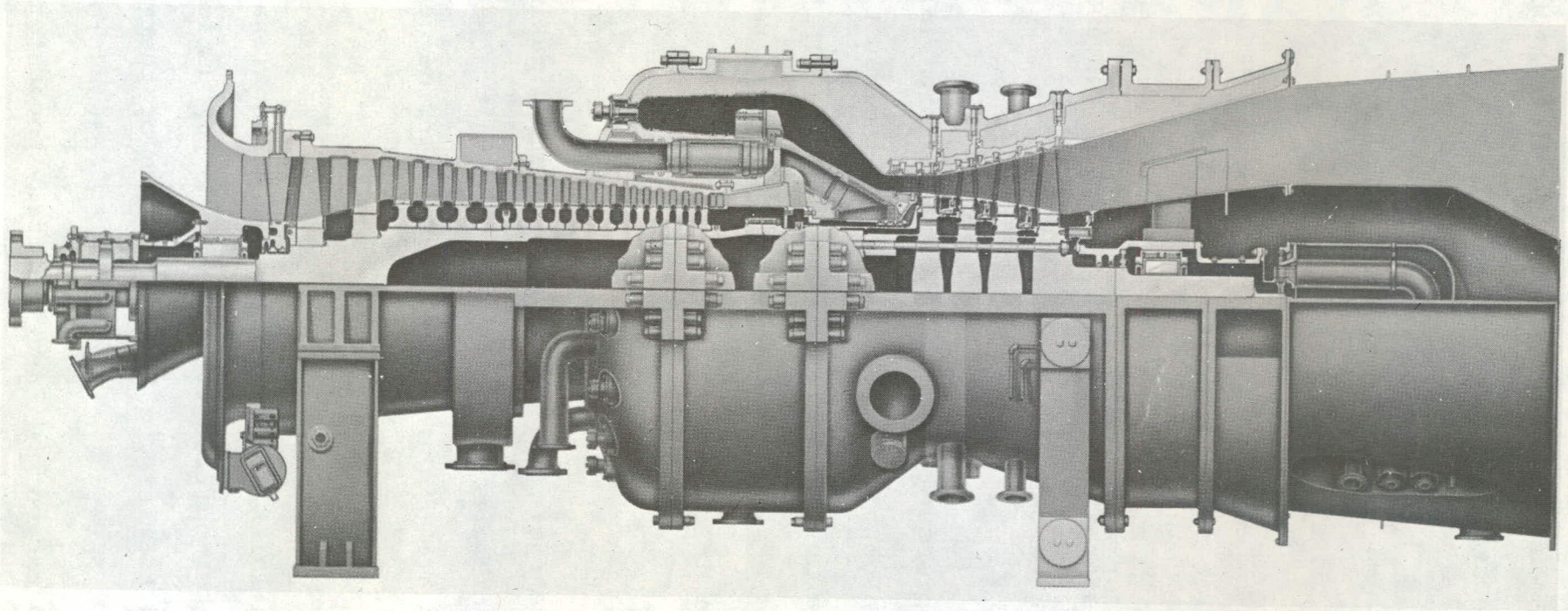

Figure 5-34 GAS TURBINE (WESTINGHOUSE W-501)

coupled. Shaft-mounted axial blowers circulate hydrogen cooling through the generator.

The gas turbine-generator nameplate rating is 96 MVA at:

- 13.8 kV at 0.9 power factor
- Air inlet pressure of 93.8 kPa (13.6 psia), corresponding to 678 m (2225 ft) elevation above sea level
- Compressor airflow of 333 kg/sec (2,640,000 lbs/hr)
- Ambient temperature of 4.4C (40F)

The compressor pressure ratio is 11.8:1, turbine inlet temperature is about 1085C (1985F), and the exhaust flow temperature is about 537C (999F) when operating in the hybrid mode. The turbine exhaust is ducted to the heat recovery steam generator (HRSG) inlet.

The majority of the auxiliary equipment for the gas turbine is installed in two factory-assembled enclosures, making the gas turbine-generator a nearly self-contained unit. Water-cooled heat exchangers are used to cool the gas turbine-generator auxiliaries.

Due to the high inlet temperatures, the conventional gas turbine combustor must be modified to prevent the combustion liner from overheating and to minimize the generation of thermal NO_x. The turndown requirements, when operating on reduced fossil input at part load, also exceed the range normally encountered in

conventional gas turbine operation. These factors suggest a catalytically-enhanced mode of combustion for the conceptual design. Laboratory investigations demonstrated that typical gas turbine fuels can be burned with minimal production of thermal NO_x at high combustion efficiencies (Refs. 5-11 through 5-16).

The catalytic element is composed of a cylindrical ceramic honeycomb structure on which a proprietary noble metal catalyst is deposited. As the mixture of fuel and air passes through the catalytic element, the fuel is oxidized below the threshhold temperature 1650C (3000F) for significant thermal NO_x generation, and only the fuel-bound nitrogen is converted to NO_x.

Catalytic combustion systems are currently being developed to replace combustors in existing conventional stationary gas turbines. Since these combustors operate with constant air inlet temperature, a conventional precombustion section is needed to meet the special solar requirement of varying inlet temperatures. The resulting hybrid combustor conceptual design is shown in Figure 5-35. Sixteen such combustor cans are arranged circumferentially around the W-501 gas turbine.

All of the airflow from the receiver is passed through both sections of the combustors. The precombustor is designed to control the inlet temperature to the catalyst within a range of about 700 to 850C (1300 to 1550F). This maintains the best efficiency of the catalytic element while minimizing the pressure loss. The precombustor efficiency is not critical, since any

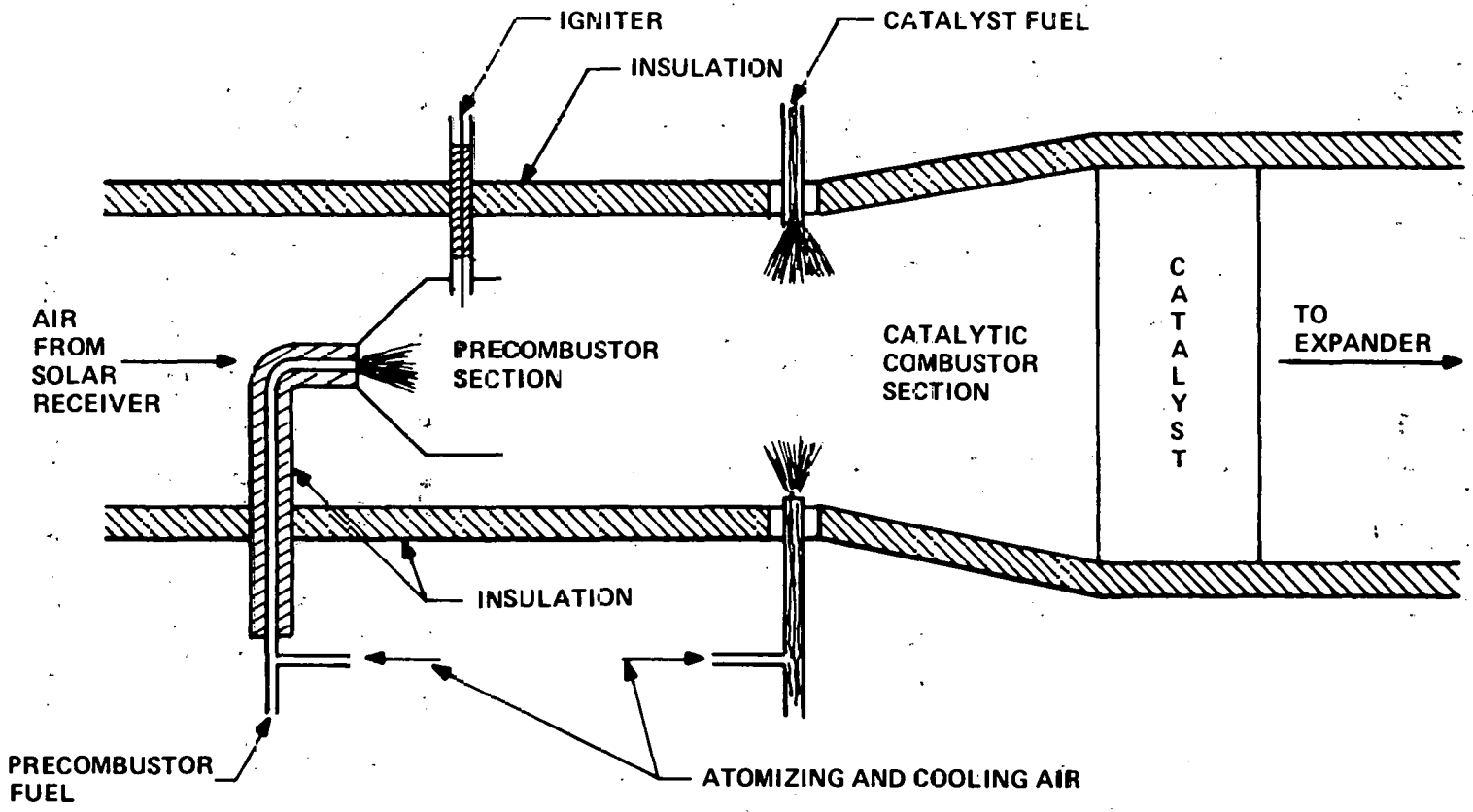

Figure 5-35 CATALYTIC COMBUSTOR SCHEMATIC

unburned fuel will be oxidized in the catalytic element. This greatly eases the fuel nozzle design for a varying temperature requirement and allows greater turndown capability for the precombustor.

The combination of the precombustor and the catalytic element can meet all the operational requirements for the solar combined cycle hybrid plant. Startup is initiated with the precombustor. The turbine is accelerated and loaded to the precombustor limit before the catalytic combustor fuel is turned on to bring the turbine inlet temperature to the design value. The precombustor fuel flow is varied to adjust to the available solar input for relatively constant inlet temperature operation of the catalyst during full load. For reduced fossil operation, the fuel flow to the catalyst is reduced, thereby lowering the turbine inlet temperature.

The NO_x generated by the precombustor parallels that of a conventional combustor, but since it burns only about one-half of the total fuel, the NO_x emissions are much less than a conventional combustor. During solar hybrid operation with high combustor inlet temperatures, less fuel is burned in the precombustor and less NO_x will be generated.

Standard auxiliary equipment and accessories supplied with the gas turbine include:

- Starting package

- 1500 hp electric motor, 5 KV-1800 rpm
- Turning gear module

- Electrical control package
- Mechanical package
  - Lube oil pumps, reservoir, and accessories
  - Generator seal oil system
  - No. 2 distillate fuel system
- Inlet air duct and silencer
- Exhaust gas silencer
- Turbine enclosure
- Cooling air cooler
- Lube oil cooler
- Hydrogen cooler
- Fire protection systems

5.6.3 Steam Turbine-Generator

The steam turbine is a single-casing, single-flow, nonreheat, 3600 rpm condensing turbine with 59.69 cm (23.5 in.) last-stage blades, designed by Westinghouse. It has an uncontrolled secondary steam inlet to the intermediate-pressure stages of the turbine and no external extractions. Internal details of a typical Westinghouse steam turbine for this service are shown in Figure 5-36. Steam conditions at 100 percent guaranteed load are 6.9 MPa/510C (1000 psia/950F) at main steam throttle and 1.7 MPa/316C (250 psia/600F) secondary steam throttle conditions. The turbine is capable of variable-pressure operation and is rated at 46 MWe.

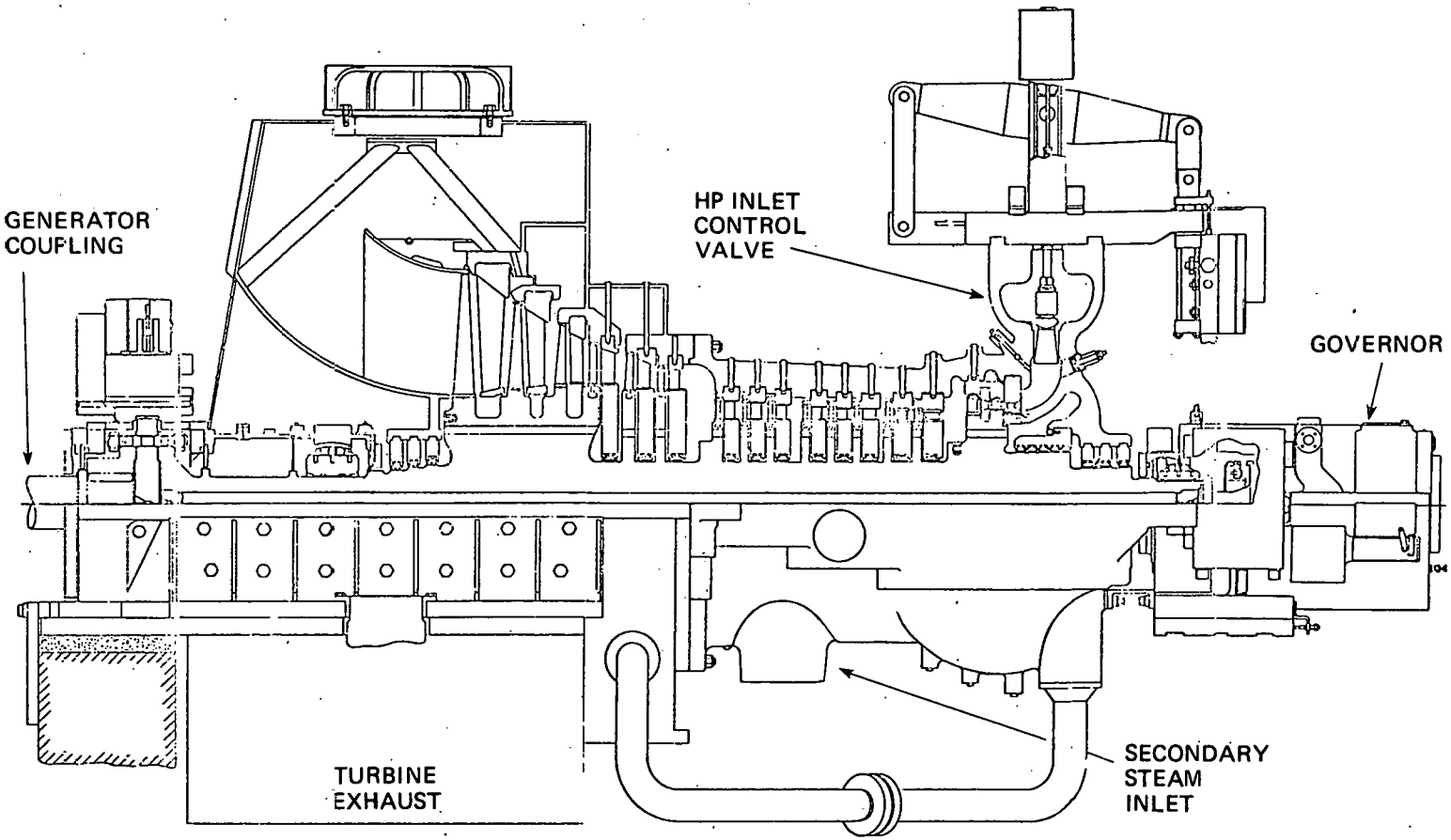

Figure 5-36 TYPICAL STEAM TURBINE CUTAWAY DRAWING

The generator and exciter are of standard design. The turbine-generator set is complete with an electrohydraulic control system to control the steam flow through the turbine and all necessary auxiliaries. The generator nameplate rating is 51 MVA at:

- 13.8 kV at 0.9 power factor
- Condenser back pressure of 8.5 kPa (2.5 in)
- Zero makeup

The electrohydraulic control provided for this turbine-generator unit combines the advantages of solid-state electronics with those of high-pressure hydraulics to control the steam flow through the turbine.

Standard steam turbine accessories include the following:

- Protective valve system
- Oil pumping system with oil reservoir, oil pumps, and oil coolers
- Steam seal equipment
- Motor-operated turning gear
- Supervisory and operating instruments
- Heat retention and metal lagging material

The electrohydraulic control accessories include:

- Electrical control circuits
- Valve operating devices
- Emergency trip devices
- High-pressure hydraulic system
- Digital electrohydraulic cabinet, operating, and test panels

Accessories for the generator include:

- Hydrogen cooler
- Instruments
- Vacuum seal system
- Hydrogen control system

5.6.4 Heat Recovery Steam Generator (HRSG)

The HRSG is a natural-circulation, dual-pressure, water tube boiler with parallel superheaters. At 100 percent design load and rated conditions, they are designed to produce 39.6 kg/sec (314,500 lb/hr) of steam at 6.9 MPa/580C (1000 psia/950F) and 7.0 kg/sec (55,500 lb/hr) of steam at 1.7 MPa/316C (250 psia/600F). Steam piping pressure and temperature losses were neglected. An additional 6.9 kg/sec (55,000 lb/hr) of steam at 207 kPa/121C (30 psia/250F) is generated in a separate low-pressure evaporator section, which is used exclusively as motive steam to the constant-pressure feedwater deaerator.

Gas flow of 333 kg/sec (2,640,000 lb/hr) at gas turbine rated conditions is horizontal through the HRSG sections. A perspective illustration of a typical HRSG is shown in Figure 5-37. More detailed HRSG design information is included in the EPGS data list in Volume III.

5.6.5 Gas Turbine Auxiliary Systems

The system shown in Figure 5-38 is designed to store and supply fossil fuel to the gas turbine safely and reliably during all operating modes. The fuel is unloaded from tank trucks or railway tank cars, transferred to storage tanks, and is pumped from these tanks to the gas turbine as well as to the plant auxiliary boiler and the emergency diesel generator.

Component Description. The unloading pump transfers fuel oil from the transporting tanks into the storage tanks. It can deliver oil at 1.1 m^3/sec (550 gpm) at a head of 30 m (100 feet) and is controlled by local on/off switches.

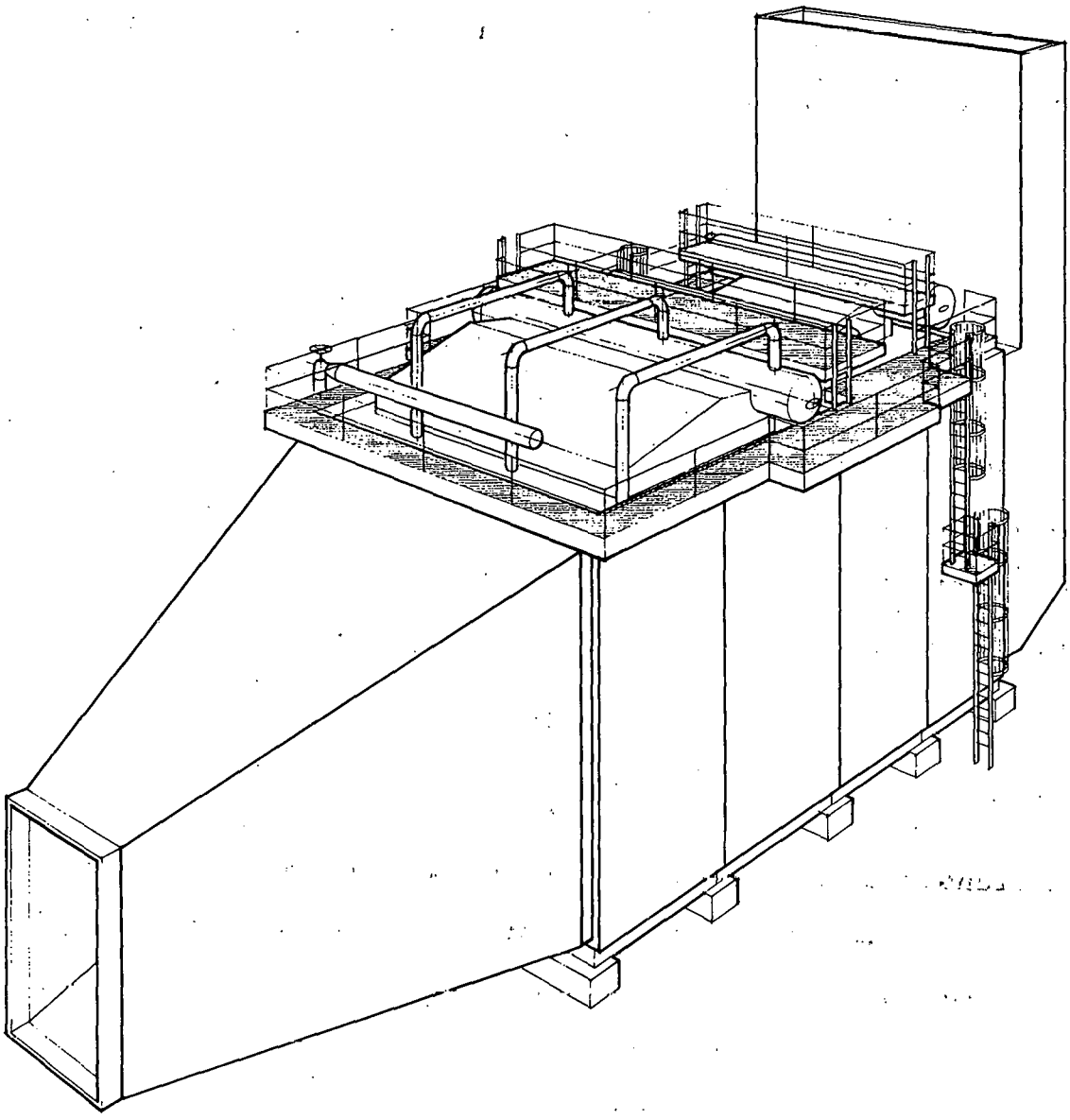

Figure 5-37 PERSPECTIVE DRAWING OF HRSG

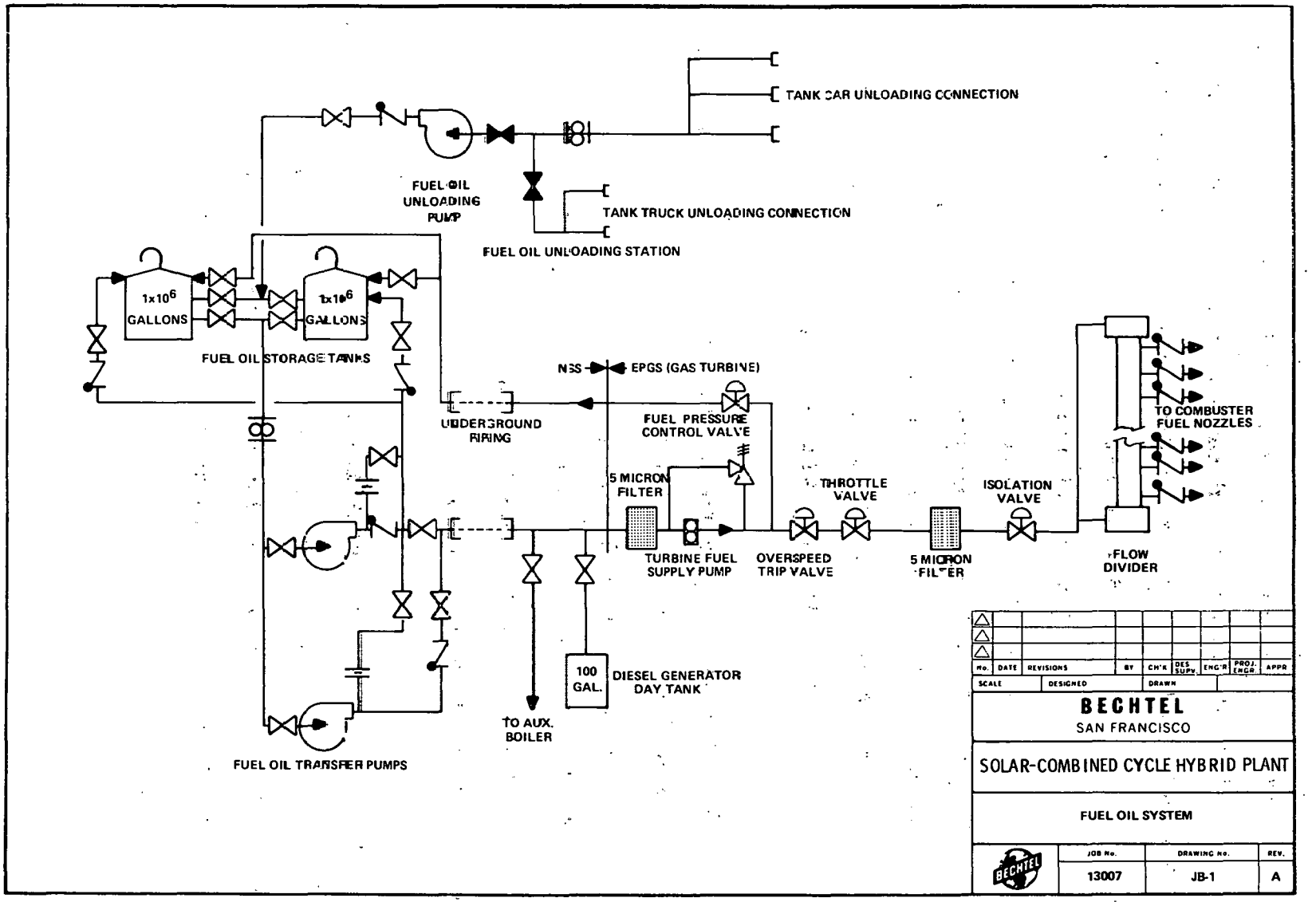

Figure 5-38 FUEL STORAGE AND SUPPLY SYSTEM

Each of two storage tanks has a one-million-gallon capacity and is sized for 30-day normal operation of the plant. A diked area around each tank is sized to contain the full volume of fuel in the tank in case of its rupture. The tanks are fitted with nozzles for connections to the unloading pump, the transfer pumps, recirculation lines, drain lines, breather and flame arrestor, and local level indicators. Low levels and high temperatures in the tanks are both annunciated in the main control room. A manually actuated mechanical foam system is provided for fire protection with each tank.

Fuel transfer pumps supply the required fuel to the gas turbine and the diesel generator day tank. Two full-capacity centrifugal pumps are provided for redundancy. Each pump can deliver 0.67 m^3/sec (300 gpm) at a head of 76 m (250 feet). A minimum flow recirculation orifice on the discharge side of each pump protects against overheating.

The diesel generator day tank has 0.38 m^3 (100 gal) capacity. It is filled from the transfer pump discharge header via a manual valve. With the use of the day tank, emergency operation of the diesel generator does not depend on operation of the transfer pumps.

The turbine fuel supply pump is a positive displacement rotary type that raises the oil pressure to 4.1 MPa (600 psia). A relief valve at the pump discharge prevents overpressurization of the system. A discharge pressure control valve is provided to bypass excess fuel back to the storage tanks.

The flow divider distributes equal flow for each fuel nozzle in the combustor.

System Operation. The fuel oil transfer pumps take suction from the storage tanks to deliver fuel to the turbine fuel supply pump, which develops adequate pressure to meet combustor requirements. The throttle valve in the supply pump discharge header controls the fuel flow, in response to a signal from the gas turbine control system. Excess oil is returned to the storage tanks by the pump discharge pressure control valve.

An overspeed trip valve operates in response to the loss of pressure in the hydraulic overspeed trip system, which is interlocked with all other emergency trips. Thus a turbine trip causes fuel supply to the combustor to be shut off. The transfer pumps are controlled by on/off automatic switches in the main control room. In automatic mode the standby pump starts automatically in response to pressure loss in the discharge header.

5.6.6 Steam Cycle Auxiliary Systems

Constant-Pressure Deaerator. The spray-type feedwater deaerator has two stages with an internal vent condenser and was sized to accommodate approximately 46.6 kg/sec (370,000 lb/hr) of condensate at rated conditions. Motive steam flow of approximately 6.9 kg/sec (55,000 lb/hr) is supplied from the HRSG low-pressure (LP) evaporator at a constant 207 kPa (30 psia) pressure over the entire load range. This ensures a minimum feedwater temperature of about 121C (250F) to the intermediate-pressure (IP) economizer sections of the HRSG. Storage tank capacity is about 24.6 m^3 (6500 gal), which is equivalent to 9 minutes of storage. The tank size is part of a standard design for deaerators of this type and size.

Additional feedwater heating is done in the HP and LP economizer sections of the HRSG. There are no external feedwater heaters and no steam turbine extractions, since there is enough energy in the gas turbine exhaust to do all feedwater heating.

Condensate-Feedwater Pump Requirements. Two nominal half-capacity, vertical, motor-driven, canned, turbine pumps deliver condensate to the constant-pressure deaerator. The 24 l/sec (380 gpm) capacity condensate pumps operate in parallel. The pumps supply water at 163 m (535 ft) head at the operating point.

Two nominal half-capacity, motor-driven, feedwater booster pumps take suction from the deaerator storage tank and discharge

through the IP economizer to the LP boiler steam drum and the suction of the main feedwater pumps. These centrifugal, horizontal split-case pumps operate in parallel. They have three stages and a capacity of 25.2 l/sec (400 gpm) each, at 218 m (715 ft) head at the operating point.

Two nominal half-capacity, motor-driven, feedwater pumps take suction from the booster pump discharge and supply feedwater through the high-pressure economizer to the high-pressure boiler steam drum. The feedwater pumps operate in parallel. They are centrifugal, horizontal split case type with eight stages and a rated capacity of 23.3 l/sec (370 gpm) and discharge head of 808 m (2650 ft) at the operating point.

Main Condenser. The main condenser is a single-pressure, two-pass surface condenser with a divided water box and a hotwell storage capacity of approximately 13 m^3 (460ft^3), which is equivalent to about 5 minutes of storage.

The condenser design duty is 102.6 MWt (350 MBtu/hr). The condensing surface is approximately 3480 m^2 (37,475 ft^2). A water temperature rise across the condenser of 8.3C (15F) is assumed and cooling water requirements are approximately 2945 l/sec (46,700 gpm).

Cooling Tower. The cooling tower is a mechanical draft evaporative tower consisting of four cells, with drift eliminators. Cooling tower duty is 112.8 MWt (385 MBtu/hr) and the approach to the design wet bulb temperature is 6.1C (11F). Circulating water flow to the tower is approximately 3236 l/sec (51,300 gpm), with an estimated makeup flow of 82 l/sec (1300 gpm).

Two half-capacity circulating water pumps circulate the cooling water from the cooling tower basin to the main condenser and to the service water pump suction. At the operating point, each pump has an approximate rating of 1892 l/sec (30,000 gpm) at 15.2 m (50 ft) head. The cooling tower cells are fan-equipped. The power requirement for each fan is approximately 100 kW (140 hp).

The entire heat rejection system, including cooling tower, condenser, circulating water system, chemical treatment, and tower blowdown, is shown schematically in Figure 5-39.

Water Treatment and Condensate Makeup. The raw water makeup to the cooling towers is chlorinated and acid-treated at the cooling tower basin. Water required for station makeup is chlorinated, lime-softened, clarified, and filtered using normal cold process treatment procedures. Condensate makeup is supplied from the raw water system and is processed in the makeup demineralizers prior to storage in the condensate storage tank.

5.6.7 Site Power Distribution

The main functions of the site power distribution system are to:

- Receive and control electric energy from the gas-turbine-driven generator and the steam-turbine-driven generator
- Provide electric power to the plant subsystems, including auxiliary power requirements to the receiver and collector subsystems
- Provide standby and emergency power to essential loads during loss of offsite power
- Deliver generated power to the utility grid during normal operating periods and supply offsite power to plant auxiliaries during startup, shutdown, and standby operating modes

As shown on the single-line diagram in Figure 5-40, the following major electrical equipment items are included:

- The electric portion of the steam turbine-generator
- The electric portion of the gas turbine-generator
- 13.8/115 kV main transformer for each generator circuit
- 13.8/4.16 kV main station auxiliary transformer
- Reserve auxiliary step-down transformer
- 4.16 kV, 1200 A metal-clad switchgear
- 37.5 kVA transformers for heliostat drive circuits
- 1000 kVA 4160/480 V step-down transformers
- 37.5 kVA, single-phase 4160-120/240 V step-down transformers
- 120/240 V distribution panel
- 650 kW standby diesel generator

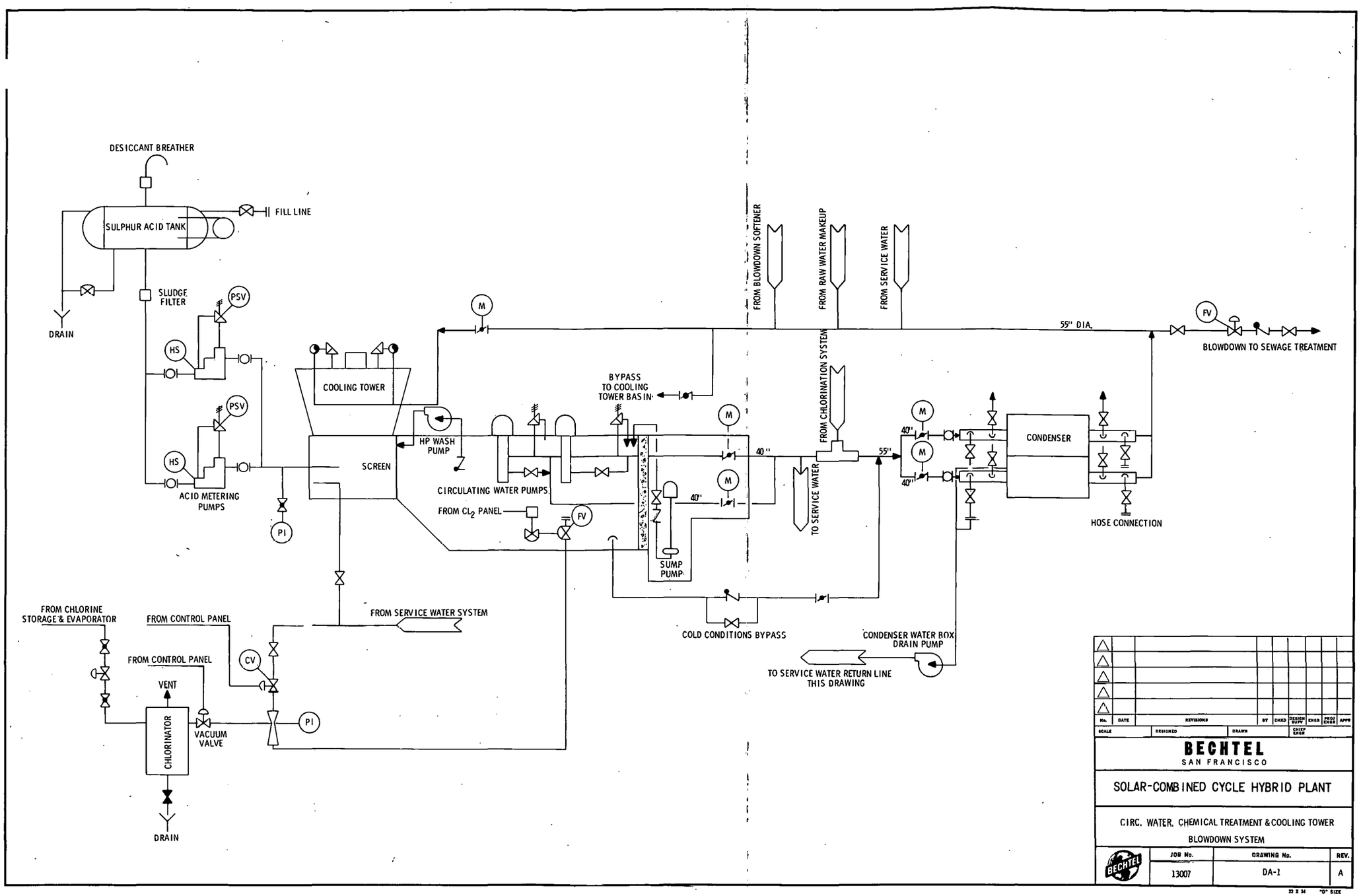

Figure 5-39 CIRCULATING WATER, CHEMICAL TREATMENT, AND COOLING TOWER BLOWDOWN SYSTEM

THIS PAGE

WAS INTENTIONALLY

LEFT BLANK

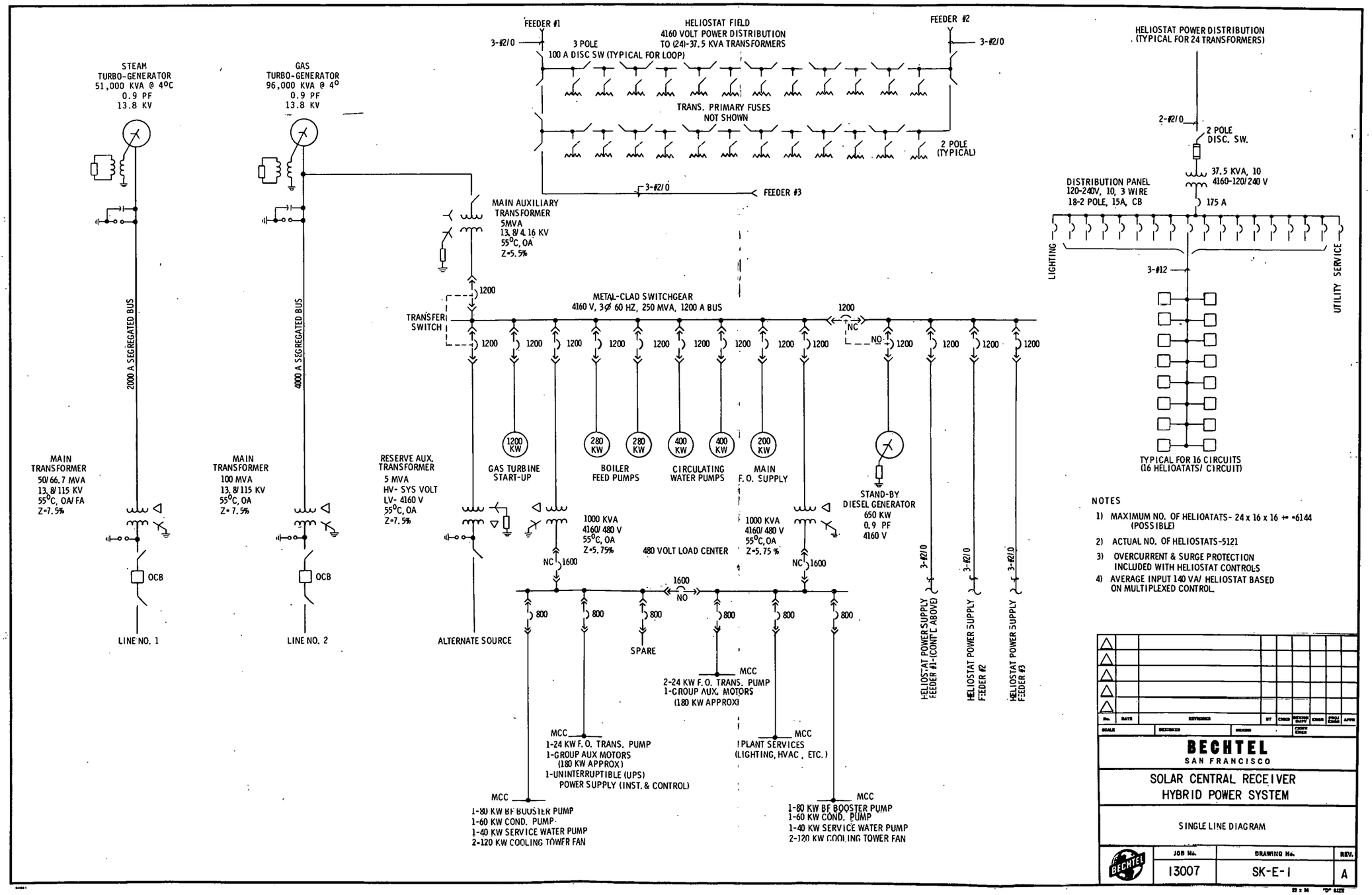

Figure 5-40 SINGLE LINE DIAGRAM

THIS PAGE

WAS INTENTIONALLY

LEFT BLANK

A grounding system is provided to protect against lightning, static electricity, and faults in electrical equipment. This grid consists of major grounding cables along each heliostat row with perpendicular cross connections spaced approximately 140 m (460 ft) or every tenth heliostat.

5.7 MASTER CONTROL SUBSYSTEM

The primary function of the master control subsystem (MCS) is to integrate the operation of various plant subsystems in response to external grid demands or changes in insolation. A secondary function is to perform data logging and performance trending of system parameters.

5.7.1 Requirements

The MCS must conform to accepted power plant design practices. Consistent with these practices, the subsystem must be able to:

- Interface between the MCS and other subsystem controls
- Use proven designs and off-the-shelf equipment as much as possible
- Eliminate single-point failures through redundant elements when cost-effective
- Separate operational controls from data logging and evaluation function
- Allow manual operation of the plant if the MCS fails
- Be flexible
- Be cost-effective

In general, control decisions affecting only one plant subsystem and its related auxiliaries should be made within that subsystem, while decisions affecting overall plant performance should be made by the MCS. Plant operator action is required to initiate plant mode selection. Table 5-15 indicates the operational status of the major subsystems for various plant operating modes.

5.7.2 Collector Subsystem Controls

Of the two primary configurations evaluated in the parametric studies, the intermediate level control configuration, (Figure 5-41), was selected for conceptual design. This system is composed of a heliostat array controller (HAC), heliostat field controller (HFC), and heliostat controller (HC). Components, hardware, and software needed for this configuration are currently being produced for technically similar equipment. This system was selected because it has:

- Low capital cost
- High reliability
- Low operation and maintenance cost
- System flexibility
- Available components

Since the decentralized system offers potential simplicity and low cost at high production levels, it should be reevaluated as experience with the intermediate-level system accumulates.

TABLE 5-15

SUBSYSTEM STATUS FOR VARIOUS PLANT OPERATING MODES

Plant Operating Mode	Subsystem Operating Status					
	Collector	Receiver	Electrical Power Generation Subsystem			Nonsolar
			Gas Turbine	Steam Turbine	Steam Generation	
Startup	Off	Off	Warm-up	Warm-up	Warm-up	On
Standby	Off	Warm-up	Idle	Warm-up	On	On
Long-Term Fossil	Off	Off	On	On	On	On
Hybrid	On	On	On	On	On	On
Shutdown	Off	Cool-down	Cool-down	Cool-down	Cool-down	Off

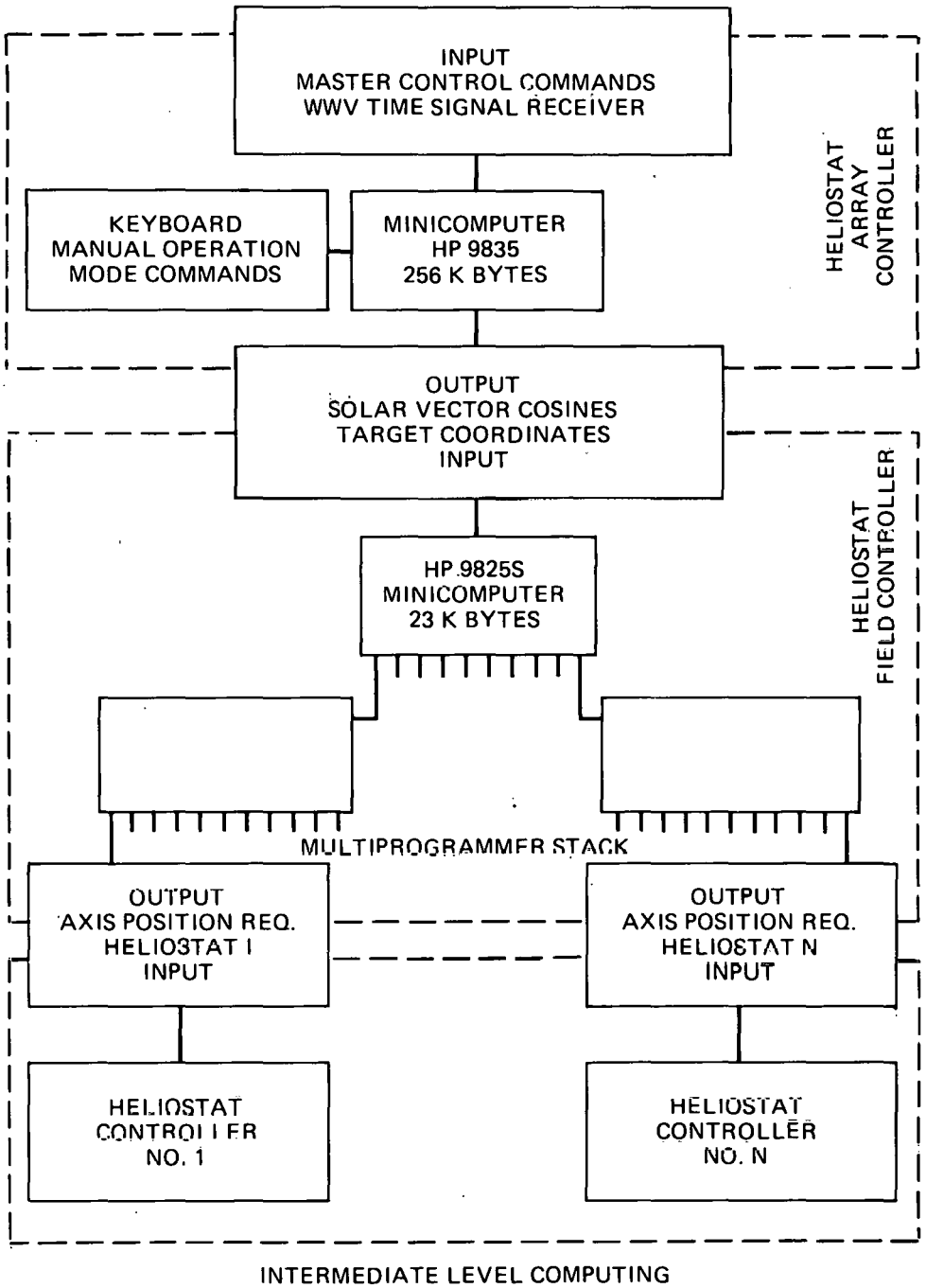

Figure 5-41 COLLECTOR SUBSYSTEM CONTROL CONFIGURATION

The central feature of the intermediate-level system is the HAC. This consists of a 256,000 byte memory version of a Hewlett-Packard HP9835A computer interfaced with the master control subsystem, a time signal generator, and approximately 20 heliostat field controllers. The HAC calculates and transmits to the HFCs solar vector direction cosine data, operating mode specification, and target coordinate data.

The HFCs make up a Hewlett-Packard HP9825S minicomputer and multiprogrammer network, interfaced at the minicomputer with the HAC and at the multiprogrammer with the individual HC's. The minicomputer receives control data from the HFC, performs the steering algorithm, and communicates individual heliostat requirements to the multiprogrammer for communication with each of the approximately 256 heliostats under its supervision.

The HC consists of a microprocessor, translator, power supply, and azimuth and elevation stepper motors for execution of the position commands. Position commands consist of stepping pulses and the azimuth and elevation position is based on step count with baseline position knowledge derived from limit switches.

The pointing accuracy budget, set at 0.75 mrad per axis, is split between mechanical backlash (0.38 mrad in the elevation drive and 0.45 mrad in the azimuth drive) and the control dead band (0.3 mrad). Since a one-step movement of the drive motor results in a minimum potential control increment of 0.0075 mrad for the elevation axis and 0.0089 mrad for the azimuth axis, control

pulses as large as 30 steps are possible within the control dead band and will be typical while operating in the tracking mode.

The selection of 256 heliostats for unit HFC control results in flux steps of 5 percent of full power. Using a stepper motor speed of 1000 steps per second results in a maximum travel time of 6.9 minutes for 3.14 rad (180 degrees) in elevation and 10.4 minutes for 4.71 rad (270 degrees) in azimuth. Defocusing within 120 seconds can be accomplished with a large margin at speeds of 1000 steps per second.

A study of the tracking speed and tracking angle rates for ten selected heliostats at summer solstice, equinox, and winter solstice showed that at all locations where singularities were encountered, the tracking speed was sufficient to maintain tracking during these periods.

5.7.3 Receiver Subsystem Controls

The receiver subsystem control functions are to:

- Proportion the receiver airflow so that the outlet temperature of each panel is equalized
- Bypass the receiver during long-term fossil mode

The first function is accomplished with modulating butterfly dampers located in the inlet pipe to each receiver panel. The dampers are wide open on the central panels with the highest

incident flux, while the flow through the other panels is restricted until all the outlet temperatures are equal. Adjustment of air flow to the cavities is accomplished by valves in the riser piping which compensate for the diurnal motion of the sun from east to west. With constant airflow, the overall receiver temperature control is accomplished by focusing or defocusing the collectors. Each of the three receivers has separate temperature sensing systems that send a demand signal through the MCS to its respective collector field.

Bypassing the receiver during long-term fossil mode operation is accomplished by valves in the riser and bypass piping. Control input is initiated by the operator when the plant operating mode is changed.

Since these controls have predetermined set points on the control elements, an analog approach provides the simplest and least expensive control scheme. The analog logic is activated or deactivated upon signal from the MCS.

No special controls are necessary to handle cloud passage transients. Using the specified cloud velocity of 20 m/sec, it will take a minimum of 50 sec to obscure the collector field from the sun. Once solar flux is completely removed from the receiver, more than 5 minutes is required for the receiver outlet temperature to fall below 425C (800F). The gas turbine fuel rate can be increased within a few seconds to keep the turbine inlet temperature constant. The response rate of the gas turbine to

compensate for the loss in solar energy is much faster than the rate of change in solar energy. This feature allows the gas turbine to compensate for solar input transients without upset to the remainder of the EPGS and does not require buffer thermal storage.

5.7.4 EPGS Controls

The function of the EPGS control system is to regulate the conversion of thermal and fossil fuel energy to electric power. EPGS control consists of three independent control packages:

- Gas turbine control
- Steam generation control
- Steam turbine control

These packages use commercially available equipment, integral to the gas turbine and steam turbine. The autonomous nature of these control packages is consistent with the requirements for manual backup of the MCS and allows a high degree of operational flexibility. Table 5-16 summarizes the EPGS subsystem control packages, the equipment controlled, and the control functions.

Gas turbine control regulates all functions of the gas turbine-generator, and the related auxiliary systems. It is an analog control package with the following capabilities:

- Automatic fuel control during acceleration and loading

TABLE 5-16

EPGS CONTROLS

Control Package	Equipment Controlled	Control Functions
Gas Turbine (GTC)	Gas turbine-generator, and auxiliary equipment	Controls turbine speed, generator load, exhaust temperature, fuel, and auxiliaries.
Steam Turbine (STC)	Steam turbine-generator, and auxiliary equipment	Controls turbine speed, generator load, steam pressure, and auxiliary equipment.
Steam Generation (SGC)	HRSG, feedwater pumps, deaerator, water treatment, condenser, condensate pump, and circulating water system	Controls steam temperature and flow to meet STC requirements.

- Closed-loop control of speed, generator output, and exhaust temperature
- Inputs for turbine speed, compressor discharge pressure, generator load, selected cycle and auxiliary system temperatures, combustion turbine status, and operator mode selections
- Automatic generator synchronization
- Generator circuit-breaker control

In addition to the packaged control system, there is a turbine overspeed protection in event of loss of generator load. To prevent overspeeding of the turbine due to the compressed air in the riser and downcomer a fast-acting butterfly dump valve located immediately upstream from the combustion chamber is activated. This valve lowers the air pressure to equalize the turbine power output with the compressor power input, which keeps the turbine from accelerating. Airflow is then maintained through the receiver system until the plant returns on line or is shut down by operator decision.

Steam turbine control regulates all functions of the steam turbine-generator and the related auxiliary systems. It is an analog control system with the following capability:

- Closed-loop control of steam pressure, speed, and generator output
- Inputs for turbine speed, turbine inlet pressure, generator load, selected cycle and auxiliary system temperatures, and operator mode selections
- Automatic generator synchronization
- Generator circuit-breaker control

Steam generation control regulates all functions of the HRSG, feedwater pumps, condensate pumps, and deaerator. It is an analog control system that features closed-loop control of steam temperature, feedwater and condensate flows, and steam and deaerator levels. In addition to controlling the HRSG and related auxiliaries, it also controls the remaining FPGS auxiliary systems, such as the condensate makeup water treatment system and the condenser circulating water system including the cooling tower.

5.7.5 Fuel Supply Controls

The fuel supply system controls consist of panel-mounted level gauges, fuel storage tank low-level alarms, and an interlock to start the fuel oil transfer pumps prior to startup of the gas turbine. All other fuel system controls are provided with the gas turbine. The fuel supply controls are of the standard analog type with predetermined set points, controlled by the gas turbine control within the FPGS.

5.7.6 Master Control

Although a complete parametric study was not conducted to select the best master control concept, several approaches were investigated. A centralized computer system was rejected due to poor utility acceptance of this type of system for packaged combined cycle plants. A modified central computer approach was examined which uses distributed digital microprocessors rather

than large central computers. This concept retains the best features of a central computer system without its inherent problems. A conventional analog master control system was also examined for comparison.

The selected MCS uses distributed micro-computers which can be used in quantity with the control functions distributed to many small computers (CPU). The result is that a single CPU failure, like a single control failure in an analog system, requires manual operation of only those loops that are associated with the failed CPU. The remainder of the MCS is not affected. Digital controls are used where feasible within the various plant subsystems. However, if simplicity or availability of hardware indicates the desirability of analog systems, these can be interfaced with the digital controls.

The current cost of conventional analog is approximately equal to distributed digital for the master control. Selection was therefore based on the operational advantages of the digital MCS. However, by 1990 the distributed digital approach should be significantly cheaper than the equivalent analog system, due to the rapid development of the microelectronics industry.

Description of Selected MCS. The configuration of the distributed digital MCS is shown in Figure 5-42. The design is based on the Westinghouse "Q-Line" series of microprocessor hardware for the master control and a Westinghouse 2500 computer for the data acquisition system.

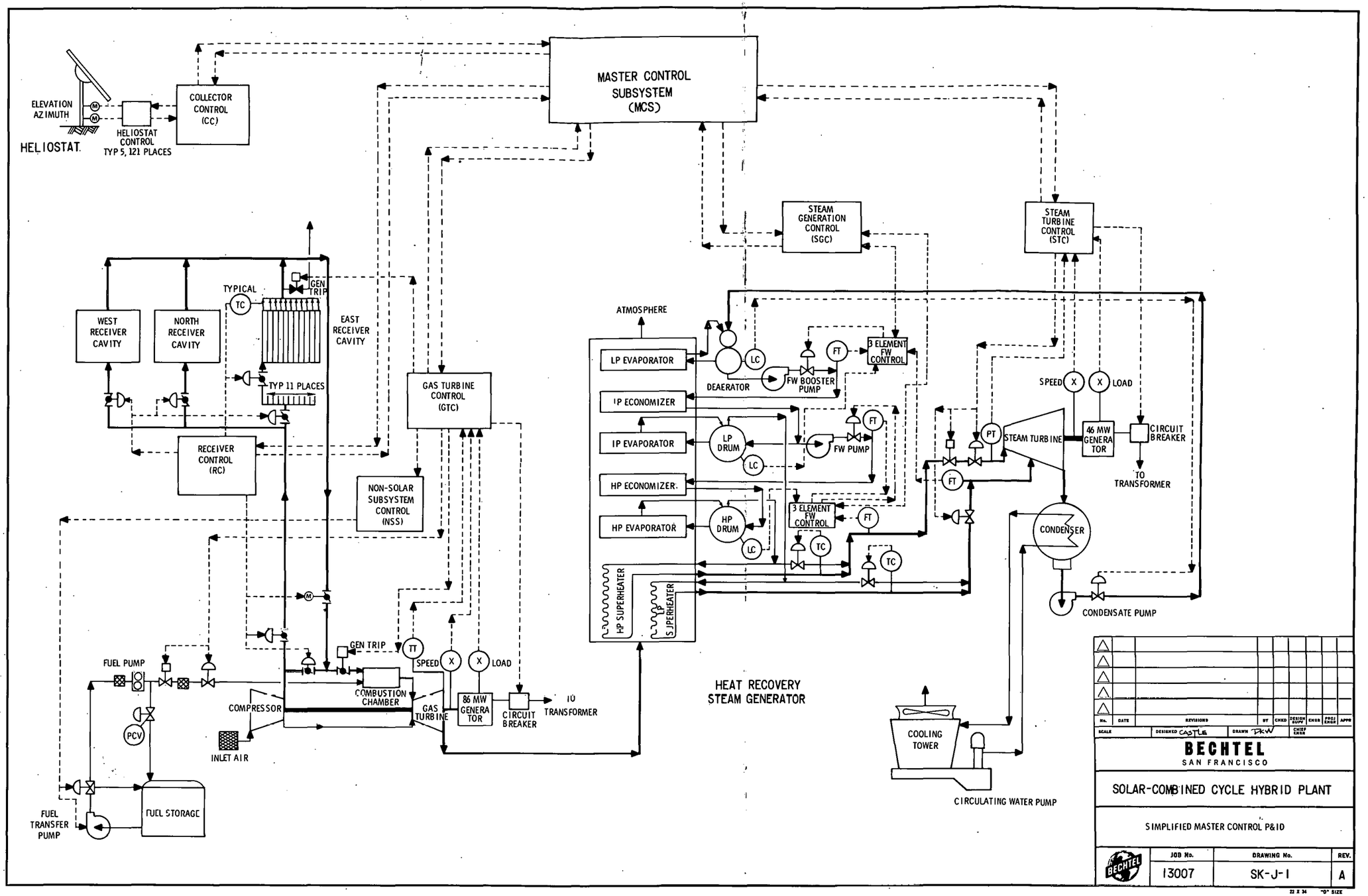

Figure 5-42 CONCEPTUAL MASTER CONTROL SUBSYSTEM

THIS PAGE

WAS INTENTIONALLY

LEFT BLANK

The configuration of a typical 10-loop distributed digital master control is shown in Figure 5-43. It is composed of individual microcomputers which operate independent control loops but allow the sharing of information. The information exchange is accomplished through the in-out (I/C) bus and the memory bus. The I/O bus provides the means of information exchange between the process variable printed circuit boards and the microcomputer. The memory bus provides the vehicle for information exchange between the microcomputer and its memory.

Redundancy. One of the benefits of a microprocessor-based system is the relatively low cost of the CPU when compared to the process I/O and software. Thus, redundancy of microcomputers that perform the control algorithms and logic function becomes economically more attractive. A typical redundant MCS configuration is shown in Figure 5-44.

The microprocessor arrangement allows the most economical backup of the control loops. While a failure in the process interface control circuits or the sensor would still force the control loop into manual mode, the control processor and logic would be redundant. The operator manual control mode is always available as a final backup.

Data Logger. The plant data logger is a computer, separate from the MCS, which monitors and records plant status and alarms abnormal conditions. The operator is provided with information

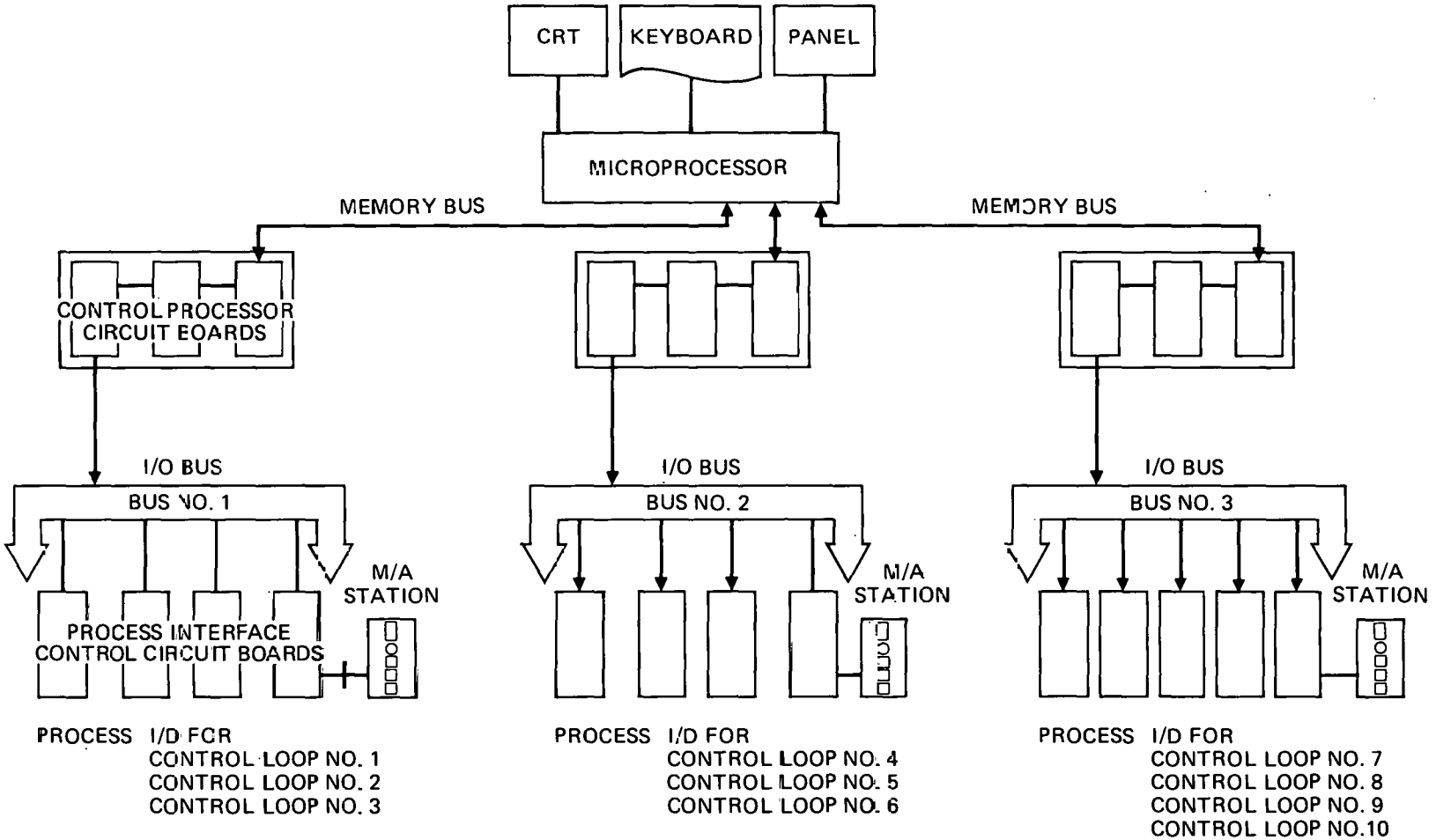

Figure 5-43 TYPICAL 10-LOOP MASTER CONTROL

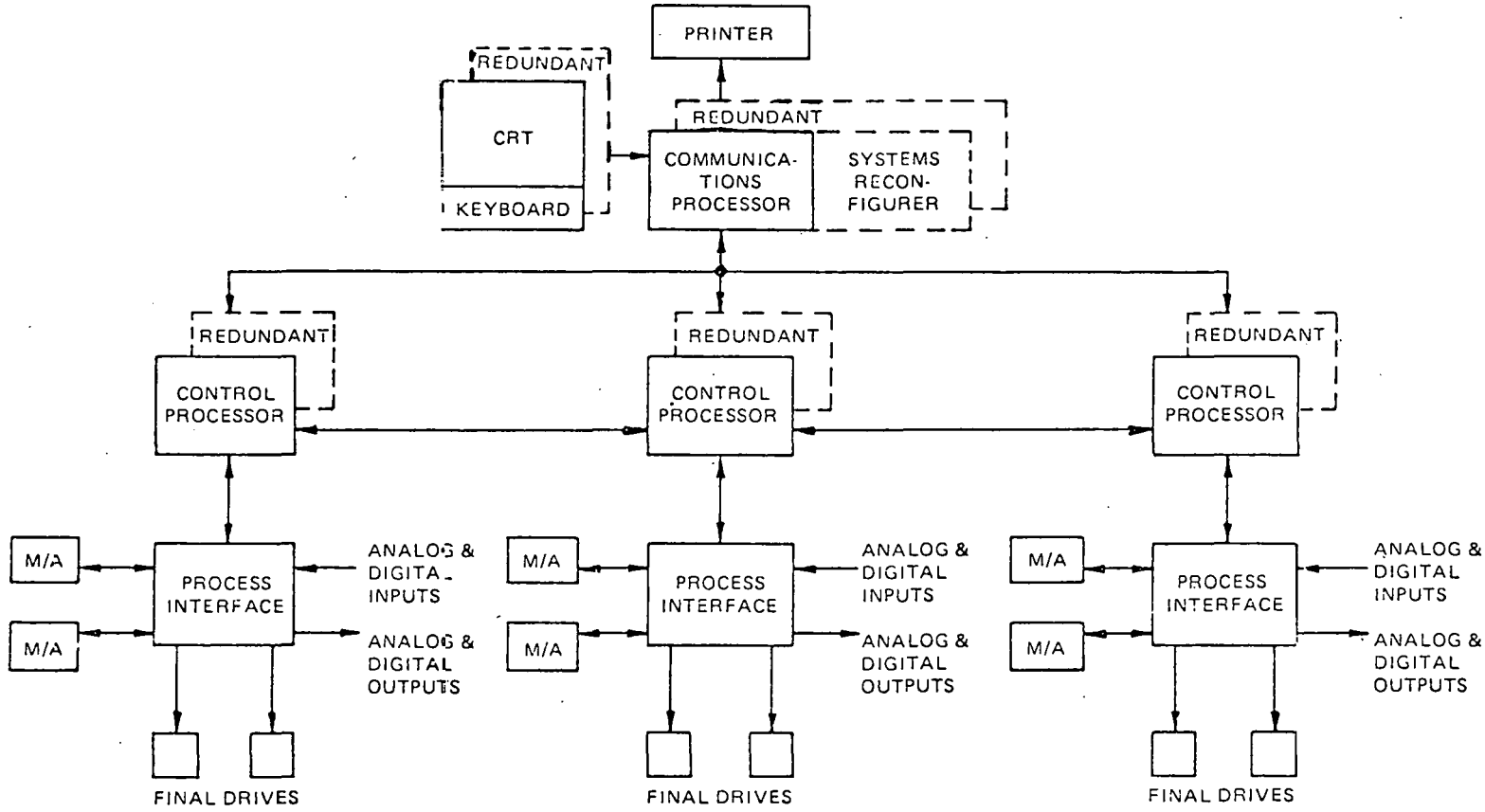

Figure 5-44 CONTROL SYSTEM OVERVIEW WITH REDUNDANT CONTROL PROCESSORS

in engineering units which can be immediately correlated to the data provided in the CRT, also in engineering units.

The plant data logger includes four color graphic CRTs with 25 displays. The system is designed for 100 analog and 250 digital inputs, and includes a 50-point sequence-of-events program printout on one of the three loggers.

Philosophy of Control. The power plant is controlled from a central control room. Operators monitor plant operation and are available to provide remote manual control as backup to the master control system.

The control CRT and keyboard provide the operator with immediate communication with the microprocessor controlled subsystem for establishing plant load requirements, rate of load changes, and startup and shutdown commands. In addition, the control CRT and keyboard facilitate simplified diagnosis and location of failures in system hardware or software. The operator supervises the automatic control of the MCS and only intervenes when abnormal conditions occur. The set point of each control loop can be changed by the operator from his control CRT. Loops can be tuned from this central location, permiting optimization in establishing control loop response. Changing control loop characteristics can be accomplished on or off line.

5.8 PLANT ARRANGEMENT

5.8.1 Plot Plan

Figure 5-45 is a partial site plan with emphasis on the power block, administrative, and service buildings. All buildings are grouped around the base of the receiver tower, within the 200 m diameter circle where heliostat placement is impractical. The administration building is located for easy access from the power block perimeter roadway. The gas turbine, heat recovery steam generator (HRSG), and steam turbine are arranged to minimize air piping runs from the receiver tower and process piping runs from the HRSG to the steam cycle equipment. The control building is located and constructed in a manner that provides a central location and observation point for the turbine areas and the tower base. The service building is close to the tower base with easy access to all major equipment; it is also convenient to the access roads into the heliostat field.

The cooling towers are located in the southeast quadrant of the site. They are at the maximum practical distance from the heliostat field perimeter and located so as to minimize cooling tower drift and plume on heliostat performance. Fuel oil storage tanks are in the southeastern quadrant of the plant site at a distance in compliance with safety regulations and good engineering practice.

5.8.2 Major Equipment

Relative location and orientation of major process equipment within the plant area were selected to enhance operability and to minimize capital and O&M costs. The gas turbine-generator is as close as possible to the receiver tower to minimize air piping runs from the tower base to the combustor air inlet. The steam turbine-generator is close to the heat recovery steam generator to minimize main steam and condensate-feedwater piping runs.

Figure 5-46 shows elevation views of the plant looking north and east, indicating the relative size and position of the major equipment.

5.8.3 Architectural Considerations

The buildings, structures, and enclosures associated with the plant are designed to minimize intrusion on the local landscape. The administration and control room buildings are made of concrete blocks; the remaining buildings and enclosures are of prefabricated insulated steel with finished exterior. All building and enclosure exteriors are finished to blend with the locale and be aesthetically pleasing. Any items of equipment that detract from this scheme will be provided with enclosures to achieve minimum impact and possibly enhance the predominant landscape features.

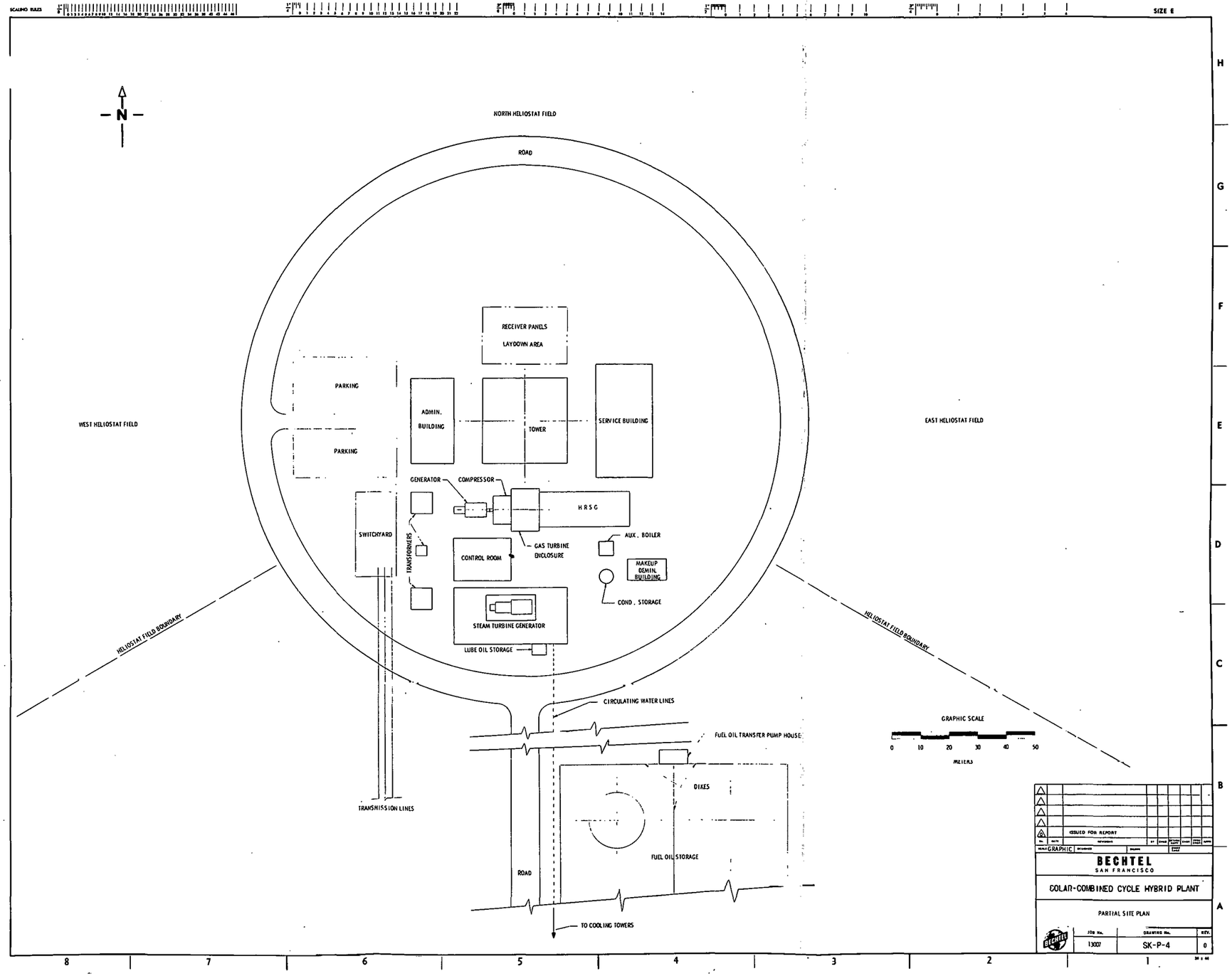

Figure 5-45 PARTIAL SITE PLAN

THIS PAGE

WAS INTENTIONALLY

LEFT BLANK

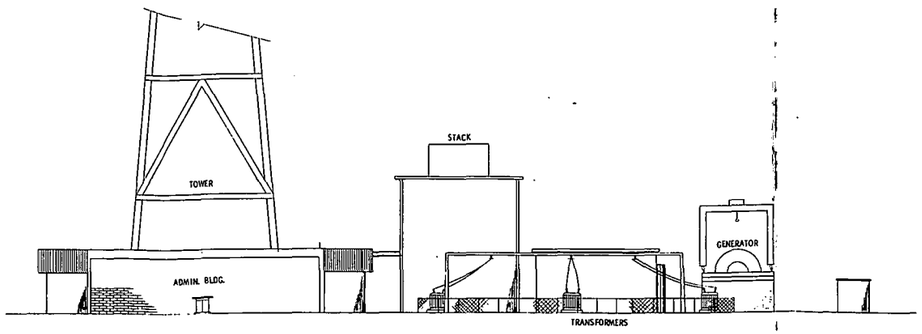

EAST ELEVATION

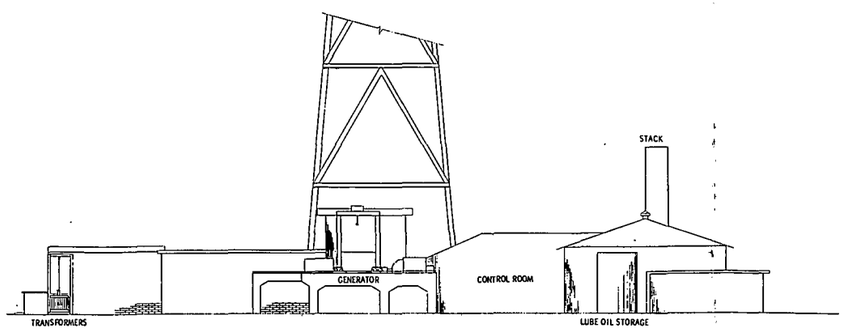

NORTH ELEVATION

GRAPHIC SCALE:
0 5 10 15
METERS

BECHTEL
SAN FRANCISCO

SOLAR-COMBINED CYCLE HYBRID PLANT

ELEVATIONS

JOB No.	DRAWING No.	REV.
13007	SK-P-2	A

Figure 5-46 ELEVATIONS

THIS PAGE

WAS INTENTIONALLY

LEFT BLANK

Paved and secondary roadway construction is limited so that associated cost and environmental impacts are minimized. Access to the individual heliostats for washing, maintenance, and removal will be achieved by marginal-terrain vehicles.

5.9 SYSTEM OPERATION

This section discusses the operation of the solar combined cycle hybrid power system. The gas turbine is the center of system operation, since the combustor fuel control has the flexibility to accommodate any solar heat input without upsetting the EPGS. The steam turbine simply follows the gas turbine, absorbing as much energy as the HRSG is able to extract from the gas turbine exhaust.

5.9.1 Daily Operating Cycle

Since the solar hybrid plant is considered to be an intermediate-load unit, it is expected to operate during the day and early evening hours with reasonably constant power output. A typical daily operating cycle would generally follow the sequence described below.

Diurnal Startup. The plant is started up on fossil fuel with the receiver bypassed early in the morning, before adequate insolation is available. The gas turbine is brought on line first, followed shortly thereafter by the steam turbine. A short time before the acquisition of trackable insolation, air flow

through the receiver is established. Then the heliostat groups are brought into focus in a sequenced manner. At this time, the highest air flow is directed to the west cavity, since it receives almost half of the solar input in the early morning, as shown in Figure 5-47.

Hybrid Operation. The plant continues to operate in this mode throughout the major portion of the day, with the receiver outlet temperature varying with the level of insolation. The receiver outlet air is held to a maximum of 843C (1550F) by defocusing heliostats if necessary. The proportion of airflow to the east and west cavities of the receiver is adjusted periodically to follow the shift of power during the day.

The actual output of the plant may vary throughout the day according to the load demand in the utility grid. At reduced loads, the fossil input is reduced until only solar heat is being used. It is not expected that the dispatcher would reduce power beyond the solar-only condition if he has a choice.

Diurnal Shutdown. When the sun reaches the minimum trackable angle in the late afternoon, with almost half of the solar input into the east cavity, the heliostats are sequentially defocused. After this, the receiver is bypassed and the system is brought to long-term fossil mode. Operation continues as long as necessary to satisfy system demand. At the end of daily operation the gas turbine is shut down completely, but the steam turbine seals and

condenser vacuum are maintained to allow expeditious resumption of operation the following day.

5.9.2 Startup and Shutdown Sequence

The normal startup of the gas turbine is automatically sequenced and takes about 27 minutes from cold shutdown to full load. The starter motor first accelerates the rotor to approximately 2400 rpm and at that point the combustor is ignited. The turbine is then accelerated, synchronized, and loaded to 4 percent within 13 minutes of initiation. The normal loading rate is 7 percent per minute to full load and rated exhaust temperature. During operation, instantaneous load changes of 25 percent are allowed normally or 50 percent in emergencies without trip.

Water circulation through the HRSG is established with pumps at minimum flow and the deaerator pegged. At this point the steam turbine bypass is opened to the condenser and the main turbine valves are closed. The turbine is on turning gear with seal steam and condenser vacuum established. When sufficient steam pressure and superheat have been established, the turbine is rolled by admitting HP steam and accelerated to rated speed, synchronized, and loaded to 5 percent of rating. From this point, the load can be increased at a rate of 2 percent per minute to rated load. The entire process from ignition of the gas turbine to rated load of the steam turbine is estimated to take 120 minutes.

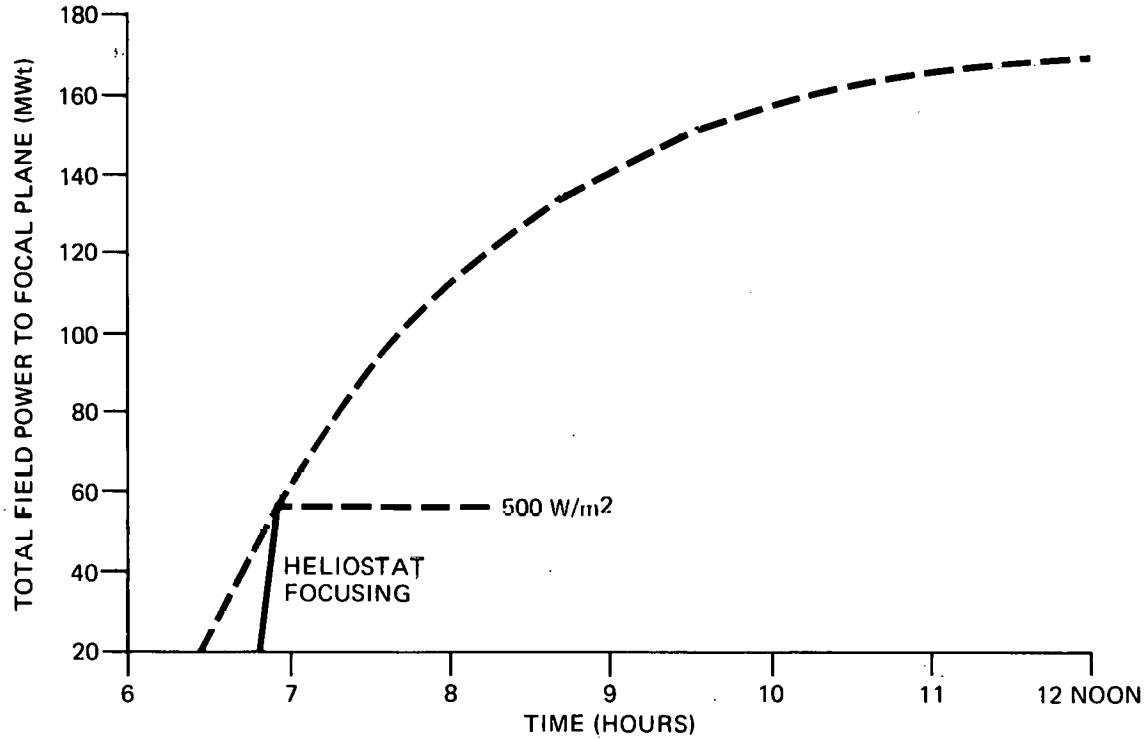

Figure 5-47 SOLAR POWER TO RECEIVERS DURING STARTUP (EQUINOX MORNING)

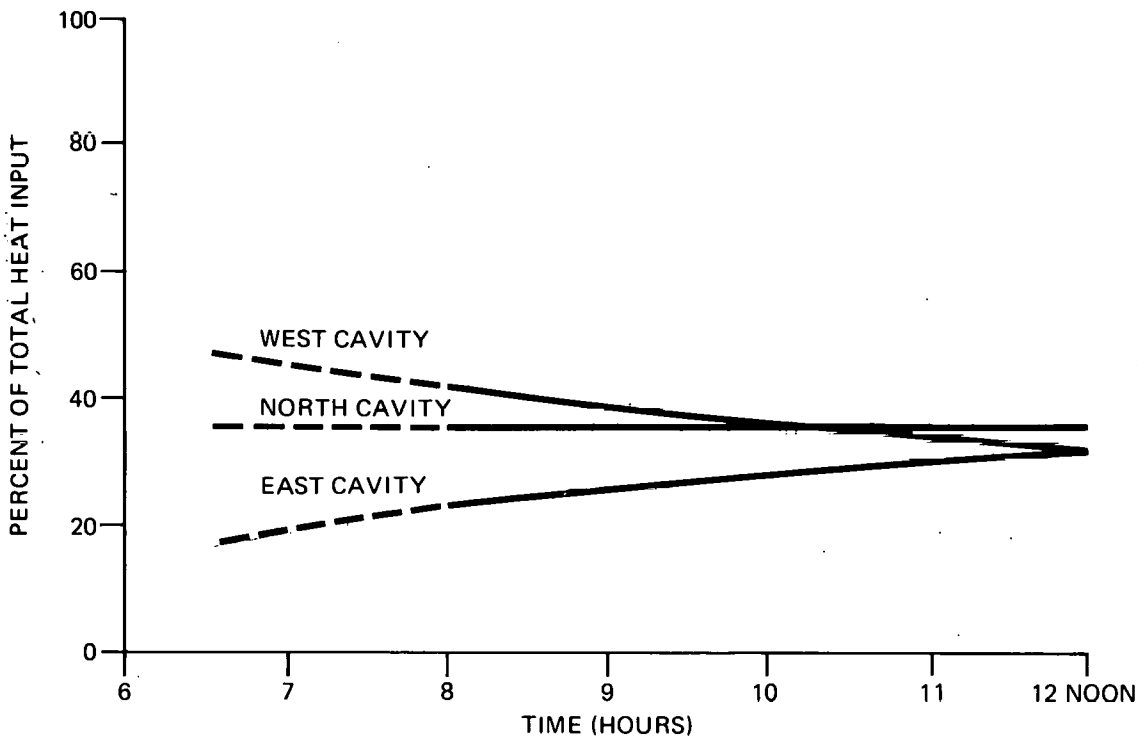

Figure 5-48 POWER SPLIT AMONG CAVITIES DURING STARTUP (EQUINOX MORNING)

During gas turbine startup, the receiver is bypassed, although a warmup valve can be used to pressurize and preheat the receiver and air piping. Air is routed to the receiver in anticipation of solar input reaching 500 W/m². After flow in the receiver is established, the heliostats will be sequentially focused and the combustor is used to automatically adjust the fossil input to maintain turbine equilibrium. Figure 5-48 illustrates the approximate loading sequence of the receiver for a normal startup.

Normal shutdown of the turbines is accomplished by reducing load to the minimum value with the normal ramp rate and then opening the generator breakers and allowing the rotors to coast down. The gas turbine remains on turning gear until cool and the steam turbine remains on turning gear as long as steam seals and vacuum are continued.

5.9.3 System Transients

Events such as steam turbine trip have the same impact on the system as for a conventional combined cycle plant. Further work is necessary during detailed design to make sure that all contingencies are covered. However, two significant transients, described below, have been identified that have unique implications for this plant.

Cloud Passage. A large cloud travelling at 20 m/sec could reduce the solar input from design value to zero in about 50 or

60 seconds. The combustor can easily adjust the fossil fuel flow to maintain stable operation of the EPGS. It is estimated that the receiver and air piping can handle the adverse thermal effects without damage. The receiver would probably be bypassed to limit the rate of cooling after the heliostats were defocused or are shaded. During detailed design, the actual operating parameters for the receiver must be established based on site-specific parameters.

Gas Turbine Trip. Since the gas turbine is the cornerstone of the power system, trip represents the most significant system upset in the hybrid plant. Several actions must be taken automatically in the event of a trip. The heliostats must be defocused quickly to limit the solar heat input, which requires operation of the diesel generator if the trip is combined with loss of offsite power. In addition, the amount of compressed air stored in the system must be prevented from causing the gas turbine to overspeed. To achieve this, maximum flow through the compressor is maintained while a portion of the stored air is vented through the air dump valves. The turbine trip valve, unique to this type of system, must act quickly to limit the pressure available at the gas turbine inlet.

5.10 COST ESTIMATES

5.10.1 Introduction

Costing Bases. The hybrid plant cost estimates are based on the conceptual design and engineering information prepared for the study. This includes subsystem descriptions, flowsheets, equipment lists, plot plans, single-line diagrams, and tower drawings. Bulk material quantities were developed from subsystem descriptions and in-house historical data for similar facilities, or from quantity take-offs where details were available.

Second quarter 1979 pricing levels were used for all equipment, subcontracts, and bulk materials. No allowance was made for future escalation.

Cost of major mechanical equipment, significant subcontracts, and major bulk items were based on written or telephone quotes supplied for estimating purposes by vendors. Pricing for all other items was based on in-house historical data.

The labor cost estimates are based on productivity and wages for unionized, direct-hire construction forces. Labor rates were developed from craft agreement information published by the Associated General Contractors of California, Inc. The overall labor rate is built up from a direct rate of $13.00 and an indirect rate of $8.00 for craft benefits, payroll burdens, and

subsistence. Manhour rates for installation work were developed from Bechtel experience in Southern California.

Indirect field costs were developed from Bechtel experience on previous jobs in the U.S. west coast and modified to reflect the specific characteristics of this project.

An allowance has been made based on in-house historical and study information for combined cycle power plants and other projects of a similar nature.

An average contingency of 12 percent and a fee of 3 percent are included in the capital cost totals.

Qualifications. For estimating purposes it was assumed that:

- Permanent plant equipment and materials will be available at present-day lead times, and manual and nonmanual personnel will be available in numbers and skills as required for engineering and construction.
- The turbines will be delivered to the jobsite with all internal piping and electrical systems preassembled at the factory.
- Existing water sources and power will be adequate for the requirments of this installation.

Exclusions. The following cost items were not included in the estimates:

- Equipment spares and mobil equipment
- Sales tax

- Owner's costs, such as costs of financing or interest during construction, owner's licensing and engineering, royalties, and the like
- Assistance to the owner in obtaining EPA clearances, permits, and authorizations from the Department of Energy or any other government agencies
- Costs of this and previous studies
- Initial charges and stocks of operating supplies
- Ecological and environmental considerations other than those incorporated in the present conceptual design
- Training plant operating personnel
- Escalation

5.10.2 Costing Geographical Boundaries

Figure 5-49, depicts each of the subsystem geographic boundaries as they are included in the construction cost estimate, excluding the 5100 account. Because of the difficulty involved in schematically illustrating all of the interfaces between subsystems, the following discussion is intended to clarify specifically what items are included in each account.

5100 Land and General Site Preparation. This is composed of all general plant equipment and facilities not specifically related to or included in other subsystems:

- Land purchase
- Clearing and rough grading
- Fencing
- Landscaping and finish grading

- Roads
- Fire water and foam system
- Water wells, pumps and pipeline
- Sewage treatment plant
- Yard lighting, grounding, and instrumentation

5200 Administrative Areas. This is composed of the plant administration building (including all building fixtures and electric), service/warehouse building (including all building fixtures, electrics, and service/warehouse equipment), and all miscellaneous structures not related to other subsystems:

- Guard shacks
- Lunch rooms
- Gate house
- Change house

5300 Collector Subsystem. This is composed of:

- Heliostats
- Foundations
- Power/control equipment and wiring
- Lightning protection and grounding
- Alignment system

5400 Receiver Subsystem. This is composed of:

- Receiver

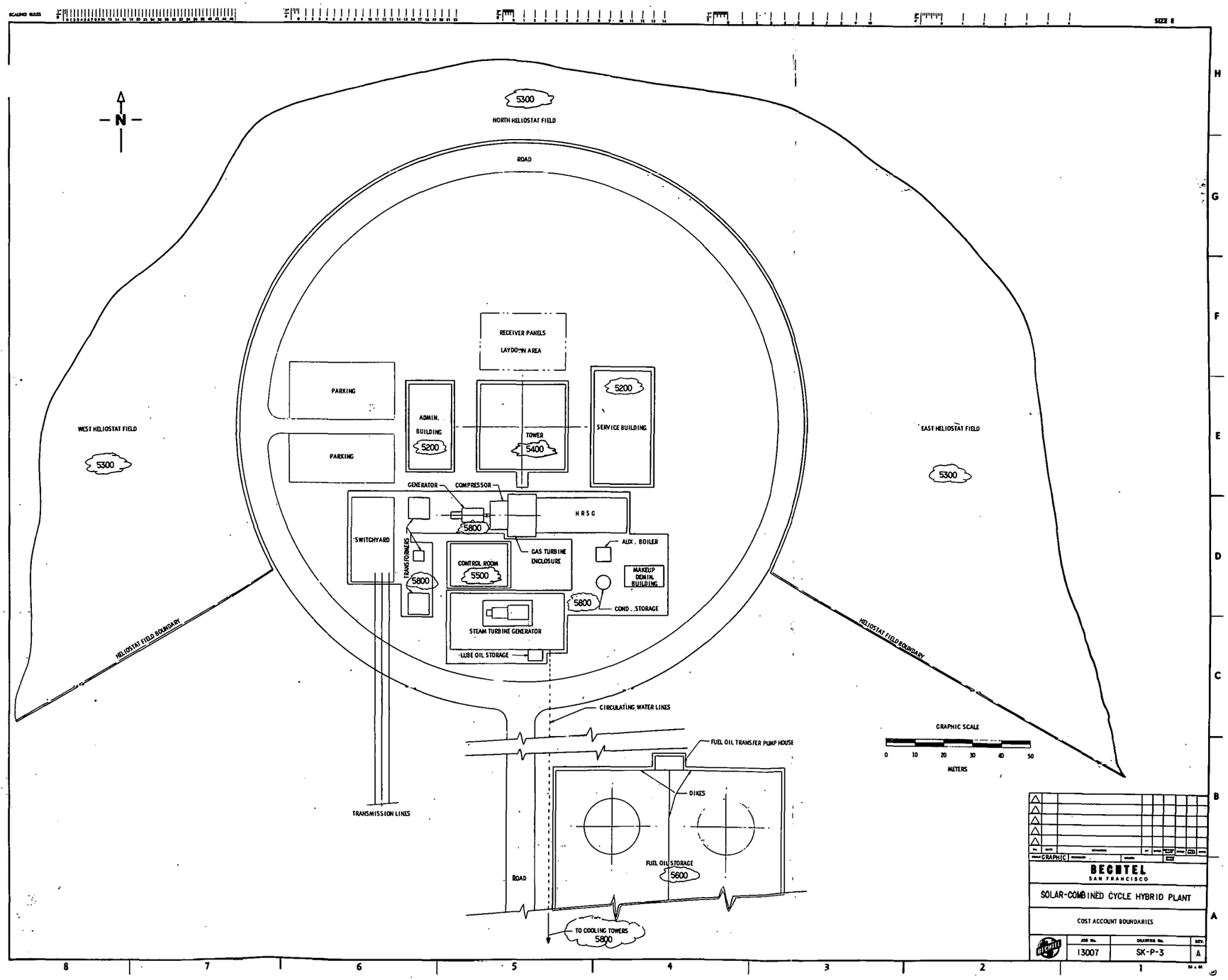

Figure 5-49 COST ACCOUNT BOUNDARIES

THIS PAGE

WAS INTENTIONALLY

LEFT BLANK

- Tower with elevator
- Riser and downcomer
- Valves and instrumentation
- Miscellaneous lighting and grounding

5500 Master Control Subsystem. This is composed of the control room building (including all building fixtures and electrics), and all control equipment/panels necessary for the operation of the solar central receiver hybrid power systems:

- Microprocessor - base system
- Data logger
- CRT auto plant startup
- Plant control panels and miscellaneous controls

5600 Nonsolar Subsystem. This is composed of all the facilities necessary for receiving, storing, and transferring fuel oil:

- Fuel oil tanks, foundations, and dikes
- Unloading and transfer pumps
- Fuel oil piping and instrumentation
- Power/control equipment and wiring
- Miscellaneous lighting and grounding

5800 Electric Power Generating Subsystem. This is composed of all equipment and bulk materials necessary for converting the thermal output of the receiver and the chemical energy in the fossil fuels to electric power, and all equipment and bulk

material required to distribute power throughout the plant (excluding the collector subsystem) and to integrate the EPGS into a typical electric power system network:

- Civil/structural and buildings
- Gas and steam turbine generators
- Heat reconvert steam generator
- Condenser and cooling tower
- Tanks (excluding main fuel oil)
- Pumps
- Auxiliary boiler
- Cranes and other miscellaneous equipment
- Piping and instrumentation
- Power/control equipment and wiring
- Switchyard and main transformers
- Miscellaneous lighting and grounding

5.10.3 Capital Costs

A summary of system and subsystem construction costs in manhours and second quarter 1979 dollars is given in Table 5-17. The detailed construction cost estimate is given Table 5-18.

5.10.4 Operating and Maintenance Costs (O&M)

The annual operating and maintenance cost for the solar hybrid power plant is 2.4 million dollars, which represents 1.58 percent

TABLE 5-17

CONSTRUCTION COST SUMMARY
(thousands)

Cost Item	Man-hours	2nd Quarter 1979 Dollars			
		Labor	Sub-contract	Material	Total
5100: Land and general site preparation	120	813	2,798	627	4,238
5200: Administrative areas	61	485	1,380	863	2,728
5300: Collector subsystem	190	-	30,370	-	30,370
5400: Receiver subsystem	188	2,209	1,157	24,208	27,574
5500: Master control subsystem	34	225	873	2,171	3,269
5600: Nonsolar energy subsystem	13	122	300	99	521
5800: Electric power generator subsystem	322	4,183	-	29,099	33,282
Total direct field costs	928	8,037	36,878	57,067	101,982
Indirect field cost					13,140
Total field costs					115,122
Engineering and other home office services					5,756
Total field and office costs					120,878
Contingency					14,647
Fee					4,065
Total construction cost					139,590
Cost per kWe (112,600 kWe net)					1,240

TABLE 5-18

CONSTRUCTION COST ESTIMATE

CLIENT DOE/SANDIA

LOCATION BARSTOW, CA

PROJECT SOLAR HYBRID

DESCRIPTION ACCOUNT 5100 LAND AND GENETICAL SITE PREPARATION

CONT. NO.

MADE BY MGG

APPROVED

A/C NO.	ITEM & DESCRIPTION	MAN HOURS	ESTIMATED COST IN $1000s LABOR	SUBCONTRACTS	MATERIALS	TOTALS
5100	SUMMARY	(MH)		(S/C)		
A	Excavation & Civil S/C MH 54360	54460	708	2543	348	3599
B	Concrete					
C	Structural Steel					
D	Buildings					
E	Machinery					
F	Piping S/C MH 3200	2500	33	255	155	443
G	Electrical	2200	29	—	50	79
H	Instruments	3330	43	—	74	117
J	Painting					
K	Insulation					
	DIRECT FIELD COSTS	62490	813	2798	627	4238
	S/C MH 57560					
L	Temporary Construction Facilities					195
M	Construction Services, Supplies & Expense					225
N	Field Staff, Subsistence & Expense					187
P	Craft Benefits, Payroll Burdens & Insurances					524
Q	Equipment Rental					195
	INDIRECT FIELD COSTS					1329
	TOTAL FIELD COSTS					5567
R	Engineering @ 5%					278
	Design & Engineering					
	Home Office Costs					
	R & D					
	TOTAL OFFICE COSTS					278
	TOTAL FIELD & OFFICE COSTS					5845
V	Contingency @ ~10%					582
W	Fee @ 3%					193
	TOTAL CONSTRUCTION COST					5620

DATE 7-20-79 REVISION NO. REVISION DATE PAGE NO. 10

TABLE 5-18 (Continued)

CONSTRUCTION COST ESTIMATE

CLIENT DOE/SANDIA

OCATION BARSTOW, CA

PROJECT SOLAR HYBRID

DESCRIPTION ACCOUNT 5200 ADMINISTRA-TIVE AREAS

CONT. NO.

MADE BY MGG

APPROVED

A/C NO.	ITEM & DESCRIPTION		MAN HOURS	ESTIMATED COST IN $1000s LABOR	SUBCONTRACTS	MATERIALS	TOTALS
5200	SUMMARY		(MH)		(S/C)		
A	Excavation & Civil						
B	Concrete						
C	Structural Steel						
D	Buildings						
E	Machinery	ADMIN BLDG	20000	260	986	254	1500
F	Piping	SERVWARE	13300	173	312	573	1058
G	Electrical	MISC BLDG	4000	52	82	36	170
H	Instruments						
J	Painting						
K	Insulation						
	DIRECT FIELD COSTS		37300	485	1380	863	2728
	S/C MH 23400						
L	Temporary Construction Facilities						116
M	Construction Services, Supplies & Expense						136
N	Field Staff, Subsistence & Expense						112
P	Craft Benefits, Payroll Burdens & Insurances						[illegible]
Q	Equipment Rental						116
	INDIRECT FIELD COSTS						773
	TOTAL FIELD COSTS						3501
R	Engineering @ 5%						176
	Design & Engineering						
	Home Office Costs						
	R & D						
	TOTAL OFFICE COSTS						176
	TOTAL FIELD & OFFICE COSTS						3697
V	Contingency @ ~10%						371
W	Fee @ 3%						122
	TOTAL CONSTRUCTION COST						4190

DATE 7-25-79 REVISION NO. REVISION DATE PAGE NO. 1 OF 1

TABLE 5-18 (Continued)

CONSTRUCTION COST ESTIMATE

CLIENT DOE / SANDIA

LOCATION BARSTOW, CA

PROJECT SOLAR HYBRID

DESCRIPTION ACCOUNT 5300 COLLECTOR SUBSYSTEM SUMMARY

CONT. NO.

MADE BY MGE

APPROVED

A/C NO.	ITEM & DESCRIPTION	MAN HOURS	* ESTIMATED COST IN $1000s LABOR	SUBCONTRACTS	MATERIALS	TOTALS
5300	SUMMARY	(MH)		(S/C)		
A	Excavation & Civil					
B	Concrete					
C	Structural Steel					
D	Buildings					
E	Machinery & Equipment	–	–	30370	–	30370
F	Piping					
G	Electrical					
H	Instruments					
J	Painting					
K	Insulation					
	DIRECT FIELD COSTS	–	–	30370	–	30370
	S/C MH 190000					
L	Temporary Construction Facilities					
M	Construction Services, Supplies & Expense					
N	Field Staff, Subsistence & Expense	INCLUDED ABOVE				–
P	Craft Benefits, Payroll Burdens & Insurances					
Q	Equipment Rental					
	INDIRECT FIELD COSTS					
	TOTAL FIELD COSTS					30370
R	Engineering @ 5%					1519
	Design & Engineering					
	Home Office Costs					
	R & D					
	TOTAL OFFICE COSTS					1519
	TOTAL FIELD & OFFICE COSTS					31889
V	Contingency @ ~10%					3189
W	Fee @ 3%					1052
	TOTAL CONSTRUCTION COST					36130

DATE 7-31-79 REVISION NO. REVISION DATE PAGE NO. 1 OF 1

* NOTE: THIS IS A CLIENT PROVIDED COST, REF SANDIA LETTER DATED 6-27-79

TABLE 5-13 (Continued)

CONSTRUCTION COST ESTIMATE

CLIENT DOE / SANDIA

LOCATION BARSTOW, CA

PROJECT SOLAR HYBRID

DESCRIPTION ACCOUNT 5400 RECEIVER SUBSYSTEM SUMMARY

CONT. NO.

MADE BY MGE

APPROVED

A/C NO.	ITEM & DESCRIPTION	MAN HOURS	ESTIMATED COST IN $1,000			
			LABOR	SUBCONTRACTS	MATERIALS	TOTALS
5400	SUMMARY	(MH)		(S/C)		
A	Excavation & Civil	9090	118	—	—	118
B	Concrete	22430	435	—	451	886
C	Structural Steel S/C MH 12920	35740	475	305	1405	2185
D	Buildings	—	—	—	—	—
E	Machinery & Equipment S/C MH 2600	40000	520	275	20000	20795
F	Piping S/C MH 240	45890	597	12	2271	2880
G	Electrical	1950	25	—	20	45
H	Instruments	1150	15	—	35	50
J	Painting	1820	24	—	23	47
K	Insulation S/C MH 3500		—	565	—	565
	DIRECT FIELD COSTS	169070	2209	1157	24209	27574
	S/C MH 19260					
L	Temporary Construction Facilities					530
M	Construction Services, Supplies & Expense					619
N	Field Staff, Subsistence & Expense					508
P	Craft Benefits, Payroll Burdens & Insurances					1425
Q	Equipment Rental					530
	INDIRECT FIELD COSTS					3612
	TOTAL FIELD COSTS					31186
R	Engineering @ 5%					1559
	Design & Engineering					
	Home Office Costs					
	R & D					
	TOTAL OFFICE COSTS					1559
	TOTAL FIELD & OFFICE COSTS					32745
V	Contingency @ ~15%					4915
W	Fee @ 3%					1130
	TOTAL CONSTRUCTION COST					38790

DATE 8-11-79 REVISION NO. REVISION DATE PAGE NO. 1 of 4

TABLE 5-18 (Continued)

CONSTRUCTION COST ESTIMATE

CLIENT LOE/SENDIA

OCATION BARSTOW, CA

PROJECT SOLAR HYBRID

DESCRIPTION ACCOUNT 5400 RECEIVER SUBSYSTEM TOWER ONLY

CONT. NO.

MADE BY MGG

APPROVED

A/C NO.	ITEM & DESCRIPTION	MAN HOURS	ESTIMATED COST IN $1000s LABOR	SUBCONTRACTS	MATERIALS	TOTALS
	TOWER SUMMARY	(MH)		(S/C)		
A	Excavation & Civil	9000	117	—	—	117
B	Concrete	33300	433	—	449	882
C	Structural Steel S/C MH 12920	35050	466	305	1367	2138
D	Buildings					
E	Machinery & Equipment S/C MH 2600	—	—	275	—	275
F	Piping					
G	Electrical	1100	14	—	11	25
H	Instruments					
J	Painting	1820	24	—	23	47
K	Insulation					
	DIRECT FIELD COSTS	80270	1054	580	1850	3484
	S/C MH 15520					
L	Temporary Construction Facilities					
M	Construction Services, Supplies & Expense					
N	Field Staff, Subsistence & Expense					
P	Craft Benefits, Payroll Burdens & Insurances					
Q	Equipment Rental					
	INDIRECT FIELD COSTS					
	TOTAL FIELD COSTS					
R	Engineering					
	Design & Engineering					
	Home Office Costs					
	R & D					
	TOTAL OFFICE COSTS					
	TOTAL FIELD & OFFICE COSTS					
V	Contingency					
W	Fee					
	TOTAL CONSTRUCTION COST					

DATE 7-18-79 REVISION NO. 1 REVISION DATE 7-27-79 PAGE NO. 2 OF 4

TABLE 5-18 (Continued)

CONSTRUCTION COST ESTIMATE

CLIENT DOE / SANDIA

LOCATION BARSTOW, CAL

PROJECT SOLAR HYBRID

DESCRIPTION ACCOUNT 5400 RECEIVER SUBSYSTEM RECEIVER ONLY

CONT. NO.

MADE BY MGS

APPROVED

A/C NO.	ITEM & DESCRIPTION	MAN HOURS	ESTIMATED COST IN $1000's			
			LABOR	SUBCONTRACTS	MATERIALS	TOTALS
	RECEIVER SUMMARY	(MH)		(S/C)		
A	Excavation & Civil					
B	Concrete					
C	Structural Steel					
D	Buildings					
E	Machinery & Equipment	4000	520	–	20 000	20 520
F	Piping					
G	Electrical					
H	Instruments					
J	Painting					
K	Insulation					
	DIRECT FIELD COSTS	4000	520	–	20 000	20 520
L	Temporary Construction Facilities					
M	Construction Services, Supplies & Expense					
N	Field Staff, Subsistence & Expense					
P	Craft Benefits, Payroll Burdens & Insurances					
Q	Equipment Rental					
	INDIRECT FIELD COSTS					
	TOTAL FIELD COSTS					
R	Engineering					
	Design & Engineering					
	Home Office Costs					
	R & D					
	TOTAL OFFICE COSTS					
	TOTAL FIELD & OFFICE COSTS					
V	Contingency					
W	Fee					
	TOTAL CONSTRUCTION COST					

DATE 8-1-79 REVISION NO. _____ REVISION DATE _____ PAGE NO. 3 OF 4

TABLE 5-18 (Continued)

CONSTRUCTION COST ESTIMATE

CLIENT DOE / SANDIA

DESCRIPTION ACCOUNT 5400 RECEIVER SUBSYSTEM RISER + DOWNCOMER

LOCATION BARSTOW, CA

PROJECT SOLAR HYBRID

CONT. NO.

MADE BY MGG

APPROVED

A/C NO.	ITEM & DESCRIPTION	MAN HOURS	ESTIMATED COST IN $ 1000S			
			LABOR	SUBCONTRACTS	MATERIALS	TOTALS
	R+D SUMMARY	(MH)		(S/C)		
A	Excavation & Civil	90	1	–	–	1
B	Concrete	130	2	–	2	4
C	Structural Steel	690	9	–	41	50
D	Buildings					
E	Machinery & Equipment					
F	Piping S/C MH 240	45890	597	12	2271	2880
G	Electrical	850	11	–	9	20
H	Instruments	1150	15	–	35	50
J	Painting					
K	Insulation S/C MH 3500	–	–	565	–	565
	DIRECT FIELD COSTS	48800	635	577	2358	3570
	S/C MH 3740					
L	Temporary Construction Facilities					
M	Construction Services, Supplies & Expense					
N	Field Staff, Subsistence & Expense					
P	Craft Benefits, Payroll Burdens & Insurances					
Q	Equipment Rental					
	INDIRECT FIELD COSTS					
	TOTAL FIELD COSTS					
R	Engineering					
	Design & Engineering					
	Home Office Costs					
	R & D					
	TOTAL OFFICE COSTS					
	TOTAL FIELD & OFFICE COSTS					
V	Contingency					
W	Fee					
	TOTAL CONSTRUCTION COST					

DATE 8-11-79 REVISION NO. _____ REVISION DATE _____ PAGE NO. 4 OF 4

TABLE 5-18 (Continued)

CONSTRUCTION COST ESTIMATE

CLIENT DOE/SANDIA

LOCATION BARSTOW, CA

PROJECT SOLAR HYBRID

DESCRIPTION ACCOUNT 5500 MASTER CONTROL SUBSYSTEM SUMMARY

CONT. NO.

MADE BY MGS

APPROVED

A/C NO.	ITEM & DESCRIPTION	MAN HOURS	ESTIMATED COST IN $1000s LABOR	SUBCONTRACTS	MATERIALS	TOTALS
5500	SUMMARY	(MH)		(S/C)		
A	Excavation & Civil					
B	Concrete					
C	Structural Steel					
D	Buildings S/C MH	12500	163	873	297	1333
E	Machinery & Equipment 16400					
F	Piping					
G	Electrical	4800	62	—	1874	1936
H	Instruments — INCL W/G					
J	Painting — INCL W/A→F					
K	Insulation — INCL W/A→F					
	DIRECT FIELD COSTS	17300	225	873	2171	3269
	S/C MH 16400					
L	Temporary Construction Facilities					54
M	Construction Services, Supplies & Expense					63
N	Field Staff, Subsistence & Expense					52
P	Craft Benefits, Payroll Burdens & Insurances					145
Q	Equipment Rental					54
	INDIRECT FIELD COSTS					368
	TOTAL FIELD COSTS					3637
R	Engineering @ 5%					182
	Design & Engineering					
	Home Office Costs					
	R & D					
	TOTAL OFFICE COSTS					182
	TOTAL FIELD & OFFICE COSTS					3819
V	Contingency @ ~12%					453
W	Fee @ 3%					128
	TOTAL CONSTRUCTION COST					4400

DATE 8-7-79 REVISION NO. REVISION DATE PAGE NO. 1 OF 1

TABLE 5-18 (Continued)

CONSTRUCTION COST ESTIMATE

CLIENT DOE/SANDIA

LOCATION BARSTOW, CA

PROJECT SOLAR HYBRID

DESCRIPTION ACCOUNT 5600 NON-SOLAR ENERGY SUBSYSTEM

CONT. NO.

MADE BY LDS

APPROVED

A/C NO.	ITEM & DESCRIPTION	MAN HOURS	ESTIMATED COST IN $1000'S			
			LABOR	SUBCONTRACTS	MATERIALS	TOTALS
5600	SUMMARY	(MH)		(S/C)		
A	Excavation & Civil	720	9	—	17	26
B	Concrete	80	1	—	2	3
C	Structural Steel					
D	Buildings					
E	Machinery & Equipment S/C ITE 3640	230	4	300	16	320
F	Piping	7350	96	—	42	138
G	Electrical	230	3	—	7	10
H	Instruments	660	9	—	15	24
J	Painting					
K	Insulation					
	DIRECT FIELD COSTS	9320	122	300	99	521
	S/C ITE 3640					
L	Temporary Construction Facilities					29
M	Construction Services, Supplies & Expense					34
N	Field Staff, Subsistence & Expense					28
P	Craft Benefits, Payroll Burdens & Insurances					79
Q	Equipment Rental					29
	INDIRECT FIELD COSTS					199
	TOTAL FIELD COSTS					720
R	Engineering @ 5%					36
	Design & Engineering					
	Home Office Costs					
	R & D					
	TOTAL OFFICE COSTS					36
	TOTAL FIELD & OFFICE COSTS					756
V	Contingency @ ~10%					79
W	Fee @ 3%					25
	TOTAL CONSTRUCTION COST					850

DATE 7-18-79 REVISION NO. REVISION DATE PAGE NO. 1 OF 1

TABLE 5-18 (Continued)

CONSTRUCTION COST ESTIMATE

CLIENT DOE/SANDIA

OCATION BARSTOW, CA

PROJECT SOLAR HYBRID

DESCRIPTION ACCOUNT 5800 ELECTRIC POWER GENERATING SUBSYSTEM

CONT. NO.

MADE BY MGS

APPROVED

A/C NO.	ITEM & DESCRIPTION	MAN HOURS	ESTIMATED COST IN ~1000s			
			LABOR	SUBCONTRACTS	MATERIALS	TOTALS
5800	SUMMARY	(MH)		(S/C)		
A	Excavation & Civil					
B	Concrete					
C	Structural Steel	79900	1039	–	1240	2279
D	Buildings					
E	Machinery & Equipment	98600	1282	–	23469	24751
F	Piping	89700	1166	–	1480	2646
G	Electrical	46600	606	–	2580	3186
H	Instruments	6900	90	–	330	420
J	Painting – INCL WITH A→D					
K	Insulation – INCL WITH E+F					
	DIRECT FIELD COSTS	321700	4183	–	29099	33282
L	Temporary Construction Facilities					1004
M	Construction Services, Supplies & Expense					1171
N	Field Staff, Subsistence & Expense					962
P	Craft Benefits, Payroll Burdens & Insurances					2615
Q	Equipment Rental					1004
	INDIRECT FIELD COSTS					6839
	TOTAL FIELD COSTS					40121
R	Engineering @ 5%					2006
	Design & Engineering					
	Home Office Costs					
	R & D					
	TOTAL OFFICE COSTS					2006
	TOTAL FIELD & OFFICE COSTS					42127
V	Contingency @ ~12%					5058
W	Fee @ 3%					1415
	TOTAL CONSTRUCTION COST					48600

DATE 8-1-79 REVISION NO. REVISION DATE PAGE NO. 1 OF 1

of the total capital cost. This estimate is based on the following:

- The plant operates an average of 4200 hours per year (48 percent load factor).
- Collector subsystem C&M costs are based on Northrup's analysis of data released by Sandia Laboratories during a workshop held July 25 and 26, 1979.
- The estimates for the receiver are based on foster wheeler's evaluation of receiver operating and maintenance requirements.
- The EPGS and nonsolar energy subsystem O&M costs are based on an analysis of historical information for combined cycle power plants, published by the DOE (Ref. 5-17).
- O&M costs for all other subsystems have been estimated as a percentage of the total construction costs.
- Costs reflect second quarter 1979 pricing levels, and no allowance has been made for future escalation.

5.10.5 Project Schedule

The conceptual schedule for the solar hybrid plant, shown in Figure 5-50, was based on the following:

- Drawings, flowcharts, and equipment lists prepared for the study
- Equipment lead times for turbines and other mechanical equipment as provided by prospective equipment manufacturers and Bechtel's procurement department, including:

  - Steam turbine: 20 months
  - Gas turbine: 15 months
  - Condenser: 14 months
  - HRSG: 14 months

- Licensing, permits, and other lead times from in-house historical data

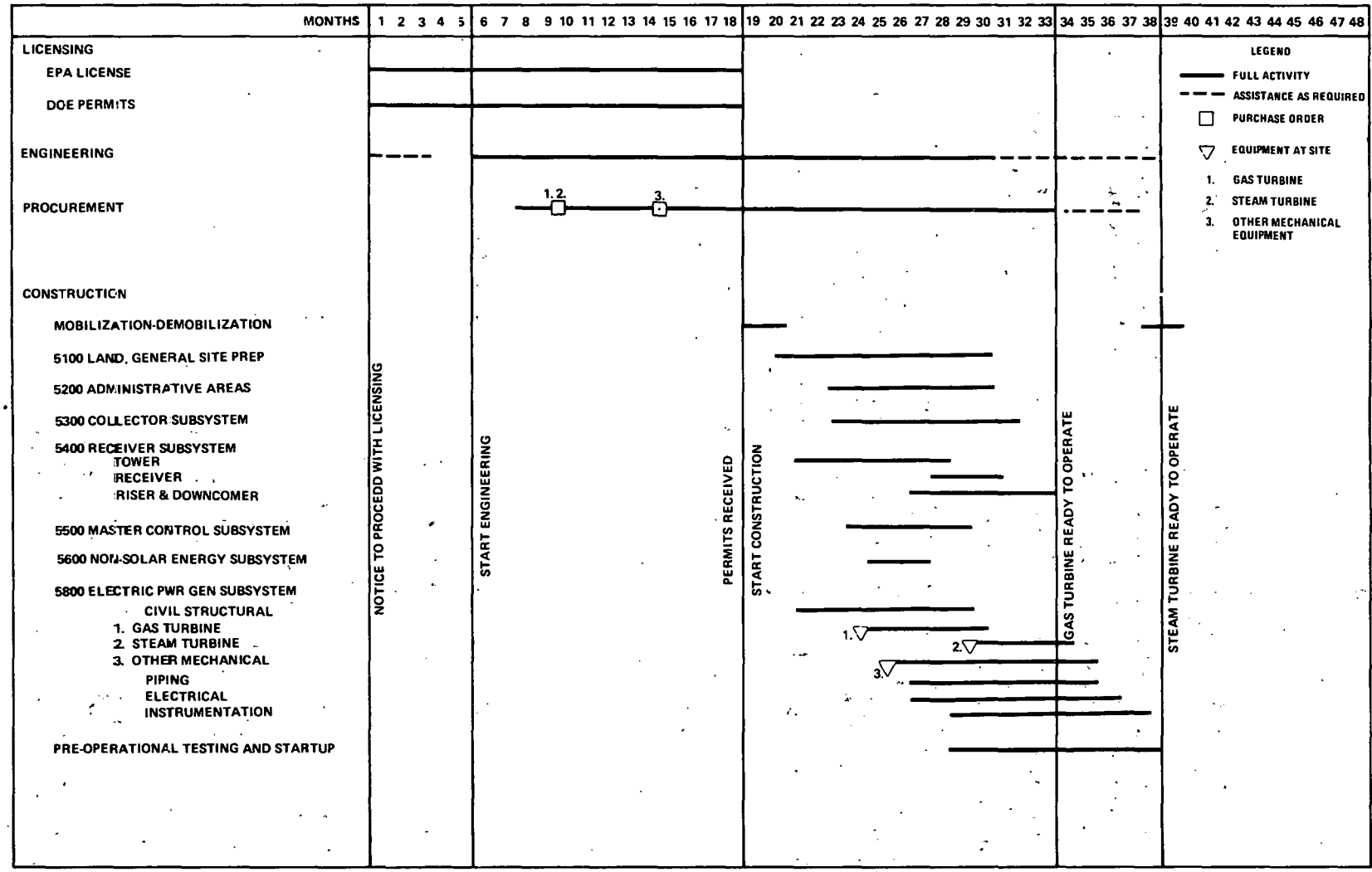

Figure 5-50 SOLAR HYBRID PLANT CONSTRUCTION SCHEDULE

- Construction workweek of 40 hours with an allowance for casual overtime
- Construction activities generally following the pattern of conventional combined cycle plants

The schedules assume availability of materials and permanent plant equipment at present-day lead times, and availability of manual and nonmanual personnel in numbers and skills as required for engineering and construction. It was further assumed that the turbines will be delivered to the jobsite with all internal piping and electrical systems preassembled at the factory.

As evident from the schedule, the total construction time, including demobilization, is 39 months. Initial operation of the gas turbine with partial output can start after 33 months, and full power operation can start after 38 months.

Section 6

ASSESSMENT OF COMMERCIAL-SCALE SOLAR CENTRAL RECEIVER HYBRID POWER SYSTEM

After the hybrid power system conceptual design was completed, the resulting system was evaluated to identify potential future improvements and technological or economic constraints that would hinder or prevent its widespread use in utility applications. The earlier market penetration analysis was also updated in light of the new cost and performance data. This section describes the areas examined and summarizes the salient findings resulting from the assessment. The present study was based on a generic site (Barstow, CA) and generic utility data; so conclusions on items related to a specific site or based on individual utility choices can only be considered as general observations that should be reevaluated in light of specific conditions prevailing at a proposed installation.

6.1 POTENTIAL IMPROVEMENTS

6.1.1 Performance

Collector Subsystem. The most significant and probably most attainable improvement in the current heliostat design is an increase in glass transmissivity and mirror reflectivity. The current baseline design and its performance are based on using a 2.4 mm (0.094 in.) low-iron glass mirror with a reflectivity conservatively estimated to be 0.87. Current projections of improvements to the mirroring process, the availability of a

thin, low-iron float glass, and an understanding of reflectivity changes due to solar aging should lead to mirrors having a reflectivity near 0.92. This 5.4 percent improvement in reflectivity will yield a somewhat greater percentage reduction in total collector field cost, because the poorer performing, long-slant-range heliostats are eliminated when fewer heliostats are required.

A facet overlap concept is being examined to increase the mirror area on a given heliostat. Most current heliostat designs exhibit a mirror "face" that contains clearance spaces between facets, providing clearance zones for gears and drive mechanisms, etc. Since wind loads are based on the envelope area, a gain in mirror area can be achieved by overlapping the facets without impacting design loads and drive hardware. For example, the Northrup II heliostat, currently in the preliminary design stage, has a 53.80 m^2 (579.13 ft^2) envelope area and a 50.54 m^2 (544 ft^2) mirror area. If all of the area could be mirrored, the reflective area per heliostat could be increased by about 6.5 percent and the number of heliostats reduced accordingly. As with improved mirror reflectivity, the cost saving would exceed 6.5 percent with preferential elimination of poorer-performing heliostats.

A mirror module design concept is also under study in which the shape of the mirror facet remains in the concave-to-flat regime for all temperature conditions and never becomes convex (i.e., beam divergent). Many current designs are based on bonded

composites of dissimilar materials. Differential thermal expansion of these materials causes the mirror to bend into a concave or convex shape at environmental temperatures above or below the assembly temperature. The improved concept would exhibit little change with environmental temperature, and never in a manner that would cause a convex shape. The end result would be better beam quality and less energy spilled at the target.

Performance and packing density could be improved by eliminating all heliostats in the "take up" rows between zones of the radially staggered collector layout. Because of the vernier effect, which varies the positioning from "fully behind" to "fully in the gaps," most heliostats in this row have degraded performance compared with those in the basic zones. Badly degraded heliostats were already eliminated in the "H" field layout. If the remainder of take-up-row heliostats were eliminated, the "H" field performance would be enhanced by about 1.5 percent. An example of this practice is evident in the layout of the 8800 heliostat "I" field shown in Figure 6-1.

Receiver Subsystem. The performance of the receiver can be improved by a more complete optimization of the aperture size and configuration. During conceptual design, only the north cavity receiver aperture was optimized for conditions of equinox noon; and to simplify cavity construction, only vertical apertures of square or octagonal shapes were considered. Full aperture

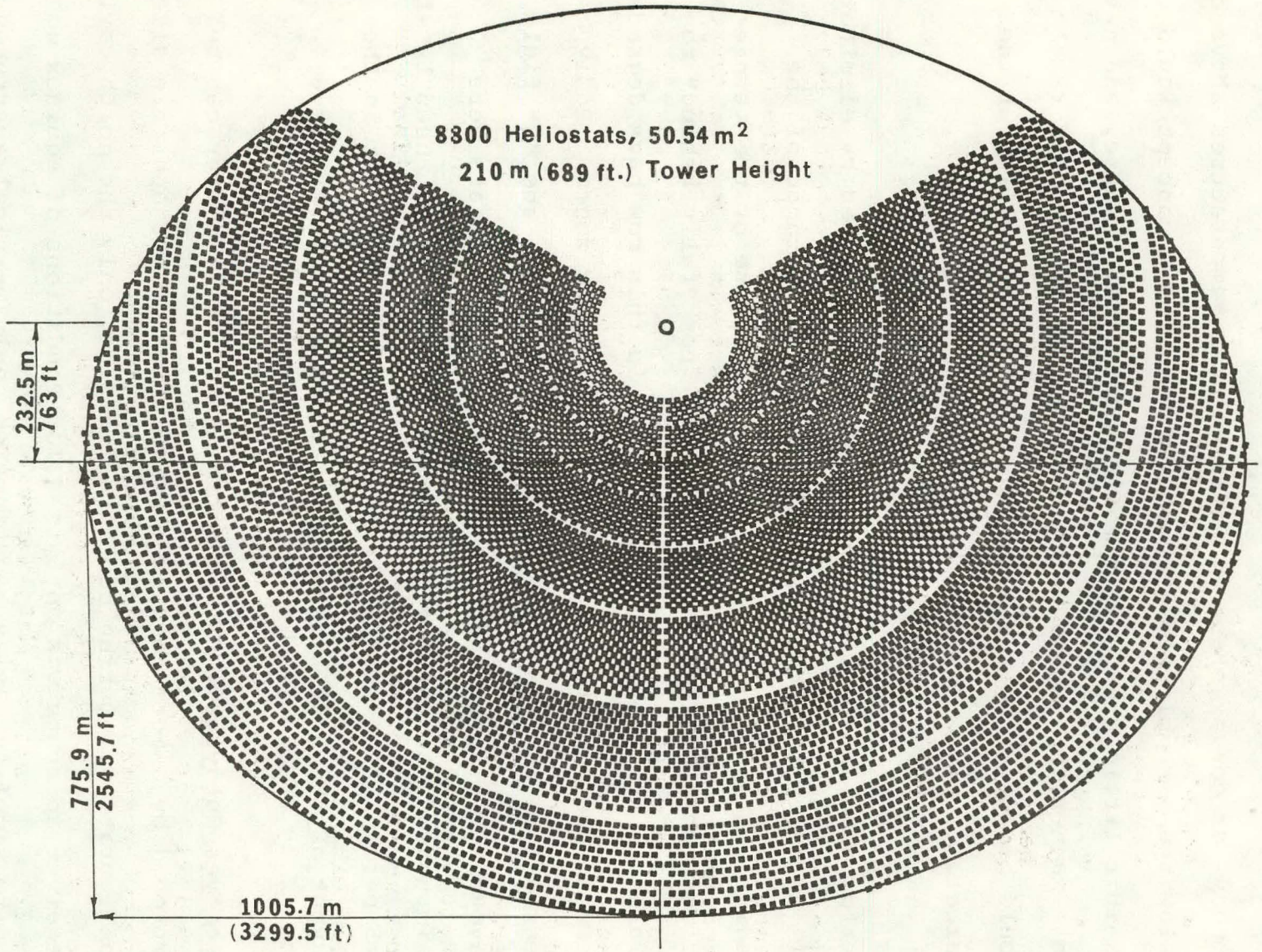

Figure 6-1 "I" FIELD RADIAL STAGGER LAYOUT

optimization should be performed in future studies by considering the following:

- Annual optimization of north, east, and west cavity apertures to maximize the year-round net receiver power
- Evaluation of circular aperture with a potential to collect more energy with lower heat losses than square or octagonal apertures of equal area
- Consideration of nonvertical apertures, which may reduce spillage losses

Conservative assumptions were used to estimate receiver heat losses in the absence of reliable correlations. Accurate determination of convection losses of a cavity-type receiver requires a substantial amount of empirical data on heat and mass transfer. However, at this time, little data are available at the high Grashof and Reynolds numbers at which the receiver will operate. The capability to estimate convection heat losses may improve in the future as a result of cryogenic wind tunnel experiments being performed by the University of Illinois and other experimental and theoretical work being performed or planned by Sandia Laboratories, Livermore.

Reradiation is by far the largest component of the receiver heat losses. Accurate estimate of these losses requires reliable prediction of heat-flux patterns within the cavity, radiation interchange factors (view factors) between the cavity interior surfaces and the aperture, and the direct and reflected energy

incident on each interior surface. A computer program will be required for the complex calculations in such analyses.

Electric Power Generation Subsystem. In the preconceptual design phase, characteristics of the EPGS were studied parametrically to quantify their impact on system costs and performance. The single characteristic found to have the most significant impact on plant performance is gas turbine inlet temperature.

Within limits, higher gas turbine inlet temperatures can improve the energy conversion efficiency and increase the solar fraction. Turbine inlet temperatures selected for the conceptual design reflect the present state of the art for industrial gas turbines. Improvement in cycle performance associated with the increased inlet temperature will require the use of more advanced gas turbine and combustor designs. A measure of potential performance improvements achievable with these modifications can be gained by comparing the 47.7 percent energy conversion efficiency of the 1316C (2400F) Advanced Strawman and the 43.5 percent efficient 1093C (2000F) Strawman cycles of the preconceptual design.

6.1.2 Fossil Fuel Displacement Potential

A major objective of introducing the solar thermal power technology is to displace scarce and depletable energy sources such as natural gas and petroleum derivatives. The hybrid system as described in Section 5 has a design point solar fraction of

.536 and an average solar fraction of .282. This means that, at the reference capacity factor of 48 percent, the annual fossil fuel requirement of the plant is 28 percent lower than for a conventional combined cycle plant.

There are several potential approaches that could increase this fuel displacement potential with some modification to the power system. The following means to increase solar fraction, and thereby the fuel displacement potential, were examined at the conceptual level:

- Energy storage
- Solar multiple and field/receiver power ratio
- Solar/nonsolar interface

Energy Storage. As discussed in Section 3, energy storage is not required for the operation of the hybrid combined cycle power system. In a 1990 time frame and for generic conditions, such a system was found to be economical only with average fuel escalation rates of 13 percent or higher. In view of its potential for increasing the solar fraction, however, energy storage should be considered as a potential future improvement. For this reason the earlier economic analyses were expanded to relate the value analyses to a specific energy storage concept and to the cost and performance of the conceptual design.

The subsystem design for the analyses was developed on the basis of a sensible-heat energy storage concept, similar to the Boeing

concept described in Ref. 6-1. A schematic of the subsystem is shown in Figure 6-2. By appropriate manipulation of valves A through G, indicated in the diagram, the subsystem can be operated through a daily operating cycle which includes charging, holding, and discharging. Utilization of energy storage in a daily operating cycle is shown in Figure 6-3. As seen from this figure, a higher solar fraction results from the stored solar energy and from increased solar contribution in the early morning and late afternoon hours. Subsystem point designs for 1, 2, and 3 hours of daily storage capacity were developed. Characteristics of these designs are shown in Table 6-1. To permit more accurate scaling of the collector subsystem costs, a collector field consisting of 8800 heliostats was also laid out. This field, with a 210 m (689 ft) tower, can provide 3 hours of energy storage at 60 percent turnaround efficiency. (The field layout is shown in Figure 6-1.)

An undesirable characteristic of the sensible-heat energy storage concept, when used in an open Brayton cycle system, is that the air temperature leaving the storage tank declines continuously during the discharge cycle, and progressively more fossil fuel must be used to boost the air temperature to meet the load demand. The energy-displacing benefit of the stored solar heat is highest at the beginning of the discharge cycle and approaches zero at the end. For this reason, the real value of energy storage must be determined in light of utility-specific conditions, particularly the daily load curve. A study of the cost effects of energy storage concludes that a sensible-heat

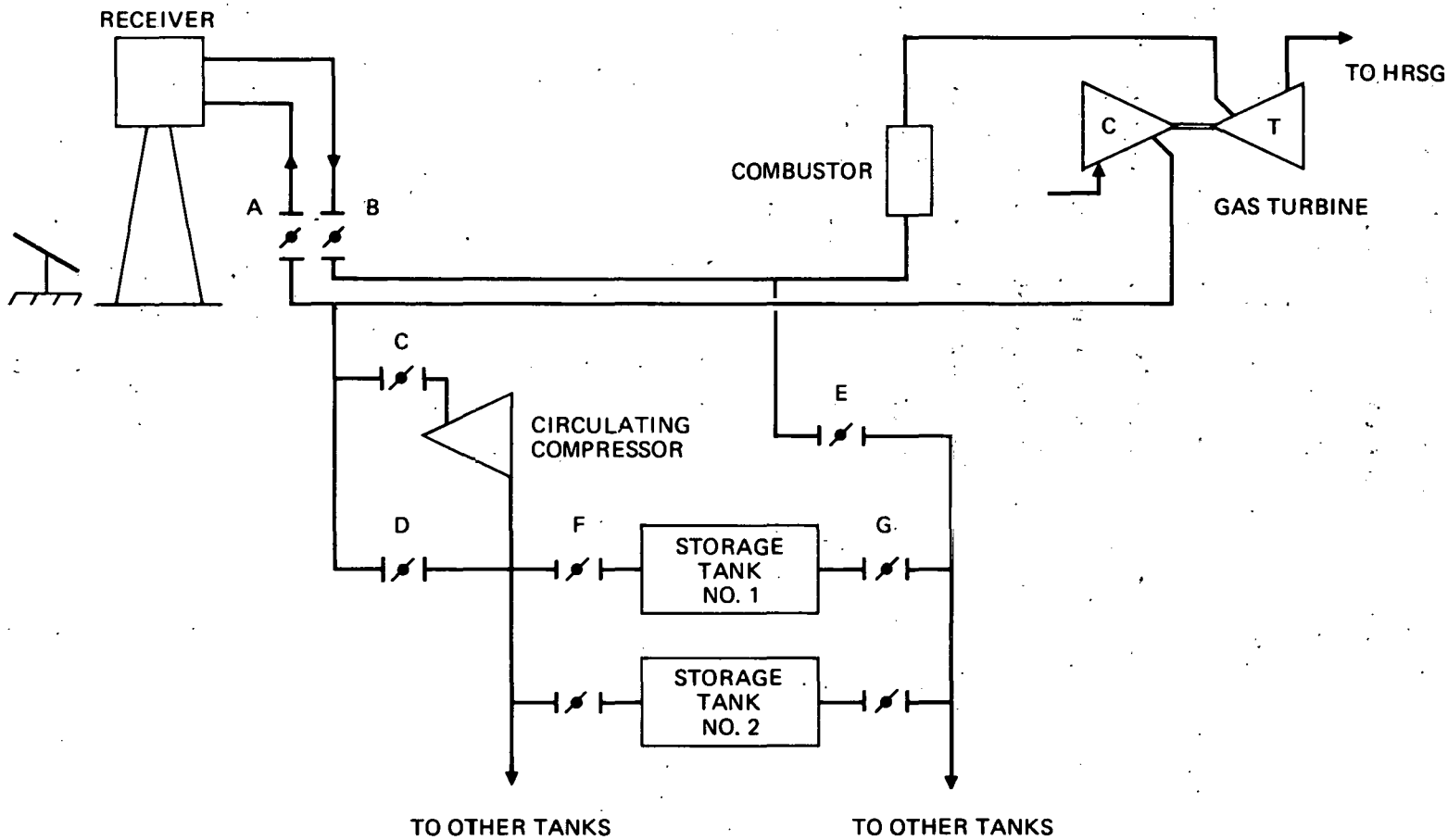

Figure 6-2 ENERGY STORAGE SUBSYSTEM SCHEMATIC

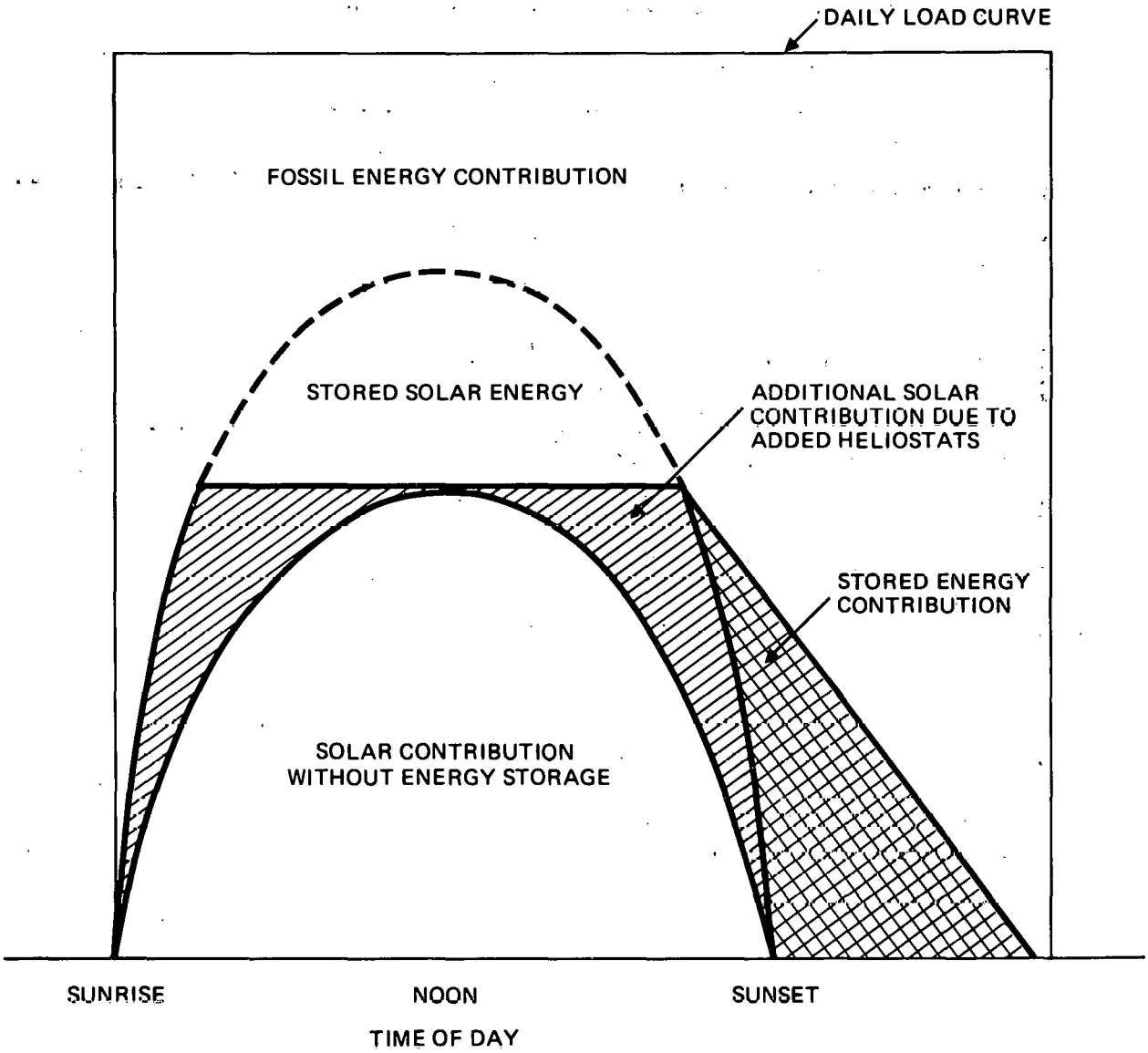

Figure 6-3 INCREASED SOLAR ENERGY CONTRIBUTIONS DUE TO ENERGY STORAGE

TABLE 6-1

CONCEPTUAL DESIGN ENERGY STORAGE SUBSYSTEM SIZING DATA

Data Item	Base System	Hours of Storage		
		1	2	3
Field multiple	1.0	1.315	1.53	1.73
Receiver air flow, kg/s	257.6	338.74	394.13	445.6
lb/s	568.0	746.9	869.1	982.7
Riser pipe ID, m	1.52	1.75	1.88	2.00
in.	60	69	74	79
Downcomer pipe ID, m	1.44	1.66	1.79	1.90
in.	57	65	71	75
Storage system air flow, kg/s	—	81.14	136.53	188.0
lb/s	—	179	301	415
No. of storage tanks		2	3	4
Storage tank dimensions				
Diameter, m	—	6.23	6.23	6.23
in.	—	245.3	245.3	245.3
Length, m	—	30.79	37.38	40.88
ft	—	101.0	122.6	134.1
Weight of alumina, metric tons	—	3175	3855	4215

energy storage subsystem coupled to the conceptual design would not break even unless fuel escalation was between 15 and 16 percent. The cost studies were based on a 70 percent turnaround efficiency and detailed cost estimates of the storage subsystems sized according to the data of Table 6-1.

The indicated fuel escalation rate for energy storage breakeven is significantly higher than the values resulting from the earlier analyses, for the following reasons:

- The new analysis is based on a specific design and cost estimates, whereas the former study only identified the escalation rate at which the first dollar could be economically spent for a storage system.
- Performance and cost of the conceptual design are somewhat worse than those assumed earlier.

Solar Multiple and Field/Receiver Power Ratio. Small increases in the solar multiple, corresponding to field/receiver power ratios greater than one, may be a cost effective way to increase average annual solar fraction and improve the plant performance. In contrast to energy storage, the modification affects only the collector subsystem.

Using the conceptual design as a base, optimal field/receiver power ratios, in terms of minimum busbar costs, were determined for a range of distillate oil escalation rates. In these analyses, the field/receiver power ratio was increased by enlarging the collector field while retaining the conceptual design receiver size. Heliostats are defocused during periods of

peak insolation to keep the receiver outlet temperature below 843C (1550F). Potential benefits, in terms of increased average solar fraction, are schematically illustrated in Figure 6-4. As shown in Figure 6-5, a significant percentage of the energy collected by the excess heliostats can be effectively utilized even at field/receiver power ratios of 1.14. Since the system is designed for peak insolation levels (950 W/m^2), small increases in field/receiver power ratio result in nearly proportional increases in average annual solar fraction.

The economic value of increased field/receiver power ratios was investigated using a modified STCRSIM computer simulation program. The results of these analyses, shown in Figure 6-6, indicate that field/receiver power ratios greater than one are economical with fuel escalation rates as low as 12 percent. With fuel escalation rates of 15 percent, the minimum busbar cost occurs at a field/receiver power ratio of about 1.2. It can be concluded that, depending on the rate of fuel escalation, field/receiver power ratios of greater than one can be a cost effective means to improve solar fraction and, with it, the fuel displacement potential.

Solar/Nonsolar Interface. In the combined cycle hybrid power system, with the receiver and combustor in series, the solar fraction is proportional to the ratio of the receiver temperature rise to the total temperature rise between the compressor outlet and turbine inlet. Therefore, the power cycle could be changed in the following ways to increase the solar fraction:

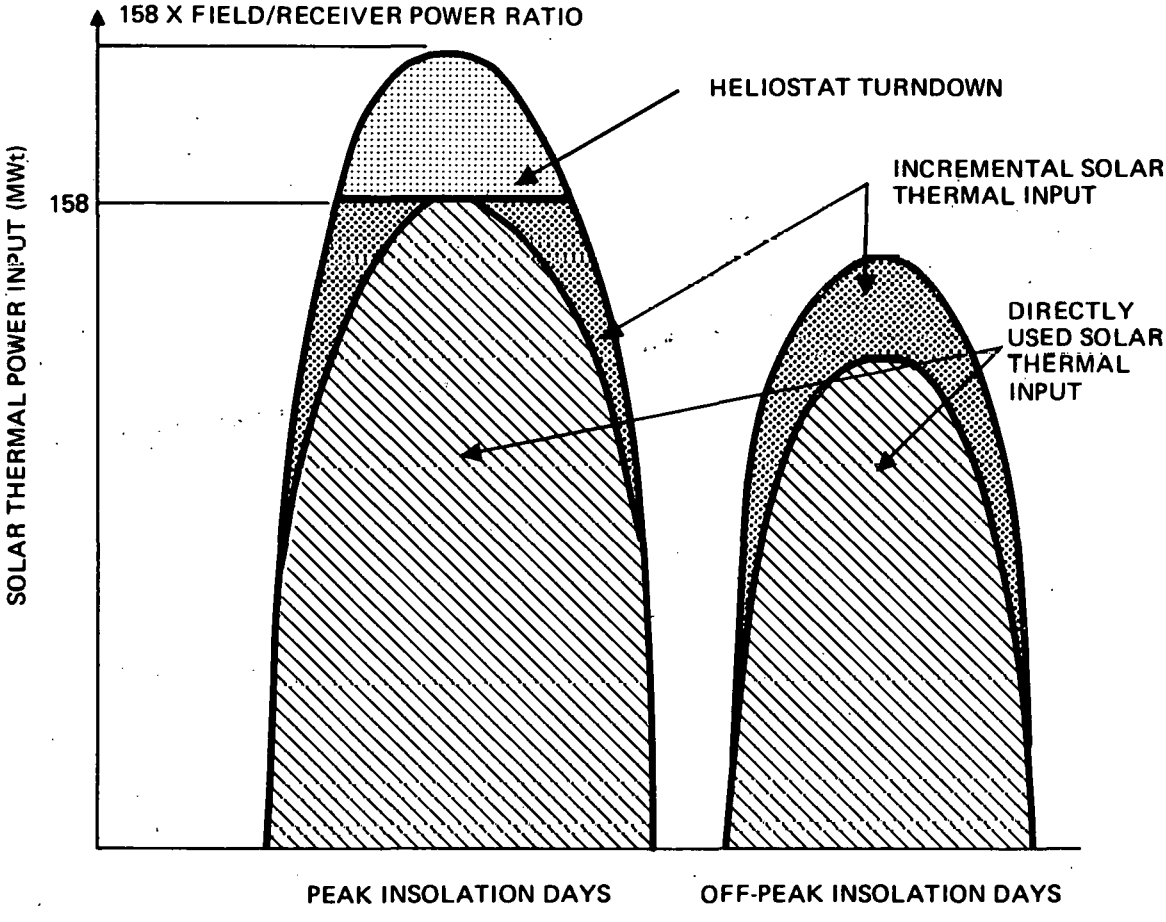

Figure 6-4 POTENTIAL FOR INCREASED SOLAR FRACTION THROUGH INCREASED FIELD/RECEIVER POWER RATIO

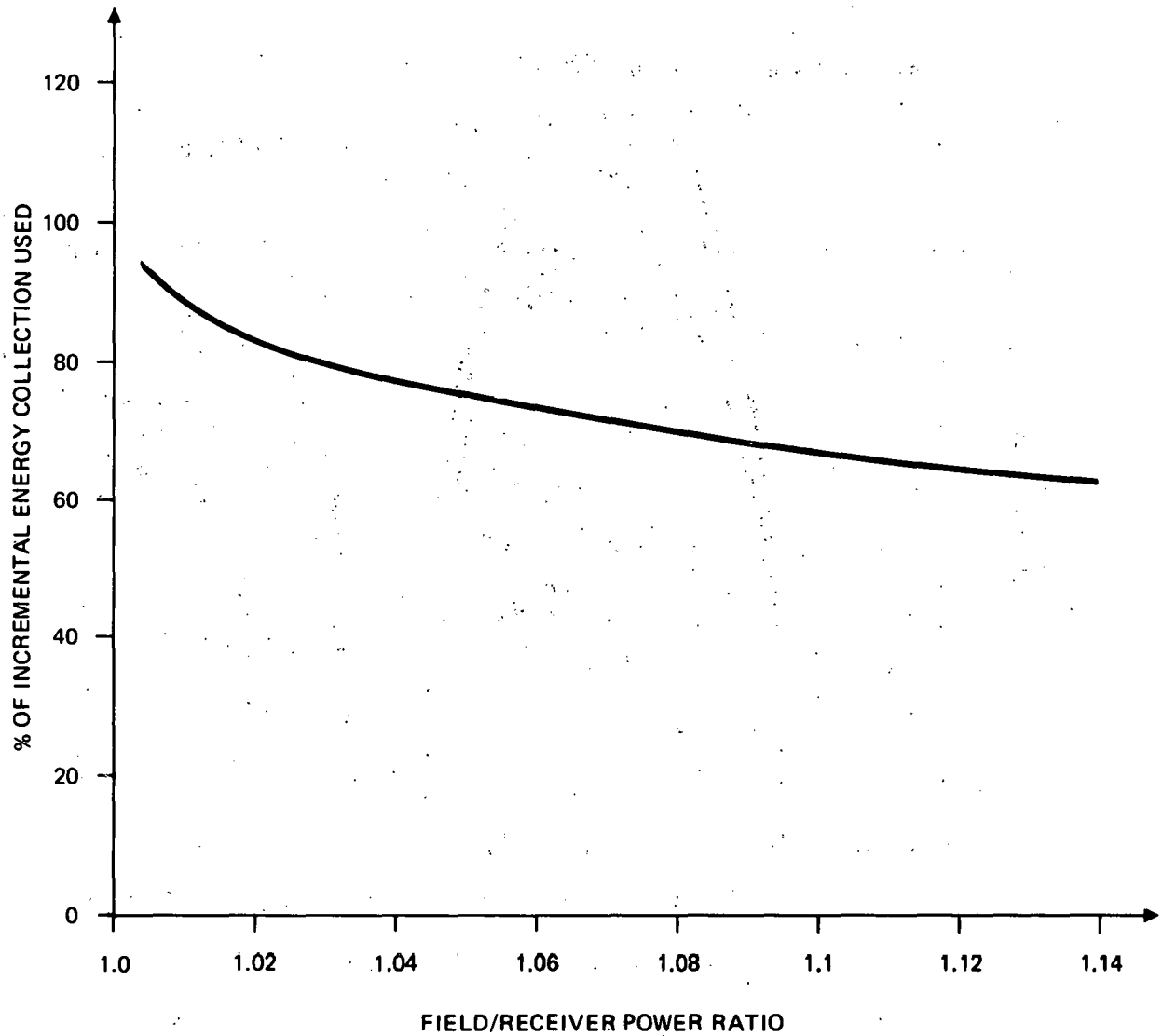

Figure 6-5 PERCENT OF INCREMENTAL ENERGY COLLECTION USED AS FUNCTION OF FIELD/RECEIVER POWER RATIO

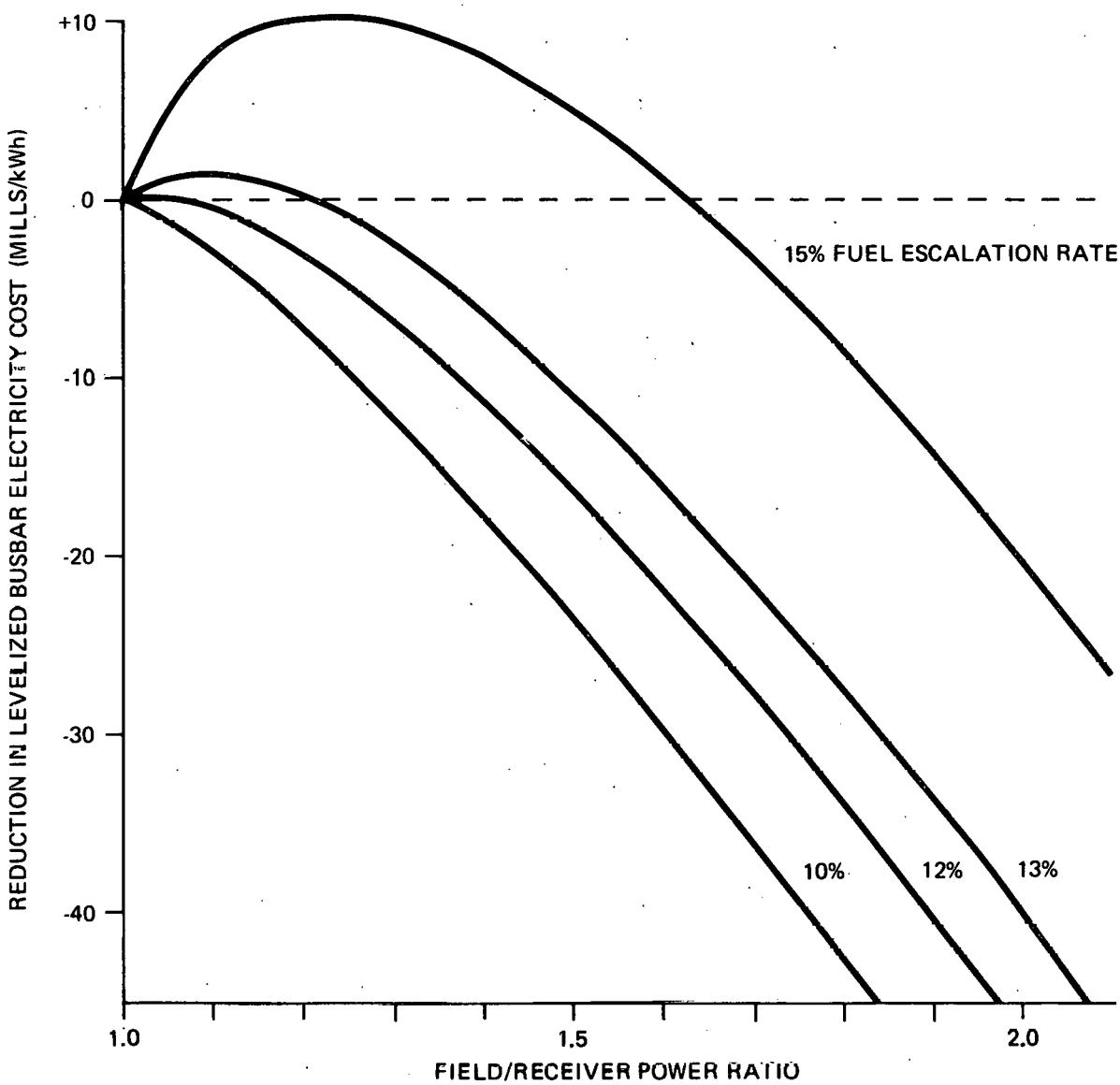

Figure 6-6 REDUCTION IN LEVELIZED COST DUE TO FIELD/RECEIVER POWER RATIOS EXCEEDING 1.0

- Decrease receiver inlet temperature
- Increase receiver outlet temperature
- Decrease turbine inlet temperature

Other design changes also affect the solar fraction, such as steam turbine reheat, which affects the cycle efficiency without affecting these key temperatures.

As discussed in Section 3.6.3, intercooling could reduce the receiver inlet temperature and improve the efficiency of the compression process. However, since the thermal energy extracted by cooling would be at a low temperature and would have to be wasted, net improvement in fuel displacement would only be marginal.

Aftercooling can reduce the receiver inlet temperature and increase the solar fraction. However, since the energy extracted from the compressor discharge would have to be used to heat the intermediate-pressure portion of the steam bottoming cycle, the additional solar energy would have to be valued at the efficiency of the intermediate-pressure portion of the steam cycle. This reduces overall cycle efficiency. For example, if the receiver inlet temperature were to be reduced from 364 to 149C (687 to 300F), the net cycle efficiency would be 40.5 percent (an 8 percent decrease), while the design point solar fraction would become .626 (a 17 percent increase). For an estimated 3 percent fuel savings, the change in total capital cost per kilowatt for this option would be about $390 (a 31 percent increase). Thus

aftercooling is not likely to be an economic way to increase solar fraction.

Another way to decrease the receiver inlet temperature is to lower the compressor pressure ratio. For the range evaluated, the economic optimum with a 12 percent fuel escalation rate was found to be approximately 12:1. For a 15 percent escalation rate, the lowest total cost is at a pressure ratio of 8:1. At this ratio, the receiver inlet temperature would be lowered from 364 to 306C (687 to 574F), the solar fraction would increase to .562 (a 5 percent increase), and the overall cycle efficiency would decrease slightly. As pressure ratios are decreased below 8:1, higher solar fractions and reduced cycle efficiencies result. However, the riser and downcomer pipe sizes would soon reach the limits of practicality.

The second method of increasing the solar fraction, namely, raising the receiver outlet temperatures, is not practical with metallic receivers. However, if a ceramic receiver with a 1093C (2000F) outlet temperature were to be used in conjunction with the conceptual design power cycle, a significant increase in solar fraction would result. Matching the receiver outlet temperature with the turbine inlet temperature would result in a design point solar fraction of 1.0, while the annual average solar fraction would be about .52, representing a major improvement in fuel displacement potential. The average energy conversion efficiency would be higher than that of the conceptual design. The added heliostats and larger capacity receiver would

account for most of the approximately 53 percent increase in the plant capital cost. Based on parametric cost data, the installed cost would be about $1920/kWe. The added capital cost would equal the cost of the fuel saved at escalation rates of 13 to 14 percent. The breakeven escalation rate would be even lower if fuel costs were to be escalated from mid-1979 prices rather than from those of the economic guidelines.

To reach this desirable fuel displacement capability, a reliable ceramic receiver must be developed. In addition, the gas turbine design would have to be upgraded to accept a 1093C (2000F) inlet air temperature or, alternately, the receiver and combustor would have to be operated in parallel in place of the series operation in the conceptual design.

Another way to reduce the air temperature difference between the receiver outlet and the turbine inlet is to lower the turbine inlet temperature to 843C (1550F), which is achievable with a heat pipe receiver. Adequate evaluation of this option would require a reoptimization of the entire system, which is beyond the scope of this study. But the following is indicative of the trend of cost and performance effects.

Assuming that the gas turbine inlet temperature was lowered to 871C (1600F), the design point solar fraction would increase to approximately 0.92, and the overall net cycle efficiency would drop to about 37 percent (a 16 percent decrease). This is a 7.5 percent lower cycle efficiency than would be achievable with a

standard 16.55 MPa/538C/538C (2400 psig/1000F/1000F) steam cycle. The installed cost of such a steam plant is likely to be much lower than that of the combined cycle plant. Therefore, a combined cycle system with significantly lower turbine inlet temperature would probably not be competitive with an equivalent hybrid plant based on the Rankine cycle.

6.1.3 Cost Reduction

Cost optimizations during the parametric and system-level studies and in the subsequent conceptual design resulted in significant capital and operating cost improvements for the hybrid power system. Items of potential cost savings were also identified for future, more detailed analyses. These items are discussed below.

Collector Subsystem. The cost of heliostats represents more than 80 percent of the subsystem costs. A major reduction in the cost of heliostats can be expected as the manufacturing volume approaches mass production levels. However, there is a significant divergence of opinion as to the probable cost benefits of mass production. In Northrup studies, where the heliostat costs were built up from estimates of individual components such as gears and motors, the collector field costs for an annual production rate of 125,000 units were estimated to be \$73.80 per m^2 of reflective area. This is in good agreement with the 80th plant unit cost of \$72 per m^2 projected by Sandia Laboratories, Livermore. Using the Northrup unit cost figures with 87 percent reflectivity, the plant cost would drop to

$1087/kWe compared with the conceptual design value of $1256/kWe. Cost benefits derived from collector improvements would represent additional savings.

Receiver Subsystem. The heat pipe and panel material, Inconel 617, is an expensive alloy. There are surcharges of up to $6.6/kg ($3.0/lb) being currently applied because of the present shortage of cobalt and molybdenum, which account for 17.5 and 9.0 percent of the weight, respectively. The receiver cost could be significantly reduced by using Inconel 617 only in the high-temperature portions of the panels and a less expensive material in the lower-temperature portions. If the surcharges persist or are even further increased, the selection of the receiver outlet temperature should be reevaluated. Reducing the receiver outlet temperature by about 29C (50F), would allow the replacement of Inconel 617 with less expensive materials, such as Inconel 610 or Incoloy 800H. An additional incentive to replace Inconel 617 as much as possible, is that about 98 percent of cobalt and 55 percent of molybdenum consumed in the U.S. are imported.

The semicircular shape of the receiver cavity rear wall was originally conceived to accommodate the removable panel concept and the reinforcement required between panels. Since in the conceptual design receiver the panels are welded together, there is no longer need for the side wall reinforcements. Therefore, it might be cost effective to substitute a less expensive flat rear wall for the presently used curved configurations. As with

the collector subsystem, cost benefit accrued from potential performance improvements would add to the above cost savings.

EPGS. The HRSG and turbine costs were furnished by the manufacturers as budgetary estimates. Competitive bid prices for actual orders may vary from these costs. However, the magnitude and direction of this variation will depend on the competitive environment at the time of such orders. Incorporation of catalyltic combustors is not expected to cause major cost variations.

6.1.4 Economies of Scale

Experience with conventional power plants indicates that increasing the capacity ratings of a unit within practical limits improves performance and yields a lower capital cost per unit of installed capacity ($/kWe). The solar hybrid power system was reviewed to determine if this observation is valid for that system as well. The assessment, conducted by subsystem, is summarized in this section.

Collector Subsystem. The average geometric efficiency of the collector field declines as heliostats are added to increase the amount of solar energy collected. Atmospheric attenuation is a function of the slant range, so the attenuation efficiency declines as the slant range increases with larger fields. The average packing density also becomes lower as the number of heliostats increases, because of the larger spacing required for

the peripheral heliostats. The impact of these factors is that the reflective area per unit of energy collected increases and the field packing density decreases as the plant rating increases. As a consequence, the collector field scaling exponent is expected to range from 1.05 to 1.1.

Receiver Subsystem. Assuming that the three-cavity receiver configuration is retained, the rear wall (panel face) area must be increased in direct proportion to the additional solar energy collected, and the focal-plane-to-rear-wall distance must be adjusted to maintain the same peak flow for each heat pipe. Thus the overall cavity dimensions will be larger. As a current best estimate, the receiver weight and cost are directly proportional to the increase in collected energy.

The receiver tower height varies in direct proportion to changes in the collector field radius (assuming identical rim angles). Due to the increased receiver and piping weight, the entire tower must also be made stronger. The receiver air flow is directly proportional to the system power rating. The pipe length also changes with the tower height. The riser and downcomer flow cross section, therefore, must be increased to maintain an acceptable pressure drop. Considering the relative costs of the receiver, tower, and piping, the scaling exponent of the receiver subsystem ranges from 0.7 to 0.9.

EPGS. According to common estimating practice, the scaling exponent for turbine generators and HRSG ranges from of 0.7 to 0.8.

Balance of Plant. The cost of the master control subsystem and plant support represents a small fraction of the plant cost and in the scaling analyses it was assumed to vary linearly with the power rating.

Overall Power System. Curves representing the variation of installed cost with plant capacity are shown in Figure 6-7. It is evident from the figure that the economies of scale favor large solar hybrid plants. But the rate of capital cost improvement with increased size decreases markedly with large multiples of the conceptual design power rating. It is also expected that plant performance will improve with increased power rating, since efficiencies of turbine generators and HRSG improve with larger sizes. There is also a step improvement in power cycle efficiency as the steam bottoming cycle output reaches 75 MWe (total plant capacity of 230 MWe) where reheat turbines become available.

Since the maximum rating of industrial gas turbines is about 100 MWe, two or more units would be required in larger plants. Depending on the specific plant requirements, each turbine could have a dedicated HRSG or several turbines could be connected to a single HRSG. Because a wide range of steam turbine sizes are available, a single turbine per plant would be used.

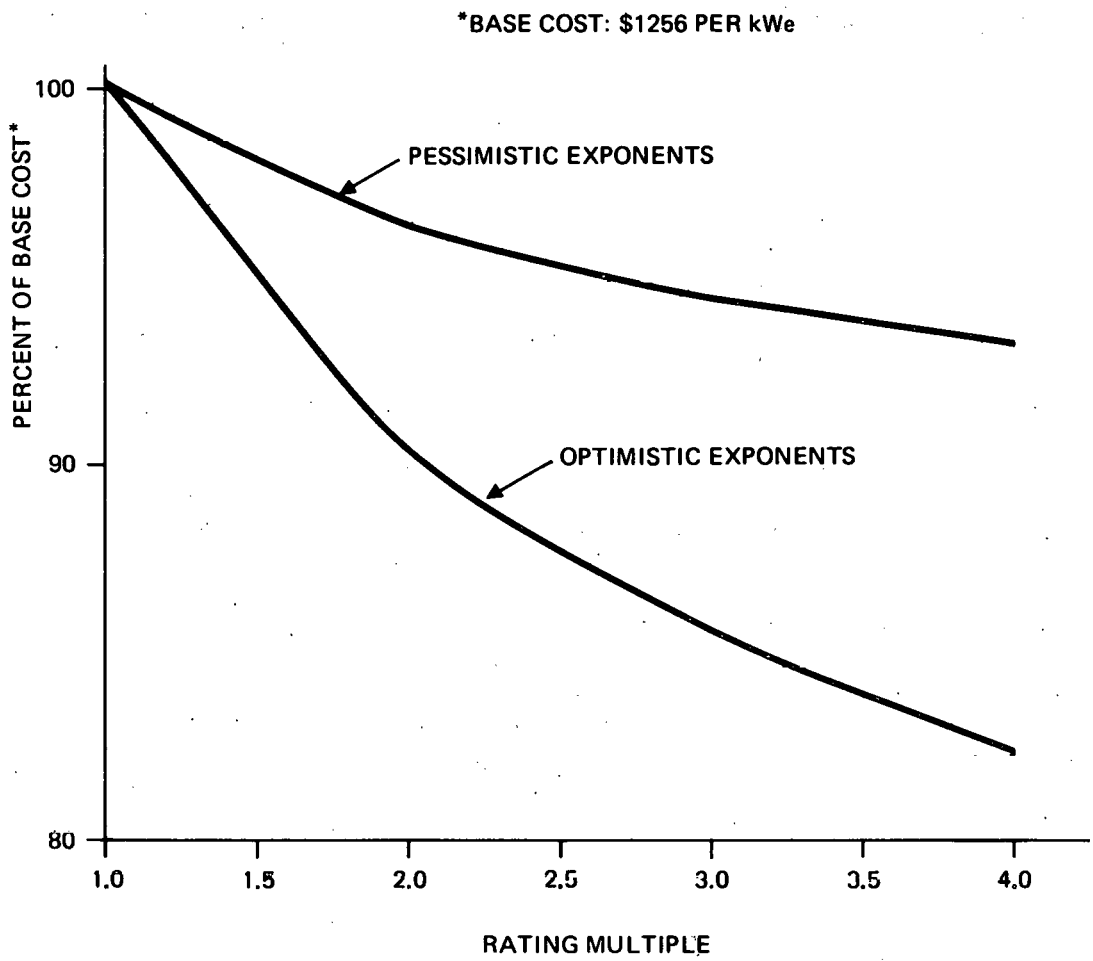

Figure 6-7 CAPITAL COST EFFECTS OF ECONOMIES OF SCALE

It is reasonable to conclude that economies of scale can be used to reduce busbar cost of electricity from hybrid plants. The potential cost reduction, however, is relatively modest. In addition, the economies of scale are no longer effective where the plant becomes large enough to require more than one collector field and receiver. In the absence of other constraining factors, such as utility need or land availability, the optimum plant size is expected to range from 300 to 400 MWe.

6.2 POTENTIAL LIMITATIONS

In this section potential limitations to implementing the commercial-scale solar hybrid power system are discussed. Issues addressed include environmental effects, land use, natural resources, state of materials technology, commercial availability of power conversion equipment, manufacturing and marketing capacity constraints, institutional constraints, and safety. Some of these issues are site-specific. Only a generalized assessment can be given at this time, since the study was based on a generic site.

6.2.1 Environmental Effects

The physical aspects of the environment considered in evaluating the impact of a solar hybrid system include topography, soils, hydrology and surface water management, local drainage patterns, surface and ground water quality, air pollution, and ambient noise.

Construction of the plant will require surface grading of approximtely 350 acres. If the surface of the selected site is relatively flat, large-scale changes in the topographic features will not be necessary. Construction will also cause some alteration of the soils on the site. Heliostats will shade the soil to varying degrees, which will alter cycles of natural soil heating and cooling and will affect air circulation at or near the soil surface. Access roads, constructed with road oil and gravel or asphalt, will alter drainage patterns and eliminate these areas as biological substrate.

The modifications to natural topography will alter the runoff pattern for the site. When local precipitation rates exceed the permeability of the surface soils, new runoff channels will develop to reflect the change in surface configuration. In certain areas of the collector field, rainfall runoff may be concentrated into high-volume, high-velocity flows, which could erode the site.

If the plant is in a groundwater recharge area, recharge of the aquifer system on the site could be altered. Infiltration depends on chemical and physical soil characteristics, which vary greatly from site to site. The alteration in surface runoff patterns on the site would probably channel surface runoff downslope and may limit infiltration onsite. There are economical mitigating measures that can be applied to minimize or eliminate any adverse ecological effects.

Construction and operation of the hybrid plant is not expected to have a direct impact on water quality. But since localized erosion may occur during periods of peak snowmelt, increased turbidity in nearby streams and ponds may result. Soil stabilization measures can reduce erosion and turbidity problems. These measures depend largely on the facility location and topography.

Mirror washing with solvents or detergents could contaminate the soil, but by judiciously selecting the chemicals used this will not significantly impair surface water resources. If large volumes of water are required for washing, groundwater resources may be impaired. Since groundwater resources at a particular site may vary from drinking water quality to unusable saline or brackish water, "impairment" must be related to specific site conditions. It is assumed that wastewater from heliostat washing operations can be collected and recycled. Other waste streams will have to be treated prior to release.

Solar hybrid plants have a smaller condenser cooling load than fossil or nuclear plants of equal capacity. Makeup water requirements to the cooling tower will be correspondingly lower. Cooling tower and HRSG blowdown can be evaporated, resulting in a zero discharge plant.

During construction there will be some temporary increase in the site noise level. The ambient noise levels will be high near the gas turbine during operation. The compressor air intake will

require a filter silencer. There are well established noise abatement procedures used in conventional combined cycle systems, which may be employed to reduce this nuisance if the plants are located near populated areas.

During construction, the site work is expected to generate some temporary airborne dust. Operation of the gas turbine cycle will result in atmospheric discharge of combustion products. Environmental Protection Agency or local air quality control regulations limit these emissions, and the plant will have to meet the applicable regulations. It is expected that control of nitrous oxide emissions will require mitigating measures, such as catalytic combustors, to stay within discharge limits applicable in the 1990s. In comparison with conventional plants of equal rating, the hybrid plant would cause about 30 percent less emission.

Clearing a site of standing vegetation also involves eliminating animals and insects. Larger predators like the fox and coyote are expected to migrate to other locations. Smaller animals, such as rodents, various reptiles, and some of the typical desert-dwelling amphibians, will be only temporarily displaced, but will be able to reestablish on the site after construction activity ends. Resident birds at the site would be displaced during construction, but would probably not be affected outside the perimeter of the heliostat field. Birds flying into the focal zone during the day would probably not survive. At night, the local birds may mistake the collector field for water and

crash into the heliostats. Field surveys will have to be conducted to determine the site-specific impact on plants and animals.

Some operating and construction personnel will probably be drawn from the area the facility serves. Other workers will come into the area and will affect housing and other community services. This impact will be minor due to the comparatively small labor force required. The regional economy would benefit from the consumption of local goods and services by workers. Long-term benefits to the local economy are employment at the facility and the secondary demands for goods and services generated by the workers. Employment levels during operation are estimated at 30 people.

In summary, the environmental impact of the solar/hybrid plant is similar in nature to other solar power plants and is minimal when compared to other less efficient power generating systems. Major advantages of the solar/hybrid plant over conventional plants include the displacement of fossil fuels with solar energy, reduced combustion emissions, smaller condenser cooling load with a related reduction of the cooling tower plume, and reduced makeup water requirements.

6.2.2 Land Use Constraints

Land use constraints vary from site to site and their impact must be evaluated in the context of each specific site. Most of the

more common constraints are similar in nature to those of other solar power plants.

Land requirement for the conceptual design solar hybrid facility is approximately 350 acres, less than half of what is needed for stand-alone solar thermal power plants of comparable rating. The ideal site topography is generally level or, at most, gently sloping. Its characteristics include a maximum height of 2 feet between the bottom and top of soil swells, with a wave length of at least 100 feet, and a 0 to 10 degree maximum inclination running downhill in a north to south direction.

Soil conditions influence the foundation design and costs. The soil must have sufficient load-bearing capacity for the receiver. Seismic characteristics will affect the tower and receiver design. The type and quantity of vegetation will affect the site clearing cost and may also be a continuing maintenance requirement in view of the potential fire hazard.

Site selection for solar plants must also consider conditions such as the potential for prolonged cloud cover, and shadowing by forests, bluffs, hills, or buildings which would reduce the number of hours of operation for the facility. Strong wind forces and snows loads add to the cost of structures.

Convenient tie-in to a nearby utility grid is desirable. Water is required for cooling and mirror washing operation and for potable services. If a water supply is not available from the

local water district, the plant must be located near an aquifer of sufficient flow capacity, and the water from wells must be purified. The selected site should be near adequate transportation routes to facilitate shipment of equipment and supplies.

Zoning regulations are not expected to have a substantial effect since the probable sites will be away from population centers. However, the plants should be located away from airports and their landing and takeoff patterns to avoid interference with air traffic and potential hazards of blinding light from straying heliostats. Also, any nearby industrial or farming operation, generating large amounts of airborne dust, would be undesirable for the hybrid plant.

Candidate sites must be investigated for historical significance, due to increased public awareness of this issue. Acceptance by the local community will influence the ease with which the necessary permits can be obtained. And their acceptance will be affected in part by identification and mitigation of any adverse environmental impacts.

6.2.3 Natural Resources Constraints

Depletable or domestically scarce material resources used in construction and operation of hybrid plants include water, distillate oil, and such alloying elements as cobalt and molybdenum.

Water is used as working fluid in the steam cycle, for condenser cooling, heliostat washing and shop and domestic consumption. The estimated total water usage in the plant is 1350 gpm. The largest water use is for condenser cooling. The expected rate of water usage is comparable to that of conventional combined cycle power plants, but is only about a third of the usage rate in conventional steam electric plants. If water of sufficient quantity cannot be obtained at an otherwise desirable site, the water requirement could be significantly reduced by using dry cooling towers. With these, however, the plant performance would be lower during the warm season. This performance penalty would not be as severe with the combined cycle plants, since only the steam cycle portion would be affected.

Distillate oil (No. 2 fuel oil) was selected as the reference fuel for the hybrid plant. This fuel was found to be the most economical and offered a number of advantages in storage and handling as well. Petroleum distillates fall under the jurisdiction of the National Energy Act of 1978, which became law while the project was in progress. Regulations implementing this law are now in the draft stage. According to current draft regulations, oil-fired plants may be licensed under a simplified procedure if they use at least 25 percent nondepletable (e.g., solar) energy. Since at a 48 percent load factor, the hybrid plant uses better than 28 percent solar energy, it can qualify for these simplified procedures.

It was estimated that the conceptual design hybrid plant would displace about 17,000 barrels of fuel oil annually. There are several options to increase the solar fraction and improve the fuel displacement potential, as discussed in Section 6.1.1. Furthermore, the cost penalty associated with using coal-derived alternative fuels ranges from 1 to 2.5 percent of the equivalent capital cost. With such a small cost penalty the plant economics would not be severely affected if it were converted, in the future, to coal-derived fuels or methanol, once these become available in sufficient quantity.

Approximately 400 metric tons of Inconel 617 is required to build the heat pipe receiver. This material contains 17.5 percent cobalt and 9 percent molybdenum as alloying elements. About 98 percent of the cobalt and 55 percent of the molybdenum used in the U.S. is imported, mainly from Africa. Due to limited production capacity and uncertainties at the source, surcharges up to $6.6/kg ($3.0/lb) are currently charged on Inconel 617 orders. There are several other nickel alloys (such as Inconel 601 and Incoloy 800) with somewhat poorer high-temperature strength properties, which do not contain either of the scarce alloying elements. As described in Section 6.2.1, cost reductions, as well as less dependence on imported materials, would be attained by substituting one of these alloys, in part or completely, for Inconel 617.

6.2.4 Status of Materials Technology

Most of the materials used in the solar hybrid power system are commercially available. However, certain high-temperature, high-strength materials will require testing to verify their suitability for application in the proposed design.

Collector Subsystem. All materials and processes used in the heliostats are within present state of the art and, generally, are commercially available stock items. The mirror module design, materials, and bonding process are virtually identical to those presently used on the Northrup I heliostats, which have been built and are currently undergoing testing. While the electronic collector field control and computer software is unique to the heliostat requirements, the subcomponents are again commercially available stock items.

In summary, no unique or advanced-technology materials or processes are required for the collector subsystem.

Receiver Subsystem. Although Inconel 617 is a commercially available alloy, it has not yet been approved by the ASME Boiler and Pressure Vessel Code, and is not covered by other existing codes. Its mechanical properties are not yet well documented at high temperatures. Development of the necessary data for code application and the process of code approval, however, can be accomplished in time to permit use of this material in solar hybrid plants with startup in 1990.

The heat pipes are the most critical components of the receiver. They must operate at high temperature, with large thermal gradients, under severe cycling conditions. Because of the importance of this concept to the success of the receiver, laboratory tests simulating solar receiver operation must be carried out to support the final conceptual design.

Combustor. The proposed design uses a catalytic combustor concept being developed by Westinghouse and several other companies. It employs a ceramic honeycomb of large surface area on which a catalyst is deposited. The materials of construction being tested for this service are currently available. The remaining technical issues pertain to the development of ceramic structures capable of withstanding the thermal cycles and vibrations, and to the service life of the catalyst.

Other Components. All other components use current materials technology, are commercially available, and require no developmental work.

6.2.5 Power Conversion Equipment Availability

Gas Turbine. The gas turbine unit is similar to Westinghouse's current production model W-501, modified as described in Section 5. The modifications in the compressor discharge and turbine inlet areas to permit series connection of the receiver are similar to those required for closed-cycle or regenerative gas turbine and, therefore, are considered current technology.

Combustor development work, supported by several organizations, is under way to reduce NO_x emissions to levels required by late-1980 air quality standards for stationary combined cycles and aircraft engine applications. It is expected that this effort will result in commercial availability of the desired technology by 1990, when the solar hybrid system is proposed to start operation.

Other Equipment. All other power conversion equipment, including HRSG and steam turbine, is commercially available and presents no restrictions to widespread application of the proposed solar hybrid system.

6.2.6 Manufacturing and Market Capacity Constraints

Manufacturing techniques required to fabricate and install conventional equipment of the hybrid plant are not significantly different from those required for conventional combined cycle power plants. An adequate manufacturing capacity and a competitive market for this equipment are in place. Constraints for the solar components are related to the need to establish a manufacturing industry of sufficient production capacity located close to the Pacific Southern and South Mountain regions, where the bulk of the central receiver solar power plants will probably be installed. For this to occur, potential suppliers must be guaranteed a sufficient market for their product, and a reasonable rate of return on investments in new production facilities must be assured. Low production rates expected in the

beginning years will result in higher unit costs, and government incentives may be necessary to defray costs related to establishing a new industry.

Collector Subsystem. A manufacturing plant to produce heliostats for the hybrid power plant would probably be sized for an annual production of 25,000 to 50,000 units. At this level of output, a facility designed exclusively to manufacture heliostats can be built and operated efficiently. Because the area is the prime market site for solar hybrid plants, the manufacturing site should be centrally situated in the Southwestern United States so that shipping distances can be minimized. Even if highly automated, a plant of this capacity would probably require about 800 employees.

Locating heliostat manufacturing facilities in the Southwest would have a disadvantage, however, since the manufacturing facility will be material-intensive (using upwards of 100,000 tons of raw materials annually). The market source for steel, glass, gears, bearings, and other high-weight/bulk materials is generally in the Midwest or in the Eastern US, and intermittent spot-shipping problems could develop. It is not anticipated, however, that supplier production capacities for glass, motors, electronic assemblies, machined parts, and steel structural stock will be a problem, provided that there is an adequate lead-time for first shipment and that a normal production flow of 500 to 1000 units per week can be maintained.

Receiver Subsystem. Materials used in the receiver are available in the quantities required, except for Inconel 617. The current production capacity of Inconel 617 is probably too small to meet the required demand. However, increased production of Inconel 617 is being planned. Projected plant expansion is also expected to alleviate the current cobalt and molybdenum shortage by 1985. Nevertheless, these alloying elements will still have to be imported.

The receiver can be manufactured using standard practices. Heat pipes of the type and size used in the receiver have never been manufactured in large quantities. But capacity could be expanded to adequately meet the demand by using existing metal fabrication facilities for the conventional manufacturing steps and expanding the final assembly facility.

6.2.7 Legal, Regulatory, Fiscal, and Institutional Constraints

Legal and Regulatory Constraints. Government constraints can come from the federal, state, and local levels. State and local regulations are often more restrictive than federal regulations. Table 6-2 summarizes potential legal and regulatory constraints applicable to the solar hybrid plant. Local and regional regulations shown are typical for the Barstow site.

As shown in Table 6-2, the list of potential regulators is considerable. Time and cost of licensing could represent a major constraint to the introduction and widespread use of solar hybrid

TABLE 6-2

POTENTIAL LEGAL AND REGULATORY CONSTRAINTS

Government Agency	Jurisdiction	Constraint on Plant
Federal		
Environmental Protection Agency	Air quality Water quality Noise	EIS review. Wastewater treatment. Noise at plant boundary.
OSHA	Health and safety	Noise, light, and general working conditions in and around plant.
Bureau of Land Management	BLM lands	Management plans and right-of-way permits.
Federal Power Commission	Power generation	Approval for electric power generation.
FAA	Airspace	Permit for towers over 200 feet.
State		
Public Utilities Commission	Utilities	Power plant certification. Public convenience certification.
Energy Commission	State energy development	Notice of intent. Power plant certification.
Solid Waste Management Board	Solid waste	Permit for waste disposal.
Department of Water Resources	State waters	Permit to appropriate water.
Lands Commission	State lands	Permit or lease for state lands and right-of-way.
Department of Architecture and Construction	Occupied structures	Certification of buildings for handicapped person access (applicable if structure receives state funds).
Local and Regional		
Air Quality Management Board	Air quality	New source performance review. Prevention of significant deterioration permit to construct and offset.
Regional Water Quality Control Board	Water quality	National pollution discharge elimination system. Water certification.
County	Licensing Zoning Compliance	Rezoning and use permits. Environmental impact report.
County and City		Right-of-way. Building permit.
Los Angeles Metropolitan Water District or County Flood Control and Water Conservation District	Water use	Water allocation.

technology. A simplified procedure, preferably "one step licensing", needs to be established early. Ease of licensing could become a significant incentive to promote favorable utility consideration of solar technologies.

Fiscal Constraints. Introduction of the solar hybrid technology into commercial utility application hinges on the resolution of two major fiscal constraints, namely, the cost of development and the alleviation of economic risks associated with this emerging technology.

For the moment, a major share of the solar development costs is borne mainly by the Department of Energy, although some private heliostat development is in progress and industry is carrying some of the cost of developing low emission combustors. In addition to the development of low-cost heliostats (a generic need for all central receiver solar power systems), the combined cycle hybrid plant also requires development of receivers for high-temperature service and combustors that can limit the formation of thermal NO_x. Solution of the low-emission combustor issue is a generic one, common to gas turbine applications, and expected to benefit the hybrid plant as well. Thus, the only major development need specific to this hybrid system is the high-temperature receiver. It is expected that, as a minimum, a critical system-level experimental power system will also have to be built and operated before commercialization can be successfully launched.

Establishing an overall development plan and timely funding of work needed to achieve the planned milestones are required to assure that the combined cycle hybrid plant will be available for commercialization in the 1990s.

From the point of view of utility economics, the hybrid power system represents a departure from many conventional technologies which require lower initial investment but continuing high fuel costs. New technologies, such as solar, typically require high initial capital expenditures but have little or no fuel charges. The capital cost of the hybrid plant is lower than that of stand-alone solar plants by virtue of its smaller solar component. Conversely, fuel costs to compensate for the lower solar contribution must be considered in the busbar cost of electricity.

Successful introduction of new technologies into the utility market usually requires some form of risk and cost sharing or credible demonstration of their technical and economic viabilities. Considering the urgent need to displace scarce and imported fuel, the extended time required for the latter is undesirable. Risk- and cost-sharing appear more likely to encourage utility interest, as confirmed by utility comments (Section 6.3). In this respect, the combined cycle hybrid plant is in an advantageous position, since the EPGS is essentially a conventional plant, capable of full power operation. As such, power generation with fossil fuel can be maintained even if the

solar portion of the plant failed for some reason. Thus, the technical risk is minimized.

Institutional Constraints. A review of institutional constraints included the examination of public and utility acceptance, industrial interest, availability of codes and standards, and availability of trained engineering and operating personnel to support introduction of the solar hybrid technology.

The use of solar energy is strongly endorsed by various environmental groups and elected government officials. For the time being, media coverage is largely favorable. General public acceptance is also good. However, expectations in terms of timing, cost, and degree of implementation are often unrealistic. The potentials of solar energy are discussed more often than all its limitations.

Judging from the admittedly limited survey of utilities conducted as part of this project, a general awareness of solar technology exists. Solar power plants are being considered by utilities in their generation planning work, although utility readiness to buy solar plants will remain moderate. This is true even though the technical and economic viability of solar power generation can be demonstrated in successfully operating solar plants.

A number of engineering and component manufacturing firms have participated in government- and EPRI-sponsored solar study and development projects. Given sufficient market incentives, most

of these are interested in future participation as constructors or equipment suppliers for commercial solar plants. To support the development of a sufficient industrial base for solar plants, engineering and manufacturing standards must be established to assure reliable performance of solar products.

At this time only a limited pool of trained personnel exist to design, construct, operate, and maintain solar power plants. Formal and on-the-job training must be initiated soon, since the number of trained personnel will have to be expanded by an order of magnitude to staff future solar power plants.

6.2.8 Safety Considerations

An extensive review of the safety aspects of a Brayton cycle central receiver power plant (in most respects very similar to the hybrid power system) was performed by the Boeing Engineering and Construction Company (Ref. 6-1). It identified specific hazards and safety measures that would either lessen the probability of an accident occurring or limit economic losses and personal injury. Major hazards were identifed as:

- Stored energy in high-temperature and pressurized working fluids (e.g., air and steam)
- Reflected high-intensity sunlight
- Exposed surfaces at high temperatures
- Noise and missiles from high-speed rotating machinery
- Elevated work locations

Safe practices and protective gear to prevent injury or losses in case of accident were identified. Most of the preventive and mitigating measures are consistent with current standard industry safety practices. A notable safety advantage of the combined cycle hybrid plant in comparison with some other proposed solar power systems is that its operation does not require circulation of large quantities of toxic or hazardous materials. Failure of a heat pipe would expose only about .1 kg (.2 lb) of sodium or potassium to the atmosphere. Since the internal pressure in the heat pipes is below atmospheric, most of this small amount would become oxidized inside the pipes.

6.3 MARKET ANALYSIS UPDATE

The market analysis results, reported in Section 2, were updated after consideration of the cost and performance of the hybrid power system conceptual design. In addition, representative utilities in the four regions considered in the market analysis, as well as the Solar Energy Research Institute and Electric Power Research Institute, were contacted for comments on the market analysis methodology. Comments were sought on the market analysis results and the prospects of solar energy utilization in their respective service areas. This section summarizes the results of the market analysis update and the utility comments.

6.3.1 Busbar Costs and Market Potential

Table 6-3 shows the capital cost estimate totals for the Modified and Advanced Strawman systems and the conceptual design. The estimates were normalized for mid-1979 dollars and 112.6 MWe capacity. (The AFDC was excluded.) Since the conceptual design uses a heat pipe receiver, comparisons with the Modified Strawman are the most appropriate. As evident from Table 6-1, the conceptual design is about 13 percent more expensive than the preconceptual Modified Strawman. The majority of the difference relates to the use of first-of-a-kind $160/m^2 heliostat costs and higher receiver costs.

Based on the cost sensitivity curves of Figure 2-6, the levelized busbar electricity cost increase due to the higher capital cost would vary from 13 percent at the lowest capacity factors to 3 percent at the highest.

Operating and maintenance cost estimates for the Modified Strawman, Advanced Strawman, and Conceptual Design are shown in Table 6-4. As before, the estimates have been normalized to mid-1979 dollars and 112.6 MWe capacity. The conceptual design O&M costs were estimated from Bechtel's historical data for combined cycle power plants and were based on analyses by subsystem. The estimated costs amount to 1.6 percent of the capital costs, compared with 1.0 percent stated in the Requirement Definition (Ref. 6-2). This accounts for the nearly 60 percent higher O&M costs indicated for the conceptual design. More detailed O&M

TABLE 6-3

CAPITAL COST COMPARISON
(1000's of mid-1979$)

Concept	Cost
Modified Strawman	124,800
Advanced Strawman	139,600
Conceptual Design	141,400
Percent Change from Modified Strawman to Conceptual Design	+13

TABLE 6-4

OPERATING AND MAINTENANCE COST COMPARISON
(1000's of mid-1979$)

Concept	Fixed O&M Cost (per year)	Variable O&M Cost (mills/kWh)	Total (per yr at 48% capacity factor)
Modified Strawman	910	1.08	1,420
Advanced Strawman	1,210	.91	1,640
Conceptual Design	860	2.92	2,240
% Change from Modified Strawman to Conceptual Design	-5	+170	+58

cost estimates also changed the relative size of the fixed and variable O&M cost components; the fixed component decreased from 65 to 40 percent at the 48 percent capacity factor. The major reason for this change is that a variable component has been included in solar plant O&M costs.

Even relatively large changes in O&M costs have only a minor impact on levelized busbar electricity costs. For example, if all else were unchanged, the indicated 58 percent increase in annual O&M costs would result in only a 2 percent increase in levelized busbar electricity cost. The percentage change would be higher at larger capacity factors and smaller at lower capacity factors.

Levelized busbar electricity costs were calculated from performance data shown in Table 6-5. As discussed in Section 5, the conceptual design has slightly lower plant efficiency because of turbine cooling flow requirements and the 7 percent decrease in the average annual solar fraction. These changes are expected to increase levelized busbar electricity cost at 48 percent capacity factor by 2 and 1 percent, respectively.

Figure 6-8 shows the net impact of the above changes on the levelized busbar electricity cost. The curves show busbar costs in mill/kWh for the Pacific Southern region for the Conceptual Design and the Modified Strawman design at 12 percent fuel escalation. The results for first-year operation in 1990 have been converted from current $/kWyr to the more familiar current

TABLE 6-5

REVISED PERFORMANCE DATA

Plant Characteristics	Modified Strawman	Advanced Strawman	Conceptual Design	Percent Change from Modified Strawman to Conceptual Design
Capacity (MWe)	100	100	112.6	+12.6
Life (yr)	30	30	30	—
Daytime Average Heat Rate (Btu/kWh)	7,679	7,355	7,969	+3.8
Nightime Average Heat Rate (Btu/kWh)	7,743	7,423	8,162	+5.41
Average Annual Solar Fraction (%)	31.2	40.8	28.8	-7.7

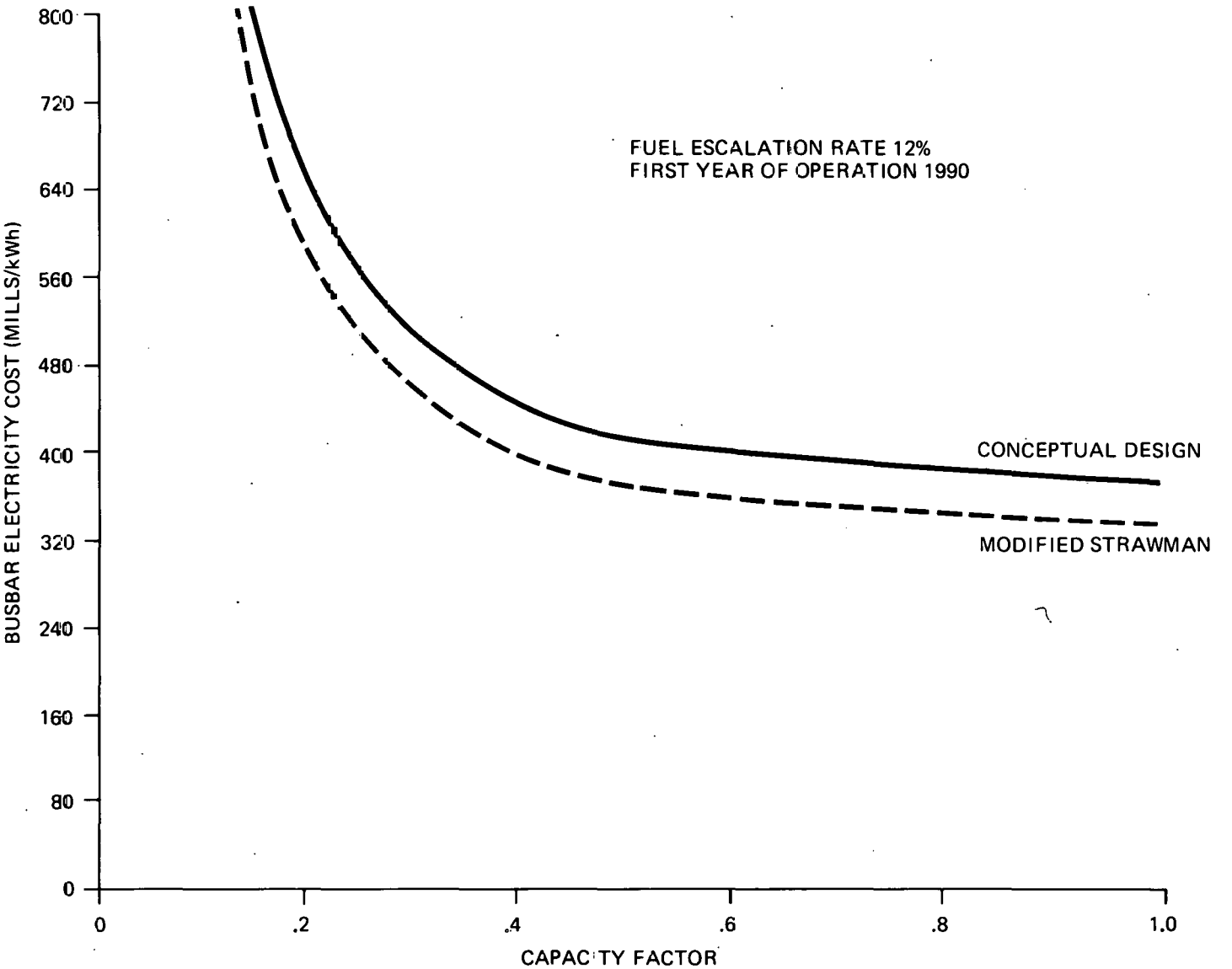

Figure 6-8 LEVELIZED BUSBAR COSTS FOR SOLAR HYBRID PLANTS

dollar mill/kWh used by many electric utilities. At the 40 to 60 percent capacity factors envisioned for the intermediate-load hybrid plant, levelized costs of the conceptual design are from 10 to 11 percent higher than that of the Strawman concept. This correlates well with the overall change of 11.75 percent implied by the sum of the independent percentage changes in busbar cost calculated from the previously defined sensitivity curves.

The impact of higher busbar costs of the conceptual design on the projected market penetration is illustrated by Figure 6-9. This curve shows that, in comparison with the Modified Strawman concept, the cost/performances changes results in a 15 to 18 percent reduction in expected cumulative solar hybrid market penetration in the Pacific Southern region. Proportional reductions occur in all cumulative penetration profiles.

The projected market penetration should be considered pessimistic because of the following:

- The calculated busbar costs of the hybrid system are based on first plant costs without considering the benefits of cost and performance improvements outlined in Section 6.1. In contrast, the conventional technology costs relate to well established technologies and a competitive market.
- Some of the economic parameters specified by the Requirement Definition and used in the analyses, such as high fixed charge rates, tend to penalize the hybrid plant because of its comparatively high capital cost.
- The mid-1978 cost of fuel oil used in the analyses is unrealistically low in light of the rapid escalation in recent months. Higher fuel costs increase the value of the solar contribution, and economic breakeven can be expected at lower escalation rates.

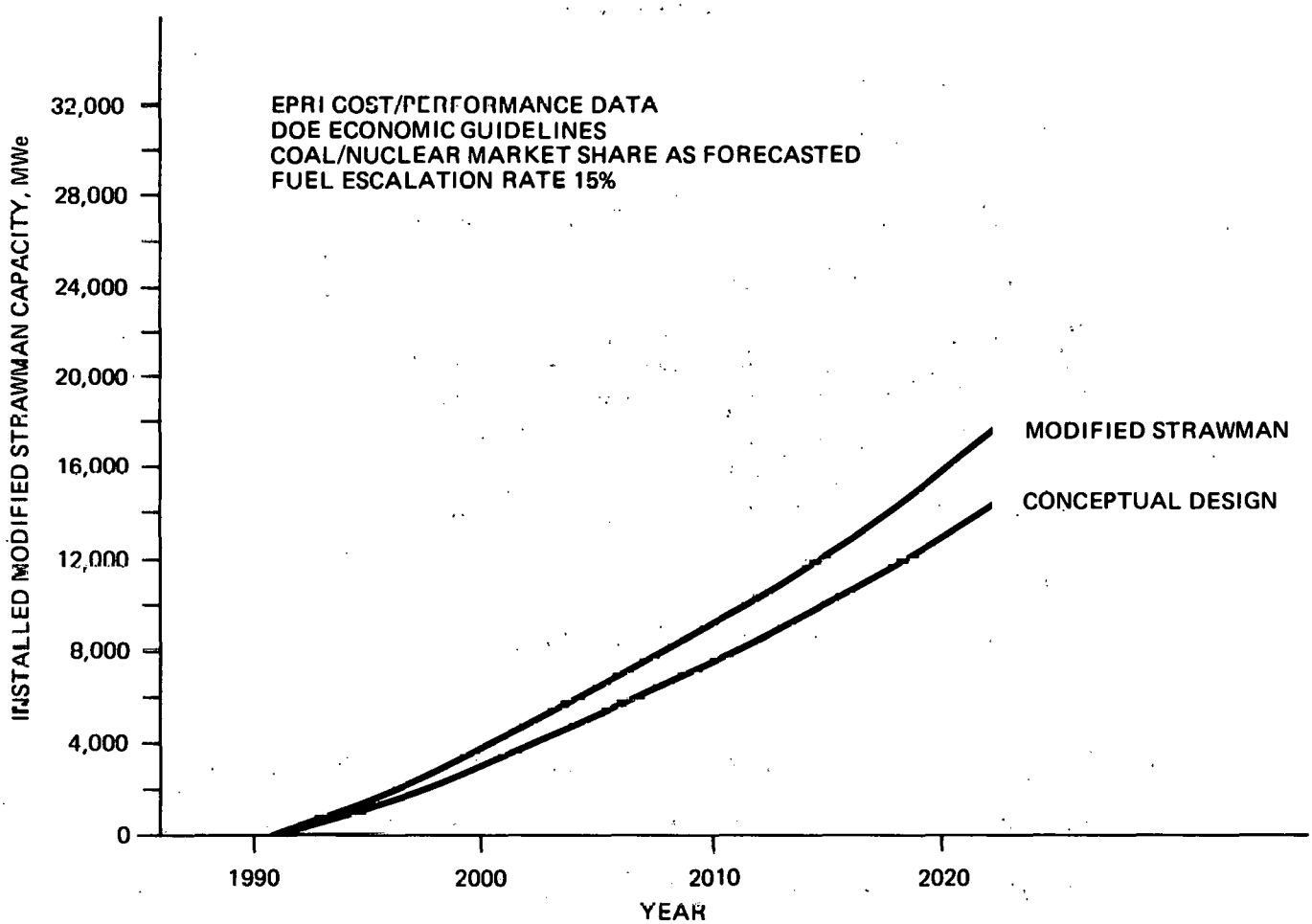

Figure 6-9 SIMULATED MARKET PENETRATION FOR PACIFIC SOUTHERN REGION

6.3.2 Utility Survey

To complement and confirm the analytical results, SERI, EPRI, and selected utility companies from the Mid-Atlantic, South Central, South Mountain, and Pacific Southern regions were requested to respond to a questionnaire shown in Appendix E. Utility companies included in the survey were:

- Pacific Southern Region
  - Pacific Gas and Electric
  - Southern California Edison Company
- South Mountain Region
  - Arizona Public Service
  - Nevada Power Company (Las Vegas)
  - Public Service Company
- South Central Region
  - Texas Electric Service Company
- Mid-Atlantic Region
  - Pennsylvania Power and Light Company

Although based on a small sample, the survey provided a reasonable basis for comparing many of the data used in the market analysis with those used by utilities.

Response to questions relative to the economic bases used by utility companies indicated a remarkable consistency in some of the economic assumptions used to compare technologies. Table 6-6 summarizes these assumptions. The indicated use of 14 to 16 percent fixed charge rates implies that most utilities expect the investment tax credit to be extended indefinitely. Most of the

TABLE 6-6

TYPICAL UTILITY ECONOMIC ASSUMPTIONS

Item	Typical Assumption
Discount rate	11 percent
Fixed charge rate	15 percent
Economic life	25 to 40 years
Capital escalation rate	
Short-term	9 to 10 percent
Long-term	7 to 8 percent
O&M escalation rate	
Short-term	8 to 9 percent
Long-term	7 to 8 percent
Distillate escalation rate	
Short-term	10 to 16 percent
Long-term	7 to 11 percent
Coal escalation rate	
Short-term	7 to 9 percent
Long-term	6 to 8 percent
U_{238} escalation rate	7 to 9 percent

utilities also use different fixed charge rates for different power technologies. These range from about 14.5 percent for combustion turbines to 16 percent for light water reactors. There is also intertechnology variation in assumed mean economic life. Combustion peaking turbines are typically assumed to have a 20 to 25 year life, combined cycle plants a 30 year life, and base-loaded coal and nuclear plants 35 to 40 year lives.

There was somewhat less agreement about projected price behavior of capital equipment, operating and maintenance costs, and fuel. Most utilities assumed different rates of escalation for short-term and long-term planning. Higher short-term nominal escalation rates are typically used over a 3 to 5 year horizon, with lower rates applicable thereafter. This treatment is consistent with an expectation that market action will reduce real price differentials over a longer period of time. As might be expected, the expected nominal oil price escalation exhibited the largest variance.

The survey sample proved too small to make reliable conclusions about specific capital costs ($/kW) and efficiencies of the conventional technologies used in the market analysis. This probably occurs because the reported values are averages over systems which differ in age and duty. Similarly, it was impossible to validate the regional cost variations. However, many of the cost/performance data furnished by the utilities agreed reasonably well with the EPRI data used in the market analysis. Overall, there did not appear to be any gross

discrepancies in the market analysis data. Moreover, several utilities stated that they actually use screening curve/load duration curve techniques for preliminary expansion planning studies.

Utility opinion on the market potential of the hybrid plant seemed to support the analytical results of the market analysis:

- In the Middle Atlantic region, there was no foreseeable market penetration. Winter load peaks, poor overall insolation, and limited land availability were cited as the major problems.
- The South Central region was seen as slightly more promising, with the possibility of a few plants prior to 2000. It was emphasized that the hybrid plants would not be considered unless they proved cost competitive (either on their own merits or through government subsidy). One utility pointed out that the hybrid concept might provide a useful way to extend the useful lives of existing combustion turbine capacity as part of a repowering scheme.
- South Mountain region utilities gave the hybrid plant its most favorable reception. Although solar was seen as accounting for no more than 2 to 10 percent of installed capacity before 2000, Arizona and New Mexico utilities believe that there may be a good demand for combined cycle solar hybrid plants after the year 2000. Stand-alone solar facilities, on the other hand, would probably not achieve a significant market share prior to 2020. The major reasons for favoring the hybrid plant in the short term is 100 percent capacity credit and less operational uncertainty. These utilities also felt that solar plants would be quite compatible with their grid systems (they are summer peaking utilities) and land availability in that region.
- Pacific Southern region utilities see only limited near-term prospects for any significant solar capacity, although the hybrid system was, once again, seen as an appropriate first step toward large-scale solar thermal power generation.

Both SERI and the utilities emphasized that the hybrid system would be used primarily for intermediate-load duty, with only limited use in peaking and base-load applications. The cumulative list of possible competing technologies indicated by the utilities include:

- Advanced combined cycle
- Advanced combustion turbine
- Syn-fuel-fired conventional oil units
- Pumped hydro
- Cycling coal
- Cogeneration
- Wind

This agrees with the market analysis assumption, which excluded base-loaded coal and nuclear plants from direct price competition in the intermediate-load range.

All of the utilities expressed concerns about some common issues:

- It was generally agreed that cost would be a primary consideration in making investments in any solar technology; unless some type of subsidy (notably investment tax credits) was forthcoming, market penetration would be considerably delayed.
- Technical and economic risks were cited as important determinants of commercial feasiblity. Most of the utilities would be hesitant to undertake construction of a hybrid plant before commercial-scale demonstration of the technology. Operational uncertainties involved in an emerging technology imply a higher level of economic risk than is currently acceptable. Unless some compensation for assuming this increased risk is provided, most utilities would not take chances with relatively unproven technologies.

- Fuel availability and fuel price were also major concerns. The domestic and foreign institutional uncertainty surrounding future distillate oil availability prompted two utilities to suggest that a coal-fired hybrid, perhaps incorporating fluidized bed technology, might be more acceptable.

- Five of the seven utilities thought that environmental laws could hinder solar plant construction, but utilities in Arizona and New Mexico said that according to their studies, land constraints were minimal.

- All of the utilities agreed that there would have to be significant new legislation at both the state and federal level if commercial-scale hybrid plants were to become a reality in the near term.

6.4 SUMMARY ASSESSMENT AND CONCLUSIONS

This study was the first DOE-sponsored project on combined cycle solar power systems. Limitations of time and scope prevented detailed considerations of all the technical and economic issues affecting the value of such systems to utilities. There are, however, some salient observations that can be made based on this limited study.

6.4.1 The Conceptual Design

Based on conservative assumptions, the specific cost of the first hybrid plant is $1256/kWe. Its net annual average energy conversion efficiency is 42.8 percent. With 48 percent load factor and 90 percent availability, the annual average solar fraction is .282. The plant can be constructed over 39 months with potential to generate useful power starting after the 33rd month. Based on a preassigned coal/nuclear market share as projected from Department of Commerce data, the hybrid plant can

successfully compete in certain regions with conventional combined cycle and gas turbine plants around the year 2000, at fuel escalation rates of as low as 12 percent.

6.4.2 Potential Improvements

The performance of the conceptual design was determined from conservative estimates for the subsystems. Specific areas where performance improvements may be achieved in the future include:

- Improved mirror reflectivity and higher packing density in the collector subsystem
- Increased receiver efficiency through more comprehensive aperture optimization, reduction of convective losses, and extension of operating temperature limits (and with it the solar fraction) by developing ceramic receivers for temperature up to 1093 C (2000 F)
- More modern gas turbines, now being developed, which promise better energy conversion efficiencies

Major cost reduction can be expected from:

- Automated, high-volume production of heliostats
- Reduced use of Inconel 617 by substituting less expensive alloys in the low temperature zones of the receiver
- Optimized receiver tower design for a specific site and for realistic deflection limits
- Larger plants, taking advantage of economies of scale

6.4.3 Potential Constraints to Widespread Application

A broad range of constraining influences was reviewed but it was concluded that none would stop introduction of the hybrid plant

by 1990. However, some major constraints require early resolution, including:

- Establishment of sufficient heliostat and heat pipe manufacturing capacity
- Completion of heat pipe and catalytic combustor development activities
- Development of a favorable legal and regulatory framework
- Demonstration of technical and economic viability through successful operation of representative-scale plants
- Establishment of engineering and manufacturing standards
- Training of personnel for design, construction, and operation of solar hybrid plants

6.4.4 Conclusions

Based on the system assessment and on the market analysis update, the following conclusions can be drawn about combined cycle solar hybrid power systems and their value to utilities:

- The hybrid plant offers a cost effective alternative to conventional gas turbine and combined cycle generating plants.
- At 15 percent fuel escalation, and within the expected range of coal/nuclear market share, the combined cycle hybrid plants can successfully penetrate the imtermediate-load market.
- Because of potentially lower busbar costs and lower risks of interruptions in generating capability, commercialization of hybrid plants will likely precede the stand-alone solar plants.
- The combined cycle hybrid plants offer significant operating advantages as a result of a simple solar/nonsolar interface, short startup cycles, minimum lag in responding to load changes, flexibility to use a wide range of fuels efficiently, and assured full generating capacity with or without sun.

- Energy storage for the combined cycle hybrid plants is not required and is not economically justified at this time, but its development must be pursued if the national goal for solar energy usage is to be attained.

- The cost and performance of the hybrid plant can be improved through further optimizations and technological development.

- Major technical issues that require future development efforts include the reliability and performance of heat pipes, ceramic receivers for higher temperature operation, and the performance of catalytic combustors.

- Major technical issues that require continuation of study at the system and subsystem level include:

  - Preparation and assessment of system designs with gas turbine inlet temperatures matching the peak receiver temperatures possible with heat pipe and with ceramic receivers

  - Reassessment of earlier engineering decisions in light of up-to-date fuel costs and economic scenarios closer to those used by utilities

  - Optimization of receiver and receiver tower designs

In summary, the study results indicate that the potential value to utilities offered by the combined cycle hybrid plant is considerable; and they show that development work should continue through preliminary design, initial system-level experiment, and detailed design, construction, and operation of the first commercial plant.

Section 7

REFERENCES

1-1 Radosevich, L. (Sandia Laboratories, Livermore, CA), Solar Central Receiver Hybrid Power Systems Requirements Definition, Rev. C, November 6, 1978.

2-1 Technical Assessment Guide, EPRI PS-866-SR, Electric Power Research Institute, Palo Alto, CA, June 1978.

2-2 Park, W. et al. (METREK Division of the MITRE Corporation, McKean, VA), Benefit/Cost Analysis of Accelerating R&D Activities Directed at Near Term Electric Utility Applications, Volume I, Methodology, Analysis, and Results, U.S. ERDA Contract EX-77-V-01-6002, May 1978.

2-3 United States Department of Energy, Summary of the National Energy Act, November 1978.

2-4 Henchling, T. P., Torbot, W. H., and Kern, D. H. (Arthur D. Little, Inc., Cambridge, MA), Implications of Lower Electric Power Growth Through 1990, February 1979.

2-5 Gustaferro, J. F. et al. (Office of Ocean, Resource and Scientific Policy Coordination, U.S. Department of Commerce), Preliminary Forecast of Likely U.S. Energy Consumption/Production Balances for 1985 and 2000 by States (Working Document), November 1978.

3-1 Letter from K.W. Battleson to J. H. Westsik dated March 2, 1979: Subject - "Cost and Earthquake Loads for Conical, Concrete Towers for Solar Central Receivers."

3-2 (Martin Marietta Corporation, Denver, CO), Central Receiver Solar Thermal Power System, Phase I, Preliminary Design Report, SAN-1110-77-2, April 1977.

3-3 (Boeing Engineering and Construction Company, Seattle, WA), Closed-Cycle, High Temperature Central Receiver Concept for Solar Electric Power, EPRI Report ER-629, January 1978.

3-4 Bienert, W. and Wolf, D. (Dynatherm Corp., Cockeysville, MD), Final Technical Report - Heat Pipe Central Solar Receiver, Vol. I, Contract EY-76-C02-2839, 1978.

3-5 (Black & Veatch Consulting Engineers, Kansas City, MO), Solar Thermal Conversion to Electricity Utilizing a Central Receiver Open-Cycle Gas Turbine Design, EPRI Report ER-652, March 1978.

3-6 Poivier, A. (Sanders Associates Inc., Nashua, NH), "Brayton Cycle Receiver Test Results," presented at DOE Large Power Systems Semi-Annual Meeting, Reston, VA, March 20-21, 1979.

3-7 Jarvinen, P.O. (MIT/Lincoln Laboratory, Lexington, MA), "Novel Ceramic Receiver for Solar Brayton Systems," presented at the International Gas Turbine and Solar Energy Conference, San Diego, CA, March 12-15, 1979.

3-8 Hunt, A.J. (Lawrence Berkeley Laboratories, Berkeley, CA), Small Particle Heat Exhangers, LBL-7841, June 1978.

3-9 (Bechtel Power Corp., San Francisco, CA), Combined Cycle Power Plant Capital Cost Estimate, EPRI AF-610, December 1977.

3-10 Brown, D.H. and Corman, J.C. (General Electric Co., Schenectady, NY), Energy Conversion Alternatives Study (ECAS), General Electric Phase I Final Report, Volume II, Part 1, Open Cycle Gas Turbines, Contract No. NAS3-19406, February 1976.

3-11 Letter from L.G. Radosevill to J.H. Westsik dated December 15, 1978.

5-1 Radosevich, L. (Sandia Laboratories, Livermore, CA), Solar Central Receiver Hybrid Power Systems Requirements Definition, Rev. C, November 6, 1978.

5-2 "Wind Forces on Structures," American Society of Civil Engineers Paper No. 3269, Transactions, Volume 126, Part II, 1961.

5-3 AISC Manual, Steel Construction, American Institute of Steel Construction, New York, 1962.

5-4 Central Receiver Solar Thermal Power System Phase I, Volume IV, Receiver Subsystem, Preliminary Draft Report, SAN-1110-77-2, MCR-77-156 (Martin Marietta, Bechtel, Foster Wheeler, and Georgia Tech.), April 1977.

5-5 Receiver Tower Conceptual Design, Stearns-Roger, Sandia Contract 18-8446.

5-6 "Recommended Practice for Planning, Designing, and Constructing Fixed Offshore Platforms," American Petroleum Institute, API RP2A, Sixth Edition, January 1975.

5-7 The NASTRAN Theoretical Manual (Level 15.0), Scientific and Technical Information Office, National Aeronautics and Space Administration, Washington, D.C., NASA SP-221 (01), December 1972.

5-8 (Black & Veatch Consulting Engineers, Kansas City, MO), Solar Thermal Conversion to Electricity Utilizing a Central Receiver, Open-Cycle Gas Turbine Design, EPRI Report ER-652, March 1978.

5-9 Davidson, W.S. et al. (Boeing Engineering and Construction Company, Seattle, WA), Closed Brayton Cycle Advanced Central Receiver Solar-Electric Power System - Final Report, Volume II, SAN/1726-1, November 1978.

5-10 (Foster Wheeler Development Corporation, Livingston, NJ), CFCC Development Program, Commercial Plant Hot Gas Shrouded Ducting Evaluation (Task 2.2), prepared for the Energy Systems Programs Department, General Electric Company, Schenectady, NY, FE-2357-33, June 1978.

5-11 Szaniszlo, A.J. (NASA-Lewis Res. Center, Cleveland, OH), "The Advanced Low-Emissions Catalytic-Combustion Program: Phase 1 - Description and Status," ASME Paper No. 79-GT-192, March 1979.

5-12 DeCorso, S.M., et al. (Westinghouse Gas Turbine Division, Lester, PA and Engelhard Industries, Menlo Park, NJ), "Catalysts for Gas Turbine Combustors - Experimental Test Results," ASME Journal of Engineering for Power, April 1977.

5-13 Mumford, S.E., Hung, W.S.Y., and Singh, P.P. (Westinghouse Electric Corp., Lester, PA), "A Potential Low NO_x Emission Combustor for Gas Turbines Using the Concept of Hybrid Combustion," ASME Journal of Engineering for Power, October 1977.

5-14 Cerkanowicz, A.E., Cole, R.B., and Stevens, J.G., "Catalytic Combustion Modeling; Comparisons with Experimental Data," ASME Journal of Engineering Power, October 1977.

5-15 Hung, W.S.Y., Dickson, W.H., and DeCorso, S.M. (Westinghouse Combustion Turbine Systems Division, Philadelphia, PA), "Preliminary Design Analysis of a Catalytic Ceramic Structure in a Turbine Combustor," ASME Paper No. 78-WA/GT-10, December 1978.

5-16 Lew, H.G., et al. (Westinghouse Combustion Turbine Systems Division, Philadelphia, PA and Engelhard Industries, Menlo Park, NJ), "Experimentally Determined Catalytic Reactor Behavior and Analysis for Gas Turbine Combustors," ASME Paper No. 79-GT-150, March 1979.

5-17 "Steam Electric Plant Construction Cost and Annual Production Expenses 1976," U.S. Department of Energy, 29th Annual Supplement, August 1978.

6-1 Davidson, W.S. et al. (Boeing Engineering and Construction Company, Seattle, WA), Closed Brayton Cycle Advanced Central Receiver Solar-Electric Power System - Final Report, Volume II, SAN/1726-1, November 1978.

6-2 Radosevich, L. (Sandia Laboratories, Livermore, CA), Solar Central Receiver Hybrid Power System Requirement Definition, Rev. C, November 6, 1978.

☆U.S. GOVERNMENT PRINTING OFFICE: 1980-640-258/2187